

SYSTEMS APPROACH TO UNDERSTANDING THE BIOLOGY OF COLD STRESS RESPONSES IN PLANTS

EDITED BY: Rosalyn B. Angeles-Shim, Sunchung Park, Dhruv Lavana and
Andy Pereira

PUBLISHED IN: Frontiers in Plant Science





frontiers

Frontiers eBook Copyright Statement

The copyright in the text of individual articles in this eBook is the property of their respective authors or their respective institutions or funders. The copyright in graphics and images within each article may be subject to copyright of other parties. In both cases this is subject to a license granted to Frontiers.

The compilation of articles constituting this eBook is the property of Frontiers.

Each article within this eBook, and the eBook itself, are published under the most recent version of the Creative Commons CC-BY licence.

The version current at the date of publication of this eBook is CC-BY 4.0. If the CC-BY licence is updated, the licence granted by Frontiers is automatically updated to the new version.

When exercising any right under the CC-BY licence, Frontiers must be attributed as the original publisher of the article or eBook, as applicable.

Authors have the responsibility of ensuring that any graphics or other materials which are the property of others may be included in the CC-BY licence, but this should be checked before relying on the CC-BY licence to reproduce those materials. Any copyright notices relating to those materials must be complied with.

Copyright and source acknowledgement notices may not be removed and must be displayed in any copy, derivative work or partial copy which includes the elements in question.

All copyright, and all rights therein, are protected by national and international copyright laws. The above represents a summary only. For further information please read Frontiers' Conditions for Website Use and Copyright Statement, and the applicable CC-BY licence.

ISSN 1664-8714

ISBN 978-2-88976-917-9

DOI 10.3389/978-2-88976-917-9

About Frontiers

Frontiers is more than just an open-access publisher of scholarly articles: it is a pioneering approach to the world of academia, radically improving the way scholarly research is managed. The grand vision of Frontiers is a world where all people have an equal opportunity to seek, share and generate knowledge. Frontiers provides immediate and permanent online open access to all its publications, but this alone is not enough to realize our grand goals.

Frontiers Journal Series

The Frontiers Journal Series is a multi-tier and interdisciplinary set of open-access, online journals, promising a paradigm shift from the current review, selection and dissemination processes in academic publishing. All Frontiers journals are driven by researchers for researchers; therefore, they constitute a service to the scholarly community. At the same time, the Frontiers Journal Series operates on a revolutionary invention, the tiered publishing system, initially addressing specific communities of scholars, and gradually climbing up to broader public understanding, thus serving the interests of the lay society, too.

Dedication to Quality

Each Frontiers article is a landmark of the highest quality, thanks to genuinely collaborative interactions between authors and review editors, who include some of the world's best academicians. Research must be certified by peers before entering a stream of knowledge that may eventually reach the public - and shape society; therefore, Frontiers only applies the most rigorous and unbiased reviews.

Frontiers revolutionizes research publishing by freely delivering the most outstanding research, evaluated with no bias from both the academic and social point of view. By applying the most advanced information technologies, Frontiers is catapulting scholarly publishing into a new generation.

What are Frontiers Research Topics?

Frontiers Research Topics are very popular trademarks of the Frontiers Journals Series: they are collections of at least ten articles, all centered on a particular subject. With their unique mix of varied contributions from Original Research to Review Articles, Frontiers Research Topics unify the most influential researchers, the latest key findings and historical advances in a hot research area! Find out more on how to host your own Frontiers Research Topic or contribute to one as an author by contacting the Frontiers Editorial Office: frontiersin.org/about/contact

SYSTEMS APPROACH TO UNDERSTANDING THE BIOLOGY OF COLD STRESS RESPONSES IN PLANTS

Topic Editors:

Rosalyn B. Angeles-Shim, Texas Tech University, United States

Sunchung Park, United States Department of Agriculture, United States

Dhruv Lavana, University of Alberta, Canada

Andy Pereira, University of Arkansas, United States

Citation: Angeles-Shim, R. B., Park, S., Lavana, D., Pereira, A., eds. (2022). Systems Approach to Understanding the Biology of Cold Stress Responses in Plants. Lausanne: Frontiers Media SA. doi: 10.3389/978-2-88976-917-9

Table of Contents

- 05** *Biochar's Leacheates Affect the Abscissic Acid Pathway in Rice Seedlings Under Low Temperature*
Jun Yuan, Jun Meng, Xiao Liang, Yang E, Xu Yang and Wen-fu Chen
- 14** *Comparative Metabolomic and Transcriptomic Studies Reveal Key Metabolism Pathways Contributing to Freezing Tolerance Under Cold Stress in Kiwifruit*
Shihang Sun, Jinbao Fang, Miaomiao Lin, Chungeng Hu, Xiujuan Qi, Jinyong Chen, Yunpeng Zhong, Abid Muhammad, Zhi Li and Yukuo Li
- 33** *Genome-Wide Characterization of B-Box Gene Family and Its Roles in Responses to Light Quality and Cold Stress in Tomato*
Xin Bu, Xiujie Wang, Jiarong Yan, Ying Zhang, Shunyuan Zhou, Xin Sun, Youxin Yang, Golam Jalal Ahammed, Yufeng Liu, Mingfang Qi, Feng Wang and Tianlai Li
- 51** *Cold Stress in Wheat: Plant Acclimation Responses and Management Strategies*
Muhammad A. Hassan, Chen Xiang, Muhammad Farooq, Noor Muhammad, Zhang Yan, Xu Hui, Ke Yuanyuan, Attiogbe K. Bruno, Zhang Lele and Li Jincai
- 66** *Nitric Oxide Functions as a Downstream Signal for Melatonin-Induced Cold Tolerance in Cucumber Seedlings*
Yiqing Feng, Xin Fu, Lujie Han, Chenxiao Xu, Chaoyue Liu, Huangai Bi and Xizhen Ai
- 86** *An R2R3-MYB Transcription Factor RmMYB108 Responds to Chilling Stress of Rosa multiflora and Conferred Cold Tolerance of Arabidopsis*
Jie Dong, Lei Cao, Xiaoying Zhang, Wuhua Zhang, Tao Yang, Jinzhu Zhang and Daidi Che
- 100** *Seasonal Metabolic Investigation in Pomegranate (Punica granatum L.) Highlights the Role of Amino Acids in Genotype- and Organ-Specific Adaptive Responses to Freezing Stress*
Parisa Yazdanpanah, Parisa Jonoubi, Mehrshad Zeinalabedini, Homa Rajaei, Mohammad Reza Ghaffari, Mohammad Reza Vazifeshenas and Somayeh Abdirad
- 114** *Integrated Transcriptomics and Metabolomics Analysis Reveal Key Metabolism Pathways Contributing to Cold Tolerance in Peanut*
Xin Wang, Yue Liu, Zhongkui Han, Yuning Chen, Dongxin Huai, Yanping Kang, Zhihui Wang, Liying Yan, Huifang Jiang, Yong Lei and Boshou Liao
- 129** *Functional Characterization of Cotton C-Repeat Binding Factor Genes Reveal Their Potential Role in Cold Stress Tolerance*
Jiangna Liu, Richard Odongo Magwanga, Yanchao Xu, Tingting Wei, Joy Nyangasi Kirungu, Jie Zheng, Yuqing Hou, Yuhong Wang, Stephen Gaya Agong, Erick Okuto, Kunbo Wang, Zhongli Zhou, Xiaoyan Cai and Fang Liu

- 145** *Integration of Metabolome and Transcriptome Studies Reveals Flavonoids, Abscissic Acid, and Nitric Oxide Comodulating the Freezing Tolerance in Liriope spicata*
Zhen Peng, Ye Wang, Wen-Tian Zuo, Yue-Rong Gao, Run-Zhi Li, Chun-Xin Yu, Zi-Yan Liu, Yi Zheng, Yuan-Yue Shen and Liu-Sheng Duan
- 160** *Transcriptome Analysis Revealed a Cold Stress-Responsive Transcription Factor, PaDREB1A, in Plumbago auriculata That Can Confer Cold Tolerance in Transgenic Arabidopsis thaliana*
Wenji Li, Suping Gao, Ting Lei, Liqiong Jiang, Yifan Duan, Zian Zhao, Jiani Li, Lisha Shi and Lijuan Yang
- 176** *Inositol Improves Cold Tolerance Through Inhibiting CBL1 and Increasing Ca²⁺ Influx in Rapeseed (Brassica napus L.)*
Lei Yan, Liu Zeng, Ali Raza, Yan Lv, Xiaoyu Ding, Yong Cheng and Xiling Zou



Biochar's Leacheates Affect the Absciscic Acid Pathway in Rice Seedlings Under Low Temperature

Jun Yuan^{1,2}, Jun Meng^{1*}, Xiao Liang^{1,2}, Yang E¹, Xu Yang¹ and Wen-fu Chen¹

¹ Liaoning Biochar Engineering and Technology Research Center, Shenyang Agricultural University, Shenyang, China,

² Eastern Liaoning University, Dandong, China

OPEN ACCESS

Edited by:

Sunchung Park,
Crop Improvement and Protection
Research (USDA-ARS), United States

Reviewed by:

Salar Farhangi-Abriz,
University of Tabriz, Iran
Kazuo Nakashima,
Japan International Research Center
for Agricultural Sciences (JIRCAS),
Japan

*Correspondence:

Jun Meng
mengjun1217@syau.edu.cn

Specialty section:

This article was submitted to
Plant Abiotic Stress,
a section of the journal
Frontiers in Plant Science

Received: 28 December 2020

Accepted: 03 February 2021

Published: 04 March 2021

Citation:

Yuan J, Meng J, Liang X, Yang E,
Yang X and Chen W (2021) Biochar's
Leacheates Affect the Absciscic Acid
Pathway in Rice Seedlings Under Low
Temperature.
Front. Plant Sci. 12:646910.
doi: 10.3389/fpls.2021.646910

Organic molecules of biochar's leacheates are known to increase the cold resistance of rice seedlings. Yet, it remains unclear whether the organic molecules of biochar leacheates can interact with the absciscic acid (ABA) signaling pathway associated with low temperature. This study used experiments and bioinformatics (molecular docking) to determine which of the organic molecules of biochar's leacheates could influence the ABA signaling pathway. Specifically, we investigated whether these molecules affected ABA, a plant hormone linked to cold resistance. The contents of endogenous ABA and its precursor carotenoids were determined under low-temperature stress (10°C) and treatment with different concentrations of biochar leacheates. With increased leachate concentrations, the endogenous ABA and carotenoid contents also increased, as did the expression of ABA- and cold-related genes. When rice seedlings were instead treated with exogenous ABA, it also affected the above-measured indexes; hence, we surmised that certain water-soluble organic molecules of biochar could exert a similar effect as ABA. We first used gas chromatography/mass spectrometry (GC/MS) to identify the organic molecules in the biochar extract, and then we used molecular docking software Autodock to show how they interact. We found that the molecule (1R, 2R, 4S)-2-(6-chloropyridin-3-yl)-7-azabicyclo(2.2.1)heptane was simplified, as Cyah could dock with the ABA receptor protein OsPYL2 in rice, which shows Cyah in biochar is probably an analog of ABA, with a similar function. Based on these results, we conclude that organic molecules of biochar's leacheates could enter into rice plants and interact with ABA-related proteins to affect the ABA signaling pathway, thereby improving the cold stress resistance of plants.

Keywords: absciscic acid, biochar, cold stress, molecular docking, rice seedlings

INTRODUCTION

Biochar is the product of heating biomass in the absence of or with limited air to above 250°C in a process called charring or pyrolysis (Lehmann and Joseph, 2015). Biochar is often used as an additive to improve the quantity of the environment and amend the soil (Lehmann and Joseph, 2015), and such additions can reportedly enhance plant growth characteristics (Waqas et al., 2018). For example, biochar treatments increased both plant height and leaf size in tomato (Graber et al., 2010); treatment with attapulgitic clay/yak dung (50/50) biochar resulted in the highest pasture yield

and promoted the nutritional quality of grass (Rafiq et al., 2017); and biochar alone or in a co-application stimulated growth in halophyte plants, including their germination, root development, and biomass (Zheng et al., 2018).

Biochar can affect plant growth *via* several plausible mechanisms: (1) by improving soil and regulating the soil microbial environment, which indirectly or directly affects plant root growth and thus affects the whole plant (Lehmann and Joseph, 2015; Zheng et al., 2018); (2) by providing nutrients for plants to uptake (Wang et al., 2018); (3) by organic molecules on the surface of biochar that can promote or inhibit plant growth (Graber et al., 2010; Lievens et al., 2014; Gale et al., 2016; Yuan et al., 2017); and (4) by affecting endogenous plant hormones, which can impact plant development and physiology (Yang et al., 2015; French and Iyerpascuzzi, 2018; Waqas et al., 2018). Recently reported effects of biochar on plant hormones include changes to jasmonic acid levels in two rice varieties that altered their resistance to herbivory (Waqas et al., 2018) and evidence suggesting that biochar promotes growth, in part, *via* stimulation of the Gibberellic acid (GA) pathway (French and Iyerpascuzzi, 2018). The previous paper dealt with low temperature (cold), yet the relationship between biochar and abscisic acid (ABA)—which is closely related to low temperature—has not been reported on.

Low temperature may negatively impact agricultural crop productivity (Li et al., 2015). ABA is an essential phytohormone that not only regulates seed dormancy, germination, and seedling growth but also is involved in plant responses to environmental stresses, such as drought, high salinity, and chilling (He et al., 2014). In the presence of ABA, the ABA receptor PYR1/PYL-like (PYL)/regulatory components of ABA receptor (RCAR) undergoes conformational changes and mediates interactions with the negative regulator type 2C protein phosphatase (PP2C), thus inhibiting their phosphatase activity, which then activates the positive regulator Class III SNF1-related protein kinase 2 (SnRK2s) to turn on downstream gene expression (Hubbard et al., 2010; Cao et al., 2013). The rice (*Oryza sativa*) ortholog of the ABA receptor in OsPYL/RCAR5 was recently identified as a positive regulator in seed germination and early seedling growth (Kim et al., 2012, 2014). He et al. (2014) determined the crystal structure of the ABA–OsPYL2–OsPP2C06 ternary complex, and the first structure of the ABA receptor in rice revealed a molecular mechanism of ABA sensitivity and phosphatase inhibition of OsPYLs (He et al., 2014).

Naturally occurring small molecules have long been foci for study due to their diverse biological activities (Bhuiya et al., 2017). One way to investigate these molecular and protein interactions is through molecular docking, which is now the most frequently used computational method for studying the interactions between organic molecules and biological macromolecules (Yang et al., 2015). In this context, docking is able to predict the preferred position of a ligand inside a receptor binding site (Ramirez and Caballero, 2018).

In previous work, we showed that biochar additions have a positive impact on cold stress resistance in rice plants (Yuan et al., 2017). Yet, it remains unclear whether the organic molecules of biochar can interact with the ABA signaling pathway associated with cold resistance. This study treated rice

seedlings with different leachates of biochar and combined the use of experiments and bioinformatics (molecular docking) to determine which of the organic molecules of biochar's leachates could influence the ABA signaling pathway. A mechanism was postulated: organic molecules of biochar's leachates can successfully connect with the ABA receptor protein, thereby affecting the ABA pathway of rice, which eventually fosters their resistance to cold.

MATERIALS AND METHODS

Preparation of Biochar Leachates and Exogenous Absciscic Acid Treatment

The biochar used in our experiments was generated from fast pyrolysis of rice husks (Shen-nong 9816), conducted at the Rice Research Institute of Shenyang Agriculture University, China. Rice husks were heated to 400°C at a rate of 10°C/min before the temperature was held constant for 1 h. The selected concentrations of biochar leachates were 0, 1, 3, 5, and 10%. In the control group (0%, no biochar) we used 25 g of dry soil to cultivate the rice seedlings. To prepare the 1, 3, 5, and 10% concentrations of biochar leachates, we, respectively, weighted 0.25, 0.75, 1.5, and 2.5 g of biochar and put them into separate beakers containing 50 ml of distilled water; these were stirred at 25°C for 72 h, and then filtered through a 0.22-μm sieve. All bacteria were removed from leachates and soils by autoclaving at 121°C for 60 min, and all samples were stored at 4°C prior to further analysis.

For the exogenous ABA treatment, 0, 10, 20, and 30 mg of ABA was placed into respective Eppendorf (EP) tubes, with a little anhydrous ethanol (500 μl) added in to help dissolve them. Then, each mixture was transferred to a beaker containing 1,000 ml of distilled water and stirred well.

Planting and Treatment of Rice Seedlings

The Japonica Super Rice “Shen-nong 9816,” a cultivar with strong resistance to stress and wide adaptability was used in this study, sourced from the Rice Research Institute, Shenyang Agricultural University, China. Its seeds were germinated in a culture dish with distilled water. Germinated seedlings were sown into small 7-cm-diameter pots containing 25 g of dry soil, and each pot received 50 ml of one of the five biochar leachate concentrations. The properties of the soil are described in a previous paper (Yuan et al., 2017). All these samples were kept in growth chambers for 5 days at 28°C day and night but subject to a 12-h/12-h light/dark cycle at 75% relative humidity and the light intensity was maintained at 12,000–14,000 lux. The 5-day-old seedlings were kept at 10°C all day and night in another growth chamber (under the same light–dark cycle and relative humidity conditions) for 21 days to simulate the cold stress treatment. The four concentrations of the exogenous ABA treatment were sprayed onto the 5-day-old rice seedlings under a normal temperature (28°C) after which they were kept at 10°C for 21 days. Treatment time was based on when the plants developed obvious phenotypes at low temperatures or under control conditions. The experimental

temperature and protocol used in this study follow those used by Challam et al. (2015). The response variables measured included plant height, dry weight, and root length for both the control and the four treatment groups. These data were used to evaluate the effects of low temperature on rice plant growth. Finally, some samples were kept in growth chambers for 7 days at 28°C day and night to serve as the normal temperature control.

Measurement of Carotenoids and Absciscic Acid

Carotenoids were extracted from 0.1 g of rice seedling leaves *via* incubation for 72 h in 3 ml of 100% dimethyl sulfoxide at 65°C. The concentrations were calculated using an absorbance measurement of the extract at 480, 649, and 665 nm and the equations described in Pompelli et al. (2013). Endogenous ABA analysis was carried out using high-performance liquid chromatography (HPLC) (Agilent 1200 Series, United States) with an Agilent C18 column. The mobile phase was methanol:acetonitrile:acetic acid (60:5:35), the flow rate was 0.8 ml/min, and the injection volume was 10 microns, with samples detected at an absorbance of 262 nm (Cheng et al., 2013).

Quantitative Real-Time PCR

Absciscic acid - and cold-regulated genes were identified in this study by using the National Center for Biotechnology Information (NCBI) database¹, while the primers for the quantitative real-time PCR (qRT-PCR) genes were designed and amplified using the Primer 3 software. The qRT-PCR was carried out in a 20-μl reaction vessel that contained 10 μl of 2 × *TransScript*[®] Top Green qPCR SuperMix (TransGen Biotech, China), 0.4 μl of passive reference dye, 0.4 μl of both forward and reverse primers, 4.2 μl of nuclease-free water, and 5 μl of diluted cDNA (1:10). The PCR amplification was performed using System LightCycler 480 equipment (Roche Applied Science, Germany), and the qRT-PCR procedure steps were 94°C for 30 s, followed by 45 cycles of 94°C for 5 s, 55°C for 15 s, and 72°C for 10 s. Values for gene expression were calculated following the method outlined by Ramakers et al. (2003) and used delta-delta Ct (Ramakers et al., 2003). The gene primers used for qRT-PCR are listed in **Supplementary Table 1**.

¹ www.ncbi.nlm.nih.gov

Molecular Docking Analysis

We identified those proteins involved in ABA pathways as influenced by biochar organic molecules *via* comparison with the NCBI database and then utilized the Research Collaboratory for Structural Bioinformatics (RCSB) protein database to obtain their structures. The three-dimensional (3D) structures of small organic molecules were reported in our previous paper (Yuan et al., 2017), while specified target proteins and organic molecules for the docking analysis were determined using AutoDock tools v.1.5.6 in AutoDock software v.4.2 (Scripps Research Institute, United States) and the procedures recommended by Trott and Olson (2009).

Statistical Analyses

Phenotypic parameters and ABA and carotenoid contents were derived from 30 biological replicates and were expressed as means ± SE. Expression of genes in rice plants were repeated independently for at least three times, and data are shown as means ± SE. All numerical data were analyzed using SPSS software (v17.0) and Microsoft Excel 2003. The use of * and ** denotes different mean concentrations of biochar and ABA that exhibited significant differences at the $P < 0.05$ and $P < 0.01$ alpha levels when compared to the control group only.

RESULTS

Biochar Affects the Absciscic Acid Signaling Pathway of Rice Seedlings

Several groups of experiments were conducted, and the results showed the same trend. A group of data and some rice seedlings were selected for the results and phenotypes presented in this paper. Rice plants treated with different concentrations of biochar leacheates (i.e., control, 1, 3, 5, and 10%) were grown in the same pots under well-watered conditions, and all of them developed the same phenotype after 5 days of growth at 28°C. While under cold stress, compared with the control; the 1% leacheate treatment reduced their plant height by 21.8% and root length by 14.58% (**Table 1**). However, greater leacheate concentrations (i.e., 3, 5, and 10%) led to continuous enhancement of rice plant growth (**Figure 1A**), though only the 5 and 10% concentrations significantly increased plant height (by 17.46 and 30.45%, respectively) and root length (by 22.05 and 34.91%, respectively). Changes in dry weight among leacheate concentrations were not significant, however (**Table 1**).

TABLE 1 | Phenotypic parameters (mean ± SE) for one part of each 5-day-old rice seedling treated with biochar leacheates and grown at 10°C for 21 days.

Parameters	Biochar treatment concentrations				
	Control (0%)	1%	3%	5%	10%
Plant height (cm)	10.87 ± 0.60	8.50 ± 1.57*	10.93 ± 0.60	13.17 ± 2.02*	15.63 ± 0.42**
Root length (cm)	3.43 ± 0.25	2.93 ± 0.31	3.67 ± 0.25	4.4 ± 0.66**	5.27 ± 0.21**
Dry weight (mg)	0.0292 ± 0.0035	0.0235 ± 0.0037	0.0292 ± 0.0071	0.0309 ± 0.0085	0.0348 ± 0.0042

Asterisks indicate statistically significant differences from the control ($n = 30$, * $P < 0.05$, and ** $P < 0.01$).

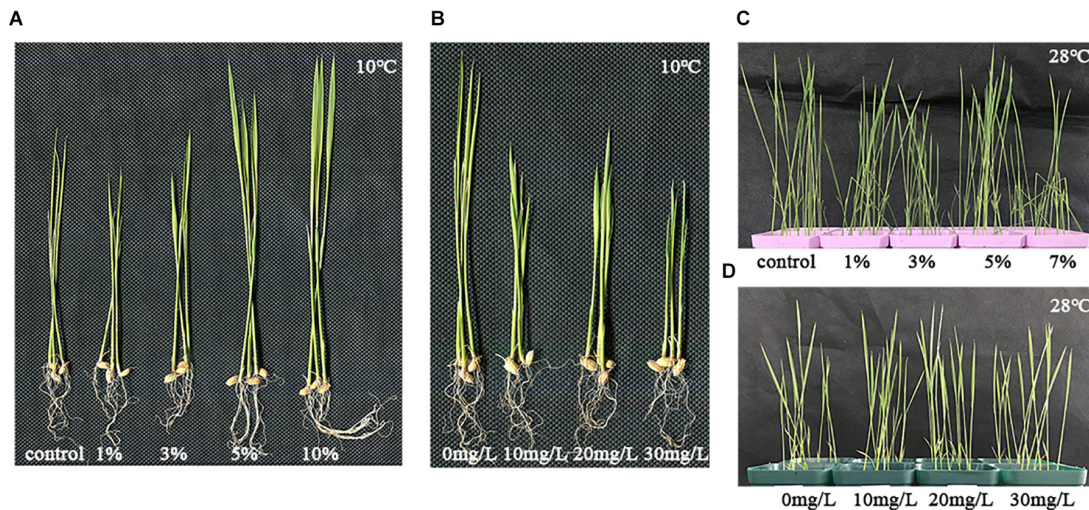


FIGURE 1 | Phenotypes of plants treated with abscisic acid (ABA) and biochar leachates under low and normal temperature. One part of each 5-day-old rice plants was then grown at 10°C for 21 days. This figure shows the different plant phenotypes that ensued under cold stress. **(A)** Rice plants were subjected to different concentrations of biochar leachates (i.e., control, 1, 3, 5, and 10%). **(B)** Rice plants were subjected to different concentrations of ABA (0, 10, 20, and 30 mg/L). One part of rice plant was then grown at 28°C for 7 days, as the normal temperature control. **(C)** Biochar leachates (i.e., control, 1, 3, 5, and 10%) and **(D)** rice plants were subjected to different concentrations of ABA (0, 10, 20, and 30 mg/L).

The phenotypic parameters of plants treated with different concentrations of exogenous ABA at 10°C are summarized in **Table 2**. Plant height in the 10, 20, and 30 mg/l ABA treatments was lower than in the 0 mg/l treatment; however, no significant changes were found in root length and dry weight relative to the control (**Figure 1B** and **Table 2**).

One part of rice seedlings was treated with biochar leachates and grown at 28°C for 7 days as the normal temperature control. Compared with 0%, there were no significant changes found in plant height, root length, nor dry weight under the different concentrations of leachates, except for the 3% leachate treatment for plant height (**Figure 1C** and **Table 3**).

However, there were no significant changes found in plant height, root length, and dry weight under different concentrations of exogenous ABA treatments (**Figure 1D** and **Table 4**).

Quantitative Real-Time PCR Analysis

To further elucidate the influence of biochar on cold tolerance, we selected seven important ABA- and cold-related genes (i.e., *ABF1*, *ABF2*, *OsPsbR1*, *OsPsbR3*, *OsABA45*, *LEA3*, and *RAB16A*) known for their involvement in the ABA and cold signaling pathways. Relative expression analysis using qRT-PCR revealed that the proportion of these transcription factors changed depending on the biochar leachate concentrations applied (i.e., 1, 3, 5, and 10%) when compared with the control. In this experiment, relative to the control, the expression of *OsABF1* under high concentrations of biochar leachates (5 and 10% treatments) was upregulated, whereas it was downregulated at low concentrations (1 and 3% treatments); however, no significant differences were detected (**Figure 2A**). Likewise, *OsABF2* expression levels in the treatments with 3, 5, and 10% biochar leachates

were upregulated but downregulated in the 1% concentration treatment (**Figure 2B**). The expression of *OsPsbR1* in all biochar leachate treatments except that of 10% was similar to that of the control (**Figure 2C**). *OsPsbR3* expression was significantly upregulated under greater biochar leachate concentrations (**Figure 2D**), while *OsABA45* was upregulated only under the 5 and 10% concentrations of biochar leachates and downregulated in the other two treatments (**Figure 2E**). The expression of *LEA3* was significantly upregulated and downregulated in the 10 and 1% concentration treatments, respectively (**Figure 2F**). With more biochar applied, the expression level of *RAB16A* gradually increased, differing significantly from that of the control in the 5 and 10% concentration treatments (**Figure 2G**).

Figure 3 shows the expression levels of the same seven genes in rice seedlings treated with different concentrations of exogenous ABA. Compared with the control (treated with 0 mg/L exogenous ABA), in rice seedlings treated with 10, 20, and 30 mg/L exogenous ABA, the expression levels of *OsABF1*, *OsABF2*, *OsABA45*, *OsPsbR1*, and *OsPsbR3* were gradually upregulated (except the expression levels of *OsABF2* in 30 mg/L exogenous ABA), while the expression of *LEA3* and *RAB16A* genes was not induced by 10 nor 30 mg/L, but slightly upregulated by 20 mg/L ABA.

Exogenous Abscisic Acid Treatment Analysis

Under low-temperature stress, 21-day-old rice seedlings grown with different biochar leachate concentrations (control, 1, 3, 5, and 10%) or different exogenous ABA concentrations (0, 10, 20, and 30 mg/L) were sent to the Wanze biotechnology company (Shenyang, China) to measure their contents of ABA and ABA-precursor substances (carotenoid). Compared with

TABLE 2 | Phenotypic parameters (mean \pm SE) for one part (subsample of rice seedlings) of each 5-day-old rice seedling treated with ABA and grown at 10°C for 21 days.

Parameters	Exogenous ABA concentrations			
	0 mg/L	10 mg/L	20 mg/L	30 mg/L
Plant height (cm)	10.87 \pm 0.60	6.83 \pm 0.86**	7.47 \pm 1.08**	6.05 \pm 0.72**
Root length (cm)	2.47 \pm 0.38	2.27 \pm 0.25	2.1 \pm 0.26	2.21 \pm 0.28
Dry weight (mg)	0.0291 \pm 0.0021	0.0255 \pm 0.0061	0.0249 \pm 0.0025	0.0231 \pm 0.0019

Asterisks indicate statistically significant differences from the control ($n = 30$, * $P < 0.05$, and ** $P < 0.01$).
ABA, abscisic acid.

TABLE 3 | Phenotypic parameters (mean \pm SE) for one part of rice seedlings treated with biochar leacheates and grown at 28°C for 7 days.

Parameters	Biochar treatment concentrations				
	Control (0%)	1%	3%	5%	10%
Plant height (cm)	15.89 \pm 0.15	15.78 \pm 0.2635	14.30 \pm 0.13**	16.28 \pm 0.25	15.54 \pm 0.23
Root length (cm)	5.34 \pm 0.31	5.17 \pm 0.48	5.25 \pm 0.27	5.47 \pm 0.20	5.50 \pm 0.27
Dry weight (mg)	0.0322 \pm 0.0014	0.0312 \pm 0.0019	0.0338 \pm 0.0020	0.0395 \pm 0.0016	0.0332 \pm 0.0022

Asterisks indicate statistically significant differences from the control ($n = 30$, * $P < 0.05$, and ** $P < 0.01$).

TABLE 4 | Phenotypic parameters (mean \pm SE) for one part of rice seedlings treated with ABA and grown at 28°C for 7 days.

Parameters	Exogenous ABA concentrations			
	0 mg/L	10 mg/L	20 mg/L	30 mg/L
Plant height (cm)	12.61 \pm 0.49	13.01 \pm 0.93	13.32 \pm 1.34	12.41 \pm 0.75
Root length (cm)	2.48 \pm 0.14	2.70 \pm 0.15	2.77 \pm 0.47	2.78 \pm 0.21
Dry weight (mg)	0.0293 \pm 0.0044	0.0329 \pm 0.0031	0.0367 \pm 0.0035	0.0286 \pm 0.0028

Asterisks indicate statistically significant differences from the control ($n = 30$, * $P < 0.05$, and ** $P < 0.01$).
ABA, abscisic acid.

the control, both ABA and carotenoid were lower in rice seedlings treated with 1% biochar leacheate, but with greater leacheate concentrations (3–10%), they gradually increased (**Figure 4A**). The ABA and carotenoid contents were promoted by ABA applied to the plants, reaching their maximum value at 20 mg/L (**Figure 4B**).

Docking Analysis

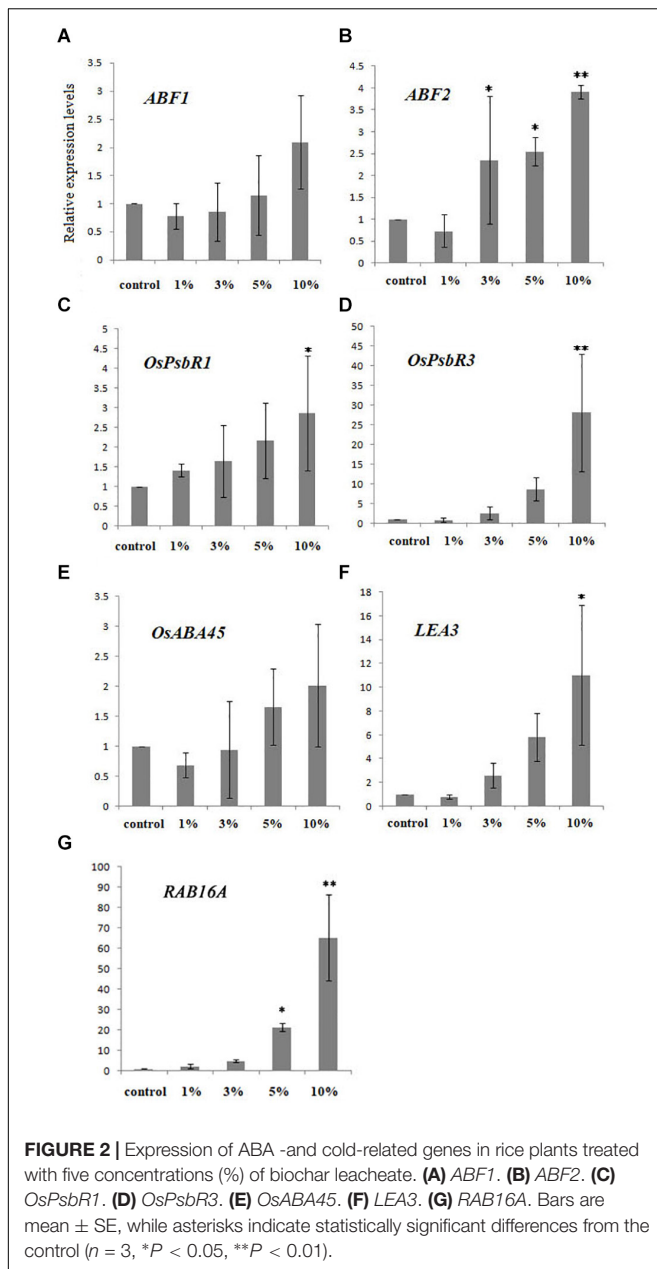
In our prior study, we had used the gas chromatography/mass spectrometry (GC/MS) method to extract 20 organic molecules from the surface of biochar, of which 14 kinds of organic molecules with a relatively small relative molecular weight were used for subsequent molecular docking (Yuan et al., 2017). Here, we used the Plant Metabolic Pathway (PMN) database to identify the potential biological activities of these candidate compounds (**Table 5**).

We searched for the ABA-related receptor protein in the RCSB database and found that the protein OsPYL2 (ID:4OIC) from rice had a known 3D structure (He et al., 2014). All the candidate organic molecules (**Table 5**) were docked with the OsPYL2 protein, and the organic molecule (1R, 2R, 4S)-2-(6-chloropyridin-3-yl)-7-azabicyclo[2.2.1]heptane was simplified as Cyah (white molecules in **Figure 5A**), which could be successfully docked with protein OsPYL2. Cyah is linked to the amino acid

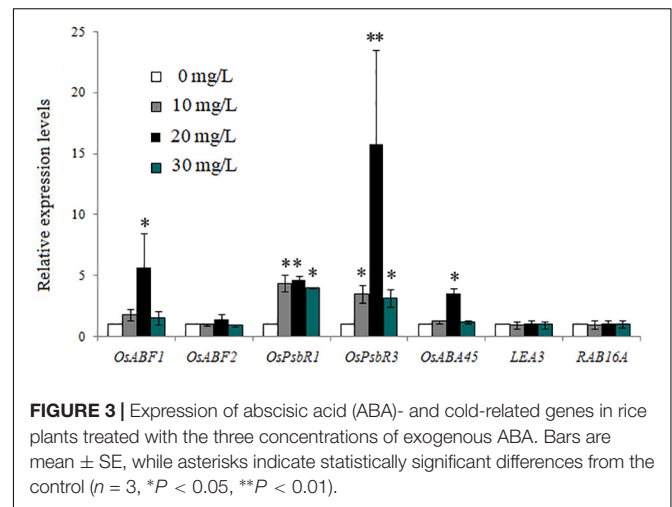
residue SER-107 of the protein by a hydrogen bond (yellow dashed line). The binding mode of the OsPYL2 protein to the original ligand ABA (yellow molecule, depicted in **Figure 5B**) is also a hydrogen bond, while ABA is linked to the amino acid residue LYS-74 in the protein by hydrogen bond. Because the association of Cyah and OsPYL2 is *via* hydrogen bonding, like that of ABA and OsPYL2, we reasonably speculate that the function of Cyah may be similar to that of ABA.

DISCUSSION

High concentration of biochar enhanced the growth of a bean under saline condition, which may have contributed to the reduction of Na uptake and enhancement of K, Ca, and Mg contents (Farhanqi-Abriz and Torabian, 2018), and application is known to preserve rice pollen given high-temperature stress (Fahad et al., 2015). Our results also reveal high concentrations of biochar leacheates led to enhancement of rice plant growth under low-temperature stress (**Figure 1A**). The heights of the plants treated with 10, 20, and 30 mg/L exogenous ABA were less than those lacking ABA and those of 20 mg/L treatment were slightly better (**Figure 1B**). This phenotype (**Figure 1B**) may arise because although ABA apart from a gradual increase in a certain



low concentration can affect cold resistance in plants, its primary role is to slow plant growth (Mega et al., 2015). In this way, when temperatures are low and the plant grows slowly, it can better protect itself from this temporary stress (Mega et al., 2015). Under low temperature, both biochar and ABA can influence the growth and development of rice. However, within a certain concentration range, the biochar does not have the inhibiting effect of ABA (Figures 1A,B). Biochar and ABA can play their roles better under adverse environmental conditions (Kim et al., 2014; Fahad et al., 2015). Thus, in our study, there were no significant changes found in plant phenotypes under different concentrations of biochar leachates and exogenous ABA treatments in the normal temperature control (Figures 1C,D).



A number of basic leucine zipper (bZIP) transcription factors are known to function in stress signaling in plants, but to date, few have been functionally characterized in rice: the *OsABF1* and *OsABF2* genes do encode a bZIP transcription factor (Hossain et al., 2010a,b). Their expression in seedling shoots and roots is reportedly induced by various abiotic stress treatments, such as anoxia, salinity, drought, oxidative stress, cold, and ABA (Hossain et al., 2010a,b). However, under the same low temperature, the expression of *OsABF1* and *OsABF2* genes within a plant may differ, since they can each respond to ABA (Figures 2A,B).

PsbR is known as the 10-kDa Photosystem II polypeptide. Although this plant PsbR is thought to play important roles in photosynthesis, little is actually known about its contribution to abiotic stress resistance (Li et al., 2017). In a recent study, the *OsPsbR1* gene was upregulated in response to cold stress, while the upregulation of *OsPsbR3* gene was observed when plants were treated with ABA (Li et al., 2017). We found that the expression of *OsPsbR1* in each biochar treatment was similar to that of the control, except under the 10% concentration treatment (Figure 2C), while that of *OsPsbR3* increased with all leachate concentrations tested (Figure 2D). When ABA changes, the expression level of *OsPsbR3* gene also changes, indicating that the surface substances of biochar may affect the endogenous ABA in rice. The *OsABA45* gene in rice seedlings can be induced by low temperature, dehydration, high salt, and ABA (Rabbani et al., 2003); *LEA3* and *RAB16A* genes are associated with stress and can be induced by ABA (Zou et al., 2008; Hossain et al., 2010b). At the same low temperature, the expression of *OsABA45*, *LEA3*, and *RAB16A* genes differed in response to ABA (Figures 2E–G). Therefore, we speculate that substances in the biochar leachates can affect the ABA pathway.

As a phytohormone, ABA is extensively involved in plant responses to abiotic stresses, such as drought, low temperature, and osmotic stress. In response to cold stress, plants usually accumulate an increased amount of ABA, and many stress-inducible genes are regulated by the endogenous ABA that accumulates during conditions of stress (Shinozaki et al., 2003).

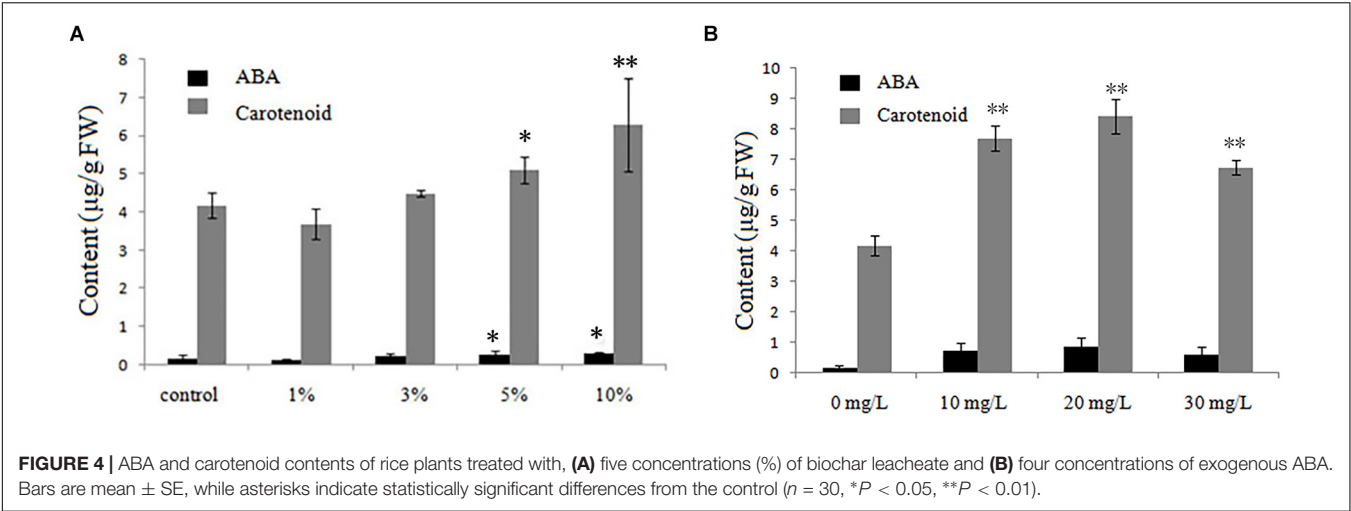


TABLE 5 | Candidate organic molecules obtained from biochar surface extracts.

Name	Potential biological activity
6-(Methylthio)hexa-1,5-dien-3-ol	No function has been reported
Formamide, N, N-diethyl-	No function has been reported
1-Oxa-4-azaspiro(4.5)decan-4-oxyl, 3,3-Dimethyl-8-oxo-	No function has been reported
2-Propanamine, N,N-dimethyl-	Involved with enzyme compensation system reaction
Ethanamine, N-pentylidene-	Takes part in some chemical reactions
Acetamide, N,N-diethyl-	Involved with enzyme compensation system reaction
Cyclopentanone, 2-(1-methylpropyl)-	No function has been reported
Cyclopentane, 1,2,3-trimethyl-	Biosynthesis of jasmonic acid
Pyrrole, 2-(4-methyl-5-cis-phenyl-1,3-oxazolidin-2-yl)-	Four pyrrole synthesis pathways Four pyrrole degradation pathways
1,2-Dimethylaziridine	No function has been reported
(1R,2R,4S)-2-(6-chloropyridin-3-yl)-7-azabicyclo(2.2.1)heptane (Cyah)	Takes part in most chemical reactions
2-Acetyl-5-methylfuran	No function has been reported
Pyridine	Participates in some conventional chemical reactions
Trans-2,4-Dimethylthiane, S,S-dioxide	Involved with enzyme compensation system reaction

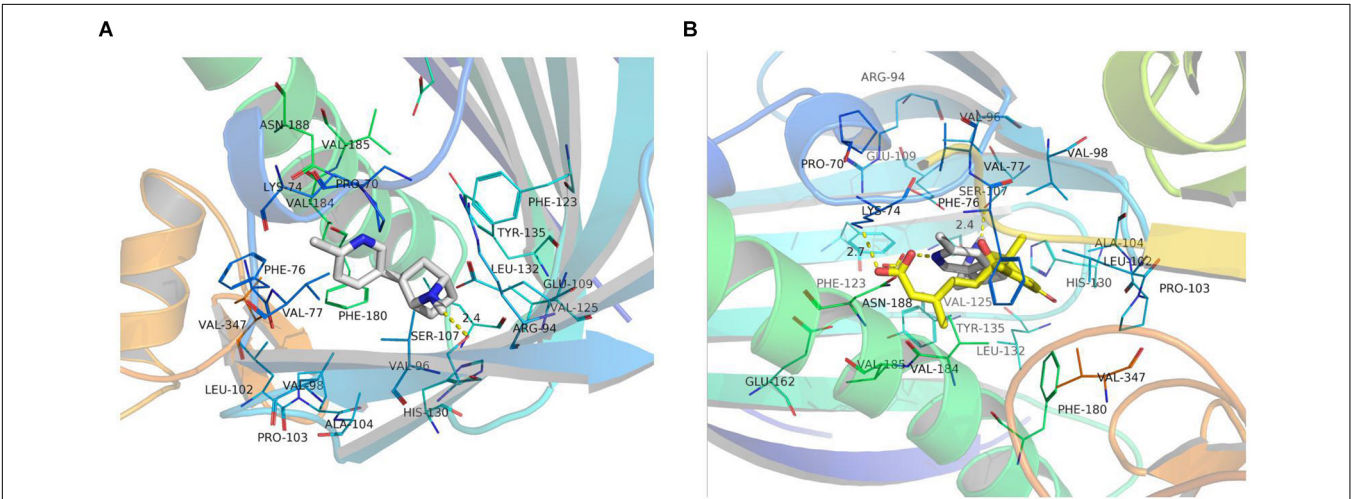


FIGURE 5 | Docked OsPYL2 active site with Cyah and absciscic acid (ABA). **(A)** Cyah docked with the OsPYL2 active site. **(B)** Cyah and ABA docked with OsPYL2. These images were drawn using the software program PyMOL.

We found that a high concentration of biochar leachates could improve the content of ABA and its precursors carotenoids in rice seedlings (**Figure 4A**), as well as the expression of ABA and the cold-related genes *OsABF1*, *OsABF2*, *OsABA45*, *OsLEA3*, *RAB16A*, *OsPsbR1*, and *OsPsbR3* (**Figure 2**). This result indicates that adding more biochar leachate can induce endogenous ABA biosynthesis in rice seedlings, and this increased ABA could influence corresponding biological functions to help plants resist cold stress. High concentrations of biochar could affect the ABA signaling pathway, and exogenous ABA could also affect the ABA signaling pathway, indicating that some ABA analogs may exist on the surface of biochar. These ABA analogs likely caused a series of physiological and biochemical processes related to ABA and cold resistance within a certain concentration range, which eventually promoted the cold resistance of rice plants.

Working with tomato, Graber et al. (2010) found that biochar treatments positively enhanced its plant height and leaf size without any effect on its flower and fruit yield (Graber et al., 2010). Yet these positive impacts of biochar on plant responses were not due to direct or indirect effects on plant nutrition *per se*, as there were no differences between control and treatments in their leaf nutrient contents (Graber et al., 2010). Therefore, those authors considered that the organic molecules in biochar were impacting the growth of crops. In the absence of interference from other factors, we also think that the organic molecules of biochar's leachates are crucial for altering the growth of rice seedlings under low-temperature stress. To explore the mechanism by which such organic molecules could influence rice seedlings cold tolerance, we recently identified them (Yuan et al., 2017). In researching the direct effects of biochar on plants, most studies have now identified organic molecules from biochar via GC/MS and then determined whether they can affect plants' growth and by which possible mechanism (Graber et al., 2010; Gale et al., 2016).

We used biochar leachates to eliminate other interferences, so we believe that the organic molecules contained in biochar are indeed an important factor influencing the growth of rice seedlings under low temperature. But admittedly, the underlying mechanism of these organic molecules is not yet known. In recent years, the interaction between molecules and proteins has become a hot research topic. In plants, the function of organic molecules can include hormone response, signal transduction, or ligand interaction with proteins to exercise a series of related biological functions (Antunes et al., 2011; Yang et al., 2015; Bhuiya et al., 2017; Haruta and Sussman, 2017). Therefore, we put forward an experimental hypothesis: organic molecules of biochar's leachates can enter cells of the plant and interact with corresponding proteins in them, thereby driving a series of physiological and biochemical reactions that enable plants to resist the cold. We suspected our identified organic molecules may have interacted mechanistically with stress or ABA-related proteins to generate the cold stress effects we observed.

The direct homologous receptor OsPYL/RCAR5 has been shown to positively impact the growth of rice seedlings (Kim et al., 2012, 2014). He et al. (2014) identified the structure of OsPYL2 in rice, and its 3D structure was found in the

RCSB database (He et al., 2014). We concluded that the organic molecule Cyah in biochar could be successfully docked with OsPYL2 (**Figure 5**). The organic molecule Cyah has been recorded in the PMN database given its participation in a variety of chemical reactions (**Table 5**), but whether it interacts with the ABA receptor protein remains unknown. Nevertheless, the interaction between the ABA ligand and ABA receptor protein can reduce abiotic stress (Cao et al., 2013). The ABA analogs and ABA ligands are the same as ABA receptor proteins, and the interaction between ABA analogs and ABA receptor proteins can prompt plant responses to abiotic stress, thus indicating that ABA analogs also function much like ABA ligands. Cyah and ABA are the same as the ABA receptor protein OsPYL2, in that they are combined with hydrogen bonds, so Cyah may also be analogs to ABA, with the same function as ABA in regulating OsPYL2 to produce a series of related effects. A plausible mechanism is that the organic molecule Cyah in biochar combines with OsPYL2 of rice, and the combination of PP2C and Cyah-OsPYL2 then inhibits the activity of PP2C itself; this activates SnRK2 and regulates the ion channel, second messenger, and the expression of related ABA genes, which together improves the cold resistance of plants.

DATA AVAILABILITY STATEMENT

The original contributions presented in the study are included in the article/**Supplementary Material**, further inquiries can be directed to the corresponding author/s.

AUTHOR CONTRIBUTIONS

JY designed and carried out the experiments, analyzed the results, and wrote the manuscript. JM, YE, XL, XY, and WC designed the experiments. All authors contributed to the article and approved the submitted version.

FUNDING

This work was supported by the National Key Research and Development plan "Biochar Based Fertilizer and Microbial Fertilizer Development" (2017YFD0200800), the earmarked fund for Modern Agro-industry Technology Research System (CARS-01-46), the research and demonstration of key technology of straw biochar resource utilization in Shenyang science and technology planning project (17-182-9-00), the Doctoral Scientific Research Foundation of Liaoning Province (2019-BS-105), and the Doctoral Scientific Research Foundation of Eastern Liaoning University (2019BS020).

SUPPLEMENTARY MATERIAL

The Supplementary Material for this article can be found online at: <https://www.frontiersin.org/articles/10.3389/fpls.2021.646910/full#supplementary-material>

REFERENCES

- Antunes, M. S., Morey, K. J., Smith, J. J., Albrecht, K. D., Bowen, T. A., Zdunek, J. K., et al. (2011). Programmable ligand detection system in plants through a synthetic signal transduction pathway. *PLoS One* 6:e16292. doi: 10.1371/journal.pone.0016292
- Bhuiya, S., Haque, L., Pradhan, A. B., and Das, S. (2017). Inhibitory effects of the dietary flavonoid quercetin on the enzyme activity of zinc(ii)-dependent yeast alcohol dehydrogenase: spectroscopic and molecular docking studies. *Int. J. Biol. Macromol.* 95, 177–184. doi: 10.1016/j.ijbiomac.2016.11.047
- Cao, M., Liu, X., Zhang, Y., Xue, X., Zhou, X. E., Melcher, K., et al. (2013). An ABA-mimicking ligand that reduces water loss and promotes drought resistance in plants. *Cell Res.* 23, 1043–1054. doi: 10.1038/cr.2013.95
- Challam, C., Ghosh, T., Rai, M., and Tyagi, W. (2015). Allele mining across DREB1a and DREB1b in diverse rice genotypes suggest a highly conserved pathway inducible by low temperature. *J. Genet.* 94, 231–238. doi: 10.1007/s12041-015-0507-z
- Cheng, J., Bi, Y., Tian, S., Li, M., and Li, S. (2013). Simultaneous determination of GA3, IAA, and ABA contents in potato tuber by high performance liquid chromatography. *J. Gansu Agric. Univ.* 48, 26–29. doi: 10.3969/j.issn.1003-4315.2013.02.006
- Fahad, S., Hussain, S., Saud, S., Tanveer, M., Bajwa, A. A., Hassan, S., et al. (2015). A biochar application protects rice pollen from high-temperature stress. *Plant Physiol. Biochem.* 96, 281–287. doi: 10.1016/j.plaphy.2015.08.009
- Farhanqi-Abri, S., and Torabian, S. (2018). Effect of biochar on growth and ion contents of bean plant under saline condition. *Environ. Sci. Pollut. Res. Int.* 25, 11556–11564. doi: 10.1007/s11356-018-1446-z
- French, E., and Iyerpascuzzi, A. S. (2018). A role for the gibberellin pathway in biochar-mediated growth promotion. *Sci. Rep.* 8:5389. doi: 10.1038/s41598-018-23677-9
- Gale, N. V., Sackett, T. E., and Thomas, S. C. (2016). Thermal treatment and leaching of biochar alleviates plant growth inhibition from mobile organic compounds. *Peer J.* 4:e2385. doi: 10.7717/peerj.2385
- Graber, E. R., Harel, Y. M., Koltun, M., Cytryn, E., Silber, A., David, D. R., et al. (2010). Biochar impact on development and productivity of pepper and tomato grown in fertigated soilless media. *Plant Soil* 337, 481–496. doi: 10.1007/s11104-010-0544-6
- Haruta, M., and Sussman, M. R. (2017). Ligand receptor-mediated regulation of growth in plants. *Curr. Top. Dev. Biol.* 123, 331–363. doi: 10.1016/bs.ctdb.2016.11.007
- He, Y., Hao, Q., Li, W., Yan, C., Yan, N., and Yin, P. (2014). Identification and characterization of ABA receptors in *Oryza sativa*. *PLoS One* 9:e95246. doi: 10.1371/journal.pone.0095246
- Hossain, M. A., Cho, J. I., Han, M., Ahn, C. H., Jeon, J. S., An, G., et al. (2010a). The ABRE-binding bZIP transcription factor *OsABF2* is a positive regulator of abiotic stress and ABA signaling in rice. *J. Plant Physiol.* 167, 1512–1520. doi: 10.1016/j.jplph.2010.05.008
- Hossain, M. A., Lee, Y., Cho, J. I., Ahn, C. H., Lee, S. K., Jeon, J. S., et al. (2010b). The bZIP transcription factor *OsABF1* is an ABA responsive element binding factor that enhances abiotic stress signaling in rice. *Plant Mol. Biol.* 72, 557–566. doi: 10.1007/s11103-009-9592-9
- Hubbard, K. E., Nishimura, N., Hitomi, K., Getzoff, E. D., and Schroeder, J. I. (2010). Early abscisic acid signal transduction mechanisms: newly discovered components and newly emerging questions. *Genes Dev.* 24, 1695–1708. doi: 10.1101/gad.1953910
- Kim, H., Hwang, H., Hong, J. W., Lee, Y. N., Ahn, I. P., Yoon, I. S., et al. (2012). A rice orthologue of the ABA receptor, OsPYL/RCAR5, is a positive regulator of the ABA signal transduction pathway in seed germination and early seedling growth. *J. Exp. Bot.* 63, 1013–1024. doi: 10.1093/jxb/err338
- Kim, H., Lee, K., Hwang, H., Bhatnagar, N., Kim, D. Y., Yoon, I. S., et al. (2014). Overexpression of PYL5 in rice enhances drought tolerance, inhibits growth, and modulates gene expression. *J. Exp. Bot.* 65, 453–464. doi: 10.1093/jxb/ert397
- Lehmann, J., and Joseph, S. (2015). *Biochar for Environmental Management*, 2nd Edn. London: Routledge.
- Li, L., Li, J., Shen, M., Zhang, X. L., and Dong, Y. H. (2015). Cold plasma treatment enhances oilseed rape seed germination under drought stress. *Sci. Rep.* 5:13033. doi: 10.1038/srep13033
- Li, L., Ye, T., Gao, X., Chen, R., Xu, J., Xie, C., et al. (2017). Molecular characterization and functional analysis of the OsPsbR, gene family in rice. *Mol. Genet. Genomics* 292, 271–281. doi: 10.1007/s00438-016-1273-1
- Lieven, C., Mourant, D., Gunawan, R., Hu, X., and Wang, Y. (2014). Organic compounds leached from fast pyrolysis mallee leaf and bark biochars. *Chemosphere* 139, 659–664. doi: 10.1016/j.chemosphere.2014.11.009
- Mega, R., Meguromaoka, A., Endo, A., Shimosaka, E., Murayama, S., Nambara, E., et al. (2015). Sustained low abscisic acid levels increase seedling vigor under cold stress in rice (*Oryza sativa* L.). *Sci. Rep.* 5:13819. doi: 10.1038/srep13819
- Pompelli, M. F., França, S. C., Tigre, R. C., Oliveira, M. T. D., Sacilot, M., and Pereira, E. C. (2013). Spectrophotometric determinations of chloroplastidic pigments in acetone, ethanol and dimethylsulphoxide. *Rev. Bras. Biol.* 11, 52–58.
- Rabbani, M. A., Maruyama, K., Abe, H., Khan, M. A., Katsura, K., Ito, Y., et al. (2003). Monitoring expression profiles of rice genes under cold, drought, and high-salinity stresses and abscisic acid application using cDNA microarray and RNA gel-blot analyses. *Plant Physiol.* 133, 1755–1767. doi: 10.1104/pp.103.025742
- Rafiq, M. K., Joseph, S. D., Li, F., Bai, Y., Shang, Z., Rawal, A., et al. (2017). Pyrolysis of attapulgite clay blended with yak dung enhances pasture growth and soil health: characterization and initial field trials. *Sci. Total Environ.* 607, 184–194. doi: 10.1016/j.scitotenv.2017.06.186
- Ramakers, C., Ruijter, J. M., Deprez, R. H., and Moorman, A. F. (2003). Assumption-free analysis of quantitative real-time polymerase chain reaction (PCR) data. *Neurosci. Lett.* 339, 62–66. doi: 10.1016/S0304-3940(02)01423-4
- Ramirez, D., and Caballero, J. (2018). Is it reliable to take the molecular docking top scoring position as the best solution without considering available structural data? *Molecules* 23:1038. doi: 10.3390/molecules23051038
- Shinozaki, K., Yamaguchi-Shinozaki, K., and Seki, M. (2003). Regulatory network of gene expression in the drought and cold stress responses. *Curr. Opin. Plant Biol.* 6, 410–417. doi: 10.1016/S1369-5266(03)00092-X
- Trott, O., and Olson, A. J. (2009). Autodock vina: improving the speed and accuracy of docking with a new scoring function, efficient optimization, and multithreading. *J. Comput. Chem.* 31, 455–461. doi: 10.1002/jcc.21334
- Wang, C., Alidoust, D., Yang, X., and Isoda, A. (2018). Effects of bamboo biochar on soybean root nodulation in multi-elements contaminated soils. *Ecotoxicol. Environ. Saf.* 150, 62–69. doi: 10.1016/j.ecoenv.2017.12.036
- Waqas, M., Shahzad, R., Hamayun, M., Asaf, S., Khan, A. L., Kang, S. M., et al. (2018). Biochar amendment changes jasmonic acid levels in two rice varieties and alters their resistance to herbivory. *PLoS One* 13:e0191296. doi: 10.1371/journal.pone.0191296
- Yang, E., Jun, M., Haijun, H., and Wenfu, C. (2015). Chemical composition and potential bioactivity of volatile from fast pyrolysis of rice husk. *J. Anal. Appl. Pyrolysis* 112, 394–400. doi: 10.1016/j.jaap.2015.02.021
- Yuan, J., Meng, J., Liang, X., Yang, E., Yang, X., and Chen, W. (2017). Organic molecules from biochar leachates have a positive effect on rice seedling cold tolerance. *Front. Plant Sci.* 8:1624. doi: 10.3389/fpls.2017.01624
- Zheng, H., Wang, X., Chen, L., Wang, Z., Xia, Y., Zhang, Y., et al. (2018). Enhanced growth of halophyte plants in biochar-amended coastal soil: roles of nutrient availability and rhizosphere microbial modulation. *Plant Cell Environ.* 41, 517–532. doi: 10.1111/pce.12944
- Zou, M., Guan, Y., Ren, H., Zhang, F., and Chen, F. (2008). A bZIP transcription factor, OsABI5, is involved in rice fertility and stress tolerance. *Plant Mol. Biol.* 66, 675–683. doi: 10.1007/s11103-008-9298-4

Conflict of Interest: The authors declare that the research was conducted in the absence of any commercial or financial relationships that could be construed as a potential conflict of interest.

Copyright © 2021 Yuan, Meng, Liang, Yang, Yang and Chen. This is an open-access article distributed under the terms of the Creative Commons Attribution License (CC BY). The use, distribution or reproduction in other forums is permitted, provided the original author(s) and the copyright owner(s) are credited and that the original publication in this journal is cited, in accordance with accepted academic practice. No use, distribution or reproduction is permitted which does not comply with these terms.



Comparative Metabolomic and Transcriptomic Studies Reveal Key Metabolism Pathways Contributing to Freezing Tolerance Under Cold Stress in Kiwifruit

Shihang Sun^{1,2}, Jinbao Fang^{1*}, Miaomiao Lin^{1*}, Chungeng Hu², Xiujuan Qi¹, Jinyong Chen¹, Yunpeng Zhong¹, Abid Muhammad¹, Zhi Li¹ and Yukuo Li¹

OPEN ACCESS

Edited by:

Andy Pereira,
University of Arkansas, United States

Reviewed by:

Wricha Tyagi,
Central Agricultural University, India
Ulrike Bechtold,
University of Essex, United Kingdom

*Correspondence:

Jinbao Fang
fangjinbao@caas.cn
Miaomiao Lin
linmiaomiao@caas.cn

Specialty section:

This article was submitted to
Plant Abiotic Stress,
a section of the journal
Frontiers in Plant Science

Received: 21 January 2021

Accepted: 06 April 2021

Published: 01 June 2021

Citation:

Sun S, Fang J, Lin M, Hu C, Qi X, Chen J, Zhong Y, Muhammad A, Li Z and Li Y (2021) Comparative Metabolomic and Transcriptomic Studies Reveal Key Metabolism Pathways Contributing to Freezing Tolerance Under Cold Stress in Kiwifruit. *Front. Plant Sci.* 12:628969. doi: 10.3389/fpls.2021.628969

¹ Key Laboratory for Fruit Tree Growth, Development and Quality Control, Zhengzhou Fruit Research Institute, Chinese Academy of Agricultural Sciences, Zhengzhou, China, ² Key Laboratory of Horticultural Plant Biology (Ministry of Education), College of Horticulture and Forestry Science, Huazhong Agricultural University, Wuhan, China

Cold stress poses a serious threat to cultivated kiwifruit since this plant generally has a weak ability to tolerate freezing tolerance temperatures. Surprisingly, however, the underlying mechanism of kiwifruit's freezing tolerance remains largely unexplored and unknown, especially regarding the key pathways involved in conferring this key tolerance trait. Here, we studied the metabolome and transcriptome profiles of the freezing-tolerant genotype KL (*Actinidia arguta*) and freezing-sensitive genotype RB (*A. arguta*), to identify the main pathways and important metabolites related to their freezing tolerance. A total of 565 metabolites were detected by a wide-targeting metabolomics method. Under (−25°C) cold stress, KEGG (Kyoto Encyclopedia of Genes and Genomes) pathway annotations showed that the flavonoid metabolic pathways were specifically upregulated in KL, which increased its ability to scavenge for reactive oxygen species (ROS). The transcriptome changes identified in KL were accompanied by the specific upregulation of a codeinone reductase gene, a chalcone isomerase gene, and an anthocyanin 5-aromatic acyltransferase gene. Nucleotides metabolism and phenolic acids metabolism pathways were specifically upregulated in RB, which indicated that RB had a higher energy metabolism and weaker dormancy ability. Since the LPCs (LysoPC), LPEs (LysoPE) and free fatty acids were accumulated simultaneously in both genotypes, these could serve as biomarkers of cold-induced frost damages. These key metabolism components evidently participated in the regulation of freezing tolerance of both kiwifruit genotypes. In conclusion, the results of this study demonstrated the inherent differences in the composition and activity of metabolites between KL and RB under cold stress conditions.

Keywords: kiwifruit, freezing tolerance, RNA-Seq, metabolome, cold stress, UPLC-ESI-MS/MS

INTRODUCTION

Low temperature stress is one of the main factors that restricts the development and growth of plants, limits their distribution and causes significant losses in yield (Peng et al., 2015). Enhancing the cold tolerance of fruit trees via breeding is a prerequisite to better cope with frequent extremely low temperatures (Xiaoming et al., 2019). A plant's cold tolerance mechanism can be divided into two parts: its chilling tolerance and the freezing tolerance (FT) (Sun et al., 2020). Chilling tolerance reflects the ability of a plant to respond to 0–15°C growing conditions (Chen et al., 2020), whereas FT is its ability to respond to subzero temperatures (Zhang et al., 2020). While the chilling tolerance mechanism has been elucidated at transcriptional and metabolic level (Jingyu et al., 2016), the mechanism of FT still remains largely unknown.

Moreover, the FT mechanism differs between annual plant and perennial plant species. For annuals, such as *Arabidopsis*, FT is a multigenic and quantitative trait that relies more on changes in metabolites levels. Many metabolites linked to the FT trait, such as osmolytes (proline, betaine, putrescine) and reactive oxygen species (ROS)-scavenging systems (catalase, peroxidase, superoxide dismutase, lignan and ascorbic acid), are known to have an important role in maintaining the survival of annual plants under cold conditions (Li et al., 2017; Ding et al., 2018; Yao et al., 2020). FT mainly derives from timely osmotic adjustments and an ability to scavenge reactive oxygen species (ROS). Unlike for annuals, the studies of FT in perennial plants have mainly focused on the seedling stage rather than adults; however, the responses to cold stress in seedlings likely differ between them in actual field situations (Chai et al., 2019). To resolve this imbalance, we designed an experiment using 3-year-old (i.e., adult stage) kiwifruit which had already entered the dormant stage, thus offering an identical situation to that in a field setting.

Recently, metabolic responses to cold stress in plants have garnered more attention, since numerous metabolites are considered to play vital roles in FT (Singh et al., 2020). In the process of adjusting to cold stress, the plant produces secondary metabolites as a kind of excretory compound, and these metabolites are the real driver of plant stress responses (Lee et al., 2019). Accordingly, changes in metabolites contents are considered to be ultimate response of plants to abiotic stresses (Ma et al., 2016). The metabolomics technique is a powerful tool for detecting and analyzing metabolites in plants under cold stress, and this approach can shed new light on the their response mechanisms to a low-temperature environment (Clemente-Moreno et al., 2020). For example, the accumulation of sugars and amino acids can occur in this cold response according to a recent metabolome study (Hannah et al., 2006). Cold stress can also influence the nucleic acid and protein stability, enzyme activity, and cytoskeleton structure (Cook et al., 2004). Slowed or even stunted plant growth due to cold stress will generally decrease the amplitude of energy utilization, by causing the formation of ROS (Dreyer and Dietz, 2018), and a low temperature induces the accumulation of anthocyanin to scavenge ROS (An et al., 2018). It has been reported as

well that polyamines are involved in potato's cold response to eliminate ROS (Kou et al., 2018). Plants produce osmolytes—i.e., proline, betaine, raffinose, trehalose and inositol—to deal with the low temperature stress, since these metabolites under cold conditions have protective functions toward alleviating damage from freezing (Zhao et al., 2019). Similarly, plants accumulate suberin and lignin to adjust themselves to cold stress and reduce its adverse effects (Jian et al., 2020). The fluidity of membrane composition plays an central role in temperature perception, which reduces to form a solid gel capable of sensing cold stress (Gilad et al., 2018; Yang et al., 2019), while changes in the content of soluble sugars may play a key role in cold signaling transduction by regulating the expression of cold-responsive genes (Krasensky and Jonak, 2012). Besides metabolomics, high-throughput sequencing techniques like transcriptomics have been widely used to explore the problem of coping with abiotic stress in a wide range of plants (Bahrmann et al., 2019). The ICE-CBF-COR regulation network response to cold stress was discovered using RNA-Seq technology, in which cold stress induces the expression of transcriptional factors, including AP2-domain protein CBFs, which activate the expression of various downstream cold responsive (COR) genes (Stockinger et al., 1997; Wanqian et al., 2018). The ICE (bHLH transcription factors) controls the CBF genes via sumoylation and polyubiquitylation that is mediated by SUMO-E3-ligase SIZ1 and ubiquitin-E3-ligase HOS1, respectively (Zhang et al., 2016). In this way, by combining profiling of the metabolome and transcriptome, a more extensive and more comprehensive understanding of metabolites and genes co-regulation of cold stress was elucidated.

Kiwifruit (*Actinidia*) is an economic plant domesticated in recent decades that is mainly distributed in subtropical and temperate regions (Yukuo et al., 2018). In these climatic zones, the winter always entails extremely low temperatures, which makes the kiwifruit vulnerable to freezing damage during the overwintering period. This freezing injury results in reduced kiwifruit yield and it can also detrimentally affects the survival of the whole plant. *Actinidia arguta* is a special species that has a large range, from northeast to south of China (Lin et al., 2020). Two contrasting genotypes in *A. arguta* have been identified, these being KL and RB. While former grows naturally in higher latitude regions and exhibits a relatively strong FT, the latter typically occurs in lower latitude areas and its FT is weak. The divergence of the two kiwifruit genotypes in terms of their FT trait renders them an ideal model for studying how plants respond to a low-temperature environment.

Here, a naturally existing experimental system—two kiwifruit genotypes with significantly different freezing tolerance ability—was used to study the mechanism of FT in kiwifruit. We conducted comparative metabolomic and transcriptomic analyses at a series of time points to identify global dynamic changes and uncover the metabolic models underlying their cold response. These results improve our understanding of kiwifruit's FT mechanism, and provide useful information for enhancing the FT in kiwifruit.

MATERIALS AND METHODS

Plant Material and Cold Stress Treatments

To discern FT mechanism, we used two kiwifruit (*A. arguta*) genotypes known to differ greatly in their tolerance of freezing: the high-freezing tolerance genotype KL and the low freezing tolerance genotype RB. The mature (3-year-old) plants of each genotype (individually planted in a 3-L-pot) were placed in a field for 3 years at Zhengzhou fruit research institute (113°E, 34°N). Zhengzhou city has a temperate climate with short-day in winter and temperature reaches to -15°C . All the shoots were collected in early January 2020, then the detached shoots were placed in a -25°C freezer chamber without light (Suzhou Zhihe Instrument Factory, China), when three biological replicates of shoots for metabolic profiling and for RNA sequencing (RNA-Seq) were collected randomly from all plants of each genotype at time points of 0 h, 1 h, 4 h, and 7 h under a -25°C treatment. At the same times, shoots were collected to assess their vegetative budbreak (VB), relative electrolyte leakage (REL) and other physiological parameters. The collected samples were immediately frozen in liquid nitrogen and stored at -80°C until their RNA and metabolite extractions.

Relative Electrolyte Leakage Assay

After receiving the low temperature treatment, the kiwifruit shoots were cut into 1–2-mm thick slices. Then 0.2 g of these slices per sample per genotype were incubated in 30 ml of double-distilled water (ddH₂O) for 2 h, with shaking at 200 rpm at 25°C . Initial electrolyte leakage (C1) was measured using a digital conductivity meter (DDS-307, Rex, China), with their second electrolyte leakage (C2) likewise measured after the samples had been boiled at 100°C for 30 min, then cooled down at 25°C with 30 min of shaking. The REL was calculated this way:

$$REL(\%) = (C1/C2) \times 100\% \quad (1)$$

The LT₅₀ (i.e., the semi-lethal temperature at which REL reaches 50%) was calculated by fitting a logistic sigmoid function to the REL values:

$$y = k / (1 + ae^{-bx}) \quad (2)$$

where x is given treatment temperature; y is the REL value; k is the maximum value when x approaches infinity; 'a' and 'b' are the estimated equation parameters.

Evaluation of Vegetative Budbreak

To examine the differences in freezing tolerance, the VB was evaluated at each collection time point in three shoots (length ≥ 20 cm) having five or more vegetative buds per shoot (at least 15 buds in total) that were pruned from both genotypes (Zhao et al., 2020). For budbreak induction, three shoots were placed in 100 ml tissue-culture bottles containing ddH₂O, then incubated in a controlled-climate chamber at $24 \pm 1.0^{\circ}\text{C}$ under a 16-h/8-h photoperiod, to induce budbreak. The ddH₂O in the bottles was changed every 2 to 3 days. The VB was determined

for each collection time points after the samples spent 20 days in the controlled chamber. The statistical differences in VB were tested with ANOVAs implemented in SPSS (IBM Corp., Armonk, NY, United States).

Measurement of Anti- $\text{O}_2^{\cdot-}$ Capacity and Contents of Procyanidin, Flavonoid

The anti- $\text{O}_2^{\cdot-}$ capacity, the contents of procyanidin, flavonoid were measured using corresponding assay kits according to the manufacturer's instructions (Nanjing Jiancheng Bioengineering Institute, China). The principle of anti- $\text{O}_2^{\cdot-}$ determination was based on the reaction of 'xanthine'-xanthine oxidase-'gross chromogenic agent' and anti- $\text{O}_2^{\cdot-}$ was determined by detecting the absorption value at 560 nm. The procyanidin was determined by reacting it with vanillin to produce the colored compounds, the absorption value was determined at 500 nm. The flavonoid determination was done by reacting it with aluminum ions until produced the red compounds, the absorption value was measured at 502 nm. The activity of anti- $\text{O}_2^{\cdot-}$ was indicated as unit (U) per g fresh weight. The contents of procyanidin and flavonoid were shown as mg per g fresh weight.

Metabolomic Profiling and Statistical Analysis

The freeze-dried shoots were crushed in a mixer mill (MM 400, Retsch, Germany) with zirconia beads for 1.5 min at a frequency of 30 Hz. From the ensuring power, 100 mg was weighted and extracted overnight at 4°C with 0.6 ml of 70% aqueous methanol. Following centrifugation at $10\,000 \times g$ for 10 min, the extracts were absorbed and filtrated before their UPLC-MS/MS (ultra performance liquid chromatography/tandem mass spectrometry) analysis. The sample extracts were examined in an UPLC-ESI-MS/MS system (UPLC, Shim-pack UFLC SHIMADZU CBM30A system; MS, Applied Biosystems 4500 Q TRAP). For its analytical conditions, a UPLC Agilent SB-C18 column (1.8 μm , 2.1 mm*100 mm) was used with a mobile phase consisting of solvent A (pure water with 0.1% formic acid) and solvent B (acetonitrile). Sample measurements were performed with a gradient program whose starting conditions was 95% A, 5% B; within 9 min, a linear gradient inversion to 5% A, 95% B was programmed, and this latter composition held for 1 min. Then, a composition of 95% A, 5.0% B was adjusted within 1.1 min and kept for 2.9 min. The column oven was set to 40°C and the injection volume was 4 μl . The effluent was alternatively connected to an ESI-triple quadrupole-linear ion trap (QTRAP)-MS.

LIT and triple quadrupole (QQQ) scans were acquired on a triple quadrupole-linear ion trap mass spectrometer (Q TRAP [API 4500 Q TRAP UPLC/MS/MS System]) equipped with an ESI Turbo Ion-Spray interface, operating in the positive and negative ion mode and controlled by Analyst 1.6.3 software (AB Sciex, Washington, DC, United States). The ESI source operation parameters were as follows: ion source, turbo spray, source temperature of 550°C , ion spray voltage (IS) of 5500 V (positive ion mode)/ -4500 V (negative ion mode), for which the ion source gas I (GSI), gas II(GSII), and curtain gas (CUR) were

set at 50, 60, and 30.0 psi, respectively; the collision gas(CAD) was set to high. Instrument tuning and mass calibration were performed with 10 and 100 $\mu\text{mol/L}$ polypropylene glycol solutions in the QQQ and LIT modes, respectively. QQQ scans were acquired as MRM experiments with a collision gas (nitrogen) set to 5 psi. The DP and CE for individual MRM transitions was done with further DP and CE optimization. A specific set of MRM transitions were monitored for each period according to the metabolites eluted within this period. The qualitative identification of metabolites was obtained from the metabolite information available on public database (MassBank, KNAPSACk, and METLIN) and private MVDB database (Wuhan Metware Biotechnology Corporation, China).

Unsupervised PCA (principal component analysis) was performed using the statistics function 'prcomp' within R¹. The data was unit variance-scaled before conducting the unsupervised PCA. The HCA (hierarchical cluster analysis) results of samples and metabolites were presented as heat maps with dendrograms, while Pearson correlation coefficients (PCC) between samples were calculated by the 'cor' function in R and presented as heat maps only. Both HCA and PCC were carried out by R package 'pheatmap'. For the HCA, the normalized signal intensities of metabolites (unit variance scaling) were visualized as a color spectrum. Significantly regulated metabolites between groups were designated as those with a VIP (variable importance in projection) ≥ 1 and absolute Log₂FC (fold change) ≥ 1 . The VIP values were extracted from OPLS-DA (Orthogonal Partial Least Squares Discrimination Analysis) results; the latter included score plots and permutation plots, as generated by the R package 'MetaboAnalystR'. The data was log transform (log₂) and mean-centered before applying the OPLS-DA. To avoid overfitting, a permutation test ($n = 200$ resamplings) was performed. Identified metabolites were annotated using the KEGG Compound database², and latter mapped to the KEGG Pathway database³. Those mapped pathways with significantly regulated metabolites were then fed into MSEA (metabolite sets enrichment analysis); their statistical significance was determined by p -values from hypergeometric tests.

RNA-Seq and Statistical Analysis

Total RNA was isolated from the shoots (100 mg per sample) with a plant total RNA purification kit (Waryoung, Beijing, China) by following the manufacturer's instructions. Samples from the four collection time points were subjected to RNA-Seq. In all, 24 samples were used for this RNA-Seq (2 cultivars \times 4 collection times \times 3 biological replicates). RNA quality was determined in a NanoDrop 1000 spectrophotometer, after which the mRNA was extracted using dynabeads oligo (dT) and a fragmentation buffer. Double-stranded cDNAs were synthesized using reverse-transcriptase and random hexamer primers, and the cDNAs' fragments were purified with a QIA quick PCR extraction kit. These purified fragments were washed with an EB buffer for end reparation of the poly (A) addition and then ligated to sequencing

adapters. Following agarose gel electrophoresis and extraction of cDNAs from the gels, the cDNAs' fragments were purified and enriched by PCR to construct the final library of cDNAs. This library was then sequenced on the Illumina sequencing platform (Illumina Hi-Seq™ 2500) by using paired-end technology.

After removing the adapter and any low-quality sequences, the clean reads were obtained and mapped to the transcripts assembled by Trinity. The mapping were done using bowtie2 (RSEM). The FPKM (fragments per kilobase of exon per million mapped fragments) was used to calculate gene expression levels, and differentially expressed genes (DEGs) were screened by Cuffdiff according to these two criteria: having (i) a false discovery rate (FDR) corrected P -value < 0.05 and (ii) a $|\log_2(\text{fold change})| \geq 1$. Based on the 'blastp' analysis, the annotated genes in kiwifruit were screened for further analysis. Finally, all sequencing data obtained in this study has been uploaded to NCBI.

RESULTS

Freezing Tolerance Assessment and Low Temperature Treatment of the KL and RB Genotypes

The KL came from Jilin province (125°E, 44°N), and the RB was from Henan province (113°E, 34°N) (**Figure 1A**). The lowest winter temperature is about -30°C in Jilin province, while it is about -15°C in Henan province (data from <http://data.cma.cn/>). Their LT₅₀ values of dormant shoots were -25°C (KL) and -19°C (RB), respectively (**Figures 1B–D**), which indicated that KL and RB were respectively tolerant of and sensitive to cold stress. The distinct FT trait between the two genotypes makes them an excellent model for investigating the underlying mechanisms of kiwifruit' FT.

After the freezing treatment (-25°C), four time-points corresponding to no freezing (0 h), mild freezing (1 h), moderate freezing (4 h), and severe freezing (7 h) were chosen for relative electrolyte leakage (REL), vegetative budbreak (VB), anti- O_2^- capacity and the contents of procyanidin, flavonoid measurements (**Figure 2A**). The REL of both genotypes gradually increased with a longer duration of the treatment (**Figure 2C**); however, the REL of KL was continuously lower than that of RB throughout the treatment. At 4 h, the REL of KL was below 50% while that of RB was above 50%. The REL of both genotypes was $> 50\%$ after 7 h at -25°C .

The VB rate was also assessed at the same four time points for both genotypes. Under the no freezing treatment (0 h/ -25°C), the budbreak rate of both genotypes was above 60% and similar. At the second collection time point (1 h/ -25°C), KL had a significantly higher budbreak rate than RB ($P < 0.05$). For the third time point (4 h/ -25°C), compared to KL, the budbreak rate significantly decreased significantly to 20% in RB ($P < 0.01$). At the last collection time (7 h/ -25°C), there was no VB (i.e., rates = 0%) in both plant genotypes. However, the shoots of KL were not completely dead and did generate new calluses, whereas the shoots of RB had thoroughly decayed (**Figures 2B,D**).

¹ www.r-project.org

² <http://www.kegg.jp/kegg/compound>

³ <http://www.kegg.jp/kegg/pathway.html>

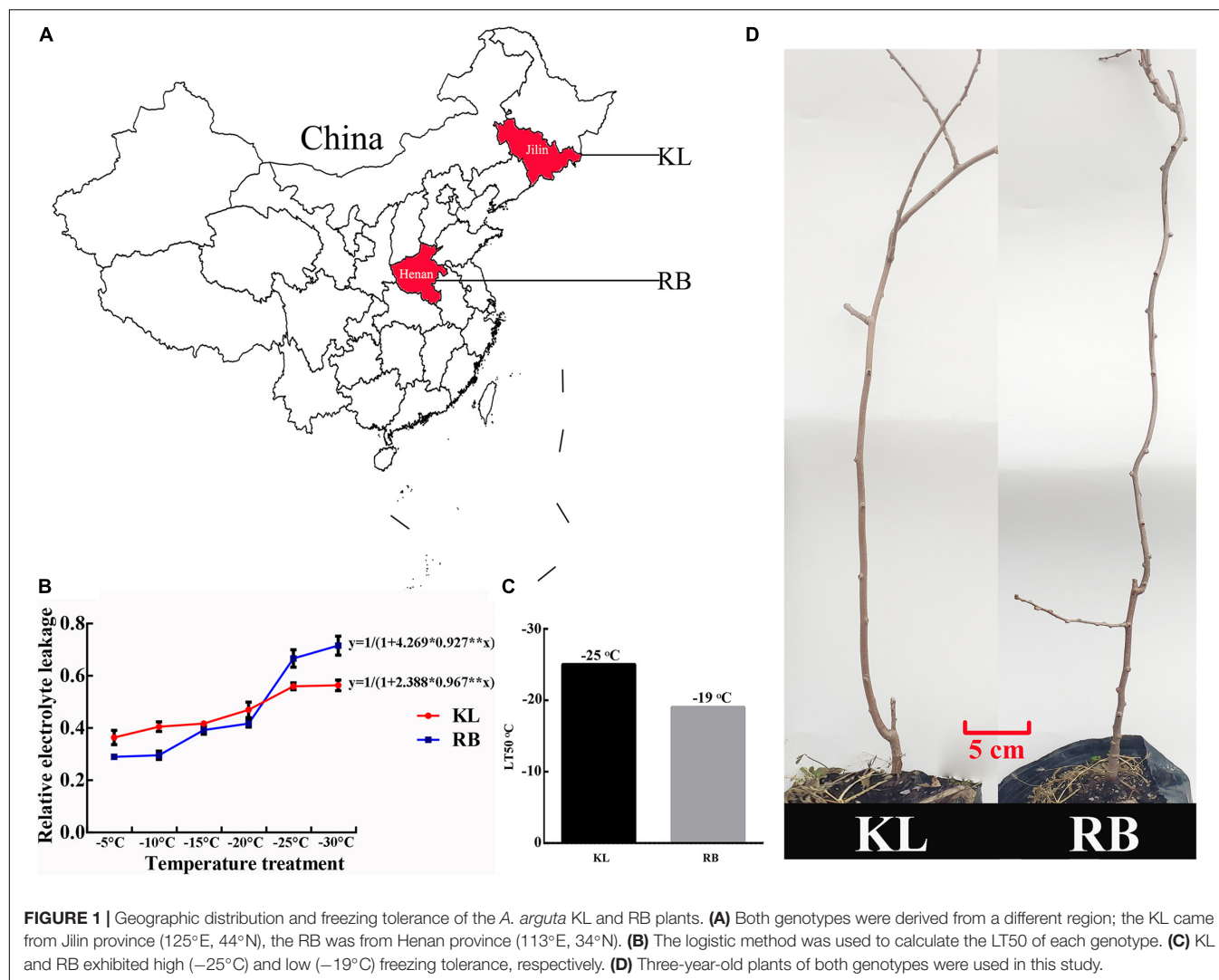


FIGURE 1 | Geographic distribution and freezing tolerance of the *A. arguta* KL and RB plants. **(A)** Both genotypes were derived from a different region; the KL came from Jilin province (125°E, 44°N), the RB was from Henan province (113°E, 34°N). **(B)** The logistic method was used to calculate the LT50 of each genotype. **(C)** KL and RB exhibited high (−25°C) and low (−19°C) freezing tolerance, respectively. **(D)** Three-year-old plants of both genotypes were used in this study.

The anti- $O_2^{\cdot-}$, procyanidin, and flavonoid were measured to evaluate the ROS scavenging ability of kiwifruit. An increasing trend for anti- $O_2^{\cdot-}$ capacity in kiwifruit genotypes was observed under cold stress, however the KL had significantly stronger ability to scavenge ROS (Figure 2E). Low temperature accelerated the accumulation of procyanidin, and flavonoid in kiwifruit. The content of procyanidin in KL increased 3-fold from 0 h to 4 h, whereas the content of procyanidin in RB showed no changes during cold stress (Figure 2F). The content of flavonoid in KL initially showed increased and finally decreased trend, while no changes was observed in RB under cold stress. These results indicated that the high FT genotype had the high ROS scavenging ability compared with the low FT genotype (Figure 2G). For the further investigation, the four time points were also used in the metabolomic and transcriptomic analysis.

Overview of Metabolic Profiles

We performed wide-targeted metabolic profiling based on UPLC-ESI-MS/MS. A total of 565 metabolites were identified among all the samples (Figure 3A), including phenolic acids

(17%), lipids (13%), flavonoids (12%), amino acids, derivatives (11%), organic acids (11%), nucleotides and derivatives (7%), alkaloids (6%), lignans and coumarins (4%), tannins (3%), terpenoids (2%), and others (17%). In the heat map (Figure 3B), all the biological replicates were grouped together, which indicated a robust correlation between replicates and the high reliability of our data. The heat map also showed that some metabolites were specifically accumulated in the KL, yet some only existed in the RB. Further, disparate accumulation patterns of metabolites could be observed in both genotypes under cold stress, which implied that the intraspecific divergence of FT in *A. arguta* may be caused by differential metabolite contents. The clustering results of all samples showed that the time points clustered into two distinct groups (0 h vs. those at 1 h, 4 h, 7 h) in both KL and RB, which indicated their metabolic changes were consistent under low temperature stress. Moreover, after this treatment, the KL_{4-h} and $KL_{1,7-h}$ were clustered into two categories and likewise RB_{4-h} and $RB_{1,7-h}$; this revealed that the 4 h (i.e., moderate freezing) duration is when specific metabolites changes occurred in both genotypes.

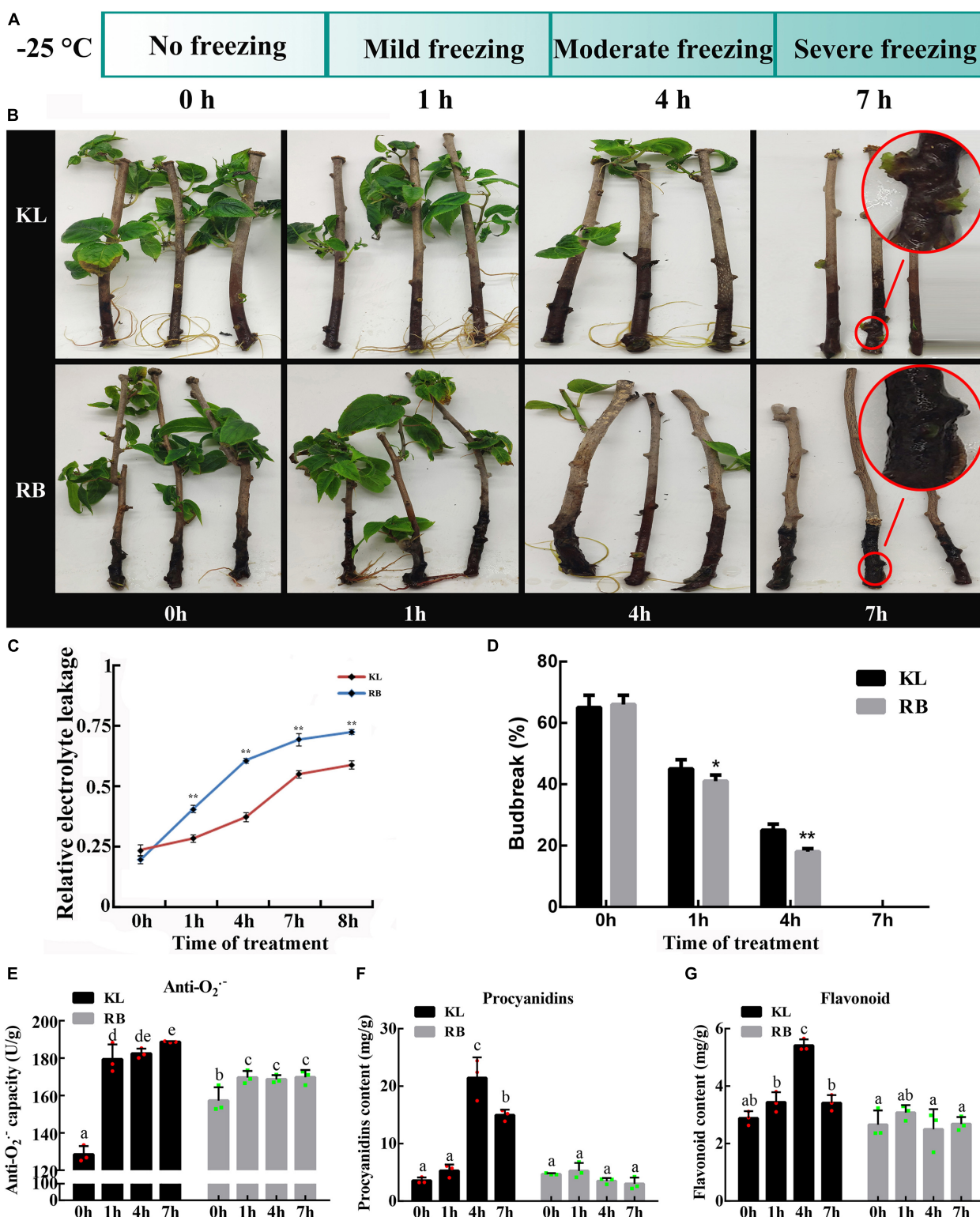
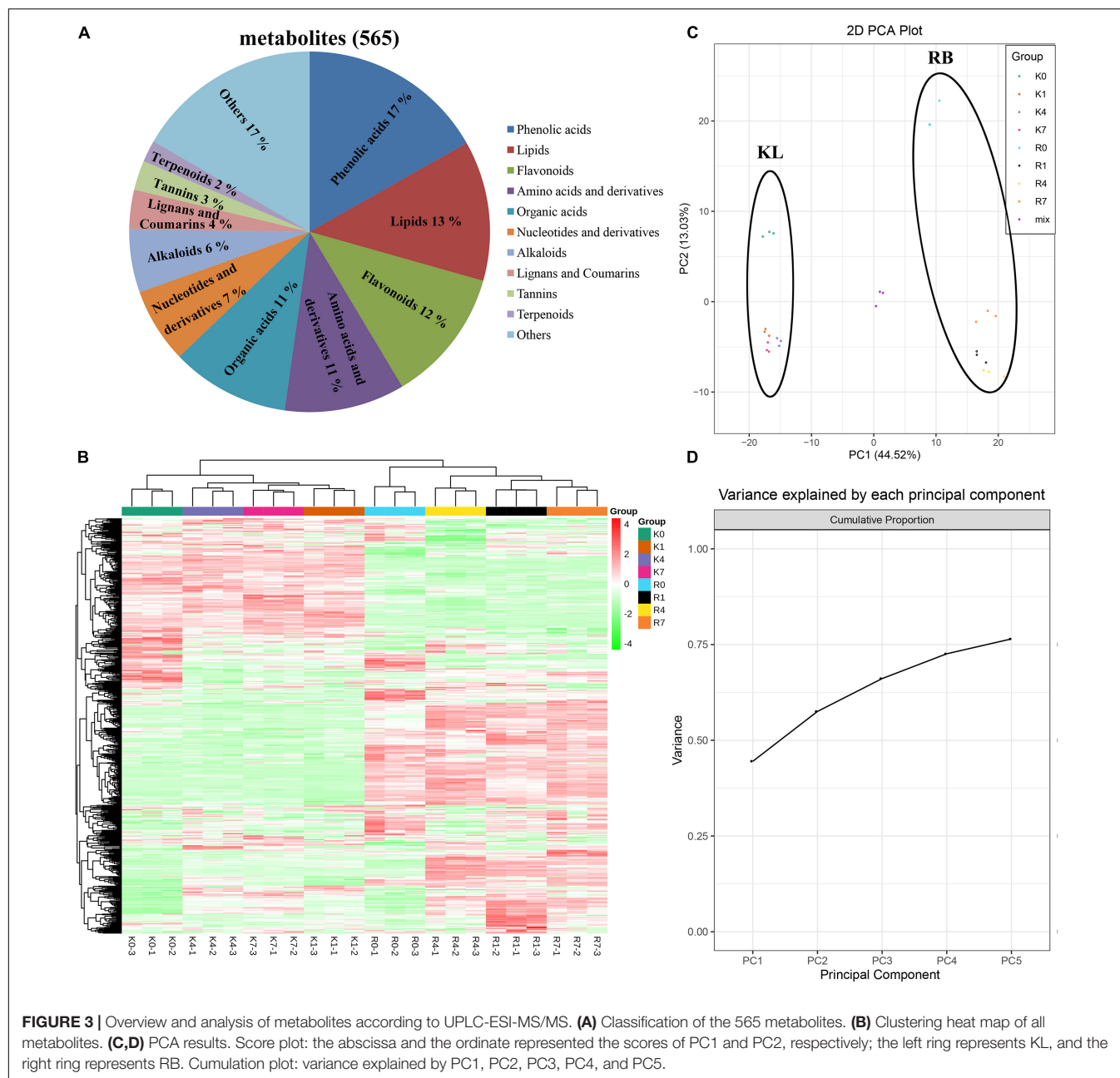


FIGURE 2 | Different REL (relative electrolyte leakage) and VB (vegetative bud) between the KL and RB genotypes under the -25°C treatment. **(A)** Metabolomic and transcriptomic analysis of both genotypes were performed at four time points: 0 h, 1 h, 4 h, 7 h. **(B)** Representative images of KL and RB at 0 h, 1 h, 4 h, 7 h. **(C)** The REL at different treatment time points under -25°C. VB rates after the -25°C treatment, given as the mean of three independent replicate experiments in both genotypes. **(D)** VB rates after the -25°C treatment, given as the mean of three independent replicate experiments in both genotypes. **(E)** The anti-O₂⁻ capacity at different treatment. **(F)** The content of procyanidins at different treatment. **(G)** The content of flavonoid under -25°C.



The data for the 565 metabolites were subjected to PCA analysis. The PCA score plot indicated that the first principal component (PC1) and the second principal component (PC2) represented 44.52% and 13.03% of the total variance, respectively (Figure 3C). The cumulative variance explained by PC1 to PC5 was above 75% (Figure 3D). Since the repeated samples and mixed samples were gathered tightly together, this indicated our experiment was reproducible and reliable. The two genotypes clearly separated along PC1 and PC2 under the normal condition without stress (0 h/−25°C) in the PCA score plot, indicating they had a distinguishable chemical composition under the no-freezing condition. For KL, its samples shifted to and clustered beneath of the no-freezing samples

along PC2 after incurring cold stress. For RB, its samples showed the same pattern as KL but moved farther along PC2 than that in KL.

Overview of Transcriptional Profiles

Twenty-four RNA libraries were built from RNA samples extracted from the two contrasting kiwifruit genotypes, KL (freezing-tolerant) and RB (freezing-sensitive), under the −25°C treatment applied. The Illumina sequencing of the 24 samples generated 171.39 Gb of clean reads. As shown in **Supplementary Table 1**, total mapped reads accounted for 63%–70% of the clean reads. Moreover, clean reads were assembled into 822 851 transcripts with a minimum length of 200 bp

(**Supplementary Figure 1a**). Following a quality control analysis of the transcriptome assembly, 670 190 unigenes were conserved for further analyses. Unigenes could be annotated in the NR database, Nt database, KEGG Ortholog (KO), SwissProt, Pfam, Gene Ontology (GO), and eukaryotic Ortholog Groups (KOG) (**Supplementary Figure 1b**). The unigenes annotated in the NR database can convey the species distribution statistics (**Supplementary Figure 1c**), for which the top species was *Quercus suber*, with 60 311 transcripts, followed by *Vitis vinifera* (403,80, 10.99%). Annotation of the kiwifruit unigenes in the GO database classified 295 300 transcripts in the three main ontologies: biological processes, molecular functions, and cellular components (**Supplementary Figure 1d**). The terms having the largest numbers of transcripts were in the biological process category for which the most abundant terms were cellular process (181 963 transcripts) and metabolic process (160 737 transcripts), followed by biological regulation (73 475 transcripts) and response to stimulus (71 154 transcripts). For molecular function, the binding (178 271) and catalytic activity (156 437) processes were the most abundant terms found, while for cellular component, membrane change (104 070) was also a highly accumulated term.

In the KOG database, a total of 224 673 transcripts were annotated and divided 25 categories (**Supplementary Figure 1e**). Among those categories, only general function prediction had the largest number of transcripts (50 687), followed by post-translational modification, protein turnover, chaperones (247,41), with cell motility having the least number (72). In the classification of KOG annotations, carbohydrate transport and metabolism (12 554), amino acids transport and metabolism (9385), and lipid transport and metabolism (9457) were most pronounced, this result indicated that the sugar, amino acid, and lipid metabolism in *A. arguta* were relatively active, which could constitute the foundation for the healthy overwintering of *A. arguta*. The correlations tested between the samples replicates had Pearson $|r|$ -values > 0.8 , thus confirming the RNA-Seq data were repeatable and that our screening of differential genes by transcriptome data was reliable (**Supplementary Figure 1f**).

DEGs (differential expression genes) in both contrasting genotypes were screened. Comparison of the expression levels of DEGs between every groups were based on FPKM values. There were 1 856 DEGs between KL–0 h and KL–1 h, 2 632 DEGs between KL–0 h and KL–4 h, 1 708 DEGs between KL–0 h and KL–7 h, 4 011 DEGs between RB–0 h and RB–1 h, 4 309 DEGs between RB–0 h and RB–4 h, 2 798 DEGs between RB–0 h and RB–7 h (**Supplementary Figure 2**). These results indicated that DEGs were abundantly enriched at 4 h treatment in both genotypes.

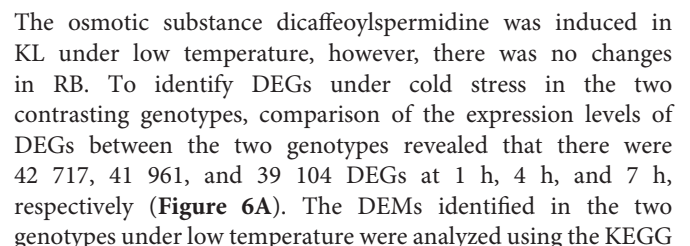
Comparison of Metabolite and Gene Levels Between KL and RB Under the No-Freezing Condition (0 h/–25°C)

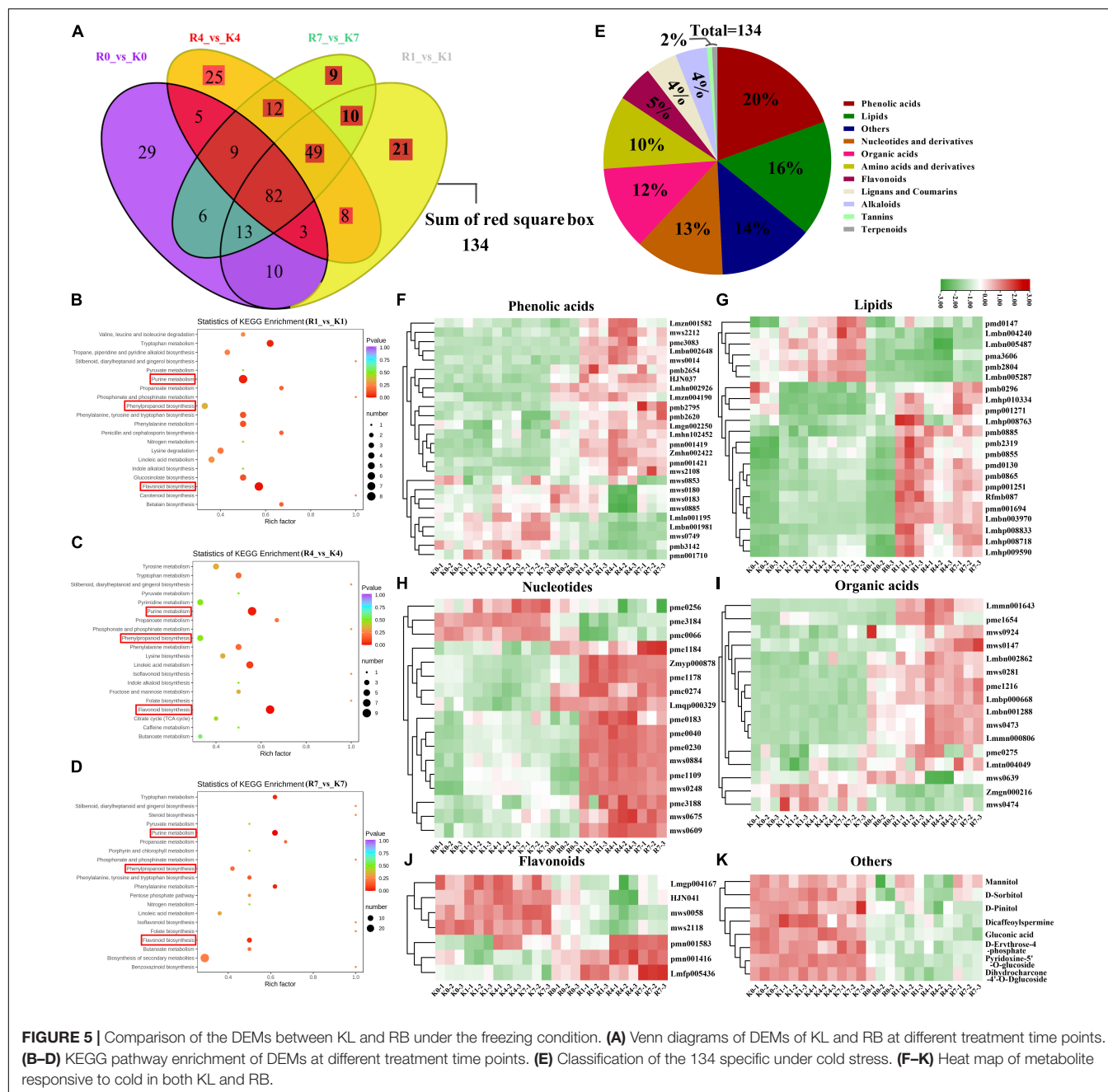
Under the no-freezing condition (0 h/–25°C), the differentially expressed metabolites (DEMs) and genes (DEGs) between the two genotypes amounted to 157 and 40 452, respectively. KEGG enrichment results of DEMs showed that flavonoid biosynthesis,

propanoate metabolism, and biosynthesis of unsaturated fatty acids differed between the two genotypes (**Figure 4A**). For flavonoid biosynthesis, both procyanidin (HJN074) and procyanidin-A6 (HJN048) had higher concentrations in KL than RB (**Figure 4B**). For propanoate metabolism, the succinic acid (mws0192) and succinic anhydride (Lmqp000873), involved in propanoate metabolism, RB had higher contents than did KL (**Figure 4B**). Propanoate metabolism, a component of the TCA cycle, plays a main role in diminishing tolerance to freezing. For the biosynthesis of unsaturated fatty acids, γ -linolenic acid (mws0366), α -linolenic acid (mws0367), linolenic acid (mws1491), 2- γ -linolenoyl-glycerol (Lmhp011388), and 2-linoleoylglycerol (Lmhp012042) in KL were higher than the corresponding amount detected in RB (**Figure 4B**). Other metabolites, namely betaine (mws0191), spermidine (pma07702), and proline (mws0216), were also found involved in FT to increase KL tolerance (**Figure 4B**). Compared with RB, the KL genotype had higher concentrations of flavonoid and lignan among the top 10 metabolites based on the fold-change between KL and RB. By contrast, RB accumulated higher contents of phenolic acid among the top 10 metabolites when compared with KL (**Figure 4C**). The total of 40 452 DEGs were identified in RB–0 h and KL–0 h, then the most of them were enriched in secondary metabolites (**Supplementary Figures 3A,B**). An overview of cellular metabolism was gleaned via the Mapman results for the DEGs; evidently, abundant DEGs between KL and RB were involved in the TCA cycle, nucleotides metabolism, and secondary metabolism (**Figure 4D**). These DEGs were enriched in the mechanism of flavonoids and betaines metabolism among secondary metabolism; though, more up-regulated DEGs were involved in KL with respect to flavonoid metabolism (**Figure 4E**). Other DEGs were found enriched in the cold response and redox metabolism. For the latter, more DEGs were identified for thioredoxin, ascorb/glutha, glutaredoxin, and dismutase/catalase (**Figure 4F**). Taking a combined view of the metabolome and transcriptome, the relative contents of DEMs including flavonoids, propanoate, lipids, betaines, and lignans were all consistent with the expression of DEGs involved in flavonoids, TCA, lipids, and betaines pathways.

Comparison of Metabolite and Gene Levels Between KL and RB Under the Freezing Condition

Comparison of the DEMs between the two genotypes revealed that there were 196, 193, and 190 DEMs at 1 h, 4 h, and 7 h, respectively (**Figure 5A**). The DEMs identified in the two genotypes under low temperature were analyzed using the KEGG pathway database. KEGG pathway analysis revealed that the most predominant subcategory among various pathways was ‘Purine metabolism’, followed by ‘Phenylpropanoid biosynthesis’, and ‘Flavonoid biosynthesis’ at 1 h, 4 h, and 7 h (**Figures 5B–D**). The 134 DEMs were specifically induced by low temperature, the classification of 134 DEMs showed that phenolic acids, lipids, nucleotides, organic acids, and flavonoids were the most abundant metabolites involved in the low temperature response of kiwifruit (**Figure 5E**). Most





pathway database. KEGG pathway analysis revealed that the most predominant subcategory among various pathways was ‘Starch and sucrose metabolism’, followed by ‘Phenylpropanoid biosynthesis’, ‘Flavonoid biosynthesis’, and ‘Biosynthesis of secondary metabolites’ at 1 h, 4 h, and 7 h (Figures 6B–D). The 29 200 DEGs were specifically induced by low temperature, 29 200 DEGs were mapped in the pathways including secondary metabolism, mitochondrial-electron-transport, TCA, inositol phosphates, spermine synthesis (Figures 6E–I). The DEGs involved in Flavonoids and phenylpropanoids, inositol phosphates, and spermine synthesis pathways had higher expression in KL than that in RB. however, The DEGs

involved in mitochondrial-electron-transport and TCA had higher expression in RB than that in KL.

Commonly and Specifically Responding Metabolites in KL and RB Under the Cold Treatment

The Venn diagram showed that the DEMs common to KL and RB totaled 43 under cold stress, with most of the DEMs having a specific accumulation in both genotypes: 62 in RB and 47 in KL (Figure 7A). The classification of common DEMs showed that lipids were the metabolites most involved in

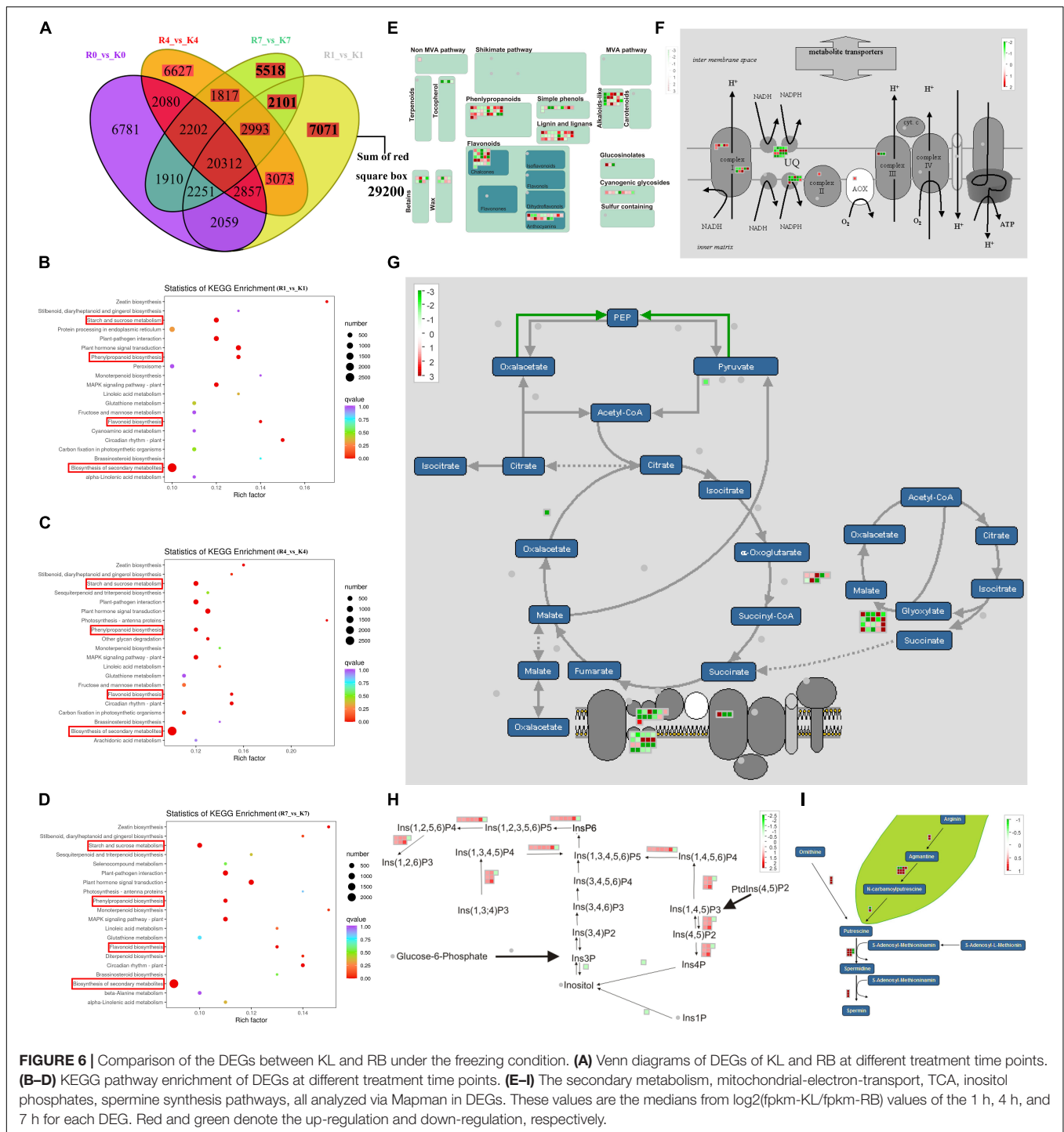
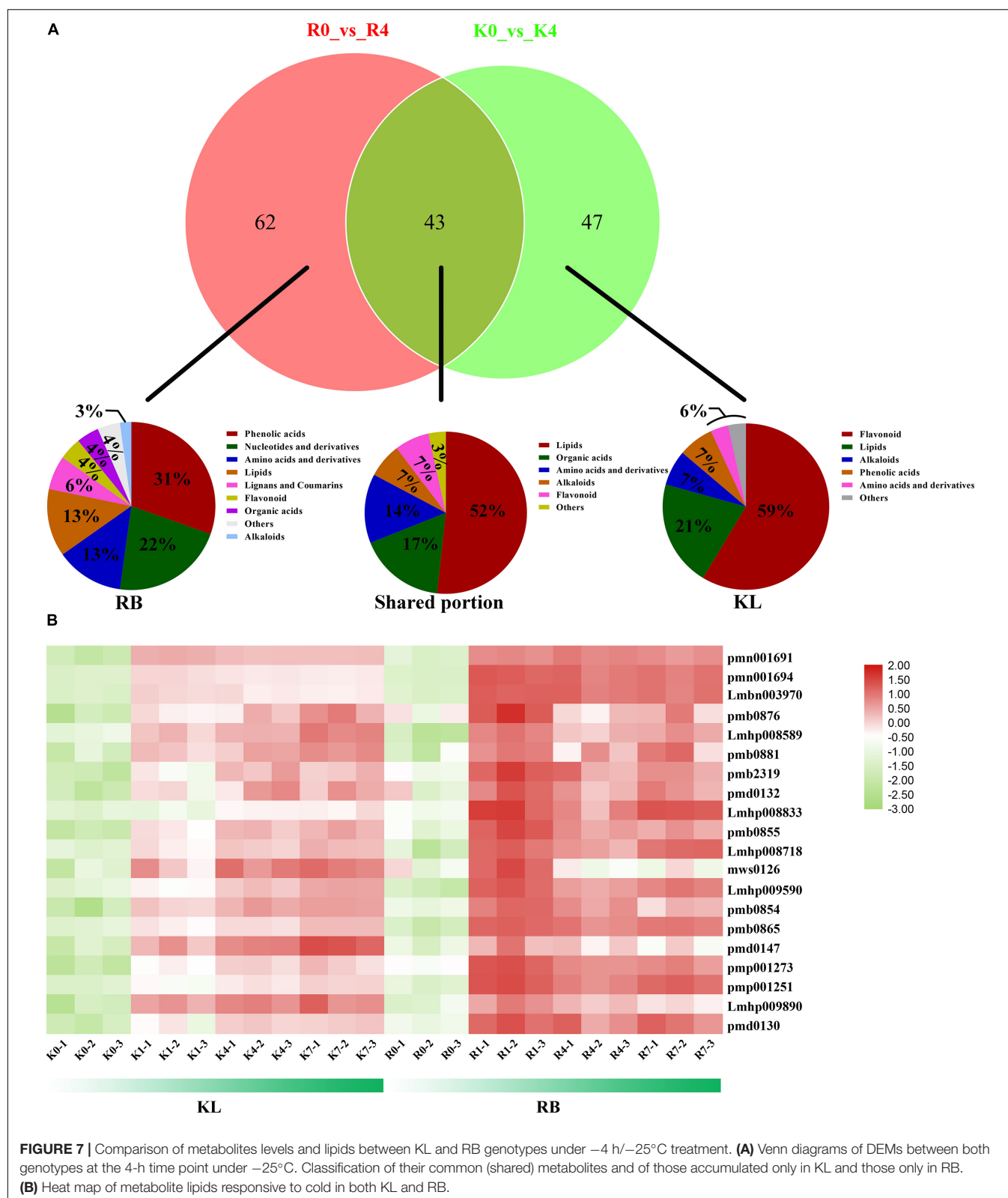


FIGURE 6 | Comparison of the DEGs between KL and RB under the freezing condition. **(A)** Venn diagrams of DEGs of KL and RB at different treatment time points. **(B–D)** KEGG pathway enrichment of DEGs at different treatment time points. **(E–I)** The secondary metabolism, mitochondrial-electron-transport, TCA, inositol phosphates, spermine synthesis pathways, all analyzed via Mapman in DEGs. These values are the medians from $\log_2(\text{fpkm-KL}/\text{fpkm-RB})$ values of the 1 h, 4 h, and 7 h for each DEG. Red and green denote the up-regulation and down-regulation, respectively.

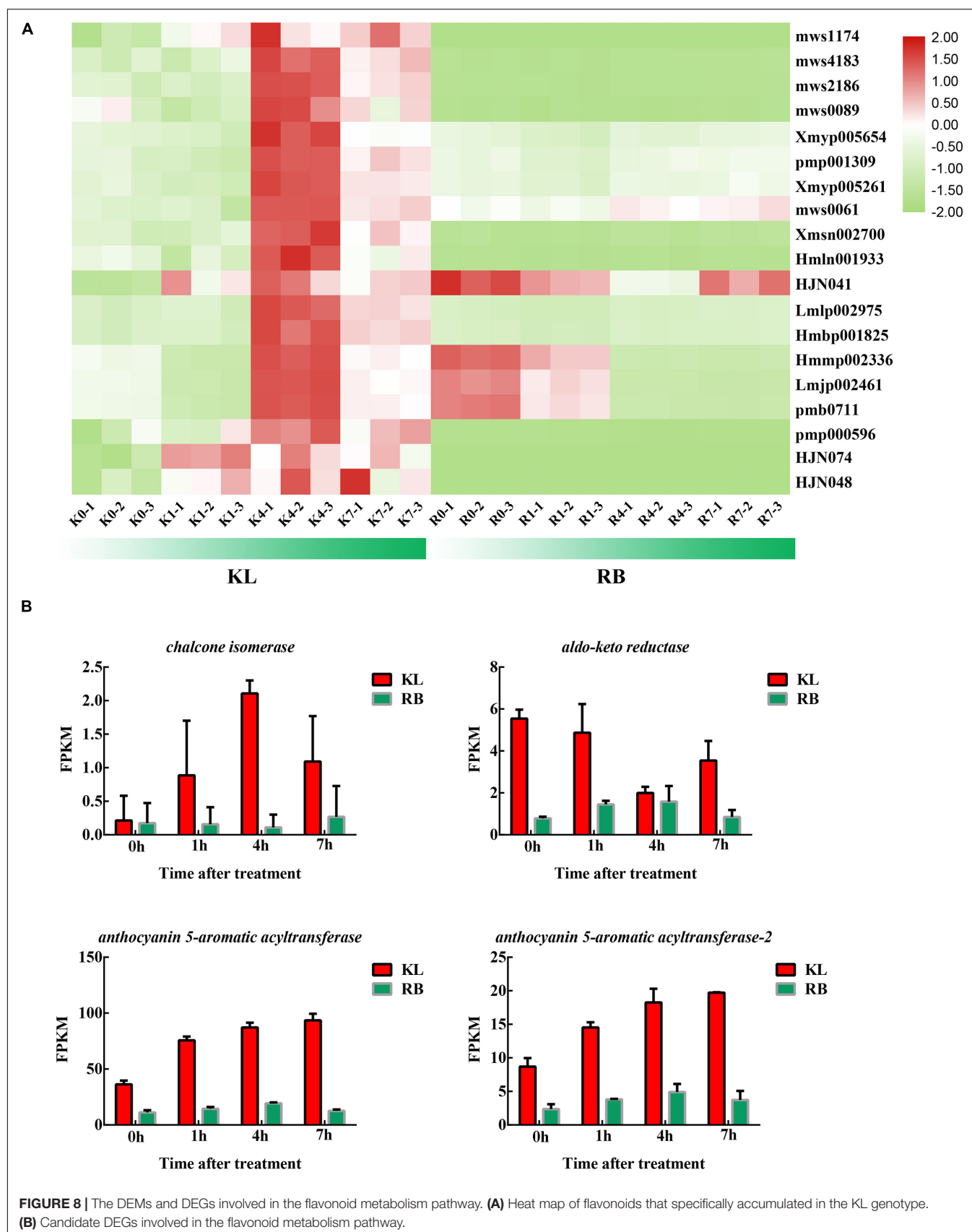
the low temperature response of kiwifruit (Figure 7A). Those DEMs that only accumulated in KL were classified into five categories, for which flavonoid species were the most prevalent (Figure 7A). For the RB-specific DEMs, the classification results showed that phenolic acid mechanism and nucleotide metabolism were the most involved in the low temperature stress (Figure 7A). A total of 20 lipids (LysoPC 14:0, LysoPC 15:0, LysoPC 16:0, LysoPC 17:1, LysoPC 18:3, LysoPE 18:3,

and so on) increased significantly in both genotypes after incurring cold stress when compared with their levels in the no-freezing condition (Figure 7B; Supplementary Table 2). With a longer exposure time to the freezing treatment, lipids was rapidly induced in first 1 h for RB and then gradually increased through the 4 h and 7 h. In contrast, the lipids accumulated continuously for KL under cold stress, but to lower level than that in RB.



Under cold stress, 19 flavonoids were upregulated remarkably in KL (**Figure 8A**; **Supplementary Table 3**), whereas flavonoids did not significantly change in RB. The flavonoids' content in

KL exceeded that in RB. Two flavonoids (HJN074, HJN048) were procyanidines, which could be induced by cold stress and have undergone specific accumulation in KL. The four DEGs



involved in the flavonoid metabolism were induced by cold stress; moreover, 4 DEGs had higher expression levels in KL than in RB (**Figure 8B**).

The two types of metabolites, namely five nucleotides and 11 phenolic acids, increased significantly only in RB under cold

stress (**Figure 9A**). The nucleotides' metabolite level in RB was consistently higher than that in KL but also increased with longer exposure time to the low temperature treatment (**Supplementary Table 4**). The metabolic level of phenolic acid was similar to that of nucleotides; this was also moderately maintained at a high

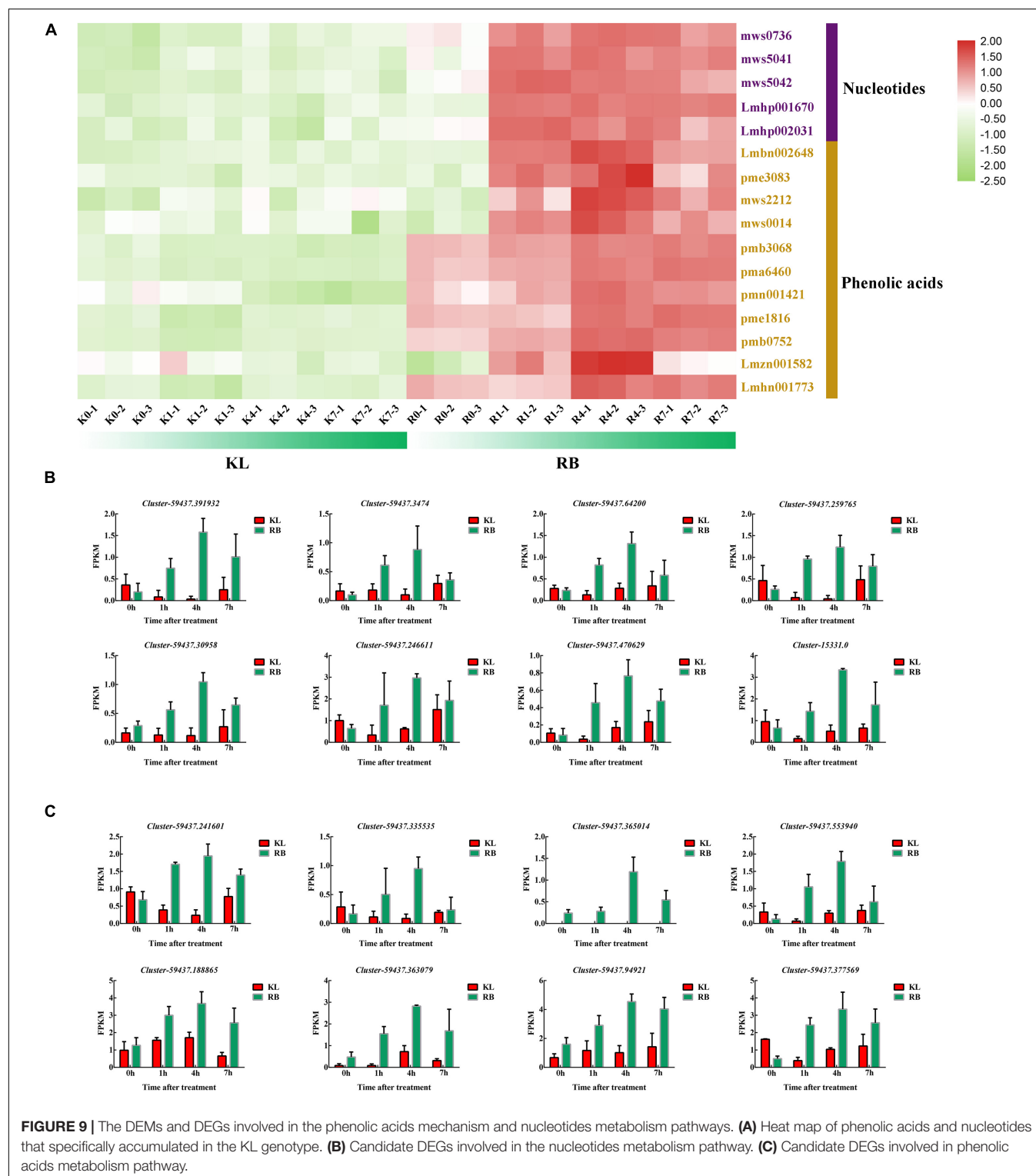


FIGURE 9 | The DEMs and DEGs involved in the phenolic acids mechanism and nucleotides metabolism pathways. **(A)** Heat map of phenolic acids and nucleotides that specifically accumulated in the KL genotype. **(B)** Candidate DEGs involved in the nucleotides metabolism pathway. **(C)** Candidate DEGs involved in phenolic acids metabolism pathway.

level in RB (Supplementary Table 5). In KL, however, it did not respond to the low temperature imposed. Eight DEGs were involved in nucleotides metabolism, and their gene expression levels were similar to those of metabolites (Figure 9B), being higher in RB than KL. Those eight DEGs are involved in phenolic acid metabolism, and their expression levels were also positively correlated with phenolic acid content (Figure 9C). The expression levels in RB significantly surpassed those in KL and displayed a trend of induction under prolonged low temperature exposure (Supplementary Table 6).

DISCUSSION

For perennial woody plants in temperate regions, the annual growth cycle can be divided into a growth stage (chilling tolerance) and dormancy stage (freezing tolerance, FT) (Owens et al., 1977). There is huge difference, however, in the tolerance mechanism at work between the growth and dormancy stages. It is therefore essential to separate these two stages when studying their molecular mechanisms for how plants respond to low temperature. In addition, to date, many previous studies have focused on the chilling tolerance (growth stage) of plants exposed to low temperatures, whereas their freezing tolerance in dormancy stage has received comparatively little attention.

The *A. arguta* species is widely distributed kiwifruit plant, and it has adapted to a broad range of environmental temperatures. The geographical distribution of KL and RB indicates that substantial divergence in their FT. The latter was quantified by the semi-lethal temperature (LT50), which confirmed this trait divergence, which amount to a 6°C between the genotypes. However, the LT50 of KL was lower than expected, perhaps because KL was planted in Henan, where the winter temperatures might have been insufficient for KL to reach its maximum FT. ROS scavenging ability is an important indicator of FT, KL had higher capacity to scavenge $-O_2^{\cdot-}$ and accumulate higher contents of procyanidin and flavonoid compared with RB, which indicated ROS scavenging ability was the key factor to distinguish differences in FT. In this study, the REL and VB rates were also useful for evaluating the FT. Prior exposure to a -25°C , this temperature can stimulate the tolerance of KL and cause damage to RB, which could distinguish the differential FT of both genotypes. Moreover, varying the duration of this low temperature treatment let us better discern the FT in the both genotypes, which provided physiological evidence for our further omics experiment. In PCA results of 565 metabolites (Figure 3C), under cold stress, RB was positioned farther along PC2 than was KL when compared with untreated samples (0h at -25°C), which indicated the metabolite content of RB had a greater variation range under cold stress compared with KL. Based on above results, we may speculate that RB was sensitive to cold stress and strongly responded to damage from cold.

Roles of Different Metabolism in the Kiwifruit Plant Response to Cold Stress

Both genotypes were cold acclimated to a maximum FT through the natural cooling of the field during the winter

before treating them at -25°C . We uncovered differences in flavonoid metabolism, unsaturated fatty metabolism and TCA cycle between KL and RB under the no-freezing condition (0 h at -25°C). Flavonoid metabolites, acting as antioxidants to remove ROS, can increase FT (Li et al., 2019), while unsaturated fatty metabolism, by enhancing the cell membrane fluidity, can increase plant resistance to cold (Li et al., 2020). The TCA cycle represents energy metabolism, while energy metabolism meant that plant dormancy was weak (Wang et al., 2021). Betaine, arginine and proline can be used as osmotic stress substances to improve plants' FT (Meilong et al., 2020). We found four lignans in KL that had higher concentrations than in RB. Lignans are known to have the ability to scavenge ROS and resist oxidation stress (Khan et al., 2020). In conclusion, osmotic ability and ROS scavenging ability were major factors driving the different FT of the kiwifruit genotypes. In the process of both genotypes responding to low temperature stress, differential metabolites were enriched in flavonoids metabolism and phenylpropanoid biosynthesis metabolism pathways; in this respect, flavonoids metabolism can improve plant cold resistance, while phenylpropanoid biosynthesis metabolism, especially phenolic acid metabolism, and TCA mechanism can also decrease plants' FT to the cold (Huang et al., 2015; Thalmann and Santelia, 2017). Concerning polysaccharide and spermine, both can promote osmotic ability and make cold stress response more effective (Sebastián et al., 2018). For RB's response under low temperature stress, both lipid metabolism and energy metabolism were more induced in RB than those in KL, which meant that RB's energy metabolism remained operational in the freezing cold. While high-energy metabolism confers weak dormancy, leaving plants comprised in their ability to withstand injury from low temperatures.

Lipid Metabolism as a Biomarker of Lipid Damages in the Plant Response to Cold Stress

Under cold stress, a contrasting FT was detected between KL (tolerant) and RB (sensitive) using the LC-MS/MS and RNA-Seq analyses. The compounds accumulated in both genotypes under cold stress represented fundamental metabolites responsive to cold stress. These metabolites, including various secondary metabolites, are known to contribute to cold stress tolerance and some of them metabolites were known to accumulate in other plant species (Colinet et al., 2012). Changes in these metabolites suggested conserved reconstruction in metabolome levels in plants in response to cold stress. In this study, the plasma membrane had crucial roles in the response to low temperature stress, as lipids are the major component of the plasma membrane. From our the metabolism analysis, we find that LPCs, LPEs, and free fatty acids were accumulated in both genotypes. Interestingly, three free fatty acids (pmn001691, pmn001694, Lmbn003970) all accumulated in RB more than in KL. The free fatty acids are the principal toxins of plant membrane lipid systems; while three LPEs, including LPE 16:0 (pmb0876), LPE 18:3 (Lmhp008589), and LPE 18:2 (pmb0881),

were significantly accumulated only in RB under mild freezing (1 h at -25°C), then, these changes were becoming disordered. However, LPEs gradually increased in the KL genotype, which indicated that cold stress caused much more damage to the RB genotype. The LPCs' results were the same as those found for LPEs. These suggested that lipid metabolism figures prominently in how kiwifruit responds to cold stress. In particular, the LPE 18:0 (2n isomer) (Tri760) was associated with phospholipids, and studies have shown it to be an isomer of lysophosphatidylethanolamine, which is a component of phospholipids and related to biofilm synthesis; moreover, cold resistance in plants is closely related to the fluidity of biofilms. LPCs can be produced by the non-enzymatic oxidation of phospholipids; LPCs are also produced by phospholipase A2 (PLA2), which cleaves phospholipids into LPC and fatty acids with specificity on the sn-2 position. Lipoxygenase (LOX) was found to be a key enzyme involved in lipid-signaling, adding oxygen to linoleic and linolenic acids to produce highly reactive lipid hydroperoxides (Alferez et al., 2010). The rapid accumulation of LPC and LPE has been reported in many plant species that incur by stress (Narvaez-Vasquez et al., 1999). Additionally, in research on blackberry red drupelet disorder research, phospholipids were a major constituent of cell membranes and the increased LPC level in red drupelet disorder indicated a loss of cell membrane integrity (Kim et al., 2019). Therefore, a higher LPC content may be an important biomarker for cold damage to plants.

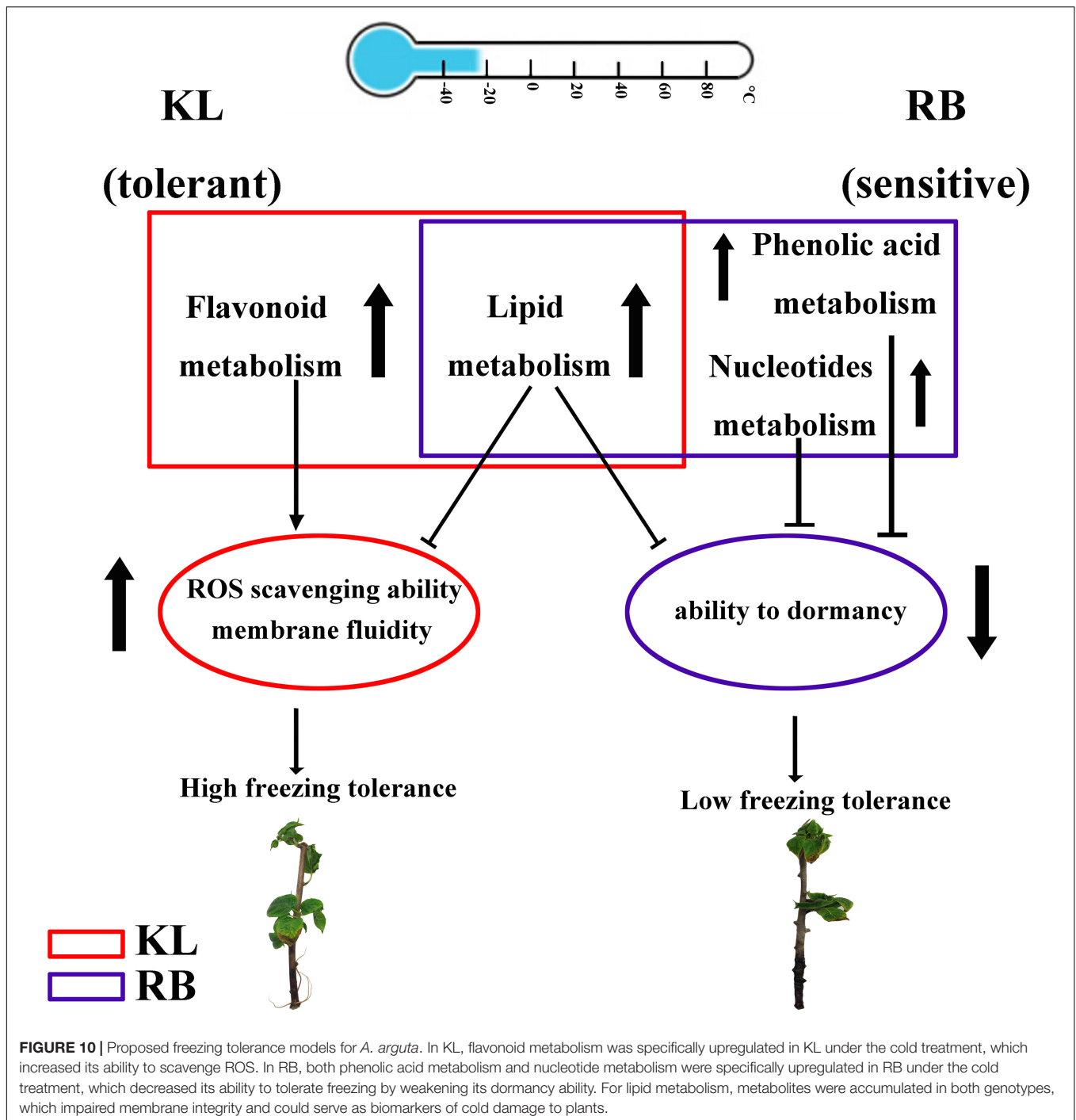
Induction of Flavonoid Metabolism Specifically in KL in Response to Cold Stress

A subset of metabolites specifically accumulated in KL. Genes involved in secondary metabolism, including those for flavonoid biosynthesis as well as flavone and flavonol biosynthesis, may have critical functions in a plant's response to cold stress (Wei et al., 2019). For the flavonoid biosynthesis process, quercetin glycoside levels were dramatically increased (more than 10-fold) in the KL whereas the changes in RB were negligible. Quercetin glycosides showed a high ROS-scavenging activity. In addition, quercetin-3-O-arabinoside, quercetin-3-O-glucoside, quercetin-3-O-xylosyl-galactoside, quercetin-3-O-sambubioside, quercetin-O-feruloyl-pentoside, quercetin-3-O-neohesperidoside, quercetin-7-O-rutinoside, and quercetin-3,7-O-diglucoside all featured different antioxidant activities. Kaempferol glycosides also have an ROS-scavenging activity, and we found that kaempferol-7-O-glucoside, kaempferol-4'-O-glucoside, 6-hydroxykaempferol-7-O-glucoside were increased in KL. Therefore, perhaps the high quercetin and kaempferol contents in this more tolerant plant under the cold treatment contributed to higher antioxidant activity compared with RB. The increased accumulation of these compounds might be due to the upregulated expression of flavonoid biosynthesis genes. Anthocyanins are type of flavonoid compound that have crucial roles in plant survival by protecting cells against damage caused by various stress conditions (Xie and Chen, 2018). Anthocyanin biosynthesis

was also affected by low temperatures, which influenced the expression of genes for flavonoid biosynthesis. The genes involved in anthocyanin biosynthesis were found affected by cold in this study, in that the genes of Cluster-59437.264203 (codeinone reductase), Cluster-59437.286871 (chalcone isomerase), Cluster-59437.250404, and Cluster-59437.316559 (anthocyanin 5-aromatic acyltransferase) were all upregulated in the KL. These results suggested that an increase in the expression level of a specific gene involved in the anthocyanin pathway would probably result in anthocyanin accumulation; they also indicated that anthocyanins could enhance the FT of kiwifruit. In grapevine (*Vitis*), it was reported that the loss of anthocyanin in grape berries at high temperatures arose from non-enzymatic degradation and inhibition of transcription in anthocyanin biosynthetic genes (Mori et al., 2007; Schulz et al., 2015). Taken together, we reasonably inferred that the mechanisms of anthocyanin synthesis in kiwifruit plants differ under low-temperature stresses, and this aspect of the FT trait merits further researched.

Induction of Phenolic Acid and Nucleotides Metabolism, Particularly in RB, in Response to Cold Stress

One of the simplest ways to assess cold injuries in plant tissues is by observing the typical browning associated with membrane rupture. As compartmentalized phenolic compounds and enzymes are simultaneously released into the cell, the phenolics lose their esterified moieties and are then free to react with proteins, forming insoluble brown complexes (Chalker-Scott and Fuchigami, 1989). In this respect, α -hydroxycinnamic acid, 2-(formylamino)benzoic acid, caffeic acid, coniferyl alcohol, ferulic acid, 1-O-p-coumaroylquinic acid, 4-O-p-coumaroylquinic acid, 3-O-(E)-p-Coumaroylquinic acid, caffeoylquinic acid, 3-O-feruloylquinic acid, 5'-glucosyloxyjasmanic acid, caffeoylnicotinoyltartaric acid and syringoylcaffeoylquinic acid O-glucose were all found increased in the RB genotype after it incurred cold stress. Phenolic acids may be useful as an index damage index to gauge and evaluate cold damage to plants (Figure 9A). In addition, since ferulic acids and caffeic acids are downstream metabolites of TCA metabolism, this indicated that RB harbors a strong energy metabolism under cold stress conditions. Nucleotide metabolism could be attributed to cold-induced damage, and we found that adenine, 2-hydroxy-6-aminopurine, cytidine, adenosine, 2-hydroxyadenosine, guanosine, β -nicotinamide mononucleotide, guanosine monophosphate and cyclic AMP (adenosine monophosphate) were increased in RB exposed to cold. This cold stress caused damage to nucleotides damage that spurred an increase in nucleotide metabolism. Overall, eight genes involved in phenolic acids metabolism, plus another eight genes involved in nucleotides metabolism, for a total of 16 gene were up-regulated under cold stress conditions in RB, with no changes detected in KL. These differences may point to key metabolism features that have caused the divergence in FT between the KL and RB genotypes.



CONCLUSION

In this study, both the DEGs and DEMs in two kiwifruit genotypes differing in FT (freezing tolerance) were identified by metabolome and transcriptome analyses after imposing a cold stress treatment. In addition, unique metabolites and genes were detected in each genotype. Although lipid metabolites were common between KL and RB, they were significantly higher in RB and might be linked to cell membrane integrity

and cold damage. Therefore, lipids could serve as a damage index to evaluate FT. Flavonoid metabolism, induced in KL only, could be involved in scavenging for ROS to enhance FT trait in KL. Both phenolic acid metabolism and nucleotide metabolism were induced in RB only, decreasing its FT. This comprehensive study thus provides new evidence and insights into how differing genotypes of the same species respond to cold stress at metabolomic and transcriptomic levels (Figure 10).

DATA AVAILABILITY STATEMENT

The datasets presented in this study can be found in online repositories. The names of the repository/repositories and accession number(s) can be found below: <https://www.ncbi.nlm.nih.gov/>, PRJNA681641.

AUTHOR CONTRIBUTIONS

SS, ML, XQ, JC, YZ, AM, ZL, and YL conducted the experiments. JF organized and supervised the overall project. SS and ML performed the data analysis and wrote the manuscript. CH edited the manuscript. All authors contributed to the article and approved the submitted version.

FUNDING

This study was funded by the National Key Research and Development Project of China (Grant No. 2019YFD1000800); the National Natural Science Foundation of China (Grant No. 31801820); The Special Engineering Science and Technology Innovation, Chinese Academy of Agricultural Sciences (Grant No. CAAS-ASTIP-2015-ZFRI); and the Modern Agricultural Industrial Technology System of Henan Province (Grant No. S2014-11).

REFERENCES

- Alferez, F., Singh, S., Umbach, A. L., Hockema, B., and Burns, J. K. (2010). Citrus abscission and *Arabidopsis* plant decline in response to 5-chloro-3-methyl-4-nitro-1H-pyrazole are mediated by lipid signalling. *Plant Cell Environ.* 28, 1436–1449. doi: 10.1111/j.1365-3040.2005.01381.x
- An, J. P., Li, R., Qu, F. J., You, C. X., Wang, X. F., and Hao, Y. J. (2018). R2R3-MYB transcription factor MdMYB23 is involved in the cold tolerance and proanthocyanidin accumulation in apple. *Plant J.* 96, 562–577. doi: 10.1111/tj.14050
- Bahrman, N., Hascot, E., Jaminon, O., Dépta, F., and Legrand, S. (2019). Identification of genes differentially expressed in response to cold in *Pisum sativum* Using RNA sequencing analyses. *Plants-Basel* 8:288. doi: 10.3390/plants8080288
- Chai, F., Liu, W., Xiang, Y., Meng, X., Sun, X., Cheng, C., et al. (2019). Comparative metabolic profiling of *Vitis amurens* and *Vitis vinifera* during cold acclimation. *Hortic. Res. England* 6:8. doi: 10.1038/s41438-018-0083-5
- Chalker-Scott, L., and Fuchigami, L. H. (1989). *The Role of Phenolic Compounds in Plant Stress Responses*. Boca Raton, FL: CRC Press.
- Chen, L., Hu, W., Mishra, N., Wei, J., and Shen, G. (2020). AKR2A interacts with KCS1 to improve VLCFAs contents and chilling tolerance of *Arabidopsis thaliana*. *Plant J.* 103, 1–43. doi: 10.1111/tj.14848
- Clemente-Moreno, M. J., Omranian, N., Saez, P. L., Figueroa, C. M., Del-Saz, N., Elso, M., et al. (2020). Low-temperature tolerance of the Antarctic species *Deschampsia antarctica*: a complex metabolic response associated with nutrient remobilization. *Plant Cell Environ.* 43, 1376–1393. doi: 10.1111/pce.13737
- Colinet, H., Larvor, V., Laparie, M., and Renault, D. (2012). Exploring the plastic response to cold acclimation through metabolomics. *Funct. Ecol.* 26, 711–722. doi: 10.1111/j.1365-2435.2012.01985.x
- Cook, D., Fowler, S., Fiehn, O., and Thomashow, M. F. (2004). A prominent role for the CBF cold response pathway in configuring the low-temperature

SUPPLEMENTARY MATERIAL

The Supplementary Material for this article can be found online at: <https://www.frontiersin.org/articles/10.3389/fpls.2021.628969/full#supplementary-material>

Supplementary Figure 1 | Overview and analysis of the transcriptome.

(a) Distribution of transcripts sequence length. (b) Unigenes were annotated in 7 databases. (c) Unigenes were annotated in Nr database and species distribution statistics. (d) Unigenes were annotated in GO and classified into Biological process, Cellular component and Molecular Function. (e) Unigenes were annotated in KOG and classified into different function. (f) Pearson's correlation coefficient analysis in different samples.

Supplementary Figure 2 | Summary of differential expression analysis of kiwifruit under cold stress.

Supplementary Figure 3 | Overview of DEGs in RB-0 h VS. KL-0 h. (a) The volcano plot between the RB-0 h and KL-0 h. (b) Enrichment of DEGs in the KEGG pathway.

Supplementary Table 1 | The statistical results of clean reads mapped into reference.

Supplementary Table 2 | Common responding metabolites lipids in KL and RB.

Supplementary Table 3 | Flavonoids that specifically accumulated in KL.

Supplementary Table 4 | Phenolic acids specific accumulated in RB.

Supplementary Table 5 | Nucleotides specific accumulated in RB.

Supplementary Table 6 | Candidate DEGs involved in flavonoid metabolism pathway, phenolic acid metabolism pathway and nucleotide metabolism pathway.

- metabolome of *Arabidopsis*. *Proc. Natl. Acad. Sci. U.S.A.* 101, 15243–15248. doi: 10.1073/pnas.0406069101
- Ding, Y., Lv, J., Shi, Y., Gao, J., and Hua, C. (2018). EGR2 phosphatase regulates OST1 kinase activity and freezing tolerance in *Arabidopsis*. *EMBO J.* 38:e99819. doi: 10.15252/embj.201899819
- Dreyer, A., and Dietz, K. J. (2018). Reactive oxygen species and the redox-regulatory network in cold stress acclimation. *Antioxidants Basel* 7, 1–15. doi: 10.3390/antiox7110169
- Gilad, G., Adi, F., Yardena, D., Yacov, I., Maxim, I., Sergey, M., et al. (2018). Transcriptome analysis and metabolic profiling reveal the key role of α -linolenic acid in dormancy regulation of European pear. *J. Exp. Bot.* 70, 1017–1031. doi: 10.1093/jxb/ery405
- Hannah, M. A., Wiese, D., Freund, S., Fiehn, O., Heyer, A. G., and Hincha, D. K. (2006). Natural genetic variation of freezing tolerance in *Arabidopsis*. *Plant Physiol.* 142, 98–112. doi: 10.1104/pp.106.081141
- Huang, X.-S., Zhang, Q., Zhu, D., Fu, X., and Wang, M. (2015). ICE1 of *Poncirus trifoliata* functions in cold tolerance by modulating polyamine levels through interacting with arginine decarboxylase. *J. Exp. Bot.* 66, 3259–3274. doi: 10.1093/jxb/erv138
- Jian, H., Xie, L., Wang, Y., Cao, Y., and Liu, L. (2020). Characterization of cold stress responses in different rapeseed ecotypes based on metabolomics and transcriptomics analyses. *PeerJ* 8:e8704. doi: 10.7717/peerj.8704
- Jingyu, Z., Luo, W., Zhao, Y., Xu, Y., Song, S., and Chong, K. (2016). Comparative metabolomic analysis reveals a reactive oxygen species-dominated dynamic model underlying chilling environment adaptation and tolerance in rice. *New Phytol.* 211, 1295–1310. doi: 10.1111/nph.14011
- Khan, I., Khan, M. A., Shehzad, M. A., and Ali, H. (2020). Micropropagation and production of health promoting lignans in *Linum Usitatissimum*. *Plants-Basel* 9:728. doi: 10.3390/plants9060728
- Kim, M. J., Lee, M. Y., Shon, J. C., Kwon, Y. S., Liu, K. H., Lee, C. H., et al. (2019). Untargeted and targeted metabolomics analyses of blackberries – Understanding postharvest red drupelet disorder. *Food Chem.* 300:125169. doi: 10.1016/j.foodchem.2019.125169

- Kou, S., Chen, L., Tu, W., Scossa, F., Wang, Y., Liu, J., et al. (2018). The arginine decarboxylase gene ADC1, associated to the putrescine pathway, plays an important role in potato cold-acclimated freezing tolerance as revealed by transcriptome and metabolome analyses. *Plant J.* 96, 1283–1298. doi: 10.1111/tj.14126
- Krasensky, J., and Jonak, C. (2012). Drought, salt, and temperature stress-induced metabolic rearrangements and regulatory networks. *J. Exp. Bot.* 63, 1593–1608. doi: 10.1093/jxb/err460
- Lee, J. H., Kwon, M. C., Jung, E. S., Lee, C. H., and Oh, M. M. (2019). Physiological and metabolomic responses of kale to combined chilling and UV-A treatment. *Int. J. Mol. Sci.* 20, 4950–4967. doi: 10.3390/ijms20194950
- Li, H., Ding, Y., Shi, Y., Zhang, X., and Yang, S. (2017). MPK3- and MPK6-mediated ICE1 phosphorylation negatively regulates ICE1 stability and freezing tolerance in *Arabidopsis*. *Dev. Cell* 43, 630–642. doi: 10.1016/j.devcel.2017.09.025
- Li, J., Yang, P., Yang, Q., Gong, X., Ma, H., Dang, K., et al. (2019). Analysis of flavonoid metabolites in buckwheat leaves using UPLC-ESI-MS/MS. *Molecules* 24:1310. doi: 10.3390/molecules24071310
- Li, Q., Xiang, C., Xu, L., Cui, J., Fu, S., Chen, B., et al. (2020). SMRT sequencing of a full-length transcriptome reveals transcript variants involved in C18 unsaturated fatty acid biosynthesis and metabolism pathways at chilling temperature in *Pennisetum giganteum*. *BMC Genomics* 21:3. doi: 10.1186/s12864-019-6441-3
- Lin, M. M., Fang, J. B., Hu, C. G., Qi, X. J., Sun, S. H., Chen, J. Y., et al. (2020). Genome-wide DNA polymorphisms in four *Actinidia arguta* genotypes based on whole-genome re-sequencing. *PLoS One* 15:e0219884. doi: 10.1371/journal.pone.0219884
- Ma, X., Hui, X., Liu, Y., Haibin, W., Zheng, X., Song, C., et al. (2016). Transcriptomic and metabolomic studies disclose key metabolism pathways contributing to well-maintained photosynthesis under the drought and the consequent drought-tolerance in rice. *Front. Plant Sci.* 7:1886. doi: 10.3389/fpls.2016.01886
- Meilong, X., Qian, T., Yi, W., Zemin, W., Guangzhao, X., Kirabi, E. G., et al. (2020). Transcriptomic analysis of grapevine LEA gene family in response to osmotic and cold stress, and functional analyses of VamDHN3 gene. *Plant Cell Physiol.* 61, 775–786.
- Mori, K., Goto-Yamamoto, N., Kitayama, M., and Hashizume, K. (2007). Loss of anthocyanins in red-wine grape under high temperature. *J. Exp. Bot.* 58, 1935–1945. doi: 10.1093/jxb/erm055
- Narvaez-Vasquez, J., Florin-Christensen, J., and Ryan, C. A. (1999). Positional specificity of a phospholipase A activity induced by wounding, systemin, and oligosaccharide elicitors in tomato leaves. *Plant Cell* 11, 2249–2260. doi: 10.1105/tpc.11.11.2249
- Owens, J. N., Molder, M., and Langer, H. (1977). Bud development in *Picea glauca*. I. Annual growth cycle of vegetative buds and shoot elongation as they relate to date and temperature sums. *Can. J. Bot.* 55, 2728–2745. doi: 10.1139/b77-312
- Peng, T., Zhu, X., Duan, N., and Liu, J. H. (2015). PtrBAM1, a β -amylase-coding gene of *Poncirus trifoliata*, is a CBF regulon member with function in cold tolerance by modulating soluble sugar levels. *Plant Cell Environ.* 37, 2754–2767. doi: 10.1111/pce.12384
- Schulz, E., Tohge, T., Zuther, E., Fernie, A. R., and Hinch, D. K. (2015). Natural variation in flavonol and anthocyanin metabolism during cold acclimation in *Arabidopsis thaliana* accessions. *Plant Cell Environ.* 38, 1658–1672. doi: 10.1111/pce.12518
- Sebastián, R., Ximena, N., and Pérez, F. J. (2018). Absciscic acid (ABA) and low temperatures synergistically increase the expression of CBF/DREB1 transcription factors and cold-hardiness in grapevine dormant buds. *Ann. Bot. London* 123, 681–689. doi: 10.1093/aob/mcy201
- Singh, A. K., Dhanapal, S., and Yadav, B. S. (2020). The dynamic responses of plant physiology and metabolism during environmental stress progression. *Mol. Biol. Rep.* 47, 1459–1470. doi: 10.1007/s11033-019-05198-4
- Stockinger, E. J., Gilmour, S. J., and Thomashow, M. F. (1997). *Arabidopsis thaliana* CBF1 encodes an AP2 domain-containing transcriptional activator that binds to the C-repeat/DRE, a cis-acting DNA regulatory element that stimulates transcription in response to low temperature and water deficit. *Proc. Natl. Acad. Sci. U.S.A.* 94, 1035–1040. doi: 10.1073/pnas.94.3.1035
- Sun, S., Qi, X., Wang, R., Lin, M., and Fang, J. (2020). Evaluation of freezing tolerance in *Actinidia* germplasm based on relative electrolyte leakage. *Hortic. Environ. Biotechnol.* 61, 755–765. doi: 10.1007/s13580-020-00272-4
- Thalman, M., and Santelia, D. (2017). Starch as a determinant of plant fitness under abiotic stress. *New Phytol.* 214, 943–951. doi: 10.1111/nph.14491
- Wang, Y., Xin, H., Fan, P., Zhang, J., Liu, Y., Dong, Y., et al. (2021). The genome of *Shanputao* (*Vitis amurensis*) provides a new insight into cold tolerance of grapevine. *Plant J.* 105, 1495–1506. doi: 10.1111/tj.15127
- Wanqian, F., Jing, L., Sixin, L., and Shanjun, W. (2018). A DREB1 gene from zoysiagrass enhances *Arabidopsis* tolerance to temperature stresses without growth inhibition. *Plant Sci.* 278, 20–31. doi: 10.1016/j.plantsci.2018.10.009
- Wei, L., Sun, X., Qi, X., Zhang, Y., and Xu, Y. (2019). Dihydromyricetin ameliorates cardiac ischemia/reperfusion injury through Sirt3 activation. *BioMed. Res. Int.* 2019, 1–9. doi: 10.1155/2019/6803943
- Xiaoming, S., Langlang, Z., Darren, C., Jan, W., and Yi, W. (2019). The ethylene response factor VaERF092 from Amur grape regulates the transcription factor VaWRKY33, improving cold tolerance. *Plant J.* 99, 988–1002. doi: 10.1111/tj.14378
- Xie, Y., and Chen, P. (2018). An atypical R2R3 MYB transcription factor increases cold hardiness by CBF-dependent and CBF-independent pathways in apple. *New Phytol.* 218, 1–18. doi: 10.1111/nph.14952
- Yang, M., Yang, J., Su, L., Sun, K., and Guo, T. (2019). Metabolic profile analysis and identification of key metabolites during rice seed germination under low-temperature stress. *Plant Sci.* 289:110282. doi: 10.1016/j.plantsci.2019.110282
- Yao, L., Hao, X., Cao, H., Ding, C., Yang, Y., Wang, L., et al. (2020). ABA-dependent bZIP transcription factor, CsbZIP18, from *Camellia sinensis* negatively regulates freezing tolerance in *Arabidopsis*. *Plant Cell Rep.* 39, 553–565. doi: 10.1007/s00299-020-02512-4
- Yukuo, L., Jinbao, F., Xiujuan, Q., Miaomiao, L., Yunpeng, Z., Leiming, S., et al. (2018). Combined analysis of the fruit metabolome and transcriptome reveals candidate genes involved in flavonoid biosynthesis in *Actinidia arguta*. *Int. J. Mol. Sci.* 19:1471. doi: 10.3390/ijms19051471
- Zhang, R. F., Guo, Y., Li, Y. Y., Zhou, L. J., Hao, Y. J., and You, C. X. (2016). Functional identification of MdSIZ1 as a SUMO E3 ligase in apple. *J. Plant Physiol.* 198, 69–80. doi: 10.1016/j.jplph.2016.04.007
- Zhang, Z., Zhu, L., Song, A., Wang, H., Chen, S., Jiang, J., et al. (2020). *Chrysanthemum* (*Chrysanthemum morifolium*) CmICE2 conferred freezing tolerance in *Arabidopsis*. *Plant Physiol. Bioch.* 146, 31–41. doi: 10.1016/j.plaphy.2019.10.041
- Zhao, L., Yang, T., Xing, C., Dong, H., and Huang, X. (2019). The β -amylase PbrBAM3 from pear (*Pyrus betulaefolia*) regulates soluble sugar accumulation and ROS homeostasis in response to cold stress. *Plant Sci.* 287:110184. doi: 10.1016/j.plantsci.2019.110184
- Zhao, Y., Wang, Z. X., Yang, Y. M., Liu, H. S., Shi, G. L., and Ai, J. (2020). Analysis of the cold tolerance and physiological response differences of amur grape (*Vitis amurensis*) germplasm during overwintering. *Sci. Hortic.* 259, 1–9. doi: 10.1016/j.scienta.2019.108760

Conflict of Interest: The authors declare that the research was conducted in the absence of any commercial or financial relationships that could be construed as a potential conflict of interest.

Copyright © 2021 Sun, Fang, Lin, Hu, Qi, Chen, Zhong, Muhammad, Li and Li. This is an open-access article distributed under the terms of the Creative Commons Attribution License (CC BY). The use, distribution or reproduction in other forums is permitted, provided the original author(s) and the copyright owner(s) are credited and that the original publication in this journal is cited, in accordance with accepted academic practice. No use, distribution or reproduction is permitted which does not comply with these terms.



OPEN ACCESS

Edited by:

Rosalyn B. Angeles-Shim,
Texas Tech University, United States

Reviewed by:

Ertugrul Filiz,
Duzce University, Turkey
Rakesh K. Upadhyay,
United States Department of
Agriculture (USDA), United States
Yushi Luan,
Dalian University of Technology, China
Suhas Karkute,
Indian Council of Agricultural Research
(ICAR), India

*Correspondence:

Feng Wang
fengwang@syau.edu.cn
orcid.org/0000-0001-5351-1531
Tianlai Li
tianlaili@126.com

[†]These authors have contributed
equally to this work

Specialty section:

This article was submitted to
Plant Abiotic Stress,
a section of the journal
Frontiers in Plant Science

Received: 21 April 2021

Accepted: 28 May 2021

Published: 05 July 2021

Citation:

Bu X, Wang X, Yan J, Zhang Y,
Zhou S, Sun X, Yang Y, Ahammed GJ,
Liu Y, Qi M, Wang F and Li T (2021)
Genome-Wide Characterization of
B-Box Gene Family and Its Roles in
Responses to Light Quality and Cold
Stress in Tomato.
Front. Plant Sci. 12:698525.
doi: 10.3389/fpls.2021.698525

Genome-Wide Characterization of B-Box Gene Family and Its Roles in Responses to Light Quality and Cold Stress in Tomato

Xin Bu^{1,2,3†}, Xiujie Wang¹, Jiarong Yan¹, Ying Zhang¹, Shunyuan Zhou¹, Xin Sun⁴, Youxin Yang⁵, Golam Jalal Ahammed⁶, Yufeng Liu^{1,2,3}, Mingfang Qi^{1,2,3}, Feng Wang^{1,2,3†} and Tianlai Li^{1,2,3*}

¹ College of Horticulture, Shenyang Agricultural University, Shenyang, China, ² Key Laboratory of Protected Horticulture, Ministry of Education, Shenyang, China, ³ National & Local Joint Engineering Research Center of Northern Horticultural Facilities Design & Application Technology, Shenyang, China, ⁴ College of Land and Environment, Shenyang Agricultural University, Shenyang, China, ⁵ College of Agronomy, Jiangxi Agricultural University, Nanchang, China, ⁶ College of Forestry, Henan University of Science and Technology, Luoyang, China

Perceiving incoming environmental information is critical for optimizing plant growth and development. Multiple B-box proteins (BBXs) play essential roles in light-dependent developmental processes in plants. However, whether BBXs function as a signal integrator between light and temperature in tomato plants remains elusive. In this study, 31 *SIBBX* genes were identified from the newly released tomato (*Solanum lycopersicum*) genome sequences and were clustered into five subgroups. Gene structure and protein motif analyses showed relatively high conservation of closely clustered *SIBBX* genes within each subgroup; however, genome mapping analysis indicated the uneven distribution of the *SIBBX* genes on tomato chromosomes. Promoter *cis*-regulatory elements prediction and gene expression indicated that *SIBBX* genes were highly responsive to light, hormones, and stress conditions. Reverse genetic approaches revealed that disruption of *SIBBX7*, *SIBBX9*, and *SIBBX20* largely suppressed the cold tolerance of tomato plants. Furthermore, the impairment of *SIBBX7*, *SIBBX9*, and *SIBBX20* suppressed the photosynthetic response immediately after cold stress. Due to the impairment of non-photochemical quenching (NPQ), the excess photon energy and electron flow excited by low temperature were not consumed in *SIBBX7*-, *SIBBX9*-, and *SIBBX20*- silenced plants, leading to the over reduction of electron carriers and damage of the photosystem. Our study emphasized the positive roles of light signaling transcription factors *SIBBXs* in cold tolerance in tomato plants, which may improve the current understanding of how plants integrate light and temperature signals to adapt to adverse environments.

Keywords: BBX, light, cold stress, *Solanum lycopersicum*, photoinhibition

HIGHLIGHT

- SIBBXs function as a signal integrator between light and temperature in tomato.

INTRODUCTION

The B-box (BBX) proteins represent a unique class of zinc-finger transcription factors (TFs) that possess single or double B-box domains in their N termini and a CCT (CO, CO-like, and TOC1) domain in their C termini in some cases (Gangappa and Botto, 2014). The B-box domains are of two classes, and each of them coordinates two zinc atoms (Khanna et al., 2009). The dissimilarities in the consensus sequences of the two B-box domains are the results of evolution through the segmental duplication and deletion events (Crocco and Botto, 2013). Studies suggest that the highly conserved CCT domain is important for transcriptional regulation and nuclear transport (Gendron et al., 2012). Furthermore, the valine-proline (VP) motif of six amino acids (G-I/V-V-P-S/T-F) contained by some BBX proteins, plays a crucial role in the interaction with CONSTITUTIVELY PHOTOMORPHOGENIC 1 (COP1) (Holm et al., 2001; Datta et al., 2006). Based on the domain structures, 32 BBX proteins are divided into five subfamilies in Arabidopsis (Crocco and Botto, 2013; Gangappa and Botto, 2014).

A variety of wavelength-specific photoreceptors are involved in perceiving the light signals in plants, including phytochromes (phys), cryptochromes (CRYs), phototropins (PHOTs), ZEITLUPE family members, and UV-B resistance locus 8 (UVR8) (Galvao and Fankhauser, 2015; Paik and Huq, 2019). Light-activated photoreceptors inhibit the COP1-SUPPRESSOR OF PHYA-105 (SPA) E3 ubiquitin ligase complex, which functions for the degradation of the positive regulators of photomorphogenesis (Galvao and Fankhauser, 2015; Paik and Huq, 2019). Notably, HY5, a target of COP1-mediated protein degradation, plays a vital role in light-regulated plant growth and development (Osterlund et al., 2000; Ahammed et al., 2020). Thus, the light-dependent regulation of COP1-HY5 mediates the plant developmental transition from dark to light.

Upon light irradiation, BBX21 directly binds to *BBX22*, *HY5* and its own promoter regions and activates its transcription (Xu et al., 2016, 2018; Xu, 2020). Moreover, both BBX21 and HY5 can associate with the *BBX11* promoter to promote its transcription, while BBX11 binds to the *HY5* promoter to activate its transcription (Zhao et al., 2020). Thus, these three TFs (BBX21, HY5, and BBX11) form a positive feedback loop that precisely regulates plant photomorphogenesis. OsBBX14 induces *OsHY5L1* gene expression to stimulate photomorphogenesis in rice (Bai et al., 2019). MdBBX37 associates with *MdHY5* promoter to inhibit its expression in apple (An et al., 2019a). Additionally, MdBBX22 and MdBBX25/MdCOL4 bind to the *MdHY5* promoter to increase and decrease the transcriptional activation of *MdHY5*, respectively (An et al., 2019b). Both PpBBX16 and PpBBX18 interact with PpHY5 to increase the biochemical activity of PpHY5, while PpHY5 binds to the promoter region of *PpBBX18* to promote the transcription of *PpBBX18* in pear (Bai et al., 2019a,b). Furthermore, the

interaction of PpBBX21 with PpHY5 and PpBBX18 affects the bioactive heterodimer formation of PpHY5-PpBBX18 (Bai et al., 2019b). Tomato RIPENING INHIBITOR (SIRIN) binds to the ripening-induced *SIBBXs* (i.e., *SIBBX19*, *SIBBX20*, and *SIBBX26*) promoter (Lira et al., 2020). *SIBBX20* modulates carotenoid biosynthesis by directly activating *PHYTOENE SYNTHASE 1*, and is targeted for 26S proteasome-mediated degradation in tomato (Xiong et al., 2019). Therefore, specific BBXs and HY5 constitute an important regulatory network to precisely control normal plant growth and development.

In the darkness, CO/BBX1, BBX4, BBX10, BBX19, BBX20, BBX21, BBX22, BBX23, BBX24, BBX25, BBX28, and BBX29 are ubiquitinated by COP1 and subsequently degraded by the 26S proteasome system (Fan et al., 2012; Gangappa et al., 2013; Wang et al., 2015; Xu et al., 2016; Zhang et al., 2017; Lin et al., 2018; Ordoñez-Herrera et al., 2018; Heng et al., 2019a; Song et al., 2020). Moreover, BBX2 to 9 and BBX13 to 16 interacts with COP1 *in vitro*, indicating a role for COP1 in controlling the stability of these proteins in darkness (Ordoñez-Herrera et al., 2018). Nevertheless, COP1 preferentially stabilizes BBX11 instead of promoting its degradation (Zhao et al., 2020), which suggests that COP1 likely regulates a yet unidentified protein degrading BBX11. These studies suggest that numerous BBX proteins, along with COP1 and HY5, play critical roles in light-dependent development in plants.

BBX proteins also play vital roles in regulatory networks that control plant adaption to abiotic stress. Previous studies show that both BBX5 and BBX21 positively regulate plant tolerance to drought and salt stress in Arabidopsis (Nagaoka and Takano, 2003; Min et al., 2015). BBX24/STO directly interacts with H-protein promoter binding factor 1 (HPPBF-1), which is a salt-responsive MYB transcription factor, to enhance the root growth and salt tolerance in Arabidopsis (Nagaoka and Takano, 2003). CmBBX22 also positively regulates the plant drought tolerance (Liu Y. N. et al., 2019). In addition, MdBBX10 enhances tolerance to salt and drought by modulating ABA signaling and ROS accumulation (Liu X. et al., 2019). In Arabidopsis, BBX18 and BBX23 control thermomorphogenesis (Ding et al., 2018). Both *MdBBX20* and *MaCOL1* are responsive to low temperature in apple and banana, respectively (Chen et al., 2012; Fang et al., 2019). Furthermore, *ZFPL*, a homologous gene of *AtBBX32*, enhances cold tolerance in the grapevine (Takuhara et al., 2011). *CmBBX24* also increases plant cold tolerance in *Chrysanthemum* (Yang et al., 2014). However, whether SIBBXs are involved in light and cold response in tomato remains to be explored.

In the present study, 31 *SIBBX* genes were identified and characterized in tomato. Gene distribution, synteny analyses, the architecture of exon-intron and motifs differences were investigated. Promoter and gene expression analysis showed that *SIBBXs* played important roles in plant response to light and low temperature signaling. Meanwhile, we found that the impairment of *SIBBX7*, *SIBBX9*, and *SIBBX20* suppressed the photosynthetic response and non-photochemical quenching (NPQ) immediately after cold stress, which resulted in excess photon energy and electron flow in *SIBBX7*-, *SIBBX9*-, and *SIBBX20*- silenced plants, leading to the overreduction of electron carriers and damage of photosystem. Our study indicated that light signaling

transcription factors *SIBBX7*-, *SIBBX9*-, and *SIBBX20*- play positive roles in cold tolerance in tomato plants, which may improve the current understanding of plant integrated light and temperature signals to adapt the adverse environments.

MATERIALS AND METHODS

Genome-Wide Identification of *SIBBX* Genes in Tomato

The BBXs proteins in tomato were identified based on protein homology searches from Arabidopsis using the Hidden Markov Model (HMM) as previously described (Upadhyay and Mattoo, 2018). The protein sequence of Arabidopsis BBXs were downloaded from the TAIR database (<https://www.arabidopsis.org/>). Tomato BBX proteins were searched and downloaded from three public databases, including the NCBI database (<http://www.ncbi.nlm.nih.gov/>), the Phytozome 13.0 database (<https://phytozome.jgi.doe.gov/pz/portal.html>), and the Sol Genomics Network tomato database (version ITAG 4.0, <https://solgenomics.net/>). Tomato BBX proteins resulting from both searches (E-value, 10^{-5}) were pooled and redundant sequences were removed. InterProScan database (<http://www.ebi.ac.uk/interpro/>), SMART (<http://smart.embl-heidelberg.de/>), and Conserved Domains Database (<http://www.ncbi.nlm.nih.gov/cdd/>) were used to further confirm the existence of B-box domain in retrieved BBX sequences.

Protein Properties, Multiple Sequence Alignment, Phylogenetic, and Conserved Motifs Analysis

The various physiochemical properties of tomato BBX proteins, such as MW, polypeptide length, pI, instability index, aliphatic index, and GRAVY were investigated using the ExPASy online tool (<http://web.expasy.org/protparam/>). To estimate the subcellular localization of tomato BBX proteins, we used CELLO v.2.5: sub-cellular localization predictor (<http://cello.life.nctu.edu.tw/>) (Yu et al., 2006) and pSORT prediction software (<http://www.genscript.com/wolf-psort.html>) (Horton et al., 2007). Open Reading Frame (ORF) numbers were calculated using the NCBI website (<https://www.ncbi.nlm.nih.gov/orffinder/>).

A multiple sequence alignment of the identified tomato BBX proteins and the known BBX families from Arabidopsis, rice, and potato, was performed with the MUSCLE (<https://www.ebi.ac.uk/Tools/msa/muscle/>) (Edgar, 2004) and DNAMAN software (Version 5.2.2). We constructed phylogenetic tree using MEGA 7.0 with 1,000 bootstrap value and the maximum likelihood method (Kumar et al., 2016), and the phylogenetic tree was displayed with an online website Evolview (<http://www.evolgenius.info/evolview/#mytrees/>) (Zhang et al., 2012).

The presence of conserved BBX_N and CCT_C—domains were identified by NCBI (<https://www.ncbi.nlm.nih.gov/Structure/cdd/wrpsb.cgi>), and drawn with IBS software (Illustrator for Biological Sequences, <http://ibs.biocuckoo.org/online.php>) (Ren et al., 2009). We performed the protein structural motif annotation using the Meme program ([\[meme-suite.org/tools/meme\]\(http://meme-suite.org/tools/meme\)\) \(Bailey et al., 2009; Upadhyay and Mattoo, 2018\) and limited our search to a maximum of 20 motifs.](http://</p>
</div>
<div data-bbox=)

Chromosomal Location, Gene Structure, and Synteny Analysis

SIBBX genes were mapped to tomato chromosomes according to the Phytozome 13.0 database with the MapChart software. The chromosome distribution diagram was drawn by the online website MG2C (http://mg2c.iask.in/mg2c_v2.1/) with the information from Sol Genomics Network (<http://www.solgenomics.net/>).

Genomic DNA sequence and CDS corresponding to each identified *SIBBX* gene were retrieved from the tomato genome database. Intron-exon were displayed by comparing CDS to genomic sequences with the gene structure display server (GSDS, <http://gsds.cbi.pku.edu.cn/>) (Hu et al., 2015).

The syntenic blocks were designed from the Plant Genome Duplication Database (<http://chibba.agtec.uga.edu/duplication/>). The synteny figures were drawn by Circos-0.69 (<http://circos.ca/>) with E-value setting to $1e^{-10}$ and output format as tabular (-m 8).

Cis-Elements of Promoters Analysis

To identify potential light-, stress-, hormone-, and development-related *cis*-elements, the 2,000-bp genomic DNA sequence upstream of the start codon (ATG) of *SIBBX* genes were obtained from the tomato genome database. The *cis*-elements in these *SIBBX* genes promoter were identified by using the Plant Cis-Acting Regulatory Element (PlantCARE; <http://bioinformatics.psb.ugent.be/webtools/plantcare/html/>) (Lescot et al., 2002).

Plant Material and Growth Conditions

Seeds of tomato (*Solanum lycopersicum*) in the cv “Ailsa Craig” (Accession: LA2838A) background were obtained from the Tomato Genetics Resource Center (<http://tgrc.ucdavis.edu>) as previously reported (Wang et al., 2016). Seedlings, which grown in pots with a mixture of one part vermiculite to three parts peat, receive Hoagland nutrient solution. The growth conditions for tomato seedlings were 25/20°C (day/night) temperature with a 12 h photoperiod, light intensity of $600 \mu\text{mol m}^{-2} \text{s}^{-1}$, and 65% relative humidity. Tobacco rattle virus-based vectors (pTRV1/2) were used for the VIGS of *SIBBX* genes in tomato with the specific PCR-amplified primers listed in **Supplementary Table 3**. The PCR-amplified fragment was cloned into the pTRV2 vector. The empty vector of pTRV2 was used as the control. All constructs were confirmed by sequencing and subsequently transformed into *Agrobacterium tumefaciens* strain GV3101. VIGS was performed as described previously (Wang et al., 2016, 2019). The inoculated plants were grown under a 12 h photoperiod at 22/20°C (day/night).

Light and Cold Treatments

The six-leaf stage plants were used for all experiments. Plants grown under white light were exposed to a temperature of 25 or 4°C for the control or cold treatment, respectively, in environment-controlled growth chambers (Ningbo Jiangnan instrument factory, Ningbo, China). For different light quality treatments, plants were exposed to dark (D), white light (W),

or different wavelength [purple (P), 394 nm; blue (B), 450 nm; green (G), 522 nm; yellow (Y), 594 nm; red (R), 660 nm and far-red (FR), 735 nm, Philips] light from 6:00 a.m. to 6:00 p.m.. The light intensity was $100 \mu\text{mol m}^{-2} \text{s}^{-1}$. The Lighting Passport (Asensetek, Model No. ALP-01, Taiwan) was used to measure light intensity and light quality as a previous study (Wang et al., 2020b).

Gene Expression Analysis

Total RNA was extracted from tomato leaves as described previously (Wang et al., 2020a). The cDNA template for real-time qRT-PCR was synthesized using a Rever-Tra Ace qPCR RT Kit with a genomic DNA-removing enzyme (Toyobo). qRT-PCR experiments were carried out with an SYBR Green PCR Master Mix Kit (TaKaRa) using an Applied Biosystems 7500 Real-Time PCR System (qTOWER³G, Germany). The primer sequences are listed in **Supplementary Table 2**. The PCR was run at 95°C for 3 min, followed by 40 cycles of 30 s at 95°C, 30 s at 58°C, and 1 min at 72°C. The tomato *ACTIN* gene was used as an internal control. The relative gene expression was calculated as described previously (Livak and Schmittgen, 2001).

Cold Tolerance Assays

The relative electrolyte leakage (REL), an indicator for cellular membrane permeability, was measured as described previously (Cao et al., 2007). Chlorophyll fluorescence and P700 absorption changes were determined simultaneously using a DUAL-PAM-100 (Heinz Walz, Effeltrich, Germany) as previously described (Wang et al., 2020b). Before measurements, plants were dark-acclimated for 30 min. PSII and PSI parameters were calculated as follows: the maximum quantum yield of PSII (F_v/F_m) as (F_m - F_o)/F_m, the effective quantum yield of PSII [Y(II)] as (F_m' - F_s)/F_m', the quantum yield of non-regulated energy dissipation of PSII [Y(NO)] as F_s/F_m, the quantum yield of regulated energy dissipation of PSII [Y(NPQ)] as 1 - Y(II) - Y(NO), NPQ as (F_m - F_m')/F_m', photochemical quenching coefficient (qP) as (F_m' - F_s)/(F_m' - F_o'), the donor limitation of PSI [Y(ND)] as 1 - P700red, or P/P_m, the acceptor side limitation of PSI [Y(NA)] as (P_m - P_m')/P_m, the quantum yield of PSI [Y(I)] as 1 - Y(ND) - Y(NA), where F_m and F_o represent the maximum and minimum fluoresce yields, whereas P_m and P_m' represent the P700 signals recorded just before (P) then briefly after the onset of a saturating pulse (P_m'). P700red, which represents the fraction of overall P700 that is reduced in a given state, was determined with the help of a saturation pulse. The electron transport rate (ETRI or ETRII) was calculated as $0.5 \times \text{abs I} \times Y(\text{I})$ or $0.5 \times \text{abs I} \times Y(\text{II})$, where 0.5 is the proportion of absorbed light reaching PSI or PSII, and abs I is absorbed irradiance taken as 0.84 of incident irradiance (Wang et al., 2020b).

Statistical Analysis

All statistics were calculated using SPSS software. To determine statistical significance, we employed Tukey's test. A value of $P < 0.05$ was considered to indicate statistical significance.

RESULTS

Identification and Characterization of SIBBX Genes in Tomato

Based on the gene annotation as well as the conserved B-box motif characteristic of the BBX members, a total of 31 *SIBBX* genes were identified. The detailed information of each *SIBBX* is presented in **Table 1**. The lengths of amino acids (AA) of 31 *SIBBX*s range from 88 aa (*SIBBX18*) to 475 aa (*SIBBX27*). Thus, varied molecular weight (MW) and theoretical isoelectric point (pI) were observed among *SIBBX* proteins. The MW of *SIBBX*s varies from 9.57 (*SIBBX18*) to 53.14 kDa (*SIBBX27*). The pI ranged from 4.25 (*SIBBX5* and *SIBBX7*) to 9.28 (*SIBBX26*), with 74.2% *SIBBX*s with a pI lower than seven, which indicated that most of the *SIBBX* proteins were acidic in nature. The pI ranged from 4 to 9 in *SIBBX* proteins contained one (single) or two (double) B-box domains; however, the pI ranged from 4 to 7 when *SIBBX* proteins contained a CCT domain (**Supplementary Figure 1**), suggesting that the CCT domain in *SIBBX* proteins may decrease its pI. The majority of *SIBBX*s were grouped into unstable proteins because their instability index was greater than 40, except for *SIBBX6* in this family (**Table 1**). The predicted aliphatic index ranged from 50.05 to 97.43 in *SIBBX* proteins. All *SIBBX* proteins, with the exception of *SIBBX18*, were predicted to be hydrophilic due to the GRAVY value (<0). Subcellular localization predicted that 23 *SIBBX* proteins are located in nuclei. Among the rest 8 tomato BBXs, five (*SIBBX5*, *SIBBX6*, *SIBBX17*, *SIBBX25*, and *SIBBX31*), two (*SIBBX16* and *SIBBX18*), and one (*SIBBX19*) *SIBBX* proteins are located in chloroplast, cytoplasm, and peroxisome, respectively (**Table 1**).

Protein Sequences and Phylogenetic Analysis of SIBBXs

The domains logos and the sequences of the B-box1, B-box2, and CCT domain of the *SIBBX* proteins are shown in **Figure 1**. Eight members out of the 31 *SIBBX*s, were characterized by the occurrence of two B-box domains and also a conserved CCT domain, whereas four members of them had a valine-proline (VP) motif (**Table 2**). Only two B-box domains were found in 10 *SIBBX*s, whereas five members had one B-box domain and also a CCT domain, and eight members had only one B-box domain (**Table 2**). Among the three domains, we found that each tomato B-box motif contained ~40 residues with the consensus sequence C-X2-C-X8-C-X2-D-X4-C-X2-C-D-X3-H-X8-H (**Figure 1**). The conserved C, C, D, and H residues ligated two zinc ions (Khanna et al., 2009). Additionally, the consensus sequence of the conserved CCT domain was R-X5-R-Y-X-E-K-X3-R-X3-K-X2-R-Y-X2-R-K-X2-A-X2-R-X-R-X-K-G-R-F-X-K (**Figure 1**).

To better reveal the evolutionary relationships, we generated a phylogenetic tree with the known BBX families from Arabidopsis, rice and potato, and the identified tomato BBX protein sequences (**Figure 2**, **Supplementary Figure 2**). All sequences of tomato BBX proteins were clustered into five subfamilies (**Figure 2**). The *BBX* genes in group 1 had two concatenated B-box domains, a CCT domain and a VP motif except for *SIBBX1* and *SIBBX2*, which did not have a VP motif and a CCT domain. The members of group 2 were characterized by two B-box domains and also a

TABLE 1 | Nomenclature, identification, chromosomal location, theoretical isoelectric point (pI), molecular weight (MW), CDS, peptide length, number of exon and intron, instability and aliphatic index, gravy and subcellular localization of BBX gene family in tomato.

Name	Gene locus ID	pI	MW(kDa)	AA	Exon	Intron	Instability index	Aliphatic index	Gravy	Subcellular Localization
SIBBX1	Solyc02g089520	4.89	45.69	409	3	2	41.8	66.06	−0.630	nucl: 14
SIBBX2	Solyc02g089500	8.16	15.18	142	2	1	72.59	70.92	−0.015	nucl: 6, mito: 5, chlo: 1, cyto: 1, extr: 1
SIBBX3	Solyc02g089540	5.76	43.44	391	3	2	41.06	64.14	−0.625	nucl: 10, chlo: 2, cyto: 1, cysk: 1
SIBBX4	Solyc08g006530	5.15	38.66	349	3	2	51.34	63.75	−0.602	nucl: 8, chlo: 3, cyto: 3
SIBBX5	Solyc12g096500	4.25	29.71	358	3	2	48.52	62.96	−0.503	chlo: 10, nucl: 3, cyto: 1
SIBBX6	Solyc07g006630	6.82	42.61	386	2	1	38.63	71.04	−0.364	chlo: 7, cyto: 4, nucl: 1, mito: 1, extr: 1
SIBBX7	Solyc12g006240	4.25	29.71	269	3	2	49.44	66.90	−0.604	nucl: 8, extr: 3, chlo: 2, cyto: 1
SIBBX8	Solyc05g020020	5.49	44.53	410	5	4	58.86	63.54	−0.482	nucl: 12, cyto: 2
SIBBX9	Solyc07g045180	5.32	46.14	418	5	4	55.69	57.85	−0.524	nucl: 14
SIBBX10	Solyc05g046040	4.73	46.27	416	4	3	53.21	65.66	−0.551	nucl: 12, cyto: 1, cysk: 1
SIBBX11	Solyc09g074560	6.16	42.23	373	4	3	51.28	61.93	−0.765	nucl: 10, cyto: 2, chlo: 1, vacu: 1
SIBBX12	Solyc05g024010	7.17	49.71	452	4	3	49.44	66.90	−0.604	nucl: 11, cyto: 1, extr: 1, vacu: 1
SIBBX13	Solyc04g007210	5.13	48.72	428	2	1	45.21	61.71	−0.774	nucl: 11, chlo: 1, mito: 1, cysk: 1
SIBBX14	Solyc03g119540	4.92	46.70	408	2	1	49.49	65.78	−0.767	nucl: 10, chlo: 3, mito: 1
SIBBX15	Solyc05g009310	5.54	49.82	437	2	1	40.72	68.47	−0.774	nucl: 6, mito: 3, chlo: 2, cyto: 2, cysk: 1
SIBBX16	Solyc12g005750	7.85	12.72	109	1	0	42.52	97.43	−0.037	cyto: 8, nucl: 3, mito: 1, cysk: 1, golg: 1
SIBBX17	Solyc07g052620	8.26	14.52	130	1	0	53.75	70.62	−0.370	chlo: 7, nucl: 3, cyto: 2, plas: 1, extr: 1
SIBBX18	Solyc02g084420	5.57	9.57	96	4	3	45.42	78.75	0.194	cyto: 11, chlo: 1, mito: 1, extr: 1
SIBBX19	Solyc01g110370	5.17	26.88	241	6	5	54.64	76.89	−0.447	pero: 9, cyto: 2.5, cyto_nucl: 2, chlo: 1, golg: 1
SIBBX20	Solyc12g089240	7.40	36.4	329	3	2	54.04	67.54	−0.491	nucl: 10, cyto: 2, chlo: 1, extr: 1
SIBBX21	Solyc04g081020	7.61	33.27	299	3	2	62.74	70.43	−0.472	nucl: 6, cyto: 4, extr: 2, chlo: 1, cysk: 1
SIBBX22	Solyc07g062160	4.61	32.07	298	3	2	57.90	68.09	−0.360	nucl: 12, cyto: 1, cysk: 1
SIBBX23	Solyc12g005420	6.23	30.64	282	3	2	54.04	69.22	−0.326	nucl: 10, chlo: 3, extr: 1
SIBBX24	Solyc06g073180	4.74	25.92	233	4	3	54.31	78.76	−0.391	nucl: 7, cyto: 2, cysk: 2, chlo: 1, plas: 1, extr: 1
SIBBX25	Solyc01g110180	5.96	22.62	203	3	2	48.29	68.28	−0.485	nucl: 10, chlo: 1, cyto: 1, extr: 1, vacu: 1
SIBBX26	Solyc10g006750	9.28	12.04	104	2	1	53.39	78.75	−0.180	nucl: 10.5, cyto_nucl: 6.5, extr: 2, cyto: 1.5
SIBBX27	Solyc04g007470	5.94	53.14	475	5	4	58.77	62.84	−0.661	nucl: 14
SIBBX28	Solyc12g005660	4.63	22.27	465	2	1	55.31	69.46	−0.552	chlo: 8, nucl: 2, cyto: 2, extr: 2
SIBBX29	Solyc02g079430	4.49	20.73	185	2	1	68.52	50.05	−1.034	nucl: 8, chlo: 2, mito: 2, cyto: 1, plas: 1
SIBBX30	Solyc06g063280	8.90	28.72	261	1	0	65.08	73.64	−0.268	nucl: 11, cyto: 2, extr: 1
SIBBX31	Solyc07g053140	4.31	28.19	257	2	1	63.17	52.80	−0.840	chlo: 7, nucl: 6, mito: 1

pI, theoretical isoelectric point; MW, molecular weight; CDS, length of coding sequence; AA, amino acid; gravity, grand average of hydropathicity; nucl, nucleus; mito, mitochondria; chlo, chloroplast; cyto, cytoplasm; extr, extracellular; cysk, cytoskeleton; vacu, vacuole; golg, golgi apparatus; pero, peroxisome; plas, plasma membrane.

CCT domain with the exception for SIBBX7 and SIBBX27, which contained two B-box domains only, and SIBBX8 and SIBBX10, which only had one B-box domain and a CCT domain. In group 3, all the members contained one B-box domain as well as a CCT domain. Group 4 and 5 possessed two and one B-box domain, respectively. Additionally, BBX proteins from two species showed scattered distribution across the branches of the evolutionary tree, which implies that the duplication events occurred after the lineages diverged.

Gene Structure, Conserved Motifs, Chromosomal Localization, and Synteny Analysis of SIBBXs

The evolution of multigene families can be driven by gene structural diversity. Examination of the genomic DNA

sequences revealed that most SIBBXs contained one to five introns, while SIBBX16, SIBBX17, and SIBBX30 had no introns (Figure 3B, Table 1, Supplementary Figure 3). Among them, nine SIBBXs had one intron, followed by 10 SIBBXs with two introns, five SIBBXs with three introns, three SIBBXs with four introns, and one SIBBXs with five introns. Generally, members of each subclass, which are most closely related, exhibited analogous exon-intron structures. For instance, the members in groups 1 and 4 had one to two, and zero to one intron, respectively (Figures 3A,B, Supplementary Figure 3). However, a few SIBBX genes showed dissimilar exon-intron arrangements. For instance, SIBBX18 and SIBBX19 had high sequence similarity, but SIBBX18 and SIBBX19 contained two and five introns, respectively (Figures 3A,B, Supplementary Figure 3). These divergences indicated that both the gain and loss of introns during

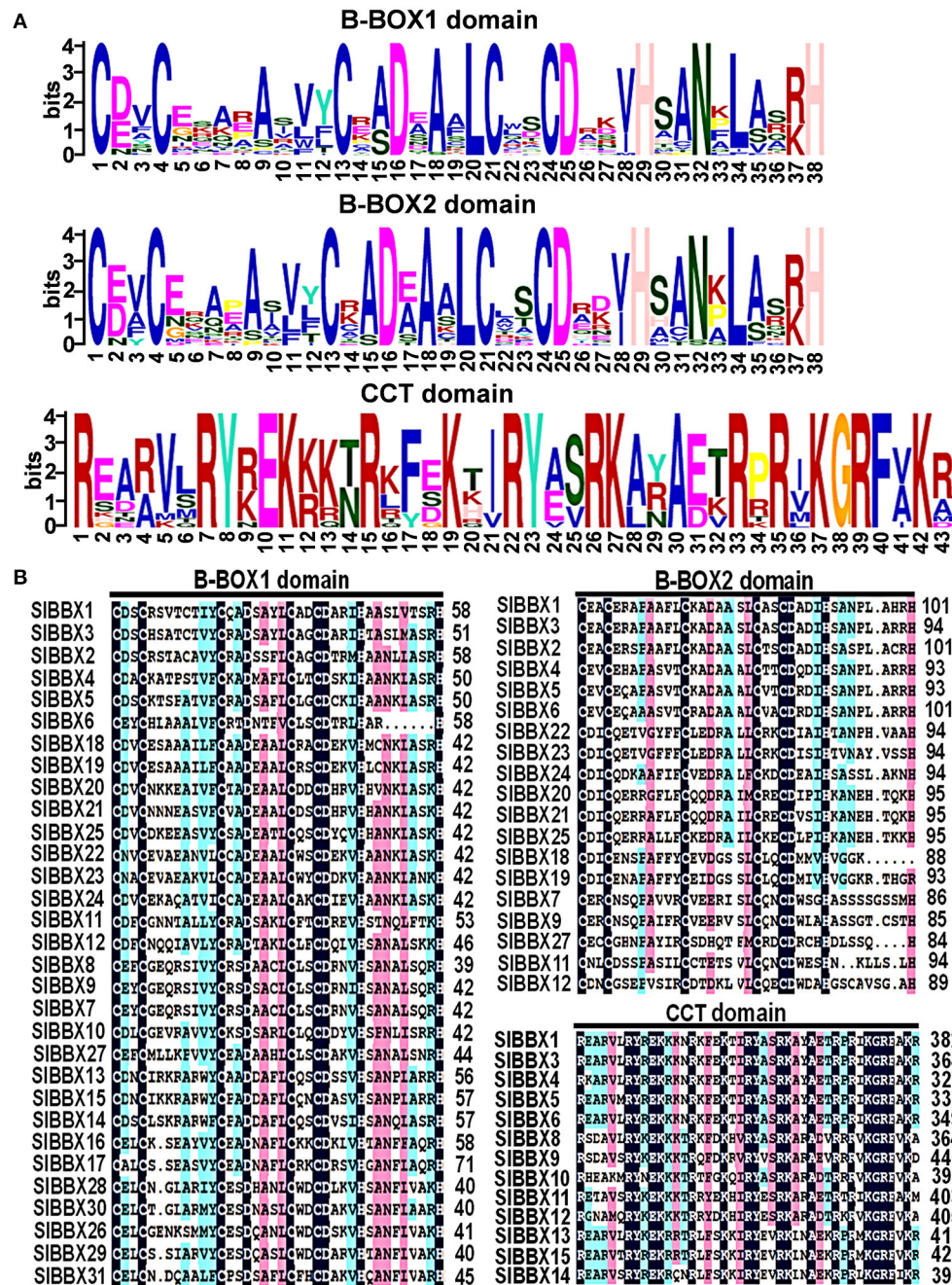


FIGURE 1 | Domain composition of SIBBX proteins. **(A)** The amino acid sequence alignment of the B-box1, B-box2, and CCT domain. The y-axis and x-axis indicated the conservation rate of each amino acid and the conserved sequences of the domain, respectively. **(B)** Multiple sequence alignments of the domains of the SIBBXs. Multiple sequence alignments of the B-box1, B-box2, and CCT domains are shown. The identical conserved amino acids were represented by black and pink shaded.

evolution, may better explain the functional diversity of *SIBBX* homologous genes.

To further examine the structural features of SIBBXs, the conserved motif distributions were analyzed. Twenty conserved motifs were predicted (Figure 3C), while multilevel consensus sequences and the E-value of them were shown in Supplementary Table 1. The results showed that motif 17



was the largest motif depending on the width, followed by motif 8 and motif 2 (Supplementary Table 1). Motif 1 was found in all the SIBBXs (Figure 3C). Notably, 74.2% and 70.1% SIBBXs contained motif 4 and motif 3, respectively. Motif 2 was unique to the group 1, 2, and 3 of SIBBXs, while motif 5 was unique to group 2 except for the SIBBX27. Motif 10 was found only in group 3 of SIBBXs. Our results showed

TABLE 2 | Structure of the tomato BBX proteins.

Name	Gene locus ID	AA(aa)	Domains	B-box1	B-box2	CCT	VP	Protein structure
SIBBX1	Solyc02g089520	409	2B-box+CCT	19–63	59–106	340–382		
SIBBX2	Solyc02g089500	142	2B-box	19–63	62–106			
SIBBX3	Solyc02g089540	391	2B-box+CCT	12–56	52–99	322–364	386–391	
SIBBX4	Solyc08g006530	349	2B-box+CCT	12–55	51–98	285–327	344–349	
SIBBX5	Solyc12g096500	358	2B-box+CCT	12–55	51–98	295–337	353–358	
SIBBX6	Solyc07g006630	386	2B-box+CCT	22–63	59–106	307–349	379–384	
SIBBX7	Solyc12g006240	269	2B-box	4–47	47–73			
SIBBX8	Solyc05g020020	410	1B-box+CCT	1–44		356–396		
SIBBX9	Solyc07g045180	418	2B-box+CCT	4–47	47–90	361–404		
SIBBX10	Solyc05g046040	419	1B-box+CCT	3–47		363–406		
SIBBX11	Solyc09g074560	373	2B-box+CCT	15–58	58–99	322–365		
SIBBX12	Solyc05g024010	452	2B-box+CCT	7–39	51–94	404–447		
SIBBX13	Solyc04g007210	428	1B-box+CCT	17–61		373–415		
SIBBX14	Solyc03g119540	408	1B-box+CCT	18–62		349–392		
SIBBX15	Solyc05g009310	437	1B-box+CCT	17–61		380–423		
SIBBX16	Solyc12g005750	110	1B-box	21–50				
SIBBX17	Solyc07g052620	130	1B-box	35–76				
SIBBX18	Solyc02g084420	88	2B-box	2–33	52–84			
SIBBX19	Solyc01g110370	241	2B-box	2–45	54–96			
SIBBX20	Solyc12g089240	329	2B-box	5–47	53–100			
SIBBX21	Solyc04g081020	299	2B-box	5–47	56–100			
SIBBX22	Solyc07g062160	311	2B-box	5–47	53–99			
SIBBX23	Solyc12g005420	282	2B-box	5–47	53–99			
SIBBX24	Solyc06g073180	233	2B-box	5–44	53–98			
SIBBX25	Solyc01g110180	203	2B-box	3–33	56–100			
SIBBX26	Solyc10g006750	104	1B-box	4–34				
SIBBX27	Solyc04g007470	475	2B-box	7–49	49–87			
SIBBX28	Solyc12g005660	202	1B-box	4–45				
SIBBX29	Solyc02g079430	185	1B-box	1–45				

(Continued)

TABLE 2 | Continued

Name	Gene locus ID	AA(aa)	Domains	B-box1	B-box2	CCT	VP	Protein structure
SIBBX30	Solyc06g063280	261	1B-box	4–50				
SIBBX31	Solyc07g053140	257	1B-box	4–45				

Numbers indicate the amino acid position of the corresponding conserved domains. The red, blue rectangles, purple circles, and gray rectangles indicate the B-box1, B-box2, CCT domain, and VP domain, respectively.

that members that are most closely related in the phylogenetic tree contained common motifs on the basis of alignment and position, which indicated that they may have a similar biological function.

Chromosomal locations showed that 31 *SIBBX* genes were unevenly distributed on the 12 chromosomes (**Figure 4A**). A maximum number of *SIBBX* genes were found on chromosome 12 (Chr12), comprising six genes. Five genes were located on Chr2 and Chr7. Four and three *SIBBX* genes were located on Chr5 and Chr4, respectively. Both Chr1 and Chr6 contained two members of *SIBBX* genes, whereas only one gene was detected on Chr3, 8, 9, and 10. Additionally, no *SIBBX* genes were found on Chr11.

Thirty-six pairs of *SIBBX*s were identified as segmental duplication in the tomato genome (**Figure 4B**). Chr2, 7, and 12 had more duplication regions, which partially explain the greater numbers of *SIBBX* genes that were located on these three chromosomes. Although *SIBBX1* and *SIBBX3* were located on the same chromosome (**Figure 4A**), and their sequence identity was 83% (**Supplementary Figure 4**), they were not tandem duplication. To further examine the evolutionary relationships between *SIBBX*s and *AtBBX*s, a synteny analysis was performed. A total of 16 of *SIBBX-AtBBX* orthologous pairs were identified (**Figure 4C**), which indicated the existence of numerous *SIBBX* genes prior to the divergence of Arabidopsis and tomato. Some members of *SIBBX*s were not localized in the syntenic block, suggesting that these genes might have certain specificity due to their evolution time.

Analysis of *cis*-Elements in the Promoter Region of *SIBBX*s

A total of 61 major *cis*-elements were predicted in promoters of *SIBBX* genes (**Figure 5A**), including 22 light responsive, 12 hormone responsive, 11 stress responsive, and 16 development. The number of light responsive *cis*-elements was the largest in the promoters of 31 *SIBBX* genes (**Figure 5B**). The number of *cis*-elements in the promoters of *SIBBX17* and *SIBBX2* was the largest and least, respectively. The major light responsive elements contained box4 (21%), G-box (17.9%), and CMA1a/2a/2b (14.3%), which were located on 87.1% (27/31), 83.9% (26/31), and 96.8% (30/31) of *SIBBX*s promoters, respectively (**Figure 5C**). The most common motifs were the JA-responsive elements (MYC), abscisic acid (ABA)-responsive element (ABRE), and ethylene-responsive element (ERE), accounting for 24.8%, 21.5%, and 17.2% of the scanned hormone responsive motifs,

respectively. The stress responsive elements MYB, STRE (stress-related elements) and WUN were located on 96.8% (30/31), 90.3% (28/31), and 77.4% (24/31) of 31 *SIBBX* genes promoters, respectively. In the development category, various growth and development related elements, such as AT-rich element (19.2%), O₂-site for zein metabolism regulation (13.7%), CAT-box for meristem expression (12.3%), GCN4_motif required for endosperm expression (9.6%), were found. Our findings suggest that the promoter regions of *SIBBX* genes that contained the *cis*-elements played a critical role in the light and stress responses.

SIBBX Genes Expression in Response to Different Light Quality

To assess whether light signaling regulates *SIBBX*s, we investigated the gene expression of *SIBBX*s in tomato plants grown at dark (D), white (W), and different light quality [purple (P), blue (B), green (G), yellow (Y), red (R), and far-red (FR)] conditions. In comparison with D, light decreased the transcripts of *SIBBX1*, *SIBBX8*, *SIBBX10*, and *SIBBX12*, while it increased the transcripts of *SIBBX7*, *SIBBX13*, and *SIBBX15* (**Figure 6**). Plants grown at R light conditions showed higher expression of *SIBBX4*, *SIBBX14*, *SIBBX23*, *SIBBX24*, and *SIBBX29* than those grown at other light qualities. Whereas, FR light significantly up-regulated the transcripts of *SIBBX7*, *SIBBX13*, *SIBBX15*, *SIBBX21*, *SIBBX25*, *SIBBX26*, and *SIBBX27*, it obviously down-regulated the transcripts of *SIBBX14*, *SIBBX16*, *SIBBX18*, *SIBBX24*, *SIBBX28*, *SIBBX30*, and *SIBBX31* (**Figure 6**). Transcripts of *SIBBX16*, *SIBBX17*, *SIBBX18*, *SIBBX30*, and *SIBBX31* were induced, while transcripts of *SIBBX5*, *SIBBX6*, *SIBBX19*, and *SIBBX20* were inhibited in plants when grown at B light conditions. *SIBBX15* was induced by G light irradiation at 6 h, whereas *SIBBX9* and *SIBBX28* were repressed (**Figure 6**). Y light led to an obvious reduction in expression of *SIBBX9* and *SIBBX31*. Obviously, the P light increased the expression of *SIBBX3*, *SIBBX5*, *SIBBX6*, *SIBBX15*, *SIBBX19*, *SIBBX20*, *SIBBX21*, *SIBBX26*, and *SIBBX27*, but decreased the expression of *SIBBX10* and *SIBBX16*. Interestingly, *SIBBX4*, *SIBBX23*, and *SIBBX29* were only responsive to R light, while *SIBBX7*, *SIBBX13*, and *SIBBX25* were induced just in response to FR light. Meanwhile, R light induced the expression of *SIBBX14* and *SIBBX24*, but FR light inhibited their expression (**Figure 6**). In general, the results showed that *SIBBX* genes might act a critical role in response to light quality signaling.

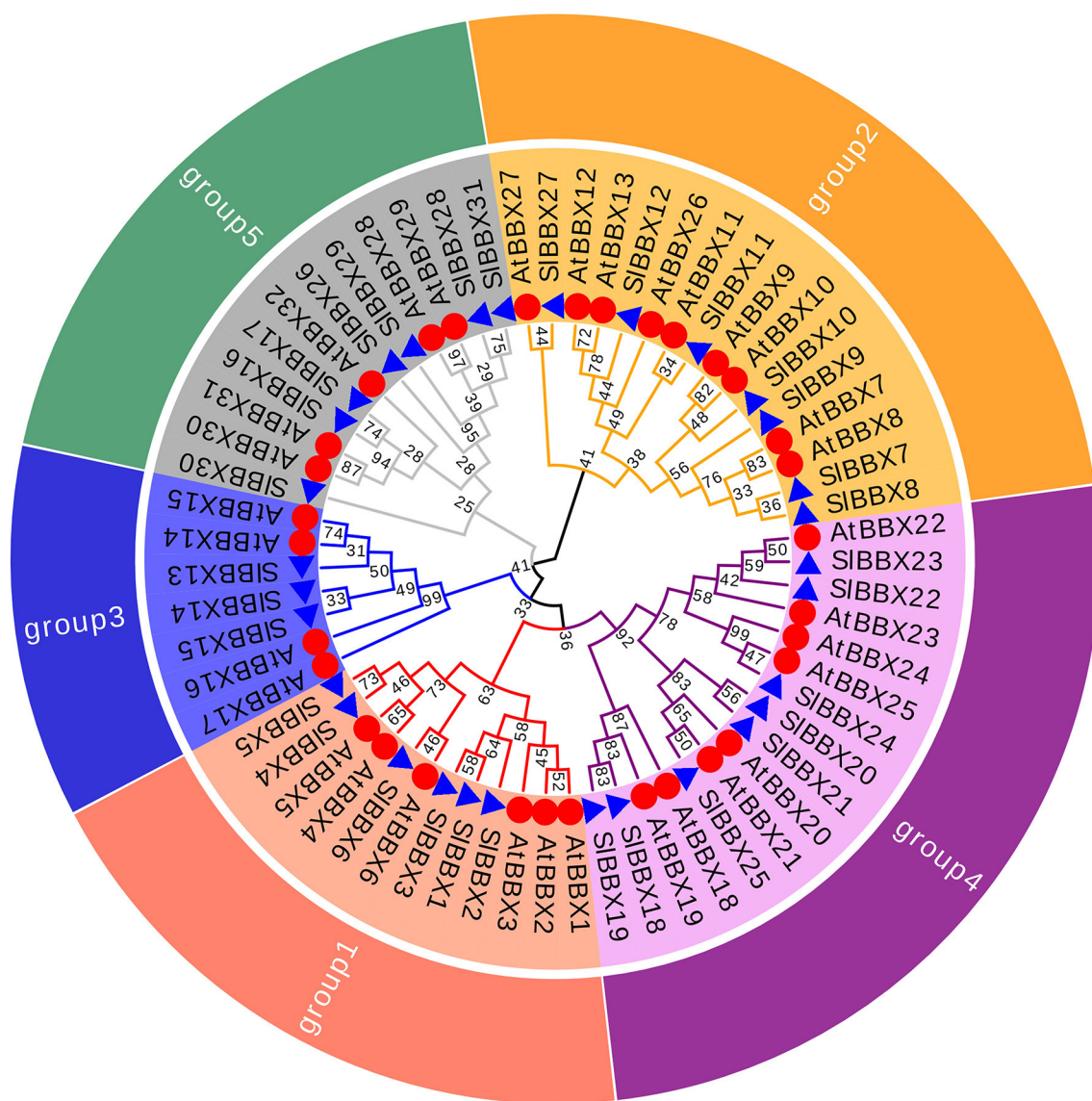
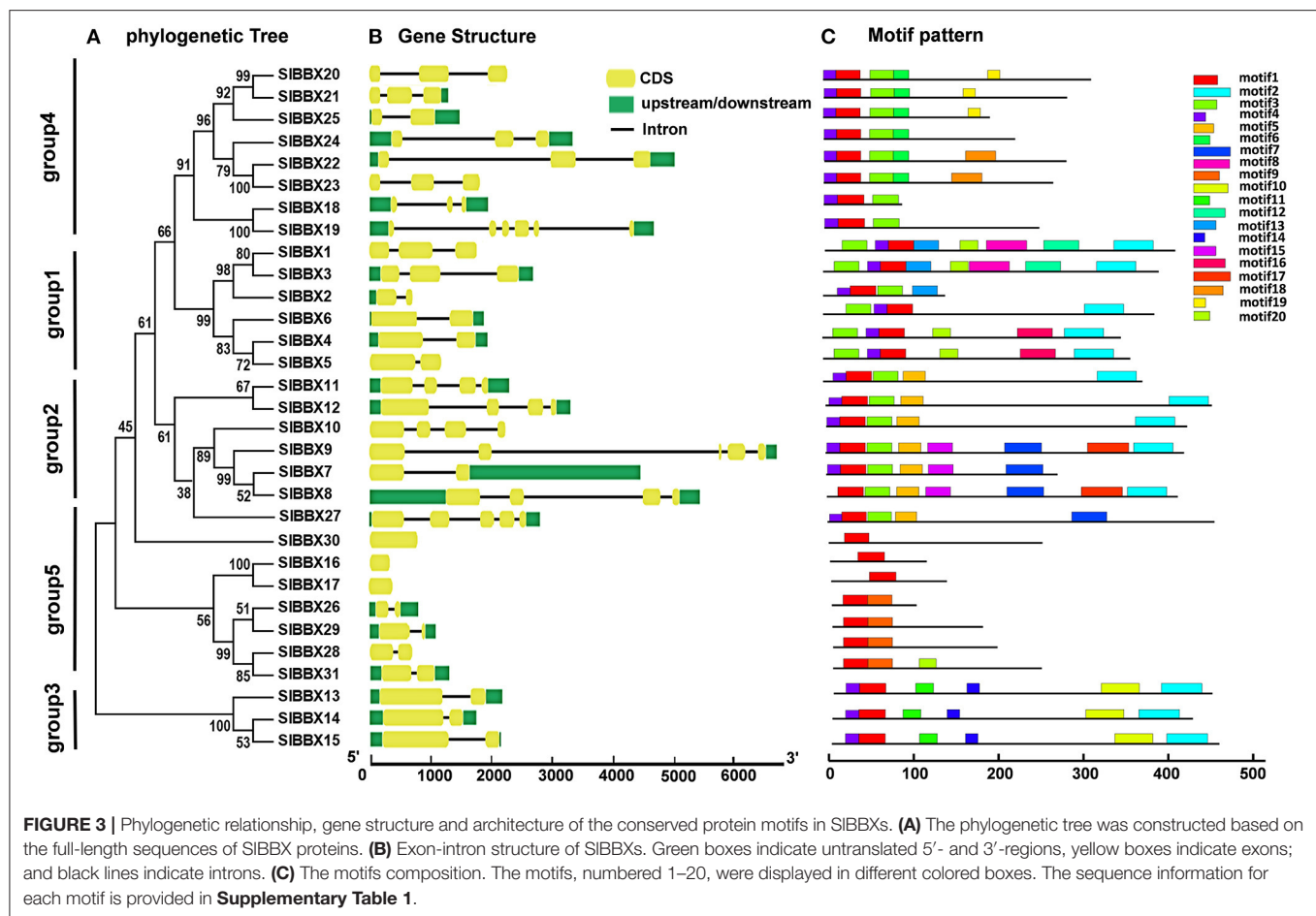


FIGURE 2 | Molecular phylogenetic analysis of *SIBBX* genes in tomato. All *SIBBX* proteins were divided into five subclasses represented by different colored clusters. Red, orange, blue, purple, and green clusters represent subclasses I, II, III, IV, and V, respectively. The evolutionary history was inferred by using the Maximum Likelihood method using MEGA7 software with 1,000 bootstrap replicates. The red circles and blue triangles represent Arabidopsis and tomato, respectively.

***SIBBX*s Act Critical Roles in Regulation of Cold Tolerance in Tomato**

To investigate whether *SIBBX* genes participated in cold stress, we analyzed the relative expression data of *SIBBX* genes in tomato plants (Chu et al., 2016), chose five genes, including *SIBBX4*, *SIBBX7*, *SIBBX9*, *SIBBX18*, and *SIBBX20*, and performed virus-induced gene silencing (VIGS) experiments to study their function under cold stress. After cold stress, the levels of relative electrolyte leakage (REL) in *SIBBX7*-silenced plants (pTRV-*BBX7*), *SIBBX9*-silenced plants (pTRV-*BBX9*) and *SIBBX20*-silenced plants (pTRV-*BBX20*) were higher than wild-type

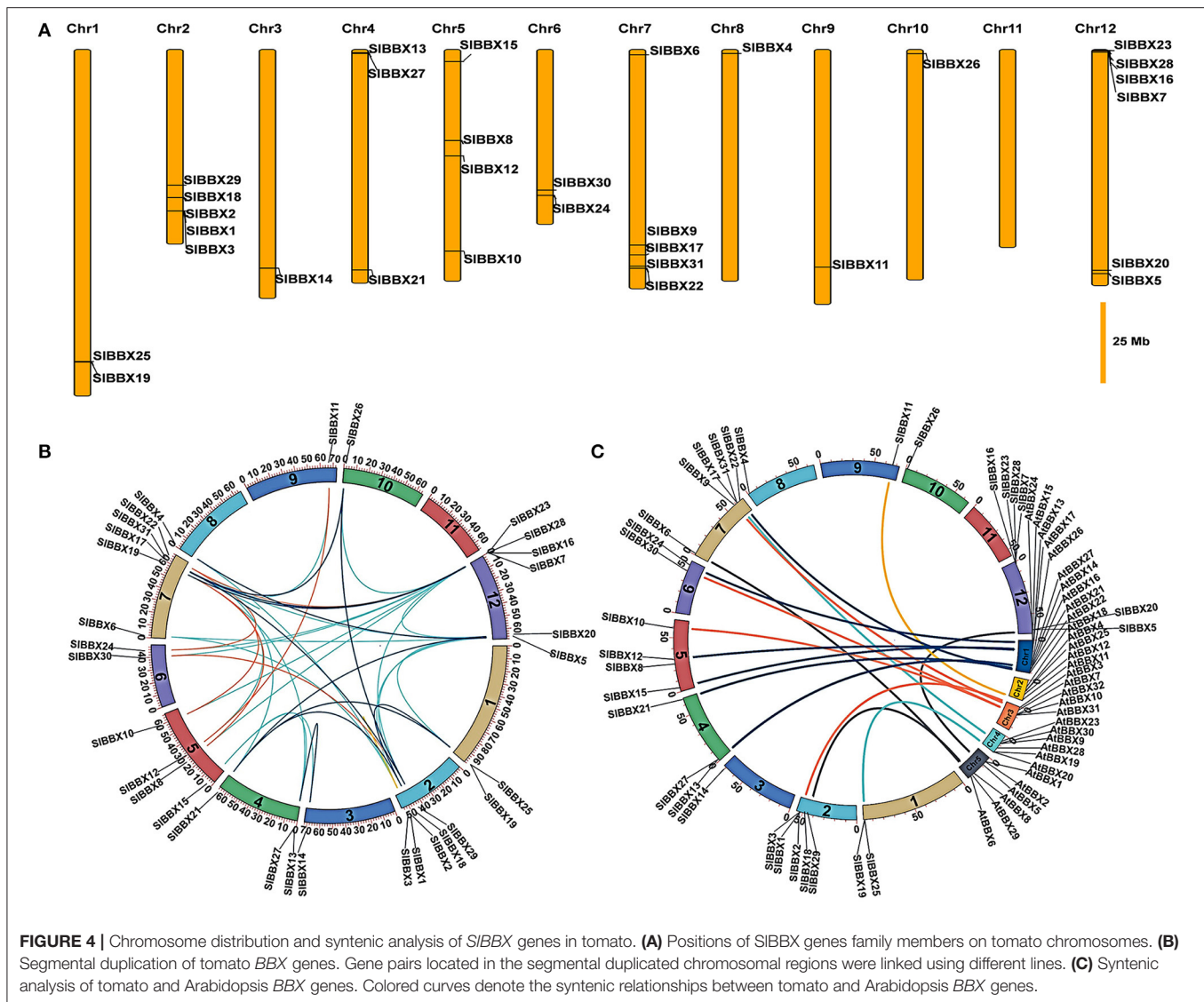
(pTRV) (Figure 7A), meanwhile, these silenced plants showed an increased sensitivity to cold stress compared with pTRV, as evidenced by a decrease in the maximum photosystem II efficiency (Fv/Fm) (Figure 7B, Supplementary Figure 5). In addition, the transcription of *COLD RESPONSIVE* (*COR*) genes, including *COR47-like* *COR413-like* was markedly lower in *SIBBX*s-silenced plants than those in control plants (pTRV) under cold stress (Figure 7C), which indicated that *SIBBX7*, *SIBBX9*, and *SIBBX20* induced cold responsive genes under cold stress. Together, these results indicated that *SIBBX7*, *SIBBX9*, and *SIBBX20* play positive roles in cold tolerance in tomato plants.



Roles of *SIBBXs* in Alleviation of Photoinhibition Under Cold Stress in Tomato

We analyzed the roles of *SIBBXs* in cold-induced photoinhibition. The maximum quantum yield of PSII (Fv/Fm) and the maximum level of the P700 signal (Pm, full oxidation of P700) in the dark were measured before and after cold treatment. Before treatment, Fv/Fm and Pm were similar among *SIBBX7*-, *SIBBX9*-, *SIBBX20*- silenced plants, and WT (pTRV) plants (**Figures 8A,F**). Fv/Fm was decreased by 27% in the pTRV plants after cold stress, while it was decreased by 51%, 48%, and 52% in *SIBBX7*-, *SIBBX9*-, and *SIBBX20*- silenced plants, respectively, after cold stress, which indicated that disruption of these three *SIBBXs* caused photoinhibition of PSII during cold stress. Furthermore, the Pm was decreased by 25% after cold stress, whereas it was decreased by 51%, 48%, and 33%, respectively, in *SIBBX7*-, *SIBBX9*-, and *SIBBX20*- silenced plants after cold stress, which suggested that the disruption of *SIBBX7* and *SIBBX9* caused obvious photoinhibition of PSI after cold stress, but the photoinhibition of PSI was slight in *SIBBX20*- silenced plants after cold stress. Together, these results indicated that these three *SIBBXs* play important roles in alleviating the photoinhibition of both photosystems during cold stress.

In order to obtain a more detailed insight into the processes affecting photoinhibition in the *SIBBX*-silenced plants after cold stress, some electron transport parameters of photosystems I and II were measured. Both ETR II (**Figures 8E, 9D**) and ETR I (**Figures 8J, 9H**) were significantly reduced after cold stress in tomato plants, showing a decrease of 50%–55% over those in plants grown at normal temperature. The ETR II and ETR I in *SIBBXs*-silenced plants were lower than those in control plants (pTRV) after cold stress, except *SIBBX7*-silenced plants, whose ETR I is close to the values of pTRV. To further explore the decrease in the ETRs, we measured Y(II), Y(NPQ), and Y(NO) for PSII and Y(I), Y(ND), and Y(NA) for PSI. We found that Y(II) values were significantly lower in pTRV-*BBX7*, pTRV-*BBX9*, and pTRV-*BBX20* plants than those in pTRV plants under cold stress (**Figures 8B, 9A**). This decrease in Y(II) appeared to be primarily due to a decrease in quantum yield of regulated energy dissipation of PSII [Y(NPQ)] and photochemical quenching coefficient (qP), and an increase in quantum yield of non-regulated energy dissipation of PSII [Y(NO)] in *SIBBXs*-silenced plants, especially in pTRV-*BBX7* and pTRV-*BBX9* plants (**Figures 8B–D, 9A–C**). Like Y(II), Y(I) was also decreased in *SIBBXs*-silenced plants, except for in pTRV-*BBX7* plants (**Figures 8G, 9E**). These decrease seemed to be due to obvious donor side limitation of PSI (due to lower ETR II in



PSII) as reflected by the elevated Y(ND), which were 29% and 47% higher in pTRV-*BBX9* and pTRV-*BBX20* plants, respectively, than in pTRV plants (Figures 8H, 9F). Although Y(ND) was 14% higher in pTRV-*BBX7* plants than in pTRV plants, its Y(I) was similar to the control plants (pTRV), which indicated that disruption of *SIBBX7* damaged the PSII rather than PSI during cold stress. Therefore, cold stress seriously reduced the capacity for photochemical energy conversion, electron transport rate and photoprotection in *SIBBX7*-, *SIBBX9*-, *SIBBX20*- silenced plants, suggesting that these three *SIBBX*s play critical roles in alleviating photoinhibition under cold stress.

DISCUSSION

In this study, we identified and characterized 31 *SIBBX* genes in tomato (Figure 1, Tables 1, 2), which contained two additional loci encoding BBX proteins in the tomato genome, that were

named *SIBBX30* and *SIBBX31*, in comparison with the previous studies (Chu et al., 2016). BBX proteins are characterized by one or two B-box domains at the N-terminal and, in some cases, a CCT domain at the C-terminal (Gangappa and Botto, 2014). Here, we found both the newly retrieved *SIBBX* proteins (*SIBBX30* and *SIBBX31*) contain a B-box domain at the N-terminal (Figure 1, Table 2), and they were also clustered in group 5 (Figure 2, Supplementary Figure 2), which further indicated these two proteins were new *SIBBX* proteins. The release of new tomato genomes and database updates may be the primary causes of this phenomenon. There were five subfamilies in the 32 members of Arabidopsis BBXs according to the combination of different conserved domains (Khanna et al., 2009). However, the conserved domain-based classification of BBX proteins in tomato was rather complex. As shown in Figure 2, *SIBBX1* to *SIBBX6* were classified into group 1, which had two B-boxes and a CCT plus a VP domains, whereas *SIBBX1* lacked a VP domain, and *SIBBX2* only contained two B-boxes

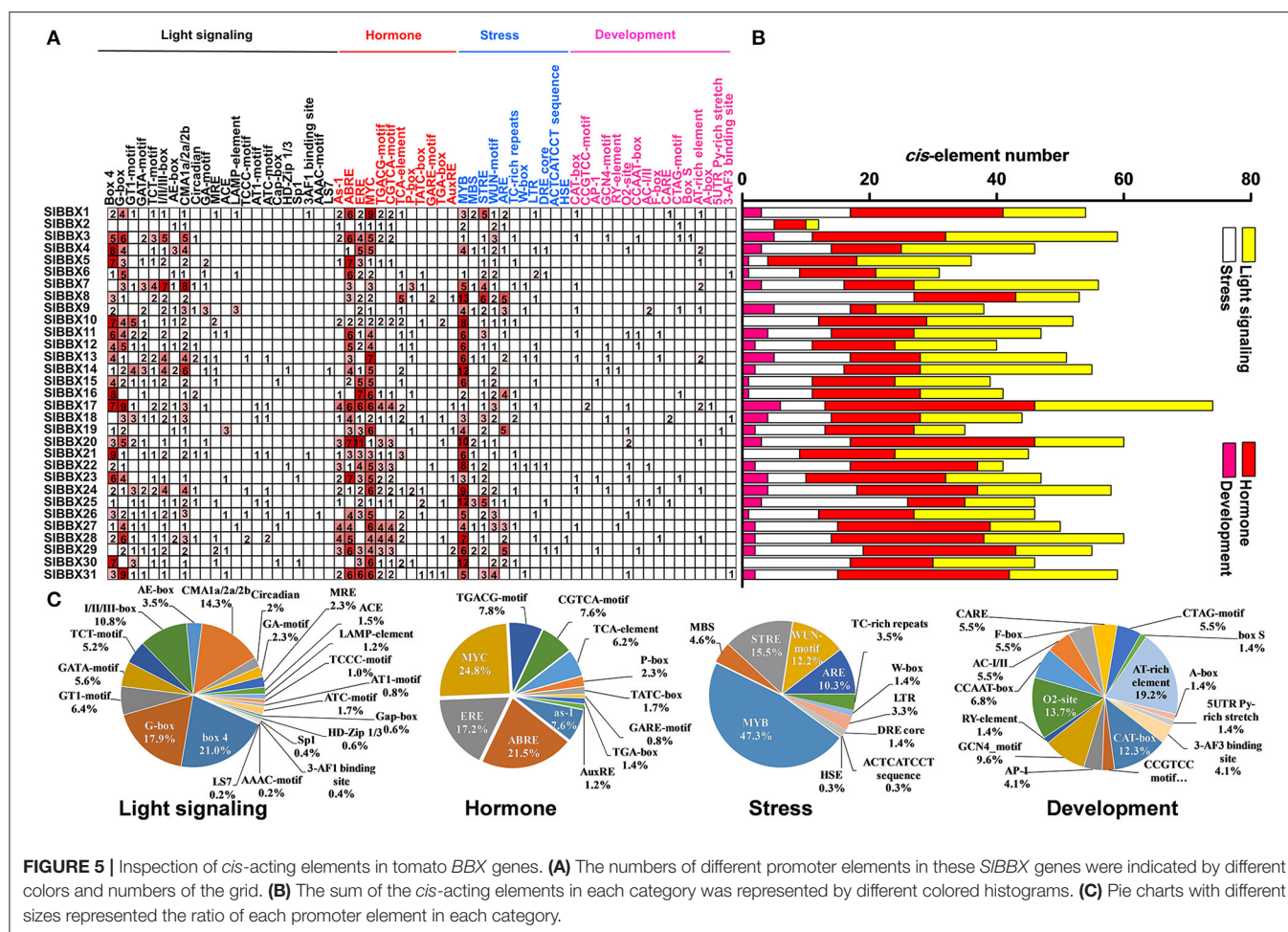


(Table 2). Meanwhile, SIBBX7 to SIBBX12 and SIBBX27 were clustered into group 2, which possessed two B-boxes and a CCT domains; however, SIBBX8 and SIBBX10 had one B-box and a CCT domains, while SIBBX7 and SIBBX27 contained two B-boxes. Group 4 contained only one B-box. We investigated the detail of sequence alignment in SIBBXs (Figure 1), and found a high degree of conservation of the B-box1 domain among SIBBX7 to SIBBX12, thus the clustering results of these proteins were similar to that based on B-box1. These results indicated that during the process of evolution, some SIBBX proteins lost the B-box2 domain.

Accumulating evidence showed that some BBX proteins act as central players in a variety of light-regulated physiological processes in plants. Here, we found that the number of light responsive *cis*-elements was the largest in the promoters of 31 SIBBX genes (Figure 5), which indicated that SIBBX genes were regulated by light signaling. Thus, we examined the gene expression of all the SIBBXs in response to different light quality. Results showed that light decreased the transcripts of SIBBX1, SIBBX8, SIBBX10, and SIBBX12, while increased the transcripts of SIBBX7, SIBBX13, and SIBBX15 compared with dark (Figure 6). Previous studies had demonstrated that COP1, which is degraded after illumination, works as an E3 ubiquitin ligase that targets

a variety of light signaling factors for ubiquitination and degradation in darkness (Osterlund et al., 2000; Han et al., 2020). For example, COP1 interacts with multiple BBXs, such as CO/BBX1 and BBX10, and subsequently degrades them by the 26S proteasome system (Liu et al., 2008; Ordoñez-Herrera et al., 2018). Nevertheless, COP1 stabilizes BBX11 rather than degrading it (Zhao et al., 2020), which suggests that COP1 likely degrades a yet unidentified component(s) targeting BBX11. Thus, COP1 may also control the stability of SIBBX proteins, including SIBBX1, SIBBX7, SIBBX8, SIBBX10, SIBBX12, SIBBX13, and SIBBX15, in the transition from dark to light. Interestingly, we found that SIBBX4, SIBBX23, and SIBBX29 were expressed only in response to R light, while SIBBX7, SIBBX13, and SIBBX25 were expressed just in response to FR light (Figure 6). These results indicate that these SIBBX proteins might directly interact with the photoreceptors, which sense R and FR light signals. Similarly, recent work has revealed that phyB directly interacts with BBX4 and positively regulates its accumulation in red light in Arabidopsis (Heng et al., 2019a), which demonstrates that photoreceptors may directly control some BBX proteins. In addition, the results showed that R light induced the expression of SIBBX14 and SIBBX24, whereas FR light inhibited their expression (Figure 6),

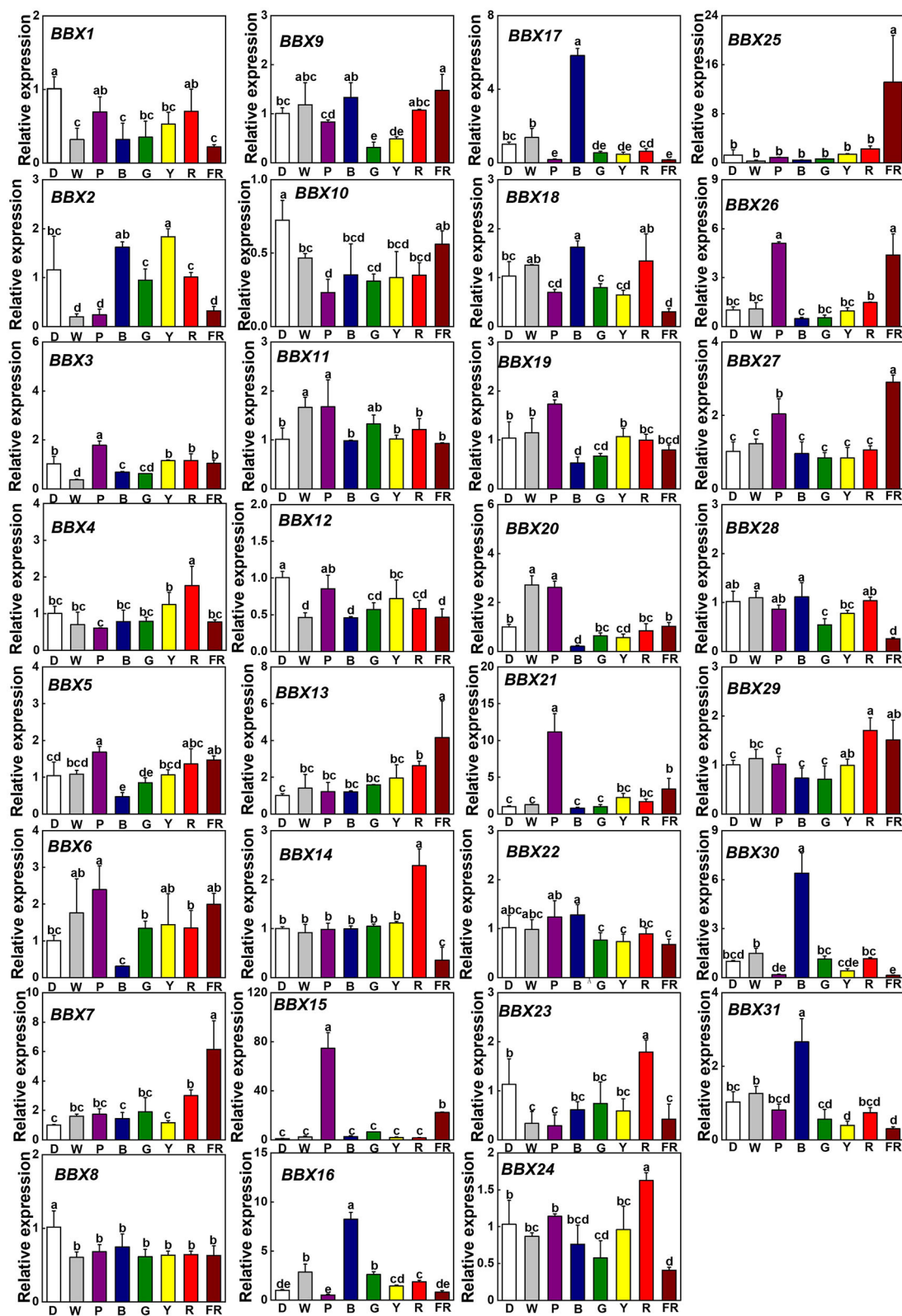
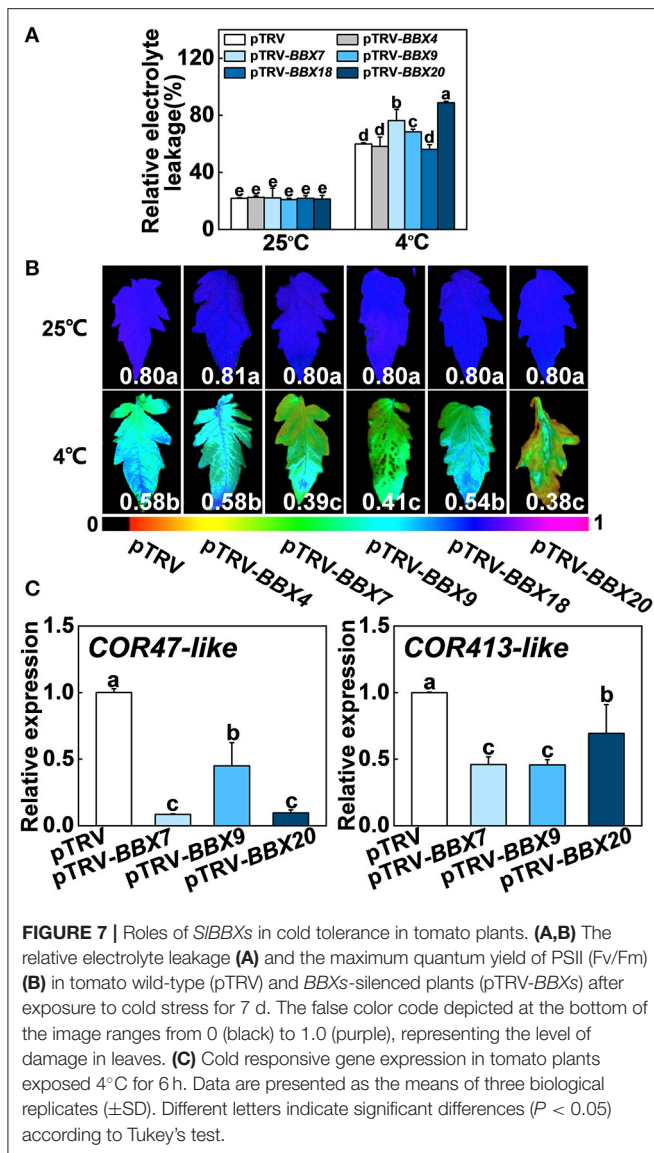
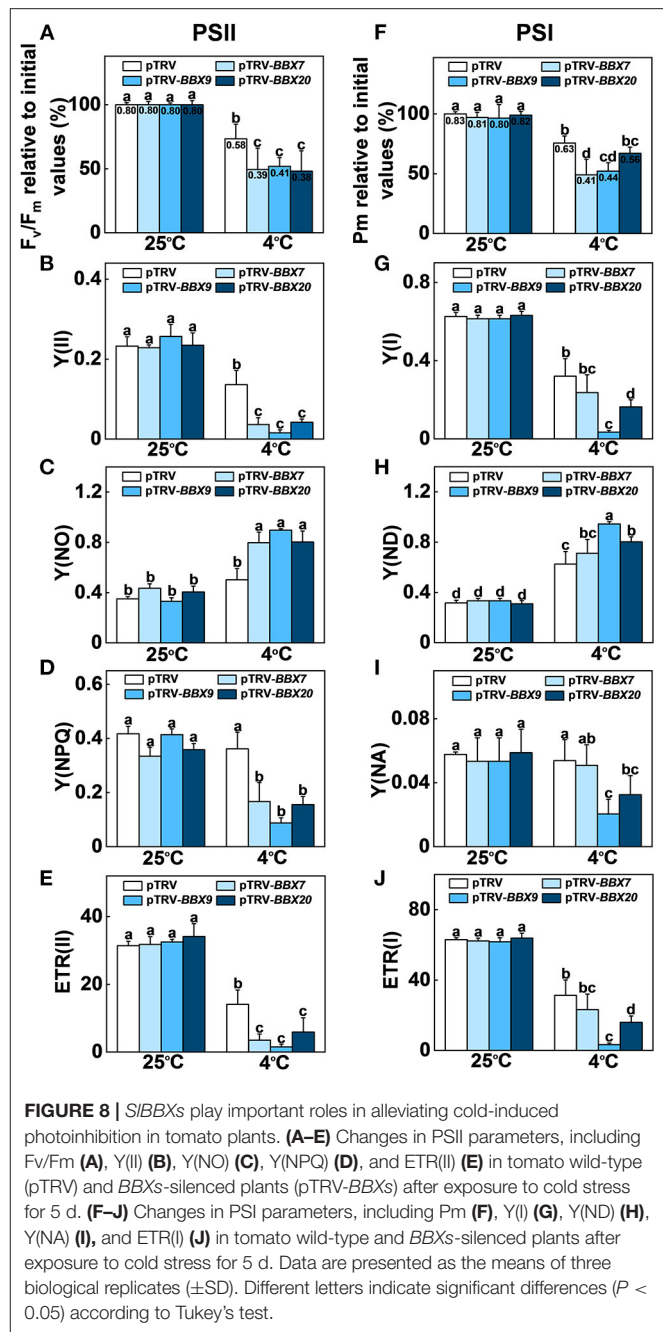


FIGURE 6 | Gene expression of *SIBBXs* in tomato leaves after the exposure of plants to different light quality for 6 h from the dark. Light quality treatments include dark (D), white light (W) or purple (P), blue (B), green (G), yellow (Y), red (R), and far-red (FR) light. The light intensity was $100 \mu\text{mol m}^{-2} \text{s}^{-1}$. Data are presented as the means of three biological replicates (\pm SD). Different letters indicate significant differences ($P < 0.05$) according to Tukey's test.

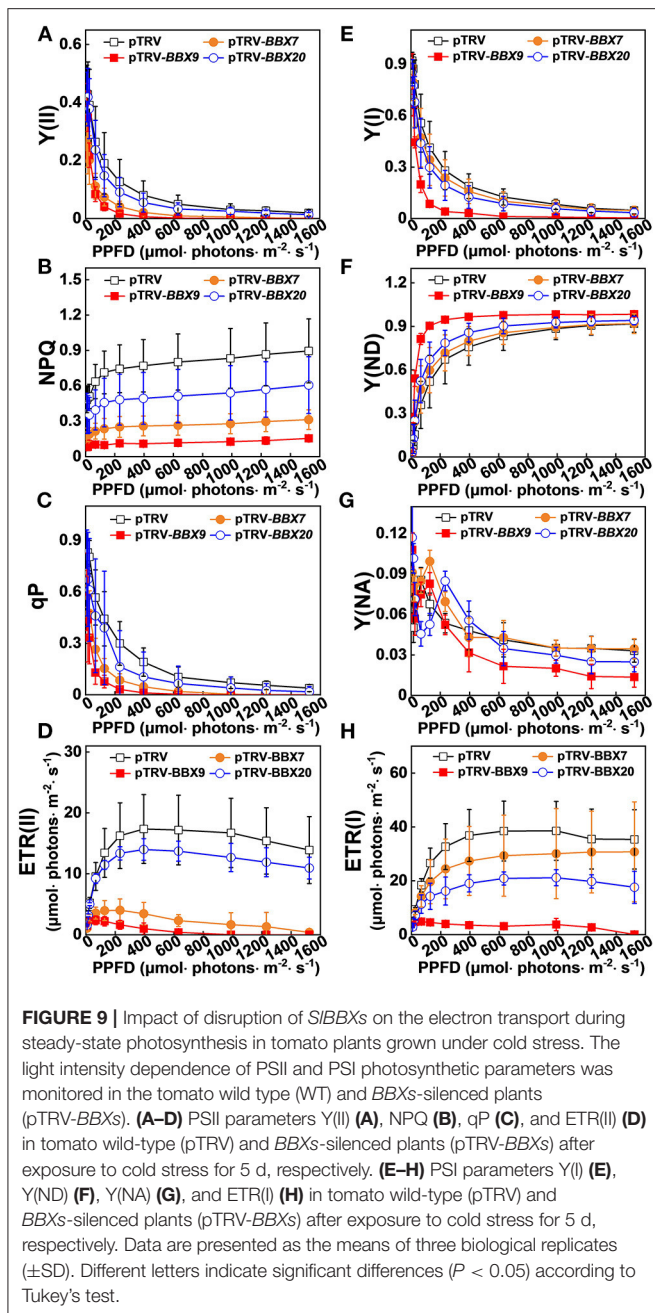


which implied that these two *SIBBX* proteins might function antagonistically to regulate some plant physiological processes, such as shade avoidance and the elongation of hypocotyls. Here, we observed that B light induced the gene expression of *SIBBX16*, *SIBBX17*, *SIBBX18*, *SIBBX30*, and *SIBBX31*, whereas inhibited the transcripts of *SIBBX5*, *SIBBX6*, *SIBBX19*, and *SIBBX20* (Figure 6). Previous work demonstrated that *BBX28/BBX29* and *BBX30/BBX31* could precisely control each other by forming a feedback loop in Arabidopsis (Lin et al., 2018; Heng et al., 2019b; Yadav et al., 2019; Song et al., 2020). Thus, these *SIBBX* proteins may work in concert with each other and some unidentified factors to regulate the plant growth in response to light signaling.

Light and temperature are more or less inter-related during plant growth and stress response (Wang et al., 2016). Here, we observed that the disruption of *SIBBX7*, *SIBBX9*, and



SIBBX20 largely reduced the cold tolerance in tomato plants as evidenced by phenotypes, REL, F_v/F_m , and cold responsive genes (Figure 7, Supplementary Figure 5), which indicated that *SIBBX7*, *SIBBX9*, and *SIBBX20* positively regulate cold tolerance in tomato plants. In addition, far-red light (FR) induced the transcription of *SIBBX7* and *SIBBX9* (Figure 6), and enhanced the cold tolerance in tomato plants (Wang et al., 2016, 2018, 2019, 2020a,b), which indicate that *SIBBXs* may play critical roles in the links between cold response and light signaling. Recent studies also showed that *BBX18* and *BBX23* are involved in the thermomorphogenesis in Arabidopsis (Ding et al., 2018). Both



MdBBX20 and *MaCOL1* are responsive to low temperature in apple and banana, respectively (Chen et al., 2012; Fang et al., 2019). *ZFPL*, a homologous gene of *AtBBX32*, enhances cold tolerance in the grapevine (Takuhara et al., 2011). *CmBBX24* also increases plant cold tolerance in *Chrysanthemum* (Yang et al., 2014). Furthermore, *MdBBX37* positively regulates JA-mediated cold-stress resistance in apples (An et al., 2021). However, whether *BBXs* are involved in cold stress-induced photoinhibition and the regulation of photoprotection during cold stress remains elusive.

Interestingly, the impairment of *SIBBX7*, *SIBBX9*, and *SIBBX20* significantly suppressed the photochemical efficiencies and energy conversion in tomato plants under cold stress, leading to the overreduction of electron carriers and damage of photosystem in tomato plants (Figures 8, 9). More recently, it has been demonstrated that heterologous expression of Arabidopsis *BBX21* in potato plants increases photosynthetic efficiency and reduces photoinhibition (Crocco et al., 2018). Therefore, *BBXs* play critical roles in photosynthesis and photoinhibition, however, the regulation mechanism is poorly understood. Previous works have revealed that *BBX20*, *BBX21*, *BBX22*, and *BBX23* interact with *HY5* to increase its transcriptional activity toward the target genes (Datta et al., 2008; Zhang et al., 2017; Job et al., 2018), whereas *BBX24*, *BBX25*, *BBX28*, and *BBX29* suppress *HY5* activity in Arabidopsis (Gangappa et al., 2013; Job et al., 2018; Lin et al., 2018; Song et al., 2020). *HY5* also positively controls *BBX22* at the transcriptional level (Chang et al., 2008), while repressing *BBX30* and *BBX31* gene expression by binding to the promoters of these two genes (Heng et al., 2019b; Yadav et al., 2019). In addition, direct interactions between *BBX32* and *BBX21* lead to inhibition in the *BBX21*-*HY5* (Holtan et al., 2011). Therefore, *SIBBXs* might alleviate the photoinhibition in tomato plants during cold stress through an *HY5*-dependent photoprotection pathway. Our previous results demonstrated that *SlHY5* alleviated photoinhibition in tomato plants under cold stress by induction of photoprotection, including increased NPQ, cyclic electron flux (CEF) around PSI and the activities of Foryer-Halliwell-Asada cycle enzymes (Wang et al., 2018). Here, we showed that the over-reduction in the flow of electrons from PSII to PSI and considerably low levels of NPQ caused a high excitation pressure in *SIBBXs*-silenced plants against cold stress, leading to a severe photoinhibition (Figures 8, 9). Thus, NPQ might function as a protective measure to prevent damage from high excitation pressure against photosynthesis and plant development (Upadhyay et al., 2013).

CONCLUSIONS

In this study, *SIBBX* family genes were identified and characterized in tomato by systematic analysis of conserved domains, phylogenetic relationship, gene structure, chromosome location. Two new members, *SIBBX30* and *SIBBX31*, were identified from the newly released tomato genome sequences. The promoter responsive *cis*-acting regulatory elements and gene expression analysis indicated that multiple *SIBBX* genes were highly responsive to light quality and low temperature. Furthermore, we found that *SIBBX7*, *SIBBX9*, and *SIBBX20* positively regulate cold tolerance in tomato plants via the prevention of photoinhibition and enhancing photoprotection. Our study emphasized the positive roles of light signaling transcription factors *SIBBXs* in cold tolerance in tomato plants, which may improve the current understanding of the integration of light and temperature signals by plants to adapt to adverse environments.

DATA AVAILABILITY STATEMENT

The original contributions presented in the study are included in the article/**Supplementary Material**, further inquiries can be directed to the corresponding author/s.

AUTHOR CONTRIBUTIONS

FW and TL designed the research. FW, XB, XW, JY, YZ, SZ, and XS performed the experiments. FW, YL, MQ, and GA analyzed the data. FW, GA, and TL wrote and revised the paper. All authors have read and approved the manuscript.

FUNDING

This research was supported by the National Natural Science Foundation of China (31801904), the Liao Ning Revitalization Talents Program (XLYC1807020), the Shenyang Young and

Middle-aged Science and Technology Innovation Talent Support Program (RC200449), National Key Research and Development Program of China (2018YFD1000800; 2019YFD1000300). Liaoning BaiQianWan Talents Program and China Agriculture Research System of MOF and MARA.

ACKNOWLEDGMENTS

We are grateful to the Tomato Genetics Resource Center at the California University for tomato seeds, and Yaofang Niu (Guhe Info technology Co. Ltd, Hangzhou, China) for assistance with syntenic analysis.

SUPPLEMENTARY MATERIAL

The Supplementary Material for this article can be found online at: <https://www.frontiersin.org/articles/10.3389/fpls.2021.698525/full#supplementary-material>

REFERENCES

- Ahammed, G. J., Gantait, S., Mitra, M., Yang, Y., and Li, X. (2020). Role of ethylene crosstalk in seed germination and early seedling development: a review. *Plant Physiol. Biochem.* 151, 124–131. doi: 10.1016/j.plaphy.2020.03.016
- An, J. P., Wang, X. F., Espley, R. V., Wang, K. L., Bi, S. Q., You, C. X., et al. (2019a). An apple b-box protein MdBBX37 modulates anthocyanin biosynthesis and hypocotyl elongation synergistically with MdMYBs and MdHY5. *Plant Cell Physiol.* 61, 130–143. doi: 10.1093/pcp/pcz185
- An, J. P., Wang, X. F., Zhang, X. W., Bi, S. Q., You, C. X., and Hao, Y. J. (2019b). MdBBX22 regulates UV-B-induced anthocyanin biosynthesis through regulating the function of MdHY5 and is targeted by MdBT2 for 26S proteasome-mediated degradation. *Plant Biotechnol. J.* 17, 2231–2233. doi: 10.1111/pbi.13196
- An, J. P., Wang, X. F., Zhang, X. W., You, C. X., and Hao, Y. J. (2021). Apple B-box protein BBX37 regulates jasmonic acid mediated cold tolerance through the JAZ-BBX37-ICE1-CBF pathway and undergoes MIEL1-mediated ubiquitination and degradation. *New Phytol.* 229, 2707–2729. doi: 10.1111/nph.17050
- Bai, B., Lu, N. N., Li, Y. P., Guo, S. L., Yin, H. B., He, Y. N., et al. (2019). OsBBX14 promotes photomorphogenesis in rice by activating OsHY5L1 expression under blue light conditions. *Plant Sci.* 284, 192–202. doi: 10.1016/j.plantsci.2019.04.017
- Bai, S. L., Tao, R. Y., Tang, Y. X., Yin, L., Ma, Y. J., Ni, J. B., et al. (2019a). BBX16, a B-box protein, positively regulates light-induced anthocyanin accumulation by activating MYB10 in red pear. *Plant Biotechnol. J.* 17, 1985–1997. doi: 10.1111/pbi.13114
- Bai, S. L., Tao, R. Y., Yin, L., Ni, J. B., Yang, Q. S., Yan, X. H., et al. (2019b). Two B-box proteins, PpBBX18 and PpBBX21, antagonistically regulate anthocyanin biosynthesis via competitive association with *Pyrus pyrifolia* ELONGATED HYPOCOTYL 5 in the peel of pear fruit. *Plant J.* 100, 1208–1223. doi: 10.1111/tjp.14510
- Bailey, T. L., Boden, M., Buske, F. A., Frith, M., Grant, C. E., Clementi, L., et al. (2009). MEME SUITE: tools for motif discovery and searching. *Nucleic Acids Res.* 37, W202–W208. doi: 10.1093/nar/gkp335
- Cao, W. H., Liu, J., He, X. J., Mu, R. L., Zhou, H. L., Chen, S. Y., et al. (2007). Modulation of ethylene responses affects plant salt-stress responses. *Plant Physiol.* 143, 707–719. doi: 10.1104/pp.106.094292
- Chang, C. S. J., Li, Y. H., Chen, L. T., Chen, W. C., Hsieh, W. P., Shin, J., et al. (2008). LZFI, a HY5-regulated transcriptional factor, functions in Arabidopsis de-etiolation. *Plant J.* 54, 205–219. doi: 10.1111/j.1365-313X.2008.03401.x
- Chen, J., Chen, J. Y., Wang, J. N., Kuang, J. F., Shan, W., and Lu, W. J. (2012). Molecular characterization and expression profiles of MaCOL1, a CONSTANS-like gene in banana fruit. *Gene* 496, 110–117. doi: 10.1016/j.gene.2012.01.008
- Chu, Z. N., Wang, X., Li, Y., Yu, H. Y., Li, J. H., Lu, Y. E., et al. (2016). Genomic organization, phylogenetic and expression analysis of the B-BOX gene family in tomato. *Front. Plant Sci.* 7:1552. doi: 10.3389/fpls.2016.01552
- Crocco, C. D., and Botto, J. F. (2013). BBX proteins in green plants: insights into their evolution, structure, feature and functional diversification. *Gene* 531, 44–52. doi: 10.1016/j.gene.2013.08.037
- Crocco, C. D., Ocampo, G. G., Ploschuk, E. L., Mantese, A., and Botto, J. F. (2018). Heterologous expression of *AtBBX21* enhances the rate of photosynthesis and alleviates photoinhibition in *Solanum tuberosum*. *Plant Physiol.* 177, 369–380. doi: 10.1104/pp.17.01417
- Datta, S., Hettiarachchi, G. H. C. M., Deng, X. W., and Holm, M. (2006). Arabidopsis CONSTANS-LIKE3 is a positive regulator of red light signaling and root growth. *Plant Cell* 18, 70–84. doi: 10.1105/tpc.105.038182
- Datta, S., Johansson, H., Hettiarachchi, C., Irigoyen, M. L., Desai, M., Rubio, V., et al. (2008). LZFI/SALT TOLERANCE HOMOLOG3, an Arabidopsis B-box protein involved in light-dependent development and gene expression, undergoes COP1-mediated ubiquitination. *Plant Cell* 20, 2324–2338. doi: 10.1105/tpc.108.061747
- Ding, L., Wang, S., Song, Z. T., Jiang, Y. P., Han, J. J., Lu, S. J., et al. (2018). Two B-Box domain proteins, BBX18 and BBX23, interact with ELF3 and regulate thermomorphogenesis in Arabidopsis. *Cell Rep.* 25, 1718–1728. doi: 10.1016/j.celrep.2018.10.060
- Edgar, R. C. (2004). MUSCLE: multiple sequence alignment with high accuracy and high throughput. *Nucleic Acids Res.* 32, 1792–1797. doi: 10.1093/nar/gkh340
- Fan, X. Y., Dong, Y. S., Cao, D. M., Bai, M. Y., Luo, X. M., Yang, H. J., et al. (2012). BZS1, a B-box protein, promotes photomorphogenesis downstream of both brassinosteroid and light signaling pathways. *Mol. Plant.* 5, 591–600. doi: 10.1093/mp/sss041
- Fang, H. C., Dong, Y. H., Yue, X. X., Hu, J. F., Jiang, S. H., Xu, H. F., et al. (2019). The B-Box zinc finger protein MdBBX20 integrates anthocyanin accumulation in response to ultraviolet radiation and low temperature. *Plant Cell Environ.* 42, 2090–2104. doi: 10.1111/pce.13552
- Galvao, V. C., and Fankhauser, C. (2015). Sensing the light environment in plants: photoreceptors and early signaling steps. *Curr. Opin. Neurobiol.* 34C, 46–53. doi: 10.1016/j.conb.2015.01.013
- Gangappa, S. N., and Botto, J. F. (2014). The BBX family of plant transcription factors. *Trends Plant Sci.* 19, 460–470. doi: 10.1016/j.tplants.2014.01.010
- Gangappa, S. N., Crocco, C. D., Johansson, H., Datta, S., Hettiarachchi, C., Holm, M., et al. (2013). The Arabidopsis B-box protein BBX25 interacts with HY5, negatively regulating BBX22 expression to suppress seedling photomorphogenesis. *Plant Cell* 25, 1243–1257. doi: 10.1105/tpc.113.109751
- Gendron, J. M., Pruneda-Paz, J. L., Doherty, C. J., Gross, A. M., Kang, S. E., and Kay, S. A. (2012). Arabidopsis circadian clock protein, TOC1, is a

- DNA-binding transcription factor. *Proc. Natl. Acad. Sci. U.S.A.* 109, 3167–3172. doi: 10.1073/pnas.1200355109
- Han, X., Huang, X., and Deng, X. W. (2020). The photomorphogenic central repressor COP1: conservation and functional diversification during evolution. *Plant Commun.* 1, 2590–3462. doi: 10.1016/j.xplc.2020.100044
- Heng, Y. Q., Jiang, Y., Zhao, X. H., Zhou, H., Wang, X. C., Deng, X. W., et al. (2019a). BBX4, a phyB-interacting and modulated regulator, directly interacts with PIF3 to fine tune red light-mediated photomorphogenesis. *Proc. Natl. Acad. Sci. U.S.A.* 116, 26049–26056. doi: 10.1073/pnas.1915149116
- Heng, Y. Q., Lin, F., Jiang, Y., Ding, M. Q., Yan, T. T., Lan, H. X., et al. (2019b). B-Box containing proteins BBX30 and BBX31, acting downstream of HY5, negatively regulate photomorphogenesis in Arabidopsis. *Plant Physiol.* 180, 497–508. doi: 10.1104/pp.18.01244
- Holm, M., Hardtke, C. S., Gaudet, R., and Deng, X. W. (2001). Identification of a structural motif that confers specific interaction with the WD40 repeat domain of Arabidopsis COP1. *EMBO J.* 20, 118–127. doi: 10.1093/emboj/20.1.118
- Holtan, H. E., Bandong, S., Marion, C. M., Adam, L., Tiwari, S., Shen, Y., et al. (2011). BBX32, an Arabidopsis B-Box protein, functions in light signaling by suppressing HY5-regulated gene expression and interacting with STH2/BBX21. *Plant Physiol.* 156, 2109–2123. doi: 10.1104/pp.111.177139
- Horton, P., Park, K. J., Obayashi, T., Fujita, N., Harada, H., Adams-Collier, C. J., et al. (2007). WoLF PSORT: protein localization predictor. *Nucleic Acids Res.* 35, W585–W587. doi: 10.1093/nar/gkm259
- Hu, B., Jin, J. P., Guo, A. Y., Zhang, H., Luo, J. C., and Gao, G. (2015). GSDS 2.0: an upgraded gene feature visualization server. *Bioinformatics* 31, 1296–1297. doi: 10.1093/bioinformatics/btu817
- Job, N., Yadukrishnan, P., Bursch, K., Datta, S., and Johansson, H. (2018). Two B-Box proteins regulate photomorphogenesis by oppositely modulating HY5 through their diverse C-terminal domains. *Plant Physiol.* 176, 2963–2976. doi: 10.1104/pp.17.00856
- Khanna, R., Kronmiller, B., Maszle, D. R., Coupland, G., Holm, M., Mizuno, T., et al. (2009). The Arabidopsis B-box zinc finger family. *Plant Cell* 21, 3416–3420. doi: 10.1105/tpc.109.069088
- Kumar, S., Stecher, G., and Tamura, K. (2016). MEGA7: molecular evolutionary genetics analysis version 7.0 for bigger datasets. *Mol. Biol. Evol.* 33, 1870–1874. doi: 10.1093/molbev/msw054
- Lescot, M., Déhais, P., Thijs, G., Marchal, K., Moreau, Y., Van, de Peer, Y., et al. (2002). PlantCARE, a database of plant cis-acting regulatory elements and a portal to tools for *in silico* analysis of promoter sequences. *Nucleic Acids Res.* 30, 325–327. doi: 10.1093/nar/30.1.325
- Lin, F., Jiang, Y., Li, J., Yan, T. T., Fan, L. M., Liang, J. S., et al. (2018). B-BOX DOMAIN PROTEIN28 negatively regulates photomorphogenesis by repressing the activity of transcription factor HY5 and undergoes COP1-mediated degradation. *Plant Cell* 30, 2006–2019. doi: 10.1105/tpc.18.00226
- Lira, B. S., Oliveira, M. J., Shiose, L., Wu, R. T. A., Rosado, D., Lupi, A. C. D., et al. (2020). Light and ripening-regulated BBX protein-encoding genes in *Solanum lycopersicum*. *Sci. Rep.* 10:19235. doi: 10.1038/s41598-020-76131-0
- Liu, L. J., Zhang, Y. C., Li, Q. H., Sang, Y., Mao, J., Lian, H. L., et al. (2008). COP1-mediated ubiquitination of CONSTANS is implicated in cryptochrome regulation of flowering in Arabidopsis. *Plant Cell* 20, 292–306. doi: 10.1105/tpc.107.057281
- Liu, X., Li, R., Dai, Y., Yuan, L., Sun, Q. H., Zhang, S. Z., et al. (2019). A B-box zinc finger protein, MdbBX10, enhanced salt and drought stresses tolerance in Arabidopsis. *Plant Mol. Biol.* 99, 437–447. doi: 10.1007/s11103-019-00828-8
- Liu, Y. N., Chen, H., Ping, Q., Zhang, Z. X., Guan, Z. Y., Fang, W. M., et al. (2019). The heterologous expression of CmBBX22 delays leaf senescence and improves drought tolerance in Arabidopsis. *Plant Cell Rep.* 38, 15–24. doi: 10.1007/s00299-018-2345-y
- Livak, K. J., and Schmittgen, T. D. (2001). Analysis of relative gene expression data using real-time quantitative PCR and the 2⁻(-Delta Delta C(T)) method. *Methods* 25, 402–408. doi: 10.1006/meth.2001
- Min, J. H., Chung, J. S., Lee, K. H., and Kim, C. S. (2015). The CONSTANS-like 4 transcription factor, AtCOL4, positively regulates abiotic stress tolerance through an abscisic acid-dependent manner in Arabidopsis. *J. Integr. Plant Biol.* 57, 313–324. doi: 10.1111/jipb.12246
- Nagaoka, S., and Takano, T. (2003). Salt tolerance-related protein STO binds to a Myb transcription factor homologue and confers salt tolerance in Arabidopsis. *J. Exp. Bot.* 54, 2231–2237. doi: 10.1093/jxb/erg241
- Ordoñez-Herrera, N., Trimborn, L., Menje, M., Henschel, M., Robers, L., Kaufholdt, D., et al. (2018). The transcription factor COL12 is a substrate of the COP1/SPA E3ligase and regulates flowering time and plant architecture. *Plant Physiol.* 176, 1327–1340. doi: 10.1104/pp.17.01207
- Osterlund, M. T., Hardtke, C. S., Wei, N., and Deng, X. W. (2000). Targeted destabilization of HY5 during light-regulated development of Arabidopsis. *Nature* 405, 462–466. doi: 10.1038/35013076
- Paik, I., and Huq, E. (2019). Plant photoreceptors: multi-functional sensory proteins and their signaling networks. *Semin. Cell. Dev. Biol.* 92, 114–121. doi: 10.1016/j.semcdb.2019.03.007
- Ren, J., Wen, L. P., Gao, X. J., Jin, C. J., Xue, Y., and Yao, X. B. (2009). DOG 1.0: illustrator of protein domain structures. *Cell Res.* 19, 271–2733. doi: 10.1038/cr.2009.6
- Song, Z. Q., Yan, T. T., Liu, J. J., Bian, Y. T., Heng, Y. Q., Lin, F., et al. (2020). BBX28/BBX29-HY5-BBX30/31 form a feedback loop to fine-tune photomorphogenic development. *Plant J.* 104, 377–390. doi: 10.1111/tpj.14929
- Takahara, Y., Kobayashi, M., and Suzuki, S. (2011). Low-temperature induced transcription factors in grapevine enhance cold tolerance in transgenic Arabidopsis plants. *J. Plant Physiol.* 168, 967–975. doi: 10.1016/j.jplph.2010.11.008
- Upadhyay, R. K., and Mattoo, A. K. (2018). Genome-wide identification of tomato (*Solanum lycopersicum* L.) lipoxygenases coupled with expression profiles during plant development and in response to methyl-jasmonate and wounding. *J. Plant Physiol.* 231, 318–328. doi: 10.1016/j.jplph.2018.10.001
- Upadhyay, R. K., Soni, D. K., Singh, R., Dwivedi, U. N., Pathre, U. V., Nath, P., et al. (2013). SLERF36, an EAR-motif-containing ERF gene from tomato, alters stomatal density and modulates photosynthesis and growth. *J. Exp. Bot.* 64, 3237–3247. doi: 10.1093/jxb/ert162
- Wang, C. Q., Sarmast, M. K., Jiang, J., and Dehesh, K. (2015). The transcriptional regulator BBX19 promotes hypocotyl growth by facilitating COP1-Mediated EARLY FLOWERING3 degradation in Arabidopsis. *Plant Cell* 27, 1128–1139. doi: 10.1105/tpc.15.00044
- Wang, F., Chen, X. X., Dong, S. J., Jiang, X. C., Wang, L. Y., Yu, J. Q., et al. (2020a). Crosstalk of PIF4 and DELLA modulates CBF transcript and hormone homeostasis in cold response in tomato. *Plant Biotechnol. J.* 18, 1041–1055. doi: 10.1111/pbi.13272
- Wang, F., Guo, Z. X., Li, H. Z., Wang, M. M., Onac, E., Zhou, J., et al. (2016). Phytochrome A and B function antagonistically to regulate cold tolerance via abscisic acid-dependent jasmonate signaling. *Plant Physiol.* 170, 459–471. doi: 10.1104/pp.15.01171
- Wang, F., Wu, N., Zhang, L. Y., Ahammed, G. L., Chen, X. X., Xiang, X., et al. (2018). Light signaling-dependent regulation of photoinhibition and photoprotection in tomato. *Plant Physiol.* 176, 1311–1326. doi: 10.1104/pp.17.01143
- Wang, F., Yan, J. R., Ahammed, G. J., Wang, X. J., Bu, X., Xiang, H. Z., et al. (2020b). PGR5/PGR1 and NDH mediate far-red light-induced photoprotection in response to chilling stress in tomato. *Front. Plant Sci.* 11:669. doi: 10.3389/fpls.2020.00669
- Wang, F., Zhang, L. Y., Chen, X. X., Wu, X. D., Xiang, X., Zhou, J., et al. (2019). SLHY5 integrates temperature, light and hormone signaling to balance plant growth and cold tolerance. *Plant Physiol.* 179, 749–760. doi: 10.1104/pp.18.01140
- Xiong, C., Luo, D., Lin, A. H., Zhang, C. L., Shan, L. B., He, P., et al. (2019). A tomato B-box protein SIBBX20 modulates carotenoid biosynthesis by directly activating PHYTOENE SYNTHASE 1, and is targeted for 26S proteasome-mediated degradation. *New Phytol.* 221, 279–294. doi: 10.1111/nph.15373
- Xu, D. Q. (2020). COP1 and BBXs-HY5-mediated light signal transduction in plants. *New Phytol.* 228, 1748–1753. doi: 10.1111/nph.16296
- Xu, D. Q., Jiang, Y., Li, J., Holm, M., and Deng, X. W. (2018). The B-Box domain protein BBX21 promotes photomorphogenesis. *Plant Physiol.* 176, 2365–2375. doi: 10.1104/pp.17.01305
- Xu, D. Q., Jiang, Y., Li, J. G., Lin, F., Holm, M., and Deng, X. W. (2016). BBX21, an Arabidopsis B-box protein, directly activates HY5 and is targeted by COP1 for 26S proteasome mediated degradation. *Proc. Natl. Acad. Sci. U.S.A.* 113, 7655–7660. doi: 10.1073/pnas.1607687113
- Yadav, A., Bakshi, S., Yadukrishnan, P., Lingwan, M., Dolde, U., Wenkel, S., et al. (2019). The B-Box-containing microprotein miP1a/BBX31 regulates

- photomorphogenesis and UV-B protection. *Plant Physiol.* 179, 1876–1892. doi: 10.1104/pp.18.01258
- Yang, Y. J., Ma, C., Xu, Y. J., Wei, Q., Imtiaz, M., Lan, H. B., et al. (2014). A zinc finger protein regulates flowering time and abiotic stress tolerance in *Chrysanthemum* by modulating gibberellin biosynthesis. *Plant Cell* 26, 2038–2054. doi: 10.1105/tpc.114.124867
- Yu, C. S., Chen, Y. C., Lu, C. H., and Hwang, J. K. (2006). Prediction of protein subcellular localization. *Proteins* 64, 643–651. doi: 10.1002/prot.21018
- Zhang, H. K., Gao, S. H., Lercher, M. J., Hu, S. N., and Chen, W. H. (2012). EvolView, an online tool for visualizing, annotating and managing phylogenetic trees. *Nucleic Acids Res.* 40, W569–W572. doi: 10.1093/nar/gks576
- Zhang, X. Y., Huai, J. L., Shang, F. F., Xu, G., Tang, W. J., Jing, Y. J., et al. (2017). A PIF1/PIF3-HY5-BBX23 transcription factor cascade affects photomorphogenesis. *Plant Physiol.* 174, 2487–2500. doi: 10.1104/pp.17.00418
- Zhao, X. H., Heng, Y. Q., Wang, X. C., Deng, X., and Xu, D. Q. (2020). A positive feedback loop of BBX11–BBX21–HY5 promotes photomorphogenic development in Arabidopsis. *Plant Commun.* 1:100045. doi: 10.1016/j.xplc.2020.100045
- Conflict of Interest:** The authors declare that the research was conducted in the absence of any commercial or financial relationships that could be construed as a potential conflict of interest.
- Copyright © 2021 Bu, Wang, Yan, Zhang, Zhou, Sun, Yang, Ahammed, Liu, Qi, Wang and Li. This is an open-access article distributed under the terms of the Creative Commons Attribution License (CC BY). The use, distribution or reproduction in other forums is permitted, provided the original author(s) and the copyright owner(s) are credited and that the original publication in this journal is cited, in accordance with accepted academic practice. No use, distribution or reproduction is permitted which does not comply with these terms.



Cold Stress in Wheat: Plant Acclimation Responses and Management Strategies

Muhammad A. Hassan^{1†}, Chen Xiang^{1†}, Muhammad Farooq², Noor Muhammad³, Zhang Yan¹, Xu Hui¹, Ke Yuanyuan¹, Attiogbe K. Bruno¹, Zhang Lele¹ and Li Jincai^{1,4*}

¹ School of Agronomy, Anhui Agricultural University, Hefei, China, ² Department of Plant Sciences, College of Agricultural and Marine Sciences, Sultan Qaboos University, Muscat, Oman, ³ Agronomy (Forage Production) Section, Ayub Agricultural Research Institute, Faisalabad, Pakistan, ⁴ Jiangsu Collaborative Innovation Centre for Modern Crop Production, Nanjing, China

OPEN ACCESS

Edited by:

Sunchung Park,
United States Department of
Agriculture, United States

Reviewed by:

Klára Kosová,
Crop Research Institute (CRI), Czechia
Dhruv Lavania,
University of Alberta, Canada

*Correspondence:

Li Jincai
ljc@ahau.edu.cn

[†]These authors have contributed
equally to this work

Specialty section:

This article was submitted to
Plant Abiotic Stress,
a section of the journal
Frontiers in Plant Science

Received: 06 March 2021

Accepted: 28 May 2021

Published: 08 July 2021

Citation:

Hassan MA, Xiang C, Farooq M,
Muhammad N, Yan Z, Hui X,
Yuanyuan K, Bruno AK, Lele Z and
Jincai L (2021) Cold Stress in Wheat:
Plant Acclimation Responses and
Management Strategies.
Front. Plant Sci. 12:676884.
doi: 10.3389/fpls.2021.676884

Unpredicted variability in temperature is associated with frequent extreme low-temperature events. Wheat is a leading crop in fulfilling global food requirements. Climate-driven temperature extremes influence the vegetative and reproductive growth of wheat, followed by a decrease in yield. This review describes how low temperature induces a series of modifications in the morphophysiological, biochemical, and molecular makeup of wheat and how it is perceived. To cope with these modifications, crop plants turn on their cold-tolerance mechanisms, characterized by accumulating soluble carbohydrates, signaling molecules, and cold tolerance gene expressions. The review also discusses the integrated management approaches to enhance the performance of wheat plants against cold stress. In this review, we propose strategies for improving the adaptive capacity of wheat besides alleviating risks of cold anticipated with climate change.

Keywords: wheat, cold stress damage, physiological mechanism, yield, stress management, cold acclimation

INTRODUCTION

Climate change is among the core problems of recent times, as it is threatening global food security (FAO, 2020). Uncertain climatic variations poses a severe challenge in fulfilling the future food demands of a growing population (Röder et al., 2014). Extreme temperature events have significantly increased over the past few decades (IPCC, 2014). Persistent cold extremes have been observed in agricultural regions worldwide with varying frequency, intensity, and duration (Kodra et al., 2011; Augspurger, 2013). This situation halts plant growth by causing mechanical injury and metabolic dysfunction through ice crystallization (Yadav, 2010). Most of the wheat-growing areas of the world often undergo low-temperature stress, such as China (Xiao et al., 2018), the United States (Holman et al., 2011), Europe (Trnka et al., 2014), and Australia (Zheng et al., 2015; Crimp et al., 2016). Even though some regions noticed reduced winter duration because of global warming as plant ecologists revealed a paradoxical connection between plant growth and climatic variations, confirming that upsurge in warm climate increased the risk of cold injury to plants (Gu et al., 2008).

Every year, 85% of the wheat sown area in the world is affected by spring frost, and it usually takes place during March and April at the early booting stage (Yue et al., 2016). In the spring season, when wheat canopy temperature falls 0°C or below, severe frost damage occurs (Frederiks et al., 2015; Zheng et al., 2015). Thakur et al. (2010) stated that frequent low-temperature spells during spring cause severe damage to the micro-organelles of the cell, resulting in excessive reactive oxygen species (ROS) and the occurrence of lipid peroxidation. A short span of freezing air during frost

stress is disastrous for the vegetative and reproductive growth of plants (Frederiks et al., 2015). Cold conditions disrupt root water uptake, and water inadequacy in the stem results in drought stress (Aroca et al., 2012). This drought condition due to imbalanced water relations causes disturbance in smooth nutrient uptake, decreases the root ion absorption rate, and limits nutrient transport to other plant parts, ultimately resulting in stunted plant growth (Nezhadahmadi et al., 2013).

In a study by Fuller et al. (2007), two wheat cultivars were subjected to cold stress in a freezing chamber with different cold stress treatments for 2 h. Consequently, severe damage to flag leaves and spikes has been observed and the damage increased with temperature decrease. Subsequently, it leads to partial to complete grain yield loss (Fuller et al., 2007). The cold stress also influences the grain number per spike and grain filling rate, leading to a substantial reduction in final wheat production (Thakur et al., 2010). The cold stress-induced yield losses are characterized by a reduced number of productive tillers, spikes, and grains per spike, biologically associated with short stems, lower leaf area, and reduced photosynthetic capacity (Valluru et al., 2012; Li et al., 2015).

The ability of plants to endure cold without damaging their growth cycle is called “cold tolerance” (Liu Y. et al., 2019). The response of plants toward cold stress induction can be classified into four different phases: (i) initial alarming response, (ii) acclimation (the increase in freezing tolerance associated with exposure to low but non-freezing temperatures), (iii) restoration, and (iv) destruction if stress prolongs or severity increases (Larcher, 2003). In addition, after cold stress (i.e., the temperature has risen from cold to optimum), an innate recovery response is activated, providing plant regeneration, an active process after stress cessation, and is vital for further growth and development of plants (Hasanfard et al., 2021). Although the regeneration capability depends on the intensity of stress earlier encountered by the plant (Puijalon et al., 2008), it can be enhanced through exogenous application of certain hormones (i.e., auxin, cytokinin, and strigolactone) (Ikeuchi et al., 2016). The temperate crop plants, including wheat, tend to overcome cold stress through cold acclimation (Theocharis et al., 2012; Li et al., 2014). Cold acclimation of winter wheat can be acquired *via* freeze hardening (the ability of a plant to withstand sub-zero temperature of up to a specific time limit) (Trischuk et al., 2014). This process is carried out through many transcriptional and physiological adjustments, including activation of cold-regulated genes (Zhu et al., 2007; Majláth et al., 2012), downstream regulation of photosynthesis, accumulation of osmoprotectants, and stimulation of antioxidant system (Theocharis et al., 2012).

To maintain yield stability and curtail the negative impact of sudden cold events, adopting proper managerial, and husbandry practices (i.e., sowing method, time, and fertilization) are pretty handy in limiting the risk of frost injury. It is also necessary to develop cold-tolerant wheat cultivars (Limin and Fowler, 2006; Zheng et al., 2015). The cold-defense mechanism of wheat can be improved by implementing integrated multi-disciplinary systems, including screening of cold-tolerant genes through modern gene mapping techniques and developing cold-tolerant cultivars, pre-sowing seed treatments, and

applying compatible osmolytes and growth hormones at critical growth stages.

This article reviews the current research findings on how extreme climatic events, particularly cold stress, negatively affect normal wheat growth, development, and yield. It first describes how cold-induced disruptions affect the morphophysiological and metabolic processes, leading to the deterioration of grain quality and lower final grain yield. Following that, it explains how wheat reacts to cold stress by expressing various kinds of adaptive responses. Stress avoidance in wheat (the avoidance of consequences of stress) involves an array of physiological and biochemical modifications (i.e., biosynthesis of compatible osmolytes, protective proteins, alteration in metabolic composition, downregulation of photosynthesis, and ROS detoxification, etc.) that occur simultaneously. Although many studies elucidated cold perception and responsive mechanism in plants, few exist on wheat; this study particularly emphasizes a better understanding of wheat cold perception, with counter-responses concerning futuristic management approaches, as it proposes suitable husbandry practices and multi-disciplinary strategies that can help to anchor the defense of wheat against climatic extremes.

RESPONSES TO COLD STRESS

Wheat needs an optimum temperature range for ideal growth and functioning, and any deviation from it will affect the normal growth process (Table 1). Cold stress severely curbs the physiological and biochemical reactions in the plant cell, which results in leaf chlorosis, wilting, and even necrosis of plant cells (Ruelland and Zachowski, 2010). This section briefly discusses how plants perceive low-temperature stress, cold-induced morpho-physiological alterations, and the survival response of the wheat plant.

Morphological Responses and Yield Losses in Wheat Vegetative Phase

When a plant undergoes cold stress, several morphological alterations occur (Equiza et al., 2001); subsequently, root-shoot growth is restricted and productivity is reduced. In winter cereals, low-temperature stress at the vegetative phase cause leaves chlorosis and wilting and ultimately leads to necrosis and inhibited growth (Janowiak et al., 2002). Cold stress severely affects germination and seedling establishment causes delayed germination, poor emergence, reduced plant density, and uneven stand establishment in wheat (Jame and Cutforth, 2004). Winter wheat initially suffers low-temperature stress when tillering begins and when photosynthate assimilation and nutrient absorption sites are under development (Rinalducci et al., 2011). Crome et al. (1998) exposed wheat plants to freezing stress (from 0 to -13°C) in a controlled chamber for 2 h, frost devastation begins at -3°C and complete burning of flag leaf and ears occurred at -7°C ; consequently, a substantial reduction in grain yield was observed. Similarly, cold exposure at jointing leads to reduced leaf size, leaf area, and lower shoot biomass

TABLE 1 | Temperature threshold values for various wheat growth stages.

#	Growth phases	Min. and Max. (Tolerable Temp. Limit)	Optimum Temp. (Ideal Growth Cond.)	Optimum duration for growth phases	References
1	Germination and emergence (E)	>4 and <40°C	12–30°C	3.5–10 d (depending on soil moisture)	Spilde, 1989; Mian and Nafziger, 1994; Jame and Cutforth, 2004
2	Floral Initiation (GS1- Prior Vernalization)	–20°C*, >20	21–16°C	20 d (Spring) 35 d (Winter)	Evans, 1975
3	Floral Initiation (GS1-Vernalization)	7 and 18°C (Spring) 0 and 7°C (Winter)	4–10°C	5–15 d (Spring) 30–60 d (Winter)	Ahrens and Loomis, 1963; Trione and Metzger, 1970; Evans, 1975
4	Heading to Anthesis (GS2)	>4.5 and <31°C	12°C	100 d (Spring) 130 d (Winter)	Fischer, 1985; Stapper and Fischer, 1990; Acevedo et al., 2009
5	Anthesis to Physiological Maturity (GS3)	>6 and <35.4°C	21°C	140 d (Spring) 170 d (Winter)	Lyons, 1973; Porter and Gawith, 1999

*Only for winter wheat, while spring wheat shows mild to no response to frost.

(Valluru et al., 2012) and limits the final output (Li et al., 2014). Additionally, applying freezing stress (–8 and –9°C) at the stem elongation stage limits the internode extension, denatures the spikelets, reduces assimilate transport, restricts the dry matter accumulation, and causes a significant reduction in grain yield (Whaley et al., 2004).

Low temperature also affects the root growth of wheat as root growth is an ecologically controlled parameter (Buriro et al., 2011; Kul et al., 2020). Root length is more sensitive to sub-optimal temperature than dry weight. It causes a significant reduction in root branching and root surface area; consequently, normal water and nutrient uptake were disrupted (Hussain et al., 2018). Restricted root surface area inhibits the ability of the plant to explore the water and nutrients resources (Richner et al., 1996).

In summary, cold stress at the initial seedling stage results in delayed emergence and poor stand establishment. Prolonged exposure to cold stress results in stunted growth, diminished root-shoot surface area, leaf chlorosis, and disturbed water and nutrient relations. Such indicators lead to a significant reduction in wheat yield and quality. Additionally, few studies have investigated roots activity with reference to low-temperature stress, which needs to be explored.

Reproductive Phase

The reproductive growth phase is more sensitive to cold stress than the vegetative phase in wheat (Thakur et al., 2010). The reproductive growth stage begins with flowering, which continues with floral differentiation (into male and female parts), sporogenesis, pollen grain and embryo development, pollination, fertilization, and, finally, grain development. Plant exposure to cold contact at the reproductive growth phase causes many structural and functional deformities, leading to a reduction in growth and development. Chilling at flowering causes flower shedding, pollen tube deformation (Chakrabarti et al., 2011), pollen sterility, and ovule distortion (Ji et al., 2017), and before anthesis, it lowers down the number of grains and disrupts the grain development (Dolferus et al., 2011; Barton et al., 2014). Such conditions lead to incomplete fruit setting, which reduces the final wheat production (Hussain et al., 2018). Though

counterresponse varies at every growth phase, collectively, all responses are not enough to resist net yield loss.

Imposing chilling and freezing stress at the jointing stage has severely damaged the morphological attributes (such as burned leaf blade, chlorosis, decreased shoot biomass, and denatured spikelets) compared with control (**Figure 1**). Assimilates accumulation during grain filling is extremely sensitive to suboptimal temperature conditions negatively influencing the grain quality and quantity (Yang and Zhang, 2006). Cold exposure at booting and flowering stages resulted in a considerable reduction in the number of grains per spike; consequently, final grain output diminished to 78% (Subedi et al., 1998). During the reproductive stage, a 1°C decrease in temperature below the threshold level may result in a 10–90% wheat crop damage (Marcellos and Single, 1984; Ji et al., 2017). A field experiment revealed that frost damage of a 5 day span (with a temperature range of 0–4°C) at the stem elongation stage might cause a nearly 15% reduction in the number of spikes and ultimately result in 14% reduction in yield loss (Li et al., 2015). If these frost spells continue, yield losses will be higher (Wu et al., 2014). In conclusion, the wheat crop is more sensitive to cold stress at the reproductive stage, especially the frost spells are disastrous, causing flower shedding, pollen infertility, denatured spikes, and incomplete/poor fruit setting, resulting in significant yield losses (**Figure 2**).

Physiological and Biochemical Responses and Wheat Yield

Plant physiological processes, such as photosynthesis and respiration, are more vulnerable to low-temperature stress (Yadav, 2010). Cold stress induces a series of changes in various biological and biochemical processes in the wheat plant cell, including photosynthesis, respiration, water relations, mineral nutrition, and other metabolic activities (**Tables 2, 3**). In this review, we briefly discussed some of these processes.

Cold-Induced Ultra-Structural Impairments

Primarily, cellular membranes are the first site of the plant, which is directly affected by cold stress repercussions, leading

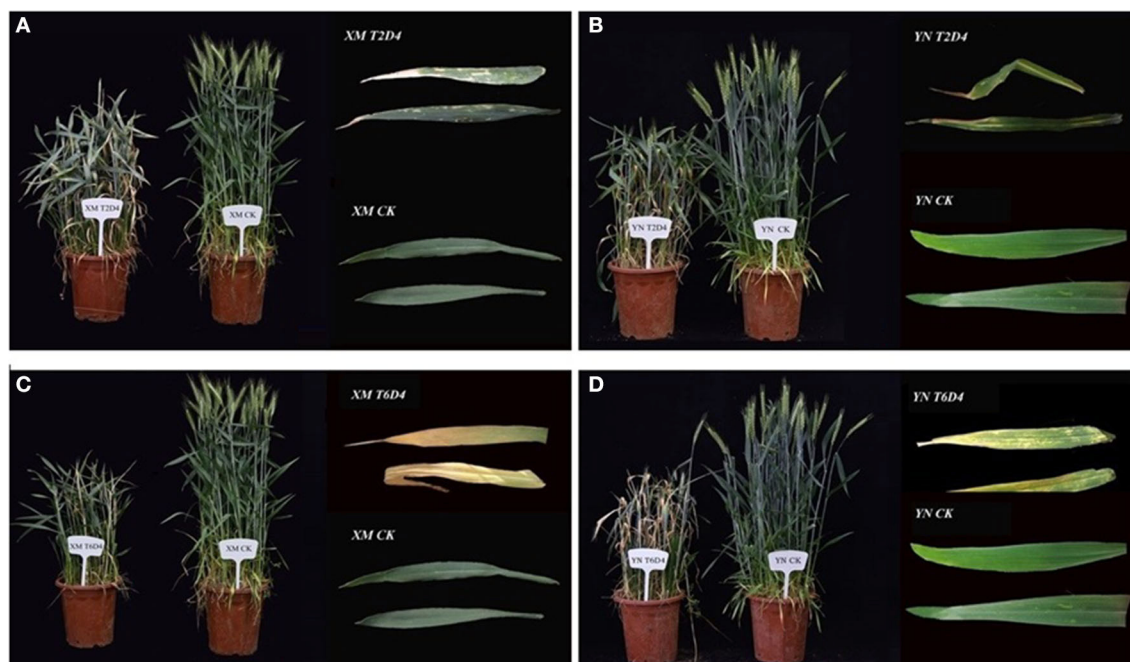


FIGURE 1 | Impacts of low-temperature stress on two winter wheat cultivars, XM and YN (XM: XinMai–Cold Sensitive and YN: YanNong–Cold Tolerant), is shown with the damage induced by cold stress, as compared with control (CK). Wheat cultivars with treatments **(A)** XMT2D4 [$T_2 = 4^\circ\text{C}$, $D_4 = 12\text{ h/3 d}$], **(B)** YNT2D4 [$T_2 = 4^\circ\text{C}$, $D_4 = 12\text{ h/3 d}$], **(C)** XMT6D4 [$T_6 = -4^\circ\text{C}$, $D_4 = 12\text{ h/3 d}$], and **(D)** YNT6D4 [$T_6 = -4^\circ\text{C}$, $D_4 = 12\text{ h/3 d}$] has clearly exhibited the damage induced by cold stress, as compared with control (CK) treatments of XM and YN. Growth Conditions: Experiment grown under field conditions, before the heading stage shifted to the controlled chamber (Humidity: 70%, *Light intensity: $0\text{ }\mu\text{mol}\cdot\text{m}^{-2}\cdot\text{s}^{-1}$) for 3 days (4 h/day, Midnight: 12:00 a.m.–4:00 a.m.) for low-temperature treatments, then shifted back to field conditions. Photos were taken before the flowering stage; extracted leaves are flag/2nd leaf. *In this experiment, in night-time, wheat plants subjected to cold stress, and light intensity set at $0\text{ }\mu\text{mol}\cdot\text{m}^{-2}\cdot\text{s}^{-1}$ because, in field conditions of Huanghuai (China), plants experience late spring cold stress after midnight. (Unpublished: Own Experiment).

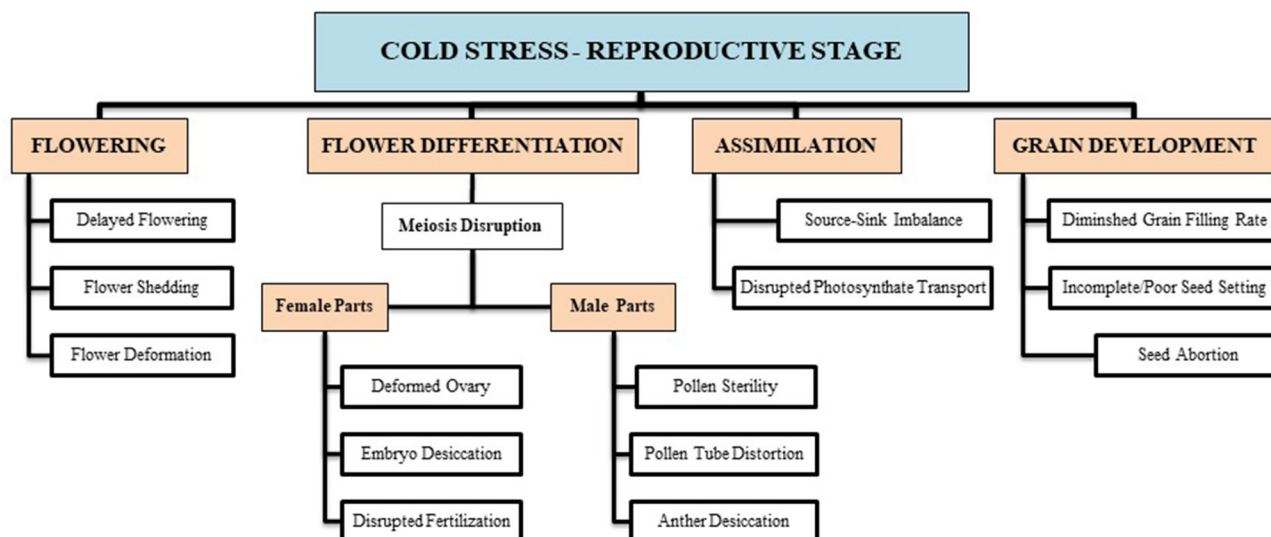


FIGURE 2 | Cold-induced reproductive deformities are briefly illustrated with respect to certain growth stages (i.e., flowering, differentiation, assimilate transport, grain filling, etc.). These growth disruptions result in a substantial decline in final wheat produce.

to other ultra-structural physiological and biochemical changes (Figure 3). Cold stress induces many ultrastructural alterations in cold-sensitive plant species (Pomeroy and Andrews, 1978;

Kratsch and Wise, 2000), which causes the imbalance of membrane fluid content and permeability that leads to disturbance to all membrane linked physiological and

TABLE 2 | Morphological traits of wheat with respect to their growth stages, influenced by cold stress.

#	Traits	Growth stage	*Low Temp. & Duration	Growth Conditions	Cold induced alterations compared to control	References
1	Germination and emergence	Initial seedling stage (Vegetative)	$\leq 2^{\circ}\text{C}$ (>2 d) Control: 30°C	Controlled (Incubator)	Delayed emergence Poor vigor	Jame and Cutforth, 2004
2	Leaf initiation	Seedling growth (Vegetative)	$\leq 5^{\circ}\text{C}$ (12 h to 1 d) Control: 20°C	Controlled (Phytotron)	Leaf initiation ↓ Growth rate ↓ Biomass ↓	Leonardos et al., 2003
3	Ground cover/stand establishment	Tillering (Vegetative)	$\leq 0^{\circ}\text{C}$ (> 5 d)	Field (Frost spells)	Number of tillers ↓ Uneven stand establishment Stem apex killed	Whaley et al., 2004
4	Peduncle development	Stem elongation (Veg. → Rep.)	≤ 2 to -9°C (≥ 2 d consecutively)	Field (Frost spells)	Internode extension ↓ Stunted peduncle extension Shoot biomass ↓	Whaley et al., 2004
5	Flag leaf and head emergence	Jointing → booting (Reproductive)	≤ 0 to -2°C (24–60 h) Control: 8°C	Controlled and Open-top Chambers	Delayed floret growth Leaf chlorosis and wilting Denatured spikelet	Li et al., 2015; Zhang et al., 2019
6	Flowering, Pollination	Anthesis (Reproductive)	≤ -2 to -6°C (2–6 d) Control: 6°C	Controlled (Phytotron)	Floret abortion Anthers desiccation Flower shedding	Ji et al., 2017
7	Final grain development	Grain filling (Reproductive)	≤ -2 to -6°C (2–6 d) Control: 6°C	Controlled (Phytotron)	Number of grains/spikes ↓ Incomplete fruit setting 1,000-grain weight ↓ Grain Yield ↓	Ji et al., 2017
8	Root growth and development	–	–	–	Surface area ↓ Thickened primary root axis. Lateral branches ↓ Hydraulic conductance ↓ Nutrient uptake ↓	Siddique et al., 2000; Farooq et al., 2009

*Temperature mentioned here is a minimum recorded field/phytotron temperature during certain growth phases [Here, ↓ indicates a decrease].

biochemical processes (Bohn et al., 2007; Los et al., 2013). Most often, these adverse effects are accompanied by structural alterations in the membrane (Bohn et al., 2007), which were subsequently followed by cellular leakage of electrolytes and amino acids, diversion of electron flow toward alternate pathways (Seo et al., 2010), alterations in protoplasmic streaming, and redistribution of intracellular calcium ions. These severe symptoms are directly correlated with injury to membrane structures of cells and changed lipid composition. Cold-induced alterations in crop plants lead to decreased ATP synthase activity, followed by inhibition of Rubisco regeneration and photophosphorylation (Yordanova and Popova, 2007). Cold-induced photo-inhibition subsequently leads to a reduction in photosynthetic activity (Groom et al., 1990; Oquist et al., 1993). If cold stress remained for a shorter duration, plants could recover their normal state, but such a situation is irreversible under prolonged duration.

Photosynthesis

In grains like wheat, photosynthesis, and bio-mass accumulations are the major sources for grain production and vital physiological processes in the crop growth phases; these processes are highly vulnerable to low-temperature stress (Rinalducci et al., 2011; Khan et al., 2017). It has been reported that cold stress causes reductions in final yield, which is associated with a decline in spike number, spike length (Karimi et al., 2011), biomass, leaf area, size, and carbohydrate metabolic reactions. Such morphological and physiological alterations are

correlated with reduced photosynthetic efficiency (Theocharis et al., 2012; Valluru et al., 2012). Research findings revealed that imposing low-temperature stress (day:night, 5°C : 5°C) at the seedling stage resulted in a 45% decrease in the photosynthetic rate of primary leaves as compared with control (day:night, 20°C : 16°C) (Leonardos et al., 2003). Similarly, in another investigation, when wheat seedlings are subjected to low temperature (4°C) in a closed chamber for 7 days, an 18% decrease in photosynthetic activity has been recorded after 5 h. Over-excitation of photosystem II has been observed under cold stress, which triggers energy dissipation through non-radiative reactions (Cvetkovic et al., 2017). The maximum efficiency of Photosystem II decreased by 18% after 1 day exposure to cold (Venzhik et al., 2011). Further, photosynthetic activity in cold-sensitive cultivars is more sensitive to cold stress than cold-tolerant cultivars (Yamori et al., 2009). During the jointing stage, cold exposure inhibits gaseous exchange, thus reducing the quantum efficiency of photosystem II, resulting in decreased photosynthesis that leads to a 5–14% reduction in yield (Li et al., 2015). Flag leaf burning due to freezing stops the photosynthetic activity that resulted in up to 100% yield losses (Rajcan and Swanton, 2001).

Cold-induced photosynthetic inhibition is due to various reasons, i.e., reduced chlorophyll synthesis, poor chloroplast development, diminished efficiency of photosynthetic apparatus, restricted carbohydrates transportation, limited stomatal

TABLE 3 | Physiological and biochemical traits influenced by cold stress.

#	Processes	Effect	*Low Temp. & Duration	Growth conditions	Cold Induced alterations compared to control	References
1	Photosynthesis	Poor photosynthetic activity	$\leq 5^{\circ}\text{C}$ at vegetative phase (1 d) Control: 20°C $\leq 4^{\circ}\text{C}$ at vegetative phase (1–7 d) Control: 22°C -2 to -6°C at reproductive phase (≥ 2 d) Control: 6°C	Controlled (Growth Chambers, Phytotrons)	Leaf Area ↓ Leaf water content ↓ Chlorophyll <i>a,b</i> synthesis ↓ CO_2 Assimilation ↓ Quantum efficiency of PSII ↓ Stomatal conductance ↓ Electron transport chain (ETR) ↓ Enzymatic activity ↓ Photo-inhibition Source-sink imbalance	Venzhik et al., 2011; Dahal et al., 2012; Liu L. et al., 2019
2	Respiration	Reduced respiration rate	$4-12^{\circ}\text{C}$ at initial vegetative phase (>12 h) Control: 22°C $\leq 5^{\circ}\text{C}$ at vegetative phase (1 d) Control: 20°C -2 to -6°C at reproductive phase (≥ 2 d) Control: 6°C	Controlled (Incubator, Phytotrons)	Damaged mitochondrial structure Kinetics of energy flow ↓ Gaseous exchange ↓ Enzymatic activity ↓ ATP production ↓ Metabolism dysfunction Energy reserves ↓	Dahal et al., 2012; Li et al., 2013
3	Nutrient relations	Decreased nutrient uptake and transport			Disturbed soil physio-chemical characteristics Disturbed microbial activity Reduced root surface area, thickened primary root axis and no lateral branching, Hydraulic conductivity ↓ Imbalanced water relations leading drought & reduced phloem activity	Siddique et al., 2000; Farooq et al., 2009

*Temperature mentioned here is the minimum recorded field/phytotron temperature during certain growth phases, while $20-25^{\circ}\text{C}$ is the optimum temperature for efficient biochemical functioning Austin, 1990 [Here, ↓ indicates a decrease].

conductivity, suppressed Rubisco activity during carbon assimilation, disrupted electron transport chain, and decreased energy stock (Bota et al., 2004; Hussain et al., 2018). The chilling conditions instigate drought stress, which reduces molecular oxygen and produces ROS that cause severe damage to photosynthetic apparatus (Basu et al., 2016). During the vegetative stage, cold stress reduced the leaf area, which is considered more critical since it reduces photosynthetic activity, resulting in a source–sink imbalance (Paul and Foyer, 2001; Liu L. et al., 2019; Liu Y. et al., 2019).

Cold stress disrupts the photosynthetic activity at every growth stage, resulting in a reduction in photo-assimilation and assimilate transportation. These conditions lead to significant yield losses.

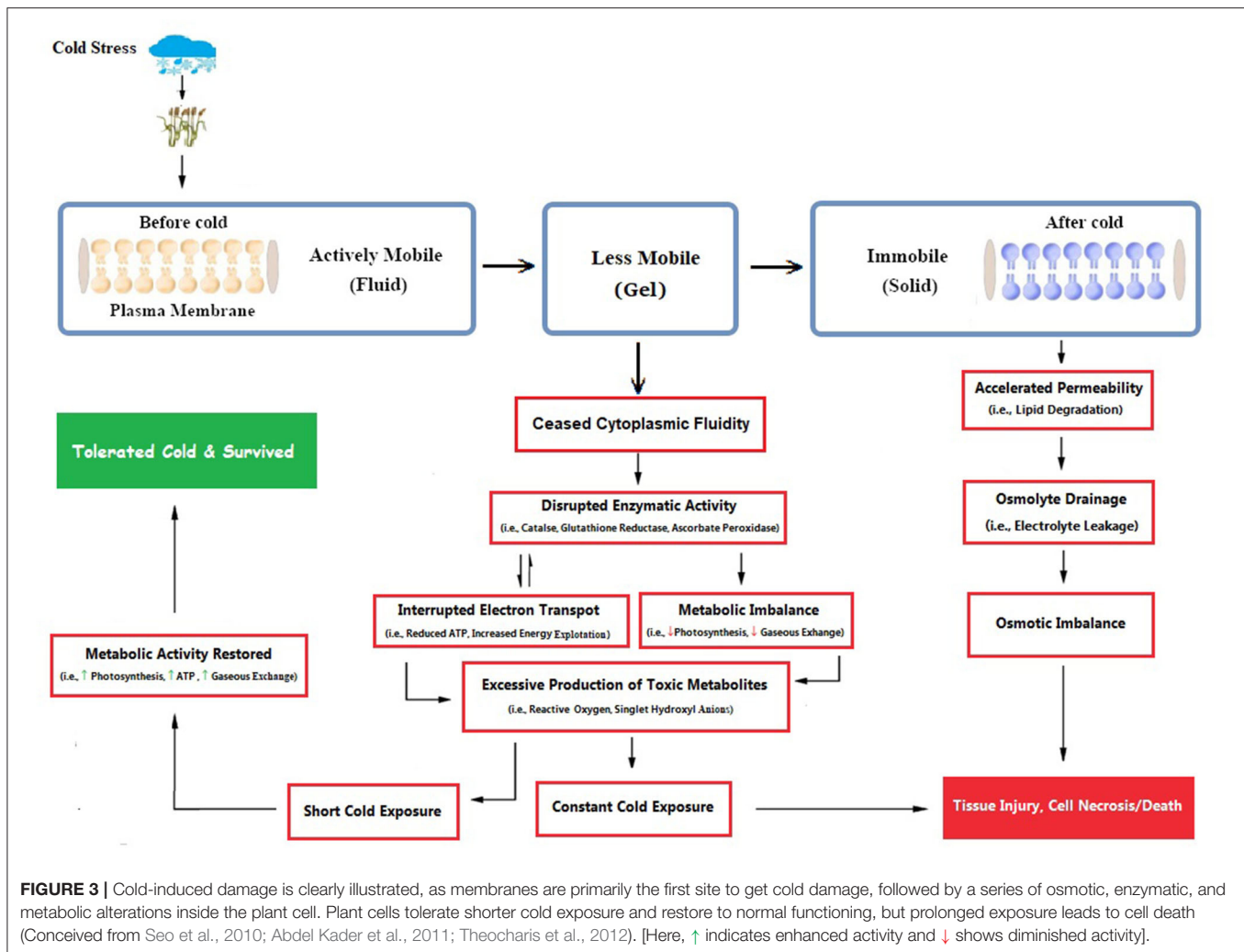
Respiration

The cold stress directly or indirectly induces a series of changes in biological and biochemical functions of the wheat plant, such as decreased respiration rate, reduced enzymatic activity, oxidative stress, and deterioration of seed reserves (Li et al., 2013; Esim et al., 2014). Cold-sensitive plant species, in general, show imbalanced homeostasis of respiration in leaves compared with tolerant species (Yamori et al., 2009). A low respiration rate at the initial seedling stage limits the ATP synthesis; subsequently, the germination process is hindered (Cheplick and Priestley,

1986). The prolonged cold stress period causes severe damage to the mitochondrial structure, slows down the flow of kinetic energy, and disrupts enzymatic activity, ultimately diminishing the respiration rate (Pomeroy and Andrews, 1975; Ikkonen et al., 2020). There are not enough literature studies found in this aspect; particularly for wheat, it is still an under-explored area.

Some studies in soybean reported increased respiration rate under prolonged cold stress; the reason for such increase is irreversible metabolism (dysfunction) and accumulation of oxidized metabolites (Yadegari et al., 2008). Furthermore, it is evident from investigations that chilling triggers the alternative respiratory systems in wheat and maize. Such alternative systems of respiration play a pivotal role in mitigating chilling stress and reducing mitochondrial structural damage (Ribas-Carbo et al., 2000; Feng et al., 2008).

Respiration and photosynthesis are vital processes that define the fate of any plant life. And both physiological processes are prone to cold stress. Structural injury to mitochondria interrupts the energy flow; subsequently, the respiration process is restricted. Such conditions compelled the plant cell to exploit the energy molecules (ATP); energy imbalance disturbed the various biochemical reactions inside the plant cell. Rare studies depict that chilling prompted respiration activity through adopting alternative respiratory pathways and prevented the plant from structural damages.



Nutrient Uptake and Transport

Low-temperature stress affects cellular turgidity and instigates drought stress (Yadav, 2010). This drought situation reduces the root hydraulic conductivity, limits the root growth, and dents the leaf turgidity in wheat (Siddique et al., 2000), which causes unavoidable wilting of leaves. Subsequently, water relations, nutrient uptake, carbohydrate metabolism, and translocation of assimilates are severely disrupted (Li et al., 1994). Apart from this, temperature fluctuation trends alter the soil physiochemical properties that disturb the beneficial microbial activity in the soil and influence plant-nutrient relationships (Jezierska-Tys et al., 2012; Massenssini et al., 2015). Further, low temperature slows down root growth and development by reducing root length and biomass. Such a reduction in root volume minimizes the root opportunities to explore new water and nutrient resources; consequently, mineral uptake is severely reduced (Al-Hamdani et al., 1990), resulting in decreased aboveground biomass. Despite the disruption of primary nutrients (NPK), water-deficient conditions also triggered the micronutrient (i.e., Mn, Zn, Fe, Mo, etc.) deficiencies in the plant (Gavito et al., 2001), which otherwise are readily available under well-watered conditions.

In conclusion, there is a direct relationship between nutrient acquisition concerning soil temperature and available soil moisture. It is well-evidenced that chilling and drought directly influence the macro and micronutrient availability, uptake, inflow transport, enzymatic activity, and other metabolic activities in plants. Only few previous studies have been reported on nutrient relations for chilling and drought stress factors; hence, there is a dire need for further investigation.

COLD TOLERANCE AND MOLECULAR RESPONSE

Most of the cereal crops tend to survive and continue their life cycle by developing their tolerance ability under increasing freezing degrees (Dubcovsky and Dvorak, 2007; Thomashow, 2010), through exhibiting a wide range of genetic expressions; such a behavior is termed as cold acclimation (Monroy et al., 2007). Plants having a higher capacity of cold acclimation have more survival chances (McKhann et al., 2008). Generally, winter cereals (wheat) have two types of cultivars: cold sensitive and cold

tolerant. Cold tolerant varieties have a higher capacity to tolerate sub-optimal cold stress; on the other hand, cold sensitive varieties cannot withstand harsh cold conditions. However, winter wheat cultivars having the ability to tolerate suboptimal conditions also requires adequate exposure to non-freezing low temperature, which is crucial for acclimatizing freezing stress (Sung and Amasino, 2005; Majláth et al., 2012). It is revealed in recent developments that the ability of plants to acclimate to the severity of winter gradually decreases with consistent changes in climatic attributes (Dalmannsdottir et al., 2017). Cold acclimation is a complex phenomenon of winter annuals that is accomplished by an extensive range of physiological, biochemical, and molecular changes (Figures 3, 4), which begins with membrane alterations and transforms it into a rigid structure (Theocharis et al., 2012; Takahashi et al., 2013).

Cold Responsive Protein Expressions

It is stated that the counter action of plants to low-temperature stress is carried out through detection (sensing) of stress followed by signal perception, transduction, and induction of cold-tolerant gene expression (Ganeshan et al., 2008). Plenty of cold responsive genes have been found in wheat (Guo et al., 2019) and are recognized as Dehydrin (DHN), Late Embryogenesis Abundance (LEA), Cold responsive (COR), and Responsive to Absciscic Acid (RBA), among others. These genes are categorized into two parts (Seki et al., 2003): first, those that directly respond to low-temperature stress, i.e., LEA (Liu et al., 2016), and second, those proteins which take part in the regulation of other molecular expressions. In response to cold conditions, these proteins have several other functions as they are also involved in countering other abiotic stresses such as drought and salinity (Seki et al., 2003). During cold tolerance, multiple gene expressions (Arabidopsis, COR and Wheat, WCS) are generated and subsequently initiate the cascade of transcriptional, biochemical, and physiological events vital for cold tolerance in the plant (Kosová et al., 2008). These cold regulatory responses include the release of Ca^{2+} , accumulation of osmolytes and reduced water content (Thakur and Nayyar, 2013), ROS scavenging (Larcher, 2003), and carbon metabolic adjustments (Ruelland and Zachowski, 2010). Gene expression, in winter wheat, against cold stress is generated after 1 day (Kurepin et al., 2013), as complete gene expression does necessarily require frequent cold exposure (Ruelland and Zachowski, 2010). The required threshold temperature for initiating this tolerant mechanism varies within two different cultivars of the same species; winter wheat cultivar Norstar and spring wheat cultivar Maintou have rational threshold temperatures of 18 and 8°C, respectively (Fowler, 2008). For the best cold acclimation, the temperature must fall below the threshold level as the acclimation rate is inverse to temperature drop (Chinnusamy et al., 2003).

Role of ABA in Gene Expression

Absciscic acid induces multiple changes in plant growth, development, and various physiological and molecular processes to cope with stress conditions. It plays a vital role in the tolerance against suboptimal temperature stress by inducing

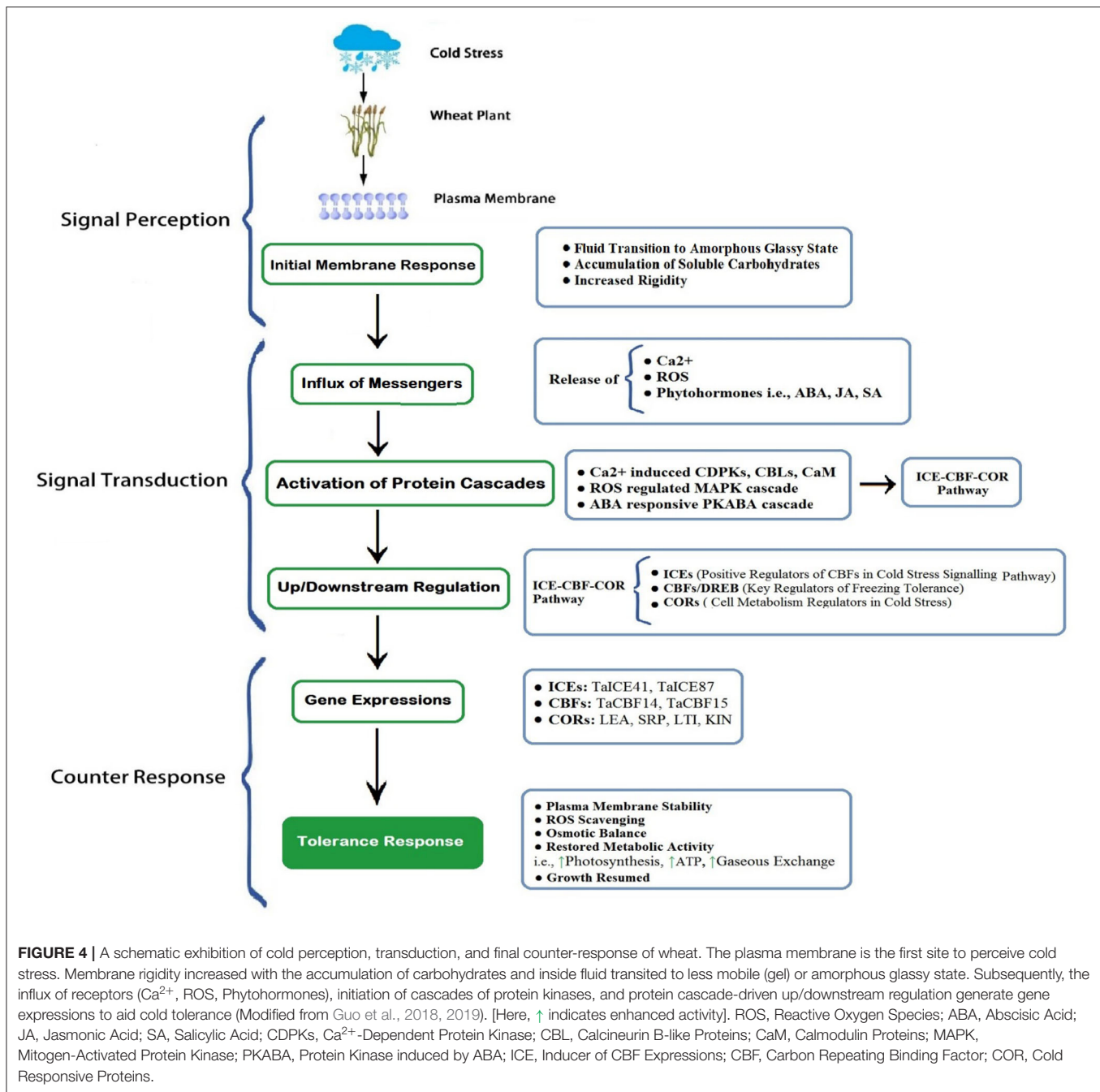
dehydration tolerance gene expressions (Shen et al., 2003). Subjecting to the role of ABA in cold tolerance mechanism (i.e., signaling, perception, and then transduction), it is categorized into two major pathways: ABA-dependent and ABA-independent pathways (Knox et al., 2008; Roychoudhury et al., 2013). ABA-dependent signaling perception of cold stress required ABA activation and vice versa. The gene expressions induced by ABA are carried out through the interaction of various transcriptional factors (such as MYC/MYB, RD22BPI, AREB1, and DREB2A) and their matching cis-elements (such as MYCRS/MYBRS, ABRE, and DRE/CRT), respectively (Tuteja, 2007; Morran et al., 2011).

Absciscic Acid-Dependent Pathway

Generally, stress accelerates the biosynthesis of ABA, followed by the closure of stomata and gene expressions (Lee and Luan, 2012). ABA is a primary intracellular receptor that stimulates the activity of secondary messengers, i.e., ROS and Ca^{2+} (Xue-Xuan et al., 2010). The instant signal perception of abiotic stress is transduced via the increased ROS and hydrogen peroxide (H_2O_2) (Saxena et al., 2016). ROS oxidative surge responded by the release of Ca^{2+} (Rao et al., 2006) that triggers the NADPH oxidase course of action and subsequently proceeds to the accumulation of antioxidant compounds (i.e., H_2O_2) (Agarwal et al., 2005). Therefore, Ca^{2+} is recognized as an essential component in signal transduction. Primarily, three types of Ca^{2+} proteins include CaM (calmodulin), Ca^{2+} dependent kinases, and calcineurin binding proteins. CaM was found to regulate the CBF regulon by binding with the regulatory element of gene promoter and help in cold tolerance (Doherty et al., 2009). Enhanced Ca^{2+} concentration initiates the calcium-regulated protein kinase (CDPKs), which helps in mitigating cold stress. Among 20 CDPKs, 7 responded to various abiotic stresses (Li et al., 2008). ABA-dependent pathway is also dependent on MYB/MYC (myeloblastosis) transcription factors (TFs) (Abe et al., 2003). Among 60 MYB genes of wheat, 15 were characterized as ABA regulated genes (Zhang et al., 2012), such as *TaMYB33*, which plays a part in the production of antioxidants, favoring ROS scavenging, assisting in proline accumulation, and modifying osmotic imbalance (Qin et al., 2012).

Absciscic Acid-Independent Pathway

Cereal crops (wheat, barley, and rye) from the Poaceae family contain a large number of DRE or CBF genes, as only wheat contains 25 various kinds of CBF genes (Badawi et al., 2007). COR gene expressions are mainly regulated by CBF TFs (CBF1, CBF2, and CBF3) (Thomashow, 2001). In wheat, the role of CBF has been well-recognized toward many signal perception pathways and enhanced cold tolerance capacity (Morran et al., 2011). Vágújfalvi et al. (2003) found a positive comparative relationship between COR expression and wheat cold acclimation. The COR proteins are labeled as hydrophilic proteins that are considered affiliated with LEA or DHNs (Close, 1997). For instance, in *Arabidopsis thaliana*, overexpression of LEA and wheat cold specific (WCS19) augments the freeze tolerance capacity (Dong et al., 2002). DHNs or LEA protein groups are highly tolerant to osmotic stress, as cold stress also



causes an osmotic imbalance in winter cereals. Hence, their accumulation is equally essential in cold acclimation (Borovskii et al., 2005). The *WCS120* is an impressive cold responsive gene of wheat; it also belongs to the LEA protein family (Fowler, 2001). Along with *WCS120*, other COR genes responsible for cold tolerance include *WCS180*, *WCS200*, *WCS66*, and *WCS40* (Sarhan et al., 1997); however, proteins that belong to *WCS120* showed higher transduction in winter cereals and were characterized as best in cold tolerance (Vítámvás and Prášil, 2008).

Accumulation of Soluble Sugars

Accumulation of soluble sugars is another easier tactic against cold stress. Plants belonging to cereals and grasses families accumulate fructans (fructose polymers derived from sucrose) upon exposure to a cold environment, which plays a stabilizer role in preventing membrane (Livingston et al., 2009). Yokota et al. (2015) also stated a positive correlation between the accumulation of fructans and cold tolerance in wheat plants with varying intensity of cold stress. Carbohydrates accumulation under suboptimal conditions partially support reaching cold

tolerance during acclimation (Yoshida et al., 1998; Janská et al., 2010).

Although their specific role at sub-optimal temperature is not fully understood, they are primarily considered as compatible osmoprotectants, ROS scavengers, and signaling compounds. Some plant studies revealed that accumulation of oligosaccharides upon cold exposure anchors the acclimation process (Janská et al., 2010; Theocharis et al., 2012). Fernandez et al. (2010) discussed the role of trehalose (glucose disaccharide) in regulating the cold-tolerant ability, and it is supposed to be involved in starch-accumulation.

Studies on photosynthesis have revealed that some cultivars of winter wheat, compared with spring wheat, sustain carbon assimilation even at cold temperatures, which is associated with increased concentrations of sucrose biosynthetic enzymes (Savitch et al., 1997). Hence, spring wheat lacks in sustaining carbon metabolism under harsh low-temperature conditions. Similarly, another investigation on spring and winter wheat depicted the increased carbohydrate (i.e., sucrose, fructose, and glucose) content in winter wheat, but no upsurge was found in spring wheat, and it also confirmed the role of carbohydrates in the inability of wheat crops to counter low-temperature stresses during spring (Hurry et al., 1995). The role of soluble sugars in responding to the cold signal in plants can be further investigated by advanced molecular techniques to examine how sugar regulates gene expression in a cold environment.

MANAGEMENT STRATEGIES

Several adaptation strategies facilitate the wheat crops to minimize the negative impacts of low-temperature extremes and are valuable in maintaining global food security. Crop husbandry practices, including the selection of cold-tolerant varieties, nutrient management, appropriate sowing technique and time, seed enhancements, exogenous application of osmoprotectants, and irrigation management, may help improve cold tolerance in wheat. Exogenous application of organic compounds, such as plant polyamines and their derivatives, are considered to be more helpful in enduring both (high and low) temperature extremes (Liu et al., 2007).

Breeding Advancement Through Implying Multi-Disciplinary Technologies

Breeders are continuously in the quest for developing new cultivars that are more compatible with changing environmental conditions. However, traditional breeding techniques require more than 10 years to develop a new variety. Sudden changes in climatic conditions, especially temperature extremes with drought, are a real challenge for breeders, as it limits the efficiency of new cultivars for a longer time. Along with conventional breeding techniques, it is necessary to implement modern disciplinary techniques in a simultaneous manner, e.g., aid of crop simulation models (i.e., CERES-Wheat Model) is handy in predicting the life duration of the particular cultivar in varying weather extremes and future development of varieties (Koç, 2020). Future assessments will sustainably ensure food security

(like availability, accessibility, and continuity) for the growing population (Ray et al., 2013), and it provides enough time for taking decisions against upcoming weather extremes (Archer, 2003). Crop simulation techniques are best in identifying the possible future threats to crop cultivation (Olesen et al., 2007). Furthermore, the addition of modern molecular strategies (like genomics, omics, gene silencing, inducing stress-specific genes, accelerated marker aided selection) and their significance count in the development of high yielding wheat cultivars (Ahmad et al., 2014; Jha et al., 2017). In contrast with traditional breeding tactics, these approaches are more advantageous in improving crop stress responses toward cold and drought conditions (Chaves and Oliveira, 2004).

Crop Husbandry Practices

Crop husbandry practices may help wheat performance under cold stress. The practices included are as follows: (1) seed enhancements (Farooq et al., 2017), (2) plant seeds of improved wheat varieties following the appropriate planting geometry at optimum sowing time with precision planting (Lamichhane and Soltani, 2020), (3) exogenous application of osmoprotectants, (4) seed inoculation with rhizobacteria (Shirinbayan et al., 2019), (5) nutrient management, and (6) irrigation management.

Positive impacts of seed priming techniques are elucidated in various crop plants under chilling stress (Jisha et al., 2013; Paparella et al., 2015). Primed seeds under low-temperature stress showed enhanced germination rate, improved vigor, and uniform stand establishment, leading to increased crop quality and produce (Paparella et al., 2015). At present, many priming techniques are in practice, such as hormonal priming, biological priming, redox priming, and chemical priming. (Wang et al., 2016). Along with cold stress, these techniques are vital in improving economic output and quality of wheat (Khaliq et al., 2015), maize (Foti et al., 2008), cotton (Casenave and Toselli, 2007), and other field crops.

The foliar application of nutrients and growth hormones is another effective agronomic approach to acclimate the low-temperature stress. Applying phytohormones [i.e., strigolactone, ABA, salicylic acid (SA), jasmonates] accelerate the various protein cascades associated with the expression of cold tolerance genes (Kolaksazov et al., 2013). It also plays a significant role in root-shoot signaling (Wilkinson et al., 2012) and is known to be efficient in minimizing the impact of chilling (Miura and Tada, 2014) and freezing stress (Taşgün et al., 2003).

Additionally, wheat growth sustainability under unfavorable environmental conditions can be achieved by following the agronomic fundamentals, such as optimum planting time, that varies for different regions and cultivars. Optimal sowing time can be determined by certain climatic factors (i.e., air temperature, soil temperature, and moisture content under different climatic conditions). As sowing time depends on climatic variables, it is too difficult to figure out conventional farming approaches under changing climate trends. Therefore, decision support tools of crop modeling are very useful in estimating the optimum sowing time for field crops (Waha et al., 2012). Crop modeling tools can make considerable

improvement in evaluating better management strategies for future climatic threats.

Thus, adapting interdisciplinary integrated approaches to tackle the several alarming fronts of climate variability and to ensure the food security of growing populations of the world is urgently needed.

CONCLUSION AND PROSPECTS

Cold stress causes morphological, physiological, biochemical, and molecular modifications in wheat. Although most winter wheat cultivars tend to tolerate such severe low-temperature extremes, prolonged exposure may result in partial or sometimes complete failure of the final produce. Such an environment/climate induces multiple alterations throughout the crop life cycle, from germination to harvesting. At the early growth stage, suboptimal temperature inhibits the seedling growth and inhibits the developmental process as reduced leaf size, diminished peduncle elongation, and decreased number of tillers and spikes. During the reproductive stage, cold stress results in pollen infertility, floret abortion, reduced fertilization, delayed maturity, and a reduced number of grains. Subsequently, it leads to significant yield losses. Besides, it is well-explained how low-temperature stress influenced physiological and biochemical events, including photosynthesis, respiration, energy imbalance, nutrients, and water relations. Further, to combat cold stress conditions, crop plants exhibit several biochemical and molecular expressions. In addition, the cold-response of wheat can be better regulated by integrating breeding and agronomic approaches, such as phenotypic screening of cold-tolerant genes, pre-sowing seed treatments, and exogenous application of growth hormones.

Due to unexpected climate changes in the last few decades, winter becomes shorter with more severity, damaging winter cereals. There is a greater need to explore and focus on the genetic traits of wheat, due to which it withstands under cold stress and continue their normal growth and development. In

this regard, traditional breeding will favor exploiting the wild wheat sources that are more adaptable to natural environmental conditions. It was further improved by identifying diversified genetic traits and mapping through various gene mapping tools, such as QTL mapping and genome-wide association studies (GWAS). In addition, precise and correct gene editing, such as the CRISPR-Cas9 system, will incorporate high yielding cultivars by using genetic engineering techniques. It will also help in ensuring global food security in both quality and quantity aspects.

Apart from this, many other osmolytes (such as glycine betaine) and plant hormones (such as brassinosteroids, ABA, SA, strigolactone) are still not well-exploited and are easier in regulating the plant responses against cold stress. That is why adopting integrated multi-disciplinary approaches to explore these missing links and explore new research horizons is currently needed.

AUTHOR CONTRIBUTIONS

MH and CX conceived the concept of the review and prepared an outline of the review. MH, CX, ZY, XH, and ZL compiled the literature and wrote the different sections. KY and AB aided in designing figures and arranging references. MF and NM provided technical assistance and editing support. All authors contributed to the article and approved the submitted version.

FUNDING

The work was supported by a grant from the China National Key Research and Development Program (No. 2017YFD0300408) and the Natural science research project of Anhui Provincial Department of Education (No. KJ2019A0174).

ACKNOWLEDGMENTS

We thank Prof. Muhammad Farooq and Dr. Noor Muhammad for proofreading and rectifying the manuscript.

REFERENCES

- Abdel Kader, D. Z., Saleh, A. A. H., Elmeleigy, S. A., and Dosoky, N. S. (2011). Chilling-induced oxidative stress and polyamines regulatory role in two wheat varieties. *J. Taibah Univ. Sci.* 5, 14–24. doi: 10.1016/S1658-3655(12)60034-X
- Abe, H., Urao, T., Ito, T., Seki, M., Shinozaki, K., and Yamaguchi-Shinozaki, K. (2003). Arabidopsis AtMYC2 (bHLH) and AtMYB2 (MYB) function as transcriptional activators in abscisic acid signaling. *Plant Cell* 15, 63–78. doi: 10.1105/tpc.006130
- Acevedo, E., Silva, P., and Silva, H. (2009). *Wheat Growth and Physiology*. FAO Corporate Document Repository. Rome: FAO, 1–31.
- Agarwal, S., Sairam, R. K., Srivastava, G. C., and Meena, R. C. (2005). Changes in antioxidant enzymes activity and oxidative stress by abscisic acid and salicylic acid in wheat genotypes. *Biol. Plant.* 49, 541–550. doi: 10.1007/s10535-005-0048-z
- Ahmad, P., Wani, M. R., Mohd, R., Azooz, M. M., and Tran, L.-S. P. (2014). *Improvement of Crops in the Era of Climatic Changes*, eds P. Ahmad, M. R. Wani, M. M. Azooz, and L.-S. P. Tran (New York, NY: Springer New York), 95–101. doi: 10.1007/978-1-4614-8824-8
- Ahrens, J. F., and Loomis, W. E. (1963). Floral induction and development in winter wheat ¹. *Crop Sci.* 3, 463–466. doi: 10.2135/cropsci1963.0011183X000300060001x
- Al-Hamdani, S. H., Todd, G. W., and Francko, D. A. (1990). Response of wheat growth and CO₂ assimilation to altering root-zone temperature. *Can. J. Bot.* 68, 2698–2702. doi: 10.1139/b90-341
- Archer, E. (2003). “Critical areas for improvement in the ability of SADC agricultural sector to benefit from seasonal forecasts,” in *Insights and Tools for Adaptation: Learning From Climate Variability Workshop* (Washington, DC: Sue Walker).
- Aroca, R., Porcel, R., and Ruiz-Lozano, J. M. (2012). Regulation of root water uptake under abiotic stress conditions. *J. Exp. Bot.* 63, 43–57. doi: 10.1093/jxb/err266
- Augsburger, C. K. (2013). Reconstructing patterns of temperature, phenology, and frost damage over 124 years: Spring damage risk is increasing. *Ecology* 94, 41–50. doi: 10.1890/12-0200.1
- Austin, R. B. (1990). *Prospects for Genetically Increasing the Photosynthetic Capacity of Crops*. New York, NY: Allan R. Liss.
- Badawi, M., Danyluk, J., Boucho, B., Houde, M., and Sarhan, F. (2007). The CBF gene family in hexaploid wheat and its relationship to the

- phylogenetic complexity of cereal CBFs. *Mol. Genet. Genomics* 277, 533–554. doi: 10.1007/s00438-006-0206-9
- Barton, D. A., Cantrill, L. C., Law, A. M. K., Phillips, C. G., Sutton, B. G., and Overall, R. L. (2014). Chilling to zero degrees disrupts pollen formation but not meiotic microtubule arrays in *Triticum aestivum* L. *Plant Cell Environ.* 37, 2781–2794. doi: 10.1111/pce.12358
- Basu, S., Ramegowda, V., Kumar, A., and Pereira, A. (2016). Plant adaptation to drought stress [version 1; referees: 3 approved]. *F1000Research* 5:1554. doi: 10.12688/f1000research.7678.1
- Bohn, M., Luthje, S., Sperling, P., Heinz, E., and Dörffling, K. (2007). Plasma membrane lipid alterations induced by cold acclimation and abscisic acid treatment of winter wheat seedlings differing in frost resistance. *J. Plant Physiol.* 164, 146–156. doi: 10.1016/j.jplph.2005.12.008
- Borovskii, G. B., Stupnikova, I. V., Antipina, A. I., Anuchina, O. S., and Voinikov, V. K. (2005). Association of dehydrins with wheat mitochondria during low-temperature adaptation. *Russ. J. Plant Physiol.* 52, 194–198. doi: 10.1007/s11183-005-0029-2
- Bota, J., Medrano, H., and Flexas, J. (2004). Is photosynthesis limited by decreased Rubisco activity and RuBP content under progressive water stress? *New Phytol.* 162, 671–681. doi: 10.1111/j.1469-8137.2004.01056.x
- Buriro, M., Wadhay Gandahi, A., Chand Oad, F., Ibrahim Keerio, M., Tunio, S., Waseem Hassan, S. U., et al. (2011). Wheat seed germination under the influence of temperature regimes. *Sarhad* 27, 539–543.
- Casenave, E. C., and Toselli, M. E. (2007). Hydropriming as a pre-treatment for cotton germination under thermal and water stress conditions. *Seed Sci. Technol.* 35, 88–98. doi: 10.15258/sst.2007.35.1.08
- Chakrabarti, B., Singh, S., Nagarajan, S., and Aggarwal, P. (2011). *Impact of Temperature on Phenology and Pollen Sterility of Wheat Varieties*. Brisbane, QLD: Southern Cross Publishing.
- Chaves, M. M., and Oliveira, M. M. (2004). Mechanisms underlying plant resilience to water deficits: prospects for water-saving agriculture. *J. Exp. Bot.* 2365–2384. doi: 10.1093/jxb/erh269
- Cheplick, G. P., and Priestley, D. A. (1986). *Seed Aging: Implications for Seed Storage and Persistence in the Soil*. Ithaca, NY: Comstock Associates, 304. doi: 10.2307/2996373
- Chinnusamy, V., Ohta, M., Kanrar, S., Lee, B., ha, Hong, X., Agarwal, M., et al. (2003). ICE1: a regulator of cold-induced transcriptome and freezing tolerance in arabidopsis. *Genes Dev.* 17, 1043–1054. doi: 10.1101/gad.1077503
- Close, T. J. (1997). Dehydrins: a commonality in the response of plants to dehydration and low temperature. *Physiol. Plant.* 100, 291–296. doi: 10.1111/j.1399-3054.1997.tb04785.x
- Crimp, S. J., Zheng, B., Khimashia, N., Gobbett, D. L., Chapman, S., Howden, M., et al. (2016). Recent changes in southern Australian frost occurrence: implications for wheat production risk. *Crop Pasture Sci.* 67, 801–811. doi: 10.1071/CP16056
- Crome, M. G., Wright, D. S. C., and Boddington, H. J. (1998). Effects of frost during grain filling on wheat yield and grain structure. *New Zeal. J. Crop Hortic. Sci.* 26, 279–290. doi: 10.1080/01140671.1998.9514065
- Cvetkovic, J., Müller, K., and Baier, M. (2017). The effect of cold priming on the fitness of Arabidopsis thaliana accessions under natural and controlled conditions. *Sci. Rep.* 7:44055. doi: 10.1038/srep44055
- Dahal, K., Kane, K., Gadapati, W., Webb, E., Savitch, L. V., Singh, J., et al. (2012). The effects of phenotypic plasticity on photosynthetic performance in winter rye, winter wheat and *Brassica napus*. *Physiol. Plant.* 144, 169–188. doi: 10.1111/j.1399-3054.2011.01513.x
- Dalmannsdottir, S., Jørgensen, M., Rapacz, M., Østrem, L., Larsen, A., Rødven, R., et al. (2017). Cold acclimation in warmer extended autumns impairs freezing tolerance of perennial ryegrass (*Lolium perenne*) and timothy (*Phleum pratense*). *Physiol. Plant.* 160, 266–281. doi: 10.1111/ppl.12548
- Doherty, C. J., Van Buskirk, H. A., Myers, S. J., and Thomashow, M. F. (2009). Roles for Arabidopsis CAMTA transcription factors in cold-regulated gene expression and freezing tolerance. *Plant Cell* 21, 972–984. doi: 10.1105/tpc.108.063958
- Dolferus, R., Ji, X., and Richards, R. A. (2011). Abiotic stress and control of grain number in cereals. *Plant Sci.* 181, 331–341. doi: 10.1016/j.plantsci.2011.05.015
- Dong, N., C., Danyluk, J., Wilson, K. E., Pocock, T., Huner, N. P. A., et al. (2002). Cold-regulated cereal chloroplast late embryogenesis abundant-like proteins. molecular characterization and functional analyses. *Plant Physiol.* 129, 1368–1381. doi: 10.1104/pp.001925
- Dubcovsky, J., and Dvorak, J. (2007). Genome plasticity a key factor in the success of polyploid wheat under domestication. *Science* 316, 1862–1866. doi: 10.1126/science.1143986
- Equiza, M. A., Miravé, J. P., and Tognetti, J. A. (2001). Morphological, anatomical and physiological responses related to differential shoot vs. root growth inhibition at low temperature in spring and winter wheat. *Ann. Bot.* 87, 67–76. doi: 10.1006/anbo.2000.1301
- Esim, N., Atici, O., and Mutlu, S. (2014). Effects of exogenous nitric oxide in wheat seedlings under chilling stress. *Toxicol. Ind. Health* 30, 268–274. doi: 10.1177/0748233712457444
- Evans, L. (1975). “Wheat. In L.T.,” in *Crop Physiology*, ed L. T. Evans (Cambridge: Cambridge University Press), 101–149.
- FAO (2020). *Responding to the Impact of the COVID-19 Outbreak on Food Value Chains Through Efficient Logistics*. Rome: FAO.
- Farooq, M., Aziz, T., Wahid, A., Lee, D. J., and Siddique, K. H. M. (2009). Chilling tolerance in maize: agronomic and physiological approaches. *Crop Pasture Sci.* 60, 501–516. doi: 10.1071/CP08427
- Farooq, M., Hussain, M., Nawaz, A., Lee, D. J., Alghamdi, S. S., and Siddique, K. H. M. (2017). Seed priming improves chilling tolerance in chickpea by modulating germination metabolism, trehalose accumulation and carbon assimilation. *Plant Physiol. Biochem.* 111, 274–283. doi: 10.1016/j.plaphy.2016.12.012
- Feng, H., Li, X., Duan, J., Li, H., and Liang, H. (2008). Chilling tolerance of wheat seedlings is related to an enhanced alternative respiratory pathway. *Crop Sci.* 48, 2381–2388. doi: 10.2135/cropsci2007.04.0232
- Fernandez, O., Béthencourt, L., Quero, A., Sangwan, R. S., and Clément Christophe, C. (2010). Trehalose and plant stress responses: friend or foe? *Trends Plant Sci.* 15, 409–417. doi: 10.1016/j.tplants.2010.04.004
- Fischer, R. A. (1985). Number of kernels in wheat crops and the influence of solar radiation and temperature. *J. Agric. Sci.* 105, 447–461. doi: 10.1017/S0021859600056495
- Foti, R., Abureni, K., Tigere, A., Gotosa, J., and Gere, J. (2008). The efficacy of different seed priming osmotic on the establishment of maize (*Zea mays* L.) caryopses. *J. Arid Environ.* 72, 1127–1130. doi: 10.1016/j.jaridenv.2007.11.008
- Fowler, D. B. (2001). Photoperiod and temperature interactions regulate low-temperature-induced gene expression in barley. *Plant Physiol.* 127, 1676–1681. doi: 10.1104/pp.010483
- Fowler, D. B. (2008). Cold acclimation threshold induction temperatures in cereals. *Crop Sci.* 48, 1147–1154. doi: 10.2135/cropsci2007.10.0581
- Frederiks, T. M., Christopher, J. T., Sutherland, M. W., and Borrell, A. K. (2015). Post-head-emergence frost in wheat and barley: defining the problem, assessing the damage, and identifying resistance. *J. Exp. Bot.* 66, 3487–3498. doi: 10.1093/jxb/erv088
- Fuller, M. P., Fuller, A. M., Kaniouras, S., Christophers, J., and Fredericks, T. (2007). The freezing characteristics of wheat at ear emergence. *Eur. J. Agron.* 26, 435–441. doi: 10.1016/j.eja.2007.01.001
- Ganeshan, S., Vitamvas, P., Fowler, D. B., and Chibbar, R. N. (2008). Quantitative expression analysis of selected COR genes reveals their differential expression in leaf and crown tissues of wheat (*Triticum aestivum* L.) during an extended low temperature acclimation regimen. *J. Exp. Bot.* 59, 2393–2402. doi: 10.1093/jxb/ern112
- Gavito, M. E., Curtis, P. S., Mikkelsen, T. N., and Jakobsen, I. (2001). Interactive effects of soil temperature, atmospheric carbon dioxide and soil N on root development, biomass and nutrient uptake of winter wheat during vegetative growth. *J. Exp. Bot.* 52, 1913–1923. doi: 10.1093/jexbot/52.362.1913
- Groom, Q. J., Long, S. P., and Baker, N. R. (1990). “Photoinhibition of photosynthesis in a winter wheat crop,” in *Current Research in Photosynthesis*, ed H. Baltscheffsky (Stockholm: Springer), 1423–1426. doi: 10.1007/978-94-009-0511-5_329
- Gu, L., Hanson, P. J., Post, W., Mac Kaiser, D. P., Yang, B., Nemani, R., et al. (2008). The 2007 eastern US spring freeze: increased cold damage in a warming world? *Bioscience* 58, 253–262. doi: 10.1641/B580311
- Guo, J., Ren, Y., Tang, Z., Shi, W., and Zhou, M. (2019). Characterization and expression profiling of the ICE-CBF-COR genes in wheat. *PeerJ* 2019, 1–19. doi: 10.7717/peerj.8190

- Guo, X., Liu, D., and Chong, K. (2018). Cold signaling in plants: Insights into mechanisms and regulation. *J. Integr. Plant Biol.* 60, 745–756. doi: 10.1111/jipb.12706
- Hasanfard, A., Rastgoo, M., Izadi Darbandi, E., Nezami, A., and Chauhan, B. S. (2021). Regeneration capacity after exposure to freezing in wild oat (*Avena ludoviciana* Durieu.) and turnipweed (*Rapistrum rugosum* (L.) All.) in comparison with winter wheat. *Environ. Exp. Bot.* 181:104271. doi: 10.1016/j.envexpbot.2020.104271
- Holman, J. D., Schlegel, A. J., Thompson, C. R., and Lingenfelter, J. E. (2011). Influence of precipitation, temperature, and 56 years on winter wheat yields in Western Kansas. *Crop Manag.* 4, 1–15. doi: 10.1094/CM-2011-1229-01-RS
- Hurry, V. M., Strand, Å., Tobiasen, M., Gardeström, P., and Öquist, G. (1995). Cold hardening of spring and winter wheat and rape results in differential effects on growth, carbon metabolism, and carbohydrate content. *Plant Physiol.* 109, 697–706. doi: 10.1104/pp.109.2.697
- Hussain, H. A., Hussain, S., Khaliq, A., Ashraf, U., Anjum, S. A., Men, S., et al. (2018). Chilling and drought stresses in crop plants: implications, cross talk, and potential management opportunities. *Front. Plant Sci.* 9:393. doi: 10.3389/fpls.2018.00393
- Ikeuchi, M., Ogawa, Y., Iwase, A., and Sugimoto, K. (2016). *Plant Regeneration: Cellular Origins and Molecular Mechanisms*. London: Company of Biologists Ltd. doi: 10.1242/dev.134668
- Ikkonen, E. N., Shibaeva, T. G., Sherudilo, E. G., and Titov, A. F. (2020). Response of winter wheat seedlings respiration to long-term cold exposure and short-term daily temperature drops. *Russ. J. Plant Physiol.* 67, 538–544. doi: 10.1134/S1021443720020065
- IPCC (2014). *The Physical Science Basis: Working Group I Contribution to the Fifth Assessment Report of the Intergovernmental Panel on Climate Change*. Cambridge: IPCC.
- Jame, Y. W., and Cutforth, H. W. (2004). Simulating the effects of temperature and seeding depth on germination and emergence of spring wheat. *Agric. For. Meteorol.* 124, 207–218. doi: 10.1016/j.agrformet.2004.01.012
- Janowiak, F., Maas, B., and Dörffling, K. (2002). Importance of abscisic acid for chilling tolerance of maize seedlings. *J. Plant Physiol.* 159, 635–643. doi: 10.1078/0176-1617-0638
- Janská, A., Maršík, P., Zelenková, S., and Ovesná, J. (2010). Cold stress and acclimation - what is important for metabolic adjustment? *Plant Biol.* 12, 395–405. doi: 10.1111/j.1438-8677.2009.00299.x
- Jezierska-Tys, S., Rachoń, L., Rutkowska, A., and Szumilo, G. (2012). Effect of new lines of winter wheat on microbiological activity in Luvisol. *Int. Agrophys.* 26, 33–38. doi: 10.2478/v10247-012-0005-y
- Jha, U. C., Bohra, A., and Jha, R. (2017). Breeding approaches and genomics technologies to increase crop yield under low-temperature stress. *Plant Cell Rep.* 36, 1–35. doi: 10.1007/s00299-016-2073-0
- Ji, H., Xiao, L., Xia, Y., Song, H., Liu, B., Tang, L., et al. (2017). Effects of jointing and booting low temperature stresses on grain yield and yield components in wheat. *Agric. For. Meteorol.* 243, 33–42. doi: 10.1016/j.agrformet.2017.04.016
- Jisha, K. C., Vijayakumari, K., and Puthur, J. T. (2013). Seed priming for abiotic stress tolerance: an overview. *Acta Physiol. Plant.* 35, 1381–1396. doi: 10.1007/s11738-012-1186-5
- Karimi, M., Golparvar, A. R., and Bahari, B. (2011). Evaluation of bread wheat varieties for chilling stress tolerance and their effective traits for higher grain yield. *Res. Crop.* 12, 633–639. Available online at: https://www.researchgate.net/publication/295646122_Evaluation_of_bread_wheat_cultivars_for_chilling_stress_tolerance_and_their_effective_traits_for_higher_grain_yield/citations
- Khaliq, A., Aslam, F., Matloob, A., Hussain, S., Geng, M., Wahid, A., et al. (2015). Seed priming with selenium: consequences for emergence, seedling growth, and biochemical attributes of rice. *Biol. Trace Elem. Res.* 166, 236–244. doi: 10.1007/s12011-015-0260-4
- Khan, T. A., Fariduddin, Q., and Yusuf, M. (2017). Low-temperature stress: is phytohormones application a remedy? *Environ. Sci. Pollut. Res.* 24, 21574–21590. doi: 10.1007/s11356-017-9948-7
- Knox, A. K., Li, C., Vágúfalvi, A., Galiba, G., Stockinger, E. J., and Dubcovsky, J. (2008). Identification of candidate CBF genes for the frost tolerance locus Fr-A m2 in *Triticum monococcum*. *Plant Mol. Biol.* 67, 257–270. doi: 10.1007/s11103-008-9316-6
- Koç, E. (2020). “Assessing climate change impacts on wheat production in Turkey and various adaptation strategies,” in *Climate Change and Food Security with Emphasis on Wheat*, eds M. Ozturk, and A. Gul (New York, NY: Elsevier), 43–54. doi: 10.1016/B978-0-12-819527-7.00003-0
- Kodra, E., Steinhäuser, K., and Ganguly, A. R. (2011). Persisting cold extremes under 21st-century warming scenarios. *Geophys. Res. Lett.* 38, 47–103. doi: 10.1029/2011GL047103
- Kolaksazov, M., Laporte, F., Ananieva, K., Dobrev, P., Herzog, M., and Ananiev, E. D. (2013). Effect of chilling and freezing stresses on jasmonate content in *Arabis alpina*. *Bulg. J. Agric. Sci.* 19, 15–17.
- Kosová, K., Prášil, I. T., and Vítámvás, P. (2008). The relationship between vernalization- and photoperiodically-regulated genes and the development of frost tolerance in wheat and barley. *Biol. Plant.* 52, 601–615. doi: 10.1007/s10535-008-0120-6
- Kratsch, H. A., and Wise, R. R. (2000). The ultrastructure of chilling stress. *Plant, Cell Environ.* 23, 337–350. doi: 10.1046/j.1365-3040.2000.00560.x
- Kul, R., Ekinci, M., Turan, M., Ors, S., and Yildirim, E. (2020). “How abiotic stress conditions affects plant roots,” in *Plant Roots [Working Title]*, ed E. Yildirim (London: IntechOpen), 6–10. doi: 10.5772/intechopen.95286
- Kurepin, L. V., Dahal, K. P., Savitch, L. V., Singh, J., Bode, R., Ivanov, A. G., et al. (2013). Role of CBFs as integrators of chloroplast redox, phytochrome and plant hormone signaling during cold acclimation. *Int. J. Mol. Sci.* 14, 12729–12763. doi: 10.3390/ijms140612729
- Lamichhane, J. R., and Soltani, E. (2020). Sowing and seedbed management methods to improve establishment and yield of maize, rice and wheat across drought-prone regions: a review. *J. Agric. Food Res.* 2:100089. doi: 10.1016/j.jafr.2020.100089
- Larcher, W. (2003). *Physiological Plant Ecology: Ecophysiology and Stress Physiology of Functional Groups*. Berlin: Springer Nature.
- Lee, S. C., and Luan, S. (2012). ABA signal transduction at the crossroad of biotic and abiotic stress responses. *Plant Cell Environ.* 35, 53–60. doi: 10.1111/j.1365-3040.2011.02426.x
- Leonardos, E. D., Savitch, L. V., Huner, N. P. A., Öquist, G., and Grodzinski, B. (2003). Daily photosynthetic and C-export patterns in winter wheat leaves during cold stress and acclimation. *Physiol. Plant.* 117, 521–531. doi: 10.1034/j.1399-3054.2003.00057.x
- Li, A. L., Zhu, Y. F., Tan, X. M., Wang, X., Wei, B., Guo, H. Z., et al. (2008). Evolutionary and functional study of the CDPK gene family in wheat (*Triticum aestivum* L.). *Plant Mol. Biol.* 66, 429–443. doi: 10.1007/s11103-007-9281-5
- Li, X., Cai, J., Liu, F., Dai, T., Cao, W., and Jiang, D. (2014). Spring freeze effect on wheat yield is modulated by winter temperature fluctuations: evidence from meta-analysis and simulating experiment. *J. Agron. Crop Sci.* 201, 288–300. doi: 10.1111/jac.12115
- Li, X., Cai, J., Liu, F., Zhou, Q., Dai, T., Cao, W., et al. (2015). Wheat plants exposed to winter warming are more susceptible to low temperature stress in the spring. *Plant Growth Regul.* 77, 11–19. doi: 10.1007/s10725-015-0029-y
- Li, X., Feng, Y., and Boersma, L. (1994). Partition of photosynthates between shoot and root in spring wheat (*Triticum aestivum* L.) as a function of soil water potential and root temperature. *Plant Soil* 164, 43–50. doi: 10.1007/BF00010109
- Li, X., Jiang, H., Liu, F., Cai, J., Dai, T., Cao, W., et al. (2013). Induction of chilling tolerance in wheat during germination by pre-soaking seed with nitric oxide and gibberellin. *Plant Growth Regul.* 71, 31–40. doi: 10.1007/s10725-013-9805-8
- Limin, A. E., and Fowler, D. B. (2006). Low-temperature tolerance and genetic potential in wheat (*Triticum aestivum* L.): response to photoperiod, vernalization, and plant development. *Planta* 224, 360–366. doi: 10.1007/s00425-006-0219-y
- Liu, J. H., Kitashiba, H., Wang, J., Ban, Y., and Moriguchi, T. (2007). Polyamines and their ability to provide environmental stress tolerance to plants. *Plant Biotechnol.* 24, 117–126. doi: 10.5511/plantbiotechnology.24.117
- Liu, L., Ji, H., An, J., Shi, K., Ma, J., Liu, B., et al. (2019). Response of biomass accumulation in wheat to low-temperature stress at jointing and booting stages. *Environ. Exp. Bot.* 157, 46–57. doi: 10.1016/j.envexpbot.2018.09.026
- Liu, Y., Dang, P., Liu, L., and He, C. (2019). Cold acclimation by the CBF-COR pathway in a changing climate: Lessons from *Arabidopsis thaliana*. *Plant Cell Rep.* 38, 511–519. doi: 10.1007/s00299-019-02376-3
- Liu, Y., Liang, J., Sun, L., Yang, X., and Li, D. (2016). Group 3 LEA protein, ZmLEA3, is involved in protection from low temperature stress. *Front. Plant Sci.* 7:1011. doi: 10.3389/fpls.2016.01011
- Livingston, D. P., Hincha, D. K., and Heyer, A. G. (2009). Fructan and its relationship to abiotic stress tolerance in plants.

- Cell. Mol. Life Sci.* 66, 2007–2023. doi: 10.1007/s00018-009-0002-x
- Los, D. A., Mironov, K. S., and Allakhverdiev, S. I. (2013). Regulatory role of membrane fluidity in gene expression and physiological functions. *Photosynth. Res.* 116, 489–509. doi: 10.1007/s11120-013-9823-4
- Lyons, J. M. (1973). Chilling injury in plants. *Annu. Rev. Plant Physiol.* 24, 445–466. doi: 10.1146/annurev.pp.24.060173.002305
- Majláth, I., Szalai, G., Soós, V., Sebestyén, E., Balázs, E., Vanková, R., et al. (2012). Effect of light on the gene expression and hormonal status of winter and spring wheat plants during cold hardening. *Physiol. Plant.* 145, 296–314. doi: 10.1111/j.1399-3054.2012.01579.x
- Marcellos, H., and Single, W. V. (1984). Frost injury in wheat ears after ear emergence. *Aust. J. Plant Physiol.* 11, 7–15. doi: 10.1071/PP9840007
- Massensini, A. M., Bonduki, V. H. A., Melo, C. A. D., Tótolá, M. R., Ferreira, F. A., and Costa, M. D. (2015). Relative importance of soil physico-chemical characteristics and plant species identity to the determination of soil microbial community structure. *Appl. Soil Ecol.* 91, 8–15. doi: 10.1016/j.apsoil.2015.02.009
- McKhann, H. I., Gery, C., Bérard, A., Lévêque, S., Zuther, E., Hinch, D. K., et al. (2008). Natural variation in CBF gene sequence, gene expression and freezing tolerance in the Versailles core collection of *Arabidopsis thaliana*. *BMC Plant Biol.* 8:105. doi: 10.1186/1471-2229-8-105
- Mian, M. A. R., and Nafziger, E. D. (1994). Seed size and water potential effects on germination and seedling growth of winter wheat. *Crop Sci.* 34, 169–171. doi: 10.2135/cropsci1994.0011183X003400010030x
- Miura, K., and Tada, Y. (2014). Regulation of water, salinity, and cold stress responses by salicylic acid. *Front. Plant Sci.* 5:4. doi: 10.3389/fpls.2014.00004
- Monroy, A. F., Dryanova, A., Malette, B., Oren, D. H., Ridha Farajalla, M., Liu, W., et al. (2007). Regulatory gene candidates and gene expression analysis of cold acclimation in winter and spring wheat. *Plant Mol. Biol.* 64, 409–423. doi: 10.1007/s11103-007-9161-z
- Morran, S., Eini, O., Pyvovarenko, T., Parent, B., Singh, R., Ismagul, A., et al. (2011). Improvement of stress tolerance of wheat and barley by modulation of expression of DREB/CBF factors. *Plant Biotechnol. J.* 9, 230–249. doi: 10.1111/j.1467-7652.2010.00547.x
- Nezhadhamadi, A., Prodhan, Z. H., and Faruq, G. (2013). Drought tolerance in wheat. *Sci. World J.* 2013, 2–7. doi: 10.1155/2013/610721
- Olesen, J. E., Carter, T. R., Díaz-Ambrona, C. H., Fronzek, S., Heidmann, T., Hickler, T., et al. (2007). Uncertainties in projected impacts of climate change on European agriculture and terrestrial ecosystems based on scenarios from regional climate models. *Clim. Change* 81, 123–143. doi: 10.1007/s10584-006-9216-1
- Oquist, G., Hurry, V. M., and Huner, N. P. A. (1993). *Low-Temperature Effects on Photosynthesis and Correlation with Freezing Tolerance in Spring and Winter Cultivars of Wheat and Rye*. Available online at: <https://plantphysiol.org> (accessed May 12, 2021). doi: 10.1104/pp.101.1.245
- Paparella, S., Araújo, S. S., Rossi, G., Wijayasinghe, M., Carbonera, D., and Balestrazzi, A. (2015). Seed priming: state of the art and new perspectives. *Plant Cell Rep.* 34, 1281–1293. doi: 10.1007/s00299-015-1784-y
- Paul, M. J., and Foyer, C. H. (2001). Sink regulation of photosynthesis. *J. Exp. Bot.* 52, 1383–1400. doi: 10.1093/jexbot/52.360.1383
- Pomeroy, M. K., and Andrews, C. J. (1975). Effect of temperature on respiration of mitochondria and shoot segments from cold hardened and nonhardened wheat and rye seedlings. *Plant Physiol.* 56, 703–706. doi: 10.1104/pp.56.5.703
- Pomeroy, M. K., and Andrews, C. J. (1978). Metabolic and ultrastructural changes in winter wheat during ice encasement under field conditions. *Plant Physiol.* 61, 806–811. doi: 10.1104/pp.61.5.806
- Porter, J. R., and Gawith, M. (1999). Temperatures and the growth and development of wheat: a review. *Eur. J. Agron.* 10, 23–36. doi: 10.1016/S1161-0301(98)00047-1
- Pujalon, S., Piola, F., and Bornette, G. (2008). Abiotic stresses increase plant regeneration ability. *Evol. Ecol.* 22, 493–506. doi: 10.1007/s10682-007-9177-5
- Qin, Y., Wang, M., Tian, Y., He, W., Han, L., and Xia, G. (2012). Over-expression of TaMYB33 encoding a novel wheat MYB transcription factor increases salt and drought tolerance in *Arabidopsis*. *Mol. Biol. Rep.* 39, 7183–7192. doi: 10.1007/s11033-012-1550-y
- Rajcan, I., and Swanton, C. J. (2001). Understanding maize-weed competition: Resource competition, light quality and the whole plant. *F. Crop. Res.* 71, 139–150. doi: 10.1016/S0378-4290(01)00159-9
- Rao, K. V. M., Raghavendra, A. S., and Reddy, K. J. (2006). *Physiology and Molecular Biology of Stress Tolerance in Plants*. Dordrecht: Springer Netherlands.
- Ray, D. K., Mueller, N. D., West, P. C., and Foley, J. A. (2013). Yield trends are insufficient to double global crop production by 2050. *PLoS ONE* 8:e66428. doi: 10.1371/journal.pone.0066428
- Ribas-Carbo, M., Aroca, R., Gonzalez-Meler, M. A., Irigoyen, J. J., and Sanchez-Diaz, M. (2000). The electron partitioning between the cytochrome and alternative respiratory pathways during chilling recovery in two cultivars of maize differing in chilling sensitivity. *Plant Physiol.* 122, 199–204. doi: 10.1104/pp.122.1.199
- Richner, W., Soldati, A., and Stamp, P. (1996). Shoot-to-root relations in field-grown maize seedlings. *Agron. J.* 88, 56–61. doi: 10.2134/agronj1996.00021962008800010012x
- Rinalducci, S., Egidi, M. G., Karimzadeh, G., Jazii, F. R., and Zolla, L. (2011). Proteomic analysis of a spring wheat cultivar in response to prolonged cold stress. *Electrophoresis* 32, 1807–1818. doi: 10.1002/elps.201000663
- Röder, M., Thornley, P., Campbell, G., and Bows-Larkin, A. (2014). Emissions associated with meeting the future global wheat demand: a case study of UK production under climate change constraints. *Environ. Sci. Policy* 39, 13–24. doi: 10.1016/j.envsci.2014.02.002
- Roychoudhury, A., Paul, S., and Basu, S. (2013). Cross-talk between abscisic acid-dependent and abscisic acid-independent pathways during abiotic stress. *Plant Cell Rep.* 32, 985–1006. doi: 10.1007/s00299-013-1414-5
- Ruelland, E., and Zachowski, A. (2010). How plants sense temperature. *Environ. Exp. Bot.* 69, 225–232. doi: 10.1016/j.envexpbot.2010.05.011
- Sarhan, F., Ouellet, F., and Vazquez-Tello, A. (1997). The wheat wcs120 gene family: a useful model to understand the molecular genetics of freezing tolerance in cereals. *Physiol. Plant.* 101, 439–445. doi: 10.1111/j.1399-3054.1997.tb01019.x
- Savitch, L. V., Gray, G. R., and Huner, N. P. A. (1997). Feedback-limited photosynthesis and regulation of sucrose-starch accumulation during cold acclimation and low-temperature stress in a spring and winter wheat. *Planta* 201, 18–26. doi: 10.1007/BF01258676
- Saxena, I., Srikanth, S., and Chen, Z. (2016). Cross talk between H₂O₂ and interacting signal molecules under plant stress response. *Front. Plant Sci.* 7:570. doi: 10.3389/fpls.2016.00570
- Seki, M., Kamei, A., Yamaguchi-Shinozaki, K., and Shinozaki, K. (2003). Molecular responses to drought, salinity and frost: common and different paths for plant protection. *Curr. Opin. Biotechnol.* 14, 194–199. doi: 10.1016/S0958-1669(03)00030-2
- Seo, P. J., Kim, M. J., Park, J. Y., Kim, S. Y., Jeon, J., Lee, Y. H., et al. (2010). Cold activation of a plasma membrane-tethered NAC transcription factor induces a pathogen resistance response in *Arabidopsis*. *Plant J.* 61, 661–671. doi: 10.1111/j.1365-313X.2009.04091.x
- Shen, Y. G., Zhang, W. K., He, S. J., Zhang, J. S., Liu, Q., and Chen, S. Y. (2003). An EREBP/AP2-type protein in *Triticum aestivum* was a DRE-binding transcription factor induced by cold, dehydration and ABA stress. *Theor. Appl. Genet.* 106, 923–930. doi: 10.1007/s00122-002-1131-x
- Shirinbayan, S., Khosravi, H., and Malakouti, M. J. (2019). Alleviation of drought stress in maize (*Zea mays*) by inoculation with *Azotobacter* strains isolated from semi-arid regions. *Appl. Soil Ecol.* 133, 138–145. doi: 10.1016/j.apsoil.2018.09.015
- Siddique, M. R. B., Hamid, A., and Islam, M. S. (2000). Drought stress effects on water relations of wheat. *Bot. Bull. Acad. Sin.* 41, 35–39.
- Spilde, L. A. (1989). Influence of seed size and test weight on several agronomic traits of barley and hard red spring wheat. *J. Prod. Agric.* 2, 169–172. doi: 10.2134/jpa1989.0169
- Stapper, M., and Fischer, R. A. (1990). Genotype, sowing date and plant spacing influence on high-yielding irrigated wheat in southern New South Wales. I Phasic development, canopy growth and spike production. *Aust. J. Agric. Res.* 41, 997–1019. doi: 10.1071/AR9900997
- Subedi, K. D., Gregory, P. J., Summerfield, R. J., and Gooding, M. J. (1998). Cold temperatures and boron deficiency caused grain set failure

- in spring wheat (*Triticum aestivum* L.). *F. Crop. Res.* 57, 277–288. doi: 10.1016/S0378-4290(97)00148-2
- Sung, S., and Amasino, R. M. (2005). Remembering winter: toward a molecular understanding of vernalization. *Annu. Rev. Plant Biol.* 56, 491–508. doi: 10.1146/annurev.arplant.56.032604.144307
- Takahashi, D., Li, B., Nakayama, T., Kawamura, Y., and Uemura, M. (2013). Plant plasma membrane proteomics for improving cold tolerance. *Front. Plant Sci.* 4:90. doi: 10.3389/fpls.2013.00090
- Taşgin, E., Atıcı, Ö., and Nalbantoglu, B. (2003). Effects of salicylic acid and cold on freezing tolerance in winter wheat leaves. *Plant Growth Regul.* 41, 231–236. doi: 10.1023/B:GROW.0000007504.41476.c2
- Thakur, P., Kumar, S., Malik, J. A., Berger, J. D., and Nayyar, H. (2010). Cold stress effects on reproductive development in grain crops: an overview. *Environ. Exp. Bot.* 67, 429–443. doi: 10.1016/j.envexpbot.2009.09.004
- Thakur, P., and Nayyar, H. (2013). “Facing the cold stress by plants in the changing environment: Sensing, signaling, and defending mechanisms,” in *Plant Acclimation to Environmental Stress* (New York, NY: Springer New York), 29–69. doi: 10.1007/978-1-4614-5001-6_2
- Theocharis, A., Clément, C., and Barka, E. A. (2012). Physiological and molecular changes in plants grown at low temperatures. *Planta* 235, 1091–1105. doi: 10.1007/s00425-012-1641-y
- Thomashow, M. F. (2001). So what's new in the field of plant cold acclimation? *Lots! Plant Physiol.* 125, 89–93. doi: 10.1104/pp.125.1.89
- Thomashow, M. F. (2010). Molecular basis of plant cold acclimation: insights gained from studying the CBF cold response pathway. *Plant Physiol.* 154, 571–577. doi: 10.1104/pp.110.161794
- Trione, E. J., and Metzger, R. J. (1970). Wheat and barley vernalization in a precise temperature gradient ¹. *Crop Sci.* 10, 390–392. doi: 10.2135/cropsci1970.0011183X001000040023x
- Trischuk, R. G., Schilling, B. S., Low, N. H., Gray, G. R., and Gusta, L. V. (2014). Cold acclimation, de-acclimation and re-acclimation of spring canola, winter canola and winter wheat: the role of carbohydrates, cold-induced stress proteins and vernalization. *Environ. Exp. Bot.* 106, 156–163. doi: 10.1016/j.envexpbot.2014.02.013
- Trnka, M., Rötter, R. P., Ruiz-Ramos, M., Kersebaum, K. C., and Olesen, J. E., Žalud, Z., et al. (2014). Adverse weather conditions for European wheat production will become more frequent with climate change. *Nat. Clim. Chang.* 4, 637–643. doi: 10.1038/nclimate2242
- Tuteja, N. (2007). Absciscic acid and abiotic stress signaling. *Plant Signal. Behav.* 2, 135–138. doi: 10.4161/psb.2.3.4156
- Vágújfalvi, A., Galiba, G., Cattivelli, L., and Dubcovsky, J. (2003). The cold-regulated transcriptional activator Cbf3 is linked to the frost-tolerance locus Fr-A2 on wheat chromosome 5A. *Mol. Genet. Genomics* 269, 60–67. doi: 10.1007/s00438-003-0806-6
- Valluru, R., Link, J., and Claupein, W. (2012). Consequences of early chilling stress in two *Triticum* species: plastic responses and adaptive significance. *Plant Biol.* 14, 641–651. doi: 10.1111/j.1438-8677.2011.00540.x
- Venzhik, Y. V., Titov, A. F., Talanova, V. V., Frolova, S. A., Talanov, A. V., and Nazarkina, Y. A. (2011). Influence of lowered temperature on the resistance and functional activity of the photosynthetic apparatus of wheat plants. *Biol. Bull.* 38, 132–137. doi: 10.1134/S1062359011020142
- Vítámvás, P., and Prášil, I. T. (2008). WCS120 protein family and frost tolerance during cold acclimation, deacclimation and reacclimation of winter wheat. *Plant Physiol. Biochem.* 46, 970–976. doi: 10.1016/j.plaphy.2008.06.006
- Waha, K., Van Bussel, L. G. J., Müller, C., and Bondeau, A. (2012). Climate-driven simulation of global crop sowing dates. *Glob. Ecol. Biogeogr.* 21, 247–259. doi: 10.1111/j.1466-8238.2011.00678.x
- Wang, H. F., Huo, Z. G., Zhou, G. S., Liao, Q. H., Feng, H. K., and Wu, L. (2016). Estimating leaf SPAD values of freeze-damaged winter wheat using continuous wavelet analysis. *Plant Physiol. Biochem.* 98, 39–45. doi: 10.1016/j.plaphy.2015.10.032
- Whaley, J. M., Kirby, E. J. M., Spink, J. H., Foulkes, M. J., and Sparkes, D. L. (2004). Frost damage to winter wheat in the UK: the effect of plant population density. *Eur. J. Agron.* 21, 105–115. doi: 10.1016/S1161-0301(03)00090-X
- Wilkinson, S., Kudoyarova, G. R., Veselov, D. S., Arkhipova, T. N., and Davies, W. J. (2012). Plant hormone interactions: innovative targets for crop breeding and management. *J. Exp. Bot.* 63, 3499–3509. doi: 10.1093/jxb/ers148
- Wu, Y. F., Zhong, X. L., Hu, X., Ren, D. C., Lv, G. H., Wei, C. Y., et al. (2014). Frost affects grain yield components in winter wheat. *New Zeal. J. Crop Hortic. Sci.* 42, 194–204. doi: 10.1080/01140671.2014.887588
- Xiao, L., Liu, L., Asseng, S., Xia, Y., Tang, L., Liu, B., et al. (2018). Estimating spring frost and its impact on yield across winter wheat in China. *Agric. For. Meteorol.* 260–261, 154–164. doi: 10.1016/j.agrformet.2018.06.006
- Xue-Xuan, X., Hong-Bo, S., Yuan-Yuan, M., Gang, X., Jun-Na, S., Dong-Gang, G., et al. (2010). Biotechnological implications from abscisic acid (ABA) roles in cold stress and leaf senescence as an important signal for improving plant sustainable survival under abiotic-stressed conditions. *Crit. Rev. Biotechnol.* 30, 222–230. doi: 10.3109/07388551.2010.487186
- Yadav, S. K. (2010). Cold stress tolerance mechanisms in plants. *A review. Agron. Sustain. Dev.* 30, 515–527. doi: 10.1051/agro/2009050
- Yadegari, L., Heidari, R., and Carapetian, J. (2008). Chilling pretreatment causes some changes in respiration, membrane permeability and some other factors in soybean seedlings. *Res. J. Biol. Sci.* 3, 1054–1059.
- Yamori, W., Noguchi, K., Hikosaka, K., and Terashima, I. (2009). Cold-tolerant crop species have greater temperature homeostasis of leaf respiration and photosynthesis than cold-sensitive species. *Plant Cell Physiol.* 50, 203–215. doi: 10.1093/pcp/pcn189
- Yang, J., and Zhang, J. (2006). Grain filling of cereals under soil drying. *New Phytol.* 169, 223–236. doi: 10.1111/j.1469-8137.2005.01597.x
- Yokota, H., Iehisa, J. C. M., Shimosaka, E., and Takumi, S. (2015). Line differences in Cor/Lea and fructan biosynthesis-related gene transcript accumulation are related to distinct freezing tolerance levels in synthetic wheat hexaploids. *J. Plant Physiol.* 176, 78–88. doi: 10.1016/j.jplph.2014.12.007
- Yordanova, R., and Popova, L. (2007). Effect of exogenous treatment with salicylic acid on photosynthetic activity and antioxidant capacity of chilled wheat plants. *Gen. Appl. Plant Physiol* 33, 155–170.
- Yoshida, M., Abe, J., Moriyama, M., and Kuwabara, T. (1998). Carbohydrate levels among winter wheat cultivars varying in freezing tolerance and snow mold resistance during autumn and winter. *Physiol. Plant.* 103, 8–16. doi: 10.1034/j.1399-3054.1998.1030102.x
- Yue, Y., Zhou, Y., Wang, J., and Ye, X. (2016). Assessing wheat frost risk with the support of gis: an approach coupling a growing season meteorological index and a hybrid fuzzy neural network model. *Sustainability* 8:1308. doi: 10.3390/su8121308
- Zhang, L., Zhao, G., Jia, J., Liu, X., and Kong, X. (2012). Molecular characterization of 60 isolated wheat MYB genes and analysis of their expression during abiotic stress. *J. Exp. Bot.* 63, 203–214. doi: 10.1093/jxb/err264
- Zhang, W., Wang, J., Huang, Z., Mi, L., Xu, K., Wu, J., et al. (2019). Effects of low temperature at booting stage on sucrose metabolism and endogenous hormone contents in winter wheat spikelet. *Front. Plant Sci.* 10:498. doi: 10.3389/fpls.2019.00498
- Zheng, B., Chapman, S. C., Christopher, J. T., Frederiks, T. M., and Chenu, K. (2015). Frost trends and their estimated impact on yield in the Australian wheatbelt. *J. Exp. Bot.* 66, 3611–3623. doi: 10.1093/jxb/erv163
- Zhu, J., Dong, C. H., and Zhu, J. K. (2007). Interplay between cold-responsive gene regulation, metabolism and RNA processing during plant cold acclimation. *Curr. Opin. Plant Biol.* 10, 290–295. doi: 10.1016/j.pbi.2007.04.010

Conflict of Interest: The authors declare that the research was conducted in the absence of any commercial or financial relationships that could be construed as a potential conflict of interest.

Copyright © 2021 Hassan, Xiang, Farooq, Muhammad, Yan, Hui, Yuanyuan, Bruno, Lele and Jincai. This is an open-access article distributed under the terms of the Creative Commons Attribution License (CC BY). The use, distribution or reproduction in other forums is permitted, provided the original author(s) and the copyright owner(s) are credited and that the original publication in this journal is cited, in accordance with accepted academic practice. No use, distribution or reproduction is permitted which does not comply with these terms.



Nitric Oxide Functions as a Downstream Signal for Melatonin-Induced Cold Tolerance in Cucumber Seedlings

Yiqing Feng, Xin Fu, Lujie Han, Chenxiao Xu, Chaoyue Liu, Huangai Bi^{†*} and Xizhen Ai^{†*}

State Key Laboratory of Crop Biology, Key Laboratory of Crop Biology and Genetic Improvement of Horticultural Crops in Huanghuai Region, College of Horticulture Science and Engineering, Shandong Agricultural University, Tai'an, China

OPEN ACCESS

Edited by:

Andy Pereira,
University of Arkansas, United States

Reviewed by:

Thomas Roach,
University of Innsbruck, Austria
Shuhua Zhu,
Shandong Agricultural
University, China
Parvaiz Ahmad,
Sri Pratap College, India
Manzer H. Siddiqui,
King Saud University, Saudi Arabia

*Correspondence:

Xizhen Ai
axz@sdau.edu.cn
Huangai Bi
bhg163@163.com

[†]These authors have contributed
equally to this work

Specialty section:

This article was submitted to
Plant Abiotic Stress,
a section of the journal
Frontiers in Plant Science

Received: 27 March 2021

Accepted: 21 June 2021

Published: 23 July 2021

Citation:

Feng Y, Fu X, Han L, Xu C, Liu C, Bi H
and Ai X (2021) Nitric Oxide Functions
as a Downstream Signal for
Melatonin-Induced Cold Tolerance in
Cucumber Seedlings.
Front. Plant Sci. 12:686545.
doi: 10.3389/fpls.2021.686545

Melatonin (MT) and nitric oxide (NO) are two multifunctional signaling molecules that are involved in the response of plants to abiotic stresses. However, how MT and NO synergize in response to cold stress affecting plants is still not clear. In this study, we found that endogenous MT accumulation under cold stress was positively correlated with cold tolerance in different varieties of cucumber seedlings. The data presented here also provide evidence that endogenous NO is involved in the response to cold stress. About 100 μ M MT significantly increased the nitrate reductase (NR) activity, NR-relative messenger RNA (mRNA) expression, and endogenous NO accumulation in cucumber seedlings. However, 75 μ M sodium nitroprusside (SNP, a NO donor) showed no significant effect on the relative mRNA expression of tryptophan decarboxylase (TDC), tryptamine-5-hydroxylase (T5H), serotonin-N-acetyltransferase (SNAT), or acetylserotonin O-methyltransferase (ASMT), the key genes for MT synthesis and endogenous MT levels. Compared with H₂O treatment, both MT and SNP decreased electrolyte leakage (EL), malondialdehyde (MDA), and reactive oxygen species (ROS) accumulation by activating the antioxidant system and consequently mitigated cold damage in cucumber seedlings. MT and SNP also enhanced photosynthetic carbon assimilation, which was mainly attributed to an increase in the activity and mRNA expression of the key enzymes in the Calvin–Benson cycle. Simultaneously, MT- and SNP-induced photoprotection for both photosystem II (PSII) and photosystem I (PSI) in cucumber seedlings, by stimulating the PsbA (D1) protein repair pathway and ferredoxin-mediated NADP⁺ photoreduction, respectively. Moreover, exogenous MT and SNP markedly upregulated the expression of chilling response genes, such as inducer of CBF expression (*ICE1*), C-repeat-binding factor (*CBF1*), and cold-responsive (*COR47*). MT-induced cold tolerance was suppressed by 2-(4-carboxyphenyl)-4,4,5,5-tetramethylimidazoline-1-oxyl-3-oxide (cPTIO, a specific scavenger of NO). However, p-chlorophenylalanine (p-CPA, a MT synthesis inhibitor) did not affect NO-induced cold tolerance. Thus, novel results suggest that NO acts as a downstream signal in the MT-induced plant tolerance to cold stress.

Keywords: melatonin, nitric oxide, antioxidant system, CO₂ assimilation, photoprotection, cold stress, signal pathway

INTRODUCTION

Cucumbers (*Cucumis sativus* L.) are sensitive to cold stress and are mainly cultivated through the winter in solar greenhouses in northern China; therefore, they often encounter cold stress. Cold stress adversely affects photosynthesis by damaging the electron transfer chain in chloroplasts and mitochondria, which naturally results in excessive reactive oxygen species (ROS) (Fan et al., 2015), and has become a major limitation to crop productivity and quality. It has been reported that plants can improve their cold tolerance to ensure growth and development mainly through stimulating antioxidant system activity and osmotic adjusting ability (Pan et al., 2020). Recently, a growing number of evidence suggest that various plant hormones, such as jasmonic acid (JA), brassinosteroids (BRs), abscisic acid (ABA), and salicylic acid (SA) (Kagale et al., 2007; Hu et al., 2013; Zhang et al., 2014; Ding et al., 2015), are also involved in responses to cold stress and regulating plant cold tolerance.

Melatonin (MT) is a small indoleamine molecule that plays a prominent role in regulating various physiological processes, including seed germination, plant growth, flower development, and root system structure (Murch and Saxena, 2002; Hernández-Ruiz et al., 2005; Wang et al., 2012; Arnao, 2014). In recent years, many reports have emphasized the importance of MT in response to abiotic stresses, such as extreme temperature, drought, osmotic stress, salinity/alkalinity, heavy metals (Cui et al., 2017, 2018; Ahammed et al., 2018; Fan et al., 2018; Nawaz et al., 2018; Qi et al., 2018; Yan et al., 2019; Kong et al., 2020; Siddiqui et al., 2020). To date, almost all studies consider that MT plays a critical role in ROS scavenging, either as a stress-induced agent or a protective molecule (Arnao and Hernandez-Ruiz, 2015; Erland et al., 2018; Martinez et al., 2018; Li et al., 2021). Additionally, reliable evidence suggests that MT achieves its antioxidant capacity through direct detoxification of ROS and reactive nitrogen species and indirect stimulation of antioxidant enzymes (Wang et al., 2017). Ahammed et al. (2018) found that MT-deficient caffeic acid O-methyltransferase1 (*COMT1*)-silenced tomato plants were more sensitive to heat-induced oxidative stress, and exogenous MT-pretreated plants showed an increase in the activity and messenger RNA (mRNA) expression of antioxidant enzymes in *COMT1*-silenced plants. Al-Huqail et al. (2020) suggested that MT induced plant defense mechanisms by enhancing Pro, TSCs, TPC, nutrient (N and P) uptake, and enzymatic and non-enzymatic antioxidants. Li et al. (2019) demonstrated that MT alleviates abiotic stress-induced damage in tea plants by scavenging ROS and regulating antioxidant systems. Recently, some evidence has indicated that MT, acting as a phytohormone-like molecule or secondary messenger, participates in many signaling events, including the response to abiotic stress in plants (Yan et al., 2019). MT appears to act as a key molecule in the plant immune response, together with other well-known molecules, such as nitric oxide (NO), and hormones, such as JA and SA (Arnao and Hernandez-Ruiz, 2018).

Previous studies have shown that NO, an important endogenous gas signaling molecule, is involved in almost all biological processes in plants, including seed germination

(Wimalasekera et al., 2011), plant maturation, and senescence (Guo and Crawford, 2005; Mishina et al., 2007). Additionally, NO has been shown to regulate numerous plant responses to a variety of biotic and abiotic stresses and to relieve the damage caused by oxidative stress (Siddiqui et al., 2011; Ahanger et al., 2020; Kaya et al., 2020b,c; Singh et al., 2020). According to previous studies, some shared physiological functions of MT and NO have been verified in their regulation of plant tolerance to stress conditions; in particular, both are involved in ROS signaling pathways in plants (Park et al., 2013; Scheler et al., 2013; Kaya et al., 2019, 2020a).

Recently, it was reported that MT can increase the resistance of plants to biotic stress *via* the NO-mediated signaling pathway (Shi H. T. et al., 2015). Exogenous MT increased NO accumulation in alkaline-stressed tomato roots, but exogenous NO showed little effect on MT content, suggesting that NO, acting as a downstream signal, is involved in MT-induced alkaline tolerance in tomatoes (Liu et al., 2015). However, limited information has been provided about the relationship between MT and NO in plants under cold stress, and the physiological and molecular mechanisms of interaction between MT and NO during detoxifying cold stress are still unclear. Therefore, in this study, we investigated the interrelationship between MT and NO as well as their role in ROS scavenging, CO₂ assimilation, and photoprotection under cold stress. Our research aimed to elucidate the mechanism of the effects of MT and its signaling pathways in the cold stress response of cucumbers.

MATERIALS AND METHODS

Plant Materials and Treatments

Cucumber [*C. sativus* L. “Jinyou 35” (JY35) and “Zhongnong 6” (ZN6)] seeds were soaked in water for 6 h, followed by incubation on moistened filter papers in the dark for 24 h at 28°C for germination. The germinated seeds were sown in a growth medium, which consisted of peat, vermiculite, and perlite (5:3:1, v/v) in a climate chamber. The growth environment conditions were maintained as follows: 25/18°C day/night temperature, 80% relative humidity, and 11 h photoperiod with photon flux density (PFD) of 600 $\mu\text{mol m}^{-2}\cdot\text{s}^{-1}$.

Chilling and MT or NO Treatment

To examine the effect of MT and sodium nitroprusside (SNP, a NO donor) on cold tolerance of cucumber, seedlings with three leaves were foliar sprayed with 0 (control), 25, 50, 75, 100, or 125 μM MT or pretreated with 0 (control), 25, 50, 75, 100, or 125 μM SNP (10 ml per plant). At 24 h after pretreatment with MT or SNP, the seedlings were exposed to 5°C for 72 h for the analysis of malondialdehyde (MDA) content and electrolyte leakage (EL). The seedlings were pretreated with 100 μM MT, 75 μM SNP, or distilled water (control) for examining the effect of MT on endogenous NO generation and that of NO on MT biosynthesis. To analyze the interaction between MT and NO, seedlings with three leaves were pretreated with 100 μM MT, 75 μM SNP, 100 μM 2-(4-carboxyphenyl)-4,4,5,5-tetramethylimidazoline-1-oxyl-3-oxide (cPTIO, a specific scavenger of NO) + 100 μM MT, 50 μM p-chlorophenylalanine

(p-CPA, MT synthesis inhibitor) +75 μM SNP, or deionized water (control). At 24 h after cold stress, the pretreated seedlings were subjected to 5°C in growth chambers. At 24 h after chilling treatment, the gas exchange parameter, fluorescence parameters, and the key enzymes in the Calvin-Benson cycle were detected. At 48 h after cold stress, the accumulation of ROS and gene expression and the activity of antioxidant enzymes were measured. The deionized water treatment under cold stress was considered as H₂O treatment to distinguish from the control at normal temperature conditions.

Measurement of MT and Activity of Its Synthase Enzymes

Endogenous MT was detected by using high-performance liquid chromatography-triple quadrupole mass spectrometry (HPLC-MS, Thermo Fisher Scientific, TSQ Quantum Access, Waltham, MA, USA) according to the method of Bian et al. (2018). Briefly, freeze-dried leaves (0.1 g) were ground in 9 ml 100% methanol, extracted with cryogenic ultrasound for 15 min, and vortexed in darkness at 4°C for 24 h. The homogenates were centrifuged at $10,000 \times g$ for 15 min at 4°C, and the supernatants were dried with nitrogen gas. The residues were dissolved in 3 ml 5% methanol, centrifugated at $10,000 \times g$ for 15 min to remove pigment and impurities, and then purified further with a C₁₈ solid-phase extraction column (Bond Elut C₁₈, 100 mg 1 ml, 100/pk, Agilent Technologies, Inc., Folsom, Santa Clara, CA, USA). The residue was dissolved in 1 ml 90% chromatographic methanol (containing 0.05% acetic acid), and the filtrate was used for the HPLC-MS analysis. The samples were separated by using a Hypersil Gold C₁₈ column (Thermo Fisher Scientific, Waltham, MA, USA, 100 \times 2.1 mm, 1.9 μm) at a flow rate of 0.3 ml·min⁻¹ and a column temperature of 25°C. About 90% chromatographic methanol and 0.05% acetic acid were used as mobile phases. The separated components were further quantitatively analyzed by MS using triple quadrupole MS with electrospray ionization (ESI) in the positive mode. The MT and 2-hydroxymelatonin in cucumber leaves were determined by an external standard method and were calculated according to the peak area.

The activities of tryptophan decarboxylase (TDC) and acetylserotonin O-methyltransferase (ASMT) were measured by the ELISA method using ELISA kits for TDC and ASMT in plants (SU-B91337 and SU-B91345, Quanzhou Kenuodi Biotechnology Co., Ltd., Quanzhou, China), respectively.

Determination of Chlorophyll Fluorescences

After seedlings were dark adapted for 45 min, the maximum photochemical efficiency of photosystem II (PSII) (F_v/F_m) and the actual photochemical efficiency of PSII (Φ_{PSII}) were detected using an Imaging-PAM Chlorophyll Fluorometer (IMAGING-PAM, Walz, Wurzberg, Germany). F_v/F_m and Φ_{PSII} were calculated as follows: $F_v/F_m = (F_m - F_0)/F_m$; $\Phi_{\text{PSII}} = (F_m' - F_s)/F_m'$ (Demmig-Adams and Adams, 1996). The initial fluorescence (F_0) was estimated after turning on the measuring beam, followed by a 0.8-s saturation pulse (3,000 $\mu\text{mol m}^{-2}\cdot\text{s}^{-1}$) to obtain maximum fluorescence (F_m). Steady-state fluorescence (F_s) was

recorded using the actinic light intensity of 400 $\mu\text{mol m}^{-2}\cdot\text{s}^{-1}$ for 5 min. The chlorophyll fluorescence imaging of cucumber leaves was visualized using the method of Tian et al. (2017), with a variable chlorophyll fluorescence imaging system (Imaging PAM, Walz, Wurzberg, Germany), which consists of a CCD camera, LED lights, and a controlling unit connected to a PC running a dedicated software (Imaging Win 2.3, Walz, Wurzberg, Germany).

The dark-adapted leaves were used to determine the transient chlorophyll fluorescence and 820 nm reflection with an integral multifunctional plant efficiency analyzer (M-PEA, Hansatech, King's Lynn, Norfolk, UK) as described by Liu et al. (2020). The parameters were calculated as follows (Chen et al., 2016): relatively variable fluorescence at time t (V_t) = $(F_t - F_0)/(F_m - F_0)$, $\Delta V_t = V_t - V_{t(\text{control})}$; the performance index on the absorption basis (PI_{ABS}) = $\text{RC}/\text{ABS} \times [\phi_{\text{P0}}/(1 - \phi_{\text{P0}})] \times [\psi_0/(1 - \psi_0)]$; the efficiency of an electron moving beyond Q_A (ψ_0) = $\text{ET}/\text{TR} = 1 - V_J$; and the quantum for heat dissipation (ϕ_{D0}) = F_0/F_m . The amplitude of the 820 nm reflection is ($\Delta I/I_0$) = $(I_0 - I_m)/I_0$ (Salvatori et al., 2014), where I_0 is the initial reflection signal between 0.4 and 10 ms and I_m is the minimum reflection signal under 820 nm far-red illumination (Zhang et al., 2011).

Measurement of MDA Content, EL, and Chilling Injury Index

Malondialdehyde content was determined using the TBA colorimetric method as described by Dong et al. (2013). EL was measured using the method of Dong et al. (2013). A total of 0.3 g of each leaf sample was incubated in a tube with 20 ml of deionized water at 25°C, and electrical conductivity (EC) of the bathing solution was estimated at 3 h, which was named EC1, using a conductivity meter (DDB-303A, Shanghai Precision Scientific Instrument Co., Ltd., Shanghai, China). Then, the samples were boiled for 30 min, and EC of the bathing solution was measured after cooling to room temperature, and named EC2. EL was calculated as follows: $\text{EL} = \text{EC1}/\text{EC2} \times 100$. The stressed seedlings were graded according to Semeniuk et al. (1986), and the chilling injury index (CI) was calculated as follows: $\text{CI} = \Sigma (\text{plants of different grade} \times \text{grade})/[\text{total plants} \times 5 (\text{the maximum grade})]$.

NO Content and Nitrate Reductase Activity Assay

Nitric oxide was extracted from the second apical leaves and quantified using the method specified in the NO kit (Nanjing Jiancheng Bioengineering Institute, Nanjing, China). The intracellular NO was visualized using the NO fluorescent probe diaminofluorescein-FM diacetate (DAF-FM DA; Beyotime, Shanghai, China) for localization according to the instructions. Fluorescent was formed in the presence of NO (excitation at 495 nm and emission at 515 nm) and visualized using an inverted fluorescence microscope (Leica DMI8; Leica, Wetzlar, Germany). Nitrate reductase (NR) activity was detected using the method of Zhao et al. (2002).

Gas Exchange Parameters Assay

The photosynthetic rate (P_n) for the second apical leaves was detected using a portable photosynthetic system (Ciras-3, PP-systems International, Hitchin, Hertfordshire, UK). The determination conditions were maintained as follows: 600 $\mu\text{mol m}^{-2}\cdot\text{s}^{-1}$ PFD, 380 $\text{mg}\cdot\text{L}^{-1}$ CO_2 concentration, and $25 \pm 1^\circ\text{C}$ leaf temperature. Following the method of Ethier and Livingston (2004), the light-saturated photosynthetic rate (Asat) was detected.

Quantitative and Histochemical Detection of ROS

Hydrogen peroxide (H_2O_2) was extracted from 0.5-g leaf samples and quantified according to the instructions specified in the H_2O_2 kit (A064-1, Nanjing Jiancheng Bioengineering Institute, Nanjing, China). The superoxide anion (O_2^-) content was measured as described by Wang and Luo (1990). Cellular H_2O_2 and O_2^- were visualized at the subcellular level using the H_2O_2 fluorescent probe 2', 7'-dichlorodihydrofluorescein diacetate (H_2DCFDA) (MCE, Cat. No. HY-D0940, Shanghai, China) and dihydroethidium (DHE) (Fluorescence Biotechnology Co., Ltd., Cat. No. 15200, Beijing, China), respectively, using the method of Zhang et al. (2020).

Measurement of Antioxidant Enzyme Activity

Fresh samples (0.5 g) were ground in 5 ml of 50 mM ice-chilled phosphate buffer solution (pH 7.8) containing 0.2 mM EDTA and 1% (w/v) PVP. The homogenates were centrifuged at $12,000 \times g$ for 20 min at 4°C , and the supernatant was used to determine the activity of antioxidant enzymes. Superoxide dismutase (SOD) activity was measured using the method of Stewart and Bewley (1980). Peroxidase (POD) activity was determined following the method of Omran (1980) and was quantified using the absorbance changes at 470 nm over 1 min. Ascorbate peroxidase (APX) activity was determined as described by Nakano and Asada (1987) and was determined by the changes of absorbance at 290 nm over 1 min. Glutathione reductase (GR) activity was assayed based on the method of Foyer and Halliwell (1976) and was expressed as the decreasing rate in the absorbance of NADPH at 340 nm over 1 min.

Glutathione and Ascorbic Acid Content Assays

We measured the contents of reduced glutathione (GSH) and oxidized glutathione (GSSG) using a GSH content kit (GSH-2-W, and GSSG-2-W, Suzhou Keming Biotechnology Co., Ltd., Suzhou, China) according to the instructions. The contents of ascorbic acid (AsA) and dehydroascorbic acid (DHA) were estimated using the method of Law et al. (1983).

Activity of the Key Enzymes in Calvin–Benson Cycle

Ribulose-1,5-bisphosphate carboxylase (RuBPCase) activity was assayed spectrophotometrically using the RuBPCase

TABLE 1 | The primer sequences of quantitative real-time PCR (qRT-PCR).

Primer names	Sequences(5'→ 3')
<i>β-Actin</i>	F: CCACGAACTACTTACAACCTCCATC R: GGGCTGTGATTTCCTTGCTC
<i>TDC</i>	F: ATAAATGGTCTCTCTCGGCGCCAG R: GTTAATCATATTCGACTTCTGGT
<i>T5H</i>	F: AGCTTGTGCGAGGCTACCAACT R: GAACGTTGGAACAACTTGTG
<i>SNAT</i>	F: AGTCCCTGTTTCAGAGGAGAAT R: AGATTCGATAAACTCTACCAC
<i>ASMT</i>	F: ATTGGAAGTTTAGTTGATGTGGGA R: AGCATCAGCCTTGGGAATGGAAT
<i>NR</i>	F: CAAGAAAGAGCTGGCTATGG R: CTACATGGGATGGCAAGACT
<i>SOD</i>	F: GGAAAGATGTGAAGGCTGTGG R: GCACCATGTTGTTTCCAGCAG
<i>POD</i>	F: GGTTTCTATGCCAAAAGCTGCC R: CAGCTTGGTTGTTTGAGGTGGAG
<i>APX</i>	F: GTGCTACCCTGTTGTGAGTG R: AACAGCGATGTCAAGGCCAT
<i>GR</i>	F: TGATGAGGCTTTGAGTTAGAGGAG R: AACTTTGGCACCCATACCATTC
<i>rbcl</i>	F: GCTATGGAATCGAGCCTGTTG R: CCAAATACATTACCCACAATGGAAG
<i>RCA</i>	F: AAAGTGGGCTGTAGGCGTTG R: CTTTCTATTGTCATCTTCGGTTGG
<i>ICE1</i>	F: CGCATCGAGTTGGCTCTGGTG R: GTCCTCATCGCCGTTTCATCTCC
<i>CBF1</i>	F: TACAGAGGAGTCAGGAGGA R: AGAATCGGCGAAATTGA
<i>COR47</i>	F: CACTTTGAGAGGACATTTGATG R: AGAAGCTCCAATTTTGACTTG

kit (RUBPS-2A-Y, Suzhou Keming Biotechnology Co., Ltd., Suzhou, China) according to the instructions. Rubisco activase (RCA) activity was detected by ELISA with an RCA ELISA kit (SU-B91104, Quanzhou Kenuodi Biotechnology Co., Ltd., Quanzhou, China).

RNA Extraction and Gene Expression Analysis

Total RNA was extracted using TransZol reagent (Transgen, Beijing, China) and reverse transcribed with the HiScript[®] III RT SuperMix for qPCR (+gDNA wiper) (Vazyme, Nanjing, China). Quantitative real-time PCR (qRT-PCR) for *TDC*, *T5H*, *SNAT*, *ASMT*, *NR*, antioxidant genes, key genes of the Calvin–Benson cycle, and cold stress-responsive genes in cucumber seedlings were analyzed using ChamQ[™] Universal SYBR[®] qPCR MasterMix (Vazyme, Nanjing, China) according to the instructions. We used the cucumber β -actin gene (Gene ID: Solyc11g005330) as a constitutively expressed internal control. The synthesis of primers by BGitech is shown in Table 1.

SDS-PAGE and Immunoblot Analysis

Fresh leaves were ground in liquid nitrogen and homogenized in extraction buffer (20 mM tricine, 1 mM sodium ascorbate, 400 mM sorbic alcohol, 10 mM NaHCO_3 , 5 mM $\text{EDTA}\cdot\text{Na}_2$, and 5 mM MgCl_2) for protein extraction and then centrifuged at $2,000 \times g$ for 15 min. After adjusting to the same concentration, the proteins were mixed with $5\times$ loading buffer (CW0027S, Beijing ComWin Biotech Co., Ltd., Beijing, China) and boiled at 100°C for 15 min. The proteins were separated using 10% sodium dodecyl sulfate-polyacrylamide gradient gel electrophoresis (SDS-PAGE). For D1, Photosystem I reaction center subunit II (PsaD), RbcL, and RCA detection, antibodies specific to the D1, PsaD, RbcL, and RCA proteins (ATCG00020, AT1G03130, ATCG00490, AT2G39730, PhytoAB Company, San Francisco, CA, USA) were used, followed by incubation with horseradish POD-conjugated anti-rabbit IgG antibody (ComWin Biotech Co., Ltd., Beijing, China). For C-repeat-binding factor (CBF1) detection, an antibody specific to CBF1 proteins (GenScript Co, Nanjing, China) was used, followed by incubation with a horseradish POD-conjugated anti-rabbit IgG antibody (ComWin Biotech Co., Ltd., Beijing, China). The immunoreaction was detected with an eECL Western Blot Kit (CW00495, ComWin Biotech Co., Ltd., Beijing, China). We recorded chemiluminescence on blots using the ChemiDoc™ XRS imaging system (Bio-Rad Laboratories, Inc., Hercules, CA, USA).

Statistical Analysis

All experiments were performed at least in triplicate, and the results are shown as mean \pm one SD. All data were analyzed statistically using DPS software. Statistical analysis of the values was performed by Duncan's multiple range test (DMRT), and comparisons with $p < 0.05$ were considered significantly different.

RESULTS

The Response of Endogenous MT to Cold Stress and Its Relationship With Cold Tolerance in Cucumber

We first determined whether endogenous MT levels are related to cold tolerance by comparing the changes in endogenous MT, the activity and relative mRNA expression of MT synthase enzymes in response to cold stress, and the F_v/F_m , Φ_{PSII} , MDA content, EL, and CI in different varieties of cucumber. As shown in **Figure 1**, cold stress induced greater activities and relative mRNA expression of *TDC* and *ASMT* (key enzymes of MT biosynthesis) and consequently promoted endogenous MT and its metabolite accumulation, 2-hydroxymelatonin, in cucumber seedlings. The increases in MT content and the activities and relative mRNA expression of *TDC* and *ASMT* were most significant after 12 h at 5°C , but an increase in 2-hydroxymelatonin was most significant after the exposure of seedlings to cold stress for 6 h. Compared to the “ZN6” seedlings, the “JY35” seedlings exhibited significantly higher activities and relative mRNA expressions of *TDC* and

ASMT, as well as MT content ($p < 0.05$), but much lower 2-hydroxymelatonin accumulation ($p < 0.05$) following cold stress.

Cold stress caused a remarkable decrease ($p < 0.05$) in F_v/F_m and Φ_{PSII} and an increase in MDA content, EL, and CI. The decreases in F_v/F_m and Φ_{PSII} and increases in MDA content, EL, and CI in the “JY35” seedlings were significantly lower than those in the “ZN6” seedlings (**Figures 2A,B,D–F**). Histochemical observation using an inverted fluorescence microscope for F_v/F_m and Φ_{PSII} (**Figures 2A,B**) agreed with the results determined by a chlorophyll fluorometer. **Figure 2C** shows that cold stress resulted in visible damages such as wilting and necrosis in cucumber leaves. The “JY35” seedlings exhibited minor damage compared to the “ZN6” seedlings, as evidenced by the unaided visual observations. These data indicated that MT is induced by cold stress and is involved in the response of cucumber seedlings to cold stress. Amplitude variation of endogenous MT in different varieties is positively correlated with cold tolerance.

MT Improves Cold Tolerance and NO Accumulation in Cucumber Seedlings

We then examined the effect of different concentrations of MT on the seedling symptoms, F_v/F_m , Φ_{PSII} , P_n , MDA content, and EL under cold stress. **Figure 3A** reveals that exogenous MT alleviated the foliar damage in cucumber seedlings caused by cold stress, and $100\ \mu\text{M}$ treatment was most noticeable. MT also increased F_v/F_m , Φ_{PSII} , and P_n but decreased MDA accumulation and EL. This increase in F_v/F_m , Φ_{PSII} , and P_n or a decrease in MDA and EL in seedlings was enhanced at a low concentration of MT but was inhibited when MT concentration exceeded $100\ \mu\text{M}$ (**Figures 3B–F**). The seedlings treated with $100\ \mu\text{M}$ MT displayed significantly higher F_v/F_m , Φ_{PSII} , and P_n but much lower MDA and EL than other treated seedlings ($p < 0.05$). These data indicate that MT improves the cold tolerance of cucumber in a concentration-dependent manner. Hence, $100\ \mu\text{M}$ MT was used in subsequent experiments.

Interestingly, $100\ \mu\text{M}$ MT significantly increased NO content, NR (a key enzyme for NO biosynthesis) activity, and NR-relative mRNA expression in cucumber seedlings (**Figures 4A–C**; $p < 0.05$). However, p-CPA-treated seedlings showed lower or similar NO content, NR activity, and relative mRNA expression compared with H_2O -treated seedlings. The NO accumulation observed by inverted fluorescence microscope (**Figure 4D**) was consistent with the results of biochemical analysis. This finding implies that NO may play a crucial role in MT-induced cold tolerance of cucumber seedlings. To verify this inference, we measured the response of endogenous NO to cold stress, and the effect of exogenous NO on chilling injury symptoms, F_v/F_m , Φ_{PSII} , ROS accumulation, and EL in cucumber seedlings. We found that NR activity, NR-relative mRNA expression, and NO accumulation in cucumber seedlings also increased under cold stress, and the highest values were reached after 9 h of cold stress (**Figure 5**). Importantly, SNP (NO specific donor) increased F_v/F_m and Φ_{PSII} while decreasing MDA accumulation and EL in cucumber seedlings, confirming that endogenous NO also enhances the cold tolerance of cucumber seedlings. Seedlings treated with $75\ \mu\text{M}$ SNP exhibited the highest F_v/F_m

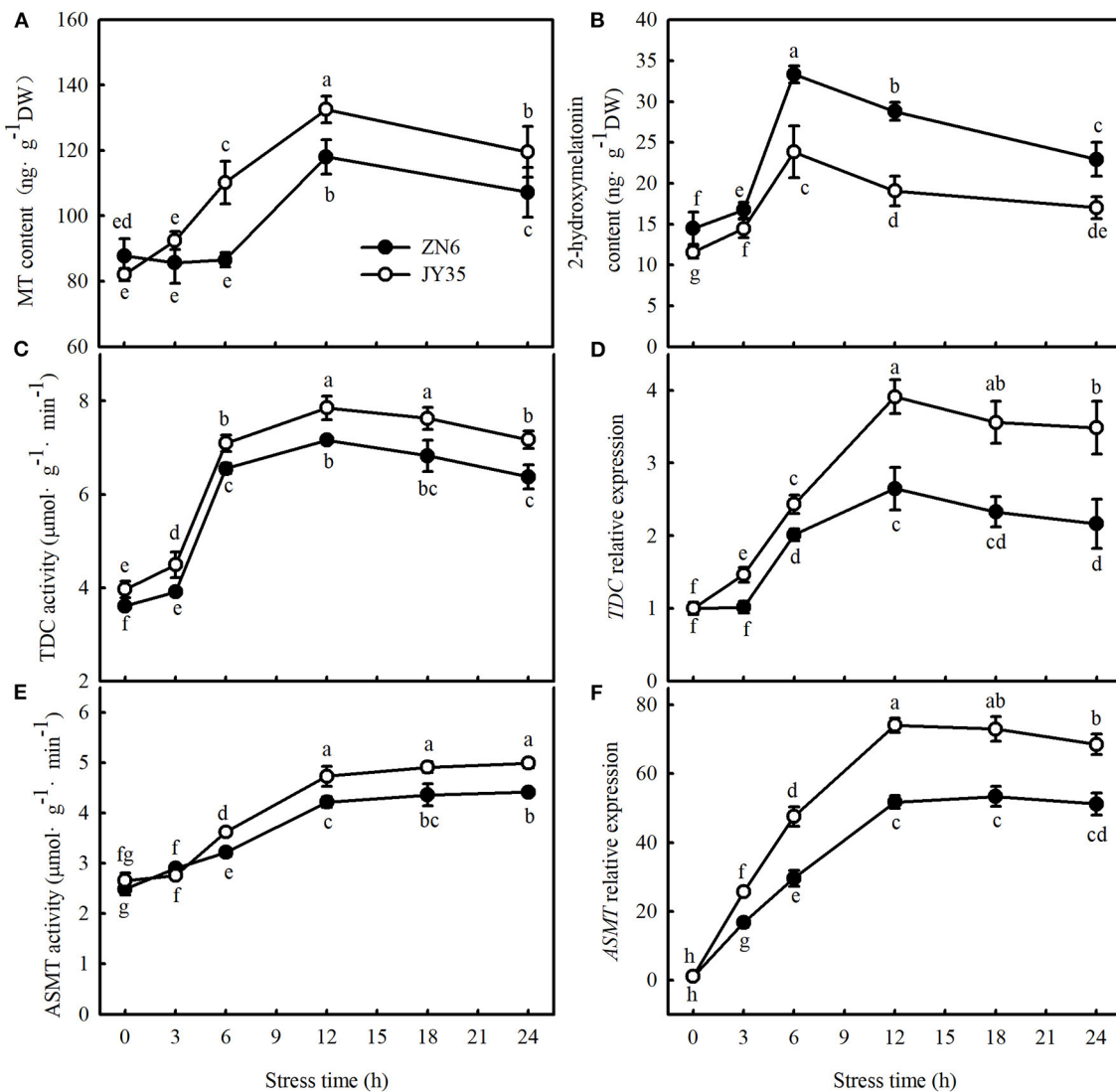


FIGURE 1 | Response of endogenous melatonin (MT) to cold stress in cucumber seedlings. **(A)** MT content; **(B)** 2-hydroxymelatonin content; **(C)** tryptophan decarboxylase (TDC) activity; **(D)** relative messenger RNA (mRNA) expression of *TDC*; **(E)** acetylserotonin O-methyltransferase (ASMT) activity; and **(F)** relative mRNA expression of *ASMT*. Seedlings were treated at 5°C for 24 h and sampled every 3 h. Data are the means \pm SD ($n = 3$). Different letters indicate a significant difference between samples according to Duncan's new multiple range test ($p < 0.05$).

and Φ_{PSII} but the lowest ROS accumulation and EL among the six SNP treatments (Figure 6), so 75 μ M SNP was used in subsequent experiments.

To further explore the upstream and downstream relationship of MT and NO signals under cold stress, we determined the effect of SNP on the mRNA abundance of key genes of MT biosynthesis and MT content in cucumber seedlings at normal temperature. No differences were observed in the relative mRNA expression of *TDC*, *T5H*, *SNAT*, and *ASMT* and in the MT content between SNP, cPTIO, or control treatments (Figure 7). These results indicate that NO may function as a downstream signal for MT-induced cold tolerance in cucumber seedlings.

Exogenous MT and SNP Increased ROS Scavenging Activity in Cucumber Seedlings Under Cold Stress

To explore whether MT alleviates oxidative damage from cold stress and whether NO is involved in the process of MT-induced antioxidation under cold stress, we examined ROS accumulation and antioxidant system activity in stressed seedlings pretreated with 100 μ M MT, 75 μ M SNP, 100 μ M cPTIO + 100 μ M MT, 50 μ M p-CPA + 75 μ M SNP, or deionized water. The results showed that MT- and SNP-treated seedlings exhibited far fewer damage symptoms caused by cold stress (Figure 8A). The mitigation of MT in chilling injury of cucumber seedlings was weakened by cPTIO, a specific scavenger of NO. However,

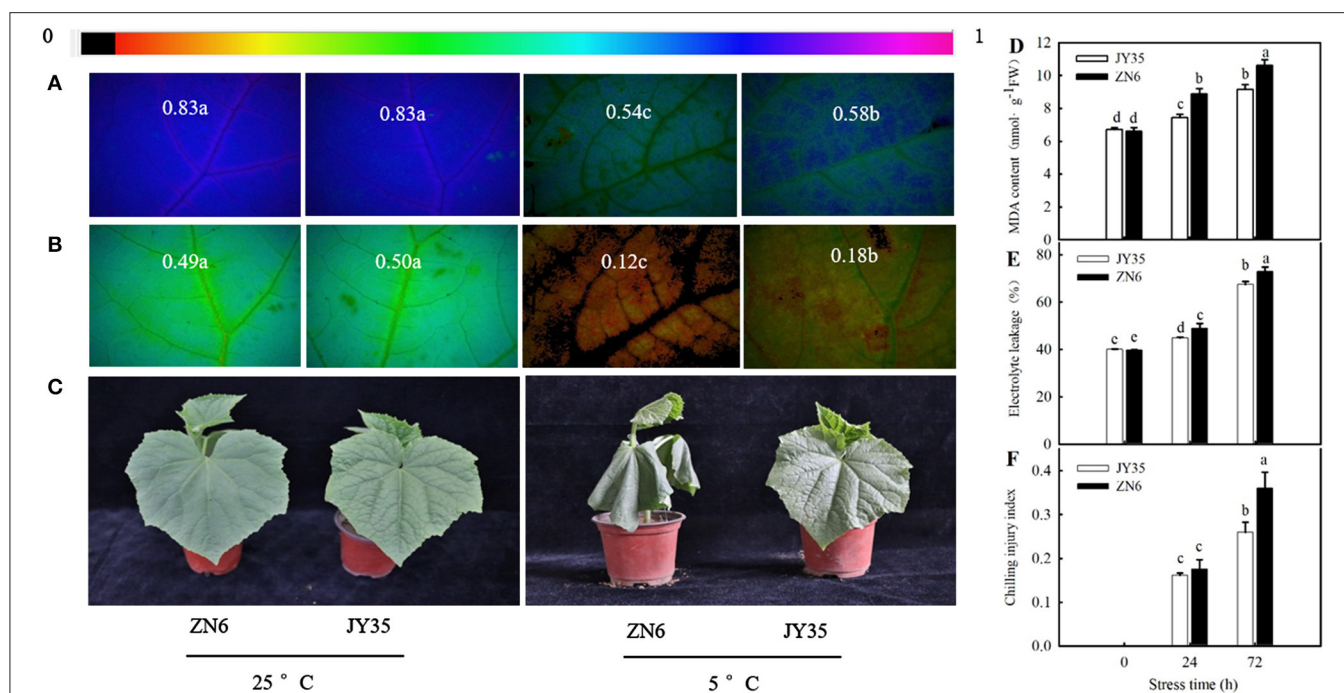


FIGURE 2 | Comparison of cold tolerance in the two different cucumber varieties. Images of (A) F_v/F_m and (B) Φ_{PSII} , respectively. The false color code depicted at the top of the image ranging from 0 (black) to 1 (purple) represents the degree of photoinhibition at photosystem II (PSII). (C) Seedling phenotype. Three-leaf stage seedlings were treated at 5°C for 24 h; (D) Malondialdehyde (MDA) accumulation, (E) Electrolyte leakage (EL) rate, and (F) Chilling injury index (CI), respectively. Seedlings were exposed to 5°C for 72 h. Data are represented as mean \pm SD ($n = 3$). Different letters indicate a significant difference between samples according to Duncan's new multiple range test ($p < 0.05$).

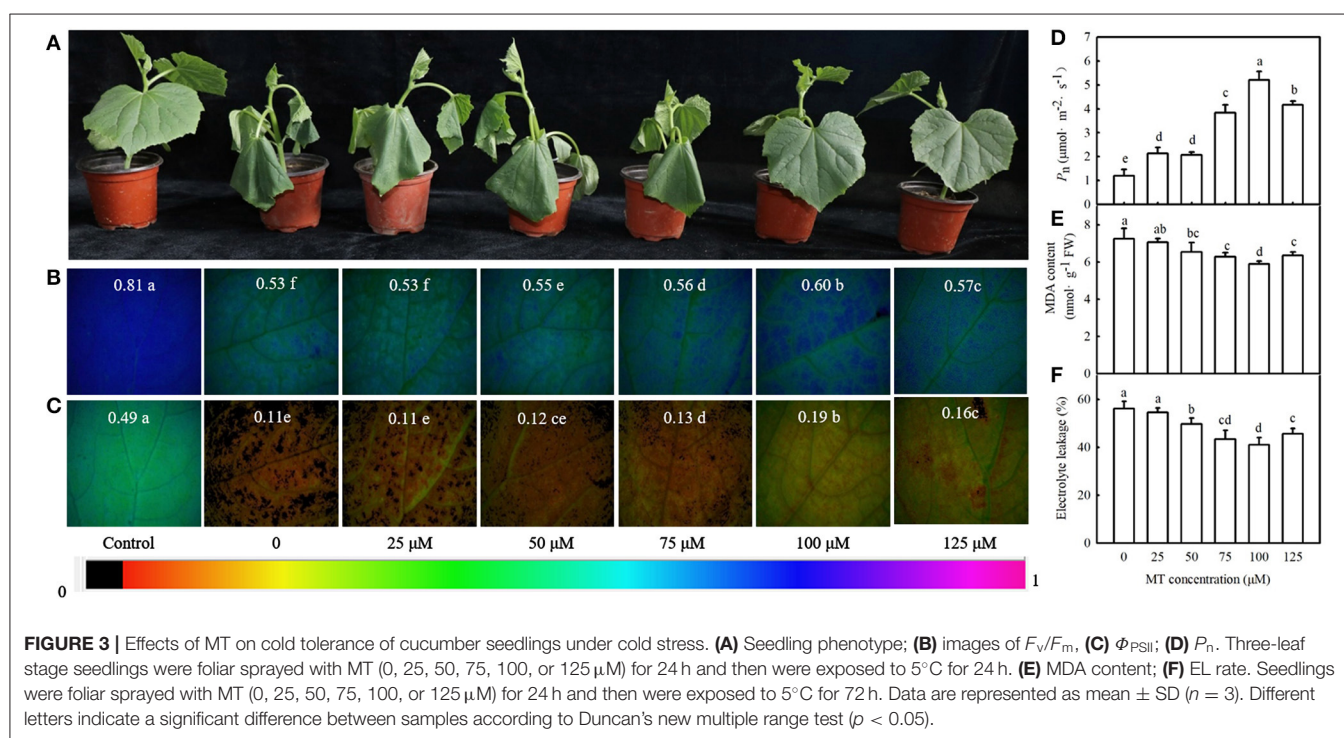
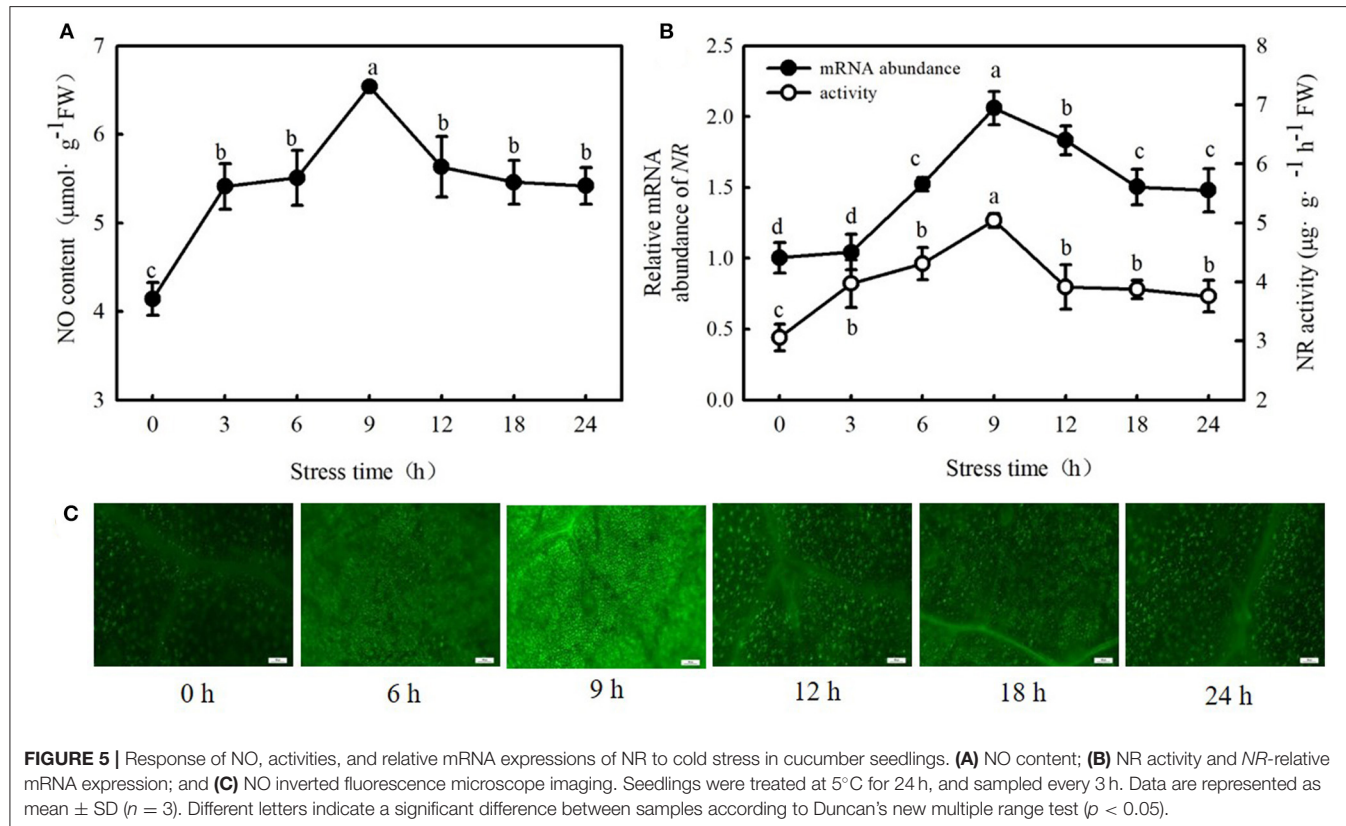
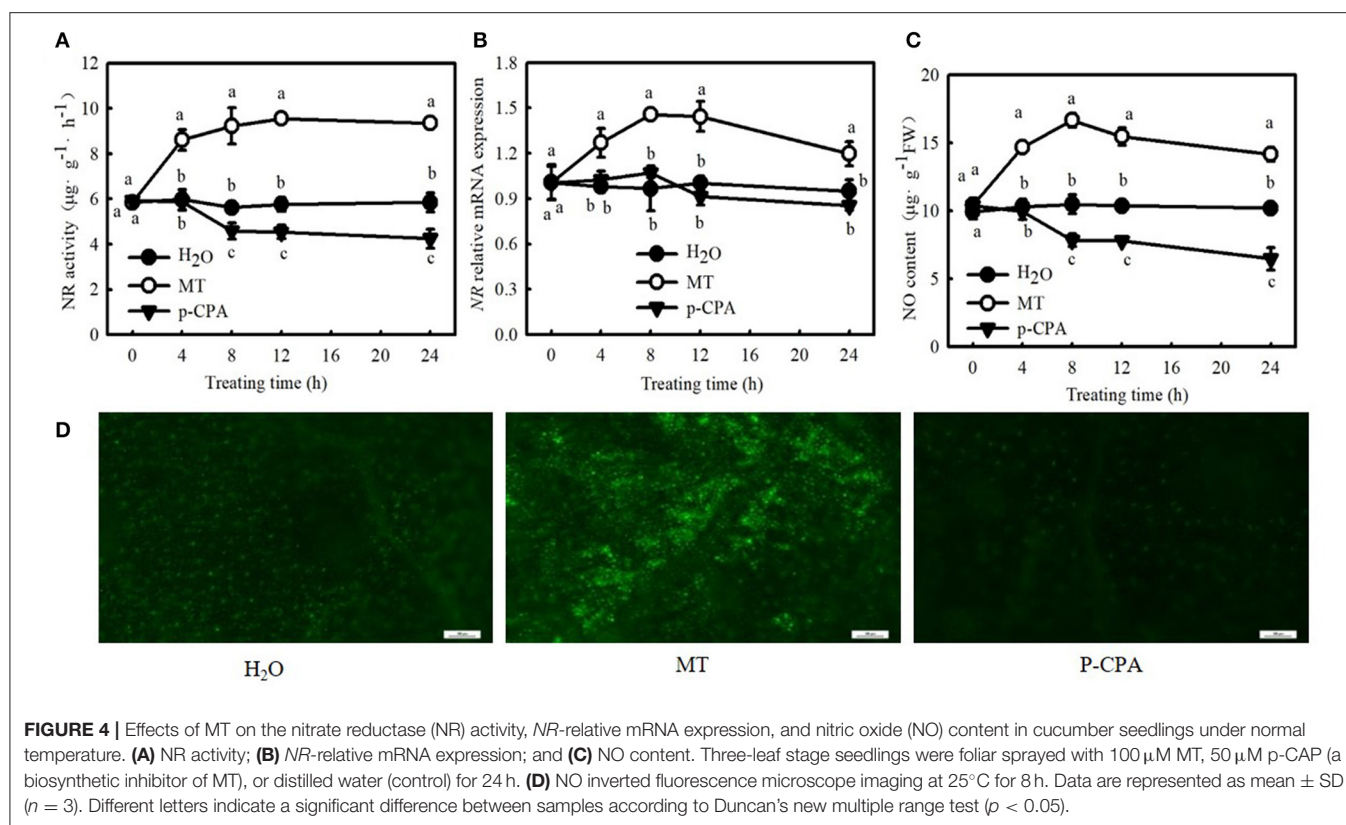
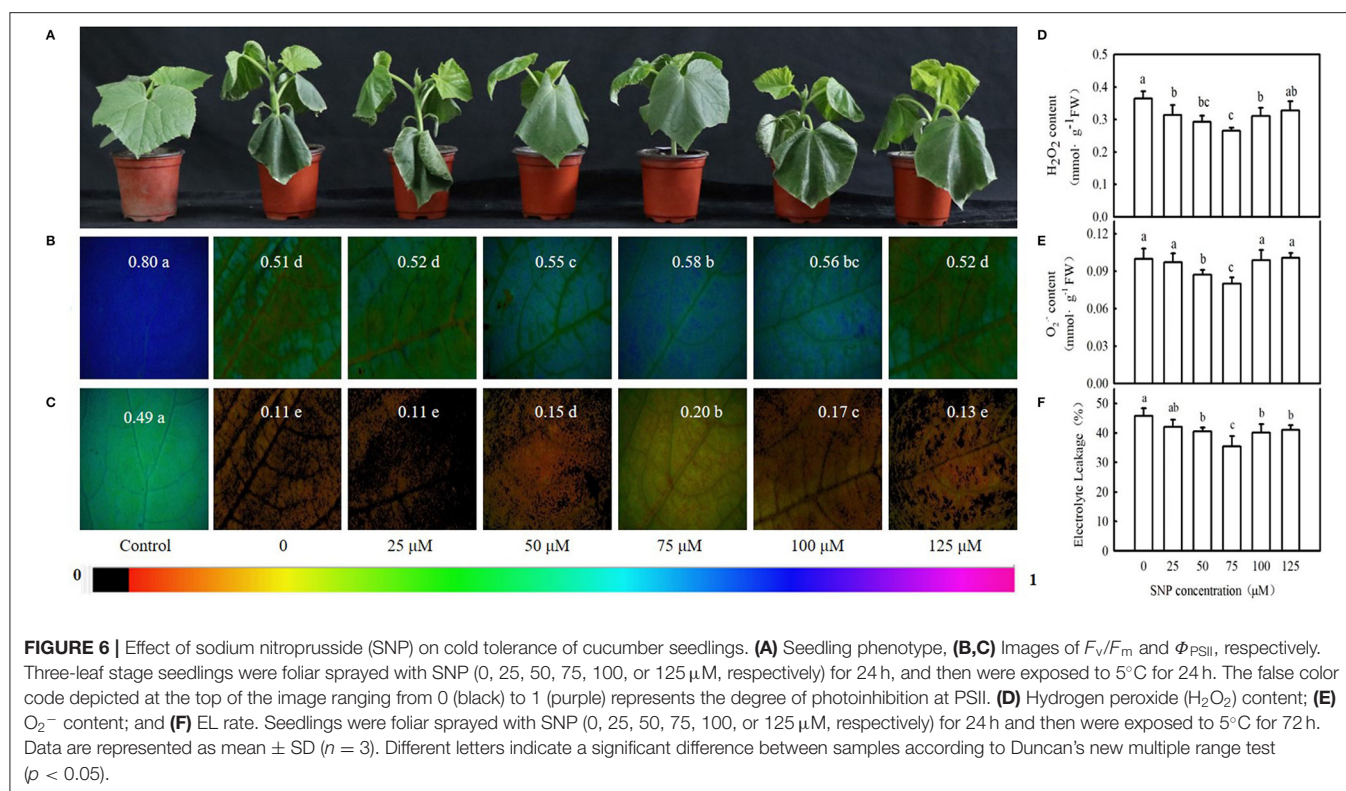


FIGURE 3 | Effects of MT on cold tolerance of cucumber seedlings under cold stress. (A) Seedling phenotype; (B) images of F_v/F_m , (C) Φ_{PSII} ; (D) P_n . Three-leaf stage seedlings were foliar sprayed with MT (0, 25, 50, 75, 100, or 125 μM) for 24 h and then were exposed to 5°C for 24 h. (E) MDA content; (F) EL rate. Seedlings were foliar sprayed with MT (0, 25, 50, 75, 100, or 125 μM) for 24 h and then were exposed to 5°C for 72 h. Data are represented as mean \pm SD ($n = 3$). Different letters indicate a significant difference between samples according to Duncan's new multiple range test ($p < 0.05$).





the MT synthetic inhibitor p-CPA had little effect on NO-induced alleviation of chilling injury. **Figures 8B–D** show that cold stress significantly increased the generation of H_2O_2 and O_2^- , and as a result of excess ROS accumulation, the stressed seedlings revealed lipid peroxidation, as evidenced by increased EL (**Figure 8E**). Exogenous MT or SNP dramatically decreased the accumulation of H_2O_2 and O_2^- and markedly reduced EL in cucumber seedlings under cold stress. MT-induced decreases in the accumulation of H_2O_2 and O_2^- and EL were blocked by cPTIO, but the decrease caused by SNP in stressed seedlings was not affected by p-CPA. These data suggest that MT-induced cold tolerance is connected with increased ROS scavenging activity. To test the speculation that NO may be involved in MT-induced antioxidant activities, we determined the changes in the antioxidant system in cucumber seedlings after exposure to 5°C for 48 h. As shown in **Figures 9A–D**, cold significantly increased in the activities of SOD, POD, APX, and GR in cucumber seedlings. Compared with H_2O -treated seedlings, the activities of SOD, POD, APX, and GR in MT-treated seedlings increased by 6.9, 29.1, 31.6, and 29.4%, respectively, and those in SNP-treated seedlings increased by 5.0, 26.9, 21.7, and 36.0%, respectively. cPTIO significantly repressed MT-induced activities of antioxidant enzymes ($p < 0.05$), but p-CPA showed little effect on NO-induced activities of antioxidant enzymes. Cold stress also increased the mRNA abundances of SOD, POD, APX, and GR, and this increase was markedly greater in MT and SNP treatments. Compared to MT treatment alone, cPTIO + MT treatment resulted in significant reduction of the mRNA abundances of SOD, POD, APX, and GR. However, p-CPA +

SNP treatment caused no remarkable difference in the mRNA abundances of SOD, POD, APX, and GR relative to SNP treatment (**Figures 9E–H**). We also found that the contents of AsA and GSH were significantly decreased in H_2O -treated seedlings after exposure to 5°C for 48 h. Seedlings pretreated with MT and SNP showed dramatically higher AsA and GSH contents than H_2O -treated seedlings ($p < 0.05$) during cold stress. With the application of cPTIO, the positive effect of MT on the generation of GSH and AsA was obviously blocked; however, p-CPA did not inhibit the positive effect of SNP on GSH and AsA generation. Similarly, cold stress led to a significant decrease in GSH/GSSG and AsA/DHA. Both MT and SNP treatments showed higher GSH/GSSG and AsA/DHA than the H_2O treatment under cold stress ($p < 0.05$). cPTIO markedly reduced the effect of MT on GSH/GSSG and AsA/DHA, while p-CPA showed little influence on the SNP-induced regulation of GSH/GSSG and AsA/DHA (**Supplementary Figure 1**). These results indicate that MT and SNP can scavenge ROS by increasing the activity of antioxidant enzymes the contents of AsA and GSH, as well as GSH/GSSG and AsA/DHA, alleviating oxidative damage caused by cold stress in cucumber seedlings. NO may function as a downstream signal of MT and play a role in ROS scavenging.

The Role of NO in MT-Induced CO_2 Assimilation

When seedlings were subjected to chilling for 24 h, P_n and A_{sat} in the H_2O treatment were decreased by 74.2 and 53.0% (**Figures 10A,B**), respectively, in comparison to those of the

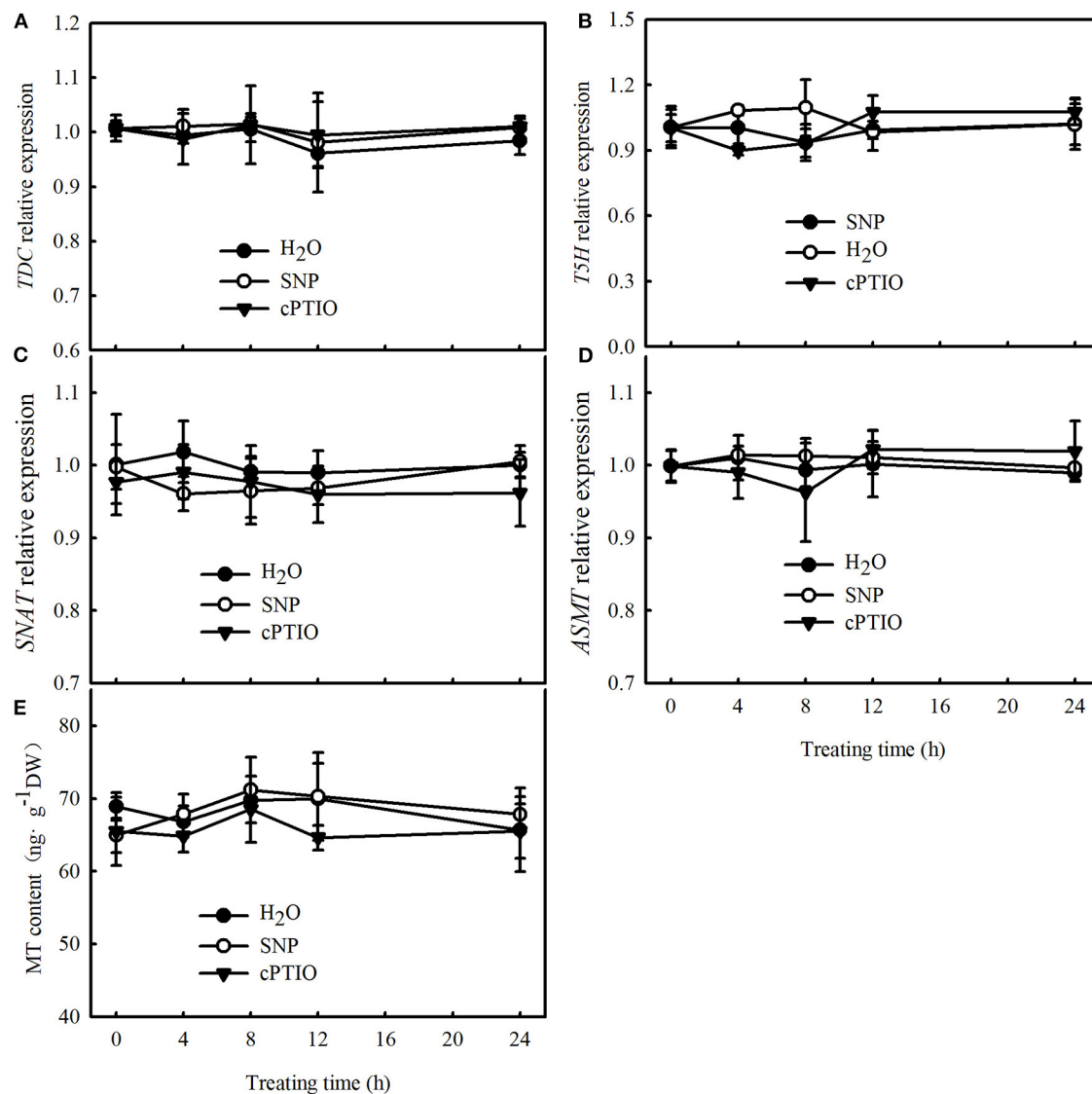


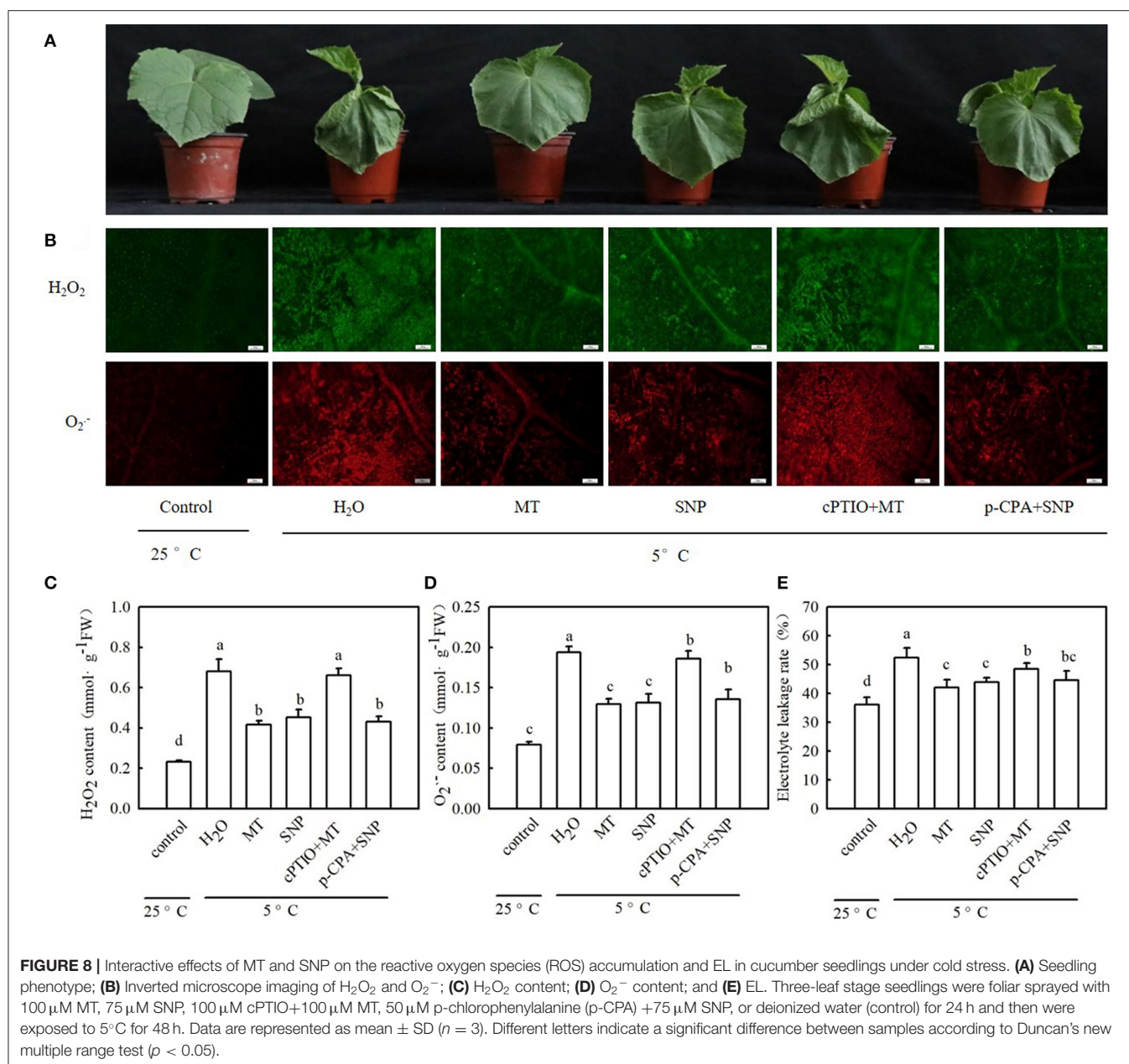
FIGURE 7 | Effects of SNP on MT content and key genes of MT biosynthesis, relative mRNA expression in cucumber seedlings. **(A–D)** Relative mRNA expression of *TDC*, *T5H*, *SNAT*, and *ASMT*, respectively; **(E)** MT content. Three-leaf stage seedlings were foliar sprayed with 75 μM SNP, 100 μM 2-(4-carboxyphenyl)-4,4,5,5-tetramethylimidazoline-1-oxyl-3-oxide (cPTIO) (a NO biosynthetic inhibitor), or distilled water (control) for 24 h. Data are represented as mean ± SD ($n = 3$).

control. MT- and SNP-treated seedlings exhibited a significant increase in P_n and A_{sat} relative to H₂O-treated seedlings under cold stress. The increases in P_n and A_{sat} in MT treatment were weakened by cPTIO, whereas those in NO-treated seedlings were not distinctly affected by p-CPA. After exposure to 5°C for 24 h, the activities of RuBPCase and RCA also distinctly decreased in all treatments (**Figures 10C,E**). Compared to H₂O treatment, MT and SNP increased the RuBPCase and RCA activity under cold stress ($p < 0.05$). The application of cPTIO significantly weakened MT-induced activities of RuBPCase and RCA, but p-CPA did not produce a noticeable effect on NO-induced RuBPCase or RCA activity. Similarly, relative expression at the mRNA and protein levels of *rbcl* in H₂O-treated seedlings was decreased by 53.8 and 43.0%, respectively (**Figures 10D,G**), and that of *RCA* in H₂O-treated seedlings

was reduced by 58.5 and 52.0%, respectively (**Figures 10F,H**), relative to those of the control. MT and SNP treatments showed significantly higher relative expression of *rbcl* and *RCA* at both the mRNA and protein levels than H₂O treatment ($p < 0.05$). The upregulation in relative expression of *rbcl* and *RCA* in MT treatment was also severely curtailed by cPTIO while that in SNP-treated seedlings was not affected by p-CPA.

The Role of NO in MT-Induced Photoprotection

To explore whether exogenous MT is relevant to photoprotection, we compared the degree of photoinhibition at photosystem I (PSI) and PSII in different treatment seedlings



under cold stress. Both MT and SNP significantly increased F_v/F_m and Φ_{PSII} relative to H_2O treatment ($p < 0.05$) during cold stress. The increases in F_v/F_m and Φ_{PSII} in MT treatment were markedly weakened by cPTIO, but those in SNP treatment were not remarkably influenced by p-CPA (Supplementary Figures 2A,B). In addition, histochemical observations with an inverted fluorescence microscope for F_v/F_m and Φ_{PSII} agreed with the detected results. From the chlorophyll fluorescence transients of dark-adapted leaves, we found that the chlorophyll transients fluorescence showed significant modifications when seedlings were subjected to 5°C for 24 h (Supplementary Figure 2C). Cold-stressed leaves revealed an increase in F_0 (O) while revealing a decrease in

F_m (IP) relative to the control leaves. The values of F_0 were significantly lower, but those of F_m were dramatically higher in MT-, SNP-, and p-CPA + SNP-treated seedlings than in H_2O -treated seedlings ($p < 0.05$); no differences were observed in F_0 and F_m between cPTIO + MT- or H_2O -treated seedlings. Cold stress led to an increase in variable fluorescence (F_v) of the O-J part but resulted in a decrease in the J-I and I-P phases. To avoid the production of any interference and heterogeneity, owing to different F_0 and F_m , we performed normalization at F_m . As shown in Supplementary Figure 2D, the increase in the O-J phase decreased in MT-, SNP-, and p-CPA + SNP-treated seedlings than in H_2O -treated seedlings, whereas those in cPTIO + MT-treated seedlings showed no significant difference

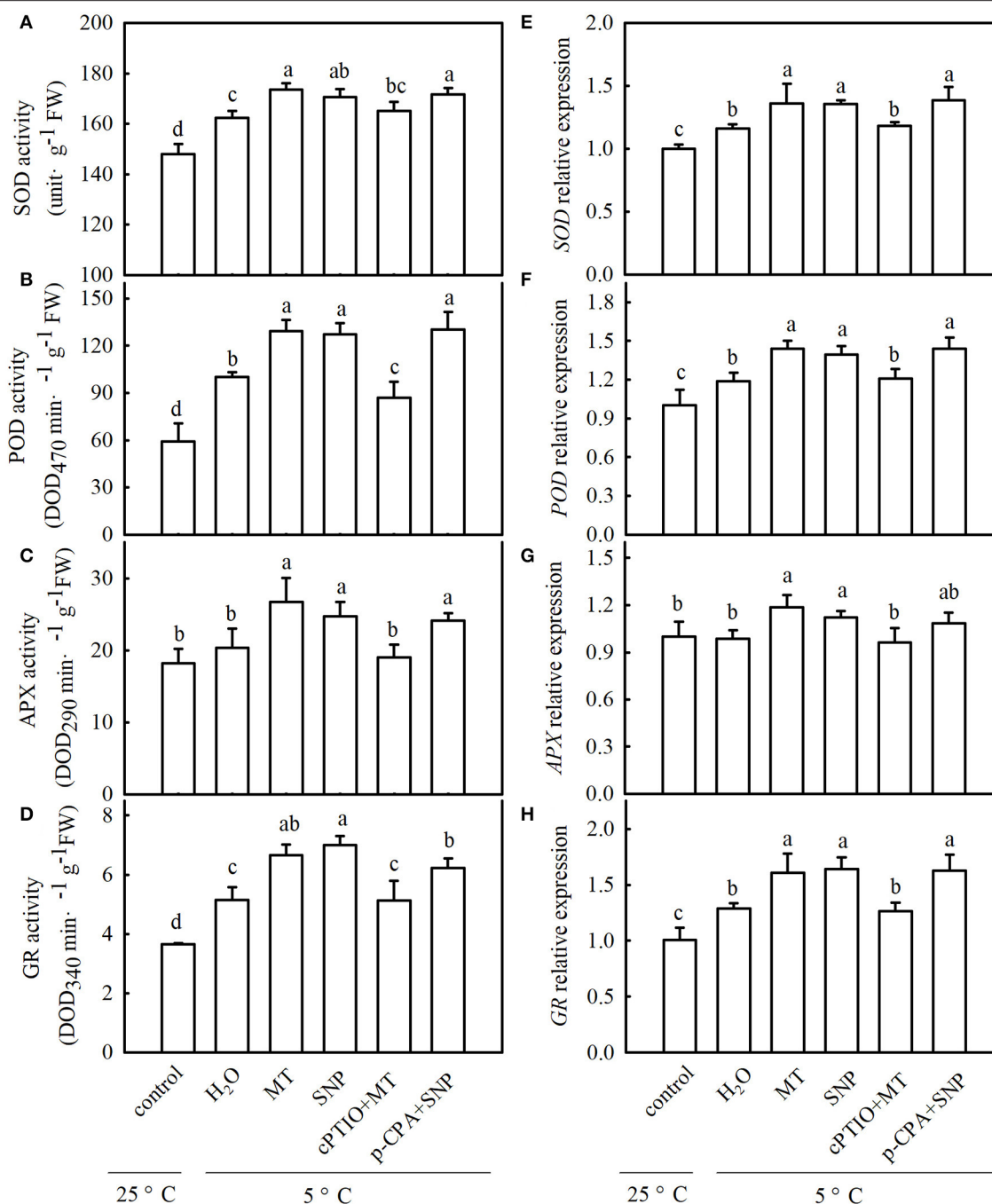


FIGURE 9 | Interactive effects of MT and SNP on activities and relative mRNA expression of antioxidant enzymes in cucumber seedlings under cold stress. **(A–D)**

Activities of superoxide dismutase (SOD), peroxidase (POD), ascorbate peroxidase (APX), and glutathione reductase (GR), respectively. **(E–H)** Relative mRNA expression of SOD, POD, APX, and GR, respectively. Three-leaf stage seedlings were foliar sprayed with 100 μ M MT, 75 μ M SNP, 100 μ M cPTIO+100 μ M MT, 50 μ M p-CPA + 75 μ M SNP, or deionized water (control) for 24 h and then were exposed to 5°C for 48 h. Data are represented as mean \pm SD ($n = 3$). Different letters indicate a significant difference between samples according to Duncan's new multiple range test ($p < 0.05$).

relative to H₂O-treated seedlings. Step J (2 ms) is a specific sign of limited electron transport for Q_A to Q_B and D1 protein damage (Liu et al., 2020). The ΔV_t curve showed that MT and SNP significantly decreased the amplitude of step J relative to H₂O

treatment. The decrease in step J in MT treatment was blocked by cPTIO, but p-CPA showed little effect on the SNP-induced reduction in the amplitude of step J (**Supplementary Figure 2E**). **Supplementary Figure 2F** reveals that cold stress reduced PI_{ABS}

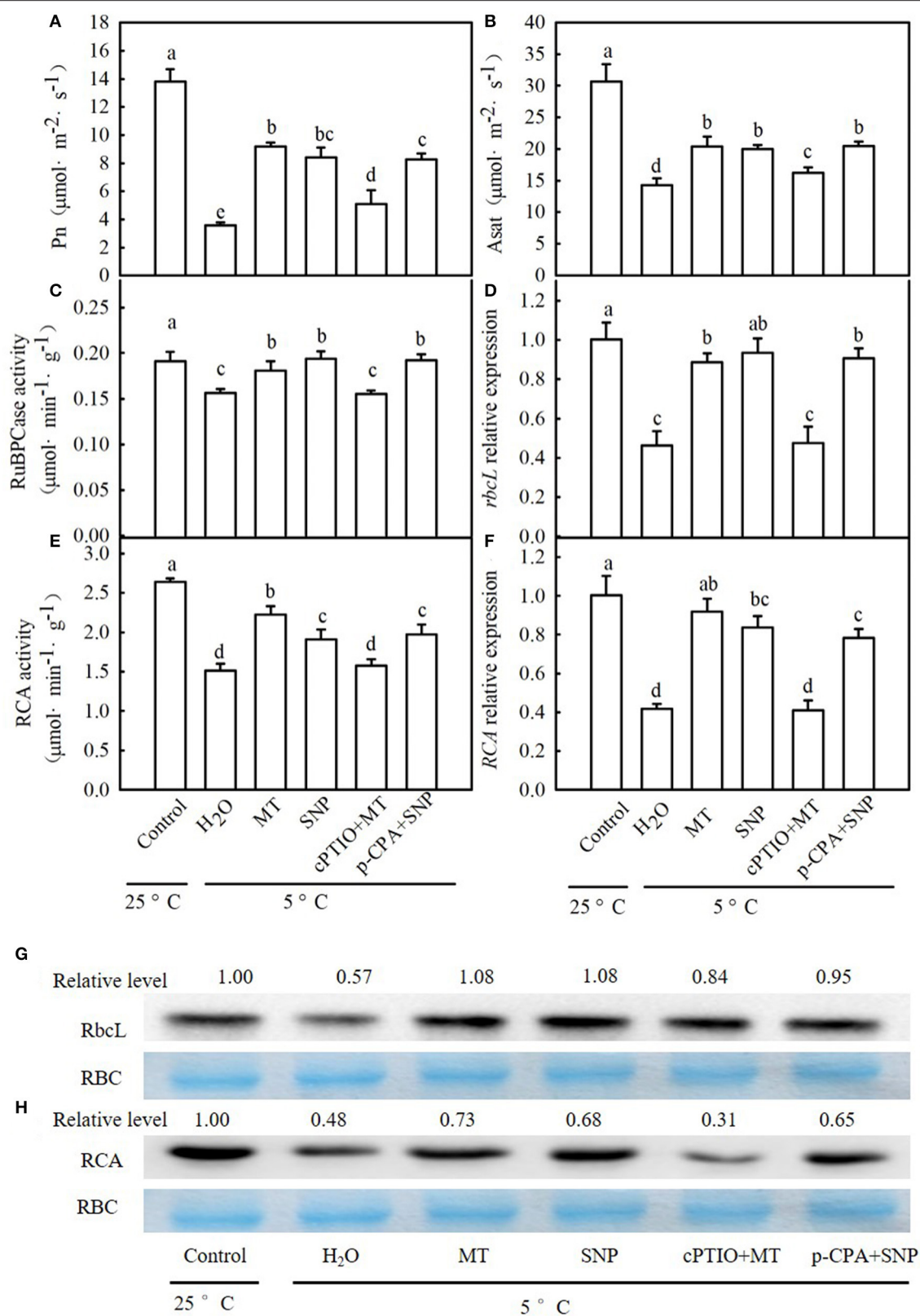


FIGURE 10 | Interactive effects of MT and SNP on P_n , A_{sat} , activity of Ribulose-1,5-bisphosphate carboxylase (RuBPCase) and Rubisco activase (RCA), and relative expression of *rbcL* and *RCA* in mRNA and the protein level in cucumber seedlings under cold stress. **(A)** P_n , **(B)** A_{sat} ; **(C,D)** activity of RuBPCase and RCA, **(E,F)** relative expression of *rbcL* and *RCA* in mRNA, **(G,H)** relative protein level of RbcL and RCA in cucumber seedlings under cold stress. **(Continued)**

FIGURE 10 | respectively; **(E,F)** Relative mRNA expression of *rbcl* and *RCA*, respectively; and **(G,H)** Protein level of *rbcl* and *RCA*, respectively. Coomassie Brilliant Blue staining Rubisco (RBC) protein is shown for equal loading control. Western blotting was performed three times with three independent biological samples, and similar results were obtained. Three-leaf stage seedlings were foliar sprayed with 100 μ M MT, 75 μ M SNP, 100 μ M cPTIO+100 μ M MT, 50 μ M p-CPA+75 μ M SNP, or deionized water (control) for 24 h and then were exposed to 5°C for 24 h. Data are represented as mean \pm SD ($n = 3$). Different letters indicate a significant difference between samples according to Duncan's new multiple range test ($p < 0.05$).

in cucumber seedlings ($p < 0.05$), and the decrease in PI_{ABS} of seedlings following 24 h stress was 98.5, 71.7, 61.0, 94.7, and 61.8% in the H₂O, MT, SNP, cPTIO + MT, and p-CPA + SNP treatment, respectively, compared with the control. Cold stress resulted in a significant decrease in Ψ_0 but an obvious increase in Φ_{D0} (**Supplementary Figures 2G,H**). Compared with H₂O treatment, a decrease in Ψ_0 and an increase in Φ_{D0} were significantly attenuated in MT and SNP treatments ($p < 0.05$). MT-induced variations in Ψ_0 and Φ_{D0} were repressed by cPTIO, whereas SNP-induced variations in Ψ_0 and Φ_{D0} were only marginally affected by p-CPA.

To validate the above results and to further explore the effect of exogenous MT on photoprotection in response to chilling and the role of NO in MT-induced photoprotection, we analyzed the protein levels of D1 and Psd in stressed seedlings. Cold stress largely downregulated the protein levels of D1 and Psd in all treatment seedlings (**Supplementary Figure 2I**). In comparison to H₂O-treated seedlings, MT- and SNP-treated seedlings displayed a significantly higher accumulation of D1 and Psd proteins after exposure to cold stress for 24 h. On the application of cPTIO, the positive effect of MT on the accumulation of D1 and Psd proteins was blocked, while p-CPA did not inhibit the effect of SNP on D1 or Psd protein levels. As shown in **Supplementary Figure 2J**, we found that $\Delta I/I_0$ was decreased by 67.2% in H₂O-treated seedlings when exposed to 5°C for 24 h. The decrease in $\Delta I/I_0$ in MT and SNP treatments was significantly less than that in H₂O treatment, indicating that MT and SNP play a positive role in protecting the PSI reaction center against photodamage caused by cold stress. cPTIO + MT-treated seedlings displayed an evidently lower $\Delta I/I_0$ than MT-treated seedlings ($p < 0.05$), but p-CPA + SNP-treated seedlings showed little difference in $\Delta I/I_0$ compared with SNP-treated seedlings under cold stress. These data suggest that MT and NO alleviated the inhibition of photosynthetic electron transport and the damage to D1 protein and the PSI reaction center caused by cold stress. NO acts as a downstream signal of MT and plays an important role in the process.

MT and SNP Upregulate the Expression of Cold-Responsive Genes Under Cold Stress

To examine whether the ICE1-CBF-COR transcriptional cascade contributed to MT- and SNP-induced cold tolerance in cucumber seedlings, we compared the responses of the *CBF1*, an inducer of *CBF* expression (*ICE1*), and cold-responsive (*COR47*) genes to cold stress among different treatments. **Figure 11** shows that cold stress largely upregulated relative mRNA expression of *ICE1*, *CBF1*, and *COR47* as well as *CBF1* protein accumulation in stressed seedlings, which was more obvious in MT and SNP treatments than in H₂O treatment. For example, relative

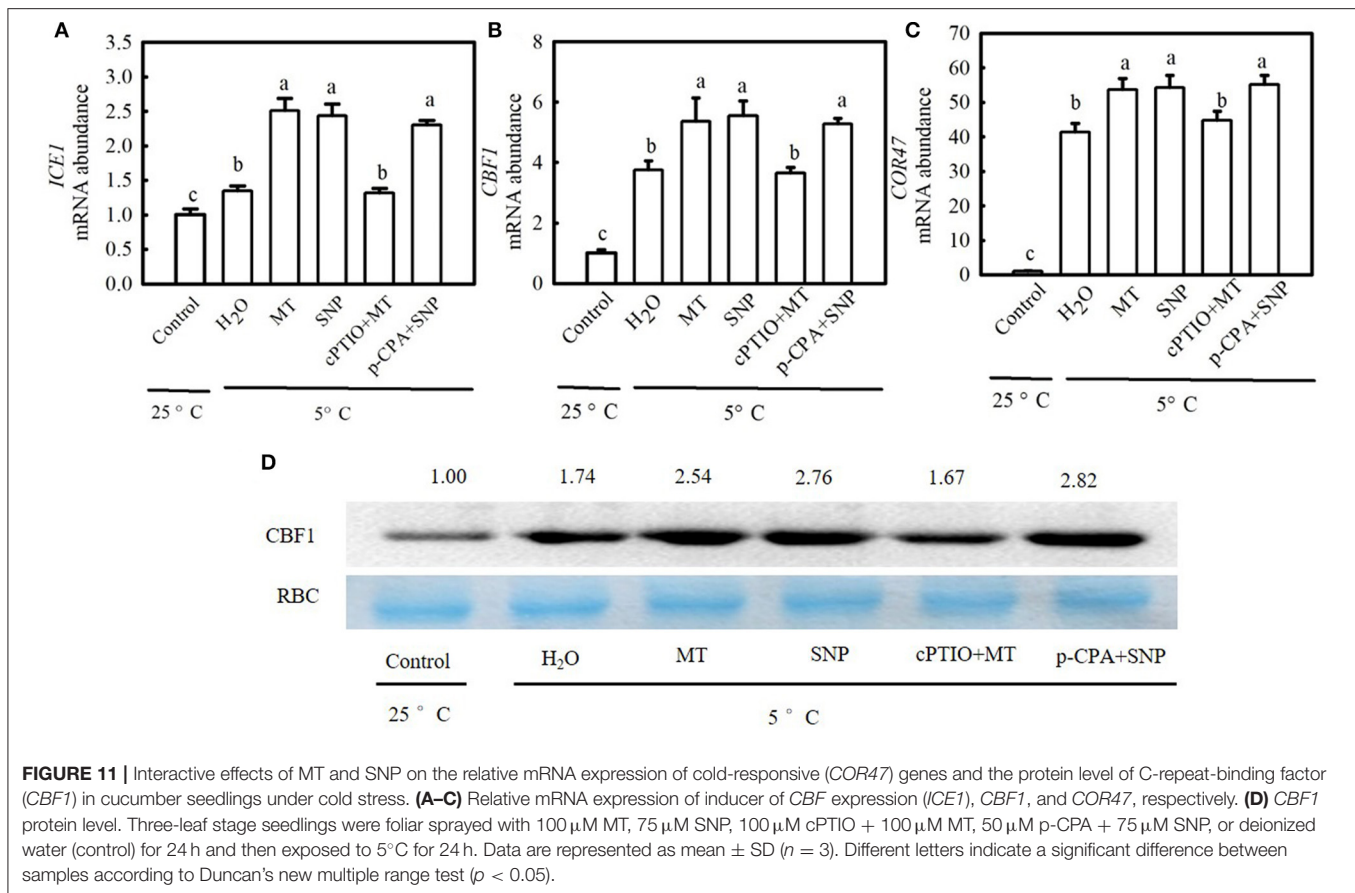
mRNA expression of *CBF1* in MT- and SNP-treated seedlings increased by 4.3- and 4.5-fold, respectively, but that in H₂O-treated seedlings only increased by 2.8-fold after exposure to 5°C for 48 h. The treatment with cPTIO significantly weakened the positive effect of MT on the expression of *COR47* genes, whereas the application of p-CPA showed little effect on NO-induced regulation of the expression of the above genes.

DISCUSSION

In the present study, we found that the endogenous MT emission system was activated by cold stress in the “JY35” and “ZN6” cucumber seedlings. The activities of TDC and ASMT, relative mRNA expression of *TDC* and *ASMT*, and MT accumulation in the “JY35” seedlings were significantly higher than those in the “ZN6” seedlings whereas 2-hydroxymelatonin accumulation in the “JY35” seedlings was markedly lower than that in the “ZN6” seedlings ($p < 0.05$) during cold stress (**Figure 1**). The “JY35” seedlings also exhibited higher F_v/F_m and Φ_{PSII} , lower MDA, EL, and CI, and minor damage than the “ZN6” seedlings following cold stress (**Figure 2**). These data suggest that endogenous MT accumulation under cold stress is positively correlated with cold tolerance in different varieties of cucumber seedlings.

Lei et al. (2004) first reported that exogenous MT attenuated cold-induced apoptosis in carrot suspension cells probably through upregulating polyamine levels. Afterward, Posmyk et al. (2009) revealed that MT alleviated lipid peroxidation in plant cell membranes caused by cold stress, but excessive MT concentration in cucumber seeds provoked oxidative changes in proteins. Heterologous human *SNAcT* expression in rice promoted the accumulation of endogenous MT, and the transgenic rice seedlings showed elevated chlorophyll synthesis and greater cold tolerance (Kang et al., 2010). Exogenous MT also induces the expression of *COR47* factors, such as *CBFs*, *DREBs*, and *COR15a* (Bajwa et al., 2014), indicating that MT has the physiological function of responding to cold stress and transcriptional activation of related metabolic processes. Seed pretreated with MT seemed to limit H₂O₂ accumulation during germination under cold stress and recovery periods (Bałabusta et al., 2016). The present study revealed that exogenous MT is involved in the regulation of cold tolerance in a concentration-dependent manner, as 100 μ M MT increased F_v/F_m , Φ_{PSII} , and P_n , decreased MDA accumulation and EL, and alleviated foliar damage in cucumber seedlings caused by cold stress; however, a higher concentration inhibited these positive effects (**Figure 3**).

Zhang et al. (2019) found that NR-derived NO synthesis was also involved in chilling acclimation and freezing tolerance in forage legumes. Liu et al. (2015) illustrated that exogenous MT treatment increased NO accumulation in tomato roots



under alkaline stress, and MT-induced NO production was accompanied by improvement of alkaline tolerance. Kaya et al. (2019) also observed that MT increased the tolerance of wheat seedlings to Cd toxicity by promoting endogenous NO. Tolerance to iron deficiency and salt stress induced by MT in pepper may be involved in downstream signal crosstalk between NO and H₂S (Kaya et al., 2020a). Our present data indicated that the endogenous NO emission system was also induced by cold stress (Figure 5), and 100 μ M MT significantly increased NR activity and relative mRNA expression, as well as NO accumulation in cucumber seedlings (Figure 4). However, no significant differences were observed among SNP, p-CPA, and control treatments in MT content and relative mRNA expression of the key genes of MT biosynthesis (Figure 7). Both MT and SNP markedly enhanced cold tolerance, and the F_v/F_m and Φ_{PSII} reached maximum, but EL reduced to the minimum value under 100 μ M MT or 75 μ M SNP treatments relative to the control and with other concentrations of MT or SNP (Figures 4, 6). The addition of cPTIO reduced MT-induced cold tolerance, whereas NO-induced cold tolerance was not affected by p-CPA (Figure 8). By detecting the antioxidant system, photosynthetic carbon assimilation, photoprotection, and the ICE-CBF-COR pathway, we speculated that NO, as a downstream signal, plays a crucial role in MT-induced cold tolerance in cucumber seedlings.

Generally, cell membrane dysfunction and excessive ROS production are the two main events of chilling injury (Chongchatuporn et al., 2013). When ROS accumulation is higher than the level that the defense mechanism can handle, cells experience oxidative stress (Schipper et al., 2016). Previous studies have demonstrated that MT and NO act as antioxidative signaling molecules to defend against abiotic stress by declining ROS production and enhancing the activity of antioxidative enzymes (Lei et al., 2004; Siddiqui et al., 2011; Bařabusta et al., 2016; Nawaz et al., 2018; Yan et al., 2019). Under arsenic (As) toxicity conditions, the application of Mel and Ca²⁺ synergistically suppressed the programmed cell death features of plants (nuclear condensation and nuclear fragmentation) in guard cells of stomata, DNA damage, and the formation of ROS in guard cells, leaves, and roots (Siddiqui et al., 2020). Here, we confirmed that cold stress triggered a burst of H₂O₂ and O₂⁻, enhanced EL and MDA accumulation, and subsequently caused ROS-associated injury in cucumber seedlings. Exogenous MT and SNP distinctly decreased ROS accumulation and ROS-induced damage in cucumber seedlings during cold stress (Figure 8). Furthermore, MT and SNP also increased the activity of antioxidant enzymes and their relative mRNA expression (Figure 9), suggesting that they can protect the cellular membrane and subcellular structures of cucumber under cold.

Ascorbic acid and GSH, the key cellular redox signal elements, are usually used for both ROS detoxification and redox signal transmission. In the AsA–GSH cycle, reduced ascorbate (AsA) is oxidized to unstable radical monodehydroascorbate (MDHA), and MDHA rapidly generates dehydroascorbate (DHA) (Smirnoff, 2000). Subsequently, DHA is converted back to AsA with the usage of reduced GSH as the electron donor (Fotopoulos et al., 2010). It is believed that maintaining higher proportions of AsA/DHA and GSH/GSSG is very important to ensure the normal participation of AsA and GSH in the AsA–GSH cycle and other physiological processes under abiotic stress. Therefore, higher proportions of AsA/DHA and/or GSH/GSSG might be the key factors for effective protection against abiotic stress-induced ROS accumulation (Fotopoulos et al., 2010; Balabusta et al., 2016). Kaya et al. (2020b,c) found that NO upregulated the activities of the AsA–GSH cycle and antioxidant enzymes, so it may play a central role as a signaling molecule in salt and Cd tolerance in pepper plants. Here, we found that cold-stressed cucumber seedlings exhibited a significant decrease in AsA, GSH, AsA/DHA, and GSH/GSSG. The application of MT and SNP notably enhanced AsA, GSH, AsA/DHA, and

GSH/GSSG under cold stress, compared with H₂O-pretreated seedlings (**Supplementary Figure 1**). These results indicate that cold stress seriously influences the redox balance in cucumber seedlings. Exogenous MT and SNP maintain redox states by upregulating the proportion of AsA/DHA and GSH/GSSG and consequently balance ROS generation and scavenging. To further elucidate the interactive role of MT and NO in exerting effective protection against chilling-induced ROS accumulation, we also applied p-CPA and cPTIO. The positive effect of MT on the antioxidant ability during cold stress was distinctly suppressed by cPTIO, but that of SNP on NO-induced ROS scavenging capacity was not affected by p-CPA. These data indicate that NO is involved in cell membrane protection induced by MT, especially in defense against oxidative stress during chilling.

Recently, some findings on the function of MT in plant photosynthesis have been published. Liang et al. (2019) reported that MT upregulates the genes involved in CO₂ fixation, such as *PGK*, *FBA*, and *FBP*, in kiwifruit seedlings. MT also improves photosynthetic capacity by inhibiting stomatal closure, enhancing light energy absorption, promoting electron transport in PSII, and increasing the adaptability of kiwifruit

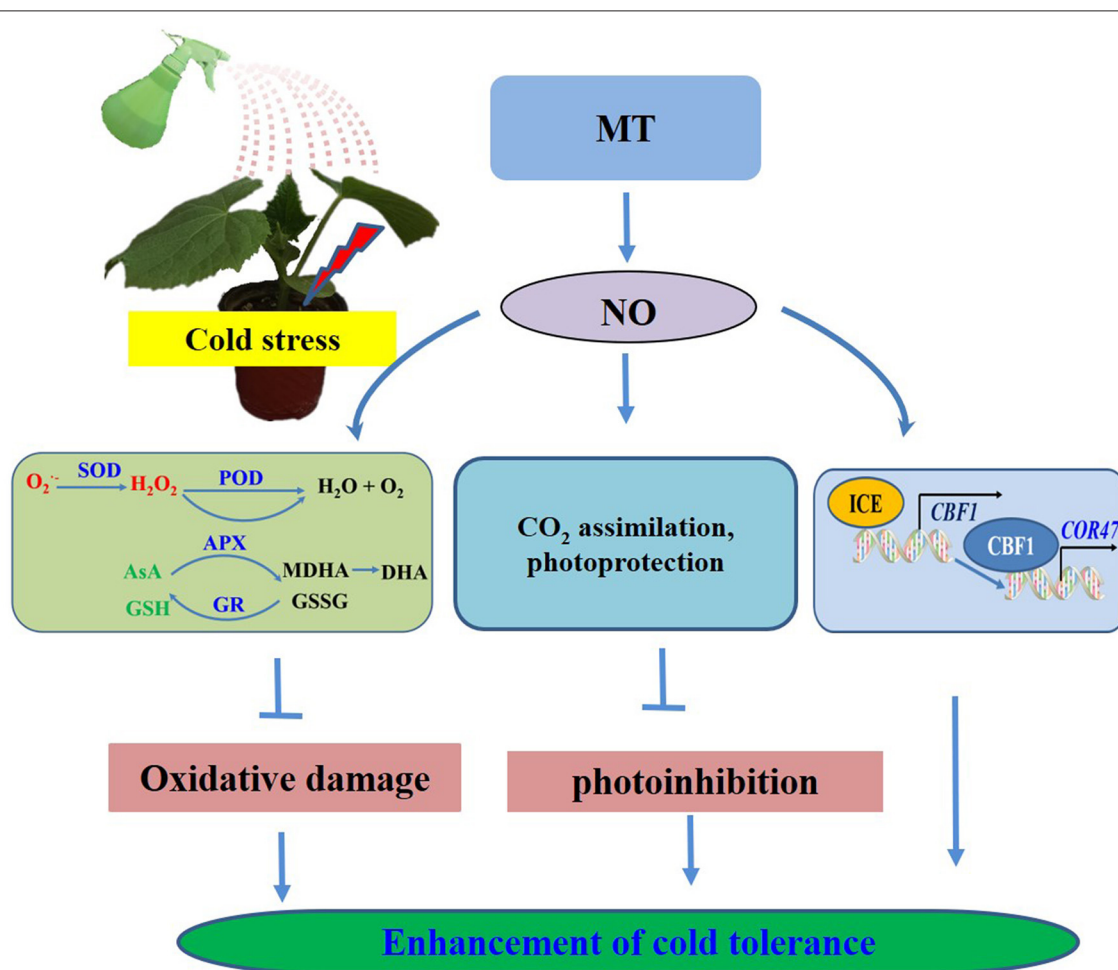


FIGURE 12 | Simplified schematic model for MT-induced cold tolerance in cucumber.

seedlings to drought stress. A similar result illustrated that the application of MT notably increased photosynthesis efficiency, upregulated chlorophyll synthesis genes, and PSII maximum efficiency (F_v/F_m) in nickel-stressed tomato plants (Jahan et al., 2020). Siddiqui et al. (2020) confirmed that MT enhanced gas exchange parameters and the activity of enzymes involved in the photosynthesis process (carbonic anhydrase and RuBisCo) and Chl biosynthesis (δ -aminolevulinic acid dehydratase) and decreased the activity of Chl degrading enzyme (chlorophyllase) under As toxicity conditions. Similarly, Tan et al. (2008) revealed that NO also increased the photosynthesis of wheat seedlings subjected to osmotic stress. In cucumber seedlings, however, a cross-talk between MT and NO in the regulation of photosynthesis under cold stress is unclear. In the present study, we observed that both MT and SNP markedly increased P_n , A_{sat} , activities of RuBPCase and RCA, relative mRNA expression of *rbcL* and *RCA*, and the protein accumulation of *rbcL* and *RCA*, compared with H₂O treatment under cold stress. cPTIO substantially abolished MT promotion in CO₂ assimilation during chilling, whereas p-CPA did not inhibit the function of SNP under stress conditions (Figure 10). Meanwhile, MT- and SNP-treated seedlings showed a significantly increased F_v/F_m , Φ_{PSII} , PI_{ABS} , ψ_0 , and D1 protein, as well as $\Delta I/I_0$ and PsaD accumulation, relative to H₂O-treated seedlings under cold stress (Supplementary Figure 2). These data support the view that MT and NO play a positive role in the photoprotection for both PSII and PSI in cucumber seedlings. The D1 protein repair pathway is considered to be conducive to cold tolerance in plants (Fang et al., 2019; Liu et al., 2020). In addition, PsaD plays distinct roles in facilitating ferredoxin-mediated NADP⁺ photoreduction on the reducing side of PSI (Chitnis et al., 1996). From this, it seems to be clear that MT- and NO-induced photoprotection may be involved in the activation of the D1 repair pathway in PSII and improvement of ferredoxin-mediated NADP⁺ photoreduction in PSI during cold stress. Considering our investigation after the application of cPTIO and p-CPA, the results suggest that NO is required as a downstream signal for MT-induced CO₂ assimilation and photoprotection in cucumber seedlings.

In higher plants, the ICE1–CBF–COR transcriptional cascade is considered the most well-understood cold acclimation signaling pathway. In this pathway, CBFs are crucial transcription factors (Zhou et al., 2018) and are essential for the induction of cold tolerance (Kang et al., 2013). Thomashow (2001) reported that the overexpression of *CBF* genes increased freezing tolerance in Arabidopsis whereas the knockdown of *CBF1* and/or *CBF3* decreased plant tolerance to freezing stress after cold acclimation (Novillo et al., 2007). Previous studies have demonstrated that hormones play a crucial role in the response of plants to cold stress. For instance, a decrease in endogenous ethylene weakens the transcriptional inhibition of *CBFs* by ethylene signaling and triggers *CBF*-dependent cold acclimation during the early stages of cold stress. Subsequently, the cold stress response promotes EIN3 accumulation to prevent overaccumulation of *CBFs* through feedback adjustment (Shi Y. T. et al., 2015). The present results revealed that cold stress increased the relative mRNA levels of *ICE1*, *CBF1*, and *COR47*, and *CBF1* protein accumulation in cucumber

seedlings (Figure 11). MT and SNP significantly upregulated the expression of *ICE1*, *CBF1*, and *COR47*, indicating that MT and NO are involved in the ICE1–CBF–COR transcriptional cascade. The application of cPTIO repressed MT-induced positive effect on the transcriptional and protein levels of *ICE1*, *CBF1*, and *COR47*, whereas p-CPA showed little influence on SNP-induced regulation of the expression of *COR47* genes. These results further illustrate that NO functions as a downstream signal to participate in MT-induced cold tolerance in cucumber seedlings.

CONCLUSIONS

Based on the present results, we proposed a model for MT-induced cold tolerance in cucumber seedlings. As shown in Figure 12, endogenous MT induced by cold or the application of MT and SNP alleviated the negative effects of growth and photosynthesis by scavenging excessive ROS, by protecting the photosynthetic apparatus and activating the ICE–CBF1–COR signaling pathway. All the investigated results indicate that NO, acting as a downstream signal, plays a critical role in MT-induced cold tolerance in cucumber seedlings. A number of evidence for the importance of exogenous MT and SNP provide potential new approaches for relieving chilling injury in cold-sensitive plants. To better reveal the detailed mechanisms and interaction of MT- and NO-induced cold tolerance in plants, further studies using advanced molecular techniques and mutant analyses are required.

DATA AVAILABILITY STATEMENT

The original contributions presented in the study are included in the article/Supplementary Material, further inquiries can be directed to the corresponding author/s.

AUTHOR CONTRIBUTIONS

YF performed most part of the experiment, analyzed the data, and completed the first draft. XA and HB designed the research and edited the manuscript. XF, LH, CX, and CL worked together with YF to accomplish the experiment. All authors contributed to the article and approved the submitted version.

FUNDING

This work was supported by the National Key Research and Development Program of China (2018YFD1000800), the Major Science and Technology Innovation of Shandong Province in China (2019JZZY010715), the Special Fund of Modern Agriculture Industrial Technology System of Shandong Province in China (SDAIT-05–10), and the Funds of Shandong Double Tops Program (SYL2017YSTD06).

SUPPLEMENTARY MATERIAL

The Supplementary Material for this article can be found online at: <https://www.frontiersin.org/articles/10.3389/fpls.2021.686545/full#supplementary-material>

REFERENCES

- Ahammed, G. J., Xu, W., Liu, A., and Chen, S. (2018). Endogenous melatonin deficiency aggravates high temperature-induced oxidative stress in *Solanum lycopersicum* L. *Environ. Exp. Bot.* 161, 303–311. doi: 10.1016/j.envexpbot.2018.06.006
- Ahanger, M. A., Aziz, U., Alsahli, A. A., Alyemeni, M. N., and Ahmad, P. (2020). Influence of exogenous salicylic acid and nitric oxide on growth, photosynthesis, and ascorbate-glutathione cycle in salt stressed vigna angularis. *Biomolecules* 10:42. doi: 10.3390/biom10010042
- Al-Huqail, A. A., Khan, M. N., Ali, H. M., Siddiqui, M. H., Al-Huqail, A. A., AlZuaib, F. M., et al. (2020). Exogenous melatonin mitigates boron toxicity in wheat. *Cototoxicol. Environ. Saf.* 201:110822. doi: 10.1016/j.ecoenv.2020.110822
- Arnao, M. B. (2014). Phyto-melatonin: discovery, content, and role in plants. *Adv. Bot.* 2014:e815769. doi: 10.1155/2014/815769
- Arnao, M. B., and Hernandez-Ruiz, J. (2015). Functions of melatonin in plants: a review. *J. Pineal Res.* 59, 133–150. doi: 10.1111/jpi.12253
- Arnao, M. B., and Hernandez-Ruiz, J. (2018). Melatonin and its relationship to plant hormones. *Ann. Bot.* 121, 195–207. doi: 10.1093/aob/mcx114
- Bajwa, V. S., Shukla, M. R., Sherif, S. M., Murch, S. J., and Saxena, P. K. (2014). Role of melatonin in alleviating cold stress in *Arabidopsis thaliana*. *J. Pineal Res.* 56, 238–245. doi: 10.1111/jpi.12115
- Balabusta, M., Szafranska, K., and Posmyk, M. M. (2016). Exogenous melatonin improves antioxidant defense in cucumber seeds (*Cucumis sativus* L.) germinated under chilling stress. *Front. Plant Sci.* 7:575. doi: 10.3389/fpls.2016.00575
- Bian, F. E., Xiao, Q. H., Hao, G. M., Sun, Y. J., Lu, W. L., Du, Y., et al. (2018). Effect of root-applied melatonin on endogenous melatonin and chlorophyll fluorescence characteristics in grapevine under NaCl stress. *Sci. Agric. Sinica.* 51, 952–963. doi: 10.3864/j.issn.0578-1752.2018.05.013
- Chen, D. D., Zhang, Z. S., Sun, X. B., Zhao, M., Sun, G. Y., and Chow, W. S. (2016). Photoinhibition and photoinhibition-like damage to the photosynthetic apparatus in tobacco leaves induced by *Pseudomonas syringae* pv. Tabaci under light and dark conditions. *BMC Plant Biol.* 16, 1–11. doi: 10.1186/s12870-016-0723-6
- Chitnis, V. P., Jung, Y. S., Albee, L., Golbeck, J. H., and Chitnis, P. R. (1996). Mutational analysis of photosystem I polypeptides: role of psad and the lysyl 106 residue in the reductase activity of photosystem I. *J. Biol. Chem.* 271, 11772–11780. doi: 10.1074/jbc.271.20.11772
- Chongchatuporn, U., Ketsa, S., and Van Doorn, W. G. (2013). Chilling injury in mango (*Mangifera indica*) fruit peel: relationship with ascorbic acid concentrations and antioxidant enzyme activities. *Postharvest Biol. Technol.* 86, 409–417. doi: 10.1016/j.postharvbio.2013.07.023
- Cui, G. B., Sun, F. L., Gao, X. M., Xie, K. L., Zhang, C., Liu, S. D., et al. (2018). Proteomic analysis of melatonin-mediated osmotic tolerance by improving energy metabolism and autophagy in wheat (*Triticum aestivum* L.). *Planta* 248, 69–87. doi: 10.1007/s00425-018-2881-2
- Cui, G. B., Zhao, X. X., Liu, S. D., Sun, F. L., Zhang, C., and Xi, Y. J. (2017). Beneficial effects of melatonin in overcoming drought stress in wheat seedlings. *Plant Physiol. Biochem.* 118, 138–149. doi: 10.1016/j.plaphy.2017.06.014
- Demmig-Adams, B., and Adams, W. W. III. (1996). Xanthophyll cycle and light stress in nature: uniform response to excess direct sunlight among higher plant species. *Planta* 198, 460–470. doi: 10.1007/BF00620064
- Ding, Y. L., Li, H., Zhang, X. Y., Xie, Q., Gong, Z. Z., and Yang, S. H. (2015). Ost1 kinase modulates freezing tolerance by enhancing ICE1 stability in *Arabidopsis*. *Dev. Cell* 32, 278–289. doi: 10.1016/j.devcel.2014.12.023
- Dong, X. B., Bi, H. G., Wu, G. X., and Ai, X. Z. (2013). Drought-induced chilling tolerance in cucumber involves membrane stabilisation improved by antioxidant system. *Int. J. Plant Prod.* 7, 67–80.
- Erland, L. A. E., Saxena, P. K., and Murch, S. J. (2018). Melatonin in plant signalling and behaviour. *Funct. Plant Biol.* 45, 58–69. doi: 10.1071/FP16384
- Ethier, G. J., and Livingston, N. J. (2004). On the need to incorporate sensitivity to CO₂ transfer conductance into the Farquhar-von Caemmerer-Berry leaf photosynthesis model. *Plant Cell Environ.* 27, 137–153. doi: 10.1111/j.1365-3040.2004.01140.x
- Fan, J. B., Hu, Z. R., Xie, Y., Chan, Z. L., Chen, K., Amombo, E., et al. (2015). Alleviation of cold damage to photosystem II and metabolisms by melatonin in *Bermudagrass*. *Front. Plant Sci.* 6:925. doi: 10.3389/fpls.2015.00925
- Fan, J. B., Xie, Y., Zhang, Z. C., and Chen, L. (2018). Melatonin: a multifunctional factor in plants. *Int. J. Mol. Sci.* 19, 1–14. doi: 10.3390/ijms19051528
- Fang, P. P., Yan, M. Y., Chi, C., Wang, M. Q., Zhou, Y. H., Zhou, J., et al. (2019). Brassinosteroids act as a positive regulator of photoprotection in response to chilling stress. *Plant Physiol.* 180, 2061–2076. doi: 10.1104/pp.19.00088
- Fotopoulos, V., Ziogas, V., Tanou, G., and Molassiotis, A. (2010). “Involvement of AsA/DHA and GSH/GSSG ratios in gene and protein expression and in the activation of defence mechanisms under abiotic stress conditions”, in *Ascorbate-Glutathione Pathway and Stress Tolerance in Plants*, eds N. Anjum, M. T. Chan, S. Umar (Dordrecht: Springer), 265–302.
- Foyer, C. H., and Halliwell, B. (1976). The presence of glutathione and glutathione reductase in chloroplasts: a proposed role in ascorbic acid metabolism. *Planta* 133, 21–25. doi: 10.1007/BF00386001
- Guo, F. Q., and Crawford, N. M. (2005). *Arabidopsis* nitric oxide synthase1 is targeted to mitochondria and protects against oxidative damage and dark-induced senescence. *Plant Cell* 17, 3436–3450. doi: 10.1105/tpc.105.037770
- Hernández-ruiz, J., Cano, A., and Arnao, M. B. (2005). Melatonin acts as a growth-stimulating compound in some monocot species. *J. Pineal Res.* 39, 137–142. doi: 10.1111/j.1600-079X.2005.00226.x
- Hu, Y., Jiang, L. Q., and Wang, F., Yu D, Q. (2013). Jasmonate regulates the inducer of CBF expression-C-repeat binding factor/DRE binding factor1 cascade and freezing tolerance in *Arabidopsis*. *Plant Cell* 25, 2907–2924. doi: 10.1105/tpc.113.112631
- Jahan, M. S., Guo, S. R., Baloch, A. R., Sun, J., Shu, S., Roy, R., et al. (2020). Melatonin alleviates nickel phytotoxicity by improving photosynthesis, secondary metabolism and oxidative stress tolerance in tomato seedlings. *Ecotoxicol. Environ. Saf.* 197:110593. doi: 10.1016/j.ecoenv.2020.110593
- Kagale, S., Divi, U. K., Krochko, J. E., and Krishna, K. P. (2007). Brassinosteroid confers tolerance in *Arabidopsis thaliana* and *Brassica napus* to a range of abiotic stresses. *Planta* 225, 353–364. doi: 10.1007/s00425-006-0361-6
- Kang, J. Q., Zhang, H., Sun, T. S., Shi, Y. H., Wang, J. Q., Zhang, B. C., et al. (2013). Natural variation of C-repeat-binding factor (CBFs) genes is a major cause of divergence in freezing tolerance among a group of *Arabidopsis thaliana* populations along the Yangtze River in China. *New Phytol.* 199, 1069–1080. doi: 10.1111/nph.12335
- Kang, K., Lee, K., Park, S., Kim, Y. S., and Back, K. (2010). Enhanced production of melatonin by ectopic overexpression of human serotonin N-acetyltransferase plays a role in cold resistance in transgenic rice seedlings. *J. Pineal Res.* 49, 176–182. doi: 10.1111/j.1600-079X.2010.00783.x
- Kaya, C., Ashraf, M., Alyemeni, M. N., and Ahmad, P. (2020b). The role of endogenous nitric oxide in salicylic acid-induced up-regulation of ascorbate-glutathione cycle involved in salinity tolerance of pepper (*Capsicum annuum* L.) plants. *Plant Physiol. Biochem.* 147, 10–20. doi: 10.1016/j.plaphy.2019.11.040
- Kaya, C., Ashraf, M., Alyemeni, M. N., and Ahmad, P. (2020c). The role of nitrate reductase in brassinosteroid induced endogenous nitric oxide generation to improve cadmium stress tolerance of pepper plants by upregulating the ascorbate-glutathione cycle. *Ecotoxicol. Environ. Saf.* 196:110483. doi: 10.1016/j.ecoenv.2020.110483
- Kaya, C., Higgs, D., Alyemeni, M. N., and Ahmad, P. (2020a). Integrative roles of nitric oxide and hydrogen sulfide in melatonin-induced tolerance of pepper (*Capsicum annuum* L.) plants to iron deficiency and salt stress alone or in combination. *Physiol. Plant* 168, 256–277. doi: 10.1111/ppl.12976
- Kaya, C., Okant, M., Ugurlar, F., Alyemeni, M. N., Ashraf, M., and Ahmad, P. (2019). Melatonin-mediated nitric oxide improves tolerance to cadmium toxicity by reducing oxidative stress in wheat plants. *Chemosphere* 225, 627–638. doi: 10.1016/j.chemosphere.2019.03.026
- Kong, X. M., Ge, W. Y., Wei, B. D., Zhou, Q., Zhou, X., Ji, S. J., et al. (2020). Melatonin ameliorates chilling injury in green bell peppers during storage by regulating membrane lipid metabolism and antioxidant capacity. *Postharvest Biol. Technol.* 170:111315. doi: 10.1016/j.postharvbio.2020.111315
- Law, M. Y., Charles, S. A., and Halliwell, B. (1983). Glutathione and ascorbic acid in spinach (*Spinacia oleracea*) chloroplasts. the effect of hydrogen peroxide and of Paraquat. *Biochem. J.* 210, 899–903. doi: 10.1042/bj2100899
- Lei, X. Y., Zhu, R. Y., Zhang, G. Y., and Dai, Y. R. (2004). Attenuation of cold-induced apoptosis by exogenous melatonin in carrot suspension cells: the possible involvement of polyamines. *J. Pineal Res.* 36, 126–131. doi: 10.1046/j.1600-079X.2003.00106.x

- Li, J. H., Yang, Y. Q., Sun, K., Chen, Y., Chen, X., and Li, X. H. (2019). Exogenous melatonin enhances cold, salt and drought stress tolerance by improving antioxidant defense in tea plant (*Camellia sinensis* (L.) O. Kuntze). *Molecules* 24:1826. doi: 10.3390/molecules24091826
- Li, X., Ahammed, G. J., Zhang, X. N., Zhang, L., Yan, P., Zhang, L. P., et al. (2021). Melatonin-mediated regulation of anthocyanin biosynthesis and antioxidant defense confer tolerance to arsenic stress in *Camellia sinensis* L. *J. Hazard. Mater.* 403:123922. doi: 10.1016/j.jhazmat.2020.123922
- Liang, D., Ni, Z. Y., Xia, H., Xie, Y., Lv, X. L., Wang, J., et al. (2019). Exogenous melatonin promotes biomass accumulation and photosynthesis of kiwifruit seedlings under drought stress. *Sci. Hortic.* 246, 34–43. doi: 10.1016/j.scienta.2018.10.058
- Liu, F. J., Fu, X., Wu, G. X., Feng, Y. Q., Li, F. D., Bi, H. G., et al. (2020). Hydrogen peroxide is involved in hydrogen sulfide-induced carbon assimilation and photoprotection in cucumber seedlings. *Environ. Exp. Bot.* 175:104052. doi: 10.1016/j.envexpbot.2020.104052
- Liu, N., Gong, B., Jin, Z. Y., Wang, X. F., Wei, M., Shi, Q. H., et al. (2015). Sodic alkaline stress mitigation by exogenous melatonin in tomato needs nitric oxide as a downstream signal. *J. Plant Physiol.* 186–187, 68–77. doi: 10.1016/j.jplph.2015.07.012
- Martinez, V., Nieves-Cordones, M., Lopez-Delacalle, M., Rodenas, R., Mestre, T., Garcia-Sanchez, F., et al. (2018). Tolerance to stress combination in tomato plants: new insights in the protective role of melatonin. *Molecules* 23:535. doi: 10.3390/molecules23030535
- Mishina, T. E., Lamb, C., and Zeier, J. (2007). Expression of a nitric oxide degrading enzyme induces a senescence programme in Arabidopsis. *Plant Cell Environ.* 30, 39–52. doi: 10.1111/j.1365-3040.2006.01604.x
- Murch, S. J., and Saxena, P. K. (2002). Melatonin: a potential regulator of plant growth and development? *In Vitro Cell. Dev. Biol. Plant* 38, 531–536. doi: 10.1079/IVP2002333
- Nakano, Y., and Asada, K. (1987). Purification of ascorbate peroxidase in spinach chloroplasts; its inactivation in ascorbate-depleted medium and reactivation by monodehydroascorbate radical. *Plant Cell Physiol.* 28, 131–140.
- Nawaz, M. A., Jiao, Y. Y., Chen, C., Shireen, F., Zheng, Z. H., Imtiaz, M., et al. (2018). Melatonin pretreatment improves vanadium stress tolerance of watermelon seedlings by reducing vanadium concentration in the leaves and regulating melatonin biosynthesis and antioxidant-related gene expression. *J. Plant Physiol.* 220, 115–127. doi: 10.1016/j.jplph.2017.11.003
- Novillo, F., Medina, J., and Salinas, J. (2007). Arabidopsis CBF1 and CBF3 have a different function than CBF2 in cold acclimation and define different gene classes in the CBF regulon. *Proc. Natl. Acad. Sci. U. S. A.* 104, 21002–21007. doi: 10.1073/pnas.0705639105
- Omran, R. G. (1980). Peroxide levels and the activities of catalase, peroxidase, and indoleacetic acid oxidase during and after chilling cucumber seedlings. *Plant Physiol.* 65, 407–408. doi: 10.1104/pp.65.2.407
- Pan, D. Y., Fu, X., Zhang, X. W., Liu, F. J., Bi, H. G., and Ai, X. Z. (2020). Hydrogen sulfide is required for salicylic acid-induced chilling tolerance of cucumber seedlings. *Protoplasma* 257, 1543–1557. doi: 10.1007/s00709-020-01531-y
- Park, S., Lee, D. E., Jang, H., Byeon, Y., Kim, Y. S., and Back, K. (2013). Melatonin-rich transgenic rice plants exhibit resistance to herbicide-induced oxidative stress. *J. Pineal Res.* 54, 258–263. doi: 10.1111/j.1600-079X.2012.01029.x
- Posmyk, M. M., Balabusta, M., Wiecek, M., Sliwinski, E., and Janas, K. M. (2009). Melatonin applied to cucumber (*Cucumis sativus* L.) seeds improves germination during chilling stress. *J. Pineal Res.* 46, 214–223. doi: 10.1111/j.1600-079X.2008.00652.x
- Qi, Z. Y., Wang, K. X., Yan, M. Y., Kanwar, M. K., Li, D. Y., Wijaya, L., et al. (2018). Melatonin alleviates high temperature-induced pollen abortion in *Solanum lycopersicum*. *Molecules* 23:386. doi: 10.3390/molecules23020386
- Salvatori, E., Fusaro, L., Gottardini, E., Pollastrini, M., Goltsev, V., Strasser, R. J., et al. (2014). Plant stress analysis: application of prompt, delayed chlorophyll fluorescence and 820 nm modulated reflectance. insights from independent experiments. *Plant Physiol. Biochem.* 85, 105–113. doi: 10.1016/j.plaphy.2014.11.002
- Scheler, C., Durner, J., and Astier, J. (2013). Nitric oxide and reactive oxygen species in plant biotic interactions. *Curr. Opin. Plant Biol.* 16, 534–539. doi: 10.1016/j.pbi.2013.06.020
- Schippers, J. H., Foyer, C. H., and Van Dongen, J. T. (2016). Redox regulation in shoot growth, SAM maintenance and flowering. *Curr. Opin. Plant Biol.* 29, 121–128. doi: 10.1016/j.pbi.2015.11.009
- Semeniuk, P., Moline, H. E., and Abbott, J. A. A. (1986). A comparison of the effects of ABA and an antitranspirant on chilling injury of coleus, cucumbers, and dieffenbachia. *J. Am. Soc. Hortic. Sci.* 111, 866–868.
- Shi, H. T., Chen, Y. H., Tan, D. X., Reiter, R. J., Chan, Z. L., and He, C. Z. (2015). Melatonin induces nitric oxide and the potential mechanisms relate to innate immunity against bacterial pathogen infection in Arabidopsis. *J. Pineal Res.* 59, 102–108. doi: 10.1111/jpi.12244
- Shi, Y. T., Ding, Y. L., and Yang, S. H. (2015). Cold signal transduction and its interplay with phytohormones during cold acclimation. *Plant Cell Physiol.* 56, 7–15. doi: 10.1093/pcp/pcu115
- Siddiqui, M. H., Alamri, S., Khan, M. N., Corpas, F. J., Al-Amri, A. A., Alsubaie, Q. D., et al. (2020). Melatonin and calcium function synergistically to promote the resilience through ROS metabolism under arsenic-induced stress. *J. Hazard. Mater.* 398:122882. doi: 10.1016/j.jhazmat.2020.122882
- Siddiqui, M. H., Al-Wahaibi, M. H., and Basalah, M. O. (2011). Role of nitric oxide in tolerance of plants to abiotic stress. *Protoplasma* 248, 447–455. doi: 10.1007/s00709-010-0206-9
- Singh, S., Husain, T., Kushwaha, B. K., Suhel, M., Fatima, A., Mishra, V., et al. (2020). Regulation of ascorbate-glutathione cycle by exogenous nitric oxide and hydrogen peroxide in soybean roots under arsenate stress. *J. Hazard. Mater.* 409:123686. doi: 10.1016/j.jhazmat.2020.123686
- Smirnov, N. (2000). Ascorbic acid: metabolism and functions of a multifaceted molecule. *Curr. Opin. Plant Biol.* 3, 229–235. doi: 10.1016/S1369-5266(00)80070-9
- Stewart, R. R. C., and Bewley, J. D. (1980). Lipid peroxidation associated with accelerated aging of soybean axes. *Plant Physiol.* 65, 245–248. doi: 10.1104/pp.65.2.245
- Tan, J. F., Zhao, H. J., Hong, J. P., Han, Y. L., Li, H., and Zhao, W. C. (2008). Effects of exogenous nitric oxide on photosynthesis, antioxidant capacity and proline accumulation in wheat seedlings subjected to osmotic stress. *World J. Agric. Sci.* 4, 307–313.
- Thomashow, M. F. (2001). So what's new in the field of plant cold acclimation? Lots! *Plant Physiol.* 125, 89–93. doi: 10.1104/pp.125.1.89
- Tian, Y. L., Ungerer, P., Zhang, H. Y., and Ruban, A. V. (2017). Direct impact of the sustained decline in the photosystem II efficiency upon plant productivity at different developmental stages. *J. Plant Physiol.* 212, 45–53. doi: 10.1016/j.jplph.2016.10.017
- Wang, A. G., and Luo, G. H. (1990). Quantitative relation between the reaction of hydroxylamine and superoxide anion radicals in plants. *Plant Physiol. Commun.* 26, 55–57.
- Wang, L., Feng, C., Zheng, X. D., Guo, Y., Zhou, F. F., Shan, D. Q., et al. (2017). Plant mitochondria synthesize melatonin and enhance the tolerance of plants to drought stress. *J. Pineal Res.* 63:e12429. doi: 10.1111/jpi.12429
- Wang, P., Yin, L. H., Liang, D., Li, C., Ma, F. W., and Yue, Z. Y. (2012). Delayed senescence of apple leaves by exogenous melatonin treatment: toward regulating the ascorbate-glutathione cycle. *J. Pineal Res.* 53, 11–20. doi: 10.1111/j.1600-079X.2011.00966.x
- Wimalasekera, R., Tebartz, F., and Scherer, G. F. E. (2011). Polyamines, polyamine oxidases and nitric oxide in development, abiotic and biotic stresses. *Plant Sci.* 181, 593–603. doi: 10.1016/j.plantsci.2011.04.002
- Yan, Y. Y., Jing, X., Tang, H. M., Li, X. T., Gong, B., and Shi, Q. H. (2019). Using transcriptome to discover a novel melatonin-induced sodic alkaline stress resistant pathway in *Solanum lycopersicum* L. *Plant Cell Physiol.* 60, 2051–2064. doi: 10.1093/pcp/pcz126
- Zhang, J. H., Wang, Y. Z., Sun, H. Y., Yang, L., and Jiang, F. C. (2014). Effects of exogenous salicylic acid on antioxidant enzymes and CBF transcription factor in apricot (*Prunus armeniaca* L.) flowers under chilling stress. *Plant Physiol. J.* 50, 171–177. doi: 10.13592/j.cnki.pj.2014.02.014
- Zhang, P. P., Li, S. S., Guo, Z. F., and Lu, S. Y. (2019). Nitric oxide regulates glutathione synthesis and cold tolerance in forage legumes. *Environ. Exp. Bot.* 167:103851. doi: 10.1016/j.envexpbot.2019.103851
- Zhang, X. W., Liu, F. J., Zhai, J., Li, F. D., Bi, H. G., and Ai, X. Z. (2020). Auxin acts as a downstream signaling molecule involved in

- hydrogen sulfide-induced chilling tolerance in cucumber. *Planta* 251, 1–19. doi: 10.1007/s00425-020-03362-w
- Zhang, Z. S., Jia, Y. J., Gao, H. Y., Zhang, L. T., Li, H. D., and Meng, Q. W. (2011). Characterization of PSI recovery after chilling-induced photoinhibition in cucumber (*Cucumis sativus* L.) Leaves. *Planta* 234, 883–889. doi: 10.1007/s00425-011-1447-3
- Zhao, S. J., Shi, G. A., and Dong, X. C. (2002). *Techniques of Plant Physiological Experiment*. (Beijing: China Agricultural Science and Technology Press), 42–44.
- Zhou, L., Li, J., He, Y. J., Liu, Y., and Chen, H. Y. (2018). Functional characterization of *SmCBF* genes involved in abiotic stress response in eggplant (*Solanum melongena*). *Sci. Hortic.* 233, 14–21. doi: 10.1016/j.scienta.2018.01.043

Conflict of Interest: The authors declare that the research was conducted in the absence of any commercial or financial relationships that could be construed as a potential conflict of interest.

The reviewer SZ declared a shared affiliation, with no collaboration, with the authors to the handling editor at the time of the review.

Publisher's Note: All claims expressed in this article are solely those of the authors and do not necessarily represent those of their affiliated organizations, or those of the publisher, the editors and the reviewers. Any product that may be evaluated in this article, or claim that may be made by its manufacturer, is not guaranteed or endorsed by the publisher.

Copyright © 2021 Feng, Fu, Han, Xu, Liu, Bi and Ai. This is an open-access article distributed under the terms of the Creative Commons Attribution License (CC BY). The use, distribution or reproduction in other forums is permitted, provided the original author(s) and the copyright owner(s) are credited and that the original publication in this journal is cited, in accordance with accepted academic practice. No use, distribution or reproduction is permitted which does not comply with these terms.



An R2R3-MYB Transcription Factor *RmMYB108* Responds to Chilling Stress of *Rosa multiflora* and Conferred Cold Tolerance of *Arabidopsis*

Jie Dong¹, Lei Cao¹, Xiaoying Zhang², Wuhua Zhang¹, Tao Yang¹, Jinzhu Zhang^{1*} and Daidi Che^{1*}

OPEN ACCESS

Edited by:

Rosalyn B. Angeles-Shim,
Texas Tech University, United States

Reviewed by:

M. A. Qibin,
South China Agricultural University,
China
Boas Pucker,
University of Cambridge,
United Kingdom
Mei Zhang,
South China Botanical Garden,
Chinese Academy of Sciences, China
Aiping Song,
Nanjing Agricultural University, China

*Correspondence:

Jinzhu Zhang
jinzhuzhang@neau.edu.cn
Daidi Che
daidiche@neau.edu.cn

Specialty section:

This article was submitted to
Plant Abiotic Stress,
a section of the journal
Frontiers in Plant Science

Received: 18 April 2021

Accepted: 30 June 2021

Published: 27 July 2021

Citation:

Dong J, Cao L, Zhang X,
Zhang W, Yang T, Zhang J and Che D
(2021) An R2R3-MYB Transcription
Factor *RmMYB108* Responds
to Chilling Stress of *Rosa multiflora*
and Conferred Cold Tolerance
of *Arabidopsis*.
Front. Plant Sci. 12:696919.
doi: 10.3389/fpls.2021.696919

¹ College of Horticulture and Landscape Architecture, Northeast Agricultural University, Harbin, China, ² Horticultural Research Institute, Hangzhou Academy of Agricultural Sciences, Hangzhou, China

A sudden cooling in the early spring or late autumn negatively impacts the plant growth and development. Although a number of studies have characterized the role of the transcription factors (TFs) of plant R2R3-myeloblastosis (R2R3-MYB) in response to biotic and abiotic stress, plant growth, and primary and specific metabolisms, much less is known about their role in *Rosa multiflora* under chilling stress. In the present study, *RmMYB108*, which encodes a nuclear-localized R2R3-MYB TF with a self-activation activity, was identified based on the earlier published RNA-seq data of *R. multiflora* plants exposed to short-term low-temperature stress and also on the results of prediction of the gene function referring *Arabidopsis*. The *RmMYB108* gene was induced by stress due to chilling, salt, and drought and was expressed in higher levels in the roots than in the leaves. The heterologous expression of *RmMYB108* in *Arabidopsis thaliana* significantly enhanced the tolerance of transgenic plants to freezing, water deficit, and high salinity, enabling higher survival and growth rates, earlier flowering and silique formation, and better seed quantity and quality compared with the wild-type (WT) plants. When exposed to a continuous low-temperature stress at 4°C, transgenic *Arabidopsis* lines-overexpressing *RmMYB108* showed higher activities of superoxide dismutase and peroxidase, lower relative conductivity, and lower malondialdehyde content than the WT. Moreover, the initial fluorescence (F_0) and maximum photosynthetic efficiency of photosystem II (F_v/F_m) changed more dramatically in the WT than in transgenic plants. Furthermore, the expression levels of cold-related genes involved in the *ICE1* (*Inducer of CBF expression 1*)-CBFs (*C-repeat binding factors*)-CORs (*Cold regulated genes*) cascade were higher in the overexpression lines than in the WT. These results suggest that *RmMYB108* was positively involved in the tolerance responses when *R. multiflora* was exposed to challenges against cold, freeze, salt, or drought and improved the cold tolerance of transgenic *Arabidopsis* by reducing plant damage and promoting plant growth.

Keywords: *Rosa multiflora*, R2R3 MYB transcription factors, *MYB108*, cold tolerance, transgenic, *Arabidopsis*

INTRODUCTION

Freezing temperatures induce cellular dehydration and limit the plant growth by inhibiting water uptake. Furthermore, chilling stress is fatal to plants, as cold thermodynamically lowers the membrane fluidity and directly inhibits several vital metabolic reactions (Mehrotra et al., 2020). In winter-hardy plants, the genes comprising a cryogenic response network mediate the physiological and biochemical changes and transcriptional modifications to maintain the cell integrity and plant survival at low temperatures (Zhao et al., 2015). We previously described that *Rosa multiflora*, a creeping thorny plant with medicinal and ornamental values, has a strong ability to withstand subzero temperatures (up to -40°C) in winter. The transcriptomic analysis of *R. multiflora* leaves exposed to different temperatures (25, 4, and -20°C) revealed that genes encoding APETALA2/ethylene-responsive factor (AP2/ERF), myeloblastosis (MYB), basic helix-loop-helix (bHLH), zinc finger protein (ZFP), NAC [NAM (NO APICAL MERISTEM)], ATAF (Arabidopsis ACTIVATION FACTOR) and CUC (CUP-SHAPED COTYLEDON)] and WRKY transcription factors (TFs) actively participate in the response to cold treatment (Zhang et al., 2016). In plants, MYB TFs form one of the largest TF families, which are characterized by 1–4 incomplete conserved repeat (R)-containing DNA-binding domain located near the N-terminus (Klempnauer et al., 1982). Each R is composed of approximately 51–53 conserved amino acid residues with three α -helices (Dubos et al., 2010). The MYB family contains four types of TFs (i.e., 1R, R2R3, 3R, and 4R), depending on the number of MYB domains (Rogers and Campbell, 2004). The R2R3-MYB TFs form the largest clade and participate in the plant growth, especially in cell differentiation, development of floral organ, specific metabolisms, and response to environmental stress (Albert et al., 2014; Li et al., 2019; Liu et al., 2021).

In *Arabidopsis thaliana*, the R2R3-MYB TFs, such as AtMYB15, AtMYB30, AtMYB44, AtMYB96, and AtMYB108, are associated with stress responses (Dubos et al., 2010). The AtMYB15 protein interacts with the Inducer of C-repeat binding factor (CBF) Expression 1 (ICE1) and binds to Myb recognition sequences in the promoters of CBF genes to repress cold tolerance (Agarwal et al., 2006). In *Rosa chinensis*, anthocyanidin synthase, flavonol synthase, orcinol O-methyltransferase 1 (RcOOMT1), and RcOOMT2 genes are highly expressed in pink petals of flower buds and open flowers (Han et al., 2019). The silencing of RcMYB84/RcMYB123 increases the susceptibility of *R. chinensis* to *Botrytis cinerea* and reduces the protective effects of treatment with jasmonic acid (JA; Ren et al., 2020). Moreover, the structural genes of proanthocyanidins and flavonoid have a high expression level in RrMYB5- and RrMYB10-overexpressed *Rosa rugosa* and tobacco (Shen et al., 2019). However, a complete understanding of how R2R3-MYB TFs respond to low-temperature stress in *Rosa* species is lacking.

Here, we identified the R2R3-MYB genes of *R. multiflora* that respond to low-temperature stress from its transcriptome data (Zhang et al., 2016). The functions of these genes were predicted based on the phylogenetic analysis of the homologs

of *R. multiflora* and *Arabidopsis* R2R3-MYB. We further investigated the RmMYB108 gene after combination of the RNA-seq data and prediction of the gene function. The overexpression (OE) of RmMYB108 in *Arabidopsis* confirmed the role of RmMYB108 in improving the tolerance against plant stress. This study provides a theoretical basis for cold-tolerance breeding in *Rosa* species.

MATERIALS AND METHODS

Plant Materials and Growth Conditions

The cuttings of *R. multiflora* were obtained from the forest botanical garden of Heilongjiang in China (45.0°N , 128.4°E) and were grown under a 16-h light/8-h dark cycle at 25°C [control (CK)]. The 1-year-old cutting seedlings of *R. multiflora* were exposed to 4°C (CT1) in an artificial climate room or to -20°C (CT2) in a freezer to induce cold stress. Additionally, plants were either not watered or watered with 150 mM NaCl to imitate drought and salt stress, respectively. The leaves and roots of *R. multiflora* were collected and immediately frozen in liquid nitrogen.

Arabidopsis thaliana ecotype Columbia-0 was used for stable genetic transformation, and tobacco (*Nicotiana benthamiana*) was used for transient transformation. *Arabidopsis* plants were grown at 23°C under 12-h light/12-h dark cycle during the vegetative period and under 14-h light/10-h dark cycle during the reproductive phase.

Bioinformatics Analysis of R2R3-MYB Proteins in *R. multiflora*

Putative R2R3-RmMYB proteins, which were queried with the MYB DNA-binding protein PF00249 in the Linux system HMMER 3.3.1 ($<1\text{E}-10$), were identified from a published RNA-seq data (SRA accession no.: PRJNA698412) and the whole genome sequence of *R. multiflora*¹ (Jung et al., 2019). The coding sequences (CDSs) of R2R3-MYB genes in *A. thaliana* and amino acid sequences of the encoded proteins were downloaded from The Arabidopsis Information Resource (TAIR)². The sequence of AtICE1 promoter was downloaded from the National Center for Biotechnology Information³, and the cis-acting elements of AtICE1 promoter were predicted using PlantCARE⁴. The conserved MYB domains were defined by using SMART⁵ (Letunic and Bork, 2018). The sequence alignments were performed using DNAMAN. A phylogenetic analysis was carried out using the maximum likelihood method with 1,000 bootstrap replicates in MEGA X. The heatmap was generated by using the Toolbox for Biologists (TBtools) software; the value in the row scale was normalized by the equation: $\text{value} = \frac{X - \mu}{\sigma}$, X is fragments per kilobase per million (FPKM), μ is mean, and σ is standard deviation of all FPKM in the row (Chen C. et al., 2020).

¹<https://www.rosaceae.org/>

²<http://www.arabidopsis.org/>

³<https://www.ncbi.nlm.nih.gov/>

⁴<http://bioinformatics.psb.ugent.be/webtools/plantcare/html/>

⁵<http://smart.embl-heidelberg.de/>

Quantitative Real-Time Polymerase Chain Reaction

The levels of gene expression were determined by using the quantitative real-time polymerase chain reaction (qRT-PCR), as described earlier (Zhang et al., 2016). The comparative Ct method was used to analyze the level of gene expression (Schmittgen and Livak, 2008). Primers used for qRT-PCR are listed in **Supplementary Table 1**. *RmUBC* (Klie and Debener, 2011) and *AtActin2* (Zhou et al., 2018) were selected as reference genes in *R. multiflora* and *Arabidopsis*, respectively. All experiments were performed in three biological replicates, each containing three technical repeats.

Subcellular Localization of RmMYB108

The *RmMYB108* CDS without the stop codon was amplified by PCR and cloned into the pBI121-green fluorescent protein (GFP) vector using ClonExpress II One Step Cloning Kit (Vazyme Biotech Co., Ltd., Nanjing, China) to generate 35S::*RmMYB108*-GFP construct. The primers used for plasmid construction are listed in **Supplementary Table 1**. The 35S::*RmMYB108*-GFP plasmid (Addgene: 173181) and 35S::GFP [positive control (PC)] plasmid were introduced into *Agrobacterium tumefaciens* strain GV3101, which was then injected into the leaves of 1-month-old *N. benthamiana* plants. The subcellular localization of 35S::*RmMYB108*-GFP and 35S::GFP was visualized by confocal laser scanning microscopy (TCS SP8, Wetzlar, Germany) 3 days post infiltration.

Transcriptional Activation of RmMYB108

The full-length CDS of *RmMYB108* was introduced into the pGBKT7 vector using *NdeI* and *BamHI* restriction endonucleases and T4 ligase (Thermo Fisher Scientific, Waltham, MA, United States). The primers that were used for plasmid construction are listed in **Supplementary Table 1**. *pGBT9* was used as a PC that could activate *HIS3*, *ADE2*, and *MEL1* reporter genes and X- α -Gal activity in the transformed yeast cells on the medium lacking tryptophan (Trp) and histidine (His). *pGBKT7* was used as a negative control (NC). The NC, PC, and *pGBKT7*-*RmMYB108* plasmids (Addgene: 173183) were transformed into the yeast strain AH109 and cultivated on synthetic-defined (SD)/-Trp or SD/-Trp/-His medium with or without X- α -Gal.

Vector Construction and Plant Transformation

To construct 35S::*RmMYB108*, the *RmMYB108* CDS was amplified using the primers listed in **Supplementary Table 1**, and then the PCR product was ligated into the *KpnI* and *BamHI* sites of the pCambia1301 vector downstream to the 35S promoter of the cauliflower mosaic virus (Addgene: 173180). The resulting vector was introduced into *A. tumefaciens* strain GV3101.

To generate *RmMYB108*-overexpressing lines, *Arabidopsis* plants were transformed with the 35S::*RmMYB108* construct using the floral dipping method (Clough and Bent, 1998). A semiquantitative reverse-transcription PCR (RT-PCR) assay was performed to select T₂ generation, which was obtained from healthy T₁ plants grown on the half-strength Murashige and

Skoog (1/2 MS)-agar medium containing 30 mg/L Hygromycin. Homozygous *RmMYB108* OE lines (#7, #9, and #11) in the T₃ generation were further identified by screening of Hygromycin resistance and PCR.

Stress Treatments of Arabidopsis

For induce stress as oxidation, dehydration, and salt, sterilized seeds or 1-week-old seedlings of *Arabidopsis* were grown in 1/2 MS medium containing 3% sugar and 0.75% agar, which was further supplemented with or without 1.2 mM hydrogen peroxide (H₂O₂), 150 mM mannitol, or 150 mM NaCl. The plates were incubated under 12-h light/12-h dark cycle at 23°C vertically. To induce cold stress, the sterilized seeds and 1-week-old seedlings in plates without any supplement were incubated in a growth chamber that was maintained at 15 or 4°C vertically. The seed germination and seedling growth were observed and measured after cultivating for 1 and 2 weeks, respectively. To test the freezing tolerance of OE lines, the 20-day-old *Arabidopsis* plants were cold-acclimated at 4°C for 12 h and then subjected to -10°C for 2.5 or 4 h. Subsequently, the plants were subjected again to 4°C for 12 h and then grown at 23°C.

Physiological Measurements of Plants

The leaves of 20-day old wild-type (WT) plants and *RmMYB108* OE lines were collected after exposure to 4°C for 0, 1, 3, 6, 12, and 24 h. The relative conductivity (RC), superoxide dismutase (SOD) activity, peroxidase (POD) activity, and malondialdehyde (MDA) content of plant leaves were measured as described earlier (Miao et al., 2010).

Measurement of Chlorophyll Fluorescence

The 20-days-old WT and transgenic *Arabidopsis* plants were exposed to 4°C for 0, 1, 3, 6, 12, and 24 h; the rosette leaves of *Arabidopsis* were used for measuring chlorophyll fluorescence. The initial fluorescence (F_0) and the highest electronic efficiency (F_v/F_m) of photosystem II (PS II) were measured using IMAGING-PAM (Walz, Germany), according to the instructions of the manufacturer. The same leaf position was used for measurements in both plant groups.

Statistics and Analysis

All data were subjected to ANOVA, followed by the least significant difference test. All statistical analyses were performed using IBM SPSS (New York, NY, United States) software. The results were displayed by graphs and charts using GraphPad Prism 8.0.

RESULTS AND ANALYSIS

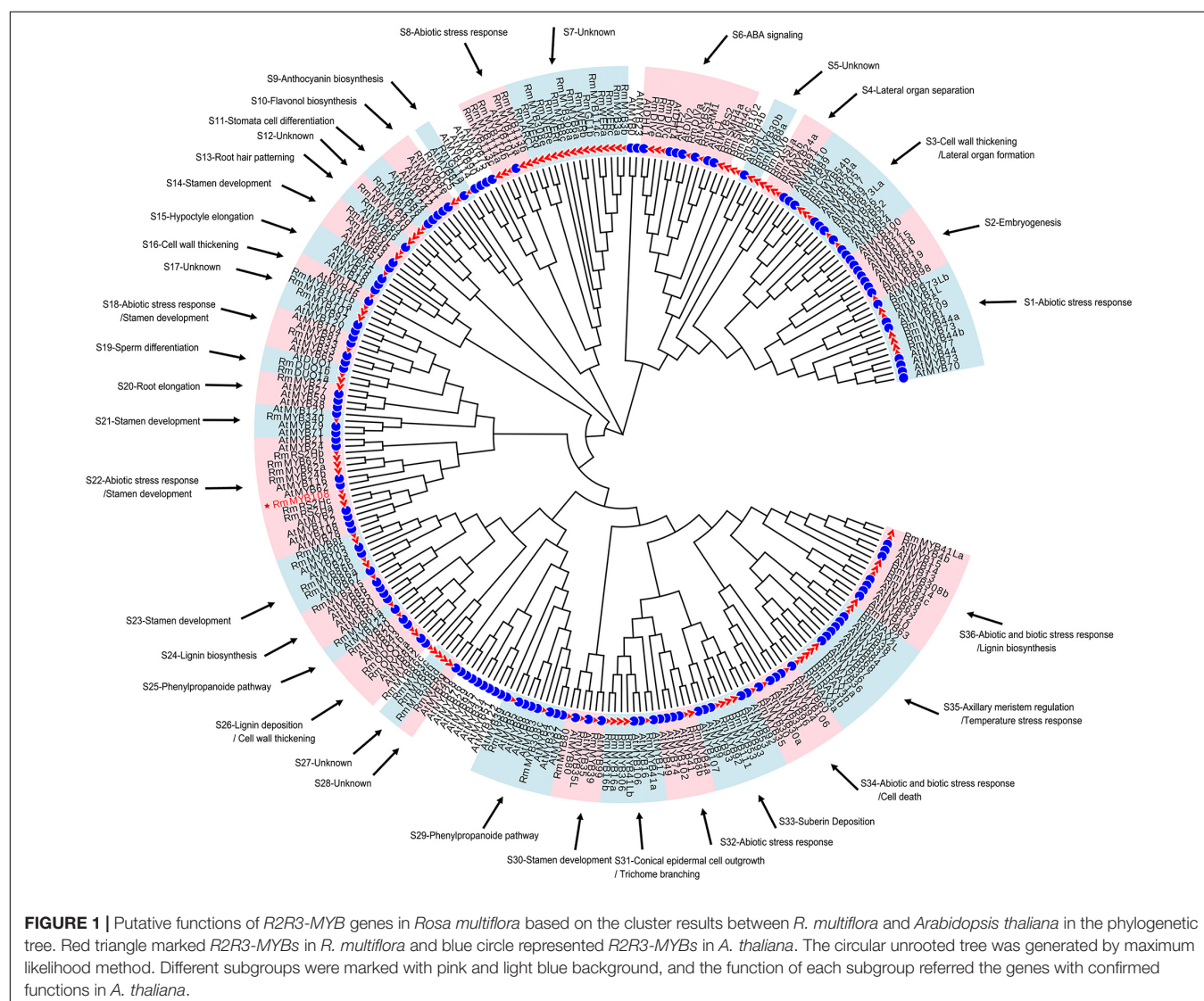
R2R3-RmMYBs Potentially Regulate Plant Growth, Development, and Stress Tolerance in *R. multiflora*

The analysis of *R. multiflora* RNA-seq data (SRA accession no.: PRJNA698412) revealed many differentially expressed genes,

which encoded TFs involved in metabolism, transcription, transport, and signal transduction in response to cold stress. For example, some genes belonging to the *AP2/ERF*, *MYB*, and *NAC* families were expressed in higher levels at both 4°C (CT1) and −20°C (CT2) than at 25°C (CK); however, the specific functions of most of these genes are unknown. In this study, we focused on how the R2R3-RmMYBs respond to low-temperature stress in *R. multiflora*. Based on the FPKM data, 37 R2R3-RmMYB genes (Supplementary Table 2 and Supplementary Figure 1) exhibited three expression trends in response to cold treatment. Genes including *RmMYB018* and *RmMYB44b* were upregulated in the CT1 and CT2 treatments, while genes such as *RmMYB308c* and *RmMYB24a* were downregulated in both treatments. Several genes including *RmMYB35* and *RmMYB106* were induced only at CT1.

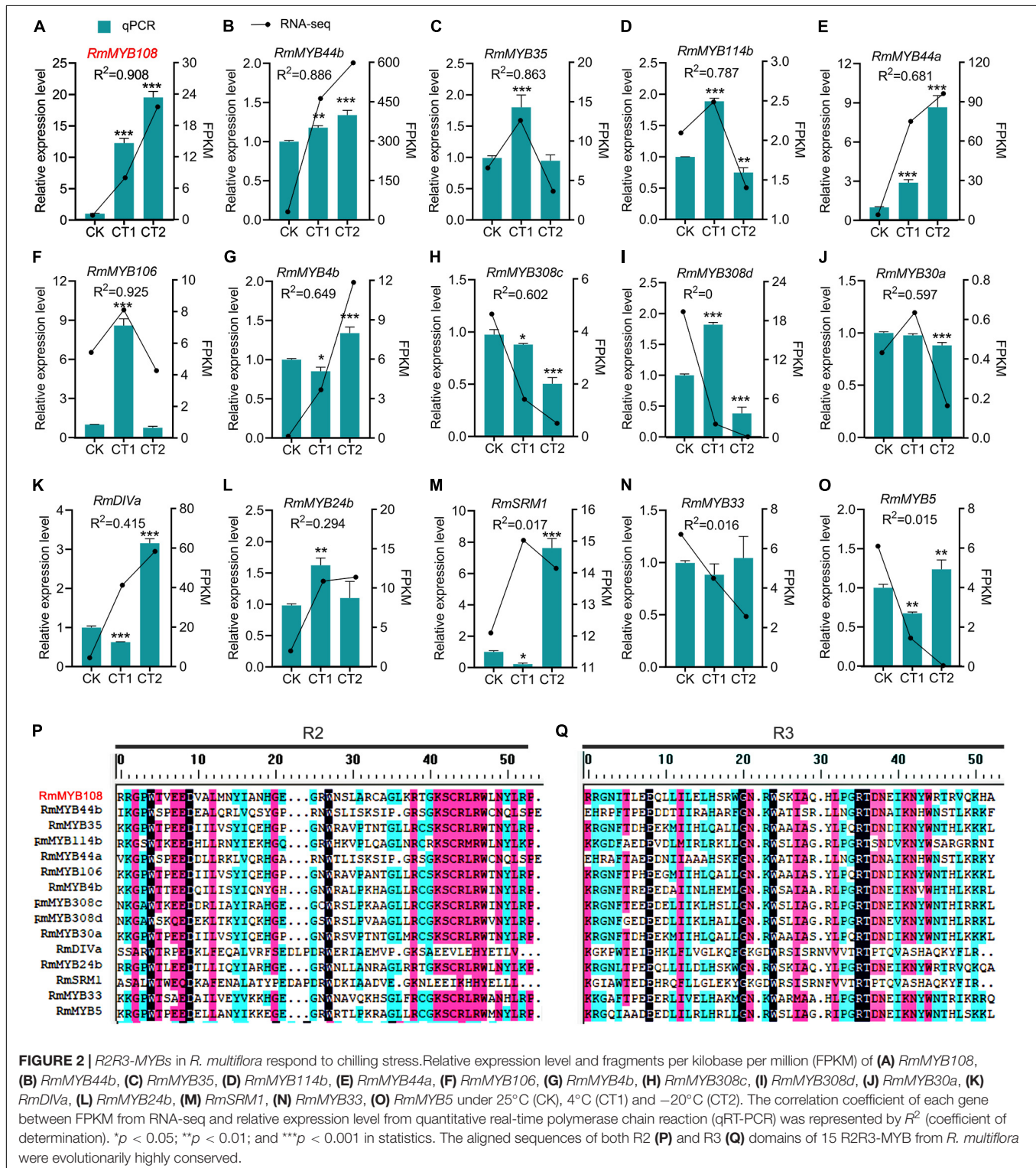
To understand the possible function as well as identifying potential chilling stress-responsive genes in this family, 119 R2R3-MYBs with complete sequences, which were extracted from 2R subgroup (Supplementary Table 3), were identified

and named by referring to the protein BLAST results and the naming principle of R2R3-MYB in *R. chinensis* (Han et al., 2019; Supplementary Figure 2). Notably, the TFs with identical names were differentiated by lowercase letters; these MYB TFs showed extremely similar sequences and blastp results (Supplementary Table 4). According to the function of 134 *Arabidopsis* R2R3-MYBs (Supplementary Table 5), 114 R2R3-MYBs in *R. multiflora* were divided and clustered to 30 function-annotated and six function-unknown subgroups, with the exception of 5 R2R3-MYBs, which shared low sequence similarity with AtMYBs in the ML phylogenetic tree (Figure 1). Based on their functional annotation, RmMYBs were divided into three classes. RmMYBs in class I were further divided into eight subgroups (i.e., S9, S10, S16, S24, S25, S26, S29, and S33) and were involved in specific metabolisms, such as the regulation of lignin, anthocyanin, and flavonol biosynthesis. For example, *RmMYB8e* clustered closely with *AtMYB11* and *AtMYB12*, which modulate flavonoid biosynthesis in favor of flavonol accumulation (Pandey et al., 2015; Wang et al., 2016). Class II contained 14 subgroups (i.e.,



S2, S3, S4, S11, S13, S14, S15, S19, S20, S21, S23, S30, S31, and S35), and *RmMYBs* in these subgroups played important roles in the fate of the plant cell, especially in the regulation of axillary meristem and stamen development. Class III *RmMYBs*, which were divided into eight clades (i.e., S1, S6, S8, S18, S22, S32, S34,

and S36), were involved in the response to biotic and abiotic stress. In class III, some *RmMYBs* showed a close relationship with *Arabidopsis* *R2R3-MYBs* involved in stress tolerance, such as *AtMYB21* (Zhang et al., 2021), *AtMYB44* (Jung et al., 2007), or *AtMYB108* (Cui et al., 2013). Furthermore, some *R2R3-MYB*



genes involved in the response to abiotic and biotic stress were also involved in the regulation of stamen development or specific metabolisms. These results suggest that *R. multiflora* *R2R3-MYBs* perform a wide range of functions including the regulation of growth and development of rose plants, as well as its tolerance to harsh environments.

Rosa multiflora *R2R3-MYB* Genes Response to Chilling Stress

The *R. multiflora* RNA-seq data analysis and prediction of gene function revealed a total of 15 stress-responsive *R2R3-MYB* genes (Figure 2). The gene expression analysis by using

the qRT-PCR confirmed that *RmMYB108*, *RmMYB44b*, and *RmMYB44a* were upregulated in response to chilling stress, while *RmMYB106*, *RmMYB35*, *RmMYB114b*, and *RmMYB308c* were upregulated at 4°C and downregulated at -20°C. Moreover, the expression trends of the abovementioned genes showed a strong correlation with the RNA-seq results. However, while some other *R. multiflora* genes such as *DIVARICATA* (*RmDIVa*), *RmMYB308d*, and *Salt-Related MYB1* were differentially expressed under low-temperature treatment, their correlation between qRT-PCR and RNA-seq data was not significant (Figures 2A–O). The alignments of the amino acid sequence of the R domains of these 15 *R2R3-MYBs* showed that the Myb

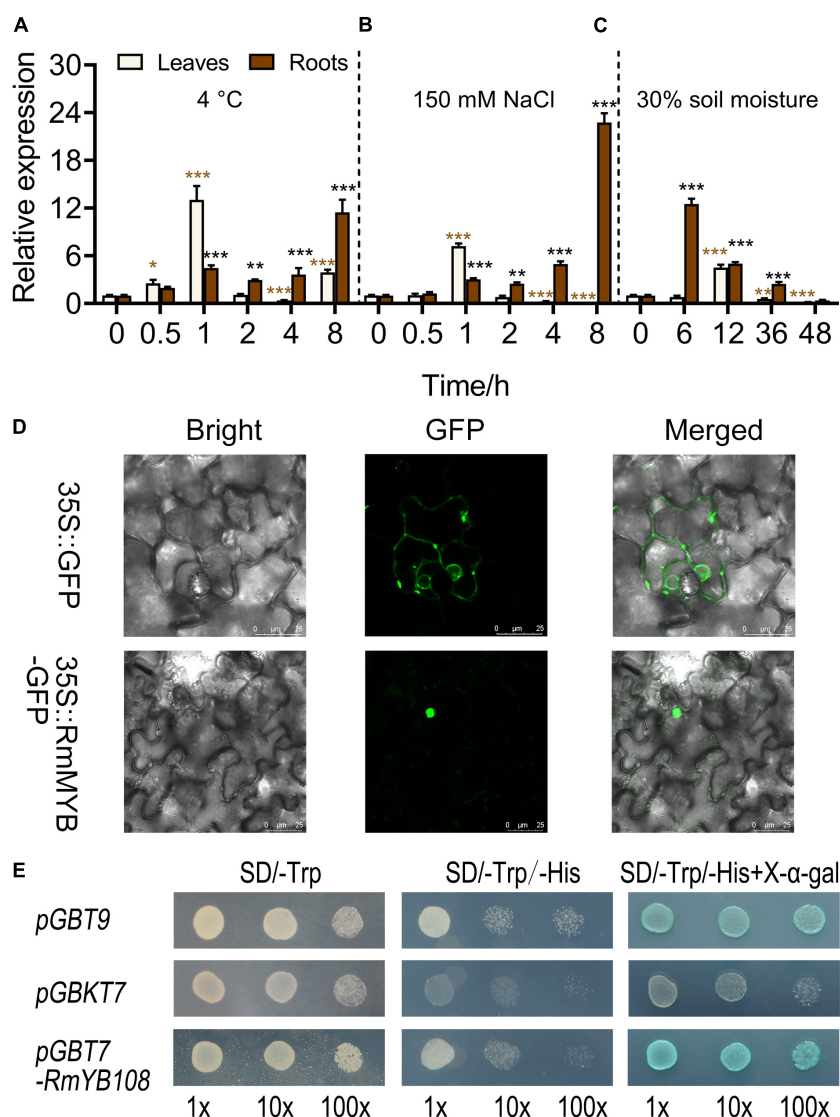


FIGURE 3 | Analysis of gene expression, localization, and transactivation assay of the *RmMYB108* transcription factor. *RmMYB108* expression patterns in *R. multiflora* leaves and roots responding abiotic stress under continuous 4°C (A), 150 mM NaCl (B), and drought (C) treatment. (D) The positive control 35S::GFP and 35S::RmMYB108 constructs were expressed in tobacco epidermal cells, showing the nuclear localization of *RmMYB108*. (E) Transcriptional activation assay of *RmMYB108*. Growth of yeast cells (strain AH109) transformed with pGBT9 vector (a positive control), pGBKT7 vector (a negative control), or pGBKT7-RmMYB108 vector on SD/-Trp or SD/-Trp/-His with or without X-α-gal. 10×, 10×, and 100× represent yeasts were diluted with original concentration (OD600 = 0.4), 10-, 100-folds, respectively. **p* < 0.05; ***p* < 0.01; ****p* < 0.001 in statistics.

domains of R2 and R3 were evolutionarily highly conserved, with spacer sequences [-W-(X19)-W-(X19)-W...-F/I-(X18)-W-(X18)-W-] (Figures 2P,Q).

Thus, the results of the prediction of gene function together with RNA-seq data revealed that the 15 *R. multiflora* R2R3-MYB genes are responsive to the cold treatment. Among those genes, *RmMYB108* showed the highest relative expression level, and its expression trend was fitted with the transcriptome result under low-temperature treatment. In addition, the effect of *RmMYB108* on plant cold tolerance has not been investigated to date although the phylogenetic tree showed that *RmMYB108* has a close relationship with R2R3-MYBs of *Arabidopsis* which are involved in stress resistance. Therefore, we further explored the potential role of *RmMYB108* in cold tolerance in *Arabidopsis*.

Molecular Characterization of *RmMYB108*

The expression of *RmMYB108* was first investigated under stress due to cold, salt, and drought using the qRT-PCR. At 4°C, *RmMYB108* expression in rose leaves was induced within 0.5–2 h of the treatment, peaked at 1 h, and then decreased to its original

level at 2 h. Furthermore, under cold stress, *RmMYB108* showed a greater increase in the expression in roots over time, with the highest value at 8 h (Figure 3A). Notably, the expression pattern of *RmMYB108* under salt stress (150 mM NaCl) was similar to that under cold stress (Figure 3B). In the drought treatment, the *RmMYB108* expression peaked at 6 h in roots and at 12 h in leaves (Figure 3C). Thus, the expression of *RmMYB108* in rose leaves and roots was affected by stress due to cold, salt, and drought at different time points. Interestingly, these results suggest that rose leaves sense environmental signals earlier than roots, although roots potentially exhibited a greater tolerance to stress than leaves.

To determine the subcellular localization of the *RmMYB108* protein, the *RmMYB108* CDS was fused with the N-terminus of the GFP gene. As expected, *RmMYB108* was localized to the nucleus in tobacco epidermal cells (Figure 3D). In addition, the experiments conducted in yeast confirmed that the full-length *RmMYB108* exhibited self-activation, as the yeast AH109 cells transformed with the pGBKT7-*RmMYB108* and pGBT9 (PC) grew well on the SD/-Trp/-His medium and turned blue on the selective medium containing X-α-Gal (Figure 3E).

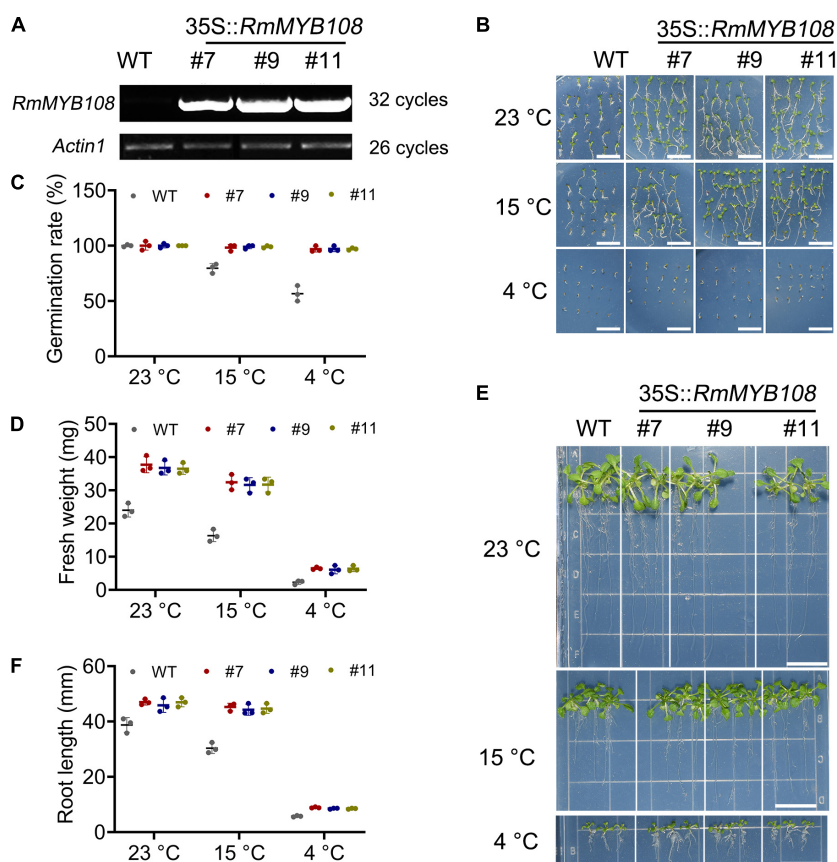


FIGURE 4 | Identification of *RmMYB108*-overexpressing *Arabidopsis* and cold tolerance contrast between wild type (WT) and #7, #9, and #11 OE lines at early growth stage of plants. (A) semiquantitative RT-PCR analysis of *RmMYB108* and *Actin1* in WT and overexpression (OE) lines showed the overexpression of *RmMYB108* in transgenic plants. The 7-days seed germination phenotype (B), seed germination rate (C), 21-day seedlings fresh weight (D), growth (E), and root length (F) of WT and OE lines under 23, 15, and 4°C, respectively, indicated OE lines had higher cold tolerance than WT. Data represent mean value + SD ($n = 30$). * $p < 0.05$; ** $p < 0.01$; *** $p < 0.001$ in statistics.

Overexpression of *RmMYB108* Enhanced the Cold Tolerance of *Arabidopsis* at the Early Growth Stage

To characterize the function of *RmMYB108*, pCambia1301-*RmMYB108* was transformed into *Arabidopsis* via the *Agrobacterium*-mediated transformation. Three *RmMYB108* OE lines (#7, #9, and #11) were identified by using the semiquantitative RT-PCR (Figure 4A). We then compared the growth and cold tolerance of WT and *RmMYB108* OE lines at the stages of germination and seedling. The rate of seed germination of the WT was similar to that of the OE lines under

normal (no stress) conditions but reduced significantly at 15 and 4°C. While 98% of the transgenic seeds stayed alive, more than 40% WT seeds showed no germination at 4°C (Figures 4B,C). Interestingly, the growth vigor of seedlings (determined by their fresh weight and primary root length) was weaker in the WT than in OE lines even at 23°C, and the growth potential of WT seedlings was affected more dramatically than that of OE lines with the decrease in temperature (Figures 4D–F). At 14 days after treatment, the weight of WT seedlings decreased by 31.78% at 15°C and by 90.27% at 4°C, whereas that of OE lines decreased by 13.6 and 82.78%, respectively. These results suggest that the OE of *RmMYB108* in *Arabidopsis* accelerated the plant

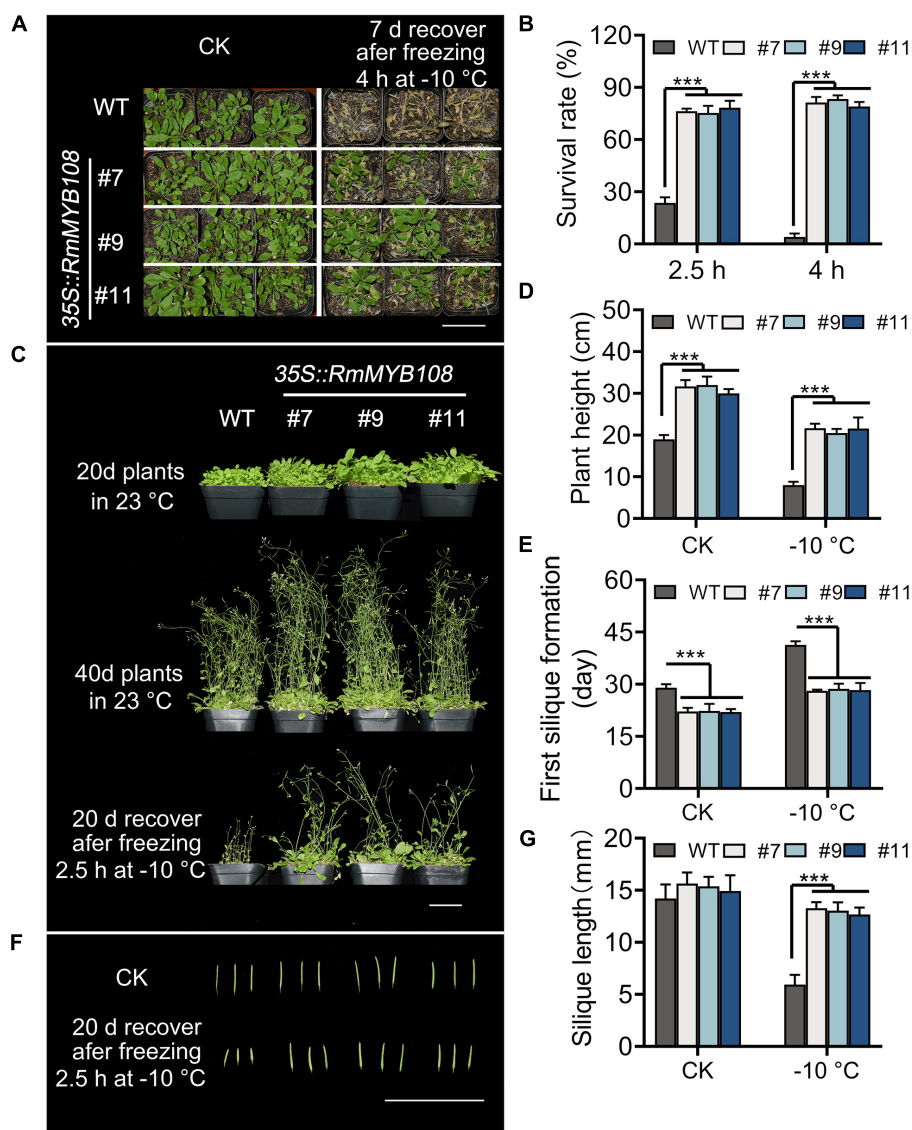


FIGURE 5 | Phenotype of transgenic *RmMYB108* plants after shortly freezing at -10°C at vegetative and reproductive growth stages of plants. **(A)** Phenotype of 20-days-old WT and OE lines that were treated at -10°C for 4 h and then recovered for 7 days. **(B)** Survival rate of recovered plants after being frozen at -10°C . The 20-day WT and OE lines were pictured after freezing 2.5 h at -10°C and recovering after 20 days **(C)**, the plant height **(D)**, first silique formation time **(E)**, and silique length **(F,G)** were measured to show that the overexpression of *RmMYB108* enhanced cold tolerance at maturity. Data represent mean value + SD ($n = 20$).

* $p < 0.05$; ** $p < 0.01$; *** $p < 0.001$ in statistics.

growth as well as enhanced tolerance to chilling temperatures by alleviating stress-induced inhibition of seed germination and plant growth.

Overexpression of *RmMYB108* Enhanced Cold Tolerance at Maturity

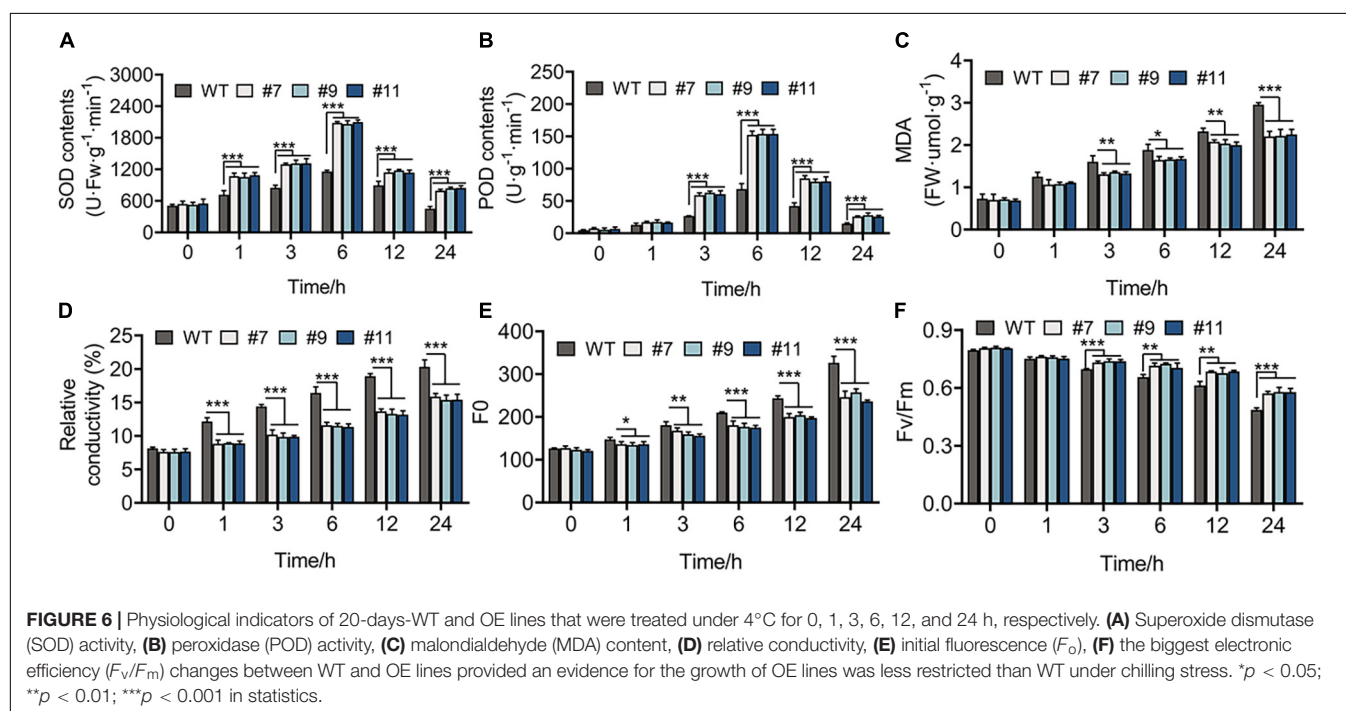
The cold tolerance assays were further carried out in mature plants of the WT and OE lines. When exposed to -10°C for 4 h, transgenic plants showed a higher survival rate and greater tolerance against freezing stress than WT plants, with several yellow leaves (Figure 5A), whereas WT plants showed the most withered leaves and less than 15% survival (Figure 5B). When the duration of freezing stress was shortened to 2.5 h, the survival rate of WT plants increased to 20%, while that of OE lines was maintained at approximately 80% (Figures 5B,C). Forty-day-old transgenic plants were more robust than WT plants with or without cold treatment. A short exposure to freezing temperatures greatly harmed WT plants, as evident from the sharp reduction in the plant height from 19 to 8 cm, whereas OE lines suffered less damage, as the plant height decreased only from 31.22 to 21.27 cm (Figure 5D). In addition, flowering and silique formation occurred earlier in OE lines than in the WT under CK and cold conditions. The first silique appeared at 29 days in the WT and 22.5 days in OE lines under normal conditions but at 41.33 and 28.43 days, respectively, under cold conditions (Figure 5E). Furthermore, after freezing, silique length of the WT was only 5.95 cm, which is much shorter than that of OE lines with 13.00 cm at average (Figures 5F,G). These results suggest that the OE of *RmMYB108* in *Arabidopsis* improved cold tolerance of the plant and shortened the plant growth cycle even after freezing.

Overexpression of *RmMYB108* Induced Physiological Changes in *Arabidopsis*

The healthy WT and OE lines were grown under the treatment at 4°C for 1 week, while the leaves of these plants were green, with no indication of wilting or dehydration. The physiological changes were observed in plants within 24 h of treatment at 4°C and indicated that all the physiological indexes of WT plants and OE lines showed the same variational trend under cold treatment in the vegetative phase. The SOD and POD activities of *Arabidopsis* peaked at 6 h after chilling stress, and their values were higher in OE lines than in WT plants at each time point, except at 0 h. For example, compared with the control at 6 h, SOD activity increased by 128.08% in the WT and by 284.20, 291.96, and 281.87% in OE lines #7, #9, and #11, respectively (Figures 6A,B). In addition, MDA content and RC, which exhibit a negative correlation with cold tolerance, showed a greater increase in WT plants than in OE lines. At 24 h, the RC of WT lines increased by 20%, whereas that of OE lines increased by an average of 15.54% (Figures 6C,D). Furthermore, the value of F_0 , which shows a linear relationship with the content of photosynthetic pigment, increased more in WT plants than in OE lines under chilling stress (Figure 6E). The value of F_v/F_m decreased over time from 0.795 to 0.490 in the WT, 0.806 to 0.570 in line #7, 0.809 to 0.579 in line #9, and 0.805 to 0.577 in line #11 (Figure 6F).

RmMYB108 Improves Plant Cold Tolerance by Upregulating the CBF Cascade

The expression of some marker genes involved in cold tolerance was tested in the WT and OE lines under chilling stress. Genes,



such as *AtICE1*, *AtCOR47A*, *AtCBF3*, *AtCOR15B*, and *AtRD29A* (Zhou et al., 2011; Thalhammer and Hinch, 2014), in the *ICE1-CBF-COR* cascade showed a similar expression in the WT and OE lines under normal conditions. Under chilling stress, all genes were upregulated, reaching peak values at 3 or 6 h (Figures 7A–E), with more drastic changes in OE lines than in the WT. No phenotypic difference was apparent between WT plants and OE lines at continuous 4°C; however, the accumulation of oxides and loss of permeability of the cell membrane were observed in plants of all genotypes. Notably, compared with WT plants, all OE lines showed a minimal injury with a similar trend in physiological indexes and expression of genes related to cold resistance.

Overexpression of *RmMYB108* Decreases Sensitivity to Other Stress

The seed germination and seedling growth of *Arabidopsis* were investigated under other stress to exemplify the essential role of *RmMYB108* in abiotic stress tolerance. In deionized water, WT and transgenic seeds showed the same germination rate (Figure 8A). However, in the presence of 1.2 mM H₂O₂, 150 mM mannitol, or 150 mM NaCl, the germination rate of WT seeds decreased to 50–70%, while that of OE lines #7, #9, and #11 remained over 95% (Figure 8B). Furthermore, the vigor of WT seedlings was lower than that of OE lines in all treatments. The fresh weight and primary root length of WT seedlings were significantly lower than those of OE lines in the treatment of stress due to oxidation, drought, and salt (Figure 8C). Under normal conditions, the average primary root length of WT seedlings was 38.79 mm, while that of OE lines was approximately 46.63 mm; however, when treated with 1.2 mM H₂O₂, 150 mM mannitol, and 150 mM NaCl, the average primary root length decreased to 11, 7.47, and 13 mm in the WT and averaged to 14.59, 13.27, and 18.82 mm in the OE lines, respectively (Figures 8D,E). Additionally, water deficiency or 200 mM NaCl treatments for 10 days significantly damaged the growth and development of *Arabidopsis* plants (Figure 8F). The survival rate of WT was less than 20% in both salt and drought treatments after returning to normal growth conditions, while that of OE lines was maintained at 60–80% (Figures 8G,H). These phenomena revealed that *RmMYB108* enhanced plant tolerance to stress due to dehydration and oxidation.

DISCUSSION

The *R2R3-MYBs* play essential roles in responses of the plant to abiotic stress. *MYB* genes in wheat [*Triticum aestivum*; *TaMYB31* and *TaMpc1-D4* (*Myb protein colorless 1 located on chromosome D*)] and cotton (*Gossypium hirsutum*; *GaMYB85*) respond to drought stress (Zhao et al., 2018; Li et al., 2020). Similarly, the *Salt Stress Regulator 1* (*PtrSSR1*) gene in poplar (*Populus trichocarpa*), *AcoMYB4* in pineapple (*Ananas comosus*), and *SiMYB305* in sesame (*Sesamum indicum*) mediate the tolerance against stress due to salt or drought through abscisic acid (ABA) signaling (Fang et al., 2017; Chen H. et al., 2020; Dossa et al., 2020). In apple (*Malus domestica*), *MdMYB308L*, *MdMYB23*,

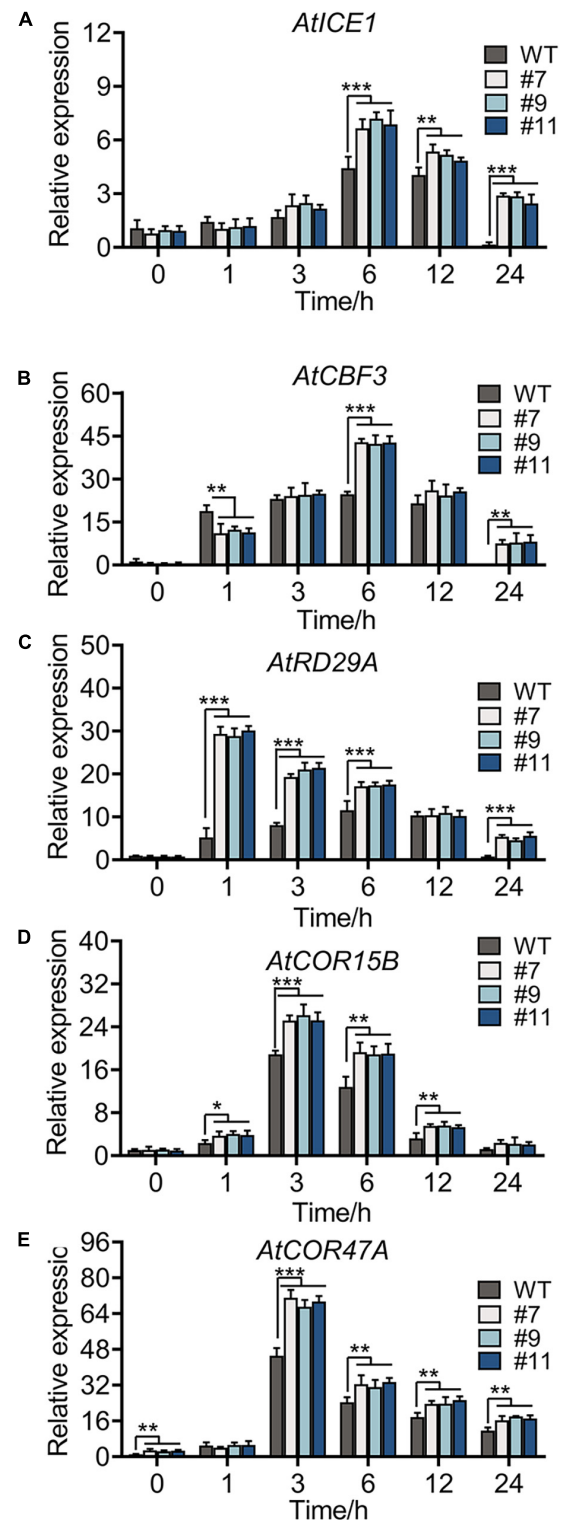


FIGURE 7 | Cold-responsive marker genes expression level of WT and OE lines under 4°C for 0, 1, 3, 6, 12, and 24 h, respectively. Relative expression level of *AtICE1* (A), *AtCBF3* (B), *AtRD29A* (C), *AtCOR15B* (D), and *AtCOR47A* (E) were measured to reveal that *RmMYB108* probably improved plant tolerance by CBF-dependent under cold treatment. **p* < 0.05; ***p* < 0.01; ****p* < 0.001 in statistics.

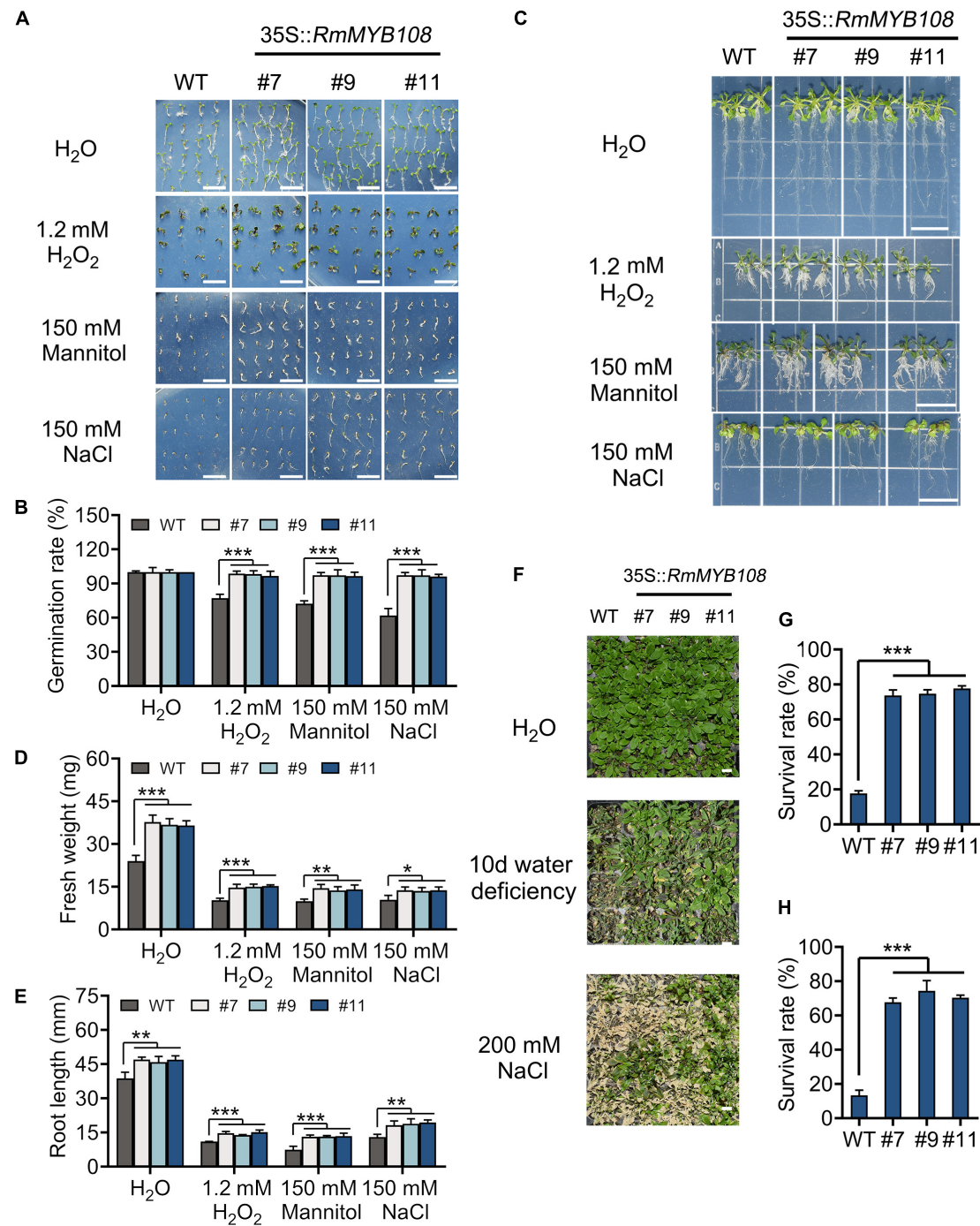


FIGURE 8 | Effects of stress due to simulated oxidation, drought, and salt on plant growth. Seed germination phenotype (A) and germination rate (B), seedlings growth (C), fresh weight (D), and root length (E) of WT and OE lines were observed and measured under deionized water (H₂O), 1.2 mM H₂O₂, 150 mM mannitol, and 150 mM NaCl, respectively. The 20-days WT and #7, #9, and #11 were not watered or watered with 200 mM NaCl for 10 days (F); the survival rate (G,H) were calculated and revealed that *RmMYB108* enhanced plant tolerance against stress due to dehydration and oxidation. Data represent mean value + SD (*n* = 30).

p* < 0.05; *p* < 0.01; ****p* < 0.001 in statistics.

MdMYB88, and *MdMYB124* regulated cold hardiness via CBF-dependent and CBF-independent pathways (An et al., 2018; Xie et al., 2018; An et al., 2020). In this study, we found that *RmMYB108*, *RmMYB44a*, and *RmMYB44b* participated in

the cold tolerance response of *R. multiflora* (Figure 1). The *ICE1*-CBF-COR gene cascade has been shown to contribute to cold acclimation by protecting plants from freezing damage in *Arabidopsis* (Zhao et al., 2015). *AtICE1*, *AtCBF3*, *AtRD29A*,

AtCOR15B, and *AtCOR47A* were upregulated in *Arabidopsis* within 24 h under chilling stress, and *RmMYB108* OE lines showed the higher expression levels of these genes than those in WT plants (Figure 7). Furthermore, the promoter of *ICE1* harbors MYB-binding sequences (Supplementary Table 6). Therefore, we predicted that *RmMYB108* enhances cold tolerance probably via the CBF-dependent pathway in *Arabidopsis* (Supplementary Figure 3).

RmMYB108 was upregulated in the transcriptome of *R. multiflora* in response to low-temperature stress, improved the ability to resist abiotic stress, and accelerated the growth of *Arabidopsis* plants by regulating changes in proteins in the cytoplasm or by indirectly maintaining the integrity of the cell membrane under stress. The stress due to low temperature, drought, and salt limits the availability of water to plant cells (Khan et al., 2018). This stress can cause membrane rupture and the outward flow of ions due to difference in osmotic pressure between the intra- and extracellular spaces, leading to plasmolysis and even cell death (Djemal and Khoudi, 2016; Ritonga and Chen, 2020). *RmMYB108*, which acts as a TF in the nucleus, regulates the expression of downstream genes probably by binding to their promoter regions on receiving the signals due to abiotic stress transmitted by the receptors. These genes generally participate in the minimization of oxidative damage, ion and water balance, osmotic stress response, and specific metabolisms to protect plant cells from water-related stress (Figure 6; Khan et al., 2018). Once the culture conditions were appropriate, the OE lines recovered and blossomed faster than WT obviously.

The recent studies showed that *MYB108* orthologs are associated with plant development, specific metabolisms, and stress response. *MYB108* is believed to be a JA-responsive TF involved in the development of stamen and pollen and defense signaling in plants (Mandaokar and Browse, 2009; Cheng et al., 2016; Xu et al., 2019). *RmMYB108* has a close relationship with *AtMYB112*, *AtMYB78*, and *AtMYB108* in *Arabidopsis* (Figure 1 and Supplementary Figure 2); *AtMYB112* responds to salinity and high-light stress (Lotkowska et al., 2015), *AtMYB78* belongs to ABA-related genes (Sun et al., 2020), and *AtMYB108* acts as a negative regulator of ABA-induced cell death, (Cui et al., 2013). In *Prunus mume*, *PmMYB108* (90% sequence similarity with *RmMYB108*) is positively associated with organ color (Zhang et al., 2018). In *R. chinensis*, *RcMYB108*, which is homologous to *RmMYB108* (94.17% sequence similarity), was upregulated during petal senescence and shedding, and silencing of *RcMYB108* altered the expression of senescence-associated genes and blocked ethylene- and JA-induced petal senescence (Zhang et al., 2019). Interestingly, when *Arabidopsis* seeds were cultured at 4°C for 6 months, we found that the speed of seed germination and plant growth was greatly reduced (data not shown). The germination rate of WT seeds was very low, whereas the seeds of most of the OE lines germinated well, and the resulting seedlings subsequently bloomed under harsh environments. After transferring to normal conditions, the transgenic plants grew well and quickly formed siliques. By contrast, WT seedlings showed a very low survival rate. Based on the evaluation of stress tolerance of OE lines and

WT plants, we speculated that the *RmMYB108* gene promotes cell division and differentiation to facilitate plant senescence, shortens the plant growth cycle, and enhances tolerance against abiotic stress.

In addition to an increasing plant yield, plant breeders focus on how to shorten the breeding period and increase the environmental stress resistance of plants (Bhatta et al., 2021). These breeding goals can generally be achieved through the genetic modification of plants by targeting genes encoding TFs (Hoang et al., 2017; Khan et al., 2018; Nowicka et al., 2018; Baillo et al., 2019). In this study, OE of *RmMYB108* in *Arabidopsis* promoted the tolerance against stress due to drought, salt, and freezing of transgenic plants, manipulated their growth cycle, and increased their biomass and seed yield under cold stress. This approach can be used to accelerate wood growth, reduce the length of the plant breeding cycle, enhance stress tolerance, and improve land utilization by developing more productive and resilient crops that can feed the global population, which is predicted to reach 10 billion by 2050 (Bhatta et al., 2021).

DATA AVAILABILITY STATEMENT

The datasets presented in this study can be found in online repositories. The names of the repository/repositories and accession number(s) can be found in the article/Supplementary Material.

AUTHOR CONTRIBUTIONS

JD designed and performed the experiments, interpreted the data, and wrote the article. DC, JZ, and LC designed the experiments and edited the article. XZ performed the experiments. WZ and TY analyzed the data. All authors contributed to the article and approved the submitted version.

FUNDING

This work was supported by the National Natural Science Foundation of China (No. 31971700) and Joint Guiding Project of Natural Science Foundation of Heilongjiang Province (No. LH2020C014).

ACKNOWLEDGMENTS

We thank Deguo Han in Northeast Agricultural University for providing the plasmids of pCambia1301 and pBI121.

SUPPLEMENTARY MATERIAL

The Supplementary Material for this article can be found online at: <https://www.frontiersin.org/articles/10.3389/fpls.2021.696919/full#supplementary-material>

Supplementary Figure 1 | The heatmap indicated row-normalized fragments per kilobase per million (FPKM) of 37 *R2R3-MYBs* from the RNA-seq database under 25°C (CK), 4°C (CT1), -20°C (CT2) in *Rosa multiflora*.

Supplementary Figure 2 | The phylogenetic tree of *R2R3-MYB* genes among *Rosa multiflora*, *Rosa chinensis*, and *Arabidopsis thaliana*. Red triangle marked *R2R3-MYBs* in *R. multiflora*, green star marked *R2R3-MYBs* in *R. chinensis*, and blue circle represented *R2R3-MYBs* in *A. thaliana*.

Supplementary Figure 3 | The putative regulation network of *RmMYB108* after encountering chilling in overexpressed *RmMYB108 Arabidopsis*.

Supplementary Table 1 | The primers names and sequences (5'–3') for quantitative real-time polymerase chain reaction (qRT-PCR), reverse-transcriptase polymerase chain reaction (RT-PCR), cloning, overexpression, subcellular localization, and self-activation.

Supplementary Table 2 | The name, raw fragments and fragments per kilobase per million (FPKM) of *R2R3-MYBs* that respond to low temperature from transcriptome sequencing of *Rosa multiflora*.

Supplementary Table 3 | The subgroups and sequences of 185 *RmMYBs* from the whole genome of *Rosa multiflora*.

Supplementary Table 4 | The names, nucleotide sequences, and encoded amino acid sequences of 119 *R2R3-MYBs* in *Rosa multiflora*.

Supplementary Table 5 | The nucleotide and encoded amino acid sequences of *R2R3-MYBs* in *Arabidopsis thaliana* from The Arabidopsis Information Resource (TAIR).

Supplementary Table 6 | The prediction of sequence and *cis*-acting elements from PlantCARE of *AtICE1* promoter.

REFERENCES

- Agarwal, M., Hao, Y. J., Kapoor, A., Dong, C. H., Fujii, H., Zheng, X. W., et al. (2006). A R2R3 type MYB transcription factor is involved in the cold regulation of CBF genes and in acquired freezing tolerance. *J. Biol. Chem.* 281, 37636–37645. doi: 10.1074/jbc.m605895200
- Albert, N., Griffiths, A., Cousins, G., Verry, I., and Williams, W. (2014). Anthocyanin leaf markings are regulated by a family of R2R3-MYB genes in the genus *Trifolium*. *New Phytol.* 205, 882–893. doi: 10.1111/nph.13100
- An, J.-P., Li, R., Qu, F.-J., You, C.-X., Wang, X.-F., and Hao, Y.-J. (2018). R2R3-MYB transcription factor MdMYB23 is involved in the cold tolerance and proanthocyanidin accumulation in apple. *Plant J.* 96, 562–577. doi: 10.1111/tbj.14050
- An, J. P., Wang, X. F., Zhang, X. W., Xu, H. F., Bi, S. Q., You, C. X., et al. (2020). An apple MYB transcription factor regulates cold tolerance and anthocyanin accumulation and undergoes MIEL1-mediated degradation. *Plant Biotechnol. J.* 18, 337–353. doi: 10.1111/pbi.13201
- Baillo, E. H., Kimotho, R. N., Zhang, Z., and Xu, P. (2019). Transcription factors associated with abiotic and biotic stress tolerance and their potential for crops improvement. *Genes* 10:771. doi: 10.3390/genes10100771
- Bhatta, M., Sandro, P., Smith, M. R., Delaney, O., Voss-Fels, K. P., Gutierrez, L., et al. (2021). Need for speed: manipulating plant growth to accelerate breeding cycles. *Curr. Opin. Plant Biol.* 60:101986. doi: 10.1016/j.pbi.2020.101986
- Chen, C., Chen, H., Zhang, Y., Thomas, H. R., Frank, M. H., He, Y., et al. (2020). TBtools - an integrative toolkit developed for interactive analyses of big biological data. *Mol. Plant* 13, 1194–1202. doi: 10.1016/j.molp.2020.06.009
- Chen, H., Lai, L., Li, L., Liu, L., Jakada, B. H., Huang, Y., et al. (2020). AcoMYB4, an ananas comosus L. MYB transcription factor, functions in osmotic stress through negative regulation of ABA signaling. *Int. J. Mol. Sci.* 21:5727. doi: 10.3390/ijms21165727
- Cheng, H.-Q., Han, L.-B., Yang, C.-L., Wu, X.-M., Zhong, N.-Q., Wu, J.-H., et al. (2016). The cotton MYB108 forms a positive feedback regulation loop with CML11 and participates in the defense response against *Verticillium dahliae* infection. *J. Exp. Botany* 67, 1935–1950. doi: 10.1093/jxb/erw016
- Clough, S. J., and Bent, A. F. (1998). Floral dip: a simplified method for *Agrobacterium*-mediated transformation of *Arabidopsis thaliana*. *Plant J.* 16, 735–743. doi: 10.1046/j.1365-3113.1998.00343.x
- Cui, F., Brosché, M., Sipari, N., Tang, S., and Overmyer, K. (2013). Regulation of ABA dependent wound induced spreading cell death by MYB108. *New Phytol.* 200, 634–640. doi: 10.1111/nph.12456
- Djamel, R., and Khoudi, H. (2016). TdSHN1, a WIN1/SHN1-type transcription factor, imparts multiple abiotic stress tolerance in transgenic tobacco. *Environ. Exp. Botany* 131, 89–100. doi: 10.1016/j.envexpbot.2016.07.005
- Dossa, K., Mmadi, M. A., Zhou, R., Liu, A., Yang, Y., Diouf, D., et al. (2020). Ectopic expression of the sesame MYB transcription factor SiMYB305 promotes root growth and modulates ABA-mediated tolerance to drought and salt stresses in *Arabidopsis*. *AoB Plants* 12:12081.
- Dubos, C., Stracke, R., Grotewold, E., Weisshaar, B., Martin, C., and Lepiniec, L. (2010). MYB transcription factors in *Arabidopsis*. *Trends Plant Sci.* 15, 573–581.
- Fang, Q., Jiang, T., Xu, L., Liu, H., Mao, H., Wang, X., et al. (2017). A salt-stress-regulator from the Poplar R2R3 MYB family integrates the regulation of lateral root emergence and ABA signaling to mediate salt stress tolerance in *Arabidopsis*. *Plant Physiol. Biochem.* 114, 100–110. doi: 10.1016/j.plaphy.2017.02.018
- Han, Y., Yu, J. Y., Zhao, T., Cheng, T. R., Wang, J., Yang, W. R., et al. (2019). Dissecting the genome-wide evolution and function of R2R3-MYB transcription factor family in *rosa chinensis*. *Genes* 10:16.
- Hoang, X. L. T., Nhi, D. N. H., Thu, N. B. A., Thao, N. P., and Tran, L. P. (2017). Transcription factors and their roles in signal transduction in plants under abiotic stresses. *Curr. Genomics* 18, 483–497.
- Jung, C., Seo, J. S., Han, S. W., Koo, Y. J., Kim, C. H., Song, S. I., et al. (2007). Overexpression of AtMYB44 enhances stomatal closure to confer abiotic stress tolerance in transgenic *Arabidopsis*. *Plant Physiol.* 146, 323–324. doi: 10.1104/pp.107.110981
- Jung, S., Lee, T., Cheng, C. H., Buble, K., Zheng, P., Yu, J., et al. (2019). 15 years of GDR: new data and functionality in the genome database for rosaceae. *Nucleic Acids Res.* 47, D1137–D1145.
- Khan, S. A., Li, M. Z., Wang, S. M., and Yin, H. J. (2018). Revisiting the role of plant transcription factors in the battle against abiotic stress. *Int. J. Mol. Sci.* 19:29.
- Klemm, K.-H., Gonda, T. J., and Michael Bishop, J. (1982). Nucleotide sequence of the retroviral leukemia gene v-myb and its cellular progenitor c-myb: the architecture of a transduced oncogene. *Cell* 31, 453–463. doi: 10.1016/0092-8674(82)90138-6
- Klie, M., and Debener, T. (2011). Identification of superior reference genes for data normalisation of expression studies via quantitative PCR in hybrid roses (*Rosa hybrida*). *BMC Res. Notes* 4:518. doi: 10.1186/1756-0500-4-518
- Letunic, I., and Bork, P. (2018). 20 years of the SMART protein domain annotation resource. *Nucleic Acids Res.* 46, D493–D496.
- Li, J., Han, G., Sun, C., and Sui, N. (2019). Research advances of MYB transcription factors in plant stress resistance and breeding. *Plant Signal. Behav.* 14:1613131. doi: 10.1080/15592324.2019.1613131
- Li, X., Tang, Y., Li, H., Luo, W., Zhou, C., Zhang, L., et al. (2020). A wheat R2R3 MYB gene TaMpc1-D4 negatively regulates drought tolerance in transgenic *Arabidopsis* and wheat. *Plant Sci.* 299:110613. doi: 10.1016/j.plantsci.2020.110613
- Liu, Z.-Y., Li, X.-P., Zhang, T.-Q., Wang, Y.-Y., Wang, C., and Gao, C.-Q. (2021). Overexpression of ThMYB8 mediates salt stress tolerance by directly activating stress-responsive gene expression. *Plant Sci.* 302:110668. doi: 10.1016/j.plantsci.2020.110668
- Lotkowska, M. E., Tohge, T., Fernie, A. R., Xue, G.-P., Balazadeh, S., and Mueller-Roeber, B. (2015). The *Arabidopsis* transcription factor MYB112 promotes anthocyanin formation during salinity and under high light stress. *Plant Physiol.* 169, 1862–1880.
- Mandaokar, A., and Browse, J. (2009). MYB108 acts together with MYB24 to regulate jasmonate-mediated stamen maturation in *Arabidopsis*. *Plant Physiol.* 149, 851–862. doi: 10.1104/pp.108.132597
- Mehrotra, S., Verma, S., Kumar, S., Kumari, S., and Mishra, B. N. (2020). Transcriptional regulation and signalling of cold stress response in plants: an overview of current understanding. *Environ. Exp. Bot.* 180:104243. doi: 10.1016/j.envexpbot.2020.104243

- Miao, B. H., Han, X. G., and Zhang, W. H. (2010). The ameliorative effect of silicon on soybean seedlings grown in potassium-deficient medium. *Ann. Bot.* 105, 967–973. doi: 10.1093/aob/mcq063
- Nowicka, B., Ciura, J., Szymańska, R., and Kruk, J. (2018). Improving photosynthesis, plant productivity and abiotic stress tolerance – current trends and future perspectives. *J. Plant Physiol.* 231, 415–433. doi: 10.1016/j.jplph.2018.10.022
- Pandey, A., Misra, P., and Trivedi, P. K. (2015). Constitutive expression of Arabidopsis MYB transcription factor, AtMYB11, in tobacco modulates flavonoid biosynthesis in favor of flavonol accumulation. *Plant Cell Rep.* 34, 1515–1528. doi: 10.1007/s00299-015-1803-z
- Ren, H., Bai, M., Sun, J., Liu, J., Ren, M., Dong, Y., et al. (2020). RcMYB84 and RcMYB123 mediate jasmonate-induced defense responses against *Botrytis cinerea* in rose (*Rosa chinensis*). *Plant J.* 103, 1839–1849. doi: 10.1111/tj.14871
- Ritonga, F. N., and Chen, S. (2020). Physiological and molecular mechanism involved in cold stress tolerance in plants. *Plants* 9:560. doi: 10.3390/plants9050560
- Rogers, L. A., and Campbell, M. M. (2004). The genetic control of lignin deposition during plant growth and development. *New Phytol.* 164, 17–30. doi: 10.1111/j.1469-8137.2004.01143.x
- Schmittgen, T. D., and Livak, K. J. (2008). Analyzing real-time PCR data by the comparative CT method. *Nat. Protocols* 3, 1101–1108. doi: 10.1038/nprot.2008.73
- Shen, Y. X., Sun, T. T., Pan, Q., Anupol, N., Chen, H., Shi, J. W., et al. (2019). RrMYB5- and RrMYB10-regulated flavonoid biosynthesis plays a pivotal role in feedback loop responding to wounding and oxidation in *Rosa rugosa*. *Plant Biotechnol. J.* 17, 2078–2095. doi: 10.1111/pbi.13123
- Sun, L., Liu, L. P., Wang, Y. Z., Yang, L., Wang, M. J., and Liu, J. X. (2020). NAC103, a NAC family transcription factor, regulates ABA response during seed germination and seedling growth in Arabidopsis. *Planta* 252:95.
- Thalhammer, A., and Hinch, D. K. (2014). A mechanistic model of COR15 protein function in plant freezing tolerance: integration of structural and functional characteristics. *Plant Signal. & Behav.* 9:e977722. doi: 10.4161/15592324.2014.977722
- Wang, F., Kong, W., Wong, G., Fu, L., Peng, R., Li, Z., et al. (2016). AtMYB12 regulates flavonoids accumulation and abiotic stress tolerance in transgenic Arabidopsis thaliana. *Mol. Genet. Genomics* 291, 1545–1559. doi: 10.1007/s00438-016-1203-2
- Xie, Y. P., Chen, P. X., Yan, Y., Bao, C. N., Li, X. W., Wang, L. P., et al. (2018). An atypical R2R3 MYB transcription factor increases cold hardness by CBF-dependent and CBF-independent pathways in apple. *New Phytol.* 218, 201–218.
- Xu, X. F., Wang, B., Feng, Y. F., Xue, J. S., Qian, X. X., Liu, S. Q., et al. (2019). AUXIN RESPONSE FACTOR17 directly regulates MYB108 for anther dehiscence. *Plant Physiol.* 181, 645–655. doi: 10.1104/pp.19.00576
- Zhang, Q., Zhang, H., Sun, L., Fan, G., Ye, M., Jiang, L., et al. (2018). The genetic architecture of floral traits in the woody plant *Prunus mume*. *Nat. Commun.* 9:1702.
- Zhang, S., Zhao, Q., Zeng, D., Xu, J., Zhou, H., Wang, F., et al. (2019). RhMYB108, an R2R3-MYB transcription factor, is involved in ethylene- and JA-induced petal senescence in rose plants. *Hortic Res.* 6:131.
- Zhang, X., Wu, S., Liu, S., and Takano, T. (2021). The Arabidopsis sucrose non-fermenting-1-related protein kinase AtSnRK2.4 interacts with a transcription factor, AtMYB21, that is involved in salt tolerance. *Plant Sci.* 303:110685. doi: 10.1016/j.plantsci.2020.110685
- Zhang, X. Y., Zhang, J. Z., Zhang, W. W., Yang, T., Xiong, Y., and Che, D. D. (2016). Transcriptome sequencing and de novo analysis of *Rosa multiflora* under cold stress. *Acta Physiol. Plantarum* 38:13.
- Zhao, C., Lang, Z., and Zhu, J.-K. (2015). Cold responsive gene transcription becomes more complex. *Trends Plant Sci.* 20, 466–468. doi: 10.1016/j.tplants.2015.06.001
- Zhao, Y., Cheng, X. Y., Liu, X. D., Wu, H. F., Bi, H. H., and Xu, H. X. (2018). The wheat MYB transcription factor TaMYB³¹ is involved in drought stress responses in Arabidopsis. *Front. Plant Sci.* 9:1426. doi: 10.3389/fpls.2018.01426
- Zhou, A., Sun, H., Feng, S., Zhou, M., Gong, S., Wang, J., et al. (2018). A novel cold-regulated gene from *Phlox subulata*, PsCor413im1, enhances low temperature tolerance in Arabidopsis. *Biochem. Biophys. Res. Commun.* 495, 1688–1694. doi: 10.1016/j.bbrc.2017.12.042
- Zhou, M. Q., Shen, C., Wu, L. H., Tang, K. X., and Lin, J. (2011). CBF-dependent signaling pathway: a key responder to low temperature stress in plants. *Crit. Rev. Biotechnol.* 31, 186–192. doi: 10.3109/07388551.2010.505910

Conflict of Interest: The authors declare that the research was conducted in the absence of any commercial or financial relationships that could be construed as a potential conflict of interest.

Publisher's Note: All claims expressed in this article are solely those of the authors and do not necessarily represent those of their affiliated organizations, or those of the publisher, the editors and the reviewers. Any product that may be evaluated in this article, or claim that may be made by its manufacturer, is not guaranteed or endorsed by the publisher.

Copyright © 2021 Dong, Cao, Zhang, Zhang, Yang, Zhang and Che. This is an open-access article distributed under the terms of the Creative Commons Attribution License (CC BY). The use, distribution or reproduction in other forums is permitted, provided the original author(s) and the copyright owner(s) are credited and that the original publication in this journal is cited, in accordance with accepted academic practice. No use, distribution or reproduction is permitted which does not comply with these terms.



Seasonal Metabolic Investigation in Pomegranate (*Punica granatum* L.) Highlights the Role of Amino Acids in Genotype- and Organ-Specific Adaptive Responses to Freezing Stress

OPEN ACCESS

Edited by:

Sunchung Park,
Crop Improvement and Protection
Research, Agricultural Research
Service, United States Department of
Agriculture, United States

Reviewed by:

Kjell Sergeant,
Luxembourg Institute of Science and
Technology, Luxembourg
Dhruv Lavania,
University of Alberta, Canada

*Correspondence:

Parisa Jonoubi
jonoubi@khu.ac.ir
Mehrshad Zeinalabedini
mzeinolabedini@abrii.ac.ir

[†]These authors have contributed
equally to this work

Specialty section:

This article was submitted to
Plant Abiotic Stress,
a section of the journal
Frontiers in Plant Science

Received: 22 April 2021

Accepted: 20 July 2021

Published: 12 August 2021

Citation:

Yazdanpanah P, Jonoubi P,
Zeinalabedini M, Rajaei H,
Ghaffari MR, Vazifeshenas MR and
Abdirad S (2021) Seasonal Metabolic
Investigation in Pomegranate (*Punica
granatum* L.) Highlights the Role of
Amino Acids in Genotype- and
Organ-Specific Adaptive Responses
to Freezing Stress.
Front. Plant Sci. 12:699139.
doi: 10.3389/fpls.2021.699139

Parisa Yazdanpanah^{1,2}, **Parisa Jonoubi**^{1*†}, **Mehrshad Zeinalabedini**^{2*†}, **Homa Rajaei**³,
Mohammad Reza Ghaffari², **Mohammad Reza Vazifeshenas**⁴ and **Somayeh Abdirad**^{1,2}

¹ Department of Plant Sciences, Faculty of Biological Sciences, Kharazmi University, Tehran, Iran, ² Department of Systems and Synthetic Biology, Agricultural Biotechnology Research Institute of Iran (ABRII), Agricultural Research, Education and Extension Organization (AREEO), Karaj, Iran, ³ Department of Biology, College of Sciences, Shiraz University, Shiraz, Iran,

⁴ Improvement Plant and Seed Department, Agricultural and Natural Resources Research and Education Center Research, AREEO, Yazd, Iran

Every winter, temperate woody plants have to cope with freezing stress. Winter hardiness is of crucial importance for pomegranate survival and productivity. A comparative morphological and metabolic study was conducted on the stems and buds of 15 field-grown mature pomegranate genotypes in seven time-points during two developmental cycles. Seasonal changes of frost hardiness, as determined by electrolyte leakage method, and metabolite analysis by HPLC and GC revealed the variability in frost hardiness and metabolic contents result from genetic background and organ, as well as seasonal condition. Morphological adaptations, as well as metabolic remodeling, are the distinct features of the hardy genotypes. Larger buds with a greater number of compressed scales and the higher number of protective leaves, together with the higher number and content of changed metabolites, especially amino acids, seem to provide a higher frost resistance for those trees. We recorded two-times the change in metabolites and several-times accumulation of amino acids in the stem compared with buds. A better potential of stem for metabolome adjustment during the hardening period and a higher level of tolerance to stress is therefore suggested. High levels of arginine, proline, glutamine, and asparagine, and particularly the accumulation of alanine, tryptophan, and histidine are responsible for excellent tolerance of the stem of tolerant genotypes. With regard to the protective roles of amino acids, a relation between stress tolerance and the level of amino acids is proposed. This points both to the importance of amino acids in the winter survival of pomegranate trees, and to the evaluation of frost tolerance in other plants, by these specific markers.

Keywords: pomegranate, primary metabolites, frost tolerance, developmental cycle, resistant genotype, fruit tree, stem, bud

INTRODUCTION

Pomegranate (*Punica granatum* L.) is an economically valuable fruit tree that originates from the region spanning Iran to the Himalayas in northern India but is cultivated in many parts of the world today (Holland et al., 2009). Despite a wide geographical distribution and adaptation, its optimal climate conditions are high exposure to sunlight, mild winter with minimal temperature, not lower than -12°C , and dry hot summers without rain, during the last stages of fruit development (Holland et al., 2009). In recent years, pomegranate cultivation and consumption greatly increased due to the dramatic progress of scientific reports on its health-promoting properties (Wu and Tian, 2017; Saeed et al., 2018).

Although Iran is one of the main producers and exporters of pomegranate fruit in the world (Erkan and Dogan, 2018), its production has recently declined due to winter frost damage. In nearly all pomegranate growth and cultivation areas in Iran, minimum winter temperatures may fall to -20°C or even lower. Therefore, winter frost, especially absolute minimum temperature, is considered the major limiting factor in pomegranate yield and productivity. For instance, severe winter frost and unprecedented temperature drops in 2007 and 2016, with the temperature down to -23 and -20°C for 3 and 2 weeks, destroyed 36,931 and 35,000 ha of pomegranate orchards in Iran, respectively. Production declined by 50–90%, in many provinces of Iran (Agricultural Statistics, 2020). According to statistical information from 1990 to 2020, in addition to year-to-year winter frosts, there was a risk of severe winter frost every 10 years in orchards of Iran. Fortunately, Iranian pomegranate germplasm is vastly rich in genetic diversity and more than 760 genotypes from different provinces of Iran have been collected in Yazd Agricultural and Natural Resources Research Center (Zahravi and Vazifeshenas, 2017). A more comprehensive understanding of pomegranate frost hardiness is needed to develop frost-hardy genotypes. The screening and selection of hardier genotypes could be of considerable help in coping with frost problems, enabling producers to reduce severe damage and huge economic losses.

Pomegranate, like other perennial deciduous woody plants, withstands winter temperature by periods of dormancy-activity during the annual cycle. The timing of the hardening/de-hardening process is well-coordinated with the seasonal dormancy-activity cycle and climate changes. Pomegranate growth cessation and entrance to a dormant state start with decreasing photoperiod and temperature. The tree gradually acquires the frost hardiness; reaching its maximum in mid-winter. In response to long days and increasing temperature, frost hardiness declines, and growth resumption occurs in late winter-early spring (Rohde and Bhalerao, 2007). Pomegranate buds develop during the growing season, and their differentiation is completed before the winter dormancy. The vegetative buds of pomegranate are composed of a shoot apex and multiple leaf primordia. A variable number of compactly arranged bud scales protect these primordia from the surrounding environment (Rajaei and Yazdanpanah, 2015).

The adaptive responses of plants to abiotic stress are diverse and involve highly dynamic metabolic and molecular pathways (Krasensky and Jonak, 2012; Preston and Sandve, 2013; Strimbeck et al., 2015; Abdirad et al., 2020). During the hardening process, plants undergo a wide range of structural, physiological, and metabolic modifications which finally lead to the acquisition of a high degree of tolerance against extreme winter temperatures (Preston and Sandve, 2013; Strimbeck et al., 2015). The changes in the level of carbohydrates, amino acids, and the composition of lipids are the most common responses of plants during the process of frost hardiness (Krasensky and Jonak, 2012; Strimbeck et al., 2015).

Frost hardiness shows variability among species, cultivars, genotypes, etc., and varies between different plant organs and tissues, based on developmental stage and plant age, and also along the year (Sakai and Larcher, 1987; Charrier et al., 2013, 2015). The frost hardiness of different plant organs has previously been studied both in gymnosperms and angiosperms: woody stems are more resistant to frost than leaves, vegetative, and reproductive buds (Sakai and Larcher, 1987; Jones et al., 1999; Sogaard et al., 2009; Charrier et al., 2013). On the other hand, the accumulation of metabolites in frost-tolerant plants in different accessions, cultivars, or species differs from those in frost-sensitive examples (Chai et al., 2019). Changes in these metabolites can be related to more tolerance, and are previously documented in other species (Hannah et al., 2006; Krasensky and Jonak, 2012; Chai et al., 2019). Metabolic profiling of more cold-tolerant *Vitis amurens* and less cold-tolerant *Vitis vinifera* cv. Muscat of Hamburg indicated the involvement of amino acids in the cold tolerance of *V. amurens* (Chai et al., 2019).

Among the laboratory-based analyses used to assess plant injury, electrolyte leakage (EL) is a common and reliable method of monitoring frost hardiness in different tissues (Charrier et al., 2013; Mayr and Améglio, 2016). This method is based on the principle that damage to cells and loss of membrane integrity results in an enhanced leakage of electrolytes from frost-injured cells. Recording the amount of leakage leads to the estimation of tissue damage (Mayr and Améglio, 2016). EL method is suitable for many woody plants (Jones et al., 1999; Morin et al., 2007; Charrier et al., 2013). The metabolic changes during low temperature stress have been analyzed in some woody plants such as *Camellia sinensis* (Yue et al., 2015) and *Vitis* sp. (Chai et al., 2019). Metabolic time-series experiments have also previously been employed for investigating seasonal changes during the acclimation/de-acclimation cycle in *Arabidopsis* (Kaplan et al., 2004), *Picea obovata* (Angelcheva et al., 2014), and *Camellia sinensis* (Yue et al., 2015).

Despite numerous studies on cold stress responses in woody plants, there is little information on pomegranate responses to frost stress. Ghasemi Soloklui et al. (2012) studied stem frost hardiness among seven 5-year-old pomegranate genotypes during one annual cycle and reported some of the tolerant and sensitive genotypes. They concluded that the content of soluble carbohydrates, especially from fall to mid-winter, is the best indicator of hardiness but, to date, the frost hardiness of mature pomegranate trees has not been reported. In particular, no information is available on the low-temperature tolerance of

the different organs of the pomegranate tree, indicating the same or different adaptation to freezing. This comparison between different pomegranate organs extends the study of stress response to the whole tree and provides information on organ-specific frost hardiness (Charrier et al., 2013). This study was conducted to compare frost hardiness of the stem and bud from 15 contrasting pomegranate genotypes in seven time-points during two developmental cycles to select frost-hardier genotypes. We investigated the commonalities and differences of a set of metabolites and their changes between two organs and among contrasting genotypes to identify the necessary compounds and mechanisms that are specific to frost tolerance. We also assessed the correlations between frost hardiness, metabolites, and minimum temperature.

MATERIALS AND METHODS

Sampling Conditions and Plant Materials

Fifteen genotypes from 25-year-old pomegranate trees (*Punica granatum* L.) grown at Yazd Agricultural and Natural Resources Research Center, Yazd province in the central part of Iran (31° 54' N and 54° 24' E) were selected from different programs (among 180 and 250 genotypes used in metabolite and morphological programs, respectively) with known frost hardiness characteristics based on expert gardeners' information and preliminary frost hardiness tests.

Full and abbreviation names of genotypes include: "Kadru Shahri Ghasr-e-dasht Fars" (KD), "Rabbab Pust-ghermez Kazerun" (RP), "Pust-siyah Abrandabad Shirin" (PS), "Khafri Jahrom Shirin" (KJ), "Torosh Goli-naz Behshahr" (GN), "Goroch Shahvar Yazdi Shahed" (GO), "Ghahveh-daneh Malas Darjazin" (GD), "Togh-gardan Yazdi Shahed" (TG), "Khusheh-nar Baharestan Sari" (KN), "Bi-tolf Daneh-sefid Malas Ramhormoz" (BT), "Barg-murdi Torosh" (BM), "Bi-hasteh Ladiz Shirin Mirjaveh" (BH), "Shirin Shahvar Yazdi Shahed" (SS), "Vashik Malas Hoshak Saravan" (VH), "Malas1 Hoshak Saravan" (MH).

The fall and winter of 2016–2017 were colder than those of 2015–2016, with mean temperatures of 6.52 and 7.35°C, respectively. The onset of temperatures below zero occurred during some nights in early December 2015 during 2015–2016, and late November 2016 during 2016–2017. The lowest air temperature of −4.1 and −5.3°C occurred in mid-January 2016 and early February 2017, respectively (**Supplementary Figure 1**). From November to March 2015–2016 and 2016–2017, 8 and 10 days had temperatures below zero, respectively.

Uniform branches (5 mm in diameter) on three different trees of each genotype were sampled from the upper part of the crown during two successive developmental cycles (2015–2017) at the seven different time-points (December 18, 2015, January 17, October 1 and December 15 2016, January 15, February 13, and April 25, 2017). Samples were immediately frozen in liquid N₂ for metabolites or packed into plastic bags and kept on crushed ice (4°C) in a cooling box for frost hardiness investigation. Further analysis was performed in the laboratory of Systems and Synthetic Biology, the Department of Agricultural Biotechnology Research Institute of Iran (ABRII).

Morphological Observations and Visual Assessment

To compare bud samples at successive time points, current branches were collected and their buds viewed with a stereo microscope (Leica MS5, Wetzlar, Germany). Thirty buds from different trees of each genotype were examined. Bud size was measured and the number of their scales was recorded during dissection.

Frost Hardiness Determination

The frost hardiness of pomegranate stem and bud was determined by the electrolyte leakage test using the method described by Charrier et al. (2013), with slight modifications. The branches were rinsed under running cold deionized water for 15 s and cut into six 5-cm-long segments without bud. Buds were kept intact on 1 mm branch segments. The samples were placed in a moistened tissue and wrapped in aluminum foil per replicate and were transferred to a temperature-controlled freezer (Electrosteel, Tehran, Iran) with a cooling rate of 2°C/h down to −10, −15, −20, and −25°C and either −5°C in spring and −30°C in winter. Each target temperature was maintained for 2 h and then samples were withdrawn and thawed overnight at 5°C. A control sample was stored at 5°C and another control was kept in a freezer at −80°C.

After freezing treatment, branches were cut into 5-mm-long segments and five buds per temperature were used. Samples were transferred into conical tubes with 15 mL of distilled-deionized water. Tubes were shaken for 24 h before the first electrical conductivity (EC1) measurement. Samples were autoclaved at 120°C for 45 min to allow maximum leakage and cooled down to room temperature and EC2 was measured again. Relative electrolyte leakage (REL) was calculated using the formula: $REL = (EC_{\text{frozen}} - EC_{\text{water}}) \times 100 / (EC_{\text{autoclave}} - EC_{\text{water}})$.

Metabolite Measurements

Soluble carbohydrates were extracted and measured according to Abdirad et al. (2020). Freeze-dried samples (100 mg) were finely ground using a mixer mill (Retsch, MM200). Samples were extracted three times with 80% ethanol followed by centrifugation at 5,000 rpm for 10 min and the aqueous phase was dried at 40°C. Then, 10 mL distilled water, 0.47 mL barium hydroxide (0.3 N), and 0.5 mL zinc sulfate (ZnSO₄) (5%) were added followed by centrifugation at 5,000 rpm for 10 min. The supernatant was evaporated and the pellet was re-dissolved in HPLC grade distilled water and filtered through 0.45 μm filters, before application to a reversed phase HPLC (Knauer, Germany) on a Eurokat H column (300 × 80 mm, 10 μm particle size). Acidic water (containing sulfuric acid, pH = 2.5) with a flow rate of 1 mL/min was used as the mobile phase. Sucrose, Glucose, and fructose were detected by the RI detector, and the peak areas were used to determine sugar contents based on their corresponding standards. Soluble carbohydrate concentrations were finally calculated through a calibration curve and expressed as milligrams/gram dry weight.

Amino acids were extracted by adding 1 mL of 80% ethanol to 100 mg of freeze-dried samples followed by heating at 80°C for 60 min and then centrifugation at 13,000 rpm for 10 min.

A solution containing 50 mg o-phthalaldehyde (OPA), 4.5 mL MeOH and 0.5 mL borate buffer (50 mM, pH = 9.5), and 50 μ L of 2-mercaptoethanol was prepared. One hundred microliter of OPA solution and 200 μ L borate buffer were added to 250 μ L of the concentrated supernatant and kept for 2 min at room temperature. The reaction was quenched by adding 50 μ L hydrochloric acid (HCl) to the solution. Amino acids were separated on a C18 column (HALO C18, 4.6 \times 50 mm, 5 μ m particle size, Advanced Materials Technology, Wilmington, USA), by HPLC. Amino acids were detected by RF-10 AXL fluorescence detector (Berlin, Germany) with excitation and emission at 330 and 450 nm, respectively. A gradient of 20–70% MeOH in sodium acetate (NaOAc) buffer (50 mM, pH = 7.0) with a flow rate of 1.1 mL/min was used as mobile phases. The amount of each amino acid was calculated by comparing its peak area with that of the corresponding standards (Abdirad et al., 2020). Amino acid concentrations were finally calculated through a calibration curve and expressed as milligrams/gram dry weight.

Fatty acids were extracted and measured according to Talebi et al. (2013). Briefly, 500 μ L of the extraction buffer containing methanol (MeOH) and 2% of concentrated H₂SO₄ was added to 100 mg of freeze-dried samples and the samples were incubated (2 h, 80°C, 750 rpm). Three hundred microliter of 0.9% NaCl solution and 150 μ L of hexane were added into the reaction tube, respectively. Then, the samples were centrifuged (3,000 rpm, 25°C, 5 min). Finally, the supernatant containing the hexane and fatty acid methyl ester (FAME) was used for GC analysis. The fatty acid determination was carried out on a Varian CP-3800 GC (Varian, Inc., Palo Alto, CA) equipped with a CP-Sill 88 fused silica column (100 m, 0.25 mm I.D., film thickness 0.25 μ m). The oven temperature was maintained at 130°C for 4 min, then programmed to increase to 180°C at a rate of 5°C/min, and kept at this temperature for 8 min. Finally, the oven temperature was programmed to rise from 180 to 220°C at a rate of 4°C/min under the following conditions: carrier gas Helium (1 mL/min), split ratio 20:1, and flame ionization detector (FID) 280°C. Fatty acid peaks were identified by comparison of the retention time with FAME standards. Standards of fatty acids (including C16:0, C16:1, C18:0, C18:1, C18:2, C18:3), were purchased from Merck Company (Darmstadt, Germany).

Statistical Analysis

Frost hardiness was expressed as LT50 by fitting response curves with the following logistic sigmoid function (Ghasemi Soloklui et al., 2012):

$$R = \frac{a}{1 + e^{b(x-c)}} + d$$

where R was REL; x was treatment temperature; b was the slope of the function at the inflection point c; and a and d determine the upper and lower asymptotes of the function, respectively.

The differences between values of LT50 and metabolite contents of stem and bud samples at each time-point were assessed with a three-way analysis of variance (ANOVA) and means were separated using LSD ($p \leq 0.05$). Comparative heat

maps, principal component analysis (PCA), partial least squares-discriminant analysis (PLS-DA), and correlation heatmaps were performed using the Metaboanalyst (5.0) online analysis software (www.metaboanalyst.ca/). The data were log₂ transformed and normalized before analysis.

RESULTS

Frost Hardiness Displayed Diversity Among Genotypes and Between Two Organs

For differential sampling and screening, we chose seven time-points during two successive developmental cycles, that are coordinated with the timing of the hardening/de-hardening cycle (Figure 1A). EL method allowed us the calculation of lethal temperature at which 50% of the total ion leakage occurs (LT50) and the evaluation of frost hardiness dynamics in the pomegranate tree. Although the changes of frost hardiness were recorded throughout the pomegranate annual cycle, we selected LT50 values of winter months, i.e., December and January of 2 successive years for representing the maximum frost tolerance of the two organs of each genotype (Figures 1B,C).

Overall, changes of frost hardiness were similar among the fifteen genotypes and between two organs. The frost hardiness level increased gradually during fall, reached a maximum level in December and January, and decreased again toward April. LT50 values ranged from -25.11 to -20.12°C and -25.64 to -20.07°C for stems and ranged from -24.15 to -19.21°C and -24.85 to -19.11°C for buds in December 2015 and 2016, respectively. The hardening/de-hardening cycle was well-accorded, with air temperature values in both years; a lower LT50 value was recorded for almost all the genotypes during winter 2016–2017, compared with winter 2015–2016, due to colder air temperatures and more freezing days (Supplementary Figure 1). One and two weeks before the second sampling (i.e., December), 4 and 7 days and nights with temperatures below zero occurred during 2015–2016 and 2016–2017, respectively.

Between the two investigated organs, the stems are harder than the buds in both years (Figures 1B,C). Although frost hardiness of the bud was higher than the stem in October for all the genotypes, the stem showed higher frost hardiness than the bud during winter and also was de-hardened later during February and April ($p \leq 0.05$ for almost all the genotypes).

Among the genotypes, KD (-25.11 and -25.64°C for the stem, -24.15 and -24.85°C for bud) and RP (-24.90 and -24.83°C for the stem, -23.10 and -23.21°C for bud) had significantly lower LT50 values and therefore the highest frost hardiness during December 2015 and 2016, respectively. KD and RP maintained high frost hardiness during winter and had a low de-hardening rate toward April. On the other hand, the lowest frost hardiness was recorded for MH (-20.12 and -20.07°C for the stem, -19.21 and -19.11°C for bud) and VH (-20.30 and -20.17°C for the stem, -19.17 and -19.18°C for bud) during December 2015 and 2016, respectively. Other genotypes were considered as the intermediate in frost hardiness level (Figures 1B,C). We designed three distinct groups based on LT50 data in the present experiment and also based on expert

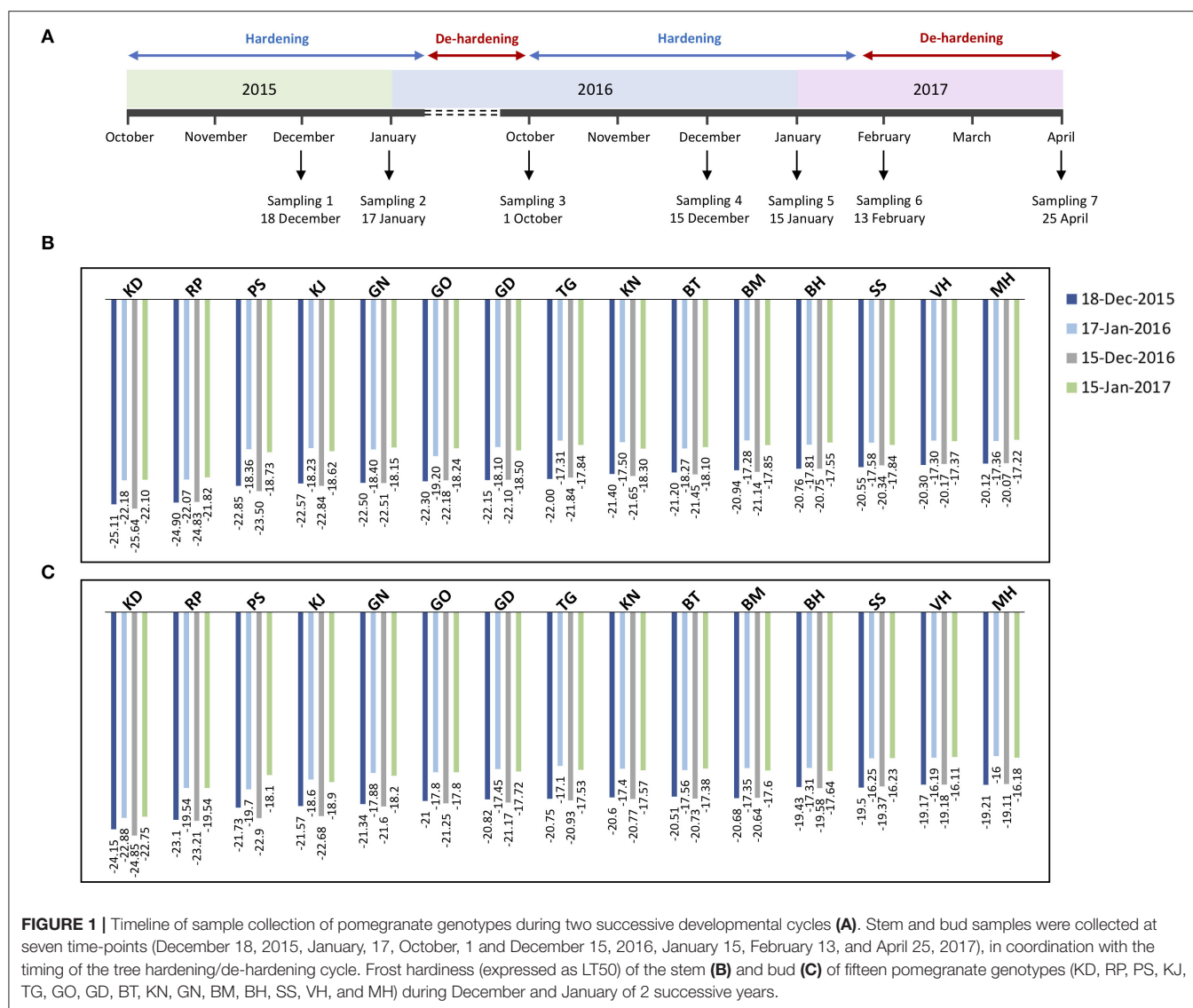


FIGURE 1 | Timeline of sample collection of pomegranate genotypes during two successive developmental cycles **(A)**. Stem and bud samples were collected at seven time-points (December 18, 2015, January, 17, October, 1 and December 15, 2016, January 15, February 13, and April 25, 2017), in coordination with the timing of the tree hardening/de-hardening cycle. Frost hardiness (expressed as LT50) of the stem **(B)** and bud **(C)** of fifteen pomegranate genotypes (KD, RP, PS, KJ, TG, GO, GD, BT, KN, GN, BM, BH, SS, VH, and MH) during December and January of 2 successive years.

gardeners' information and preliminary frost hardiness test, as well as according to Ghasemi Soloklui et al. (2012): the frost-hardy group included KD and RP, the frost-sensitive group contained VH and MH, and the intermediate group covered other genotypes: PS, KJ, TG, GO, GD, BT, KN, GN, BM, BH, and SS.

Morphological Adaptations Support Pomegranate Tree Against Frost Stress

KD and RP, as the hardest genotypes, had normal growth during the subsequent spring and early summer. MH and VH were the least hardy genotypes and suffered more winter injury with frost signs including reduced growth, bud necrosis, formation of small leaves, and leafless terminal branches with the frozen state. Hardy genotypes had larger buds while, in resistant genotypes, buds were smaller. Our microscopic observations under a stereo microscope revealed variability in the number

of scales among genotypes. The buds of hardy genotypes had more scales (6–8) that were tightly packed with primordia but in the sensitive genotypes there were fewer scale numbers (2–4). The scales were not completely packed together. The buds of hardy genotypes had more sclerenchymatous leaves (scaly leaves) than those of sensitive genotypes during dissection by removing scales.

Seasonal Metabolite Analysis Revealed Differential Responses of Two Organs and Different Genotypes

The stem and bud of 15 pomegranate genotypes at seven time-points during two developmental cycles were used for three soluble carbohydrates, twenty-two amino acids, and six fatty acids extraction followed by HPLC and GC analysis. Despite the similarity of the rhythm of seasonal changes, the content

of investigated metabolites varied depending on the genotype, organ, and sampling date.

Figures 2A,B shows a heatmap with the normalized values (expressed as \log_2) of investigated metabolites for each genotype during the annual cycle in pomegranate stem and bud, respectively. Four distinct patterns of seasonal changes were recorded for investigated metabolites during the annual cycle: (a) an increase toward December and January, a decline in February, and another rise toward April. This cluster contained eight amino acids in the stem. Metabolites in cluster (b) increased rapidly toward December and January and then declined gradually toward April. This cluster included three soluble carbohydrates and some fatty acids in both stem and buds, and fourteen amino acids in the stem. Metabolites in cluster (c) tended to

increase toward December and January and kept their rise toward February and April. This cluster contained the majority of amino acids in the buds. Metabolites in cluster (d) showed a distinct decrease toward December and January and then increased in February and April, including only some fatty acids in both stem and buds. Stearic acid was the only metabolite that represented diffuse seasonal pattern among genotypes and between organs: stem of hardy genotypes and buds of sensitive genotypes were placed in cluster (b) while, the stem of intermediate and sensitive genotypes and buds of hardy and intermediate genotypes were placed in cluster (d) (**Supplementary Tables 1, 2**).

In general, a higher number of metabolites were changed in the stem compared with the buds during the hardening period (20 vs. 10 metabolites). Metabolites that exhibited the



FIGURE 2 | The heatmaps for seasonal variation of primary metabolites in pomegranate stem (**A**) and bud (**B**). The column represents each genotype (KD, RP, PS, KJ, TG, GO, GD, BT, KN, GN, BM, BH, SS, VH, and MH) at the specific time-point (1 October and 15 December 2016, 15 January, 13 February, and 25 April 2017). Each cell represents the mean values of three biological replicates of each metabolite. The color scales from blue (low) to red (high) and is proportional to the normalized values (expressed as \log_2) of the concentration of each metabolite.

most noticeable increase in the stem of all the genotypes during the hardening period were arginine (19 to 29-fold increase), alanine (9.3–20.7×), proline (11–20.3×), tryptophan (7–19.7×), glutamine (5.2–17×), asparagine (5–13.7×), histidine (6.3–12.5×), glucose (4–8.4×), fructose (2.6–8.5×), glutamic acid (2.2–8×), sucrose (3.7–7.9×), aspartic acids (2–7.8×), serine (3–7.5×), glycine (2–6.5×), leucine (2.5–5.5×), linolenic acid, phenylalanine and isoleucine (2–5×) while, palmitoleic acid (2–6×) and linoleic acid (2–4×) showed the decline during hardening period. In the buds, glutamine (6–12×), arginine (6–10.7×), proline (5–10.6×), fructose (4.3–8.9×), glucose (4.8–7.8×), asparagine (3–7×), sucrose (2–6×), glutamic acid (2.5–4.7×), oleic acid (2.2–4×), and aspartic acids (1.6–4×) were the metabolites which exhibited the most rise during hardening period. Linoleic acid (2.2–3.5×) was the only metabolite that represented a decrease in buds during this period.

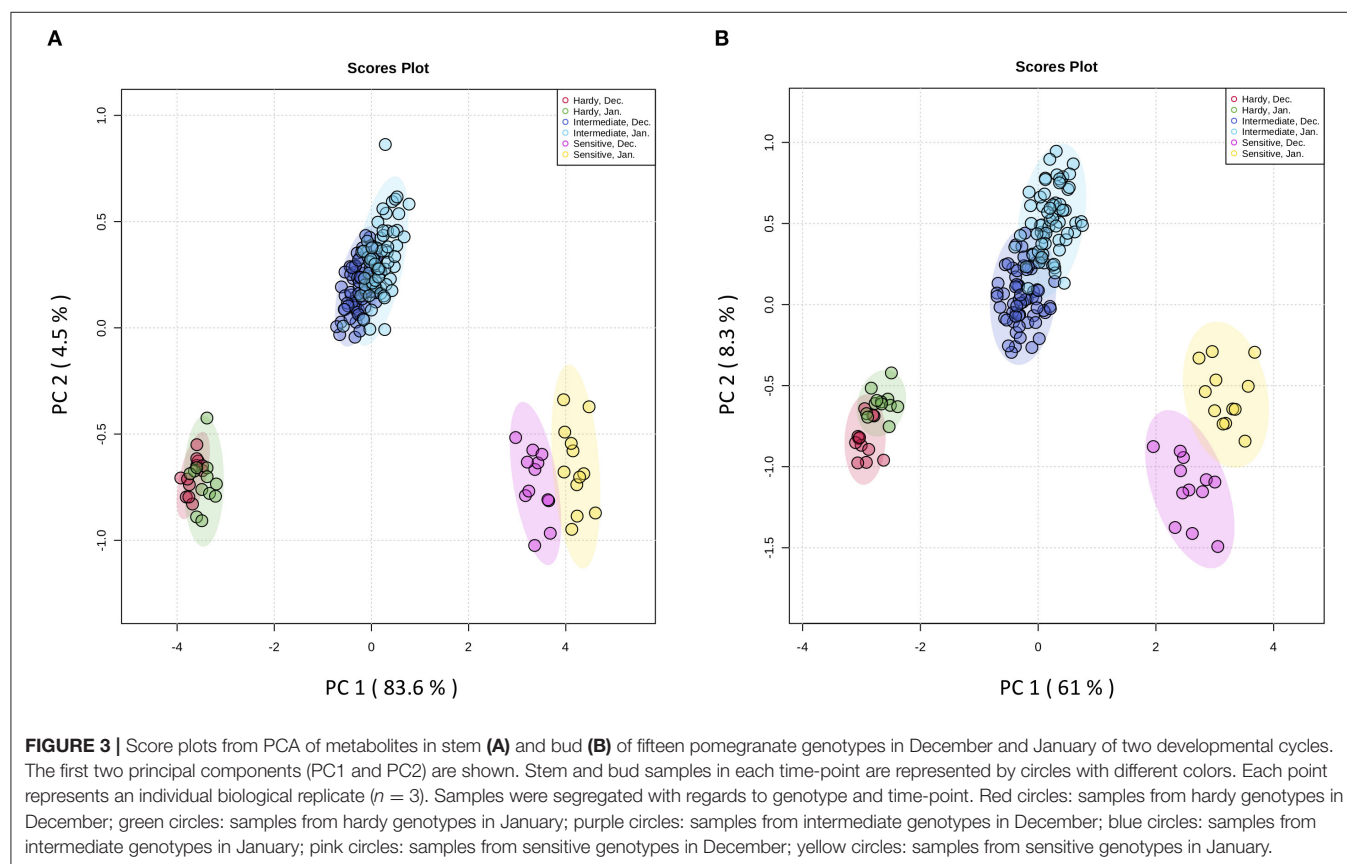
The fold change of soluble carbohydrates was similar in hardy and sensitive groups in both organs during the hardening period. The stem showed more increase in sucrose, as compared to the buds. The fold change of glucose was almost similar in both stem and bud. The buds exhibited more rise in fructose, as compared to the stem. Amino acid groups exhibited considerable accumulation in both tolerant and sensitive genotypes; however, their increase in the stem was two to several times that of the rise in the buds in both groups of genotypes. The extent of amino acid accumulation in the hardy genotypes was several times that of the increase in the sensitive genotypes. The fatty

acid changes (increase or decline) occurred more in the stem of tolerant genotypes than in the buds. This was reversed in the sensitive genotypes.

Comparing all the genotypes, the frost-hardy genotype (KD) showed the greatest fold change of soluble carbohydrates, amino and fatty acids, while frost-sensitive genotypes (MH and/or VH) had the lowest fold change in both organs during 2 years (Supplementary Tables 1, 2).

Metabolite Profile Was Impacted by Genotype and Organ

The principal aims of the present study were to identify frost-hardier genotypes and the key metabolites related to frost tolerance. We selected two time-points i.e., December and January for multivariate data analysis when pomegranate trees were fully hardened. To reveal the effect of the hardening process on metabolite modification, the metabolite data sets derived from the stem and bud samples of the 15 genotypes during December and January of 2 successive years were independently subjected to principal component analysis (PCA) (Figure 3 and Supplementary Figure 2 and Supplementary Table 3). The PCA score plot for both organs showed that principal component 1 (pc1; 83.6 and 61% of the variance for stem and bud, respectively) separated data with regard to genotype and time-points of sampling. The PCA results confirmed our designation based on LT50 data. In both organs, PC1 separated three groups of genotypes: the frost-hardy group



including KD and RP; the frost-sensitive group containing MH and VH; and the intermediate group, which covered other genotypes.

To identify the frost-responsive metabolites in the stem and buds of pomegranate, the partial least squares-discriminant analysis (PLS-DA) was performed on KD (hardest genotype) and MH (the most sensitive genotype) for data from October (control or pre-hardening stage) and December (hardening stage), separately. Frost stress explained 98.4 and 85.4% of the total variation in stem (**Supplementary Figure 3** and **Supplementary Table 4**) and 90.5 and 74.4% of the total variation in the bud (**Supplementary Figure 4** and **Supplementary Table 4**) of KD and MH, respectively. Based on a VIP (variable importance in projection) score of >1 , the important metabolites involved in frost stress were identified in the stem and bud of KD and MH genotypes. Amino acids seem to contribute to the stem hardening, while in the bud, soluble carbohydrates (fructose and glucose) and fatty acids (oleic and linoleic acid) were found as important metabolites together with amino acids (**Figure 4**).

We also performed correlation analyses on LT50 and the metabolite data sets derived from the stem and bud samples of the 15 genotypes (**Supplementary Tables 5, 6**). The correlations between frost hardiness, investigated metabolites and minimum temperature (T_{\min}) are shown in **Supplementary Figure 5**.

Hardening Process Is Associated With Remodeling of the Primary Metabolism

In October, as the pre-hardening stage, the difference of metabolite contents between the stem of KD and MH was below 1.5 times except for methionine, oleic acid, stearic acid, lysine, sucrose, and linolenic acid. The difference in metabolite values between the two cited genotypes became evident toward December and January 2016–2017 (**Figure 5**). The content of amino acid lysine in the stem of KD was 5.7 times that of MH while, palmitoleic acid in MH was 6.5 times that of KD. Fructose, methionine, aspartic and glutamic acid amounts in KD were 4–5 times that of MH. Linoleic acid amount in MH was 3.5 times that of KD. Sucrose, serine, glycine, threonine, cysteine, valine, phenylalanine, and isoleucine values in KD were 3–4 times that of MH. Glucose, asparagine, glutamine, histidine, citrulline, alanine, GABA, tryptophan, tyrosine, leucine, proline, oleic, and linolenic acid contents in KD were 2–3 times that of MH. Arginine, palmitic, and stearic acids showed a 1.5 time increase in content in KD, as compared to MH.

In the buds, similar to the stem, the difference in metabolite values between KD and MH was below 1.5 times in October except for stearic acid, cysteine, methionine, palmitoleic acid, palmitic acid, isoleucine, tyrosine, histidine, glycine, sucrose, and glucose. An increase in the content of metabolites was observed in pomegranate buds toward December and January, but their rise was very low, compared to the stem (**Figure 6**). The sucrose, glycine, aspartic acid, and phenylalanine amounts in KD were 3–4 times that of MH. Glucose, fructose, glutamic acid, asparagine, histidine, threonine, arginine, cysteine, tyrosine, methionine,

isoleucine, proline, palmitoleic, and stearic acids content in KD were 2–3 times that of MH.

DISCUSSION

Pomegranate Tree Responses to Frost Stress in a Time-Dependent Manner

Pomegranate trees established the dormancy and hardened gradually during fall, and reached maximum hardness in mid-winter and de-hardened toward late winter or early spring, in coordination with bud-break and new growth resumption. Concerning the same sampling dates in 2 successive years, we concluded that observed differences in hardness come from climate changes, as reported by Szalay et al. (2017) in *Prunus domestica* cultivars.

In the stem and bud of all the pomegranate genotypes, the sucrose, glucose, and fructose contents increased during fall, reached their peak in mid-winter, responsible for a high degree of freezing tolerance, and then declined gradually toward spring. It seems that the accumulation of the hexose including glucose and fructose, and disaccharide sucrose is a common response during cold acclimation (Kaplan et al., 2004; Bocian et al., 2015; Yue et al., 2015; Chai et al., 2019). Sugars function as osmo-protectants and stabilize the biological membranes. They are essential for the repair of freeze-induced cavitated vessels and facilitate deep supercooling at high levels (Krasensky and Jonak, 2012; Strimbeck et al., 2015; Mayr and Améglio, 2016). In the vegetative buds of *Picea abies*, primordial cells close to the ice barrier tissue accumulated an amorphous starch and di, tri, and tetra-saccharides (Kuprian et al., 2017).

All the amino acids in the stem and buds of all pomegranate genotypes increased toward December and January but three different patterns were observed toward spring: (a) metabolites which declined in February and raised again toward April, and all recorded in the stem. (b) metabolites which declined in February and April and were related to both stem and bud. (c) metabolites which kept their rise in content during February and April and were all registered in buds. Bocian et al. (2015) and Andersen et al. (2017) stated that the accumulated amino acids are not only involved in the plant survival during unfavorable conditions but can also be an important source of nitrogen and carbon required for plant resuming growth. Increasing levels of proline in developing buds can be related to its important role in flower development (Andersen et al., 2017).

Although the majority of amino acids accumulated in the stem and buds of all the pomegranate genotypes during the hardening period, most accumulations were registered for arginine, proline, glutamine, and asparagine in both stem and buds, and alanine, tryptophan, and histidine in the stem, but not in the buds. The similarity of metabolite changes between pomegranate and other plant species (Kaplan et al., 2004; Angelcheva et al., 2014; Bocian et al., 2015; Chai et al., 2019) can be related to conserved mechanisms of metabolic adjustment to increase cold tolerance (Chai et al., 2019).

Here, an increase of proline and arginine was found in the stem and buds of all the genotypes. A large body of data has

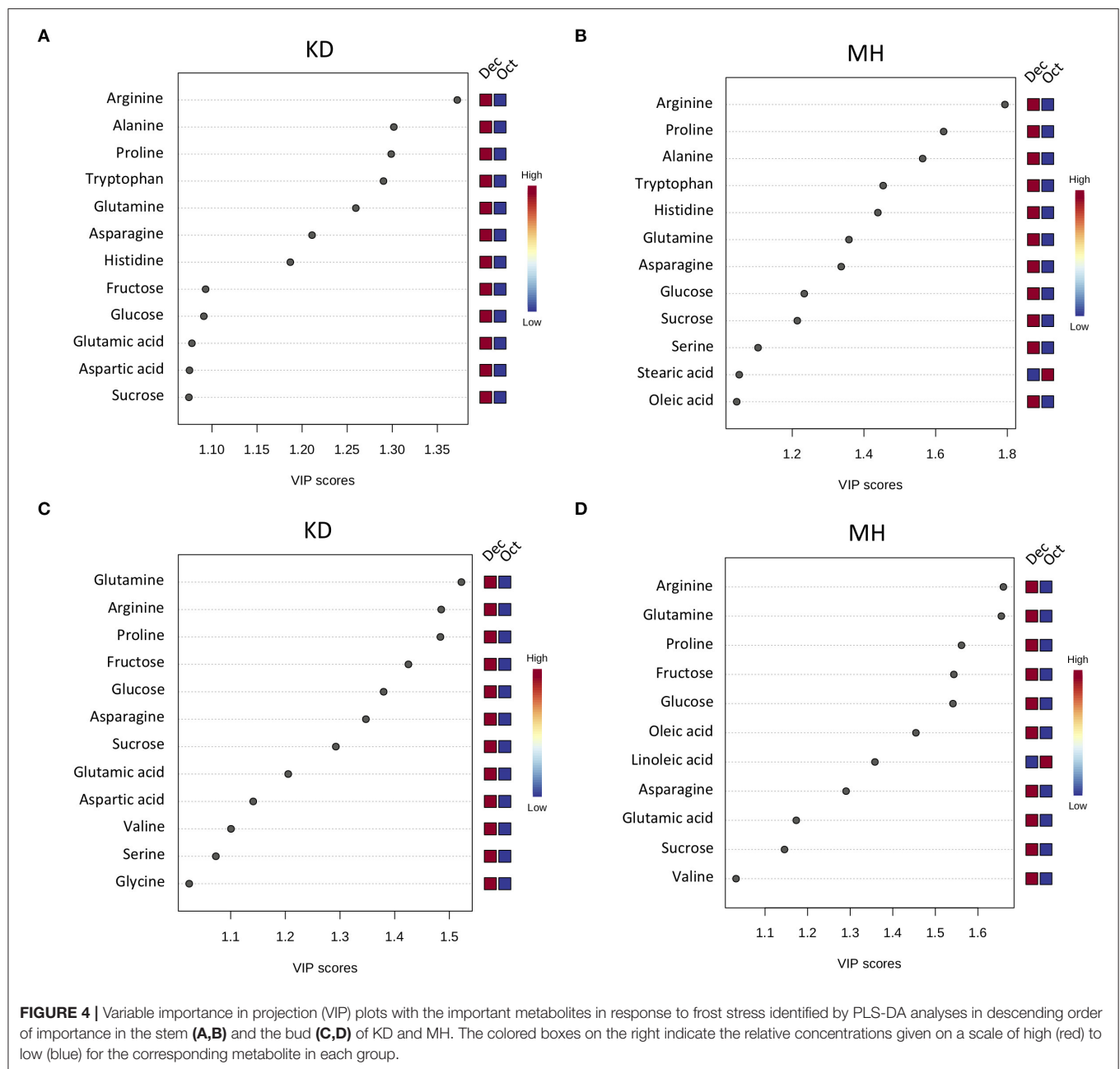


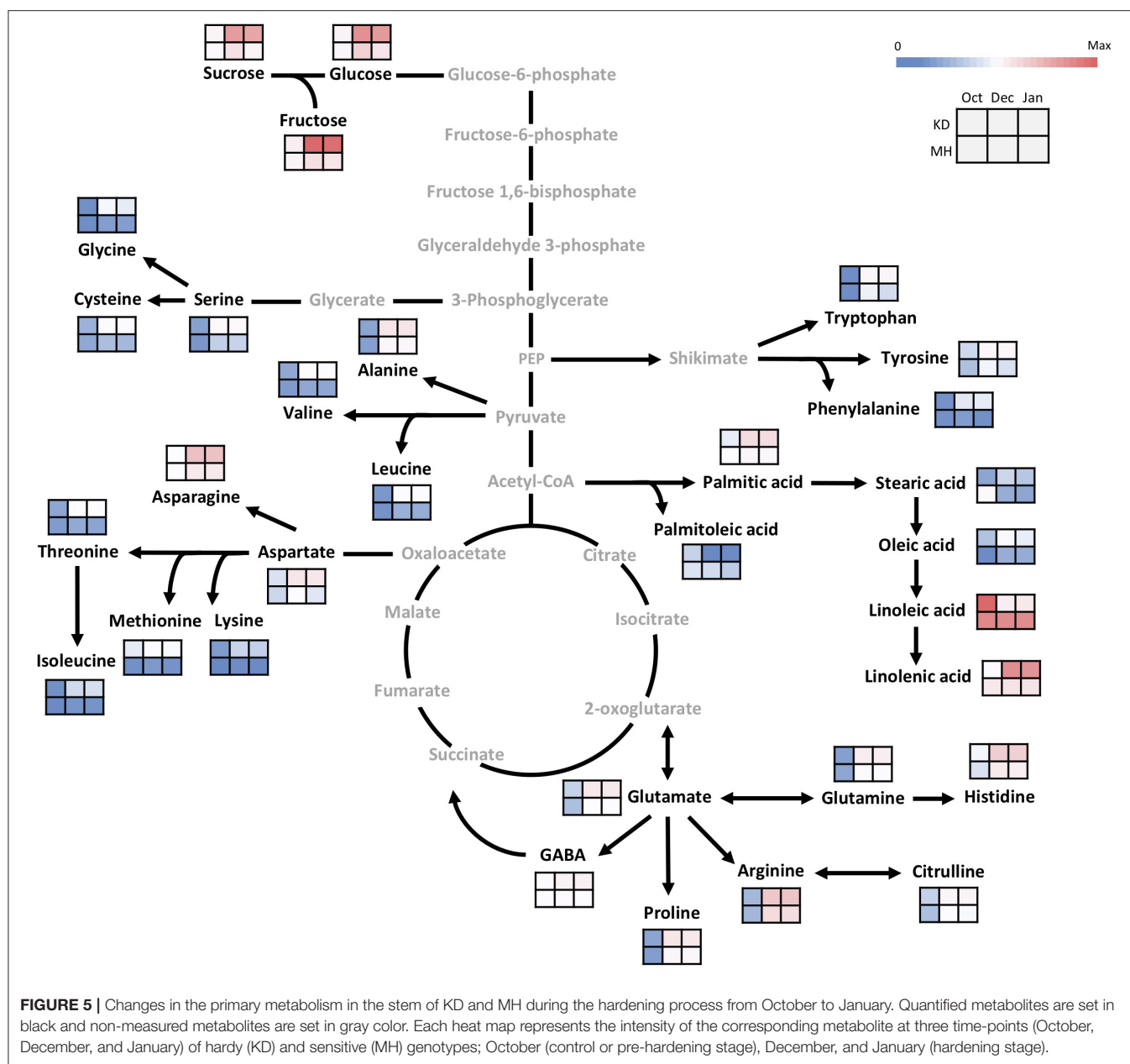
FIGURE 4 | Variable importance in projection (VIP) plots with the important metabolites in response to frost stress identified by PLS-DA analyses in descending order of importance in the stem (**A,B**) and the bud (**C,D**) of KD and MH. The colored boxes on the right indicate the relative concentrations given on a scale of high (red) to low (blue) for the corresponding metabolite in each group.

described proline accumulation under stress conditions and its function as a compatible osmolyte, stabilizer of proteins, membranes, and subcellular structures, regulator of redox potential, molecular chaperone, radical scavenger, and signaling molecule (Szabados and Savouré, 2010; Krasensky and Jonak, 2012; Casartelli et al., 2018). Arginine is a suitable storage form for organic nitrogen because of its high nitrogen to carbon ratio, which is a precursor for the biosynthesis of proline, and also a precursor for nitric oxide (NO) and polyamines, which play crucial roles in regulating abiotic stress (Winter et al., 2015).

Our results also demonstrate that an accumulation of large amounts of glutamine, asparagine, glutamic, and aspartic acids

during the hardening process. These metabolites may be used by the plant as an ammonium donor for the synthesis of other amino acids (Glutamic acid and glutamine), an active ammonium donor, and a precursor for the biosynthesis of pyrimidine and NAD (aspartic acid) and transport/storage compounds (asparagine) (Hincha et al., 2012; Casartelli et al., 2018).

Large amounts of alanine, tryptophan, and histidine were preferentially accumulated in the pomegranate stem. Other reports have proved that alanine acts as an osmo-protectant and can restore the activity of lactate dehydrogenase damaged by frost/defrost rounds (Bocian et al., 2015). The accumulation of tryptophan can be related to important roles in osmotic



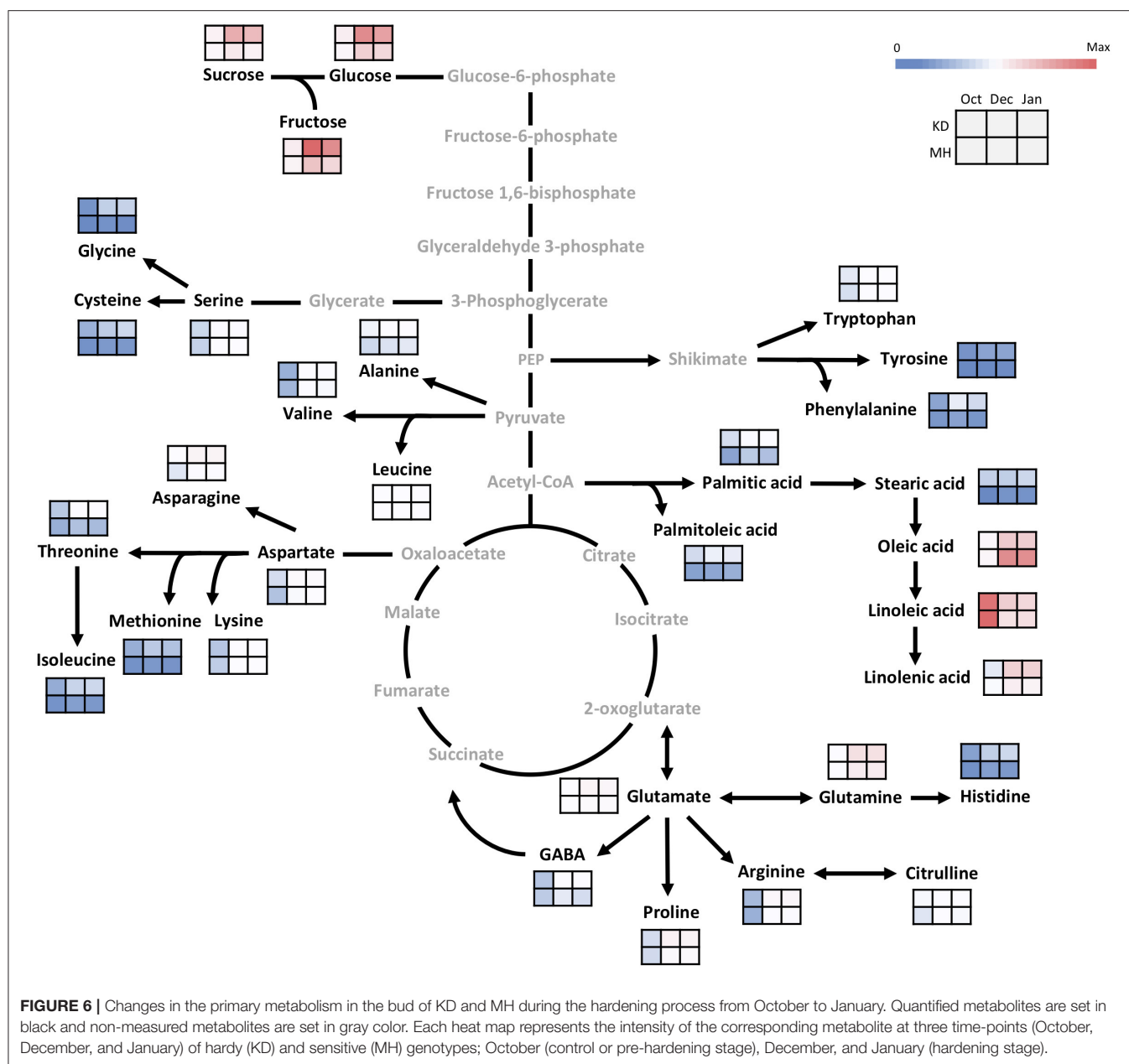
adjustment, stomatal regulation, and ROS scavenging under stress conditions (You et al., 2019).

The results presented in this study demonstrated a significant increase in the content of linolenic and oleic acids, but a decrease in linoleic acid, in both organs of all the pomegranate genotypes during the hardening stage. The changes of palmitoleic acid were different based on organ. The level of stearic acid differed not only between both organs but also changed among different groups of genotypes. The concentrations of oleic, linoleic, and linolenic acids changed notably from pre- to full-acclimation stages in *Picea obovata* needles (Angelcheva et al., 2014). Zhang et al. (2020) concluded that the accumulation of large amounts of linolenic acid in peanut plants under cold stress can be related to fatty acid β -oxidation and thus jasmonate biosynthesis

which through CBF-dependent signaling can improve plant cold tolerance. Changes in fatty acids composition and accumulation of long-chain mono- and polyunsaturated fatty acids help to maintain membrane fluidity, prevent membrane phase change, and are important for regulating the activity of membrane-associated enzymes during frost hardening (Angelcheva et al., 2014; Strimbeck et al., 2015; Zhang et al., 2020).

Differential Responses of the Stem and Bud to Frost Stress Reveal Resistance Variability Within Pomegranate Tree

Higher frost hardiness in winter and a slow rate of de-hardening at spring in the stem, allowed us to conclude that the stem



is frost harder than the buds, similar to the findings in some gymnosperms and angiosperms (Jones et al., 1999; Søgaard et al., 2009; Charrier et al., 2013). The differences in organ-specific tolerance result from the different mechanisms plants use in response to low temperatures. In grape, buds avoid extra-cellular freezing and supercool, whereas canes experience extra-cellular freezing (Jones et al., 1999).

In walnut trees and *Hedera helix* L., bark, and cambium were relatively susceptible to frost during the growing season but during winter, they were able to harden more than xylem parenchyma (Andergassen and Bauer, 2002; Charrier et al., 2013). Conversely, buds hardened but remained more sensitive than other parts during winter. The difference in cold tolerance

may be explained by the anatomical characteristics of stem bark and cambium, as compared to bud. On the other hand, frost has a remarkable impact on wood or meristematic tissues but has a low effect on bark (Charrier et al., 2013). Leaf primordia are the least differentiated and most sensitive parts of bud throughout the year (Andergassen and Bauer, 2002). Therefore, buds are more exposed to freezing events however, the bud scales and cuticle may play an essential role as water or ice proof structures (Kuprian et al., 2017).

Although buds are typically more sensitive than the stems in pomegranate, there is a difference in bud resistance between the genotypes: hardier genotypes have larger buds with more protective scales while, in less resistant genotypes, buds are

smaller and the number of protective scales is lower. Therefore, we assumed the assortment for buds of pomegranate genotypes. A decrease in water content of the shoot primordia and reduction in their size in response to decreasing temperature (Ide et al., 1998) may explain the smaller size of buds in less frost resistant genotypes.

The seasonal progress of frost hardiness differs between the two organs of the present study. Pomegranate buds started hardening earlier than the stem but other reports showed that hardiness begins slightly later in the buds than in the twigs (Sakai and Larcher, 1987). Although both stem and bud of all the genotypes achieved their maximum hardiness level at the same time, pomegranate buds de-hardened earlier. Sakai and Larcher (1987) reported that de-hardening occurs first in the flower buds, then in the leaf buds, and finally in the stems.

Although the hardening process resulted in increased levels of soluble carbohydrates, amino acids, and some fatty acids, responses to low temperature were not the same for the stem and buds of the pomegranate tree. The number of changed metabolites in the stem was twice that of the buds during the hardening period, suggesting that the stem is more influenced by frost stress, compared to buds, thus it is more prone to alteration at metabolic levels. The higher levels of amino acids in the stem compared with buds may be a part of the pre-adaptation strategy, ensuring a higher level of tolerance and guarantee protection against frost stress during winter. Schmitz et al. (2014) suggested that lateral buds were hydraulically isolated from the parent stem during winter until a few days before budburst. We suggest that buds may act as independent parts when compared with branches, reflecting their different behavior in response to frost.

Sucrose, fructose, and glucose were accumulated in both pomegranate stem and buds, suggesting that the accumulation of soluble carbohydrates is a common response of different organs of the tree. The majority of amino acid groups exhibited several times the accumulation in the stem when compared with buds, reflecting that the stem employs more amino acid pathways to improve stress tolerance. Concerning fatty acids, the changes (increase or decrease) in the stem were greater than the buds during the hardening stage. Among fatty acids, stearic acid has a different accumulation profile: its content increases in the stem, and decreases in buds of the hardy group, but it has reverse changes in the sensitive group. Although linoleic and linolenic acids represent similar changes in stem (decrease) and buds (increase), the level of their changes is different between hardy and sensitive groups. According to a comprehensive review by He and Ding (2020), unsaturated fatty acids act as ingredients and modulators of cellular membranes in glycerolipids, a reserve of carbon and energy in triacylglycerol, and stock extracellular barrier constituents (e.g., cutin and suberin), acting as precursors of various bioactive molecules (e.g., jasmonates and nitroalkenes), and regulators of stress signaling.

Pomegranate Tree Responses to Frost Stress Are Genotype-Dependent

Despite the same hardening/de-hardening timing in all the genotypes and both organs, we found genotypic differences in

the hardening/de-hardening rate and maximum frost hardiness level; similar to a previous report on 5-year-old pomegranates (Ghasemi Soloklui et al., 2012) and the other woody perennials such as oak (Morin et al., 2007) and beech trees (Lenz et al., 2016). According to this comprehensive discussion by Lenz et al. (2016), this large variability in freezing resistance in mid-winter can result from genetic differentiations, phenological differences, and phenotypic plasticity.

In agreement with the field observations, KD and MH were the hardiest and the least hardy genotypes, with different morphology during next spring and early summer. Despite a previous report by Rajaei and Yazdanpanah (2015) with four sturdy brown scales in dormant buds of pomegranate cv. Rabbab-e-Neyriz, our recent study demonstrated variability in scale number and compression with leaf primordia. The number of scaly leaves in pomegranate buds was also different in hardy and sensitive genotypes. The greater number of scales and their compression, as well as the higher number of protective leaves, can provide the necessary protection for the most sensitive parts of the trees, i.e., the shoot apex and primordial leaves, against freezing stress. This structural evidence supports greater frost resistance in the KD genotype and is concomitant with our metabolic findings. The number of bud scales in *Abies sachalinensis* increased with winter cold. In boreal conifers of Pinaceae, shoot and flower primordia are enclosed by 40 or more scales and/or modified primordial leaves, which increase the winter survival in northern continental climates (Sakai and Larcher, 1987). During the extra-organ freezing mechanism specific to buds, primordia remain stably unfrozen whereas bud scales freeze first, working as an ice sink to withdraw water from the primordia to the scales (Sakai and Larcher, 1987; Endoh et al., 2014).

During this study, some histological differences were also observed between the stem of hardy and sensitive genotypes. KD showed a thicker periderm, more granular, and massive phenolics in outer cortical layers and smaller xylem vessels, as compared with MH stem (data not shown). These structural attributes are indicative of a difference in freezing tolerance between the genotypes and are under more consideration in our lab, in combination with transmission electron microscope observations.

The same metabolite changes did not occur in all the 15 pomegranate genotypes and may be related to variation in the levels of stress tolerance. Our comparison between the hardiest and the least hardy genotypes (KD vs. MH) revealed that although the accumulation of some metabolites was common in both genotypes; the extent of their increases was higher in KD than in MH. These different responses would enable KD to maintain or improve tolerance during frost stress.

Importantly, KD changes more metabolites than MH during the hardening stage, demonstrating the establishment of strong biochemical strategies to cope with frost stress. Among the investigated metabolites, the group of amino acids shows more accumulation, in both fold change and amount, in KD when compared with MH. Concerning the protective roles of amino acids, the higher accumulation of amino acids in frost-tolerant genotypes represents a relation between stress tolerance and the

level of amino acids. This result implies that in pomegranate, amino acids and their derivatives have benefits for frost adaptation, in contrast to soluble carbohydrates and fatty acids. Despite the functional similarity of soluble carbohydrates and amino acids in stress tolerance, the reason for this preference is unclear and may be due to the energetic and/or nutritional cost to produce a large amount of metabolites belonging to these groups (Benina et al., 2013).

CONCLUSION

In conclusion, pomegranate frost sensitivity was different seasonally, genotypically, and within the tree. The metabolite quantification represented different metabolic adaptations among genotypes and between the stem and bud, indicating genotype- and organ-specific responses which lead to different levels of frost tolerance. We found that the hardening process has a dramatic impact on the content of pomegranate metabolites and that changes in metabolite levels could be important for the development of frost tolerance. The levels of the metabolites increased during the hardening period, but this was not equal between genotypes or plant organs. KD as the most frost-hardy genotype and stem as the most frost-tolerant organ has a high capacity in stress regulation by the greater accumulation of metabolites, particularly amino acids.

Increased knowledge about frost hardiness and underlying mechanisms, the timing and the rate of hardening/de-hardening, the degree and the maintenance of freezing

tolerance, as well as its relations to dormancy-growth cycle and seasonal temperature shifts under global warming could impact horticultural production systems. Parallel structural, ultrastructural, transcriptomic, and metabolomic studies on contrasting pomegranate genotypes, currently running in our lab in ABRII, will help gain a more comprehensive understanding of pomegranate freezing response and underlying mechanisms.

DATA AVAILABILITY STATEMENT

The original contributions presented in the study are included in the article/**Supplementary Material**, further inquiries can be directed to the corresponding authors.

AUTHOR CONTRIBUTIONS

PY and MZ designed the experiment. PY, MZ, and SA performed the experiment. PY, SA, and MG analyzed the data. MZ and PJ supervised the experiment. PY wrote the manuscript. HR revised the manuscript. MV identified the genotypes. All authors contributed to the article and approved the submitted version.

SUPPLEMENTARY MATERIAL

The Supplementary Material for this article can be found online at: <https://www.frontiersin.org/articles/10.3389/fpls.2021.699139/full#supplementary-material>

REFERENCES

- Abdirad, S., Majd, A., Irian, S., Hadidi, N., and Hosseini Salekdeh, G. (2020). Differential adaptation strategies to different levels of soil water deficit in two upland and lowland genotypes of rice: a physiological and metabolic approach. *J. Sci. Food. Agric.* 100, 1458–1469. doi: 10.1002/jsfa.10153
- Agricultural Statistics (2020). *Executive Committee on Management of Environmental Stresses for Horticultural Products*. Iran: Ministry of Agriculture.
- Andergassen, S., and Bauer, H. (2002). Frost hardiness in the juvenile and adult life phase of ivy (*Hedera helix* L.). *Plant Ecol.* 161, 207–213. doi: 10.1023/A:1020365422879
- Andersen, U. B., Kjaer, K. H., Erban, A., Alpers, J., Hinch, D. K., Kopka, J., et al. (2017). Impact of seasonal warming on overwintering and spring phenology of blackcurrant. *Environ. Exp. Bot.* 140, 96–109. doi: 10.1016/j.envexpbot.2017.06.005
- Angelcheva, L., Mishra, Y., Antti, H., Kjellsen, T. D., Funk, C., Strimbeck, R. G., et al. (2014). Metabolomic analysis of extreme freezing tolerance in Siberian spruce (*Picea obovata*). *New Phytol.* 204, 545–555. doi: 10.1111/nph.12950
- Benina, M., Obata, T., Mehterov, N., Ivanov, I., Petrov, V., Toneva, V., et al. (2013). Comparative metabolic profiling of *Haberlea rhodopensis*, *Thellungiella halophylla*, and *Arabidopsis thaliana* exposed to low temperature. *Front. Plant Sci.* 4:499. doi: 10.3389/fpls.2013.00499
- Bocian, A., Zwierzykowski, Z., Rapacz, M., Koczyk, G., Ciesiolka, D., and Kosmala, A. (2015). Metabolite profiling during cold acclimation of *Lolium perenne* genotypes distinct in the level of frost tolerance. *J. Appl. Genet.* 56, 439–449. doi: 10.1007/s13353-015-0293-6
- Casartelli, A., Riewe, D., Hubberten, H. M., Altmann, T., Hoefgen, R., and Heuer, S. (2018). Exploring traditional aus-type rice for metabolites conferring drought tolerance. *Rice* 11, 1–16. doi: 10.1186/s12284-017-0189-7
- Chai, F., Liu, W., Xiang, Y., Meng, X., Sun, X., Cheng, C., et al. (2019). Comparative metabolic profiling of *Vitis amurensis* and *Vitis vinifera* during cold acclimation. *Hortic. Res.* 6, 1–12. doi: 10.1038/s41438-018-0083-5
- Charrier, G., Ngao, J., Saudreau, M., and Améglio, T. (2015). Effects of environmental factors and management practices on microclimate, winter physiology, and frost resistance in trees. *Front. Plant Sci.* 6:259. doi: 10.3389/fpls.2015.00259
- Charrier, G., Poirier, M., Bonhomme, M., Lacomte, A., and Améglio, T. (2013). Frost hardiness in walnut trees (*Juglans regia* L.): how to link physiology and modelling? *Tree Physiol.* 33, 1229–1241. doi: 10.1093/treephys/tpt090
- Endoh, K., Kuwabara, C., Arakawa, K., and Seizo Fujikawa, S. (2014). Consideration of the reasons why dormant buds of trees have evolved extraorgan freezing as an adaptation for winter survival. *Environ. Exp. Bot.* 106, 52–59. doi: 10.1016/j.envexpbot.2014.02.008
- Erkan, M., and Dogan, A. (2018). “Pomegranate/Roma—*Punica granatum*,” in *Exotic Fruits Reference Guide*, eds S. Rodrigues, E. de Oliveira Silva, and E. S. de Brito (London: Academic Press), 355–361.
- Ghasemi Soloklui, A. A., Ershadi, A., and Fallahi, E. (2012). Evaluation of cold hardiness in seven Iranian commercial pomegranate (*Punica granatum* L.) cultivars. *HortScience* 47, 1821–1825. doi: 10.21273/HORTSCI.47.12.1821
- Hannah, M. A., Wiese, D., Freund, S., Fiehn, O., Heyer, A. G., and Hinch, D. K. (2006). Natural genetic variation of freezing tolerance in *Arabidopsis*. *Plant Physiol.* 142, 98–112. doi: 10.1104/pp.106.081141
- He, M., and Ding, N.-Z. (2020). Plant unsaturated fatty acids: multiple roles in stress response. *Front. Plant Sci.* 11:562785. doi: 10.3389/fpls.2020.562785
- Hinch, D. K., Espinoza, C., and Zuther, E. (2012). “Transcriptomic and metabolomic approaches to the analysis of plant freezing tolerance and cold acclimation,” in *Improving Crop Resistance to Abiotic Stress*, eds N. Tuteja, S. S. Gill, A. F. Tiburcio, and R. Tuteja (Berlin: Wiley-Blackwell), 255–287.

- Holland, D., Hatib, K., and Bar-Ya'akov, I. (2009). "Pomegranate: botany, horticulture, breeding," in *Horticultural Reviews*, ed J. Janick (New Jersey, NJ: John Wiley and Sons), 127–191.
- Ide, H., Price, W. S., Arata, Y., and Ishikawa, M. (1998). Freezing behaviors in leaf buds of cold-hardy conifers visualized by NMR microscopy. *Tree Physiol.* 18, 451–458. doi: 10.1093/treephys/18.7.451
- Jones, K. S., Paroschy, J., Mckersie, B. D., and Bowley, S. R. (1999). Carbohydrate composition and freezing tolerance of canes and buds in *Vitis vinifera*. *J. Plant Physiol.* 155, 101–106. doi: 10.1016/S0176-1617(99)80146-1
- Kaplan, F., Kopka, J., Haskell, D. W., Zhao, W., Schiller, K. C., Gatzke, N., et al. (2004). Exploring the temperature-stress metabolome of Arabidopsis. *Plant Physiol.* 136, 4159–4168. doi: 10.1104/pp.104.052142
- Krasensky, J., and Jonak, C. (2012). Drought, salt, and temperature stress-induced metabolic rearrangements and regulatory networks. *J. Exp. Bot.* 63, 1593–1608. doi: 10.1093/jxb/err460
- Kuprian, E., Munkler, C., Resnyak, A., Zimmermann, S., Tuong, T. D., Gierlinger, N., et al. (2017). Complex bud architecture and cell-specific chemical patterns enable supercooling of *Picea abies* bud primordia. *Plant Cell Environ.* 40, 3101–3112. doi: 10.1111/pce.13078
- Lenz, A., Hoch, G., and Vitasse, Y. (2016). Fast acclimation of freezing resistance suggests no influence of winter minimum temperature on the range limit of European beech. *Tree Physiol.* 36, 490–501. doi: 10.1093/treephys/tpv147
- Mayr, S., and Améglio, T. (2016). "Freezing stress in tree xylem," in *Progress in Botany*, Vol. 77, ed U. Lüttge (Switzerland: Springer International Publishing), 381–414.
- Morin, X., Améglio, T., Ahas, R., Kurz-Besson, C., Lanta, V., Lebourgeois, F., et al. (2007). Variation in cold hardiness and carbohydrate concentration from dormancy induction to bud burst among provenances of three European oak species. *Tree Physiol.* 27, 817–825. doi: 10.1093/treephys/27.6.817
- Preston, J. C., and Sandve, S. R. (2013). Adaptation to seasonality and the winter freeze. *Front. Plant Sci.* 4:167. doi: 10.3389/fpls.2013.00167
- Rajaei, H., and Yazdanpanah, P. (2015). Buds and leaves in pomegranate (*Punica granatum* L.): phenology in relation to structure and development. *Flora* 214, 61–69. doi: 10.1016/j.flora.2015.05.002
- Rohde, A., and Bhalerao, R. P. (2007). Plant dormancy in the perennial context. *Trends Plant Sci.* 12, 217–223. doi: 10.1016/j.tplants.2007.03.012
- Saeed, M., Naveed, M., BiBi, J., Kamboh, A. A., Arain, M. A., Shah, Q. A., et al. (2018). The promising pharmacological effects and therapeutic/medicinal applications of *Punica granatum* L. (Pomegranate) as a functional food in humans and animals. *Recent Pat. Inflamm. Allergy Drug Discov.* 12, 24–38. doi: 10.2174/1872213X12666180221154713
- Sakai, A., and Larcher, W. (1987). *Frost Survival of Plants: Responses and Adaptation to Freezing Stress*. Germany: Springer-Verlag.
- Schmitz, J. D., Guédon, Y., Herter, F. G., Leite, G. B., and Lauri, P. É. (2014). Exploring bud dormancy completion with a combined architectural and phenological analysis: the case of apple trees in contrasting winter temperature conditions. *Am. J. Bot.* 101, 398–407. doi: 10.3732/ajb.1300335
- Søgaard, G., Granhus, A., and Johnsen, Ø. (2009). Effect of frost nights and day and night temperature during dormancy induction on frost hardiness, tolerance to cold storage and bud burst in seedlings of Norway spruce. *Trees* 23, 1295–1307. doi: 10.1007/s00468-009-0371-7
- Strimbeck, G. R., Schaberg, P. G., Fossdal, C. G., Schröder, W. P., and Kjellsen, T. D. (2015). Extreme low temperature tolerance in woody plants. *Front. Plant Sci.* 6:884. doi: 10.3389/fpls.2015.00884
- Szabados, L., and Savouré, A. (2010). Proline: a multifunctional amino acid. *Trends Plant Sci.* 15, 89–97. doi: 10.1016/j.tplants.2009.11.009
- Szalay, L., Molnár, Á., and Kovács, S. (2017). Frost hardiness of flower buds of three plum (*Prunus domestica* L.) cultivars. *Sci. Hortic.* 214, 228–232. doi: 10.1016/j.scienta.2016.11.039
- Talebi, A. F., Mohtashami, S. K., Tabatabaei, M., Tohidfar, M., Bagheri, A., Zeinalabedini, M., et al. (2013). Fatty acids profiling: a selective criterion for screening microalgae strains for biodiesel production. *Algal Res.* 2, 258–267. doi: 10.1016/j.algal.2013.04.003
- Winter, G., Todd, C. D., Trovato, M., Forlani, G., and Funck, D. (2015). Physiological implications of arginine metabolism in plants. *Front. Plant Sci.* 6:534. doi: 10.3389/fpls.2015.00534
- Wu, S., and Tian, L. (2017). Diverse phytochemicals and bioactivities in the ancient fruit and modern functional food pomegranate (*Punica granatum*). *Molecules* 22:1606. doi: 10.3390/molecules22101606
- You, J., Zhang, Y., Liu, A., Li, D., Wang, X., Dossa, K., et al. (2019). Transcriptomic and metabolomic profiling of drought-tolerant and susceptible sesame genotypes in response to drought stress. *BMC Plant Biol.* 19:267. doi: 10.1186/s12870-019-1880-1
- Yue, C., Cao, H. L., Wang, L., Zhou, Y. H., Huang, Y. T., Hao, X. Y., et al. (2015). Effects of cold acclimation on sugar metabolism and sugar-related gene expression in tea plant during the winter season. *Plant Mol. Biol.* 88, 591–608. doi: 10.1007/s11103-015-0345-7
- Zahravi, M., and Vazifeshenas, M. R. (2017). Study of genetic diversity in pomegranate germplasm of Yazd province of Iran. *IJGPB* 6, 20–35. doi: 10.30479/IJGPB.2017.1488
- Zhang, H., Jiang, C., Ren, J., Dong, J., Shi, X., Zhao, X., et al. (2020). An advanced lipid metabolism system revealed by transcriptomic and lipidomic analyses plays a central role in peanut cold tolerance. *Front. Plant Sci.* 11:1110. doi: 10.3389/fpls.2020.01110

Conflict of Interest: The authors declare that the research was conducted in the absence of any commercial or financial relationships that could be construed as a potential conflict of interest.

Publisher's Note: All claims expressed in this article are solely those of the authors and do not necessarily represent those of their affiliated organizations, or those of the publisher, the editors and the reviewers. Any product that may be evaluated in this article, or claim that may be made by its manufacturer, is not guaranteed or endorsed by the publisher.

Copyright © 2021 Yazdanpanah, Jonoubi, Zeinalabedini, Rajaei, Ghaffari, Vazifeshenas and Abdirad. This is an open-access article distributed under the terms of the Creative Commons Attribution License (CC BY). The use, distribution or reproduction in other forums is permitted, provided the original author(s) and the copyright owner(s) are credited and that the original publication in this journal is cited, in accordance with accepted academic practice. No use, distribution or reproduction is permitted which does not comply with these terms.



Integrated Transcriptomics and Metabolomics Analysis Reveal Key Metabolism Pathways Contributing to Cold Tolerance in Peanut

Xin Wang[†], Yue Liu[†], Zhongkui Han, Yuning Chen, Dongxin Huai, Yanping Kang, Zhihui Wang, Liying Yan, Huifang Jiang, Yong Lei* and Boshou Liao*

Key Laboratory of Biology and Genetic Improvement of Oil Crops, Ministry of Agriculture and Rural Affairs, Oil Crops Research Institute of the Chinese Academy of Agricultural Sciences, Wuhan, China

OPEN ACCESS

Edited by:

Dhruv Lavania,
University of Alberta, Canada

Reviewed by:

Sibaji Kumar Sanyal,
Jawaharlal Nehru University, India
Vivek Kumar Raxwal,
Central European Institute
of Technology (CEITEC), Czechia

*Correspondence:

Yong Lei
leiyong@caas.cn
Boshou Liao
liaoboshou@caas.cn

[†]These authors have contributed
equally to this work

Specialty section:

This article was submitted to
Plant Abiotic Stress,
a section of the journal
Frontiers in Plant Science

Received: 03 August 2021

Accepted: 21 October 2021

Published: 24 November 2021

Citation:

Wang X, Liu Y, Han Z, Chen Y,
Huai D, Kang Y, Wang Z, Yan L,
Jiang H, Lei Y and Liao B (2021)
Integrated Transcriptomics
and Metabolomics Analysis Reveal
Key Metabolism Pathways
Contributing to Cold Tolerance
in Peanut.
Front. Plant Sci. 12:752474.
doi: 10.3389/fpls.2021.752474

Low temperature (non-freezing) is one of the major limiting factors in peanut (*Arachis hypogaea* L.) growth, yield, and geographic distribution. Due to the complexity of cold-resistance trait in peanut, the molecular mechanism of cold tolerance and related gene networks were largely unknown. In this study, metabolomic analysis of two peanut cultivars subjected to chilling stress obtained a set of cold-responsive metabolites, including several carbohydrates and polyamines. These substances showed a higher accumulation pattern in cold-tolerant variety SLH than cold-susceptible variety ZH12 under cold stress, indicating their importance in protecting peanut from chilling injuries. In addition, 3,620 cold tolerance genes (CTGs) were identified by transcriptome sequencing, and the CTGs were most significantly enriched in the “phenylpropanoid biosynthesis” pathway. Two vital modules and several novel hub genes were obtained by weighted gene co-expression network analysis (WGCNA). Several key genes involved in soluble sugar, polyamine, and G-lignin biosynthetic pathways were substantially higher and/or responded more quickly in SLH (cold tolerant) than ZH12 (cold susceptible) under low temperature, suggesting they might be crucial contributors during the adaptation of peanut to low temperature. These findings will not only provide valuable resources for study of cold resistance in peanut but also lay a foundation for genetic modification of cold regulators to enhance stress tolerance in crops.

Keywords: *Arachis hypogaea*, RNA-Seq, metabolome, carbohydrate, polyamine, lignin, phenylpropanoid

INTRODUCTION

Peanut (*Arachis hypogaea* L.) is an important oil and economic crop worldwide, and provides a rich source of nutrients for humans, including fat, protein, sugar, fatty acids, and free amino acids (Zhao et al., 2012; Sorita et al., 2020). Low temperature is one of the major environmental stresses that adversely affect plant development and geographic distribution (Kakani et al., 2002; Wang et al., 2003). The growth of peanut is severely inhibited below 15°C, and chilling stress (non-freezing) is deemed as a limiting factor in peanut cultivation and production (Bell et al., 1994). In northeast China, cold weather often occurs during spring sowing and autumn harvest seasons, leading to a serious decrease of peanut yields per year (Chen et al., 2014). With the increasing demand for

peanut in recent years, it is urgent to investigate the mechanism of cold tolerance and cultivate new cold-resistant varieties.

Cold stress causes excessive accumulation of reactive oxygen species (ROS) during respiration and photosynthesis processes in plant, thus increasing cell membrane permeability and the lipid peroxidation level (Zhang et al., 2019). Nevertheless, plants evolve a series of sophisticated mechanisms to defense against cold stress to some extent (Ding et al., 2020). The alterations of gene expression in response to low temperature are a common strategy to cope with cold damage in plants (Suzuki, 2019). During the last two decades, a number of components involved in the cold-responsive-signaling pathway have been isolated and characterized, including messenger molecules (e.g., Ca^{2+}), Ca^{2+} -related protein kinases and several crucial transcription factors (Yuan et al., 2018). One of the best studied examples was the plant ICE-CBF-COR-signaling module (Chinnusamy et al., 2003). C-repeat Binding Factors/Dehydration-Responsive Element-Binding proteins (CBFs/DREBs) were members of APETALA 2/Ethylene Response Factor (AP2/ERF) family and played central roles in cold acclimation (Kim et al., 2015). The transcript levels of CBFs were sharply upregulated by Inducer of CBF Expression protein (ICE), an MYC-type basic helix-loop-helix family transcription factor, and then CBFs activated the expression of downstream cold-responsive (COR) genes *via* binding to *cis*-elements in their promoters (Lee et al., 2005; Tang et al., 2020). In addition, a lot of cold-resistant proteins (e.g., late embryogenesis-abundant proteins, IEAs) and protective substances (e.g., soluble sugars and proline) were synthesized in plant cells, functioning as osmolytes to regulate osmotic potential and maintain membrane integrity (Dong et al., 2002; Zuther et al., 2004; Ma et al., 2009).

Transcriptomic analysis has been a highly efficient way to reveal cold-responsive genes in many crops, such as maize (Li et al., 2019), rice (Pan et al., 2020), *Brassica napus* (Mehmood et al., 2021) and *Brassica juncea* (Sinha et al., 2015). Microarray analysis of peanut leaves subjected to low temperature got a number of cold-regulated genes and provided some useful insights into cold signal transduction pathways in peanut (Chen et al., 2014). With the rapid development of high-throughput sequencing and mass spectrometer technologies, a massive of multi-omics data (e.g., transcriptomics and metabolomics) have been generated, and it is possible to explore the mechanism of plant cold tolerance by analyzing and mining the big data (Zhao et al., 2019; Cui et al., 2020; Du et al., 2020; Yang et al., 2020; Jiang et al., 2021). Comparative transcriptomic analysis of two peanut varieties with contrasting cold resistance (NH5 and FH18) identified several cold-responsive transcription factors, including bHLH, MYB, and NAC (Jiang et al., 2020). Furthermore, lipidomic analysis of the two varieties revealed that membrane lipid and fatty acid metabolisms contributed substantially to cold resistance in peanut (Zhang H. et al., 2020).

Although there are a few reports about cold tolerance in peanut, the molecular mechanism underlining the signal pathway and related gene networks need to be further investigated due to the complexity of the cold-resistant trait in this important crop (Wang et al., 2017, 2020; Zhang et al., 2019). In the current study, an integrated analysis of transcriptome and metabolome from

two peanut cultivars (SLH and ZH12) allowed us to obtain a set of cold-responsive metabolites/genes that possibly protect peanut from chilling damage. These results contributed to a better understanding of the molecular mechanism of cold response in peanut and will be useful for the development of cultivars with enhanced cold-stress tolerance.

MATERIALS AND METHODS

Plant Materials and Treatments

The cold-resistant peanut cultivar “Silihong” (SLH) and cold-sensitive “Zhonghua 12” (ZH12) were used in this study. Peanut seeds were soaked in distilled water for 4 h, and placed in petri dishes with moistened filter papers, and then germinated in the dark at 28°C for 2 days. The germinated seeds were sown in soil pots and transferred into a growth chamber under a 16-h/8-h (light-dark) cycle at 28°C, with a photosynthetic photon flux density of $700 \mu\text{mol m}^{-2} \text{s}^{-1}$. Two-week-old seedlings were used for cold treatment with a 16-h/8-h cycle (light/dark) at 10°C. The third leaves from seedlings were collected at 0, 3, 24, and 48 h, quickly frozen in liquid nitrogen, and stored at -80°C until use. All samples were performed in three independent biological replicates.

Physiological Index Measurements

The two varieties of peanut seeds were immersed in distilled water for 4 h, transferred to petri dishes at 2°C for 72 h, and then returned to normal temperature (28°C) for additional 3 days. The controls were continuously germinated at 28°C for 3 days. The germination rates were measured every day.

Malondialdehyde (MDA) and H_2O_2 content were determined by Lipid Peroxidation MDA Assay Kit and Hydrogen Peroxide Assay Kit (Beyotime Biotechnology Co., Ltd., Shanghai, China), respectively. The superoxide anion level was analyzed by Micro Superoxide Anion Assay Kit (Beijing Solarbio Science and Technology Co., Ltd., Beijing, China). All the experiments were performed according to the manufacturers' protocols, and data were derived from three biological replicates. Student's *T*-test was performed to calculate the *p*-values using SPSS 20.0 version.

Metabolite Extraction and Profiling

The frozen leaves were grounded into fine powder in liquid nitrogen. About 100 mg of samples was placed into 2-ml Eppendorf tubes and resuspended with 500- μl extraction liquid (80% methanol and 0.1% formic acid). After vortex for 30 s, the mixtures were incubated on ice for 5 min and then centrifuged at 15,000 rpm, 4°C for 10 min. Some of the supernatant was transferred to a fresh EP tube and diluted to final concentration containing 53% methanol by adding with LC-MS grade water. The samples were centrifuged at 15,000 g, 4°C for 20 min. Finally, the supernatant was injected into the LC-MS/MS system for analysis.

For the positive polarity mode, LC-MS/MS analyses were performed using an ExionLCTM AD system (SCIEX) on a BEH C8 Column (100 mm \times 2.1 mm, 1.9 μm), coupled with a QTRAP® 6500 + mass spectrometer (SCIEX). The mobile phase

consisted of 0.1% formic acid water (A) and acetonitrile (B) with elution gradient at a flow rate of 0.35 ml/min as follows: 5% B, 1 min; 5–100% B, 24 min; 100% B, 28 min; 100–5% B, 28.1 min; 5% B, 30 min. For the negative polarity mode, samples were injected onto an HSS T3 Column (100 mm × 2.1 mm). The flow rate was set as 0.35 ml/min with solvent gradient as follows: 2% B, 1 min; 2–100% B, 18 min; 100% B, 22 min; 100–5% B, 22.1 min; 5% B, 25 min. The main parameters of QTRAP® 6500 + mass spectrometer were set as follows: Curtain Gas of 35 psi, Collision Gas of Medium, Temperature of 500°C, Ion Spray Voltage of 5,500 V or –4,500 V in a positive or negative mode, respectively.

Metabolite identification was based on the fragmentation patterns of Q1 and Q3, retention time, decluttering potential, and collision energy. Q3 was used to quantify the metabolite according to the in-house database (Novogene Bioinformatics Technology Co., Ltd.).

Transcriptome Sequencing

Total RNA was isolated from the peanut leaves. The concentration and integrity of RNA were checked by the Bioanalyzer 2100 system (Agilent Technologies, CA, United States). About 1 µg of RNA per sample was used as input material for the transcriptome library preparation. The libraries were sequenced on an Illumina NovaSeq platform (Tianjin, China), and 150-bp paired-end reads were generated. The high-quality reads were obtained by removing reads containing adapter, reads containing poly-N, and low-quality reads from raw data. The high-quality paired-end reads were then mapped to the peanut reference genome (Tifrunner.gnm1.ann1.CCJH¹) using HISAT2 software (version 2.0.5) with default parameters (Kim et al., 2019). The feature counts program (with a parameter of v1.5.0-p3) (Liao et al., 2014) was used to count the reads numbers mapped to each gene. If a read was mapped to two or more positions in the genome, then it will be filtered out. Only uniquely mapped reads were used for quantification. The gene expression level was calculated by the FPKM values (Fragments per Kilobase of transcript per Million mapped reads) using the Cufflinks program (Trapnell et al., 2010). The Pearson correlation coefficients between different samples were calculated by the cor function in R package and presented as heatmap using pheatmap software². To identify cold-responsive genes in peanut, the differentially expressed genes (DEGs) were screened using the DESeq2 R package (1.20.0) with the criteria of | log₂FC (fold change) | > 1 and an adjusted *P*-value < 0.01 (Love et al., 2014). Gene ontology (GO) and KEGG enrichment analysis of DEGs were performed by the cluster Profiler R package (Yu et al., 2012).

Analysis of Gene Expression by Real-Time Quantitative RT-PCR

Total RNA was extracted from the peanut leaves of three replicates using an EASYspin plant RNA extraction kit (Aidlab Biotechnologies, Co., Ltd., China) according to the manufacturer's instructions. First-strand cDNA was synthesized from DNase

I-treated total RNA (about 1 µg) using an MMLV reverse transcriptase kit (ThermoFisher Scientific, United States). Quantitative RT-PCR (qRT-PCR) assays were performed on the Bio-Rad CFX96 RT-PCR Detection system (Bio-Rad, Hercules, CA, United States) using Hieff qPCR SYBR Green Master Mix (YEASEN, Shanghai, China). The relative transcript levels among different samples were quantified by the 2^{−ΔΔC_t} method (Livak and Schmittgen, 2001), using *A. hypogaea* Actin gene (accession number: Aradu.W2Y55) as a reference gene for normalization. The expression level of 0 h in SLH was used as a control, whose value was set to 1. The relative expression levels of other samples (including a 0-h time point in ZH12) were determined relative to the control. In this way, we can compare all samples across the two varieties within the same gene. The information of genes for qRT-PCR analysis is listed in **Supplementary Table 1**.

Weighted Gene Co-expression Network Analysis

Weighted gene co-expression network analysis (WGCNA) can be used for identifying genes with similar expression patterns that may participate in specific biological functions (Langfelder and Horvath, 2008). A total of 3,620 cold tolerance core genes were used as an input in the R package WGCNA (version 1.47) to construct weighted co-expression modules with following parameters: weighted network = unsigned, power = 10, minimum module size = 30, minimum height for merging modules = 0.25. Then, the calculated module eigen genes and Pearson's correlation coefficient values were used to determine the association of modules with the metabolite contents (soluble sugars, polyamines, amino acids, and phenols) for the 24 samples. The number of edges in a node represented the hubness of the gene. Hub genes were ranked based on the module eigengene values and edge numbers, and they often exhibit the most connections with other genes within a module. The gene networks and top 20 hub genes within a module were visualized by Cytoscape software (Shannon et al., 2003).

RESULTS

Physiological Differences Between SLH and ZH12 in Response to Cold Stress

Two peanut cultivars with differential cold tolerance (SLH and ZH12) were selected for investigating their physiological traits in response to chilling stress (Zhang et al., 2021). SLH has been characterized as a cold-tolerant germplasm, and it is popularly planted in northeast China (a relative high latitude region, 48°N–55°N) where cold weather often happens in the early sowing and harvest seasons. ZH12 (cold susceptible) is a representative variety released by Oil Crops Research Institute, Chinese Academy of Agricultural Sciences, and it is commonly planted in Hubei province, central China (a low latitude region, 29°N–33°N), which has a warm climate in the sowing and harvest season. It was found that the two cultivars showed similar germination rates

¹https://www.peanutbase.org/peanut_genome

²<https://cran.r-project.org/web/packages/pheatmap/>

under normal condition but were severely affected for ZH12 in comparison to SLH when they were exposed to low temperature (Figures 1A,B). Additionally, the levels of hydrogen peroxide (H_2O_2) and superoxide anion (O_2^-) were significantly higher in the seedlings of ZH12 than those of SLH within 24 h of cold treatment (10°C) (Figures 1C,D). It is known that ROS overproduction brings about lipid peroxidation, and the malondialdehyde (MDA) level is an important indicator for membrane damage (Jambunathan, 2010). In the current study, the leaf MDA contents in cold-treated ZH12 increased about 2-fold compared with control (0 h) and displayed higher levels than those of SLH after 48-h cold treatment (Figure 1E). The pronounced enhancement of MDA content in susceptible peanut cultivar ZH12 was presumably caused by excessive accumulation of O_2^- and H_2O_2 under chilling stress. Thus, the difference of physiological responses to low temperature confirmed that SLH was relatively stable, while ZH12 was more susceptible to cold damage.

Metabolome Profiling of Peanut in Response to Cold Stress

To investigate metabolome profiling of the two peanut genotypes exposed to low temperature, leaves were collected at the four different treatment time points (with three biological replicates per point), and further subjected to UPLC-MS for analyzing their metabolic changes. As a result, a total of 563 metabolites were successfully detected, and these could be mainly classified into different categories, including amino acids, carbohydrates, nucleosides, lipids, alkaloids, flavonoids, terpenoids, etc., (Supplementary Table 2). Principle component analysis (PCA) of metabolites profiling showed that the two cultivars were separated by PC1 (21.70%), and samples collected at different time points were separated by PC2 (15.97%) (Figure 2A). Moreover, the control and cold-treated samples were separated, indicating that low temperature had profound impacts on the compound accumulation patterns in peanut.

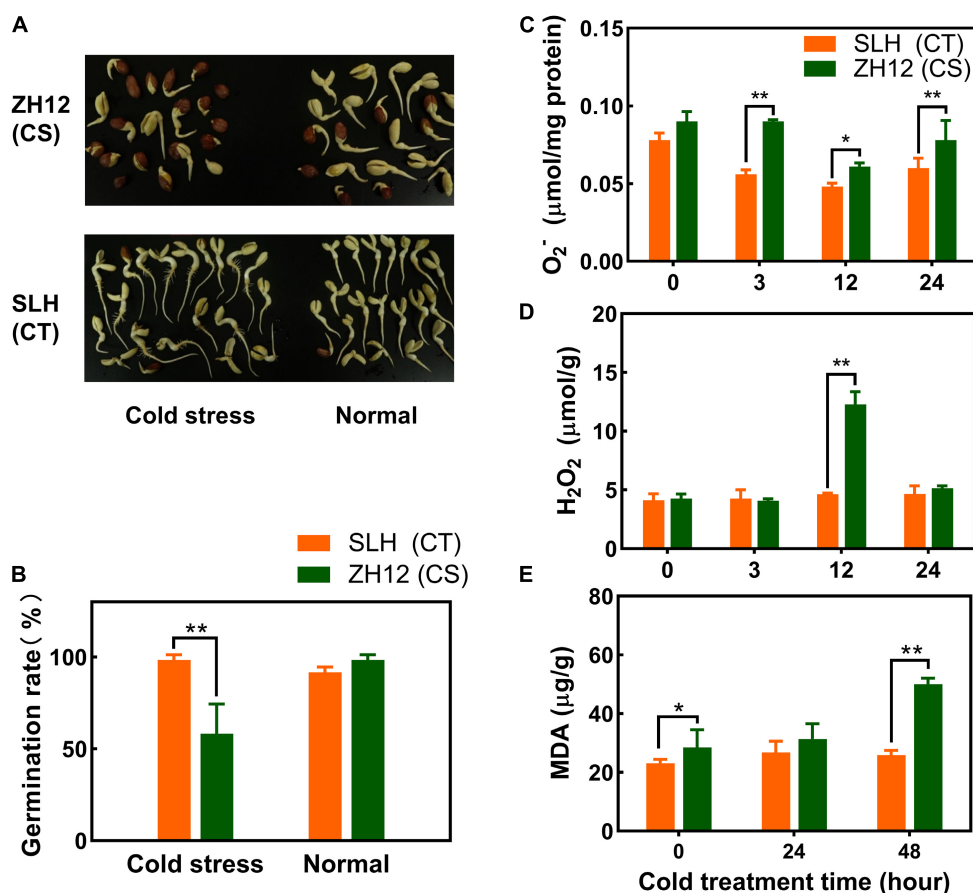


FIGURE 1 | Differential physiological responses of SLH and ZH12 peanut cultivars to cold stress. (A,B) Effects of low temperature on germination rates of the two peanut cultivars. For cold treatment, seeds were immersed in distilled water for 4 h, and then transferred to petri dishes at 2°C for 72 h in the dark, and, finally, returned to normal temperature (28°C) for additional 3 days for germination. The controls were continuously germinated at 28°C for 3 days. SLH (CT), the cold-tolerance cultivar; ZH12 (CS), the cold-susceptible cultivar. The level of O_2^- (C), H_2O_2 (D), and malondialdehyde [MDA, (E)] of peanut seedlings in response to chilling stress. Error bars represent the SD of the means of three biological replications. *An asterisk indicates significant difference between the two cultivars as determined by the Student's *T*-test (* $p < 0.05$; ** $p < 0.01$).

To identify the metabolites that contribute to cold tolerance in peanut, we performed comparative analysis of the metabolomic changes between SLH and ZH12. Using thresholds for $|\log_2(\text{fold change})| > 1$ and $P\text{-value} < 0.05$, a total of 42, 85, 63, and 56 differentially changed metabolites (DCMs) were found between the two cultivars in the four time points of cold treatment, respectively (Figure 2B and Supplementary Table 3). Altogether, we identified 145 DCMs between the two cultivars, which were mainly involved in organic acid, amino acids, nucleotides and carbohydrates (Figure 2C and Supplementary Table 4). Among the changed carbohydrates, the contents of seven sugars (e.g., raffinose, trehalose, lactose, galactinol, cellotriose, melezitose, and sucrose) were found to be significantly increased under cold stress. Moreover, it appeared that SLH exhibited at an earlier induction time point (at 24 h) and displayed more enhanced levels of the sugars compared to ZH12 in response to low temperature (Figure 2D and Supplementary Table 5). Similarly, other metabolites, such as polyamines (spermine, spermidine) and phenols (coniferin), also exhibited higher accumulation patterns in SLH than ZH12 (Figure 2E). As some soluble sugars,

polyamines and phenols were reported to be involved in plant cold response (Fuertauer et al., 2019; Alcazar et al., 2020), the differential accumulation patterns of these substances probably provided stronger cold tolerance capability in SLH.

Transcriptomic Analysis of Peanut Exposed to Cold Stress

General Description of Transcriptome Data

Total mRNA extracted from peanut leaves was subjected to construct sequencing libraries using the Illumina paired-end platform. With three biological replicates per time point, the 24 samples yielded more than 185.44 Gb high-quality data with an average Q30 score of 93.09% (Supplementary Table 6). A total of 48,374 and 46,844 unigenes were obtained from SLH and ZH12 with FPKM values > 0.1 in at least one time point, respectively (Supplementary Figures 2A,B). There were 38,741 and 37,705 transcripts expressed at all-time points in SLH and ZH12, respectively. Over 90% (45,302) of the detected transcripts were shared by the two genotypes (Supplementary Figure 2C).

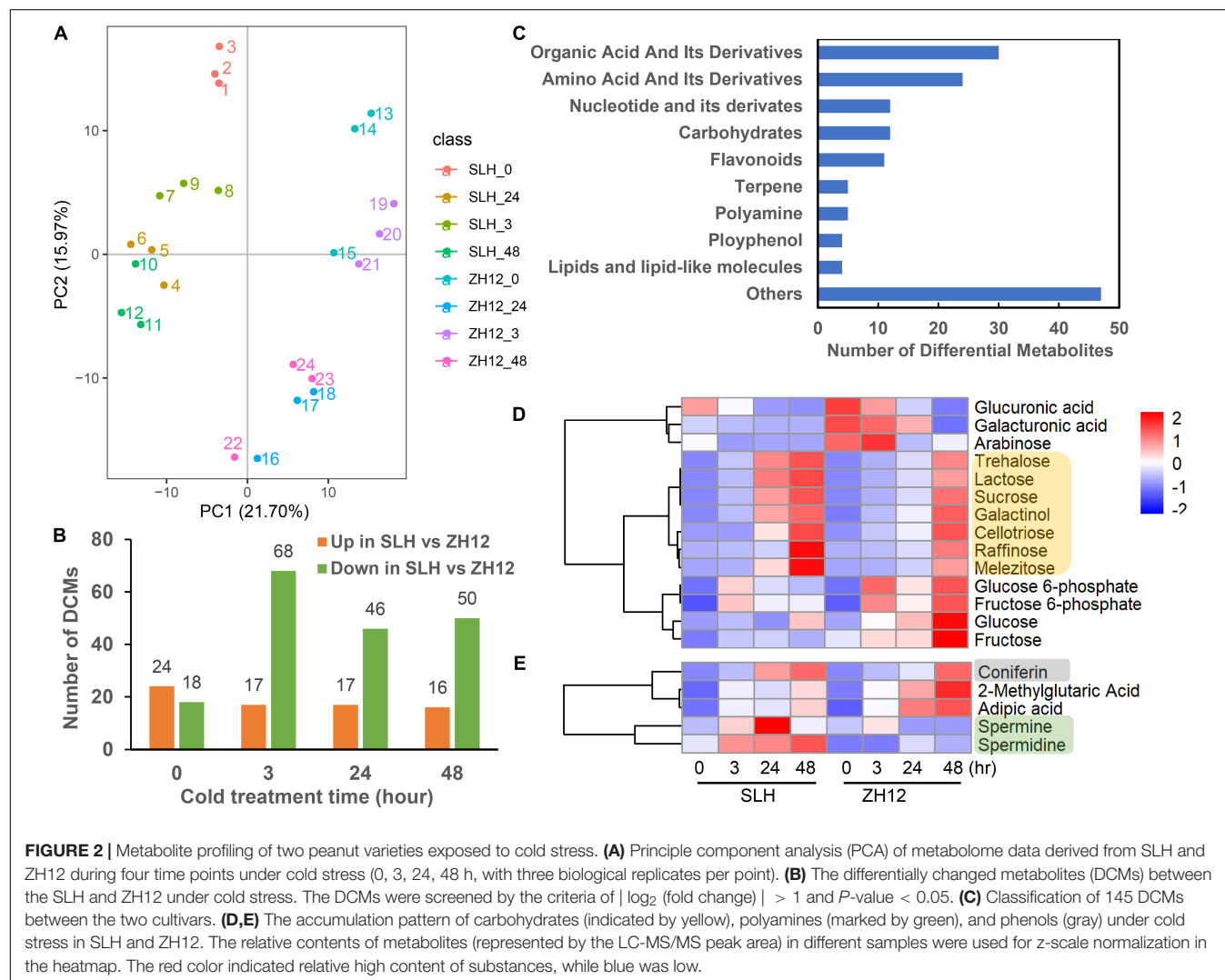


FIGURE 2 | Metabolite profiling of two peanut varieties exposed to cold stress. **(A)** Principle component analysis (PCA) of metabolome data derived from SLH and ZH12 during four time points under cold stress (0, 3, 24, 48 h, with three biological replicates per point). **(B)** The differentially changed metabolites (DCMs) between the SLH and ZH12 under cold stress. The DCMs were screened by the criteria of $|\log_2(\text{fold change})| > 1$ and $P\text{-value} < 0.05$. **(C)** Classification of 145 DCMs between the two cultivars. **(D,E)** The accumulation pattern of carbohydrates (indicated by yellow), polyamines (marked by green), and phenols (gray) under cold stress in SLH and ZH12. The relative contents of metabolites (represented by the LC-MS/MS peak area) in different samples were used for z-scale normalization in the heatmap. The red color indicated relative high content of substances, while blue was low.

Pearson correlation analysis of RNA-seq data displayed high reproducibility between biological replicates (**Supplementary Figure 3**). PCA analysis indicated that the samples from the different time points could be separated by the PC1 (41.93%), and the genotypes were separated by the PC2 (14.72%) (**Figure 3A**). Additionally, the number of cold-responsive genes in 24 or 48 h is greater than that in 3 h (**Supplementary Figure 4**). This suggested that prolonged duration of cold stress resulted in more profound changes of a transcriptome profile in peanut.

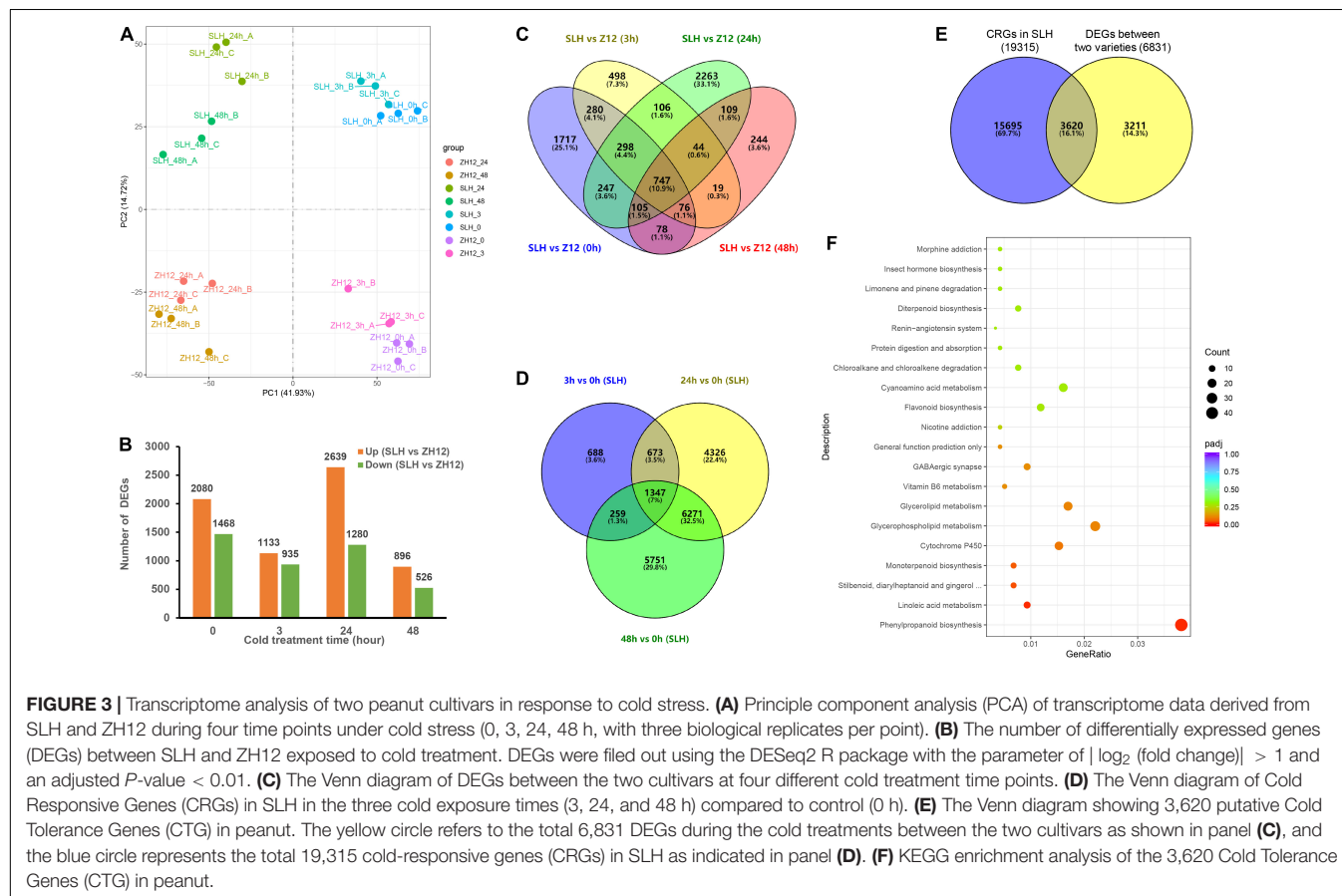
Identification of Putative Cold Tolerance Genes in Peanut

To get a deep insight into the mechanism of cold tolerance in peanut, we performed comparative analysis of the transcriptional difference between SLH and ZH12 at the four time points of cold treatment (**Figures 3B,C**). In total, 6,831 differentially expressed genes (DEGs) were found between the two contrasting cultivars (**Supplementary Table 7**). Since genes involved in cold tolerance were probably induced and/or depressed by low temperature, we identified a total of 19,315 cold-responsive genes (CRGs) in SLH by comparing the transcriptome profile in 3, 24, and 48 h with that of control (0 h) (**Figure 3D** and **Supplementary Table 8**). As a result, there were 3,620 common genes shared by DEGs between the two cultivars and cold-responsive genes in SLH (**Figure 3E**). These common genes were believed to be a putative “Cold Tolerance Gene set” (CTGs) in peanut

(**Supplementary Table 9**). Several transcription factors that were known to be involved in the regulating cold-signaling pathway were included in CTGs, such as two DREBs (Arahy.73DHNZ and Arahy.SE8WTS) and two phytochrome interacting factors (Arahy.SDDU5A and Arahy.F2RES5) (**Figure 4**). Also, some structure genes in the carbohydrate metabolism were found in CTGs, including two raffinose synthases (Arahy.UR837P and Arahy.DBZB80) and a galactinol synthase (Arahy.N6N04K). The gene expression changes of nine CTGs were analyzed by qRT-PCR. Their transcript levels were higher and/or induce a data earlier time point by cold stress in SLH (cold tolerant) than ZH12 (cold susceptible), which had a good correlation with RNA-seq results (**Figure 4** and **Supplementary Figure 5**).

Functional Enrichment Analysis of Cold Tolerance Genes in Peanut

Based on the GO enrichment analysis, the 3,620 CTGs were distributed into different known GO terms (**Supplementary Table 10** and **Supplementary Figure 6**). Among the “biological process” category, the most significantly enriched terms are “response to biotic stimulus” and “defense response.” In addition, the “metal ion transport” term included 14 genes encoding for heavy metal-associated isoprenylated plant proteins (HIPPs), which were reported to play important roles in response to biotic/abiotic stresses (Zhang et al., 2015). The top enriched GO terms in “molecular functions” were related to “transferring acyl



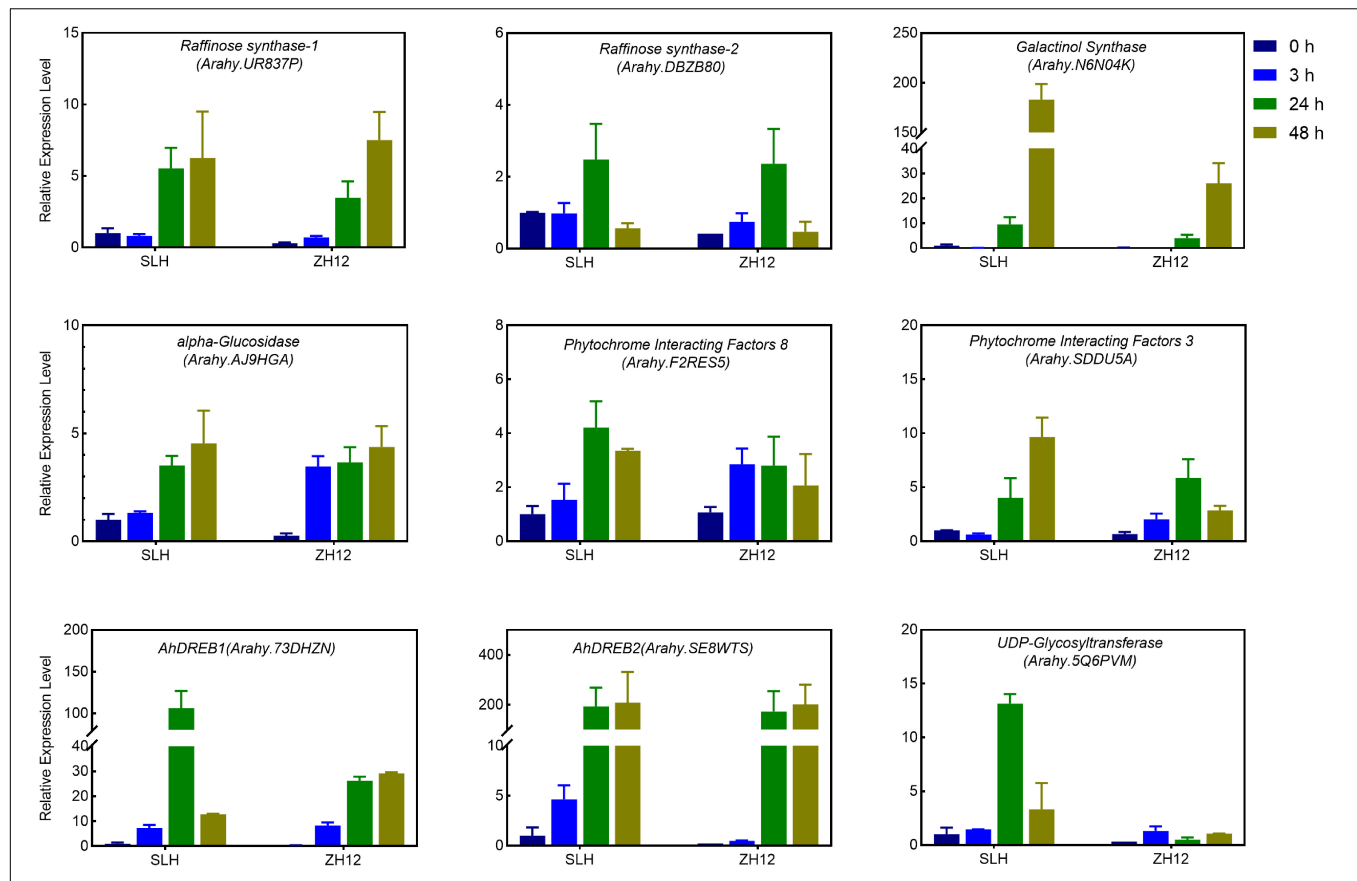


FIGURE 4 | Quantitative RT-PCR (qRT-PCR) analysis of the expression levels of selected Core Cold Tolerance Genes in the peanut seedlings subjected to cold stress. The relative transcript levels among different samples were quantified by the $2^{-\Delta\Delta C_t}$ method, with *A. hypogaea* Actin gene as the reference gene for normalization. Error bars indicate the S.D. of the means of three biological replicates.

groups” and “glycosyltransferase activity.” Of these terms, 12 genes were annotated as putative cellulose synthases involved in the biosynthesis of the hemicellulose backbone, which might be helpful to confer abiotic stress tolerance to plants (Endler et al., 2015; Huang et al., 2021; Yuan et al., 2021).

KEGG pathway enrichment analysis of CTGs showed that the top significant enriched pathways were “phenylpropanoid biosynthesis” and “linoleic acid metabolism,” and “stilbenoid, diarylheptanoid, and gingerol biosynthesis” (Figure 3F and Supplementary Table 11). As one of the major branches of the phenylpropanoid pathway, lignin biosynthetic genes were upregulated by cold stress. In addition, the “linoleic acid metabolism” pathway included 11 lipoxygenase genes that were known to be related cold acclimation in plants (Upadhyay et al., 2019). These results indicate that both lignin and lipids take a great part in response to cold stress in peanut.

Identification of Key Genes and Modules in Response to Cold Stress by Weighted Gene Co-expression Network Analysis

Weighted gene co-expression network analysis is a popular systems biology method used to not only construct gene

networks but also detect gene modules and identify the central players (i.e., hub genes) within modules. To obtain a comprehensive understanding of the molecular mechanism of cold tolerance in peanut, the 3,620 CTGs were put into the WGCNA software R package to build a gene co-expression network (Langfelder and Horvath, 2008). Based on pairwise correlations analysis of gene expression, 13 merged co-expression modules marked with different colors are shown in Figure 5A and could be further clustered into two main branches (Figure 5A and Supplementary Table 12). Analysis of the module-trait relationships for the 24 samples revealed that amino acids (Arginine and Alanine), spermidine, and two sugar compounds (raffinose and melezitose) were tightly associated with a red module ($R > 0.5$ and $p < 0.01$), while coniferin and the other three soluble sugars (trehalose, glucose, and sucrose) were more related to the tan module (Figure 5B). Based on the values of WGCNA edge weight and node scores, the top 20 hub genes were identified in the red module (Supplementary Table 13). These genes encoded some important proteins involved in abiotic stress processes, including dehydrin (araby.4JU6QM), 6-phosphogluconate dehydrogenase (6PGDH, araby.RH103U), pentatricopeptide repeat family protein (PPR, araby.97P92R), nucleoporin (araby.9L03M9), and S-adenosylmethionine

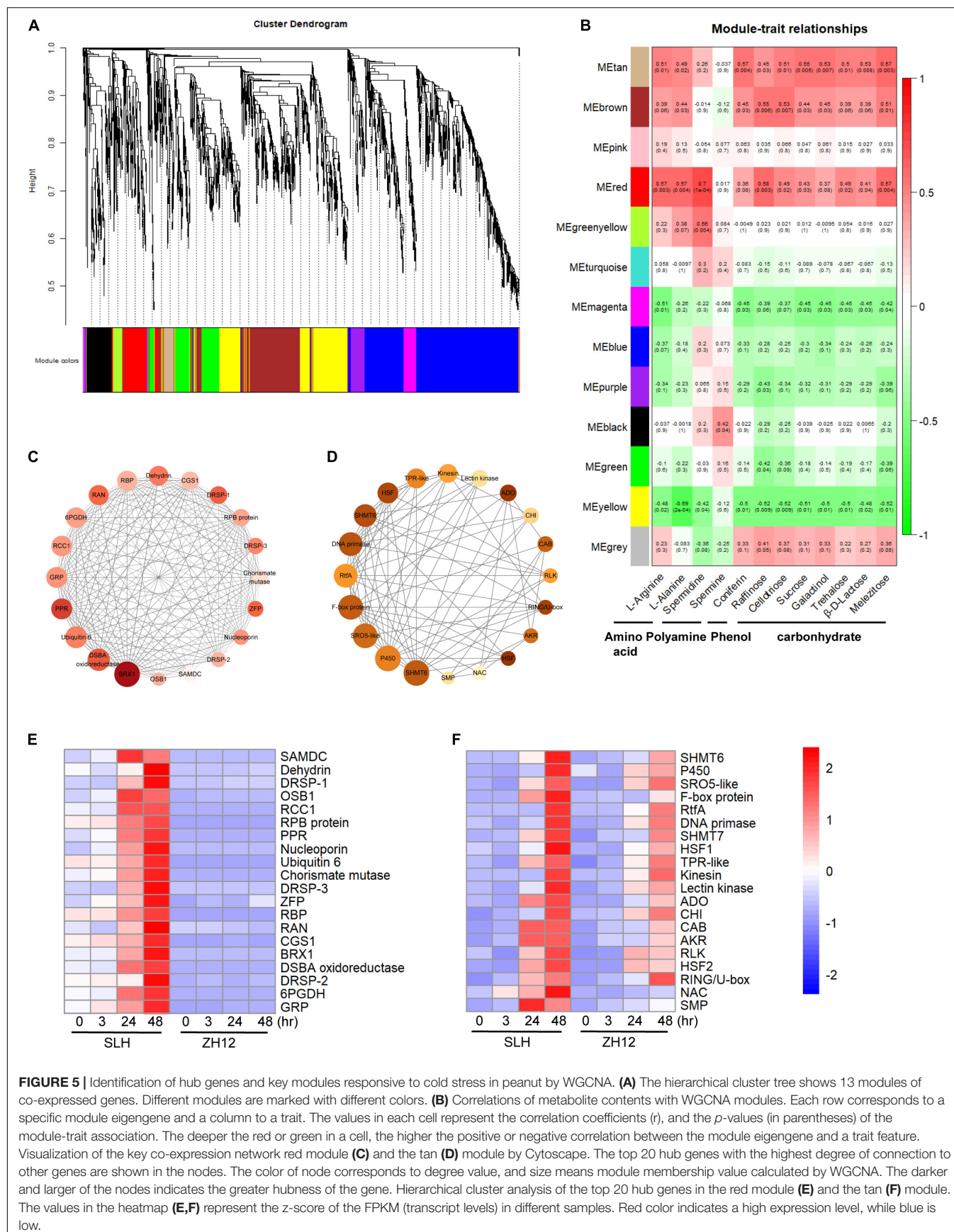


FIGURE 5 | Identification of hub genes and key modules responsive to cold stress in peanut by WGCNA. **(A)** The hierarchical cluster tree shows 13 modules of co-expressed genes. Different modules are marked with different colors. **(B)** Correlations of metabolite contents with WGCNA modules. Each row corresponds to a specific module eigengene and a column to a trait. The values in each cell represent the correlation coefficients (r), and the p -values (in parentheses) of the module-trait association. The deeper the red or green in a cell, the higher the positive or negative correlation between the module eigengene and a trait feature. Visualization of the key co-expression network red module **(C)** and the tan **(D)** module by Cytoscape. The top 20 hub genes with the highest degree of connection to other genes are shown in the nodes. The color of node corresponds to degree value, and size means module membership value calculated by WGCNA. The darker and larger of the nodes indicates the greater hubness of the gene. Hierarchical cluster analysis of the top 20 hub genes in the red module **(E)** and the tan **(F)** module. The values in the heatmap **(E,F)** represent the z-score of the FPKM (transcript levels) in different samples. Red color indicates a high expression level, while blue is low.

decarboxylase (SAMDC, arahy.0034KJ) and GTP-binding nuclear protein (Ran, arahy.G34P0I) (**Figure 5C**). For the tan module, the top 20 genes encoded transcription factors (such as heat shock transcription factor and NAC-domain protein) and several stress-related proteins/enzymes, including cytochrome P450 (P450, arahy.MG688V), serine hydroxy-methyltransferase 6 (SHMT6, arahy. HK9TK1), F-box protein (arahy.C9YQVF), and SRO5 (arahy.7WJT5G) (**Figure 5D** and **Supplementary Table 13**). Notably, the transcript levels of hub genes in both of the modules were remarkably upregulated in SLH but were hardly expressed or only slightly enhanced in ZH12 at a late treatment point (48 h) (**Figures 5E,F**).

Integrated Metabolome and Transcriptome Analysis to Reveal Crucial Pathways Responsive to Cold Stress

An integrated analysis of transcriptome and metabolome data revealed some common enriched pathways, including “carbohydrates metabolism” and “polyamines metabolism.” For carbohydrates metabolism, most of raffinose family oligosaccharides (RFOs) and sucrose-related metabolites, such as galactinol, raffinose, melibiose, and trehalose, were markedly increased in the two genotypes under cold stress. It should be noted that the fold changes of sugar compounds were consistently higher in cold-tolerant (SLH) than in cold-susceptible genotypes (ZH12), suggesting their vital roles in protection of peanut against low temperature stress (**Figures 2C, 6A**). Accordingly, the transcriptional profile of most genes involved in sugar biosynthetic pathways correlated well with the accumulation pattern in the two cultivars exposed to cold stress (**Figures 2D, 6B**). For instance, four genes-encoding galactinol synthases (EC 2.4.1.123, which catalyze the key steps for galactinol synthesis (Sengupta et al., 2015; Shimosaka and Ozawa, 2015), were greatly upregulated in SLH, but their transcripts were not changed or only slightly upregulated under cold stress in ZH12. Raffinose synthase, also called as galactinol-sucrose galactosyltransferase (EC 2.4.1.82), was a rate-limiting enzyme in biosynthesis of raffinose (ElSayed et al., 2014). Interestingly, expression levels of all the six raffinose synthase were strong cold induced in SLH, while moderately enhanced in ZH12. Besides, most of the genes involved in the biosynthesis pathways of sucrose, melibiose, and trehalose were upregulated in both genotypes in response to low temperature, but their expression levels increased more significantly in SLH than in ZH12. These results suggested that the cold tolerance of SLH might be associated with its stronger ability to regulate carbohydrates metabolism, thus leading to a higher accumulation of sucrose, raffinose, and trehalose in SLH than in cold-susceptible genotype (ZH12).

Polyamines, including putrescine, spermidine, and spermine, are aliphatic nitrogen substances with low molecular weight and polycation characteristics, which have important roles in improving abiotic stress tolerance, including low-temperature tolerance (Alcazar et al., 2011). Several key enzyme genes involved in the “spermidine biosynthetic process,” including spermidine synthase (E.C. 2.5.1.16) and spermine synthase

(E.C. 2.5.1.22), were found to be upregulated in response to cold stress (**Figures 6C,D**). This was in accordance with the accumulation pattern of polyamines in both peanut cultivars. Moreover, as compared with susceptible peanut (ZH12), the cold-tolerant one (SLH) had higher cellular levels of spermidine and spermine, suggesting it has a larger capacity to enhance polyamine biosynthesis under low temperature.

It has been reported that lignin serves as one of the major contributors to abiotic stress resistance (Cesarino, 2019). Coniferin, the glucoside of coniferyl alcohol, was considered as the most possible storage form of monolignol for G-lignin biosynthesis, which helps plants to fight against several abiotic stresses (Tsuiji et al., 2005; Sharma et al., 2019). In this study, cold stress greatly increased coniferin contents in the peanut seedlings (**Figures 2E, 6E**). Accordingly, several genes in the general phenylpropanoid pathway and downstream G-lignin biosynthesis were significantly upregulated, including two phenylalanine ammonia lyases (PALs, the entry enzyme for phenylpropanoids), four 4-coumarate-CoA ligases (4CLs), two caffeic acid 3-O-methyltransferases (COMTs), and one caffeoyl-CoA 3-O-methyltransferase (CCoAOMT) (**Figure 6F** and **Supplementary Table 12**). However, the transcript levels of these genes showed a differential expression pattern between the two cultivars. For instance, two PALs and one COMT gene had significant higher transcript levels in SLH than in ZH12, while the expression levels of four 4CLs, two hydroxycinnamoyltransferases (HCTs), and aCCoAOMT gene were higher in ZH12 compared to SLH after 24-h cold treatment (**Figure 6F**).

DISCUSSION

Cold weather accounts for serious reductions in crop yield every year, since many agriculturally important crops, including rice (*Oryza sativa*) and peanut, are chilling sensitive and can only be cultivated in tropical or subtropical regions (Wu et al., 2020). Despite the molecular mechanisms of cold-induced reprogramming of gene expression and the metabolite accumulation pattern were extensively studied in model plants (Hoermiller et al., 2016; Jin et al., 2017; Pagter et al., 2017; Dasgupta et al., 2020), only a handful of reports were related to peanut (Jiang et al., 2020; Wu et al., 2020; Zhang H. et al., 2020). In this study, we attempted to decipher the regulatory mechanisms of peanut in response to cold stress through combining transcriptome with metabolome analysis.

Analysis of Signal Transduction and Protein Kinases in Response to Cold Stress

Ca²⁺ is an important signaling messenger in response to cold stress (Yuan et al., 2018). The calmodulins (CAMs) and calcium-dependent protein kinases (CDPKs) are vital calcium sensors and could transduce cold signals to activate the expression of downstream cold-response gene (*CORs*), including *DREBs/CBFs* and other components (Yang et al., 2010; Zeng et al., 2015). Overexpression of a salt-induced peanut CDPK

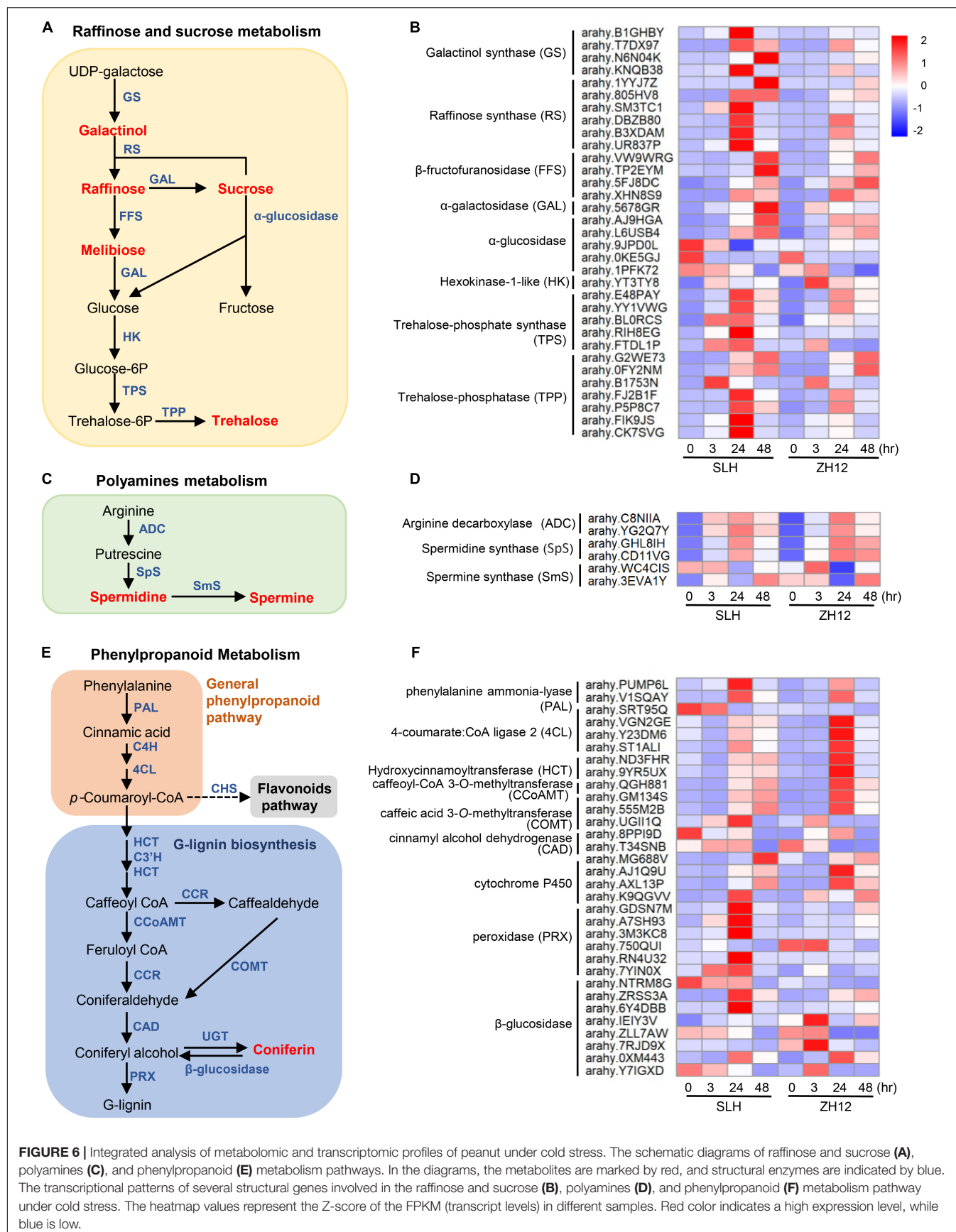


FIGURE 6 | Integrated analysis of metabolomic and transcriptomic profiles of peanut under cold stress. The schematic diagrams of raffinose and sucrose (A), polyamines (C), and phenylpropanoid (E) metabolism pathways. In the diagrams, the metabolites are marked by red, and structural enzymes are indicated by blue. The transcriptional patterns of several structural genes involved in the raffinose and sucrose (B), polyamines (D), and phenylpropanoid (F) metabolism pathway under cold stress. The heatmap values represent the Z-score of the FPKM (transcript levels) in different samples. Red color indicates a high expression level, while blue is low.

gene in tobacco could alleviate PSII photoinhibition under abiotic stress, suggesting it played an important role in stress tolerance in peanut (Li et al., 2015). In the current study, the transcription of three calmodulin-binding proteins (CBPs, Arahy.1Y8NUF, Arahy.R2NPVK, and Arahy.GM51F1) and four CDPKs (Arahy.706LQI, Arahy.D2QNFF, Arahy.D2U3E6, and Arahy.P2RW1V) were significantly induced by low temperature (Supplementary Figures 7A,B and Supplementary Table 14) and have a relative higher transcript abundance in SLH (cold tolerant) than ZH12. Also, a total of 17 CBF transcripts were identified in our RNA-seq database (Supplementary Table 15). Among them, seven CBFs were not expressed at any time points in both of the varieties, while most of the other transcripts were increased in response to cold treatment (Supplementary Figure 7). It should be noted that some of the upregulated CBFs (arahy.73DHZN, arahy.WP3ECB, and arahy.5KI8FH) were induced at an earlier time point and/or have relative higher expression levels in cold tolerance variety (SLH) than that in cold susceptible (ZH12) (Figure 4 and Supplementary Figure 7), implying their significance in cold-signal perception and transduction processes in peanut.

In the present study, the transcript expression of two Heat Shock transcription Factors (HSFs) (Arahy.8U41WB and Arahy.W19Z82) was induced by cold stress in both cultivars (Figure 5F), and their transcript levels exhibited much higher in the cold-tolerant (SLH) than susceptible cultivar (ZH12) at 24- or 48-h treatment. Plant HSFs are encoded by large gene families with variable structure, expression, and function. They control responses not only to high temperatures but also to a number of abiotic stresses, such as cold, drought, and salt stress (Andrási et al., 2021). Some reports have shown that transcript abundances of HSF (*HSFA4A*, *HSFA6B*, *HSFA8*, and *HSFC1*) were enhanced by cold stress in *Arabidopsis*, while the induction effect was reduced in the *ice1* mutant, implicating HSFs were involved in the cold-acclimation pathway (Swindell et al., 2007; Olate et al., 2018). In addition, overexpression of HSFs can stimulate the synthesis of protective metabolites, such as galactinol and raffinose, to improve abiotic stress tolerance in plants (Nishizawa et al., 2006; Lang et al., 2017). Therefore, it was proposed that the relative higher transcript levels of HSFs in SLH could be more beneficial for it to cope with cold stress.

Carbohydrate Metabolism Contributes Greatly to Cold Tolerance in Peanut

Carbohydrates are the primary products of photosynthesis. They act as nutrients as well important regulators that are required for plant growth, energy metabolism, and stress responses (Fuertauer et al., 2019). It was known that soluble sugars can not only function as osmoprotectants (Zuther et al., 2004; Lunn et al., 2014; Ma et al., 2021) but also to be ROS scavengers to provide cold tolerance in plants (Smirnoff and Cumbes, 1989; Van den Ende, 2013; Matros et al., 2015). In our study, the concentrations of soluble sugars (e.g., sucrose, trehalose, and raffinose) greatly raised in the two peanut cultivars exposed to cold stress. Notably, their contents were higher and/or induced at an earlier time point in cold-resistant peanut (SLH)

than those in susceptible cultivar (ZH12) (Figure 2D). It has been reported that chilling stress could lead to a significant increase in H₂O₂ concentration in peanut (Wu et al., 2020). Similarly, we found that low temperature caused a sudden increase in the H₂O₂ in ZH12 rather than in SLH after 12-h treatment. Thus, it was proposed that the higher accumulation of soluble sugars probably led to maintain a low level of ROS in the cold-tolerant cultivar (SLH), which facilitated to its relative stronger cold-tolerance ability than the susceptible one (ZH12). On the other hand, ROS (including O₂⁻ and H₂O₂) can be detoxified by enzymatic and non-enzymatic antioxidant systems to maintain them at non-toxic levels in a delicate balancing state. In our transcriptome data, the transcript levels of several antioxidant enzymes (including superoxide dismutase and peroxidase) were enhanced in ZH12 (and also in SLH) during the early cold treatment period (3 and 24 h) (Supplementary Figures 7D,E). Thereby, we hypothesize that the upregulation of these antioxidant enzymes might efficiently scavenge the excess H₂O₂, rendering it recovered to the normal level (0 h) in 24 h.

In addition, the accumulation patterns of raffinose and sucrose between the two cultivars correlated well with expression profiles of their structural enzyme genes in the pathway (Figures 2D,E, 6A,B). Several studies have highlighted the role of these genes in cold stress (Lunn et al., 2014; Sengupta et al., 2015). For instance, overexpression of cold-inducible wheat galactinol synthase increased levels of galactinol and raffinose, and conferred higher tolerance to chilling stress in transgenic rice (Shimosaka and Ozawa, 2015). Simultaneously, exogenous application of sucrose improved chilling tolerance in cucumber seedlings by increasing antioxidant enzyme activity, and enhanced proline and soluble sugar contents. These results indicated that genes and metabolites involved in carbohydrate metabolism contributed much to cold tolerance in peanut.

Polyamine Metabolism Plays Central Roles in Cold Resistance in Peanut

Several studies have shown that the levels of polyamine were substantially elevated in plants exposed to stressful conditions, including drought, salinity, chilling, and heat (Chen et al., 2019). The improvement of cold-stress tolerance could be achieved by exogenous application of polyamines or genetic manipulation of endogenous polyamine levels (Kou et al., 2018; Alcazar et al., 2020). In the present study, spermine and spermidine were specifically accumulated in SLH (cold resistant) under chilling stress. Meanwhile, transcriptomic and WGCNA analysis showed that several transcripts and/or hub genes in polyamines biosynthesis have a relatively higher level in SLH than ZH12. For instance, S-adenosylmethionine decarboxylase (SAMDC, arahy.0034KJ), a key enzyme in the polyamine biosynthetic process, was identified as one of the hub genes in the red module (Figures 5C,E). It has been reported that overexpression of a bermudagrass SAMDC (*CdSAMDC1*) gene in tobacco enhanced plant cold tolerance through involvement of H₂O₂ and NO signaling (Luo et al., 2017). Like the transcriptional patterns of other hub genes in this module, the expression

level of SAMDC was increased upon prolonged cold stress in SLH, but was not induced in ZH12 samples. These results suggested polyamine metabolism played crucial roles in cold resistance in peanut.

G-Lignin Biosynthesis Is Involved in Cold-Stress Response

Phenylpropanoid biosynthesis is one of the most important metabolisms in plants, generating an enormous array of secondary metabolites, such as lignin and flavonoid (Dong and Lin, 2021). Recent studies have revealed that cold stress induced the expression of structural genes in the phenylpropanoid pathway, including chalcone synthase (CHS) and 4-coumarate-CoA ligase (4CL), and, as a consequence, flavonoids and lignin accumulated to facilitate the adaptation to low-temperature environments in *A. thaliana* (Catalá et al., 2011), loquat fruit (*Eriobotrya japonica*) (Zhang J. et al., 2020), and apple (*M. domestica*) (An et al., 2020). In the current study, we found that some cold-responsive genes involved in the common phenylpropanoid metabolism and downstream G-lignin biosynthesis showed higher expression levels in cold-tolerant cultivar (SLH) than those in ZH12 (Figure 6F). For instance, PAL is the rate-limiting enzyme that catalyzes the deamination of L-phenylalanine to *trans*-cinnamate and forms the entry point into the synthesis of all phenylpropanoids. The higher transcript level of two PALs in SLH compared with those in ZH12 could drive more carbon flux into the phenylpropanoid pathway, probably leading to more coniferin accumulation and better cold tolerance in SLH.

CONCLUSION

In the present study, combining metabolomic and transcriptomic analysis of peanut seedlings exposed to chilling stress identified a set of important cold-responsive genes and metabolites, some of which showed differential expressions and/or accumulation patterns between the two cultivars. The signaling molecule Ca^{2+} and its related components first sense the cold stress, and then activate downstream pathways. During the adaptation of peanut to low temperature, soluble sugars, polyamines, and G-lignin might be the significant contributors. These results facilitate a better understanding of the molecular mechanism of cold response in peanut and could be helpful to genetic improvement of cold tolerance of crops. So far, we have heterogeneously overexpressed several peanut cold-tolerance-related genes in *Arabidopsis*, and obtained some transgenic lines. We are now analyzing their phenotypes under normal and stressful conditions. However, this part has not been finished yet. We hope to take a deep insight into the phenotypic characterization of transgenic *Arabidopsis* lines. It will be more profound if we get the relevant positive phenotypic results in the future.

DATA AVAILABILITY STATEMENT

The original contributions presented in the study are publicly available. This data can be found here: National Center for Biotechnology Information (NCBI) BioProject database under accession number PRJNA751249.

AUTHOR CONTRIBUTIONS

XW, YuL, ZH, YC, DH, YK, and ZW conducted the experiments. YoL and BL organized and supervised the overall project. XW, LY, and HJ performed the data analysis and wrote the manuscript. BL edited the manuscript. All authors contributed to the article and approved the submitted version.

FUNDING

This study was funded by the National Key Research and Development Project of China (No. 2018YFD1000900).

SUPPLEMENTARY MATERIAL

The Supplementary Material for this article can be found online at: <https://www.frontiersin.org/articles/10.3389/fpls.2021.752474/full#supplementary-material>

Supplementary Table 1 | qRT-PCR primers in this study.

Supplementary Table 2 | A list of metabolites detected in the samples.

Supplementary Table 3 | The list of differential changed metabolites between the two peanut varieties under cold stress.

Supplementary Table 4 | Classification of differential changed metabolites between two peanut cultivars under cold stress.

Supplementary Table 5 | The accumulation pattern of metabolites during cold stress in peanut.

Supplementary Table 6 | Statistical analyses and mapping results of RNA sequencing reads.

Supplementary Table 7 | Differentially expressed genes between cold-tolerant and cold-susceptible cultivars.

Supplementary Table 8 | A list of cold-responsive genes in SLH and ZH12 peanut.

Supplementary Table 9 | The detail information of 3,620 cold-tolerance genes.

Supplementary Table 10 | GO enrichment analysis cold-tolerance genes.

Supplementary Table 11 | KEGG pathway enrichment analysis of cold tolerance genes.

Supplementary Table 12 | A gene list of WGCNA modules.

Supplementary Table 13 | The top 20 hub genes in red and tan modules.

Supplementary Table 14 | The transcription levels of antioxidative genes and calcium signal genes in the two cultivars under cold stress.

Supplementary Table 15 | The transcription levels of CBF genes in the two cultivars under cold stress.

REFERENCES

- Alcazar, R., Bueno, M., and Tiburcio, A. F. (2020). Polyamines: small amines with large effects on plant abiotic stress tolerance. *Cells* 9:2373. doi: 10.3390/cells9112373
- Alcazar, R., Cuevas, J. C., Planas, J., Zarza, X., Bortolotti, C., Carrasco, P., et al. (2011). Integration of polyamines in the cold acclimation response. *Plant Sci.* 180, 31–38. doi: 10.1016/j.plantsci.2010.07.022
- An, J. P., Wang, X. F., Zhang, X. W., Xu, H. F., and Hao, Y. J. (2020). An apple MYB transcription factor regulates cold tolerance and anthocyanin accumulation and undergoes MIEL1-mediated degradation. *Plant Biotechnol. J.* 18, 337–353.
- Andrási, N., Pettkó-Szandtner, A., and Szabados, L. (2021). Diversity of plant heat shock factors: regulation, interactions and functions. *J. Exp. Bot.* 72, 1558–1575. doi: 10.1093/jxb/eraa576
- Bell, M. J., Gillespie, T. J., Roy, R. C., Micheals, T. E., and Tollenaar, M. (1994). Peanut leaf photosynthetic activity in cool field environments. *Crop Sci.* 34, 1023–1029. doi: 10.2135/cropsci1994.0011183X003400040035x
- Catalá, R., Medina, J., and Salinas, J. (2011). Integration of low temperature and light signaling during cold acclimation response in *Arabidopsis*. *Proc. Natl. Acad. Sci. U.S.A.* 108, 16475–16480. doi: 10.1073/pnas.1107161108
- Cesarino, I. (2019). Structural features and regulation of lignin deposited upon biotic and abiotic stresses. *Curr. Opin. Biotechnol.* 56, 209–214. doi: 10.1016/j.copbio.2018.12.012
- Chen, D., Shao, Q., Yin, L., Younis, A., and Zheng, B. (2019). Polyamine function in plants: metabolism, regulation on development, and roles in abiotic stress responses. *Front. Plant Sci.* 9:1945. doi: 10.3389/fpls.2018.01945
- Chen, N., Yang, Q., Hu, D., Pan, L., Chi, X., Chen, M., et al. (2014). Gene expression profiling and identification of resistance genes to low temperature in leaves of peanut (*Arachis hypogaea* L.). *Sci. Hortic.* 169, 214–225. doi: 10.1016/j.scienta.2014.01.043
- Chinnusamy, V., Ohta, M., Kanrar, S., Lee, B. H., Hong, X. H., Agarwal, M., et al. (2003). ICE1: a regulator of cold-induced transcriptome and freezing tolerance in *Arabidopsis*. *Genes Dev.* 17, 1043–1054. doi: 10.1101/gad.1077503
- Cui, P., Li, Y., Cui, C., Huo, Y., Lu, G., and Yang, H. (2020). Proteomic and metabolic profile analysis of low-temperature storage responses in *Ipomoea batata* Lam. Tuberous roots. *BMC Plant Biol.* 20:435. doi: 10.1186/s12870-020-02642-7
- Dasgupta, P., Das, A., Datta, S., Banerjee, I., Tripathy, S., and Chaudhuri, S. (2020). Understanding the early cold response mechanism in IR64 indica rice variety through comparative transcriptome analysis. *BMC Genomics* 21:425. doi: 10.1186/s12864-020-06841-2
- Ding, Y. L., Shi, Y. T., and Yang, S. H. (2020). Molecular regulation of plant responses to environmental temperatures. *Mol. Plant* 13, 544–564. doi: 10.1016/j.molp.2020.02.004
- Dong, C. N., Danyluk, J., Wilson, K. E., Pocock, T., Huner, N. P. A., and Sarhan, F. (2002). Cold-regulated cereal chloroplast late embryogenesis abundant-like proteins. Molecular characterization and functional analyses. *Plant Physiol.* 129, 1368–1381. doi: 10.1104/pp.001925
- Dong, N. Q., and Lin, H. X. (2021). Contribution of phenylpropanoid metabolism to plant development and plant-environment interactions. *J. Integr. Plant Biol.* 63, 180–209. doi: 10.1111/jipb.13054
- Du, S., Cui, M., Cai, Y., Xue, A., Hao, Y., Huang, X., et al. (2020). Metabolomic analysis of chilling response in rice (*Oryza sativa* L.) seedlings by extractive electrospray ionization mass spectrometry. *Environ. Exp. Bot.* 180:104231. doi: 10.1016/j.envexpbot.2020.104231
- ElSayed, A. I., Rafudeen, M. S., and Golldack, D. (2014). Physiological aspects of raffinose family oligosaccharides in plants: protection against abiotic stress. *Plant Biol.* 16, 1–8. doi: 10.1111/plb.12053
- Endler, A., Kesten, C., Schneider, R., Zhang, Y., Ivakov, A., Froehlich, A., et al. (2015). A mechanism for sustained cellulose synthesis during salt stress. *Cell* 162, 1353–1364. doi: 10.1016/j.cell.2015.08.028
- Fuertauer, L., Weiszmann, J., Weckwerth, W., and Naegele, T. (2019). Dynamics of plant metabolism during cold acclimation. *Int. J. Mol. Sci.* 20:5411. doi: 10.3390/ijms20215411
- Hoermiller, I., Naegele, T., Augustin, H., Stutz, S., Weckwerth, W., and Heyer, A. (2016). Subcellular reprogramming of metabolism during cold acclimation in *Arabidopsis thaliana*. *Plant Cell Environ.* 40, 602–610. doi: 10.1111/pce.12836
- Huang, T., Luo, X., Fan, Z., Yang, Y., and Wan, W. (2021). Genome-wide identification and analysis of the sucrose synthase gene family in cassava (*Manihot esculenta* Crantz). *Gene* 769:145191. doi: 10.1016/j.gene.2020.145191
- Jambunathan, N. (2010). Determination and detection of reactive oxygen species (ROS), lipid peroxidation, and electrolyte leakage in plants. *Methods Mol. Biol.* 639, 292–298. doi: 10.1007/978-1-60761-702-0_18
- Jiang, C. J., Zhang, H., Ren, J. Y., Dong, J. L., Zhao, X. H., Wang, X. G., et al. (2020). Comparative transcriptome-based mining and expression profiling of transcription factors related to cold tolerance in peanut. *Int. J. Mol. Sci.* 21:1921. doi: 10.3390/ijms21061921
- Jiang, J., Hou, R., Yang, N., Li, L., Deng, J., Qin, G., et al. (2021). Physiological and TMT-labeled proteomic analyses reveal important roles of sugar and secondary metabolism in *Citrus junos* under cold stress. *J. Proteomics* 237:104145. doi: 10.1016/j.jpro.2021.104145
- Jin, J. J., Zhang, H., Zhang, J. F., Liu, P. P., Chen, X., Li, Z. F., et al. (2017). Integrated transcriptomics and metabolomics analysis to characterize cold stress responses in *Nicotiana tabacum*. *BMC Genomics* 18:496. doi: 10.1186/s12864-017-3871-7
- Kakani, V. G., Prasad, P., Craufurd, P. Q., and Wheeler, T. R. (2002). Response of in vitro pollen germination and pollen tube growth of groundnut (*Arachis hypogaea* L.) genotypes to temperature. *Plant Cell Environ.* 25, 1651–1661. doi: 10.1046/j.1365-3040.2002.00943.x
- Kim, D., Paggi, J. M., Park, C., Bennett, C., and Salzberg, S. L. (2019). Graph-based genome alignment and genotyping with HISAT2 and HISAT-genotype. *Nat. Biotechnol.* 37, 907–915. doi: 10.1038/s41587-019-0201-4
- Kim, Y. S., Lee, M., Lee, J.-H., Lee, H.-J., and Park, C.-M. (2015). The unified ICE-CBF pathway provides a transcriptional feedback control of freezing tolerance during cold acclimation in *Arabidopsis*. *Plant Mol. Biol.* 89, 187–201. doi: 10.1007/s11103-015-0365-3
- Kou, S., Chen, L., Tu, W., Scossa, F., Wang, Y., Liu, J., et al. (2018). The arginine decarboxylase gene ADC1, associated to the putrescine pathway, plays an important role in potato cold-acclimated freezing tolerance as revealed by transcriptome and metabolome analyses. *Plant J.* 96, 1283–1298. doi: 10.1111/tj.14126
- Lang, S., Liu, X., Xue, H., Li, X., and Wang, X. (2017). Functional characterization of BnHSFA4a as a heat shock transcription factor in controlling the re-establishment of desiccation tolerance in seeds. *J. Exp. Bot.* 68, 2361–2375. doi: 10.1093/jxb/erx097
- Langfelder, P., and Horvath, S. (2008). WGCNA: an R package for weighted correlation network analysis. *BMC Bioinformatics* 9:559. doi: 10.1186/1471-2105-9-559
- Lee, B. H., Henderson, D. A., and Zhu, J. K. (2005). The *Arabidopsis* cold-responsive transcriptome and its regulation by ICE1. *Plant Cell* 17, 3155–3175. doi: 10.1105/tpc.105.035568
- Li, M., Sui, N., Lin, L., Yang, Z., and Zhang, Y. H. (2019). Transcriptomic profiling revealed genes involved in response to cold stress in maize. *Funct. Plant Biol.* 46, 830–844. doi: 10.1071/fp19065
- Li, Y., Fang, F., Guo, F., Meng, J.-J., Li, X.-G., Xia, G.-M., et al. (2015). Isolation and functional characterisation of CDPKs gene from *Arachis hypogaea* under salt stress. *Funct. Plant Biol.* 42, 274–283. doi: 10.1071/fp14190
- Liao, Y., Smyth, G. K., and Shi, W. (2014). FeatureCounts: an efficient general purpose program for assigning sequence reads to genomic features. *Bioinformatics* 30, 923–930. doi: 10.1093/bioinformatics/btt656
- Livak, K. J., and Schmittgen, T. D. (2001). Analysis of relative gene expression data using real-time quantitative PCR and the $2^{-\Delta\Delta CT}$ method. *Methods* 25, 402–408. doi: 10.1006/meth.2001.1262
- Love, M. I., Huber, W., and Anders, S. (2014). Moderated estimation of fold change and dispersion for RNA-seq data with DESeq2. *Genome Biol.* 15:550. doi: 10.1186/s13059-014-0550-8

- Lunn, J. E., Delorge, I., Figueroa, C. M., Van Dijck, P., and Stitt, M. (2014). Trehalose metabolism in plants. *Plant J.* 79, 544–567. doi: 10.1111/tpj.12509
- Luo, J., Liu, M., Zhang, C., Zhang, P., Chen, J., Guo, Z., et al. (2017). Transgenic centipedegrass (*Eremochloa ophiuroides* [Munro] Hack.) overexpressing S-adenosylmethionine decarboxylase (SAMDC) gene for improved cold tolerance through involvement of H₂O₂ and no signaling. *Front. Plant Sci.* 8:1655. doi: 10.3389/fpls.2017.01655
- Ma, S., Lv, J., Li, X., Ji, T., Zhang, Z., and Gao, L. (2021). Galactinol synthase gene 4 (*CsGolS4*) increases cold and drought tolerance in *Cucumis sativus* L. by inducing RFO accumulation and ROS scavenging. *Environ. Exp. Bot.* 185:104406. doi: 10.1016/j.envexpbot.2021.104406
- Ma, Y., Zhang, Y., Lu, J., and Shao, H. (2009). Roles of plant soluble sugars and their responses to plant cold stress. *Afr. J. Biotechnol.* 8, 2004–2010.
- Matros, A., Peshev, D., Peukert, M., Mock, H. P., and Van den Ende, W. (2015). Sugars as hydroxyl radical scavengers: proof-of-concept by studying the fate of sucralose in *Arabidopsis*. *Plant J.* 82, 822–839. doi: 10.1111/tpj.12853
- Mehmood, S. S., Lu, G., Luo, D., Hussain, M. A., Raza, A., Zafar, Z., et al. (2021). Integrated analysis of transcriptomics and proteomics provides insights into the molecular regulation of cold response in *Brassica napus*. *Environ. Exp. Bot.* 187:104480. doi: 10.1016/j.envexpbot.2021.104480
- Nishizawa, A., Yabuta, Y., Yoshida, E., Maruta, T., Yoshimura, K., and Shigeoka, S. (2006). *Arabidopsis* heat shock transcription factor A2 as a key regulator in response to several types of environmental stress. *Plant J.* 48, 535–547. doi: 10.1111/j.1365-3113X.2006.02889.x
- Olate, E., Jiménez-Gómez, J. M., Holuigue, L., and Salinas, J. (2018). NPR1 mediates a novel regulatory pathway in cold acclimation by interacting with HSF1 factors. *Nat. Plants* 4, 811–823. doi: 10.1038/s41477-018-0254-2
- Pagter, M., Alpers, J., Erban, A., Kopka, J., Zuther, E., and Hinch, D. (2017). Rapid transcriptional and metabolic regulation of the deacclimation process in cold acclimated *Arabidopsis thaliana*. *BMC Genomics* 18:731. doi: 10.1186/s12864-017-4126-3
- Pan, Y., Liang, H., Gao, L., Dai, G., Chen, W., Yang, X., et al. (2020). Transcriptomic profiling of germinating seeds under cold stress and characterization of the cold-tolerant gene LTG5 in rice. *BMC Plant Biol.* 20:371. doi: 10.1186/s12870-020-02569-z
- Sengupta, S., Mukherjee, S., Basak, P., and Majumder, A. L. (2015). Significance of galactinol and raffinose family oligosaccharide synthesis in plants. *Front. Plant Sci.* 6:656. doi: 10.3389/fpls.2015.00656
- Shannon, P., Markiel, A., Ozier, O., Baliga, N. S., Wang, J. T., Ramage, D., et al. (2003). Cytoscape: a software environment for integrated models of biomolecular interaction networks. *Genome Res.* 13, 2498–2504. doi: 10.1101/gr.1239303
- Sharma, A., Shahzad, B., Rehman, A., Bhardwaj, R., Landi, M., and Zheng, B. (2019). Response of phenylpropanoid pathway and the role of polyphenols in plants under abiotic stress. *Molecules* 24:2452. doi: 10.3390/molecules24132452
- Shimosaka, E., and Ozawa, K. (2015). Overexpression of cold-inducible wheat galactinol synthase confers tolerance to chilling stress in transgenic rice. *Breed. Sci.* 65, 363–371.
- Sinha, S., Raxwal, V. K., Joshi, B., Jagannath, A., Katiyar-Agarwal, S., Goel, S., et al. (2015). De novo transcriptome profiling of cold-stressed silques during pod filling stages in Indian mustard (*Brassica juncea* L.). *Front. Plant Sci.* 6:932. doi: 10.3389/fpls.2015.00932
- Smirnov, N., and Cumbes, Q. J. (1989). Hydroxyl radical scavenging activity of compatible solutes. *Phytochemistry* 28, 1057–1060. doi: 10.1016/0031-9422(89)80182-7
- Sorita, G. D., Leimann, F. V., and Ferreira, S. R. S. (2020). Biorefinery approach: is it an upgrade opportunity for peanut by-products? *Trends Food Sci. Technol.* 105, 56–69. doi: 10.1016/j.tifs.2020.08.011
- Suzuki, N. (2019). Temperature stress and responses in plants. *Int. J. Mol. Sci.* 20:2001.
- Swindell, W. R., Huebner, M., and Weber, A. P. (2007). Transcriptional profiling of *Arabidopsis* heat shock proteins and transcription factors reveals extensive overlap between heat and non-heat stress response pathways. *BMC Genomics* 8:125. doi: 10.1186/1471-2164-8-125
- Tang, K., Zhao, L., Ren, Y., Yang, S., Zhu, J.-K., and Zhao, C. (2020). The transcription factor ICE1 functions in cold stress response by binding to the promoters of CBF and COR genes. *J. Integr. Plant Biol.* 62, 258–263. doi: 10.1111/jipb.12918
- Trapnell, C., Williams, B. A., Pertea, G., Mortazavi, A., Kwan, G., van Baren, M. J., et al. (2010). Transcript assembly and quantification by RNA-Seq reveals unannotated transcripts and isoform switching during cell differentiation. *Nat. Biotechnol.* 28, 511–515. doi: 10.1038/nbt.1621
- Tsuji, Y., Fang, C., Yasuda, S., and Fukushima, K. (2005). Unexpected behavior of coniferin in lignin biosynthesis of *Ginkgo biloba* L. *Planta* 222, 58–69.
- Upadhyay, R. K., Handa, A. K., and Mattoo, A. K. (2019). Transcript abundance patterns of 9- and 13-lipoxygenase subfamily gene members in response to abiotic stresses (heat, cold, drought or salt) in tomato (*Solanum lycopersicum* L.) highlights member-specific dynamics relevant to each Stress. *Genes* 10:683. doi: 10.3390/genes10090683
- Van den Ende, W. (2013). Multifunctional fructans and raffinose family oligosaccharides. *Front. Plant Sci.* 4:247. doi: 10.3389/fpls.2013.00247
- Wang, C., Cheng, B., Zheng, Y., Sha, J., Li, A., and Sun, X. (2003). Effects of temperature to seed emergence, seedling growth and anthesis of peanut. *J. Peanut Sci.* 32, 7–11. doi: 10.14001/j.issn.1002-4093.2003.04.002
- Wang, X. J., Shen, Y., Sun, D. L., Bian, N. F., Shi, P. X., Zhang, Z. M., et al. (2020). iTRAQ-based proteomic reveals cell cycle and translation regulation involving in peanut buds cold stress. *Russ. J. Plant Physiol.* 67, 103–110. doi: 10.1134/s1021443720010239
- Wang, X. J., Sun, D. L., Bian, N. F., Shen, Y., Zhang, Z. M., Wang, X., et al. (2017). Metabolic changes of peanut (*Arachis hypogaea* L.) buds in response to low temperature (LT). *S. Afr. J. Bot.* 111, 341–345. doi: 10.1016/j.sajb.2017.04.009
- Wu, D., Liu, Y. F., Pang, J. Y., Yong, J. W. H., Chen, Y. L., Bai, C. M., et al. (2020). Exogenous Calcium alleviates nocturnal chilling-induced feedback inhibition of photosynthesis by improving sink demand in peanut (*Arachis hypogaea*). *Front. Plant Sci.* 11:607029. doi: 10.3389/fpls.2020.607029
- Yang, C., Yang, H., Qijun, X., Wang, Y., Sang, Z., and Yuan, H. (2020). Comparative metabolomics analysis of the response to cold stress of resistant and susceptible Tibetan hulless barley (*Hordeum distichon*). *Phytochemistry* 174:112346. doi: 10.1016/j.phytochem.2020.112346
- Yang, T., Chaudhuri, S., Yang, L., Du, L., and Poovaiah, B. W. (2010). A calcium/calmodulin-regulated member of the receptor-like kinase family confers cold tolerance in plants. *J. Biol. Chem.* 285, 7119–7126. doi: 10.1074/jbc.M109.035659
- Yu, G., Wang, L. G., Han, Y., and He, Q. Y. (2012). clusterProfiler: an R package for comparing biological themes among gene clusters. *Omics* 16, 284–287. doi: 10.1089/omi.2011.0118
- Yuan, P., Yang, T., and Poovaiah, B. W. (2018). Calcium signaling-mediated plant response to cold stress. *Int. J. Mol. Sci.* 19:3896.
- Yuan, W., Liu, J., Takac, T., Chen, H., Li, X., Meng, J., et al. (2021). Genome-wide identification of banana csl gene family and their different responses to low temperature between chilling-sensitive and tolerant cultivars. *Plants* 10:122. doi: 10.3390/plants10010122
- Zeng, H., Xu, L., Singh, A., Wang, H., Du, L., and Poovaiah, B. W. (2015). Involvement of calmodulin and calmodulin-like proteins in plant responses to abiotic stresses. *Front. Plant Sci.* 6:600. doi: 10.3389/fpls.2015.00600
- Zhang, H., Dong, J. L., Zhao, X. H., Zhang, Y. M., Ren, J. Y., Xing, L. T., et al. (2019). Research progress in membrane lipid metabolism and molecular mechanism in peanut cold tolerance. *Front. Plant Sci.* 10:838. doi: 10.3389/fpls.2019.00838
- Zhang, H., Jiang, C. J., Ren, J. Y., Dong, J. L., Shi, X. L., Zhao, X. H., et al. (2020). An advanced lipid metabolism system revealed by transcriptomic and lipidomic analyses plays a central role in peanut cold tolerance. *Front. Plant Sci.* 11:1110. doi: 10.3389/fpls.2020.01110
- Zhang, H., Jiang, C. J., Yin, D. M., Dong, J. L., Ren, J. Y., Zhao, X. H., et al. (2021). Establishment of comprehensive evaluation system for cold tolerance and screening of cold-tolerance germplasm in peanut. *Acta Agron. Sin.* 47, 1753–1767. doi: 10.3724/SP.J.1006.2021.04182
- Zhang, J., Yin, X.-R., Li, H., Xu, M., Zhang, M.-X., Li, S.-J., et al. (2020). Ethylene response factor EjERF39–EjMYB8 complex activates cold-induced lignification of loquat fruit, via the biosynthetic gene Ej4CL1. *J. Exp. Bot.* 71, 3172–3184. doi: 10.1093/jxb/eraa085
- Zhang, X., Feng, H., Feng, C., Xu, H., Huang, X., Wang, Q., et al. (2015). Isolation and characterisation of cDNA encoding a wheat heavy metal-associated isoprenylated protein involved in stress responses. *Plant Biol.* 17, 1176–1186. doi: 10.1111/plb.12344

- Zhao, X., Chen, J., and Du, F. (2012). Potential use of peanut by-products in food processing: a review. *J. Food Sci. Technol.* 49, 521–529. doi: 10.1007/s13197-011-0449-2
- Zhao, Y., Zhou, M., Xu, K., Li, J. H., Li, S. S., Zhang, S. H., et al. (2019). Integrated transcriptomics and metabolomics analyses provide insights into cold stress response in wheat. *Crop J.* 7, 857–866. doi: 10.1016/j.cj.2019.09.002
- Zuther, E., Buchel, K., Hundertmark, M., Stitt, M., Hinch, D. K., and Heyer, A. G. (2004). The role of raffinose in the cold acclimation response of *Arabidopsis thaliana*. *FEBS Lett.* 576, 169–173. doi: 10.1016/j.febslet.2004.09.006

Conflict of Interest: The authors declare that the research was conducted in the absence of any commercial or financial relationships that could be construed as a potential conflict of interest.

Publisher's Note: All claims expressed in this article are solely those of the authors and do not necessarily represent those of their affiliated organizations, or those of the publisher, the editors and the reviewers. Any product that may be evaluated in this article, or claim that may be made by its manufacturer, is not guaranteed or endorsed by the publisher.

Copyright © 2021 Wang, Liu, Han, Chen, Huai, Kang, Wang, Yan, Jiang, Lei and Liao. This is an open-access article distributed under the terms of the Creative Commons Attribution License (CC BY). The use, distribution or reproduction in other forums is permitted, provided the original author(s) and the copyright owner(s) are credited and that the original publication in this journal is cited, in accordance with accepted academic practice. No use, distribution or reproduction is permitted which does not comply with these terms.



Functional Characterization of Cotton C-Repeat Binding Factor Genes Reveal Their Potential Role in Cold Stress Tolerance

Jiangna Liu^{1,2†}, Richard Odongo Magwanga^{1,3†}, Yanchao Xu^{1†}, Tingting Wei¹, Joy Nyangasi Kirungu^{1,2}, Jie Zheng¹, Yuqing Hou¹, Yuhong Wang¹, Stephen Gaya Agong³, Erick Okuto³, Kunbo Wang¹, Zhongli Zhou^{1*}, Xiaoyan Cai^{1*} and Fang Liu^{1,2*}

OPEN ACCESS

Edited by:

Dhruv Lavania,
University of Alberta, Canada

Reviewed by:

Dayong Li,
Beijing Vegetable Research Center,
China
Suprasanna Penna,
Bhabha Atomic Research Centre
(BARC), India

*Correspondence:

Zhongli Zhou
zhonglizhou@163.com
Xiaoyan Cai
cxycri@163.com
Fang Liu
liufcri@163.com

[†]These authors have contributed
equally to this work

Specialty section:

This article was submitted to
Plant Abiotic Stress,
a section of the journal
Frontiers in Plant Science

Received: 28 August 2021

Accepted: 04 November 2021

Published: 08 December 2021

Citation:

Liu J, Magwanga RO, Xu Y, Wei T, Kirungu JN, Zheng J, Hou Y, Wang Y, Agong SG, Okuto E, Wang K, Zhou Z, Cai X and Liu F (2021) Functional Characterization of Cotton C-Repeat Binding Factor Genes Reveal Their Potential Role in Cold Stress Tolerance. *Front. Plant Sci.* 12:766130. doi: 10.3389/fpls.2021.766130

¹ Chinese Academy of Agricultural Sciences (ICR, CAAS)/State Key Laboratory of Cotton Biology, Institute of Cotton Research, Anyang, China, ² School of Agricultural Sciences, Zhengzhou University (SBPMAS), Zhengzhou, China, ³ School of Biological, Physical, Mathematics and Actuarial Sciences, Jaramogi Oginga Odinga University of Science and Technology (JOUST), Bondo, Kenya

Low temperature is a common biological abiotic stress in major cotton-growing areas. Cold stress significantly affects the growth, yield, and yield quality of cotton. Therefore, it is important to develop more robust and cold stress-resilient cotton germplasms. In response to climate change and erratic weather conditions, plants have evolved various survival mechanisms, one of which involves the induction of various stress responsive transcript factors, of which the C-repeat-binding factors (CBFs) have a positive effect in enhancing plants response to cold stress. In this study, genomewide identification and functional characterization of the cotton CBFs were carried out. A total of 29, 28, 25, 21, 30, 26, and 15 proteins encoded by the *CBF* genes were identified in seven *Gossypium* species. A phylogenetic evaluation revealed seven clades, with Clades 1 and 6 being the largest. Moreover, the majority of the proteins encoded by the genes were predicted to be located within the nucleus, while some were distributed in other parts of the cell. Based on the transcriptome and RT-qPCR analysis, *Gthu17439* (*GthCBF4*) was highly upregulated and was further validated through forward genetics. The *Gthu17439* (*GthCBF4*) overexpressed plants exhibited significantly higher tolerance to cold stress, as evidenced by the higher germination rate, increased root growth, and high-induction levels of stress-responsive genes. Furthermore, the overexpressed plants under cold stress had significantly reduced oxidative damage due to a reduction in hydrogen peroxide (H₂O₂) production. Moreover, the overexpressed plants under cold stress had minimal cell damage compared to the wild types, as evidenced by the Trypan and 3,3'-Diaminobenzidine (DAB) staining effect. The results showed that the *Gthu17439* (*GthCBF4*) could be playing a significant role in enhancing cold stress tolerance in cotton and can be further exploited in developing cotton germplasm with improved cold-stress tolerance.

Keywords: CBF4, transcription factors, cold tolerance, overexpression, cotton

INTRODUCTION

Cotton is a thermophilic crop and is more sensitive to low temperature (Hemantaranjan et al., 2014); China being the major cotton-growing country globally, the site specific regions within China, such as Xinjiang, is often affected by cold, which lasts for more than a half growing of cotton plants, which results in negative effects on plant growth and development (Rihan et al., 2017). Cold stress leads to inhibition of seed germination, reduction of plant growth, and reproduction, as well as a decrease in crop yield and quality (Körner, 2016). However, many crops, such as rice (*Oryza sativa*), maize (*Zea mays*), tomato (*Solanum lycopersicum*), soybean (*Glycine max*), and cotton (*Gossypium hirsutum*), do lack the ability to adapt to environments with low temperature, thus highly adaptive to tropical or subtropical regions (Xiong et al., 2002; Wang et al., 2017; Kumar Verma et al., 2018). In order to deter the emergence of the adverse effects, plants have evolved complex mechanisms to resist cold stress by integrating the plants' transcription factors (Diouf et al., 2017; Lu et al., 2018; Magwanga et al., 2018b, 2019). Through the integration of the physiological, biochemical, and molecular regulatory mechanisms into stress detection, signal transduction, gene expression, and metabolic modifications, plants have been found to have survival strategy for reducing or preventing the effects of cellular oxidative damage (Thomashow, 1999).

In order to understand the effect of cold stress on plants, it is important to distinguish between cold (0–15°C) and freezing/chilling stress (<0°C). Cold stress leads to metabolic injury, destruction of the stability of protein complexes, inhibition of the metabolic pathways and various cellular processes in varying degrees, and eventually, damage to the photosynthetic processes (Bruce et al., 2007; Colebrook et al., 2014; Zhao et al., 2018). Freezing/chilling temperature promotes the ice formation in intercellular spaces of plant tissues, significantly reduces the efficiency of photosynthesis, and increases the release of reactive oxygen species (ROS). Increased release of ROS leads to chloroplast membrane oxidation; moreover, increased levels of ROS initiate stress-signal mechanism in plants, which significantly alter gene expression at chloroplast and nucleus levels, thereby promoting lipid homeostasis, thereby increasing plants adaptation to chilling stress (Liu X. et al., 2018). Furthermore, when ice crystals are deposited on the cell wall, the extracellular water potential decreases, and the cell membrane is destroyed, resulting in serious cell dehydration (Uemura, 2014). The most common phenomenon to resist the adverse effects of cold is acclimatization through the evolution of stress-responsive genes, for instance, the C-repeat-binding factors (CBFs), being the CBF1 and CBF3 play a significant role in cold acclimation-dependent freezing tolerance (Zhao et al., 2016). Many plants have increased freezing resistance after a period of low non-freezing temperature, a phenomenon known as cold acclimation (Kumar et al., 2010; Hussain et al., 2018). Cold acclimation is an effective way to increase plant-freezing resistance after a period of low non-freezing temperature (Shi et al., 2018). When plants are exposed to chilling conditions, the plants do mobilize the cold-response genes (COR), which then activate.

C-repeat binding factors (CBFs), followed by the accumulation of cryoprotectants, results in the acquisition of freezing tolerance (Thomashow, 1999). When plants are exposed to non-freezing cold condition, the CBFs are rapidly induced by low temperature, and then the downstream target gene *COR* becomes activated (Zhang and Huang, 2010). In addition, as the expression of CBF is regulated by light quality, biological clock, and photoperiod, it is necessary to understand the daily and seasonal regulations of the *CBF* genes (Gong et al., 2020). The CBF/dehydration-responsive element binding factor 1 (CBF/DREB1) is well-studied as an integral transcription factor in the cold regulatory pathway. It is an adaptive response where plants increase freezing tolerance after exposure to low non-freezing temperatures (Liu et al., 1998). The CBF/DREB protein, a DNA-binding protein belonging to the AP2/ERF superfamily, was first identified in *Arabidopsis thaliana* as a cold (LT)-induced transcription factor (Jin Y. et al., 2018). The APETALA2/ethylene-responsive element binding factor (AP2/ERF) family is a large class of plant-specific transcription factors, including AP2, RAV, ERF, and CBF (Haake, 2002; Jin J. H. et al., 2018). The expression of *CBF* gene was very low at room temperature but increased rapidly within 15 min of plants exposure to cold stimulation (Wang et al., 2017; Shi et al., 2018). During cold acclimation, mobilization of the CBF activated cold response (*COR*) gene and increased accumulation levels of the cryoprotectants do significantly enhance the cold tolerance in plants (Thomashow, 1999). The *CBF/DREB* gene is activated by a *CBF* expression (ICE) inducer through specific binding of *cis*-elements to MYC (c-Myc, L-Myc, S-Myc, and N-Myc) in the promoter region (Chinnusamy et al., 2003; Jin Y. et al., 2018; Shi et al., 2018).

The cold reaction pathway of ICE-CBF-COR has been proved to be the effective defense mechanism to cold stress (Wang et al., 2017). Moreover, the known six members of the CBF family members CBF1/DREB1C, CBF2/DREB1B, and CBF3/DREB1A are induced by cold stress, while CBF4/DREB1D, DREB1E/DDF2, and DREB1F/DDF1 are induced by osmotic stresses (Ma et al., 2014). Furthermore, the CBF1, CBF2, and CBF3 are arranged in tandem in an 8.7-kb region of the short arm of chromosome 4 in *Arabidopsis* (Jin Y. et al., 2018). All the three CBF Transcription factors perhaps act as the activators of the expression of downstream *CORs* genes, but with different functions (Siddiqua and Nassuth, 2011). The CBF1/2/3 triple mutant *Arabidopsis* seedlings obtained by CRISPR/Cas9 technology are more sensitive to low temperature than the single mutant CBF2 and CBF3, as well as the double mutant CBF1/3 (Zhao et al., 2016), which is an indication that *CBF* genes play a significant role in enhancing cold stress tolerance in plants.

The CBF transcription factors have been widely identified and isolated from rice, tomato, *Brassica napus*, wheat, barley, and maize, which show that the CBF family is large in scale and complex in structure (Yu et al., 2015; Rihan et al., 2017). It has been reported that the *AtCBF* gene was overexpressed in *Brassica napus* transgenic plants and improved the cold tolerance (Huang et al., 2011; Rihan et al., 2017). The combination of the *AtDREB1A* gene with the stress-induced *RD29A* promoter improved the tolerance in transgenic tobacco to drought and cold

stress (Bhatnagar-Mathur et al., 2008; Lata et al., 2011). Through phylogenetic analysis of Arabidopsis CBFs and their orthologous genes in other plants, it was found that CBFs were highly conservative in the phylogeny (Shi et al., 2018). In understanding cold stress response among the cotton genotypes, Cai et al. (2019) found that the cotton germplasms of the D genome respond differently to drought stress, in which *Gossypium thurberi* exhibit higher levels of cold stress tolerance by mobilizing the antioxidant enzymes and induction of stress-responsive genes, such as the *CBF4* and *ICE2*. As an important oil and fiber crop, cotton has been planted in more than 70 countries and plays an important role in the global economy. However, cotton yield is often adversely affected by abiotic stresses. Therefore, studying the molecular adaptation mechanism to stress resistance in cotton is of great significance for improving cotton yield. The 21 *CBF* genes have been cloned from *G. hirsutum*, which provides useful clues for understanding the cold tolerance mechanism in cotton. However, due to the limited genome sequence, the expression profile of the *CBF* family, and its phylogenetic relationship with other plants, the role of the *CBF* members is still unclear. In order to better understand the function and evolutionary relationship of the *CBF* gene family in cotton, we analyzed the structural variation and the evolution pattern of the *CBF* family based on the genome-wide data of several cotton species and explored the molecular mechanism of cold adaptation formation in *G. thurberi*. This study provides fundamental information and reference for further research on the molecular mechanism of the *CBF* genes and their regulatory role in cold adaptation in cotton.

MATERIALS AND METHODS

Identification of CBF Family Genes in the Cotton Genomes

Wild diploid cotton species genome data were retrieved from CottonGen¹ to construct a local BLAST database². The Arabidopsis CBF protein sequences were used as probes to compare with the wild diploid cotton. The *E*-value threshold for BLASTP was set at $1e^{-10}$ to obtain the final dataset of the CBF proteins. The Pfam (Finn et al., 2014) SMART³ databases were employed to confirm each predicted CBF protein sequence (Letunic et al., 2015). Redundant sequences and incomplete sequences were removed. The sequences of 10 *Gossypioideis kirkii* and nine *Theobroma cacao* CBF proteins were obtained from the CottonGen (see text footnote 1) and the national center for biotechnology information (NCBI)⁴ databases, respectively. In addition, physicochemical parameters, including the molecular weight (MW) and isoelectric point (*pI*) of each gene product, were calculated using compute the *pI*/Mw tool from ExPASy⁵, as previously used by Magwanga et al. (2018b) in the evaluation of the physicochemical properties of the *LEA* genes in cotton.

¹<https://www.cottongen.org/>

²<https://blast.ncbi.nlm.nih.gov/Blast.cgi?PAGE=Proteins>

³<http://smart.embl-heidelberg.de/>

⁴<https://blast.ncbi.nlm.nih.gov/Blast.cgi>

⁵<http://www.expasy.org/tools/>

Sequence Alignment and Phylogenetic Analysis of the Cotton CBF Gene Family

An alignment of multiple CBF protein sequences from *A. thaliana*, *Gossypioideis kirkii*, and *Theobroma cacao* was generated using the ClustalW program⁶. A neighbor-joining (NJ) analysis of the generated alignment was performed using the unweighted pair-group method with an arithmetic mean algorithm to construct an unrooted phylogenetic tree. Bootstrap value was 1,000, and other parameters were used by default value. The tree was visualized with MEGA 7.0 software (Kumar et al., 2016).

Gene Structure and C-Terminal Conserved Motifs Analysis

Structural information for the *CBF* genes, including the chromosomal location and gene length, was determined. The exons and introns were predicted by comparing the coding sequences with genomic sequences. The conserved motif analysis of the CBF protein sequences was predicted by MEME online software⁷. Moreover, the Conserved Domains Database (CDD)⁸ was employed to search for the conserved domain information of the CBF and used the TBtools mapping tool to draw the conserved domains (Chen et al., 2020).

Retrieval and Analysis of Promoter Sequences

The 2,000-bp sequence upstream of ATG was extracted from the transcription start site of the *CBF* gene sequence and submitted the obtained sequence to the PlantCARE website⁹. Identification of possible *cis*-acting elements in the promoter region is used to identify putative *cis*-regulatory elements in the promoter sequence (Higo et al., 1999). In addition, we carried out the subcellular localization prediction of all the CBF proteins by an online tool WoLF PSORT¹⁰ (Horton et al., 2007).

RNA Extraction and qRT-PCR Analysis

At three leaf stages, cold stress was imposed by subjecting to cold stress by transferring the seedlings and kept at 4°C under normal light conditions. The leaves were then harvested for RNA extraction at 0, 0.5, 3, 6, 12, and 24 h of post-stress exposure. The total RNA was extracted using the EASYspin plus plant RNA kit (Aidlab Biotech, Beijing, China), following the instructions of the manufacturer. The quality and the concentration of each RNA sample were determined by NanoDrop 2000 spectrophotometer and RNA that fulfilled the standard at 260/280 in a range of 1.80–2.1 was used for further analysis. The primers used for qRT-PCR were designed using primer premier 5 software for all genes (Supplementary Table 3). The cotton *GhActin* gene, (forward primer sequence 5'ATCCTCCGTCTTGACCTTG3', and reverse primer sequence 5'TGTCCGTCAGGCAACTCAT3') were used

⁶<https://www.genome.jp/tools-bin/clusterw>

⁷<https://meme-suite.org/meme/>

⁸<https://www.ncbi.nlm.nih.gov/cdd/>

⁹<http://www.dna.affrc.go.jp/htdocs/PLACE/>

¹⁰<http://www.genscript.com/wolf-psort.html>

as a reference gene for the analysis. Real-time PCR reactions were carried out in a final volume of 25 μ l, using an SYBR Green master mix and an ABI 7500 thermal cycler (Applied Biosystems, Foster City, CA, United States), following the instructions of the manufacturer. The single stranded cDNA was synthesized from reverse transcriptase with TransScript-All-in-One First-Strand cDNA Synthesis SuperMix (TransGen Biotech kit, Beijing, China) for RT-qPCR in harmony with the protocol of the manufacturer. NCBI primer blast was used to design 27 LHC gene primers. The primers details are given in **Supplementary Table 1**. The 7500 fast real-time system was used for analysis, and 10 μ l of Time FastStart Universal SYBR Green Master sigma (ROX) solution (Roche Diagnostics, Mannheim, Germany) per sample was used for RT-qPCR. Total reaction mixture volume was 20 μ l, containing 2- μ l cDNA, 6- μ l RNA free water, 10- μ l green SYBR, 1 μ l of each forward and reverse primer. Ghactin7 used as a control (Artico et al., 2010). The RT-qPCR was completed with three technical repeats. The expression level of genes was calculated using the formula $E = 2^{-\Delta\Delta Ct}$.

Plant Material

The seeds of *Gossypium herbaceum*, *G. thurberi*, and *Gossypium australe* were pre-germinated in the sand at 25°C for 4 days. Then, seedlings were then transferred to the hydroponic facility equipped with Hoagland nutrient solution (Hoagland and Arnon, 1950). The greenhouse conditions were set at 28°C during the day/25°C at night, the photoperiod was 16 h, and the relative humidity was 60–70%. At the three-leaf stage, cotton seedlings were subjected to cold stress by transferring the seedlings and kept at 4°C under normal light conditions. The leaves were then harvested for RNA extraction at 0, 0.5, 3, 6, 12, and 24 h of post-stress exposure. Each treatment was repeated three times. The leaf samples were put in liquid nitrogen, frozen, and stored at –80°C, awaiting RNA extraction.

GthCBF4 Subcellular Localization Analysis

The *Agrobacterium tumefaciens* strain GthCBF4 vector was used for transformation studies. The design of GFP fusion constructs for pCambia2300-eGFP (control GFP). The total RNA (1 μ g) isolated from leaves of *G. thurberi* was used for amplification of the first strand of cDNA (TransGen Biotech, Beijing). Specific primers were used to amplify C-repeat-binding factors protein (GthCBF4) gene products from *G. thurberi*. The oligonucleotides used for amplification of GthCBF4 were forward primer 5'-GAGAACACGGGGGACTCTAGAATGGTTGATTCTGGGT CGGTTTCT3' and reverse primer 5'-ACCCATGTAA TTAAGGATCCAATAGAATAACTCCATAAAGG3' (Sigma, Henan, China). The underlined sequences (TCT AGA and GGA TCC) in the primer pair represent restriction sites for *Xba*I and *Bam*HI, respectively. The reverse primers used for amplification of GthCBF4 genes were designed in a fashion so as to eliminate stop codons of these genes. The PCR-amplified products of GthCBF4 were digested and cloned at the restriction site(s), *Xba*I, and *Bam*HI, respectively, in the vector (GFP) backbone. The PCR cycling conditions were as follows: Step (1) 95°C-3 min,

(2) 95°C-15 s, (3) 58°C-15 s, (4) 72°C-1 min, (5) a cycle to Steps 2 to 4 for 35 more times, (6) 72°C-5 min, (7) incubation at 4°C. The PCR was performed using Phanta Max Super-Fidelity DNA polymerase (Vazyme, Nanjing, China). To explore the subcellular localization of the *GthCBF4* gene, a pCambia2300-eGFP-Flag-GthCBF4 fusion vector of CBF and GFP was transiently infused in the epidermal cells of tobacco leaves; the construct was driven by the 35-s promoter and transformed *Agrobacterium* LBA4404 competent cells. In addition, *Agrobacterium* competent cells expressing only the *GFP* gene were used as a negative control. Four-week-old tobaccos cotyledon flat leaves were selected for infusion and cultivated in dark for 24–36 h after infiltration, and then fluorescence observation was performed under a laser confocal microscope.

Cloning of GthCBF4, a CBF Novel Gene in Arabidopsis

To explore the function of the *GthCBF4* gene in Arabidopsis, a constructed pBI121-GthCBF4 recombinant vector, transformed into the promoter cells of *A. tumefaciens* GV3101 (Reyes et al., 2020), as previously applied by Magwanga et al. (2018a), by adopting a freeze-thaw method (Dupadahalli, 2014), was performed. The wild-type (WT) *A. thaliana* was transformed by adopting the dipping method (Clough and Bent, 1999) by using a 50-mg/ml kanamycin for positive selection up to the third generation (T3). At the second generation, also referred to as the T2 generation, the GthCBF4 overexpressed lines were identified through a polymerase chain reaction; two high-overexpressed transgenic lines were obtained, and grown to generate the stable T3 generation.

Phenotypic Identification, Physiological and Biochemical Parameters of Wild-Type and GthCBF4 Overexpressed Plants Under Cold Stress

The transgenic and wild-type *A. thaliana* was grown in plastic bowls for 2 weeks; the growth pattern between the transgenic and the wild types was not significantly different. The two types, transgenic and wild type Arabidopsis, were placed in an environment of –15°C for 3 h. After the treatment, the treated plants were moved to a 4°C-light incubator to thaw for 4 h, and finally, they were cultivated under normal light conditions at 23°C. After 7 days, photographs were taken to aid the counting of the survival rate of the plants. The germination rate and the root length were determined under cold stress; a *t*-test was used to verify the significance of the difference in root length between the mutant and the wild types. The trypan blue staining method (Berrocal-lobo, 2016) was adopted to reflect the cell damage under cold stress. Moreover, the DAB staining was applied to reflect the accumulation of peroxidase under cold stress. DAB staining was performed using a DAB chromogenic kit (Nanjing Jiancheng Bioengineering Institute, Nanjing, China).

Statistical Analysis

The experiments were done in three biological replicates, and the data were statistically analyzed by ANOVA procedure

(Molugaram and Rao, 2017), using statistical analysis software (SAS) version 9.3. The least significant difference test ($p \leq 0.05$) was used for the mean comparison.

RESULTS

Identification of the CBF Gene Families in the Cotton Genomes

The availability of the whole sequences for the seven cotton species enabled us to identify the CBF proteins harbored in their genome. The protein family (Pfam) domain PF00847 was used as the query to obtain the CBF proteins. Finally, 29 members of the CBF genes were identified in *G. herbaceum*, 28 members in *Gossypium arboreum*, 25 members in *G. thurberi*, 21 members in *Gossypium raimondii*, and 30 members in *Gossypium turneri*, and *Gossypium longicalyx* had 26 members. In contrast, *G. australe* had 15 CBF genes. Three representative cotton species from these seven species were then chosen for further detailed analysis: *G. herbaceum* (29), *G. thurberi* (25), and *G. australe* (26). The CBF-coding sequences (CDS) length in *G. herbaceum* ranged from 306 to 1,230 bp, while, for *G. australe*, the CDS ranged from 429 to 1,077 bp. In the analysis of the physicochemical properties of the CBF proteins, the results showed a great variation; for instance, the CBF proteins obtained from the *G. herbaceum*, their molecular weights (MW) ranged from 11.24188 to 39.02073 kDa; isoelectric value (pI) ranged from 5.26 to 10.27, while, in *G. thurberi*, the MW of the proteins encoded by the CBF genes ranged from 16.17923 to 45.59153 kDa; the pI ranged from 5.11 to 10.83. Similarly, in *G. australe*, it ranged from 15.67636 to 40.86796 kDa. The CBF genes differed substantially by the encoded protein size and its biophysical properties (Supplementary Table 1).

Phylogenetic Analysis of the Cotton CBF Gene Family

To determine the phylogenetic relationship of the CBF proteins, we constructed a phylogenetic tree by MEGA 7.0, using the neighbor-joining (N.J.) method with minimal evolution and maximum parsimony. The CBF proteins were clustered into seven clades and designated as Clades 1 to 7 (Figure 1). Clade 1 contained 61 CBF protein sequences, while Clade 3 contains only seven CBF amino acid sequences. Consistent with the previous classification, all Arabidopsis CBFs were distributed among the Clade 6 (Haake, 2002; Huang et al., 2011; Rihan et al., 2017). Except *G. australe* did not appear in Clade 3, the other cotton species were distributed in all seven groups.

Chromosomal Mapping, Gene Structure, and C-Terminal-Conserved Motif Analysis

All the genes located on various chromosomes in the three cotton genomes were named according to their positions on the chromosome. In *G. herbaceum*, a member of the diploid type of the A genome, the CBF genes were mapped on all the chromosomes, except chromosome Chr01, which harbored no

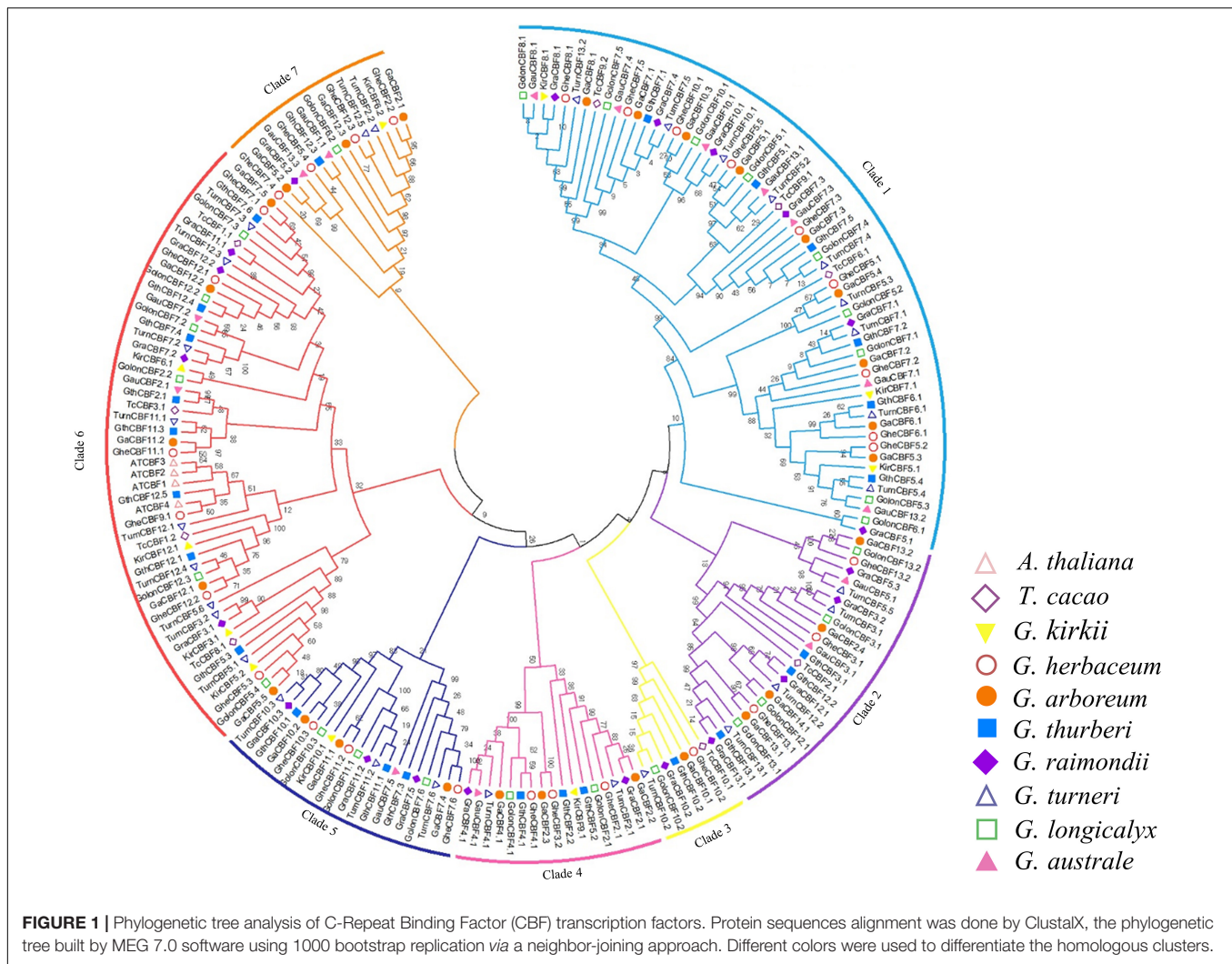
CBF genes. The highest gene loci were observed in chromosome Chr05 and Chr07 with five and six genes, respectively, while the lowest gene loci were observed in chromosome Chr04, 06, 08, and Chr09 with a single gene locus in each (Figure 2A). In the diploid of the D genome, *G. thurberi*, chromosome Gthu_1, Gthu_8, and Gthu_9 harbored no genes, while chromosomes, Gthu_5, Gthu_7, and Gthu_12 had more gene loci. However, the highest gene loci were noted in chromosome Gthu_05, 07, and 12 with four, six, and five CBF genes, respectively; similarly, the lowest gene loci were noted on chromosome Gthu_3, 6, and 13 with a single gene locus each (Figure 2B). Finally, in *G. australe* diploid cotton of the G genome, no CBF genes were found in chromosomes G6, G9, G11, and G12, but the highest gene loci were only observed in chromosome G7 with five genes (Figure 2C).

In order to analyze the motifs, we employed MEME to detect conserved motifs in the CBF family. There were 10 conserved motifs distributed in each CBF family (Figure 3A). Almost all CBF proteins had the same number of motifs; three motifs were prominent among the CBF proteins, motifs 1, 2, and 4. Analyzing the arrangement of exons and introns can provide important insights into the evolution of gene families (Colebrook et al., 2014). To study the exon/intron structure of the CBF gene, the CDS and the genome sequence were compared. The results showed that most of *G. herbaceum* and *G. australe* harbored no intron, and indication that the genes were highly conserved, but, for the *G. thurberi*, the least number of exons was two, but others contained a higher number (Figures 3B–E). Basically, the members of the same group phylogenetically harbored a similar number of the intron-exon ratio. Stress regulates the expression of primary and specialized metabolism genes at the transcriptional level via transcription factors binding to specific *cis*-elements; a number of the *cis*-regulatory elements were found to be associated with the various cotton CBF genes, for instance, MYB, ABA-responsive element (ABRE), and long-term repeat (LTR), among others (Figure 3F); the MYB and ABRE are among the top-ranked stress responsive *cis*-regulatory elements (Ambawat et al., 2013). The detection of a myriad of *cis*-regulatory elements reveals the significant role played by the members of the cotton CBF genes in enhancing stress tolerance, more so cold stress in plants.

An online tool wolf sport was employed to determine the possible cellular sublocalization of the proteins encoded by CBF genes. Among the three cotton species, the highest proportions of CBF proteins were embedded in the nucleus. Moreover, the nucleus is the central regulator of cellular activities. However, other signals were observed in different cellular compartments, such as the chloroplast, mitochondria, plasma membrane, vacuole membrane, and chloroplast (Supplementary Table 2).

RNA-Seq Analysis and RT-qPCR Validation of the CBF Genes Under Cold Stress Conditions

Gossypium thurberi transcriptome data were used to analyze the expression patterns of the 25 CBF genes under cold stress; however, out of the 25 identified CBF genes, only



17 exhibited differential expression, while the other eight showed no expression, and thus, we excluded from further analysis (**Figure 4A**). Out of the 17 differentially expressed genes under cold stress as per the RNA-seq¹¹, 12 genes were selected as per their expression patterns, upward, downward, and partially expressed genes; the 12 CBF genes exhibited differential expression; moreover, 15 and 13 CBF genes from *G. herbaceum* and *G. australe*, respectively, were also profiled through RT-qPCR (**Figure 4B**). Among the 12 genes in *G. thurberi*, 10 genes exhibited significantly higher upregulation, with only two genes being downregulated. The expression trend was consistent with the transcriptome data. In *G. herbaceum*, nine genes were upregulated, and six were downregulated. In *G. australe*, eight were upregulated and five were downregulated. But, more significantly, out of all the CBF genes profiled, GauCBF3.1 and GthCBF12.5 were most highly upregulated in the leaf across the periods in which the plants were subjected to cold stress. The leaf plays an important role in photosynthesis, and the stomata are the key to this function, for it controls both photosynthesis and

respiration processes (Hajihashemi et al., 2018). Moreover, the process of photosynthesis involves the mechanisms of capturing light energy, which is then transformed to carbohydrates; this whole process is susceptible to low temperature (Stewart et al., 2016). The higher level of upregulation among the CBF genes across the various cotton types indicates that the proteins encoded by the CBF genes could play an integral role in enhancing cold acclimatization in cotton plants. Moreover, by integrating the transcriptome data and RT-qPCR result, we selected one of the highly upregulated CBF genes, *GthCBF12.5* (*GthCBF4*), for further validation.

Experimental Validation of Subcellular Localization of Cotton CBF Proteins

The results showed that none of the pCAMBIA2300-eGFP-Flag-*GthCBF4*-infused plants showed green fluorescence signals on both the nucleus and cell membrane. In contrast, the fusion protein pCAMBIA2300-eGFP-Flag-*GthCBF4* only had green fluorescence signals in the nucleus (**Figure 5**), indicating that the protein encoded by the gene was localized in the nucleus.

¹¹<https://www.ncbi.nlm.nih.gov/sra/PRJNA554555>

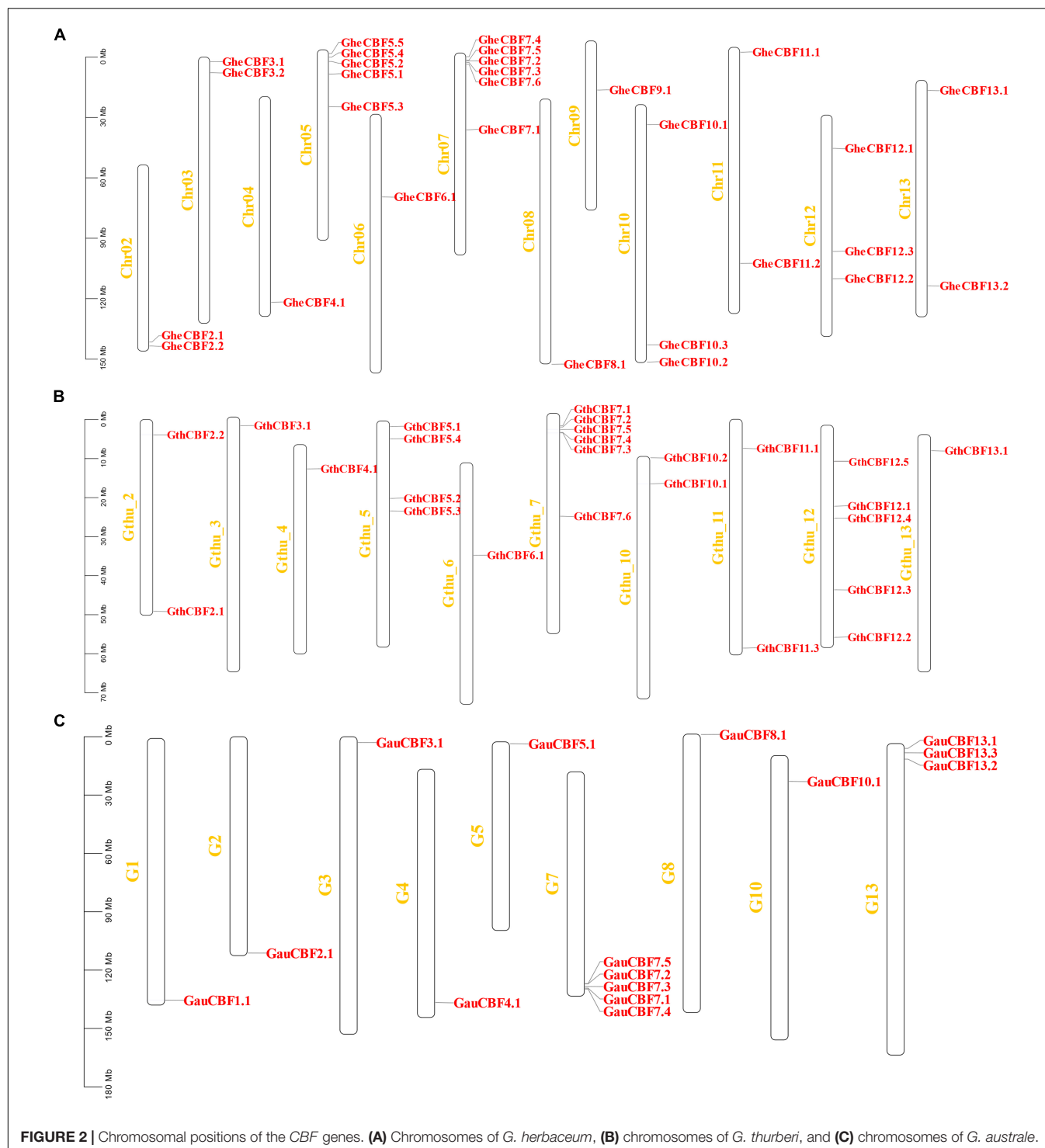


FIGURE 2 | Chromosomal positions of the *CBF* genes. **(A)** Chromosomes of *G. herbaceum*, **(B)** chromosomes of *G. thurberi*, and **(C)** chromosomes of *G. australe*.

The results were in agreement with the bioinformatics prediction of the possible cell compartmentalization of the CBF proteins. The presence of these proteins encoded by the *CBF* genes could possibly indicate that these genes have a critical role under cold stress conditions; moreover, posttranscriptional regulation at the pre-mRNA processing and export from the nucleus plays a role in cold acclimation (Chinnusamy et al., 2010).

Phenotype and Biochemical Evaluation of *GthCBF4*-Overexpressed Arabidopsis Plants Under Low Temperature

Two highly overexpressed (OE) lines OE-1 and OE-3 were selected for phenotypic and biochemical evaluation (**Figure 6A**); phenotypically, the *GthCBF4*-overexpressed lines (OE-1 and

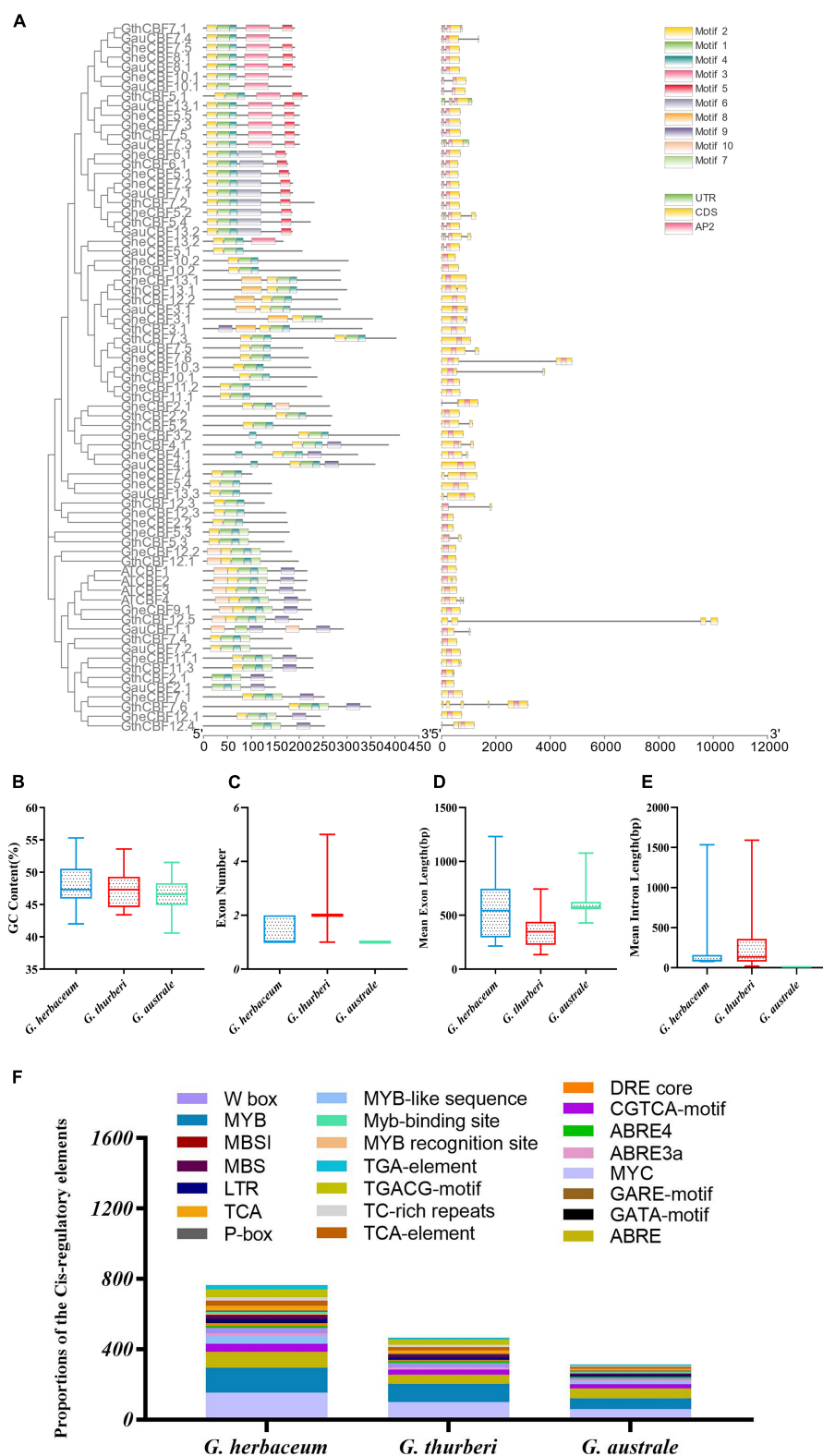
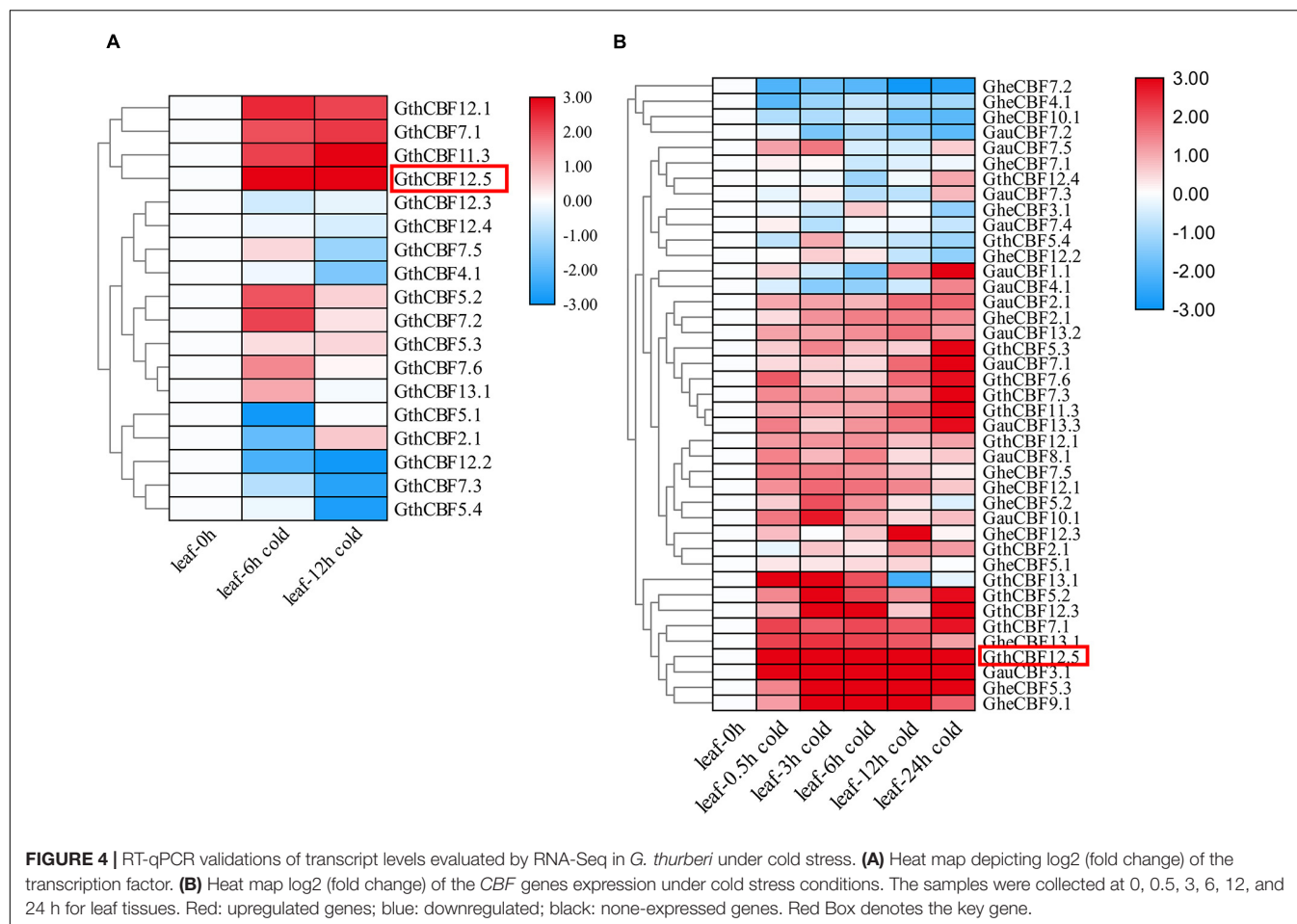


FIGURE 3 | Conserved domain and gene structure analysis of CBF family protein sequences from the evolutionary level in cotton. Different colors denote different motifs. **(A)** Physiochemical properties and *cis*-regulatory element analysis of the proteins encoded by the cotton *CBF* genes. **(B–E)** Guanine-cytosine (G.C.) content, exon number, mean exon length, and mean intron length. **(F)** *Cis*-regulatory elements obtained for the various proteins encoded by the *CBF* genes in the *G. herbaceum*, *G. thurberi*, and *G. australe*.



OE-3) showed no significant difference with the wild types under normal conditions, but, when the plants were exposed to cold stress, the survival of the WT was significantly reduced, while the OE-1 and OE-3 showed a higher level of survival (**Figure 6B**), in which the OE plants survival rate was estimated at 60% compared to the WT with only a 2% survival rate (**Figure 6C**). Similar results were obtained by Tang et al. (2019) in which the survival rate among the overexpressed lines was estimated at 64.9%, 62.2%. In determining the expression levels of the *GthCBF4*-overexpressed gene, at 0 h, the WT showed no expression, but, at 1 h and 3 h of cold-stress exposure, the *CBF* genes were partially induced but insignificantly, slightly below one, while the reverse was observed among the OE plants. The expression levels of the *GthCBF4*-overexpressed gene were significantly high, with 0 h showing expression levels close to 3-fold, while, at 1 h and 3 h, the expression levels of the *GthCBF4*-overexpressed gene were above 4-fold (**Figure 6D**). Under normal conditions, the stained blue area on the leaves of the transgenic overexpression plants and wild-type plants was minimal. While under cold treatment, the blue regions on transgenic leaves were significantly smaller than the wild type; the color depth was also lighter. Furthermore, the DAB-staining method was used to reflect the accumulation of H_2O_2 in Arabidopsis leaves. The accumulation of H_2O_2 in the transgenic overexpression leaves and the wild-type was very

low under normal conditions, and the DAB-staining region was hardly seen. But, after cold treatment, the DAB staining area on the wild-type Arabidopsis leaves was more pronounced compared to the stained region in the wild type, and the color depth was also deeper (**Figure 6E**). Knockdown of the *OsGRXS17* gene in rice significantly increased the H_2O_2 accumulation. The gene plays a critical role in the induction of ABA. ABA-induced accumulation of H_2O_2 , which is synthesized in guard cells, is essential for stomatal closure by activating plasma membrane Ca^{2+} channels. In the absence of ABA, the leaves of mutant plants exhibited slightly higher H_2O_2 levels on the basis of DAB staining than the wild-type plants (Hu et al., 2017). The results showed that the overexpression of the *CBF* gene in the transgenic lines improved the ability of the plants to oxidize the oxidative agents such as the H_2O_2 , thereby reducing the levels of oxidative damage in the plants.

Evaluation of Physio-Morphological Traits in *GthCBF4*-Overexpressed and Wild-Type Plants Under the Low-Temperature Environment

Germination of the OE and WT lines showed no significant differences under normal or controlled conditions; however,

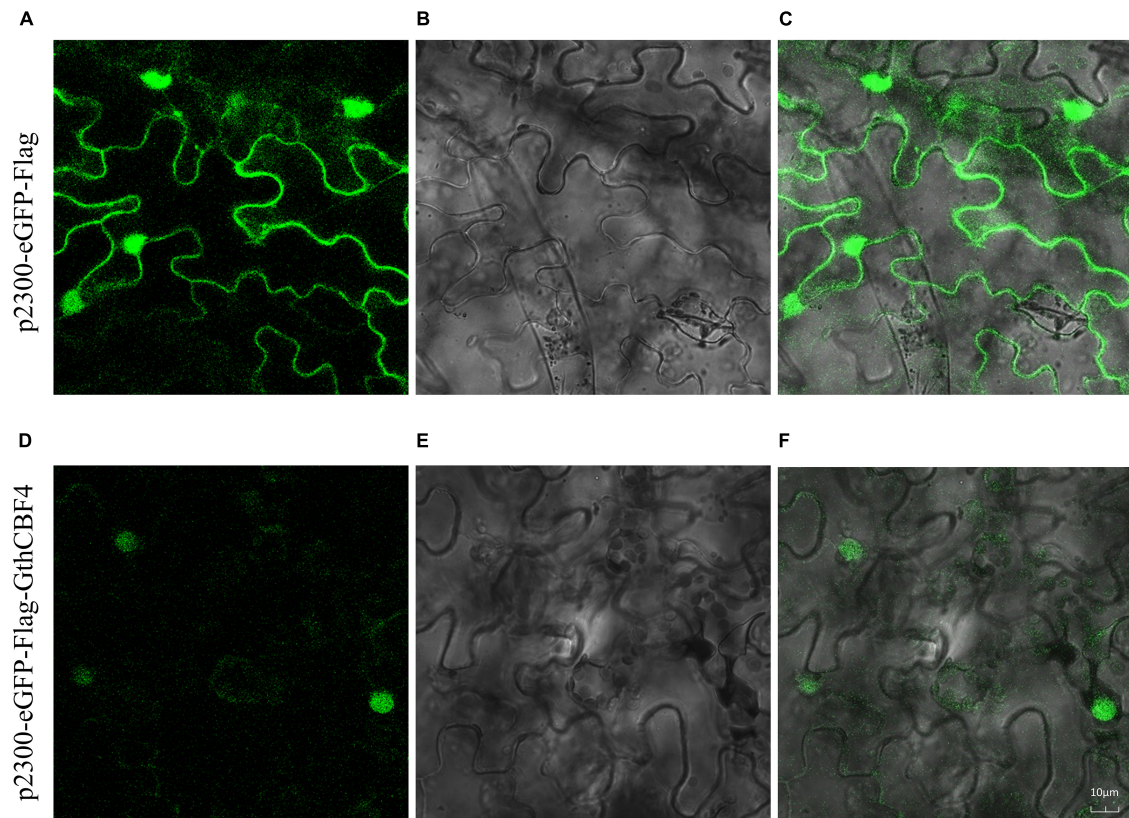


FIGURE 5 | Localization of pCAMBIA2300-eGFP-Flag-GthCBF4 in tobacco leaf. **(A–C)** Tobacco epidermal cells transformed with pCAMBIA2300-eGFP; **(D–F)** Onion epidermal cells transformed with pCAMBIA2300-eGFP-Flag-GthCBF4. **(A,D)** A light field with the magnification of X400 to display morphology. **(B,E)** Dark field images for the detection of green fluorescent protein (GFP) fluorescence. **(C,F)** Superimposed light and dark field images.

under cold stress, none of the WT germinated, while the OE lines showed some level of germination (**Figures 7A,B**), an indication that the OE lines were significantly improved and were able to adapt to cold stress condition. In the evaluation of the root lengths, no significant differences were observed under controlled conditions, but, under cold stress conditions, the OE lines showed higher root lengths compared to the WT (**Figures 7C,D**). Thus, the overexpression of the *CBF* genes could be playing a role either in the rate of cell division and or cell elongation. We further evaluated known stress-responsive genes, such as the *COR15A*, *RD29A*, *KIN1*, and *COR47* (Zhao et al., 2016). The OE lines significantly showed higher expression levels to all the stress-responsive genes profiled (**Figure 7E**). The high induction levels of the stress-responsive genes in the OE lines showed that the overexpressed genes do not suppress the expression of the stress-responsive genes, but do promote their expression, an indication that the overexpressed gene could be playing a vital role in enhancing cold stress tolerance in plants.

DISCUSSION

Cotton is an important economic crop, which supports the economies of several countries globally; moreover, it is the primary source of natural fiber critical raw material for the

textile industries (Reddy and Yang, 2009); however, in the recent past, its global production has significantly shrunk due to climate change. Rainfall has become erratic and scarce. Even the average daily temperature has increased dramatically with prolonged periods of cold weather, thereby affecting the growth and development of the plant. To improve the performance of current elite cultivars, a number of strategies have been proposed; among them is the utilization of the transcription factors and other novel genes of the plants to improve the adaptability of the current cotton germplasms to ever-changing environmental conditions. Cold stress has been a major concern in cotton production, but the climate dynamics have increased the deleterious effects of cold stress. For instance, in the 1980s, the United States loss due to the chilling impacts was estimated at 60 million dollars (Chaurasiya and Singh, 2019). Furthermore, cold stress causes considerable agricultural yield loss in very sensitive crops, particularly in sensitive crops like maize, rice, and chickpea (Thakur and Kumar, 2010). To increase the chance of survival, plants have adopted numerous mechanisms to cope with the ever-changing environmental conditions, one of which is the evolution of novel genes with tremendous effects on improving the adaptability of plants to various environmental stress factors, for instance, the *LEA* genes have been found to offer drought-stress tolerance in cotton (Magwanga et al., 2018a).

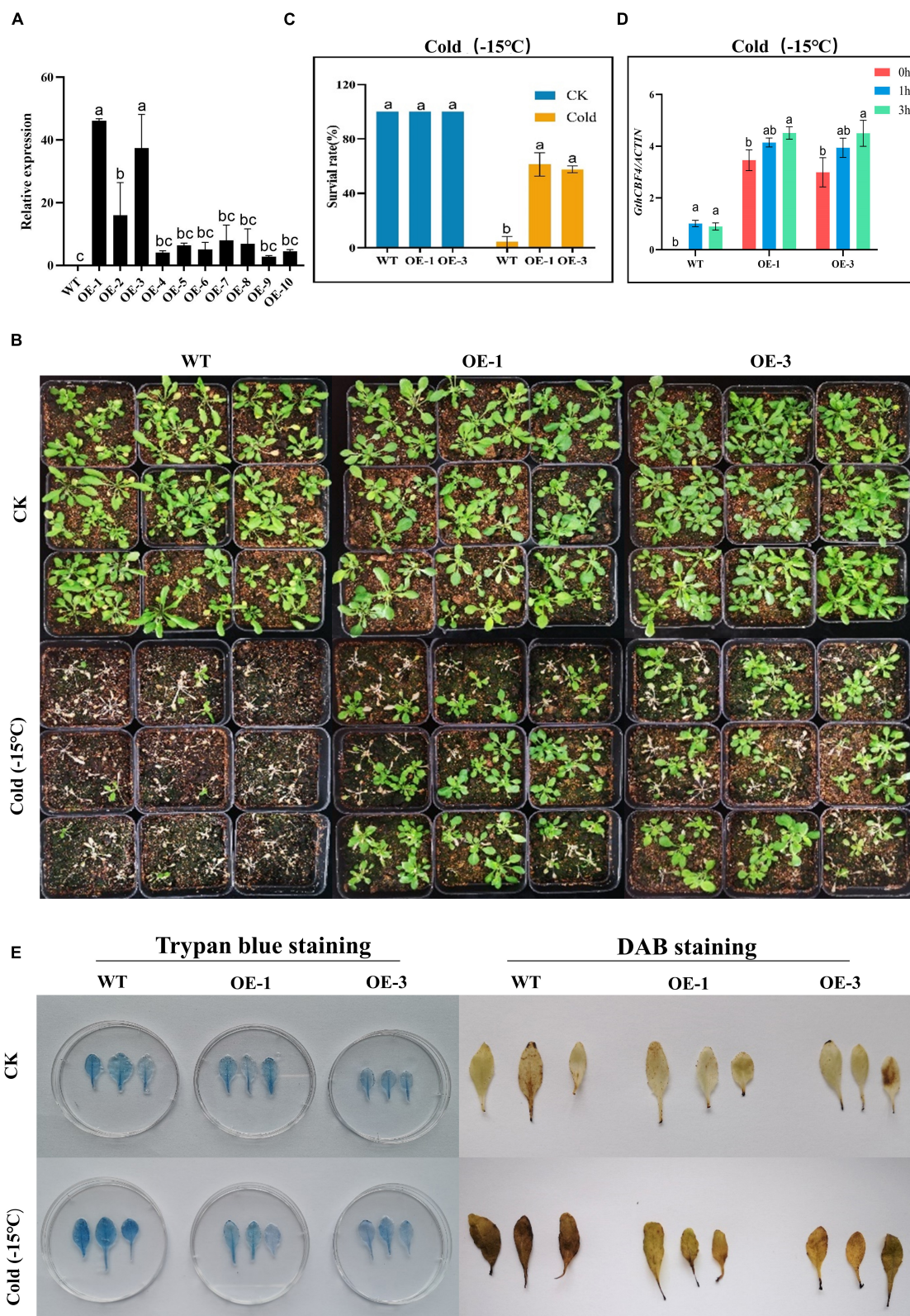


FIGURE 6 | Phenotype identification and cell damage identification of *GthCBF4*-overexpressed *Arabidopsis* under low temperature. **(A)** The quantitative expression level of *GthCBF4* gene in transgenic *Arabidopsis*. **(B)** -15°C treatment restores the growth status of wild-type and transgenic *Arabidopsis thaliana* after culture. **(C)** Freezing survival assay. **(D)** Log10 (fold change) of the *GthCBF4* genes expression in -15°C treatment. **(E)** Trypan blue staining and DAB staining. The letters a/b indicate statistically significant differences (two-tailed, $p < 0.05$) between the samples in each treatment.

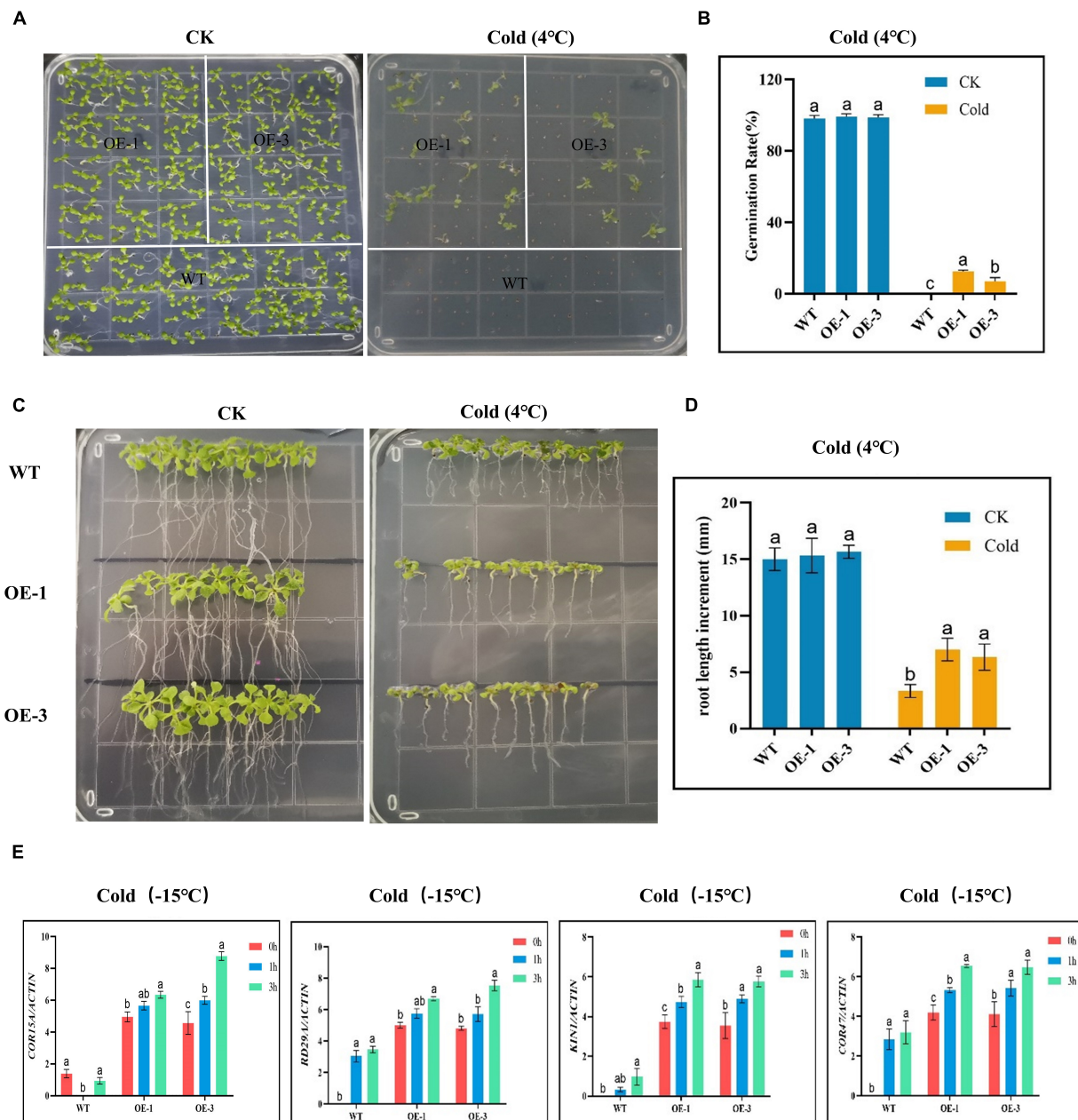


FIGURE 7 | Determination of the growth phenotypes and regulatory gene expression of transgenic Arabidopsis under cold stress conditions. **(A,B)** Germination rate determination. **(C,D)** Root length determination. **(E)** The expression levels of abiotic stress-responsive gene. The letters a/b indicate statistically significant differences (two-tailed, $p < 0.05$) between the samples in each treatment.

Although abiotic stress is a significant challenge in cotton growth, there is no detailed study on the *CBF* gene in cotton (Bo et al., 2007). In previous studies, the *CBF* family has been identified in cotton (*Gossypium hirsutum*) (Ma et al., 2014), wheat (Mohseni et al., 2012), lettuce (Sunchung et al., 2020), *Brassica napus* (Lv et al., 2020), Barley (Marquez-cedillo et al., 2005), and soybean (Kidokoro et al., 2015), but there are few studies on diploid cotton. In this work, genome-wide identification, characterization, and functional analysis of the

proteins encoded by the cotton *CBF* genes were done, in which 29, 25, and 15 *CBF* proteins encoded by the *CBF* genes were identified in *G. herbaceum*, *G. thurberi*, and *G. australe*, respectively. The results obtained showed that the proteins encoded by the *CBF* genes in cotton were higher compared to other plants, such as lettuce with 14, *Brassica napus* with 10, and soybean with 14 *CBF* genes, but less than hexaploid wheat with 65 *CBF* genes and barley with 20 *CBF* genes. The high number of the proteins encoded by the *CBF* genes

in cotton perhaps could explain the significant role they play in plants in relation to stress tolerance. Moreover, studies have found that Arabidopsis CBF family members have an AP2 domain, and each has a conserved amino acid sequence upstream and downstream of AP2. The upstream of AP2 is PKK/PKKPAGR (RAGRxxKFxETRHP), and the downstream is DSAWR (Okamuro et al., 1997). If the PKK/PKKPAGR mutation can inhibit the binding ability of CBF to the COR promoter of its downstream genes, thereby weakening the level of CBF regulation, this sequence is necessary for CBF to perform its transcription factor function. The cotton genome contains a large and complex CBF subfamily, with conserved AP2/EREBP domains and with CBF-like characteristics, indicating that cotton CBFs have a similar function with other CBFs in dicotyledons (Siddiqua and Nassuth, 2011). Phylogenetic analysis showed that the CBF families are divided into seven groups; among these genes, *CBF1*, *CBF2*, and *CBF3* are all induced by cold stress in *Arabidopsis thaliana*. Therefore, we speculate that CBF genes may also respond to abiotic stress, especially to cold. Further analysis showed that the isolated CBF gene was highly expressed under cold stress, consistent with previous research results.

The cotton CBF genes phylogenetic analysis revealed that the entire members of the cotton CBF family were grouped into seven clades; this deviates from the previous findings in which five clusters were observed among the CBF members obtained from lettuce (Sunchung et al., 2020) but were in agreement with findings obtained for the Tea Plant (*Camellia sinensis*) in which the CBF and its homologs were classified into six groups (Hu et al., 2020). In plants, the transcriptional regulation of osmotic stress response mainly depends on two main *cis*-regulatory elements related to stress response genes ABREs and dehydration response elements (DREs). The two *cis*-regulatory aspects were found to be associated with the CBF genes, which are indicators that the members of the CBF gene family could, perhaps, be playing a significant role in enhancing cold stress tolerance in plants. Moreover, the DREs are mainly involved in ABA-independent pathways (Liu S. et al., 2018), and ABRE is responsible for detecting ABA-mediated osmotic stress signals (Kim et al., 2011). In this study, the CBF genes detected for the three cotton species were rich in stress-response genes (ABRE), dehydration response element (DRE), and cold stress response element (LTR). Moreover, the C-repeat-binding factors (CBFs) are pivotal signaling genes, which are rapidly induced by cold and bond to the C-repeat/dehydration-responsive motif in the promoter region, more so in the downstream cold-responsive genes, with an important role in enhancing cold stress tolerance in plants. In the identification of the CBF genes in tea, a number of the identified genes were found to be associated with various stress responsive promoters, more importantly the CRT/DRE motif (Wang et al., 2019). It is suggested that exogenous environmental stress can induce the expression of the CBF gene through its response to *cis*-regulatory elements and further improve the resistance of plants to environmental stress.

It is universally accepted that transcription factors must be present in the nucleus to perform their functions (Wang et al., 2008). In evaluating the possible cell compartmentalization of the proteins encoded by the CBF genes, both prediction

and experimental evaluation showed that most of the CBF proteins are localized within the nucleus. Several studies have found that a number of stress-responsive proteins are sub-localized within the nucleus, for instance, calmodulin-regulated proteins; in plants, the activity of a pea apyrase, PsNTP9, is localized in the nucleus, and has a significant role in enhancing resistance to heavy metals and xenobiotic compounds (Virdi et al., 2015). Moreover, when plants are exposed to environmental stress, there is increased release of oxidizing agents, which destroys the DNA to counteract the DNA damage; plant cells evolved mechanisms for the DNA repair in both nucleus and mitochondria (Gruszka, 2015). Thus, the abundance of the CBF proteins in the nucleus could be significant in DNA repair as a result of oxidative damage.

Overexpression of Arabidopsis CBF gene in other plant species or overexpression of CBF of other species in Arabidopsis has revealed the potential of the CBF genes in enhancing frost resistance (Tondelli et al., 2011). Moreover, it has been shown that the CBF gene plays an important role in plant cold acclimatization; downregulation of *CBF1* and *CBF3* results in a 25–50% reduction in tolerance to cold stress levels in pre-cold treated mutant plants (Miura and Furumoto, 2013). In this study, the *GthCBF4* was strongly upregulated in cotton seedlings under cold treatment. The survival rate of *GthCBF4* transgenic *Arabidopsis thaliana* plants was significantly improved after freezing treatment. Furthermore, the inducer of CBF Expression (ICE) is a pioneer of cold acclimation, an MYC-type basic helix-loop-helix family transcription factor (TF; Zarka et al., 2003). It has been reported that ICE1 plays a significant role in C-repeat binding factor 3 (CBF3) cold induction (Chinnusamy et al., 2003). When plants encounter cold stress, ICE1 could be mobilized from JAZs bound by DELLAs and trigger the expression of CBF3. The CBF3 activates the expression of GA2ox7 to reduce the bioactive gibberellic acid (GA) level, which enhances the accumulation of DELLAs. Therefore, DELLAs can control the cold induction of CBF3 through ICE1 *via* JAZs. Moreover, the trypan blue staining, DAB staining, and the *GthCBF4*-overexpressed plants significantly reduced cold injury compared to the wild types, a strong indicator of the possible roles of CBF genes in enhancing cold-stress tolerance in plants. Moreover, root growth was significantly higher in *GthCBF4*-overexpressed plants. The trypan blue staining is critical to determining the level of cell death. When plants are exposed to various forms of stress factors, the cells undergo a series of effects, including cell damage, and eventually, cell death, depending on the intensity or tolerance nature of the plant. The overexpressed plants exhibit significantly low staining as compared to the wild types. The dye only enters into dead cells and not living ones; thus, the high blue color intensity in wild types showed that the level of cell death was significantly higher due to cold-stress effect (Zhang et al., 2017).

To further elucidate the critical roles played by the proteins encoded by the CBF genes, known stress-responsive genes were profiled, and the results showed that overexpression of the CBF gene significantly increased the induction levels of the stress-responsive genes. In general, the expression level of the four COR genes was significantly correlated with the freezing

tolerance level. Furthermore, *COR15A*, which encodes the chloroplast-targeted polypeptide, enhances the cold resistance of the chloroplasts (Thalhammer et al., 2014). In addition, the *CBF* genes can induce the expression of the *COR47*, *RD29A*, and *KIN1* genes, thereby improving the tolerance level of the plant to cold stress (Zhao et al., 2016). The upregulation of the stress-responsive genes further confirmed that the ability of GthCBF4-overexpressed plants to tolerate the effects of cold was significantly higher compared to the wild types. In the past two decades, the transcriptional network of CBF-signaling pathways has been extensively studied, and many *COR* genes have been identified in genome-wide expression profiles. About 10–25% of them are regulated by CBF, which implies that more early cold-regulated transcription factors are mainly involved in improving cold tolerance. Moreover, the mutational effect on the DRE motif revealed that the mutant crops were highly susceptible to cold stress as compared to non-mutant (Lei et al., 2014), which implied that mutations in DRE motifs impair the induction of the *CORs* under cold stress.

CONCLUSION

Based on the genome-wide identification and functional characterization of the proteins encoded by the *CBF* genes, a total of 69 *CBF* genes were identified among the three diploid cotton species, in which 29, 25, and 15 *CBF* proteins were identified in *G. herbaceum*, *G. thurberi*, and *G. australe*, respectively. The RNA data and the expression profiling of the *CBF* genes revealed that higher proportions were upregulated under cold stress conditions. Moreover, overexpression of the *Gth17439* (*GthCBF4*) gene in the model plant, *Arabidopsis*, revealed that the ability of the GthCBF4-overexpressed plants to tolerate cold stress was higher compared to the wild types, as evident in the germination, root growth, and induction of various stress-responsive genes. The results, therefore, provide fundamental information for future exploration of the *CBF* genes in the development of more robust cotton germplasms, which are highly resilient to cold and or chilling stress.

REFERENCES

- Ambawat, S., Sharma, P., Yadav, N. R., and Yadav, R. C. (2013). MYB transcription factor genes as regulators for plant responses: an overview. *Physiol. Mol. Biol. Plants* 19, 307–321. doi: 10.1007/s12298-013-0179-1
- Artico, S., Nardeli, S. M., Brilhante, O., Grossi-de-sa, M. F., and Alves-ferreira, M. (2010). Identification and evaluation of new reference genes in *Gossypium hirsutum* for accurate normalization of real-time quantitative RT-PCR data. *BMC Plant Biol.* 10:49. doi: 10.1186/1471-2229-10-49
- Berrocal-lobo, M. (2016). Plant tissue trypan blue staining during phytopathogen infection. *Bio Protoc.* 6:e2078. doi: 10.21769/BioProtoc.2078
- Bhatnagar-Mathur, P., Vadez, V., and Sharma, K. K. (2008). Transgenic approaches for abiotic stress tolerance in plants: retrospect and prospects. *Plant Cell Rep.* 27, 411–424. doi: 10.1007/s00299-007-0474-9
- Bo, H., Longguo, J. I. N., and Jinyuan, L. I. U. (2007). Molecular cloning and functional characterization of a DREB1 / CBF-like gene (GhDREB1L) from cotton. *Sci. China Ser. C* 50, 7–14. doi: 10.1007/s11427-007-010-8

DATA AVAILABILITY STATEMENT

The original contributions presented in the study are included in the article/**Supplementary Material**, further inquiries can be directed to the corresponding author/s.

AUTHOR CONTRIBUTIONS

JL, RM, and FL: conceptualization. JL, RM, YX, TW, and FL: methodology, software, formal analysis, investigation, writing – original draft preparation, and visualization. JL, RM, YX, TW, FL, and ZZ: validation. SA, KW, ZZ, XC, and FL: resources, supervision, project administration, and funding acquisition. JL, RM, YX, JK, EO, TW, and FL: data curation. JL, RM, YX, TW, JZ, YH, SA, KW, ZZ, XC, and FL: writing – review and editing. All authors have read and agreed to the published version of the manuscript.

FUNDING

This research was funded by the National Natural Science Foundation of China (32072023 and 32171994), Central Public-Interest Scientific Institution Basal Research Fund (1610162021017), and National Key R&D Program of China (2021YFE0101200).

ACKNOWLEDGMENTS

We are grateful for the support of the research group during this research work.

SUPPLEMENTARY MATERIAL

The Supplementary Material for this article can be found online at: <https://www.frontiersin.org/articles/10.3389/fpls.2021.766130/full#supplementary-material>

- Bruce, T. J. A., Matthes, M. C., Napier, J. A., and Pickett, J. A. (2007). Stressful “memories” of plants: evidence and possible mechanisms. *Plant Sci.* 173, 603–608. doi: 10.1016/j.plantsci.2007.09.002
- Cai, X., Magwanga, R. O., Xu, Y., Zhou, Z., Wang, X., Hou, Y., et al. (2019). Comparative transcriptome, physiological and biochemical analyses reveal response mechanism mediated by CBF4 and ICE2 in enhancing cold stress tolerance in *Gossypium thurberi*. *AoB Plants*. 11:plz045. doi: 10.1093/aobpla/plz045
- Chaurasiya, P. C., and Singh, S. (2019). A review report: Low temperature stress for crop production. *Int. J. Pure App. Biosci.* 6, 575–598. doi: 10.18782/2320-7051.3031
- Chen, C., Chen, H., Zhang, Y., Thomas, H. R., Frank, M. H., He, Y., et al. (2020). TBtools: an integrative toolkit developed for interactive analyses of big biological data. *Mol. Plant* 13, 1194–1202. doi: 10.1016/j.molp.2020.06.009
- Chinnusamy, V., Ohta, M., Kanrar, S., Lee, B., Hong, X., Agarwal, M., et al. (2003). ICE1: a regulator of cold-induced transcriptome and freezing tolerance in *Arabidopsis*. *Genes Dev.* 17, 1043–1054. doi: 10.1101/gad.1077503

- Chinnusamy, V., Zhu, J., and Zhu, J. (2010). Gene regulation during cold stress acclimation in plants. *Methods Mol. Biol.* 639, 39–55. doi: 10.1007/978-1-60761-702-0_3
- Clough, S. J., and Bent, A. F. (1999). Floral dip: a simplified method for *Agrobacterium*-mediated transformation of *Arabidopsis thaliana*. *Plant J.* 16, 735–743.
- Colebrook, E. H., Thomas, S. G., Phillips, A. L., and Hedden, P. (2014). The role of gibberellin signalling in plant responses to abiotic stress. *J. Exp. Biol.* 217, 67–75. doi: 10.1242/jeb.089938
- Diouf, L., Pan, Z., He, S. P., Gong, W. F., Jia, Y. H., Magwanga, R. O., et al. (2017). High-density linkage map construction and mapping of salt-tolerant QTLs at seedling stage in upland cotton using genotyping by sequencing (GBS). *Int. J. Mol. Sci.* 18:2622. doi: 10.3390/ijms18122622
- Dupadahalli, K. (2014). A modified freeze-thaw method for the efficient transformation of *Agrobacterium tumefaciens*. *Curr. Sci.* 93:770.
- Finn, R. D., Bateman, A., Clements, J., Coghill, P., Eberhardt, Y., Eddy, S. R., et al. (2014). Pfam: The protein families database. *Nucleic Acids Res.* 42, D222–D230. doi: 10.1093/nar/gkt1223
- Gong, Z., Xiong, L., Shi, H., Yang, S., Xu, G., Chao, D., et al. (2020). Plant abiotic stress response and nutrient use efficiency. *Sci. China Life Sci.* 63, 635–674.
- Gruszka, D. (2015). DNA damage and repair in plants – from models to crops. *Front. Plant Sci.* 6:885. doi: 10.3389/fpls.2015.00885
- Haake, V. (2002). Transcription Factor CBF4 is a regulator of drought adaptation in *Arabidopsis*. *Plant Physiol.* 130, 639–648. doi: 10.1104/pp.006478
- Hajhashemi, S., Noedoost, F., Geuns, J. M. C., and Djalovic, I. (2018). Effect of cold stress on photosynthetic traits, carbohydrates, morphology, and anatomy in nine cultivars of *Stevia rebaudiana*. *Front. Plant Sci.* 9:1430. doi: 10.3389/fpls.2018.01430
- Hemantaranjan, A., Bhanu, A. N., Singh, M. N., Yadav, D. K., Patel, P. K., Singh, R., et al. (2014). Heat stress responses and thermotolerance. *Adv. Plants Agric. Res.* 1, 62–70. doi: 10.15406/apar.2014.01.00012
- Higo, K., Ugawa, Y., Iwamoto, M., and Korenaga, T. (1999). Plant cis-acting regulatory DNA elements (PLACE) database: 1999. *Nucleic Acids Res.* 27, 297–300. doi: 10.1093/nar/27.1.297
- Hoagland, D. R., and Arnon, D. I. (1950). The Water-Culture Method for Growing Plants Without Soil. *Calif. Agric. Exp. Station* 347:32.
- Horton, P., Park, K. J., Obayashi, T., Fujita, N., Harada, H., Adams-Collier, C. J., et al. (2007). WoLF PSORT: protein localization predictor. *Nucleic Acids Res.* 35, W585–W587. doi: 10.1093/nar/gkm259
- Hu, Y., Wu, Q., Peng, Z., Sprague, S. A., Wang, W., Park, J., et al. (2017). Silencing of OsGRXS17 in rice improves drought stress tolerance by modulating ROS accumulation and stomatal closure. *Sci. Rep.* 7:15950. doi: 10.1038/s41598-017-16230-7
- Hu, Z., Ban, Q., Hao, J., Zhu, X., Cheng, Y., Mao, J., et al. (2020). Genome-Wide Characterization of the C-repeat Binding Factor (CBF) gene family involved in the response to abiotic stresses in tea plant (*Camellia sinensis*). *Front. Plant Sci.* 11:921. doi: 10.3389/fpls.2020.00921
- Huang, G. T., Ma, S. L., Bai, L. P., Zhang, L., Ma, H., Jia, P., et al. (2011). Signal transduction during cold, salt, and drought stresses in plants. *Mol. Biol. Rep.* 39, 969–987. doi: 10.1007/s11033-011-0823-1
- Hussain, H. A., Hussain, S., Khaliq, A., Ashraf, U., Anjum, S. A., Men, S., et al. (2018). Chilling and drought stresses in crop plants: implications, cross talk, and potential management opportunities. *Front. Plant Sci.* 9:393. doi: 10.3389/fpls.2018.00393
- Jin, J. H., Wang, M., Zhang, H.-X., Khan, A., Wei, A.-M., Luo, D.-X., et al. (2018). Genome-wide identification of the AP2/ERF transcription factor family in pepper (*Capsicum annuum* L.). *Genome* 61, 663–674. doi: 10.1139/gen-2018-0036
- Jin, Y., Zhai, S., Wang, W., Ding, X., Guo, Z., Bai, L., et al. (2018). Identification of genes from the ICE-CBF-COR pathway under cold stress in Aegilops-Triticum composite group and the evolution analysis with those from Triticeae. *Physiol. Mol. Biol. Plants* 24, 211–229. doi: 10.1007/s12298-017-0495-y
- Kidokoro, S., Watanabe, K., Ohori, T., Moriwaki, T., Maruyama, K., Mizoi, J., et al. (2015). Soybean DREB1/CBF-type transcription factors function in heat and drought as well as cold stress-responsive gene expression. *Plant J.* 81, 505–518. doi: 10.1111/tpj.12746
- Kim, J. S., Mizoi, J., Yoshida, T., Fujita, Y., Nakajima, J., Ohori, T., et al. (2011). An ABRE promoter sequence is involved in osmotic stress-responsive expression of the DREB2A gene, which encodes a transcription factor regulating drought-inducible genes in *Arabidopsis*. *Plant Cell Physiol.* 52, 2136–2146. doi: 10.1093/pcp/pcr143
- Körner, C. (2016). Plant adaptation to cold climates. *F1000Res.* 5:2769. doi: 10.12688/f1000research.9107.1
- Kumar Verma, J., Wardhan, V., Singh, D., Chakraborty, S., and Chakraborty, N. (2018). Genome-wide identification of the alba gene family in plants and stress-responsive expression of the rice alba genes. *Genes (Basel)* 9:183. doi: 10.3390/genes9040183
- Kumar, S., Nayyar, H., Bhanwara, R. K., and Upadhyaya, H. D. (2010). Chilling stress effects on reproductive biology of chickpea. *J. Agric. Res.* 8, 1–14.
- Kumar, S., Stecher, G., and Tamura, K. (2016). MEGA7: Molecular Evolutionary Genetics Analysis Version 7.0 for Bigger Datasets. *Mol. Biol. Evol.* 33, 1870–1874. doi: 10.1093/molbev/msw054
- Lata, C., Yadav, A., and Pras, M. (2011). “Role of plant transcription factors in abiotic stress tolerance,” in *Abiotic Stress Response in Plants - Physiological, Biochemical and Genetic Perspectives*, eds A. Shanker and B. Venkateswarlu (London: IntechOpen), doi: 10.5772/23172
- Lei, X., Xiao, Y., Xia, W., Mason, A. S., Yang, Y., and Peng, M. (2014). RNA-Seq analysis of oil palm under cold stress reveals a different C-repeat binding factor (CBF) mediated gene expression pattern in *elaeis guineensis* compared to other species. *PLoS One* 9:e114482. doi: 10.1371/journal.pone.0114482
- Letunic, I., Doerks, T., and Bork, P. (2015). SMART: recent updates, new developments and status in 2015. *Nucleic Acids Res.* 43, D257–D260. doi: 10.1093/nar/gku949
- Liu, Q., Kasuga, M., Sakuma, Y., Abe, H., Miura, S., and Yamaguchi-shinozaki, K. (1998). Two Transcription Factors, DREB1 and DREB2, with an EREBP/AP2 DNA binding domain separate two cellular signal transduction pathways in drought- and low-temperature-responsive gene expression, respectively, in *Arabidopsis*. *Plant Cell* 10, 1391–1406.
- Liu, S., Lv, Z., Liu, Y., Li, L., and Zhang, L. (2018). Network analysis of ABA-dependent and ABA-independent drought responsive genes in *Arabidopsis thaliana*. *Genet Mol Biol.* 41, 624–637.
- Liu, X., Zhou, Y., Xiao, J., and Bao, F. (2018). Effects of Chilling on the Structure, Function and Development of Chloroplasts. *Front Plant Sci.* 9:1715. doi: 10.3389/fpls.2018.01715
- Lu, P., Magwanga, R. O., Guo, X., Kirungu, J. N., Lu, H., Cai, X., et al. (2018). Genome-Wide Analysis of Multidrug and Toxic Compound Extrusion (MATE) Family in Diploid Cotton, *Gossypium raimondii* and *Gossypium arboreum* and Its expression analysis under salt, cadmium and drought stress. *G3 (Bethesda)* 8, 2483–2500. doi: 10.1534/g3.118.200232
- Lv, K., Li, J., Zhao, K., Chen, S., Zhang, W., Liu, G., et al. (2020). Plant Science Overexpression of an AP2/ERF family gene, BpERF13, in birch enhances cold tolerance through upregulating CBF genes and mitigating reactive oxygen species. *Plant Sci.* 292:110375. doi: 10.1016/j.plantsci.2019.110375
- Ma, L. F., Zhang, J. M., Huang, G. Q., Li, Y., Li, X. B., and Zheng, Y. (2014). Molecular characterization of cotton C-repeat/dehydration-responsive element binding factor genes that are involved in response to cold stress. *Mol. Biol. Rep.* 41, 4369–4379. doi: 10.1007/s11033-014-3308-1
- Magwanga, R. O., Kirungu, J. N., Lu, P., Yang, X., Dong, Q., Cai, X., et al. (2019). Genome wide identification of the trihelix transcription factors and overexpression of Gh_A05G2067 (GT-2), a novel gene contributing to increased drought and salt stresses tolerance in cotton. *Physiol. Plant.* 167, 447–464. doi: 10.1111/ppl.12920
- Magwanga, R. O., Lu, P., Kirungu, J. N., Lu, H., Wang, X., Cai, X., et al. (2018b). Characterization of the late embryogenesis abundant (LEA) proteins family and their role in drought stress tolerance in upland cotton. *BMC Genet.* 19:6. doi: 10.1186/s12863-017-0596-1
- Magwanga, R. O., Lu, P., Kirungu, J. N., Dong, Q., Hu, Y., Zhou, Z., et al. (2018a). Cotton Late Embryogenesis Abundant (LEA2) Genes Promote Root Growth and Confers Drought Stress Tolerance in Transgenic *Arabidopsis thaliana*. *G3 (Bethesda)* 3, 2781–2803. doi: 10.1534/g3.118.200423
- Marquez-cedillo, L., Filichkin, T., Amundsen, K., Stockinger, E. J., Thomashow, M. F., Chen, T. H. H., et al. (2005). Structural, functional, and phylogenetic characterization of a large CBF gene family in barley. *Plant Mol. Biol.* 59, 533–551. doi: 10.1007/s11033-005-2498-2

- Miura, K., and Furumoto, T. (2013). Cold signaling and cold response in plants. *Int. J. Mol. Sci.* 14, 5312–5337. doi: 10.3390/ijms14035312
- Mohseni, S., Che, H., Djillali, Z., Dumont, E., Nankeu, J., and Danyluk, J. (2012). Wheat CBF gene family: identification of polymorphisms in the CBF coding sequence. *Genome* 881, 865–881. doi: 10.1139/gen-2012-0112
- Molugaram, K., and Rao, G. S. (2017). “ANOVA (Analysis of Variance),” in *Statistical Techniques for Transportation Engineering*, eds K. Molugaram and G. S. Rao (Oxford: Butterworth-Heinemann), 451–462. doi: 10.1016/b978-0-12-811555-8.00011-8
- Okamura, J. K., Caster, B., Villarroel, R., Van Montagu, M., and Jofuku, K. D. (1997). The AP2 domain of APETALA 2 defines a large new family of DNA binding proteins in *Arabidopsis*. *Proc. Natl. Acad. Sci. U. S. A.* 94, 7076–7081.
- Reddy, N., and Yang, Y. (2009). Extraction and characterization of natural cellulose fibers from common milkweed stems. *Polym. Eng. Sci.* 49, 2212–2217. doi: 10.1002/pen.21469
- Reyes, F. C., Sun, B., Guo, H., Gruis, D. F., and Otegui, M. S. (2020). *Agrobacterium tumefaciens*-Mediated Transformation of Maize Endosperm as a Tool to Study Endosperm. *Plant Physiol.* 153, 624–631. doi: 10.1104/pp.110.154930
- Rihan, H. Z., Al-issawi, M., and Fuller, M. P. (2017). Advances in physiological and molecular aspects of plant cold tolerance. *J. Plant Interact.* 12, 143–157. doi: 10.1080/17429145.2017.1308568
- Shi, Y., Ding, Y., and Yang, S. (2018). Molecular Regulation of CBF Signaling in Cold Acclimation. *Trends Plant Sci.* 23, 623–637. doi: 10.1016/j.tplants.2018.04.002
- Siddiqua, M., and Nassuth, A. (2011). Vitis CBF1 and Vitis CBF4 differ in their effect on *Arabidopsis* abiotic stress tolerance, development and gene expression. *Plant Cell Environ.* 34, 1345–1359. doi: 10.1111/j.1365-3040.2011.02334.x
- Stewart, J. J., Demmig-adams, B., Cohu, C. M., Wenzl, C. A., Muller, O., and Adams, W. W. III. (2016). Growth temperature impact on leaf form and function in *Arabidopsis thaliana* ecotypes from northern and southern Europe. *Plant Cell Environ.* 39, 1549–1558. doi: 10.1111/pce.12720
- Sunchung, P., Ainong, S., and Mo, B. (2020). Genome-wide identification and expression analysis of the CBF / DREB1 gene family in lettuce. *Sci. Rep.* 10:5733. doi: 10.1038/s41598-020-62458-1
- Tang, Y., Bao, X., Zhi, Y., Wu, Q., Guo, Y., Yin, X., et al. (2019). Overexpression of a MYB Family Gene, OsMYB6, Increases drought and salinity stress tolerance in transgenic rice. *Front. Plant Sci.* 10:168. doi: 10.3389/fpls.2019.00168
- Thakur, P., and Kumar, S. (2010). Cold stress effects on reproductive development in grain crops: an overview. *Environ. Exp. Bot.* 67, 429–443. doi: 10.1016/j.envexpbot.2009.09.004
- Thalhammer, A., Bryant, G., Sulpice, R., Hinch, D. K., Planck, M., Plant, M., et al. (2014). Disordered cold regulated15 proteins protect chloroplast membranes during freezing through binding and folding, but do not stabilize chloroplast enzymes *in vivo*. *Plant Physiol.* 166, 190–201. doi: 10.1104/pp.114.245399
- Thomashow, M. F. (1999). Plant cold accliation: freezing tolerance genes and regulatory mechanisms. *Annu. Rev. Plant Physiol. Plant Mol. Biol.* 50, 571–599. doi: 10.1146/annurev.arplant.50.1.571
- Tondelli, A., Francia, E., Barabaschi, D., Pasquariello, M., and Pecchioni, N. (2011). Plant Science Inside the CBF locus in Poaceae. *Plant Sci.* 180, 39–45. doi: 10.1016/j.plantsci.2010.08.012
- Uemura, M. (2014). Plant plasma membrane proteomics for improving cold tolerance. *Front. Plant Sci.* 4:90. doi: 10.3389/fpls.2013.00090
- Virdi, A. S., Singh, S., and Singh, P. (2015). Abiotic stress responses in plants: roles of calmodulin-regulated proteins. *Front. Plant Sci.* 6:809. doi: 10.3389/fpls.2015.00809
- Wang, D.-Z., Jin, Y.-N., Ding, X.-H., Wang, W.-J., Zhai, S.-S., Bai, L.-P., et al. (2017). Gene regulation and signal transduction in the ICE-CBF-COR signaling pathway during cold stress in plants. *Biochemistry (Mosc)* 82, 1103–1117. doi: 10.1134/S0006297917100030
- Wang, P., Chen, X., Guo, Y., Zheng, Y., Yue, C., and Yang, J. (2019). Identification of CBF Transcription factors in tea plants and a survey of potential CBF target genes under low temperature. *Int J Mol Sci.* 20:5137.
- Wang, Q., Guan, A.Y., Wu, A.Y., Chen, H., Chen, A.F., and Chu, A.C. (2008). Overexpression of a rice OsDREB1F gene increases salt, drought, and low temperature tolerance in both *Arabidopsis* and rice. *Plant Mol. Biol.* 67, 589–602. doi: 10.1007/s11103-008-9340-6
- Xiong, L., Schumaker, K. S., and Zhu, J. (2002). Cell Signaling during Cold, Drought, and Salt Stress. *Plant Cell* 14, S165–S184. doi: 10.1105/tpc.000596. S166
- Yu, X., Pijut, P. M., Byrne, S., Asp, T., Bai, G., and Jiang, Y. (2015). Plant Science Candidate gene association mapping for winter survival and spring regrowth in perennial ryegrass. *Plant Sci.* 235, 37–45. doi: 10.1016/j.plantsci.2015.03.003
- Zarka, D. G., Vogel, J. T., Cook, D., and Thomashow, M. F. (2003). Cold induction of *Arabidopsis* CBF genes involves multiple ICE (Inducer of CBF Expression) promoter elements and a cold-regulatory circuit that is desensitized by low temperature. *Plant Physiol.* 133, 910–918. doi: 10.1104/pp.103.027169.of
- Zhang, L., Xin, Z., Yu, X., Ma, C., and Liang, W. (2017). Osmotic Stress Induced Cell Death in Wheat Is Alleviated by Tauroursodeoxycholic Acid and Involves Endoplasmic Reticulum Stress – Related Gene Expression. *Front. Plant Sci.* 8:667. doi: 10.3389/fpls.2017.00667
- Zhang, Z., and Huang, R. (2010). Enhanced tolerance to freezing in tobacco and tomato overexpressing transcription factor TERF2/LeERF2 is modulated by ethylene biosynthesis. *Plant Mol. Biol.* 73, 241–249. doi: 10.1007/s11103-010-9609-4
- Zhao, C., Zhang, Z., Xie, S., Si, T., Li, Y., and Zhu, J. (2016). Mutational evidence for the critical role of CBF transcription factors in cold acclimation in *Arabidopsis*. *Plant Physiol.* 171, 2744–2759. doi: 10.1104/pp.16.00533
- Zhao, Q., Xiang, X., Liu, D., Yang, A., and Wang, Y. (2018). Tobacco transcription factor NtHLH123 confers tolerance to cold stress by regulating the NtCBF pathway and reactive oxygen species homeostasis. *Front. Plant Sci.* 9:381. doi: 10.3389/fpls.2018.00381

Conflict of Interest: The authors declare that the research was conducted in the absence of any commercial or financial relationships that could be construed as a potential conflict of interest.

Publisher's Note: All claims expressed in this article are solely those of the authors and do not necessarily represent those of their affiliated organizations, or those of the publisher, the editors and the reviewers. Any product that may be evaluated in this article, or claim that may be made by its manufacturer, is not guaranteed or endorsed by the publisher.

Copyright © 2021 Liu, Magwanga, Xu, Wei, Kirungu, Zheng, Hou, Wang, Agong, Okuto, Wang, Zhou, Cai and Liu. This is an open-access article distributed under the terms of the Creative Commons Attribution License (CC BY). The use, distribution or reproduction in other forums is permitted, provided the original author(s) and the copyright owner(s) are credited and that the original publication in this journal is cited, in accordance with accepted academic practice. No use, distribution or reproduction is permitted which does not comply with these terms.



Integration of Metabolome and Transcriptome Studies Reveals Flavonoids, Abscissic Acid, and Nitric Oxide Comodulating the Freezing Tolerance in *Liriope spicata*

Zhen Peng^{1,2}, Ye Wang¹, Wen-Tian Zuo¹, Yue-Rong Gao¹, Run-Zhi Li¹, Chun-Xin Yu¹, Zi-Yan Liu¹, Yi Zheng^{1,3}, Yuan-Yue Shen^{1,2} and Liu-Sheng Duan^{1,2*}

¹ College of Plant Science and Technology, Beijing University of Agriculture, Beijing, China, ² Beijing Key Laboratory for Agricultural Application and New Technique, Beijing, China, ³ Bioinformatics Center, Beijing University of Agriculture, Beijing, China

OPEN ACCESS

Edited by:

Andy Pereira,
University of Arkansas, United States

Reviewed by:

Magda Pál,
ELKH Agricultural Institute, Centre
for Agricultural Research, Hungary
Marta A. Fernandez Reyes,
University of Concepción, Chile

*Correspondence:

Liu-Sheng Duan
18601272095@163.com

Specialty section:

This article was submitted to
Plant Abiotic Stress,
a section of the journal
Frontiers in Plant Science

Received: 25 August 2021

Accepted: 14 December 2021

Published: 27 January 2022

Citation:

Peng Z, Wang Y, Zuo W-T,
Gao Y-R, Li R-Z, Yu C-X, Liu Z-Y,
Zheng Y, Shen Y-Y and Duan L-S
(2022) Integration of Metabolome
and Transcriptome Studies Reveals
Flavonoids, Abscissic Acid, and Nitric
Oxide Comodulating the Freezing
Tolerance in *Liriope spicata*.
Front. Plant Sci. 12:764625.
doi: 10.3389/fpls.2021.764625

Liriope spicata is an evergreen perennial ornamental groundcover with a strong freezing tolerance. However, the molecular mechanism underlying the freezing tolerance in *L. spicata* remains unclear. In this study, a comprehensive investigation of *L. spicata* freezing tolerance was conducted at the levels of physiology and biochemistry, metabolite, and transcript during the stress treatment. There were 581 unique differentially expressed metabolites (DEMs) and 10,444 unique differentially expressed genes (DEGs) between freezing treatment and normal cultured plant in leaves. Integrated analysis of metabolomics and transcriptomics showed that flavonoid biosynthesis, carbohydrate metabolism, amino acid metabolism, lipid metabolism, and signal transduction pathways were prominently enriched in response to the freezing stress in *L. spicata*. Now, we identified genes and metabolites involved in the flavonoid pathway, abscissic acid (ABA) biosynthesis, and the oxidative synthesis pathway of nitric oxide (NO), which may form a regulatory network and play a synergistic effect in osmotic adjustment, reactive oxygen species (ROS) homeostasis, and stomatal closure under freezing stress. These results offer a comprehensive network of flavonoids, ABA, and NO comodulating the freezing tolerance in *L. spicata*.

Keywords: *Liriope spicata*, freezing stress, metabolomics, transcriptomics, flavonoids, ABA, NO

INTRODUCTION

Freezing stress (<0°C) is a primary factor that determines plant geographic distribution and restrains the choice of plant species in the landscape design of the ground cover. The freezing temperature forces the leaves of most groundcovers to wither, reducing the ornamental value and resulting in a large area of exposed soil, causing ecosystem problems such as flying dust. To solve the contradiction between the green landscape and the cold winter environment in the north, one of the key technologies urgently needed is to study and make full use of the rural groundcover resources with freezing tolerance. *Liriope spicata* is an evergreen perennial, tufted, or rhizomatous

ornamental groundcover in the *Asparagaceae* family. *L. spicata* is widely distributed and cultivated in vast areas of China, Japan, and Vietnam and introduced in several other countries, including the United Kingdom and United States. *L. spicata* has a strong freezing tolerance (able to survive the winter safely with green leaves even at -15°C outdoor temperature) and is the main groundcover in the cold winter in the northern China that forms green landscapes and suppresses ground dust. However, the mechanism underlying the freezing tolerance in *L. spicata* remains largely unknown.

Survival under cold stress requires the integration of adaptive metabolic, physiological, and molecular responses that are tightly associated with stress-related gene expression, enzyme activities, and the concentrations of primary and secondary metabolites (Chinnusamy et al., 2007; Guo et al., 2018; Ding et al., 2020). Cold stress affects membrane fluidity, thereby altering the structure and activity of membrane-localized proteins such as calcium (Ca^{2+}) channels (Yuan et al., 2018). Then, the cold signal is transduced to a regulatory network and triggers multiple corresponding cold responses in the cell (Guo et al., 2018; Yuan et al., 2018). The C-repeat binding factor/dehydration-responsive element-binding protein 1 (CBF/DREB1) dependent transcriptional regulatory pathway is essential for plant responses to cold stress (Jia et al., 2016; Shi et al., 2018). CBF/DREB1 is rapidly upregulated by cold stress and then activates the transcription of cold-responsive (COR) genes by binding to their promoters (Stockinger et al., 1997; Jia et al., 2016). Mitogen-activated protein kinase (MAPK) cascades, transcription factors (TFs), reactive oxygen species (ROS), flavonoids, nitric oxide (NO), and phytohormones such as abscisic acid (ABA) also play pivotal roles in the cold response process in plants (Shinkawa et al., 2013; Simontacchi et al., 2015; Schulz et al., 2016; Li H. et al., 2017; Zhao et al., 2017; Chen et al., 2018; Zhang et al., 2020).

Absciscic acid signaling plays important roles in plant development and adaptation to environmental stress. In the seedling stage, the transgenics of ABA receptor *PYL10*-overexpressed rice plants show a significantly higher survival rate under cold stress as compared with WT plants (Verma et al., 2019). MYB96-HHP (heptahelical protein) module integrates ABA-dependent and ABA-independent signals and activates the CBF pathway, ensuring plant adaptation to cold stress (Lee and Seo, 2015). Open stomata 1 (OST1)/sucrose non-fermenting 1 (SNF1) related protein kinase 2.6 (SnRK2.6) is a Ser/Thr protein kinase, which is activated by ABA and cold. OST1-overexpressing plants were more resistant, and *ost1* knockout lines were hypersensitive to freezing (Mustilli et al., 2002). ABA also interrelates with NO signaling. In guard cells, NO negatively regulates ABA signaling by inhibiting OST1/SnRK2.6 through S-nitrosylation (Wang et al., 2015).

Flavonoids are the main secondary metabolites that are involved in the plant defense abiotic response. In *Arabidopsis thaliana*, flavonoids are regarded as the determinants of freezing tolerance and cold-acclimation (CA) using the 20 mutant lines that are affected in the different steps of the flavonoid biosynthetic pathway (Schulz et al., 2016). The winter ecotype of *Brassica napus* is more resistant to low temperature compared

to the spring ecotype. In the metabonomic analysis of the *B. napus*, it was found that the content of flavonol metabolites such as quercetin and dihydromyricetin in the seedlings significantly increased after cold stress (Jian et al., 2020). In apple (*Malus domestica*), the accumulation of flavonols promotes the scavenging of ROS and plant survival under drought conditions (Wang et al., 2020). In tomato (*Solanum lycopersicum*), flavonols reduce the accumulation of ROS and modulate the ABA-dependent ROS burst in guard cells, facilitating stomatal opening to modulate leaf gas exchange (Watkins et al., 2017).

Nitric oxide is a small, gaseous signaling molecule that has been studied for decades in mammalian cells. Recent research findings have shown that NO regulates plant growth, enhances nutrient uptake, and activates stress tolerance mechanisms in most plants (Sun et al., 2021). NO is a negative regulator of the chlorophyll (Chl) catabolic pathway and positively maintains the stability of thylakoid membranes during leaf senescence (Liu and Guo, 2013). In tomato, an exogenous NO donor, sodium nitroprusside (SNP), protects the photosynthetic system from damage, thereby enhancing chilling tolerance (Diao et al., 2016). In tea plants (*Camellia sinensis* L.), exogenous NO increased flavonoid concentrations by promoting the transcription and activity of the flavonoid biosynthesis enzyme phenylalanine ammonia-lyase (PAL) in leaves (Li X. et al., 2017). NO is considered as a critical component of mediating phytohormonal actions, interacting with ROS, and modulating gene expression and protein activity under abiotic stress conditions. NO deficiency decreases the plant CA response, alters ABA content and signaling, and increases anthocyanin accumulation (Costa-Broseta et al., 2019). Emerging evidence implies that NO regulates plant growth, enhances nutrient uptake, and activates disease and stress tolerance mechanisms in most plants, making NO a potential tool for use in improving the yield and quality of horticultural crop species (Simontacchi et al., 2015; Sun et al., 2021).

In this study, we aimed to explore the molecular mechanisms at the transcriptome and metabolome levels from a wide perspective and sought the clues linking genes and marker metabolites in response to freezing stress. We globally analyzed the metabolic pathways involved in differentially expressed genes (DEGs) and metabolites when suffering freezing. In addition, we proposed a network formed by flavonoid biosynthesis, the ABA signaling pathway, and NO signaling, which comodulated the freezing tolerance in *L. spicata*.

MATERIALS AND METHODS

Plant Materials

Experiments were conducted in the greenhouse of Beijing University of Agriculture. The *L. spicata* accession BUA1032 was collected from the germplasm nursery after 2 years of good planting. The plants were divided into clusters of three buds and transplanted into containers using a 8-L loam-peat-roseite substrate. The plants were grown at $25/20^{\circ}\text{C}$ (day/night) temperature and 12/12 h (light/dark) photoperiods with fluorescent white light at $200\ \mu\text{mol m}^{-2}\text{ s}^{-1}$.

Freezing Stress Assays

The freezing tolerance program was performed in a freezing chamber. Before freezing stress, the plants were pretreated at 4°C for 5 days [cold-acclimated (CA)] or without cold treatment [non-acclimated (NA)], and the soil humidity was controlled at 40~50%. The freezing program began at 0°C, and then the temperature was dropped by 1°C per h until reaching -15°C. The temperature remained stable for 24 h, and samples were taken at 0, 2, 6, 12, and 24 h of -15°C freezing stress. After freezing treatment, the plants were then shifted to 4°C for 12 h before being transferred to 25°C normal conditions for 3 days of recovered growth. All materials were analyzed in three biological replicates in this study.

RNA Isolation and Transcriptomics Analysis

Liriope spicata samples were collected from control (25°C) and freezing-treated leaves (at 0, 2, 6, 12, and 24 h of -15°C freezing stress with CA) and quickly immersed in liquid nitrogen. Then, the high-quality total RNA (three biological replicates for each treatment) was isolated from liquid nitrogen frozen leaves using the TRIzol method, and high-throughput sequencing was implemented on an Illumina HiSeq 2500 platform. After filtering raw data, the transcripts were assembled with the Trinity software (Grabherr et al., 2011) to obtain the long-contig transcriptome. Seven databases [NR, NT, Pfam, SwissProt, GO, Kyoto Encyclopedia of Genes and Genomes (KEGG), and KOG] were used for annotating the gene function. The longest transcript in each gene was regarded as a unigene. Plant TFs were predicted using the iTAK software¹. The levels of gene expression were estimated by the fragments per kilobase of exon per million mapped reads (FPKM). DEGs were determined using DESeq2, with a screening threshold of $|\log_2(\text{Fold Change})| > 1$ and $p\text{-adj} < 0.05$ (Love et al., 2014). These DEGs were then used for enrichment analyses of the KEGG pathway².

Metabolite Extraction and Quasi-Targeted Metabolomics Analysis

Leaf material (six biological replicates for each treatment) was extracted two times with extraction solvent methanol/water [8:2 (v/v)] containing 0.1% formic acid at 0°C for 30 min. The solution was centrifuged at 12,000 rpm for 10 min at 4°C, and the supernatant samples were filtered with a 0.22-μm filter sterilizer before liquid chromatography coupled to electrospray tandem mass spectrometry (LC-MS/MS) analysis. Each experimental samples were taken in equal volumes and blended as QC samples. Blank sample is 53% methanol aqueous solution containing 0.1% formic acid instead of an experimental sample, the pretreatment process is the same as an experimental sample.

Liquid chromatography coupled to electrospray tandem mass spectrometry analyses were performed using an ExionLCTM AD system (SCIEX) coupled with a QTRAP[®] 6500+ mass spectrometer (SCIEX) in Novogene Co., Ltd. (Beijing, China).

For the positive polarity mode, samples were injected onto a BEH C8 Column (100 mm × 2.1 mm, 1.9 μm) using a 30 min linear gradient at a flow rate of 0.35 ml min⁻¹. The eluents were eluent A (0.1% formic acid-water) and eluent B (0.1% formic acid-acetonitrile). The solvent gradient was set as follows: 5% B, 1 min; 5–100% B, 24.0 min; 100% B, 28.0 min; 100–5% B, 28.1 min; and 5% B, 30 min. For the negative polarity mode, samples were injected onto a HSS T3 Column (100 mm × 2.1 mm) using a 25 min linear gradient at a flow rate of 0.35 ml min⁻¹. The eluents were eluent A (0.1% formic acid-water) and eluent B (0.1% formic acid-acetonitrile). The solvent gradient was set as follows: 2% B, 1 min; 2–100% B, 18.0 min; 100% B, 22.0 min; 100–5% B, 22.1 min; and 5% B, 25 min. QTRAP[®] 6500+ mass spectrometer was operated in a positive polarity mode with curtain gas of 35 psi, collision gas of medium, ion spray voltage of 5,500 V (positive) or -4,500 V (negative), temperature of 500°C, ion source gas of 1: 55, and ion source gas of 2: 55.

Based on the Novogene database, the sample metabolite detection was implemented in the multiple reaction monitoring (MRM) mode of the SCIEX QTRAP[®] 6500+ mass spectrometer. The compounds were quantified according to Q3 (production), and qualitative analysis was performed according to the retention time of the detected substance, the information of the production pair (Q1/Q3), and the secondary spectrum data. The data were analyzed by a principal component analysis (PCA), partial least squares-discriminant analysis (PLS-DA), and other multivariate statistical analyses to elucidate differences in metabolites between the samples.

Integrated Analysis of Metabolome and Transcriptome

The correlation analysis between the significantly different genes obtained by transcriptome analysis and the significantly different metabolites obtained by metabolomics analysis was based on the Pearson correlation coefficient to measure the degree of correlation between the different genes and the different metabolites. To determine the main biochemical pathways and signal transduction pathways in which differential metabolites and differential genes participate together, all differential genes and metabolites obtained were simultaneously mapped to the KEGG pathway database to obtain their common pathway information.

Quantitative PCR Assays

The RNA samples used for quantitative PCR (qPCR) assays were exactly the same as those used for RNA-sequencing (RNA-seq) assays. Then, the high-quality total RNA was reverse transcribed using a FastKing One Step RT-PCR kit (Tiangen, China; Cat#KR123). qPCR was performed with TB Green[®] Premix Ex TaqTM II (Takara, Japan; Cat#RR820A) on a CFX96 Touch Real-Time PCR Detection System (Bio-Rad, Hercules, CA, United States). The *ACT1* (Cluster-21629.42877) gene of *L. spicata* was used as an internal reference gene. The gene relative expression levels were calculated by the 2^(-ΔΔCT) method. All experiments were performed in three biological replicates. The

¹<http://itak.feilab.net/cgi-bin/itak/index.cgi>

²<https://www.kegg.jp/kegg/pathway.html>

primers used for qPCR analysis in this study are listed in **Supplementary Table 1**.

Analysis of Water Status in Leaf

The content of free water (FWC) and bound water (BWC) in plants is closely related to the existence of the cytoplasm. The refractometer method was used to detect the FWC and BWC of the samples. The leaves of *L. spicata* were collected at 9–10 a.m. and divided into two parts. One part was measured for the fresh weight (W_f) and dry weight (W_d) after being baked at 105°C to constant weight. The leaf total water content (TWC) was calculated as $(W_f - W_d)/W_f \times 100\%$. The other part (W_{f1}) was completely immersed in 10 ml sucrose solution (concentration of C_1 , weight of W). After sufficient water exchange, the concentration was measured as C_2 . FWC was calculated as $W \times (C_1 - C_2)/(W_{f1} \times C_2) \times 100\%$, and BWC was calculated as $TWC - FWC$.

Ion Leakage Assays

Ion leakage is a symptom of cold-induced membrane damage and is used as an indicator of freezing tolerance. Ion leakage assays were carried out as described in Lee and Zhu (2010) with slight modifications. The banded leaflets were quickly crosscut with a surgical blade and placed in 15-ml test tubes containing 10 ml of CO₂-free deionized water. The initial electrical conductivity value was recorded as S_0 . The samples were shaken at 22°C for 1 h, and the conductivity was measured as S_1 . After a water bath at 100°C for 30 min, the samples were shaken and cooled to 22°C, and the value was detected as S_2 . Ion leakage was calculated as $(S_1 - S_0)/(S_2 - S_0) \times 100\%$.

Measurement of Chl Relative Content

The leaf Chl relative content was measured by Chl meter SPAD-520 Plus (Konica Minolta, Marunouchi, Japan). The freezing treated plants were recovered at 25°C for 3 days before measuring Chl relative content. Each set of processed samples collected 50 data.

Determination of Antioxidant Enzyme Activity

After the freezing process, fresh leaves were immediately sampled to detect the antioxidant enzyme activity, including superoxide dismutase (SOD), peroxidase (POD), and catalase (CAT). The measurements were conducted using the SOD assay kit (Solarbio, China; Cat#BC0170), POD assay kit (Solarbio, China; Cat#BC0090), and CAT assay kit (Solarbio, China; Cat#BC0200) following the manufacturer's protocols. A UV-6000PC UV-Visible Spectrophotometer (Shanghai, China) was used to measure the absorbance values. Six biological replicates for each sample were carried out through the whole process.

Stomatal Aperture Assays

Microscopy images of stomatal phenotypes were obtained from freshly fixed samples and visualized using an electron fluorescence microscope (Olympus BX53, Tokyo, Japan). The abaxial epidermises of the living leaf were torn off with tweezers

and quickly fixed in absolute ethanol for 3 min. The stomata fluorescence was detected with an excitation wavelength of 488 nm. The stomatal aperture (width) was determined from the measurements of 40–60 stomata per treatment. Each experiment was replicated three times.

RESULTS

Physiological and Biochemical Responses to Freezing Stress

To evaluate the freezing tolerance in *L. spicata* accession BUA1032, we identified the phenotype of the materials cultivated in the non-protected field and greenhouse. The leaves are dark green in autumn and maintain viability, and can survive the winter safely (the lowest temperature reached −15°C or even below). *L. spicata* can maintain good plant morphology even when covered by heavy snow in winter (**Figures 1A–C**). In a controlled environment, −15°C freezing treatment was carried out under either CA or NA conditions. After 3 days of recovery of growth, the leaves of the freezing plants with CA endured the stress and remained green, but the quick-freezing leaves exhibited severe damage (**Figures 1D–F**).

The water status of the leaves was tested, and the results showed that the control leaves grown at 25°C contained 15.85% FWC and 55.22% BWC, while the leaves upon freezing treatment with CA contained 5.41% FWC and 53.40% BWC (**Figure 1G**). This result suggested that the prominent forms of high BWC and high ratio of BWC/FWC might have important roles in the freezing tolerance ability of *L. spicata*. The leaves upon freezing treatment with CA showed increased ion leakage compared to those upon treatment with CK (**Figure 1H**). Although the change reached a significant level between the leaves of CK (7.92%) and CA (16.76%), it was still safe for this plant. However, the ion leakage of quick-freezing samples (NA, −15°C, 2 h) increased to 70.13%, which reached a lethal degree (**Figure 1H**). After recovering at 25°C for 3 days, the CA plants still hold about 50 SPAD Chl content to keep the leaves green (**Figure 1I**). The determination of antioxidant enzyme activity showed that SOD, POD, and CAT were responded to freezing stress, which displayed higher levels in the CK and CA leaves compared to the NA (**Figures 1J–L**). These results indicate that *L. spicata* under CA conditions has a strong freezing tolerance to extreme low temperatures.

Transcriptomics Analysis of *L. spicata* Leaves in Response to Freezing Stress

To understand the molecular basis of the freezing tolerance in *L. spicata*, transcriptomics analysis was used to identify the DEGs in the leaves treated with −15°C freezing (CA before treatment) for duration times of 0, 2, 6, 12, and 24 h and control samples treated at 25°C. In this study, a total of 135.9 million clean reads were produced, and 315,382 transcripts were assembled through Trinity; 110,639 unigenes were functionally annotated. These genes were enriched mainly in cellular processes, environmental information processing,

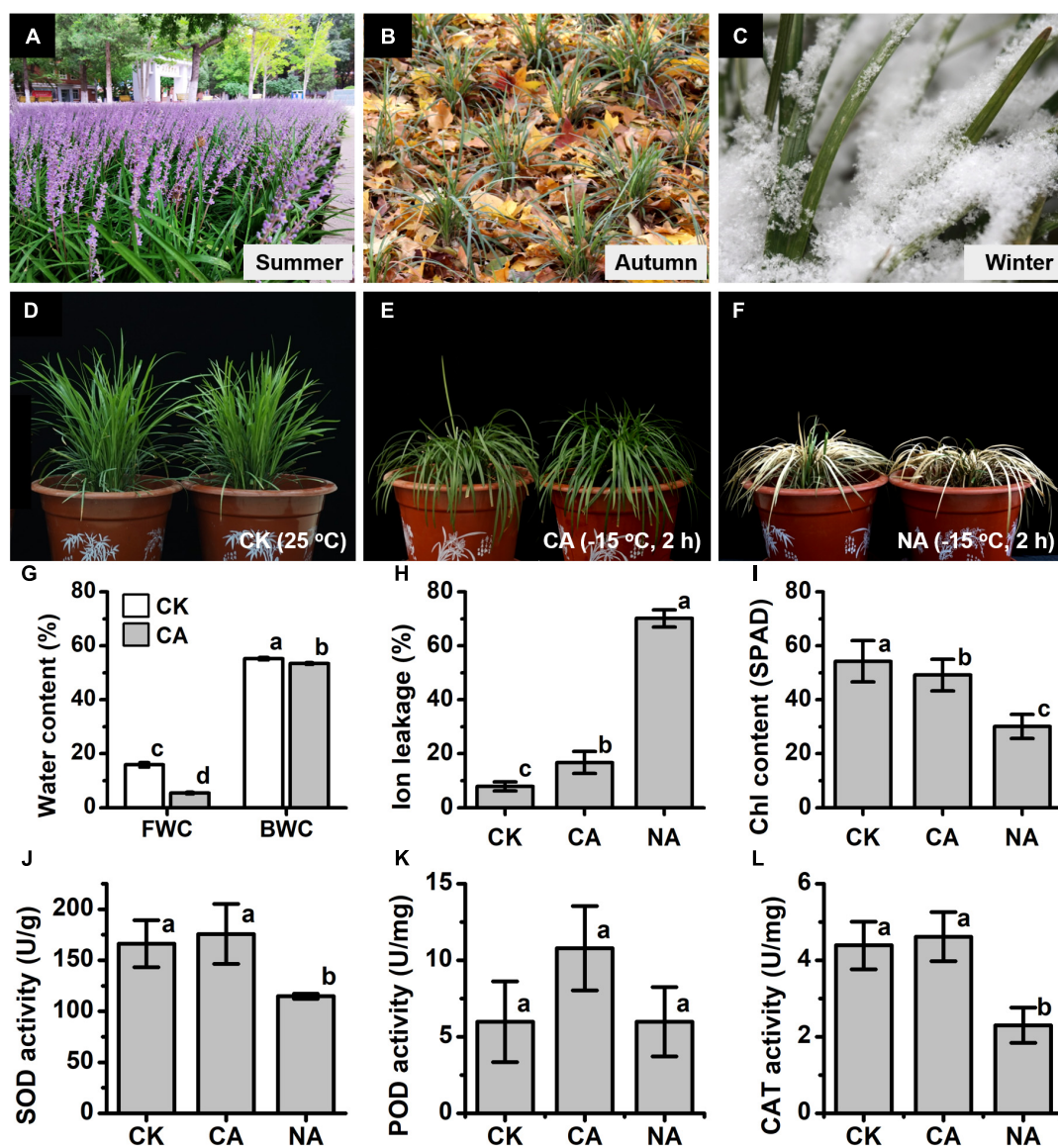
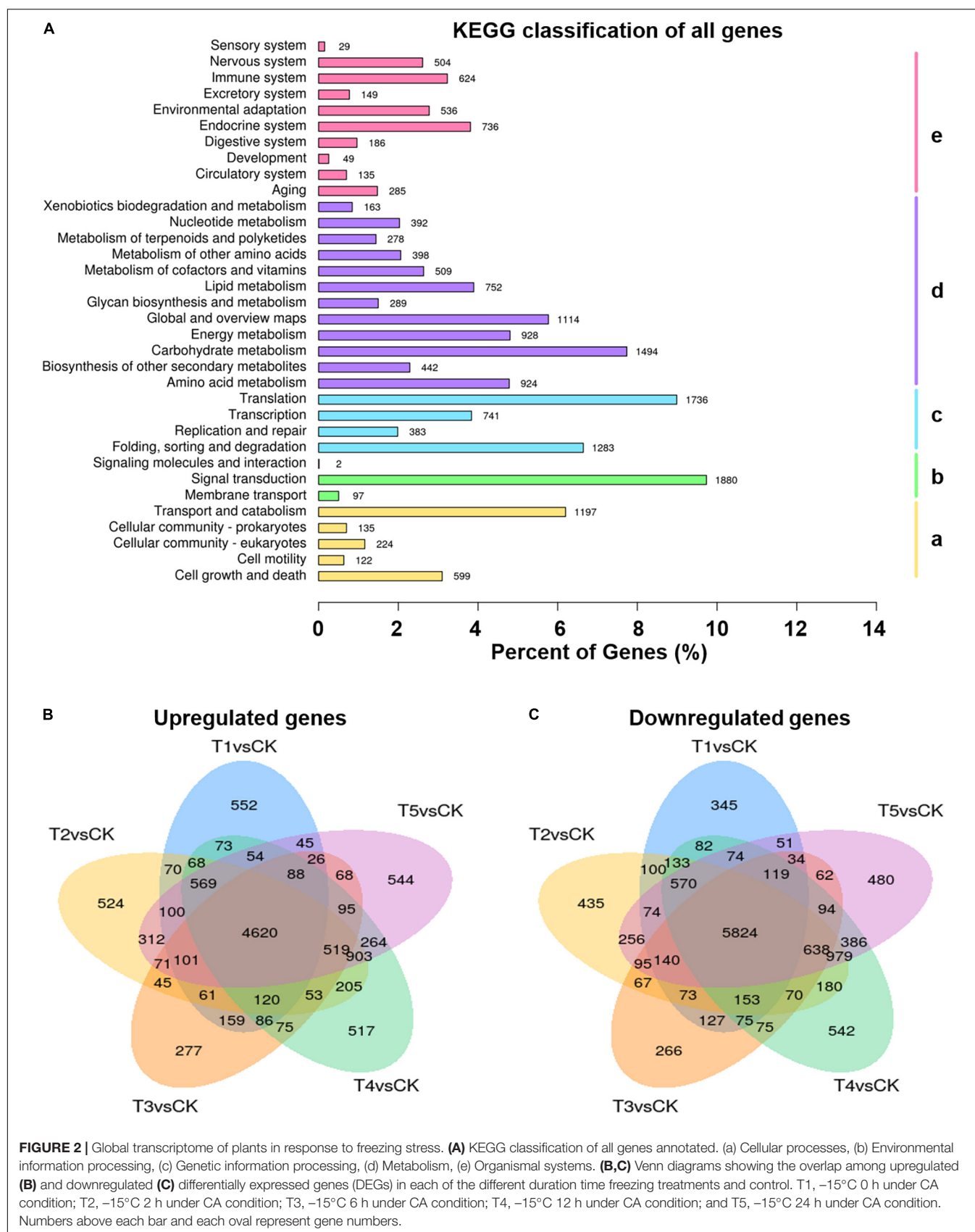


FIGURE 1 | Physiological and biochemical responses to the freezing stress in *Liriope spicata*. (A) Flowering landscape in summer. (B) Leaves of *L. spicata* do not turn yellow in autumn. (C) Leaves remain fresh and green when covered by heavy snow in winter. (D) Normal phenotype under 25°C (CK) condition. (E) Freezing phenotype under cold-acclimation (CA) conditions. (F) Freezing phenotype under non-acclimation (NA) conditions. (G) Water physiology. FWC, free water content; BWC, bound water content. (H) Ion leakage. (I) chlorophyll (Chl) relative content. (J) superoxide dismutase (SOD) enzyme activity. (K) Peroxidase (POD) enzyme activity. (L) Catalase (CAT) enzyme activity. CK, control samples that culture under 25°C; CA, freezing treatment samples under -15°C 2 h with 4°C CA for 3 days priority; NA, freezing treatment samples under -15°C 2 h without 4°C CA. The letters a,b,c in (G–L) represent significant differences among the samples; Student's *t*-test, $p < 0.05$.

genetic information processing, metabolism, and organismal systems (Figure 2A). With the DESeq2 software and the filter criteria $|\text{Log2FC}| \geq 1$, $p\text{-adj} < 0.05$, the DEGs were identified by a pairwise comparison between freezing treatment and control samples of *L. spicata* leaves (Supplementary Table 1). Furthermore, the vast majority of DEGs shared 4,620 upregulation and 5,824 downregulation between each freezing treatment and the control (Figures 2B,C), suggesting that a potentially common molecular mechanism is involved in the response to freezing stress.

Comparing DEGs between freezing samples and the control, KEGG enrichment analyses showed that the upregulated DEGs were specifically enriched in the pathways of “flavonoid biosynthesis (ko00941),” “flavone and flavonol biosynthesis (ko00944),” “fructose and mannose metabolism (ko00051),” “ascorbate and aldarate metabolism (ko00053),” “arginine and proline metabolism (ko00330),” and “cutin, suberin, and wax biosynthesis (ko00073)” (Supplementary Table 2). These results suggested that *L. spicata* accumulates osmotic adjustment substances to maintain cell homeostasis and produces a



thickened cell surface protection layer to achieve enhanced freezing resistance. The downregulated DEGs were abundant in “photosynthesis-antenna proteins (ko00196),” “plant-pathogen interaction (ko04626),” “linoleic acid metabolism (ko00591),” “alpha-linolenic acid metabolism (ko00592),” “fatty acid elongation (ko00062),” and “tryptophan metabolism (ko00380)” (Supplementary Table 3). These results imply that freezing stress restricts photosynthesis and prevents the degradation of unsaturated fatty acids. At the same time, the metabolism of tryptophan, the precursor of auxin biosynthesis, is also inhibited by the induction of freezing.

As TFs can regulate the expression of other genes and play an important role in regulating plant growth and increasing the freezing tolerance in plants, we further analyzed the expression profiles of TFs in all the samples. A total of 2,047 TFs were identified in the leaves exposed to low temperatures. Among these TFs, there were 830 genes whose expression level had changed significantly in at least one pairwise relationship that compared freezing to control samples, with 312 upregulated and 518 downregulated. These TFs were categorized into 20 main TF families, and most of these were abiotic stress-related families, such as AP2/ERF, bHLH, bZIP, HSF, MADS, MYB, NAC, and WRKY (Supplementary Table 4). There were 135 TFs upregulated in all the five freezing phases compared with the TFs at normal temperature, while 262 downregulated TFs were identified (Supplementary Table 4). These results provide some useful suggestions for further study of the functions of TFs in *L. spicata* freezing resistance.

Metabolomics Analysis Identifies Flavonoids as the Main Secondary Metabolites That Changed in *L. spicata* Leaves Under Freezing Stress

Leaf tissues of *L. spicata* with normal culture and freezing treatment were subjected to metabolomics assays using high-performance liquid chromatography with tandem mass spectrometric (HPLC-MS/MS). This analysis identified 581 metabolites in leaves. Via the KEGG pathway annotation, the metabolites were classified mainly as environmental information processing (32 annotated), genetic information processing (14 annotated), and metabolism (462 annotated) (Figure 3A). The PCA plot showed that the five freezing treatments were clearly separated from the control by PC1 and represented the altered accumulation of chemically related metabolites when suffering freezing stress (Figure 3B). By the criteria of a PLS-DA model $VIP > 1.0$, $FC > 2.0$ or $FC < 0.5$, and $p < 0.05$, 156, 169, 167, 165, and 190 significantly differentially expressed metabolites (DEMs) were detected in *L. spicata* leaves with five different lengths of freezing duration treatment (-15°C) compared with the control (25°C). Hierarchical clustering analysis showed that the enrichment patterns of freezing sample libraries were classified into the same cluster (Figure 3C). The KEGG pathway analysis of DEMs showed that these detections highlighted the enrichment in carbon fixation in photosynthetic organisms (map00710), flavone and flavonol biosynthesis (map00944), flavonoid biosynthesis (map00941), phenylpropanoid biosynthesis

(map00940), and lysine biosynthesis (map00300) ($p < 0.05$; Supplementary Table 5).

Accumulation of Flavonols in *L. spicata* Leaves Promotes Resistance to Freezing Stress

We screened the total DEMs and investigated the top 20-fold change metabolites. As a result, we found that 10 individual flavonoids were significantly upregulated in the freezing samples ($FC > 5$ and $p < 1 \times 10^{-3}$). Rutin and two kaempferol glycosides were upregulated more than 10-fold in all the five freezing samples compared with the control.

In this study, a total of 83 different flavonoids, including 26 upregulated metabolites and 7 downregulated metabolites ($VIP > 1.0$, $FC > 2.0$ or $FC < 0.5$, and $p < 0.05$), were identified to have significantly different accumulation after freezing stress. The fold changes of 33 flavonoids with significant differences in enrichment are shown in Figure 4A. Among these flavonoids, rutin and kaempferol 3-O-robinobioside showed the highest fold changes, with 14.9- to 20.1-fold and 13.1- to 20.1-fold, respectively (Figure 4B). Most genes and enzymes involved in the pathway lead to this chemical shift. Surprisingly, the flavonol biosynthesis pathway genes *C4H* (six transcripts), *CHS* (five transcripts), *CHI* (two transcripts), *F3H* (one transcript), *F3'H* (four transcripts), and *FLS* (two transcripts) consistently showed significantly increased expression levels when the plants were exposed to freezing stress (Figures 4A,C). We detected four types of quercetins (rutin, methylquercetin O-hexoside, quercetin O-malonylhexoside, and quercetin-3'-O-glucoside) and four types of kaempferols (kaempferol 3-O-robinobioside, kaempferol 7-O-D-glucopyranoside, kaempferol 3-D-glucopyranoside, and kaempferol 3-galactoside) were significantly enriched in flavonols under freezing treatments (Figure 4D). These results indicate that the flavonol biosynthesis pathway positively responds to the freezing stress in *L. spicata*.

Integrated Analysis of Absciscic Acid Responding to the Freezing Stress in *L. spicata*

Given that ABA is important in the response to abiotic stress in plants, we integratively analyzed changes in ABA biosynthesis and signaling pathway gene expression and ABA content. We found that most genes related to the ABA biosynthetic pathway, such as *LUT5* (beta-ring hydroxylase), *ZEP* (zeaxanthin epoxidase), *NCED* (9-cis-epoxycarotenoid dioxygenase), *ABA2* (xanthoxin dehydrogenase), and *AAO3* (abscisic-aldehyde oxidase), showed a significantly increased expression under freezing stress (Figure 5A). Moreover, the expression of the violaxanthin de-epoxidase (*VDE*) gene, which catalyzes the conversion of violaxanthin to zeaxanthin at the lumen side of the thylakoids, was decreased (Figures 5A,C). The expression patterns of these genes suggest that the pathway is conducive to the enrichment of ABA. The LC-MS results showed that the ABA content continued to increase and reached an extremely significant level of enrichment at T2 and

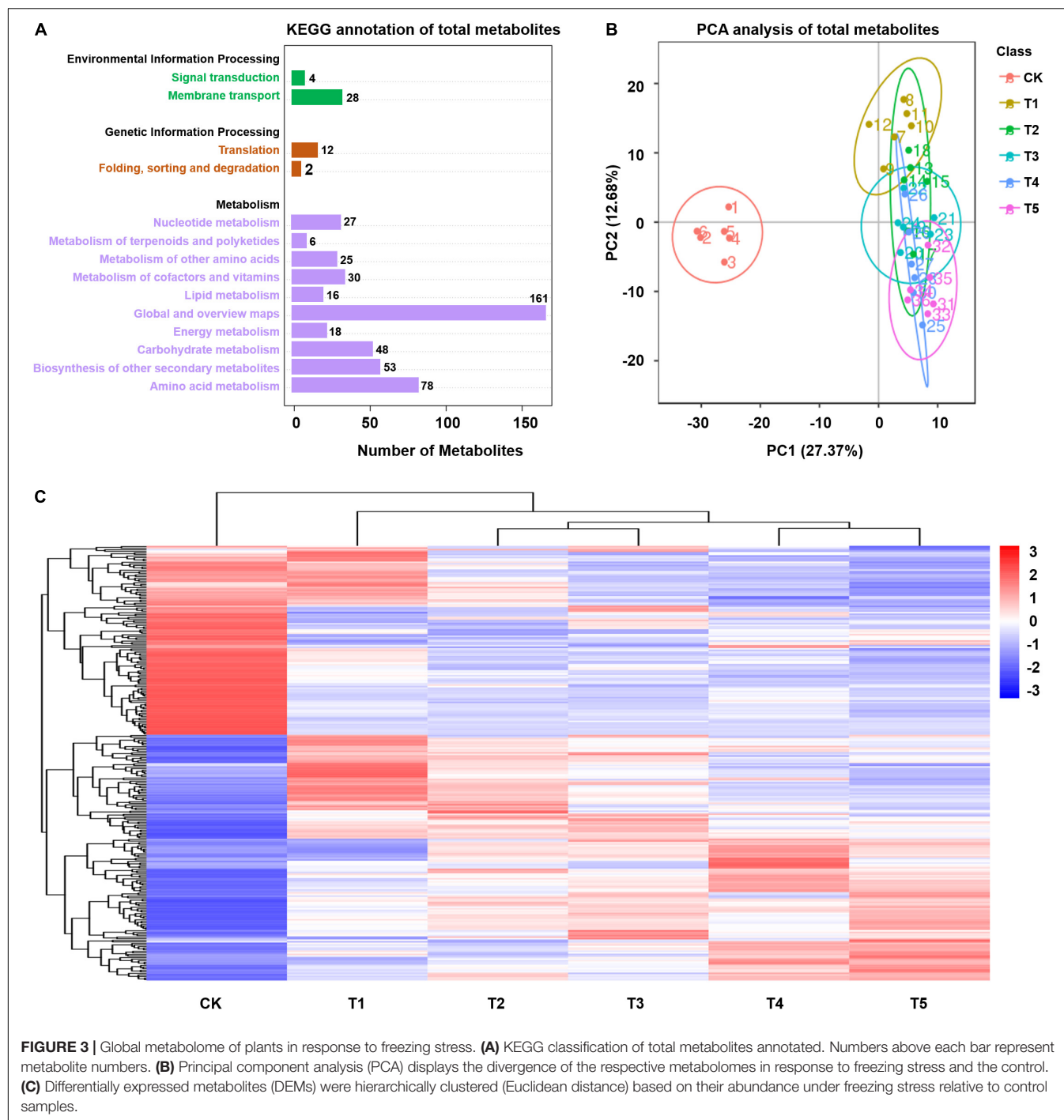


FIGURE 3 | Global metabolome of plants in response to freezing stress. **(A)** KEGG classification of total metabolites annotated. Numbers above each bar represent metabolite numbers. **(B)** Principal component analysis (PCA) displays the divergence of the respective metabolomes in response to freezing stress and the control. **(C)** Differentially expressed metabolites (DEMs) were hierarchically clustered (Euclidean distance) based on their abundance under freezing stress relative to control samples.

later periods of freezing treatment, with a 1.5–2-fold increase (Figure 5B). Genes involved in the ABA signal transduction pathway responded to the freezing stress in *L. spicata*. In this study, 18 ABA receptors, pyrabactin resistance 1/PYR1-like (PYR/PYL), were differentially expressed, with most of them downregulated when suffering freezing stress. Twenty-four PP2Cs (type 2C protein-phosphatases) were detected, and most were upregulated by freezing. Twenty-one SNF1-related protein kinase subfamily 2 (SnRK2) genes were identified, and most

were significantly induced. Eight of nine ABA-responsive element binding factor (ABF) genes displayed increased expression under freezing stress (Figures 5C,D).

One of the regulating factors of stomatal closure is the increase in ABA content in the plant. Here, we examined stomatal closure and measured the stomatal aperture (Figures 5E,F). The abaxial epidermis of leaves was quickly torn off and immediately put into absolute ethanol to fix the cell morphology after treatment. Under a fluorescence microscope, the CK (25°C) epidermis displayed

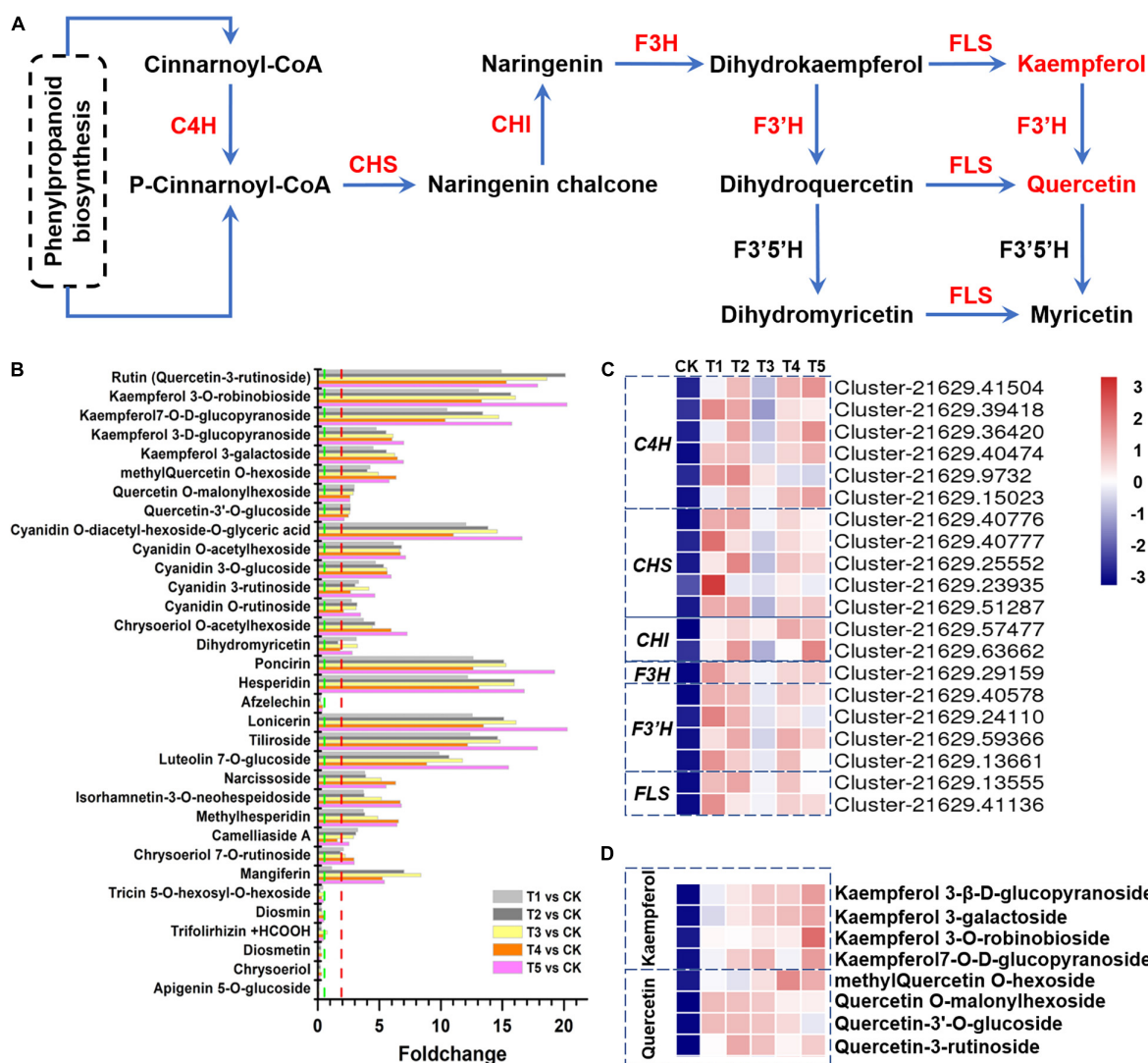


FIGURE 4 | Flavonoids in response to freezing stress. **(A)** Flavonol biosynthesis pathway and genes involved in this process. **(B)** The fold changes of flavonoid accumulation in plants subjected to each freezing stress compared with the control, including 26 upregulated and 7 downregulated flavonoid compounds. **(C)** The flavonol biosynthesis-associated genes were hierarchically clustered (Euclidean distance) based on their expression level. **(D)** The flavonols were hierarchically clustered (Euclidean distance) based on their abundance. C4H, cinnamate 4-hydroxylase; CHS, chalcone synthase; CHI, chalcone isomerase; F3H, flavanone 3-hydroxylase; F3'H, flavonoid 3'-hydroxylase; FLS, flavonol synthase.

opening stomata, and CA (-15°C 2 h) showed significantly narrower opening stomata (Figures 5E,F). However, the stomata in the quickly freezing samples of NA (-15°C 2 h) were almost closed (Figures 5E,F). These results illustrate an inverse relationship between the level of ABA and stomatal aperture, which are linked to altered rates of an ABA-dependent stomatal closure under freezing stress.

The Nitric Oxide Signaling Pathway May Regulate Compound Metabolism Under Freezing Stress

In the integrated analysis, we found that the arginine biosynthesis pathway (ko00220) and arginine metabolism pathway (ko0330)

were modulated by freezing stress. What attracted attention was that the oxidative pathway of NO synthesis by oxidizing arginine was upregulated (Figure 6A). The nitric oxide synthase (NOS, Cluster-21629.40348) gene, which encodes an enzyme that catalyzes arginine to NO, was significantly increased after the freezing stress in leaves (Figure 6B). A previous study found that NO inhibits the degradation of Chl (Liu and Guo, 2013). In this study, the expression of the *Pheophorbide a Oxygenase* (PAO, Cluster-21629.37954) gene, a key control point in the overall regulation of Chl degradation, was significantly reduced after 4 h freezing stress (Figure 6C) and negatively correlated (Pearson correlation coefficient $r = -0.52$) with the expression of the NOS gene. These results indicate that the degradation process of Chl was inhibited, which

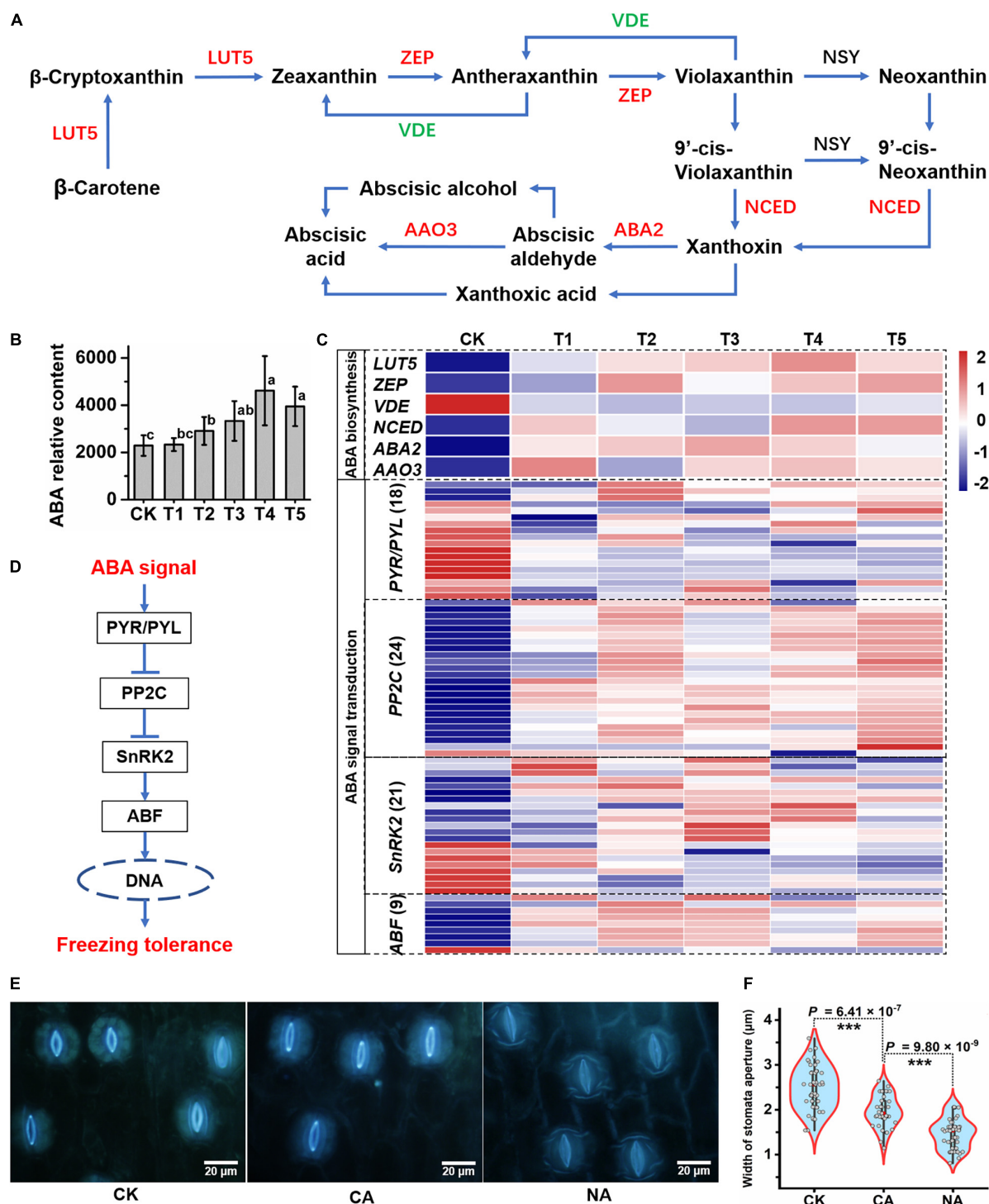


FIGURE 5 | The response of abscisic acid (ABA) biosynthesis to freezing stress. **(A)** The biosynthesis pathway of ABA was produced according to the KEGG database. LUT5, beta-ring hydroxylase; ZEP, zeaxanthin epoxidase; VDE, violaxanthin de-epoxidase; NCED, 9-cis-epoxycarotenoid dioxygenase; ABA2, xanthoxin dehydrogenase; AAO3, abscisic-aldehyde oxidase. **(B)** ABA relative content detected by liquid chromatography coupled to electrospray tandem mass spectrometry (LC-MS/MS) in each sample. The letters represent significant differences among the samples; Student's *t*-test, $p < 0.05$. **(C)** The identified ABA biosynthesis-associated genes and ABA signal transduction genes were hierarchically clustered (Euclidean distance) based on their expression level. **(D)** The pathway of ABA signaling transduction in plants. PYR1/PYL, pyrabactin resistance 1/PYR1-like; PP2C, type 2C protein-phosphatase; SnRK2, sucrose non-fermenting 1-related protein kinase subfamily 2; ABF, ABA-responsive element binding factors. **(E)** Stomatal closure and apertures of leaf abaxial epidermis are shown under control and freezing stress conditions. **(F)** Mean \pm SD of 40–60 stomata from the four separate experiments are reported as the width of stomatal aperture. Asterisks represent significant differences in stomatal aperture ($p < 0.001$; Student's *t*-test) between freezing-treated leaves and the control.

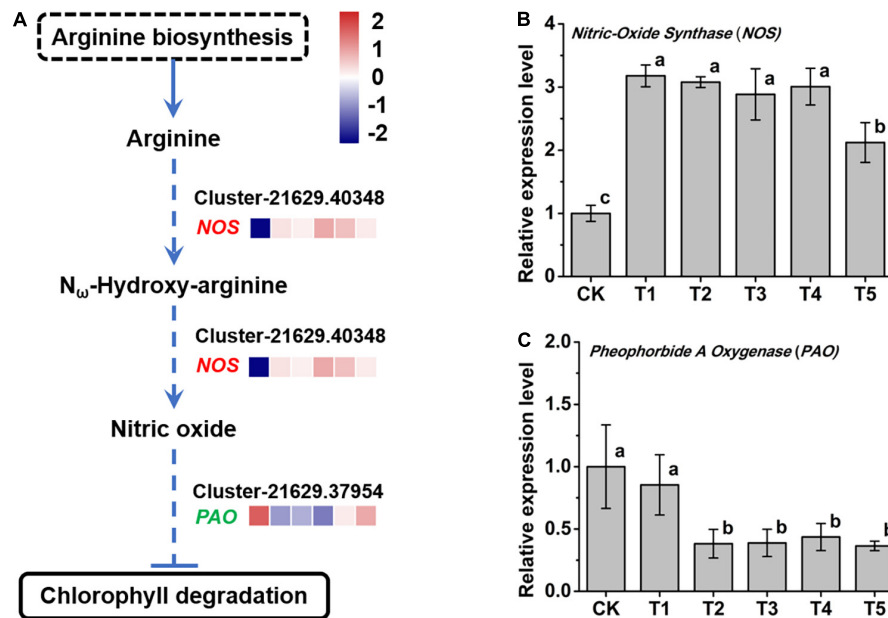


FIGURE 6 | The response of nitric oxide (NO) metabolism to freezing stress. **(A)** The biosynthesis pathway of NO was produced according to the KEGG database. **(B)** The expression of NOS, a NO synthase gene, was upregulated under freezing stress. **(C)** The expression of Pheophorbide a Oxygenase (PAO), a key gene in the Chl degradation pathway, was downregulated under freezing stress. The letters in **(B)** and **(C)** represent significant differences among the samples; Student's *t*-test, $p < 0.05$.

may explain the characteristics of *L. spicata* to stay green over the winter.

DISCUSSION

Molecular Networks Involved in the Freezing Tolerance in *L. spicata*

In this study, we performed an integrated analysis of the transcriptome and metabolome profiled from *L. spicata* leaves cultured at normal temperature and suffered from the freezing stress of five different durations. We identified 10,444 DEGs and 581 DEMs between the five freezing samples and the control, suggesting that freezing stress is a critical factor for transcriptomics and metabolomics data. The DEGs and DEMs were coenriched mainly in the pathways of carbohydrate metabolism, amino acid metabolism, cutin, suberin and wax biosynthesis, phytohormone biosynthesis, and secondary metabolite biosynthesis, such as flavonoid biosynthesis and stilbenoid, diarylheptanoid, and gingerol biosynthesis. These results suggested that freezing stress caused the comprehensive defense response of *L. spicata*, including the enrichment of osmotic adjustment substances and antioxidant compounds and signal transduction of phytohormones. ABA and indole-3-acetic acid (IAA) are important signaling molecules that regulate metabolic processes related to stress adaptation and induce stress resistance in plants (Verma et al., 2019). Numerous studies have shown that the ABA content increases under abiotic stress and induces the expression of downstream genes (Vaidya et al., 2019). The upregulated cellular defensive

substance synthesis pathways supported the maintenance of homeostasis in the cellular membrane to achieve enhanced freezing resistance (Liang Y. et al., 2020). Meanwhile, the downregulated DEGs were abundant in “photosynthesis-antenna proteins,” “plant-pathogen interaction,” “linoleic acid metabolism,” “alpha-linolenic acid metabolism,” “fatty acid elongation,” and “tryptophan metabolism,” implying that freezing stress reduced photosynthetic activity and IAA biosynthesis by the tryptophan pathway, which may constitute an energy-saving strategy under low CO₂ availability (Guo et al., 2021).

Transcription factors regulate the expression of other genes and play important roles in regulating plant growth and increasing cold tolerance in plants (Shi et al., 2018). In this study, we identified 830 TF genes that displayed a significantly different expression. These genes were classified mainly into the AP2/ERF, bHLH, bZIP, HSF, MADS, MYB, NAC, and WRKY families. In bermudagrass [*Cynodon dactylon* (L.) Pers], *CdERF1* is induced by cold, drought, and salinity stresses. The overexpression of *CdERF1* activates a subset of stress-related genes in transgenic *Arabidopsis*, such as *CBF2*, *pEARL11* (lipid transfer protein), *PER71* (POD), and lipid transfer protein (*LTP*), suggesting that *CdERF1* may be an ideal candidate in the effort to improve cold tolerance (Hu et al., 2020). In sweet orange (*Citrus sinensis*), most of the *CsbHLH* genes are responsive to cold stress, and the greatest upregulation gene *CsbHLH18* functions in the modulation of cold tolerance and the homeostasis of ROS by regulating antioxidant genes (Geng and Liu, 2018). *AtMYB15* is a transcriptional repressor of cold signaling because it negatively regulates *AtCBF3*, which is required for the freezing tolerance in *Arabidopsis*. Meanwhile, *AtMPK6*-induced

phosphorylation reduces the affinity of AtMYB15 binding to the AtCBF3 promoter (Kim et al., 2017). The homeostasis of the negative regulator MYB15 is controlled by an OST1-PUB25/26 module regulating the duration and amplitude of the cold response (Wang et al., 2019). Thus, TFs may have major roles in modulating cold-related gene expression. However, how different TFs coordinate to regulate the cold response network remains to be elucidated.

Flavonoids, Especially Flavonols, Enhance Freezing Tolerance

Flavonoid biosynthetic genes actively respond to abiotic stress and are the determinants of freezing tolerance and CA (Schulz et al., 2016; Watkins et al., 2017). Integrating the DEMs and DEGs as well as their co-expression modules, some of the modules can be potentially linked to the biosynthesis of flavonoids, including the flavone and flavonol biosynthesis pathway and flavonoid biosynthesis pathway. In this study, 83 different flavonoids, including 26 upregulated metabolites and 7 downregulated metabolites, were detected. Here, we detected that flavonol biosynthesis genes, such as *C4H*, *CHS*, *CHI*, *F3H*, *F3'H*, and *FLS*, were all upregulated by freezing stress. The most significant enrichment was rutin in *L. spicata* leaves under freezing stress (Figures 4A–D).

Rutin is an important flavonol of medicinal value and functions as an ROS scavenger and osmotic regulator (Gegotek et al., 2017). Analyzing mutant lines in the two *Arabidopsis* accessions that are affected in the different steps of the flavonoid biosynthetic pathway found that most flavonols and anthocyanins accumulate upon cold exposure, along with most transcripts encoding TFs and enzymes of the flavonoid biosynthetic pathway (Schulz et al., 2016), providing evidence for the functional role of flavonoids in plant CA (Schulz et al., 2016). *MYB12*, a TF gene that positively regulates rutin biosynthesis, is greatly induced by low temperature (Pandey et al., 2012). *MYB12*-overexpressing *Arabidopsis* lines show enhanced cold tolerance with higher root length and elevated levels of proline content and lower levels of malondialdehyde under cold stress conditions compared to wild-type plants (Zhou et al., 2015). In addition, flavonols also protect plants from other abiotic stresses to maintain survival. For example, the accumulation of flavonols can be promoted by MdHSA8a, a drought-responsive HSE, contribute to ROS scavenging, and help plants survive under drought conditions (Wang et al., 2020). When *Arabidopsis* is exposed to broadband UV-B, the flavonol biosynthesis pathway responds to UV-B stress and increases accumulation, promptly allowing plants to switch from growth to UV-B stress responses (Liang T. et al., 2020). However, the molecular network of flavonols that enhance *L. spicata* freezing tolerance and whether it is suitable as a marker metabolite of freezing tolerance remain to be explored in the future.

Abscisic Acid and Nitric Oxide May Respond to Freezing Stress

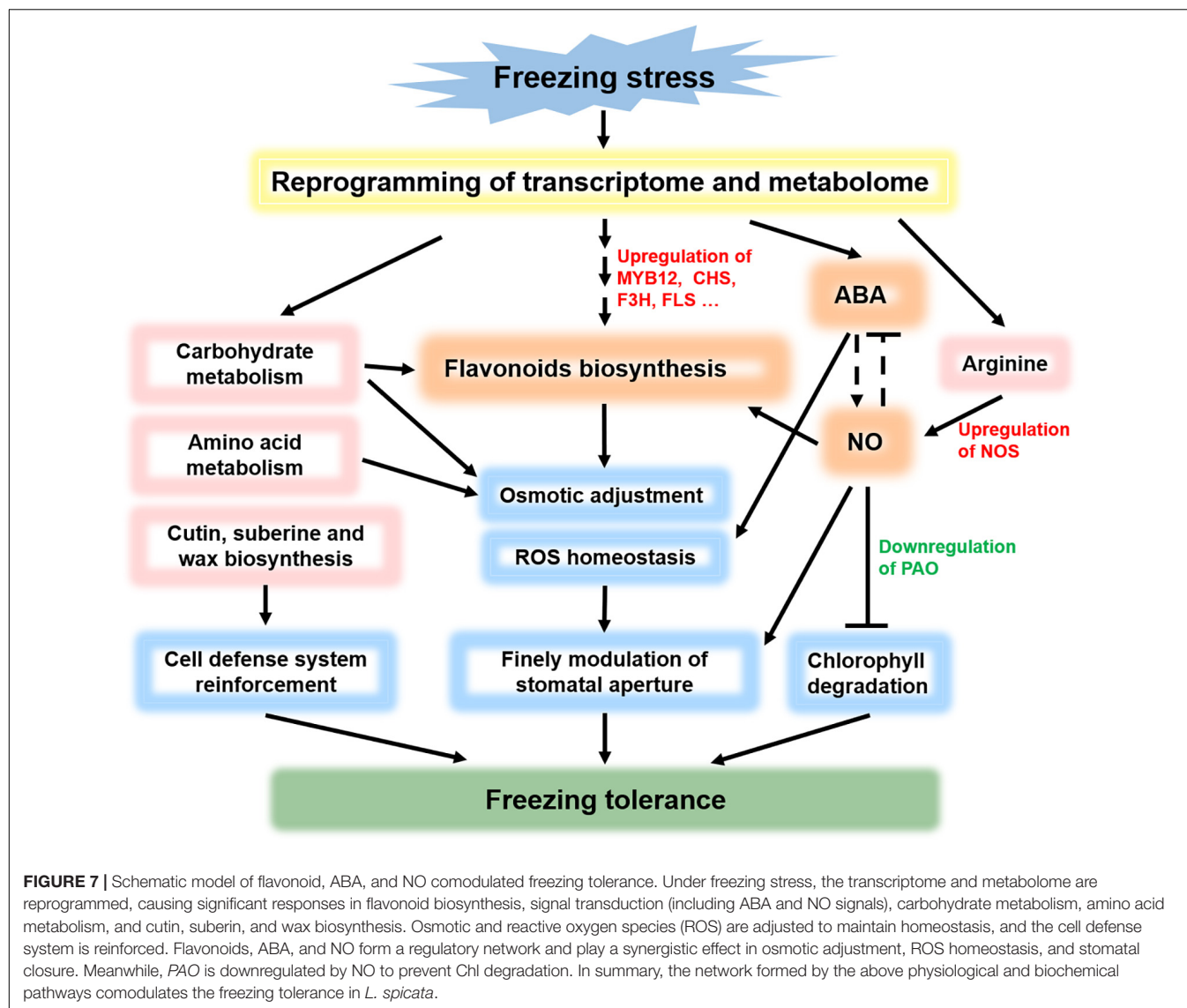
Abscisic acid plays versatile functions in regulating plant development and tolerance to various biotic and abiotic stresses.

The responses of plants to abiotic stresses are mediated mainly by ABA-dependent and ABA-independent signaling pathways, which are also intertwined (Lee and Seo, 2015). In *Arabidopsis*, the MYB96-HHP module integrates cold and ABA signaling to activate the CBF-COR pathway and response to freezing stress (Lee and Seo, 2015). In rice (*Oryza sativa*), ABA receptor PYL10 (Pyrabactin Resistance 1-like 10) overexpressing transgenic lines increase cold tolerance by maintaining a higher Chl content and membrane stability index and enriching a lower amount of H₂O₂ (Verma et al., 2019). In chilling-sensitive rice cells and seedlings, exogenous ABA can induce some levels of freezing tolerance, probably by eliciting mechanisms different from low temperature-induced CA (Shinkawa et al., 2013). In our study, the increase in ABA biosynthesis and signaling pathway gene expression and ABA content suggests that ABA is involved in the response to the freezing stress in *L. spicata* (Figures 5A–D).

Nitric oxide signaling may also respond to the freezing stress in *L. spicata*. The oxidative pathway of NO synthesis was detected, and the key gene *NOS* was upregulated under freezing stress (Figures 6A,B). A study with a *nos1/nao1* mutant showed that NO negatively regulates the activities of Chl catabolic enzymes, such as PAO, resulting in the preservation of Chl degradation and the maintenance of the stability of thylakoid membranes (Liu and Guo, 2013). Notably, we detected that the expression of *NOS* was upregulated and *PAO* was downregulated in *L. spicata* leaves, which maintained green color under freezing stress (Figures 1C,E, 6B,C). NO helps plants respond and survive under abiotic stress and is related to its interaction with ROS, the modulation of gene expression and protein activity (Simontacchi et al., 2015). Moreover, NO plays a role in regulating the biosynthesis of flavonols and inhibiting the closure of stomata (Li X. et al., 2017). Given the important roles of NO in regulating plant growth and activating stress tolerance mechanisms in most plants, NO is considered as a potential tool for use in improving the yield and quality of crops (Sun et al., 2021).

Flavonoids, Abscissic Acid, and Nitric Oxide May Play a Synergistic Effect to Comodulate Freezing Tolerance

Is there any connection among flavonoids, ABA, and NO in abiotic stress tolerance? A previous study found that ABA induces NO release in guard cells, and then NO inactivates SnRK2.6 to negatively regulate ABA signaling by S-nitrosylation of SnRK2.6 at a cysteine residue, resulting in kinase catalytic site closure and stomatal opening (Wang et al., 2015). However, NO is unlikely to be a key factor in ABA-induced rapid stomatal closure, but it allows fine tuning of stomatal aperture via different pathways (Van Meeteren et al., 2020). The regulation and feedback regulation between ABA and NO finely modulate stomatal closure under stress. In tea (*C. sinensis* L.) leaves, an increase in the endogenous concentration of NO induces the enrichment of flavonoids, and exogenous NO also increases flavonoids and NO levels dose-dependently (Li X. et al., 2017). Under stress, antioxidant flavonols accumulate in guard cells to scavenge ROS and maintain homeostasis. However, ABA induces stomatal closure by increasing ROS in guard cells. Studies



on tomatoes show that flavonols block the ABA-dependent ROS burst and facilitate stomatal opening to modulate leaf gas exchange (Watkins et al., 2017).

In summary, we propose a model in which flavonoids, ABA, and NO comodulate the freezing tolerance in *L. spicata* (Figure 7). Under freezing stress, the transcriptome and metabolome are reprogrammed, following the main significant response pathways of flavonoid biosynthesis, ABA biosynthesis, signal transduction, carbohydrate metabolism, amino acid metabolism, and cutin, suberine, and wax biosynthesis. Osmotics and ROS are adjusted to maintain homeostasis, and the cell defense system is reinforced. Flavonoids, ABA, and NO, which have all enhanced accumulation, may form a regulatory network and play a synergistic effect in osmotic adjustment, ROS homeostasis, and stomatal closure. Meanwhile, PAO, the key enzyme gene of Chl degradation, is downregulated by NO, resulting in the leaves remaining green under freezing stress. Overall, the network formed by the above physiological and

biochemical pathways comodulates the freezing tolerance in *L. spicata*.

CONCLUSION

In this study, the potential mechanism of the freezing tolerance of *L. spicata* was explored through the integration of metabolome and transcriptome studies. A total of 581 DEMs and 10,444 DEGs, including 830 TFs, were identified in leaves. The prominent response pathways of flavonoid biosynthesis, ABA biosynthesis and signal transduction, and NO signaling were characterized. The metabolite with the most significant increase in enrichment was rutin. The genes associated with flavonol biosynthesis and ABA biosynthesis, as well as the NOS gene, were found to be strongly increased by freezing stress. However, the Chl degradation gene PAO was significantly decreased. Furthermore, flavonols, ABA, and NO coordinate with each other

to regulate osmotic adjustment, ROS homeostasis, and stomatal closure in leaves for freezing tolerance. In summary, our results provide a network of flavonoids, ABA, and NO comodulating the freezing tolerance in *L. spicata*.

DATA AVAILABILITY STATEMENT

Data supporting the findings in this study are included in the article and **Supplementary Tables**. Further inquiries can be directed to the corresponding authors. The raw RNA-seq data generated in this study have been deposited in the National Center for Biotechnology Information (NCBI) Sequence Read Archive (SRA) database under accession number PRJNA761519.

AUTHOR CONTRIBUTIONS

L-SD conceived and designed the study. Y-YS edited the manuscript. YZ contributed to data analysis. ZP conducted the bioinformatic work and wrote the first draft. YW, W-TZ, and Y-RG performed the experiments. R-ZL, C-XY, and Z-YL revised the manuscript. All authors discussed the results and agreed to the published version of the manuscript.

REFERENCES

- Chen, L., Zhao, Y., Xu, S., Zhang, Z., Xu, Y., Zhang, J., et al. (2018). OsMADS57 together with OsTB1 coordinates transcription of its target OsWRKY94 and D14 to switch its organogenesis to defense for cold adaptation in rice. *New Phytol.* 218, 219–231. doi: 10.1111/nph.14977
- Chinnusamy, V., Zhu, J., and Zhu, J. K. (2007). Cold stress regulation of gene expression in plants. *Trends Plant Sci.* 12, 444–451. doi: 10.1016/j.tplants.2007.07.002
- Costa-Broseta, Á., Perea-Resca, C., Castillo, M.-C., Ruíz, M. F., Salinas, J., and León, J. (2019). Nitric oxide deficiency decreases C-repeat binding factor-dependent and -independent induction of cold acclimation. *J. Exp. Bot.* 70, 3283–3296. doi: 10.1093/jxb/erz115
- Diao, Q.-N., Song, Y.-J., Shi, D.-M., and Qi, H.-Y. (2016). Nitric oxide induced by polyamines involves antioxidant systems against chilling stress in tomato (*Lycopersicon esculentum* Mill.) seedling. *J. Zhejiang Univ. Sci. B* 17, 916–930. doi: 10.1631/jzus.B1600102
- Ding, Y., Shi, Y., and Yang, S. (2020). Molecular regulation of plant responses to environmental temperatures. *Mol. Plant* 13, 544–564. doi: 10.1016/j.molp.2020.02.004
- Gęgotek, A., Rybałowska-Kawałko, P., and Skrzydlewska, E. (2017). Rutin as a mediator of lipid metabolism and cellular signaling pathways interactions in fibroblasts altered by UVA and UVB radiation. *Oxid. Med. Cell Longev.* 2017:4721352. doi: 10.1155/2017/4721352
- Geng, J., and Liu, J.-H. (2018). The transcription factor CsbHLH18 of sweet orange functions in modulation of cold tolerance and homeostasis of reactive oxygen species by regulating the antioxidant gene. *J. Exp. Bot.* 69, 2677–2692. doi: 10.1093/jxb/ery065
- Grabherr, M. G., Haas, B. J., Yassour, M., Levin, J. Z., Thompson, D. A., Amit, I., et al. (2011). Full-length transcriptome assembly from RNA-Seq data without a reference genome. *Nat. Biotechnol.* 29, 644–652. doi: 10.1038/nbt.1883
- Guo, Q., Li, X., Niu, L., Jameson, P. E., and Zhou, W. (2021). Transcription-associated metabolomic adjustments in maize occur during combined drought and cold stress. *Plant Physiol.* 186, 677–695. doi: 10.1093/plphys/kiab050
- Guo, X., Liu, D., and Chong, K. (2018). Cold signaling in plants: insights into mechanisms and regulation. *J. Int. Plant Biol.* 60, 745–756. doi: 10.1111/jipb.12706

FUNDING

This work was financially supported by the Scientific Research Key Project of Beijing Municipal Commission of Education (KZ202110020027) and Scientific Research Common Project of Beijing Municipal Commission of Education (KM202110020009).

ACKNOWLEDGMENTS

We are grateful to Shu-Hua Yang and Yi-Ting Shi from the State Key Laboratory of Plant Physiology and Biochemistry, China Agricultural University, for providing helpful suggestions. Fluorescence electron microscopy observations were supported by the Key Laboratory of New Technology in Agricultural Application of Beijing.

SUPPLEMENTARY MATERIAL

The Supplementary Material for this article can be found online at: <https://www.frontiersin.org/articles/10.3389/fpls.2021.764625/full#supplementary-material>

- Hu, Z., Huang, X., Amombo, E., Liu, A., Fan, J., Bi, A., et al. (2020). The ethylene responsive factor CdERF1 from bermudagrass (*Cynodon dactylon*) positively regulates cold tolerance. *Plant Sci.* 294:110432. doi: 10.1016/j.plantsci.2020.110432
- Jia, Y., Ding, Y., Shi, Y., Zhang, X., Gong, Z., and Yang, S. (2016). The cbfs triple mutants reveal the essential functions of CBFs in cold acclimation and allow the definition of CBF regulons in *Arabidopsis*. *New Phytol.* 212, 345–353. doi: 10.1111/nph.14088
- Jian, H., Xie, L., Wang, Y., Cao, Y., Wan, M., Lv, D., et al. (2020). Characterization of cold stress responses in different rapeseed ecotypes based on metabolomics and transcriptomics analyses. *PeerJ* 8:e8704. doi: 10.7717/peerj.8704
- Kim, S. H., Kim, H. S., Bahk, S., Jonguk, A., Ji, Y. Y., Yean, K. J., et al. (2017). Phosphorylation of the transcriptional repressor MYB15 by mitogen-activated protein kinase 6 is required for freezing tolerance in *Arabidopsis*. *Nucleic Acids Res.* 45, 6613–6627. doi: 10.1093/nar/gkx417
- Lee, B.-H., and Zhu, J.-K. (2010). Phenotypic analysis of *Arabidopsis* mutants: electrolyte leakage after freezing stress. *Cold Spring Harb. Protocols* 2010:pdb.prot4970. doi: 10.1101/pdb.prot4970
- Lee, H. G., and Seo, P. J. (2015). The MYB96-HHP module integrates cold and abscisic acid signaling to activate the CBF-COR pathway in *Arabidopsis*. *Plant J.* 82, 962–977. doi: 10.1111/tpj.12866
- Li, H., Ding, Y., Shi, Y., Zhang, X., Zhang, S., Gong, Z., et al. (2017). MPK3- and MPK6-Mediated ICE1 phosphorylation negatively regulates ICE1 stability and freezing tolerance in *Arabidopsis*. *Dev. Cell* 43, 630–642.e4 doi: 10.1016/j.devcel.2017.09.025
- Li, X., Zhang, L., Ahammed, G. J., Li, Z.-X., Wei, J.-P., Shen, C., et al. (2017). Nitric oxide mediates brassinosteroid-induced flavonoid biosynthesis in *Camellia sinensis* L. *J. Plant Physiol.* 214, 145–151. doi: 10.1016/j.jplph.2017.04.005
- Liang, T., Shi, C., Peng, Y., Tan, H., Xin, P., Yang, Y., et al. (2020). Brassinosteroid-Activated BRI1-EMS-SUPPRESSOR 1 inhibits flavonoid biosynthesis and coordinates growth and UV-B stress responses in plants. *Plant Cell* 32:3224. doi: 10.1105/tpc.20.00048
- Liang, Y., Wang, S., Zhao, C., Ma, X., Zhao, Y., Shao, J., et al. (2020). Transcriptional regulation of bark freezing tolerance in apple (*Malus domestica* Borkh.). *Horticulture Res.* 7:205. doi: 10.1038/s41438-020-00432-8
- Liu, F., and Guo, F.-Q. (2013). Nitric oxide deficiency accelerates chlorophyll breakdown and stability loss of thylakoid membranes during dark-induced

- leaf senescence in *Arabidopsis*. *PLoS One* 8:e56345. doi: 10.1371/journal.pone.0056345
- Love, M. I., Huber, W., and Anders, S. (2014). Moderated estimation of fold change and dispersion for RNA-seq data with DESeq2. *Genome Biol.* 15:550. doi: 10.1186/s13059-014-0550-8
- Mustilli, A.-C., Merlot, S., Vavasour, A., Fenzi, F., and Giraudat, J. (2002). *Arabidopsis* OST1 protein kinase mediates the regulation of stomatal aperture by abscisic acid and acts upstream of reactive oxygen species production. *Plant Cell* 14, 3089–3099.
- Pandey, A., Misra, P., Chandrashekar, K., and Trivedi, P. K. (2012). Development of AtMYB12-expressing transgenic tobacco callus culture for production of rutin with biopesticidal potential. *Plant Cell Rep.* 31, 1867–1876. doi: 10.1007/s00299-012-1300-6
- Schulz, E., Tohge, T., Zuther, E., Fernie, A. R., and Hinch, D. K. (2016). Flavonoids are determinants of freezing tolerance and cold acclimation in *Arabidopsis thaliana*. *Sci. Rep.* 6:34027. doi: 10.1038/srep34027
- Shi, Y. T., Ding, Y. L., and Yang, S. H. (2018). Molecular regulation of CBF signaling in cold acclimation. *Trends Plant Sci.* 23, 623–637. doi: 10.1016/j.tplants.2018.04.002
- Shinkawa, R., Morishita, A., Amikura, K., Machida, R., Murakawa, H., Kuchitsu, K., et al. (2013). Absciscic acid induced freezing tolerance in chilling-sensitive suspension cultures and seedlings of rice. *BMC Res. Notes* 6:351. doi: 10.1186/1756-0500-6-351
- Simontacchi, M., Galatro, A., Ramos-Artuso, F., and Santa-Maria, G. E. (2015). Plant survival in a changing environment: the role of nitric oxide in plant responses to abiotic stress. *Front. Plant Sci.* 6:977. doi: 10.3389/fpls.2015.00977
- Stockinger, E. J., Gilmour, S. J., and Thomashow, M. F. (1997). *Arabidopsis thaliana* CBF encodes an AP2 domain-containing transcriptional activator that binds to the C-repeat/DRE, a cis-acting DNA regulatory element that stimulates transcription in response to low temperature and water deficit. *Proc. Natl. Acad. Sci. U S A.* 94:1035. doi: 10.1073/pnas.94.3.1035
- Sun, C., Zhang, Y., Liu, L., Liu, X., Li, B., Jin, C., et al. (2021). Molecular functions of nitric oxide and its potential applications in horticultural crops. *Horticulture Res.* 8:71. doi: 10.1038/s41438-021-00500-7
- Vaidya, A. S., Helander, J. D. M., Peterson, F. C., Elzinga, D., Dejonghe, W., Kaundal, A., et al. (2019). Dynamic control of plant water use using designed ABA receptor agonists. *Science* 366:eaaw8848. doi: 10.1126/science.aaw8848
- Van Meeteren, U., Kaiser, E., Malcolm Matamoros, P., Verdonk, J. C., and Aliniaefard, S. (2020). Is nitric oxide a critical key factor in ABA-induced stomatal closure? *J. Exp. Botany* 71, 399–410. doi: 10.1093/jxb/erz437
- Verma, R. K., Santosh Kumar, V. V., Yadav, S. K., Pushkar, S., Rao, M. V., and Chinnusamy, V. (2019). Overexpression of ABA receptor PYL10 gene confers drought and cold tolerance to Indica rice. *Front. Plant Sci.* 10:1488. doi: 10.3389/fpls.2019.01488
- Wang, N., Liu, W. J., Yu, L., Guo, Z. W., Chen, Z. J., Jiang, S. H., et al. (2020). HEAT SHOCK FACTOR A8a modulates flavonoid synthesis and drought tolerance. *Plant Physiol.* 184:1273. doi: 10.1104/pp.20.01106
- Wang, P., Du, Y., Hou, Y.-J., Zhao, Y., Hsu, C.-C., Yuan, F., et al. (2015). Nitric oxide negatively regulates abscisic acid signaling in guard cells by S-nitrosylation of OST1. *Proc. Natl. Acad. Sci. U S A.* 112, 613–618. doi: 10.1073/pnas.1423481112
- Wang, X., Ding, Y. L., Li, Z. Y., Shi, Y. T., Wang, J. L., Hua, J., et al. (2019). PUB25 and PUB26 promote plant freezing tolerance by degrading the cold signaling negative regulator MYB15. *Dev. Cell* 51, 222–235.e5. doi: 10.1016/j.devcel.2019.08.008
- Watkins, J. M., Chapman, J. M., and Muday, G. K. (2017). Absciscic acid-induced reactive oxygen species are modulated by flavonols to control stomata aperture. *Plant Physiol.* 175, 1807–1825. doi: 10.1104/pp.17.01010
- Yuan, P. G., Yang, T. B., and Poovaiah, B. W. (2018). Calcium signaling-mediated plant response to cold stress. *Int. J. Mol. Sci.* 19:3896. doi: 10.3390/ijms19123896
- Zhang, L., Jiang, X., Liu, Q., Ahammed, G. J., Lin, R., Wang, L., et al. (2020). The HY5 and MYB15 transcription factors positively regulate cold tolerance in tomato via the CBF pathway. *Plant Cell Environ.* 43, 2712–2726. doi: 10.1111/pce.13868
- Zhao, C., Wang, P., Si, T., Hsu, C.-C., Wang, L., Zayed, O., et al. (2017). MAP kinase cascades regulate the cold response by modulating ICE1 protein stability. *Dev. Cell* 43, 618–629.e5. doi: 10.1016/j.devcel.2017.09.024
- Zhou, M., Wang, C., Qi, L., Yang, X., Sun, Z., Tang, Y., et al. (2015). Ectopic expression of *Fagopyrum tataricum* FtMYB12 improves cold tolerance in *Arabidopsis thaliana*. *J. Plant Growth Regulation* 34, 362–371. doi: 10.1007/s00344-014-9472-7

Conflict of Interest: The authors declare that the research was conducted in the absence of any commercial or financial relationships that could be construed as a potential conflict of interest.

Publisher's Note: All claims expressed in this article are solely those of the authors and do not necessarily represent those of their affiliated organizations, or those of the publisher, the editors and the reviewers. Any product that may be evaluated in this article, or claim that may be made by its manufacturer, is not guaranteed or endorsed by the publisher.

Copyright © 2022 Peng, Wang, Zuo, Gao, Li, Yu, Liu, Zheng, Shen and Duan. This is an open-access article distributed under the terms of the Creative Commons Attribution License (CC BY). The use, distribution or reproduction in other forums is permitted, provided the original author(s) and the copyright owner(s) are credited and that the original publication in this journal is cited, in accordance with accepted academic practice. No use, distribution or reproduction is permitted which does not comply with these terms.



Transcriptome Analysis Revealed a Cold Stress-Responsive Transcription Factor, *PaDREB1A*, in *Plumbago auriculata* That Can Confer Cold Tolerance in Transgenic *Arabidopsis thaliana*

Wenji Li¹, Suping Gao^{1*}, Ting Lei^{1*}, Liqiong Jiang², Yifan Duan¹, Zian Zhao¹, Jiani Li¹, Lisha Shi¹ and Lijuan Yang¹

¹College of Landscape Architecture, Sichuan Agricultural University, Chengdu, China, ²Chengdu Academy of Agriculture and Forestry Sciences, Chengdu, China

OPEN ACCESS

Edited by:

Rosalyn B. Angeles-Shim,
Texas Tech University, United States

Reviewed by:

Joyce Cartagena,
Nagoya University,
Japan
Jing Zhang,
Nanjing Agricultural University, China

*Correspondence:

Suping Gao
gao_suping@sicau.edu.cn
Ting Lei
ting_lei85@sicau.edu.cn

Specialty section:

This article was submitted to
Plant Abiotic Stress,
a section of the journal
Frontiers in Plant Science

Received: 18 August 2021

Accepted: 09 February 2022

Published: 04 March 2022

Citation:

Li W, Gao S, Lei T, Jiang L, Duan Y,
Zhao Z, Li J, Shi L and Yang L (2022)
Transcriptome Analysis Revealed a
Cold Stress-Responsive Transcription
Factor, *PaDREB1A*, in *Plumbago*
auriculata That Can Confer Cold
Tolerance in Transgenic *Arabidopsis*
thaliana.
Front. Plant Sci. 13:760460.
doi: 10.3389/fpls.2022.760460

The tropical plant *Plumbago auriculata* can tolerate subzero temperatures without induction of apoptosis after cold acclimation in autumn, making it more cold tolerant than conventional tropical plants. In this study, we found that low temperatures significantly affected the photosynthetic system of *P. auriculata*. Using transcriptome sequencing, *PaDREB1A* was identified as a key transcription factor involved in the response to cold stress in *P. auriculata*. This transcription factor may be regulated by upstream JA signaling and regulates downstream *ERD4* and *ERD7* expression to resist cold stress. Overexpression of *PaDREB1A* significantly enhanced freezing resistance, protected the photosynthetic system, and enhanced the ROS scavenging mechanism under cold stress in *Arabidopsis thaliana*. Additionally, *PaDREB1A* significantly enhanced the expression of *CORs* and *CAT1* in *A. thaliana*, which further activated the downstream pathway to enhance plant cold tolerance. This study explored the possible different regulatory modes of *CBFs* in tropical plants and can serve as an important reference for the introduction of tropical plants to low-temperature regions.

Keywords: *Plumbago auriculata*, cold stress, transcriptome, C-repeat-binding factors, transgenic *Arabidopsis*

INTRODUCTION

According to the latest assessment report of the Intergovernmental Panel on Climate Change (IPCC), global climate change is intensifying. The frequent occurrence of extreme weather events, such as typhoons, heat waves, cold waves, and droughts, poses a severe threat to the vegetation in urban green spaces. With increasing globalization, urban dwellers are demanding more diverse urban green space vegetation (Hanson et al., 2021), and an increasing number of beautiful tropical plants are being introduced into urban green spaces. However, extreme weather, especially extremely low temperatures, poses a great threat to the survival of these tropical plants.

The photosystem is extremely sensitive to low temperatures and is an important indicator of whether plants have been subjected to cold stress (Chassot et al., 2001; Bilska and Sowiński, 2010). Cold stress has significant effects on the chloroplast structure, photosynthetic pigment content, photosynthetic rate, and other important physiological and biochemical parameters in plants. Photosynthesis in plants is severely impeded under cold stress. The main manifestation of this is inhibition of the biosynthesis of chlorophyll and the enzymatic activity associated with photosynthesis, leading to weakened photosynthesis. Under cold stress, the non-photochemical quenching (NPQ) of plants increases (Kramer et al., 2004; Ozturk et al., 2013), which hinders the heat dissipation pathway of photosystem II (PS II), resulting in the absorption of light energy by photosynthetic pigments far exceeding its consumption and resulting in photoinhibition (Liang et al., 2009). Whether photoinhibition occurs or not is often used as the evaluation standard of cold tolerance in plants (Long et al., 1994). The photosynthetic rate of most plants is significantly reduced by cold stress. Cold stress also affects chloroplast thylakoid membranes and reduces photochemical efficiency (Strauss et al., 2006). In addition, cold stress increases the accumulation of reactive oxygen species (ROS) in plants; ROS cause oxidative damage to DNA and proteins, damage the membrane structure, and decrease the fluidity of the cell membrane, affecting the exchange of information and materials. Cold stress also leads to the production of large amounts of malondialdehyde (MDA), which has cytotoxic effects (Neill et al., 2002; Dutilleul et al., 2003). Antioxidant enzymes protection systems in plants effectively scavenge ROS, and increased levels or activity of these enzymes can protect cell membranes from ROS damage. The three most important antioxidant enzymes that regulate the balance of ROS metabolism are superoxide dismutase (SOD), catalase (CAT), and peroxidase (POD; Wang et al., 2018).

The C-repeat-binding factor/dehydration-responsive element-binding factor 1 (CBF/DREB1) family is the most widely studied family of transcription factors associated with the low-temperature response of plants. Inducer of CBF expression 1 (ICE1) is a key transcriptional regulator of CBF genes, and together, they constitute the ICE1-CBF signaling pathway, which plays a critical role in the protection of plants against cold stress. CBF, belonging to the apetala2/ethylene response factor (AP2/ERF) family (Hannah, et al., 2006; Yamaguchi-Shinozaki, et al., 2006; Chinnusamy et al., 2010), binds to the promoter of the cold-related (COR) gene containing the dehydration-responsive element/C-repeat-binding element (DRE/CRT element) to induce the expression of the COR gene, which, in turn, affects the cold tolerance of plants. In the *Arabidopsis thaliana* genome, CBF1 (DREB1B), CBF2 (DREB1C), and CBF3 (DREB1A) have been successively identified as having high sequence similarity (Gilmour et al., 1998; Medina et al., 1999). Overexpression of CBF1-3 was found to significantly increase the frost resistance of *A. thaliana* (Jaglo-Ottosen et al., 1998). Approximately 100 COR genes were detected as being expressed (Stockinger et al., 1997; Liu et al., 1998), and knockdown of *cbf1* and *cbf3* resulted in a 60% reduction in frost resistance in *A. thaliana* compared to the wild type (Novillo et al., 2007).

To date, CBFs have been identified in *Brassica campestris*, *Triticum aestivum*, *Lycopersicon esculentum*, *Oryza sativa*, and *Zea mays* (Jaglo et al., 2001; Kasuga et al., 2004; Qin et al., 2004), and all these CBFs were found to exhibit cold-induced properties.

Plumbago auriculata is a tropical semishrub native to South Africa, and its optimum growth temperature is 30–35°C. This species has been widely planted as a garden plant in various countries around the world because of its beautiful and rare blue corolla and is considered to be a model for studying the evolution of heterostyly (Ferrero et al., 2009). It has also been shown that the secondary metabolite plumbagin from *P. auriculata* directly inhibits the key PI3K/Akt/mTOR pathway in cancer (Hafeez et al., 2013; Li et al., 2014). In our previous study, we found that although *P. auriculata*, as a tropical plant, is very sensitive to low temperatures and that 15°C can cause growth arrest (Li et al., 2020), after cold acclimation in autumn, the plant was able to survive the winter in Chengdu, China, with a minimum temperature of −3°C. This ability to tolerate low temperatures was shown to be much better than that of conventional tropical plants (Zhang et al., 2004). However, the key pathways and related transcription factor regulatory processes in this plant associated with the response to low temperatures have not been elucidated. In this study, we measured the physiological indices of *P. auriculata* under cold stress, and transcriptome sequencing was performed. We found that cold stress at 4°C significantly reduced the photosynthetic efficiency of *P. auriculata* leaves and increased the activity of protective enzymes related to ROS scavenging. Transcriptome analysis identified a key transcription factor, PaDREB1A, that was highly expressed under cold stress in *P. auriculata*. The sequence of this transcription factor shared high homology with genes from other species. Upregulated expression of COR genes was observed in not only *P. auriculata* but also *A. thaliana* (ERD4, ERD7, and COR15A) after overexpression of PaDREB1A. At the same time, the level of ROS scavenging was enhanced, and the ability of plants to cope with cold stress was improved in transgenic *A. thaliana*. This is the first complete report on the discovery, isolation, identification, and functional study of a *P. auriculata* gene. We believe that in the context of rapid globalization, this study can serve as a typical case study for introducing tropical plants into regions with relatively low temperatures and provides an important theoretical basis for further molecular breeding to improve the tolerance of tropical plants to cold stress.

MATERIALS AND METHODS

Plant Material Growth Conditions and Cold Stress Treatment

One-year-old *P. auriculata* plants were planted in a greenhouse at Sichuan Agricultural University (Chengdu, China) and placed in a phytotron for 6 weeks prior to the experiment. Wild-type (WT) *A. thaliana* (Columbia ecotype, Col-0) and T3 generation transgenic lines were cultivated in the phytotron for 4 weeks. The cultivation conditions were as follows: photoperiod, 8 h/16 h

(day/night); temperature, 25°C/20°C (day/night); light intensity 15,000lx; and relative humidity, 70%.

For determination of the chlorophyll content, chlorophyll fluorescence parameters, protective enzyme activities, and MDA content, cold stress treatments were performed for 0, 3, 8, 24, and 72 h at 4°C in the dark. For RNA-seq and RT-qPCR, cold stress treatments were performed at 0, 1, 3, 8, and 24 h at 4°C in the dark. For morphological observations of WT and transgenic lines of *A. thaliana* under cold stress, freezing treatment was performed for 8 h at −6°C in the dark, and photography and recording of the results were performed after 24 h of recovery at room temperature.

Determination of the Chlorophyll Content and Chlorophyll Fluorescence Parameters

The relative chlorophyll content of the leaves was measured directly using a SPAD-502 PLUS chlorophyll meter (Konica Minolta, Tokyo, Japan) via soil and plant analyzer development (SPAD) readings in the range of −9.9–199.9. Three plants were examined at each time point, and three points were randomly selected for each plant (Uddling et al., 2007).

Chlorophyll fluorescence parameters were measured using a Handy PEA plant efficiency analyzer (Hansatech, Norfolk, United Kingdom). Three plants were examined at each time point, and three points were randomly selected for each plant. Fv/Fm and PI abs were used to determine the photochemical efficiency of the leaves. The data points from 0 to 2 s were also recorded, and the fast chlorophyll fluorescence induction curve was plotted based on the data points (Rapacz, 2007).

Assays of Protective Enzyme Activities and MDA Levels

These assays were carried out according to the manufacturer's instructions. Leaves (0.1 g) were collected at each time point, with three biological replicates. Then, 0.1 ml of the extraction solution was added for milling in an ice bath, and the homogenate was centrifuged at 8000×g and 4°C for 10 min. The SOD, POD, and CAT activities were measured with a BC0170 SOD assay kit (Solarbio, Beijing, China), POD BC0090 assay kit (Solarbio, Beijing, China), and BC0200 CAT assay kit (Solarbio, Beijing, China), respectively. The MDA content was measured with a BC0025 MDA assay kit (Solarbio, Beijing, China; Spitz and Oberley, 1989; Yin et al., 2018).

RNA Preparation, RNA-Seq, and Differential Expression Analysis

One gram of leaves from each time point was collected and flash-frozen in liquid nitrogen with three biological replicates. Total leaf RNA was then extracted using a Pure Plant Kit (TIANGEN, Beijing, China), and RNA degradation and contamination were detected using 1% agarose gels. RNA quantification and qualification were performed using a Bioanalyzer 2,100 system (Agilent Technologies, CA, United States). The cDNA libraries were sequenced using the Illumina NovaSeq 6,000 System platform (Illumina, California, United States) via paired-end sequencing. Differential expression

analysis of the two conditions/groups was performed using the DESeq R package (1.10.1). KOBAS (Xie et al., 2011) software was used to test the statistical enrichment of differentially expressed genes (DEGs) in Kyoto Encyclopedia of Genes and Genomes (KEGG) pathways.

Cloning and Bioinformatic Analysis of PaDREB1A

Total RNA was extracted from *P. auriculata* leaves under cold stress, and cDNA was synthesized as a template by reverse transcription according to the instructions of the HiScript II 1st Strand cDNA Synthesis Kit (Vazyme, Nanjing, China). Primers (Supplementary Table S1) were designed with the full-length CDS obtained from RNA-seq using Primer 6 software for *PaDREB1A* gene cloning. The PCR products were detected by 1.0% agarose gel electrophoresis and subsequently recovered. The PCR products were transformed into *Escherichia coli* DH5α after construction of the pTOPO vector. The bacterial culture solution was tested again by PCR, and the screened monoclonal bacterial solution was verified by sequencing. Prediction of protein domains was performed using SMART.¹ The amino acid sequence homology of PaDREB1A was examined using BLAST.² Multiple sequence alignments were performed using DNAMAN 9.0, and ESPrnt 3.0³ was used for mapping. MEGA 7.0 was used for phylogenetic tree mapping.

Vector Construction and Generation of Transgenic Lines

To produce the 35S::PaDREB1A lines, the target gene was amplified using appropriate primers (Supplementary Table S1). The pCAMBIA1302-PaDREB1A-EGFP overexpression vector (Supplementary Figure S1) was constructed using NcoI enzyme cleavage of the vector and homologous recombination. Monoclonal bacterial solution was screened by PCR. After sequencing and verification, the plasmids were extracted and transformed into *Agrobacterium tumefaciens* GV3101 receptor cells. After incubation at 28°C for 36 h, monoclonal bacterial solution was selected for PCR identification. *A. thaliana* plants were transformed using the floral-dip transformation method. The transformed *A. thaliana* plants were cultured until seeds were harvested. The harvested seeds were sterilized and uniformly dispersed in 1/2 MS medium (with the addition of hygromycin) and cultured until the 4-leaf stage. Plants that were screened as being positive for resistance were transferred to soil for growth. The vector was also tested using universal primers (Supplementary Table S1) to identify transgenic T0 generation plants (Qiu et al., 2020).

RT-qPCR Validation

The RT-qPCR assay was divided into three parts: (1) five genes were selected for RT-qPCR to verify the reliability of RNA-seq, (2) the expression of *PaDREB1A* in 16 transgenic

¹<http://smart.embl-heidelberg.de/>

²<https://blast.ncbi.nlm.nih.gov/Blast.cgi>

³<https://esprnt.ibcp.fr/>

lines was examined, and (3) four related genes were selected to verify the regulatory effects of *PaDREB1A* on downstream *CORs* and oxidative stress-related protective enzymes (*ERD4*, *ERD7*, *COR15A*, *CAT1*). The TURScript 1st Strand cDNA Synthesis Kit (Nobelab Biotechnologies, Beijing, China) was used to synthesize cDNA following the manufacturer's instructions. Primers were designed using Premier 6. The primer sets for the target and reference genes are listed in **Supplementary Table S1**. RT-qPCR was performed with qTOWER 2.0/2.2 Quantitative Real-Time PCR Thermal Cyclers (Analytik Jena, Jena, Germany). Relative gene expression levels were calculated automatically using qPCRsoft3.2 software.

Data Analysis

Data were processed and analyzed using Microsoft Excel 365 and IBM SPSS Statistics 26. One-way ANOVA was used to determine significant differences. For RNA-seq, differential expression analysis was performed with the DESeq R package (1.10.1). Unigenes with a false discovery rate (FDR) < 0.01 and fold change (fC) ≥ 2 identified by DESeq analysis were considered DEGs.

RESULTS

Chlorophyll Content and Chlorophyll Fluorescence Parameters of *P. auriculata* Under Cold Stress

Figure 1A shows the changes in the relative chlorophyll content of *P. auriculata* after the plants were subjected to cold stress at 4°C. The relative chlorophyll content of the leaves did not vary significantly from 0 to 72 h. Two parameters, namely, PI abs and Fv/Fm, could indicate the response of plant photochemical efficiency to stress, especially PI abs, which could respond to very small changes in the environment. For PI abs (**Figure 1B**), a significant decrease started to appear after 8 h of cold stress at 4°C, but the value started to gradually rebound after 24 h. The Fv/Fm value started to decrease at 24 h. This observation indicated that cold stress at 4°C caused some degree of damage to the leaves of *P. auriculata*, but this damage was mild, and the leaves gradually recovered during plant adaptation. **Figure 1C** shows the fast chlorophyll fluorescence induction curve after different durations of cold stress. The curve showed a significant decrease at 24 h and a more pronounced decrease at 72 h. In particular, two characteristic points, J and I, showed a downward shift, indicating a decrease in photochemical efficiency at a low temperature.

Protective Enzyme Activities and MDA Content of *P. auriculata* Under Cold Stress

Relatively high antioxidant enzyme activities may reduce the oxidative damage suffered by plant leaves under stress. **Figure 2** shows the protective enzyme activity and MDA content of *P. auriculata* at different times under 4°C cold stress. The CAT and POD activities showed a significant increase at 72 h (**Figures 2A,B**). However, the SOD activity peaked at 8 h, showed

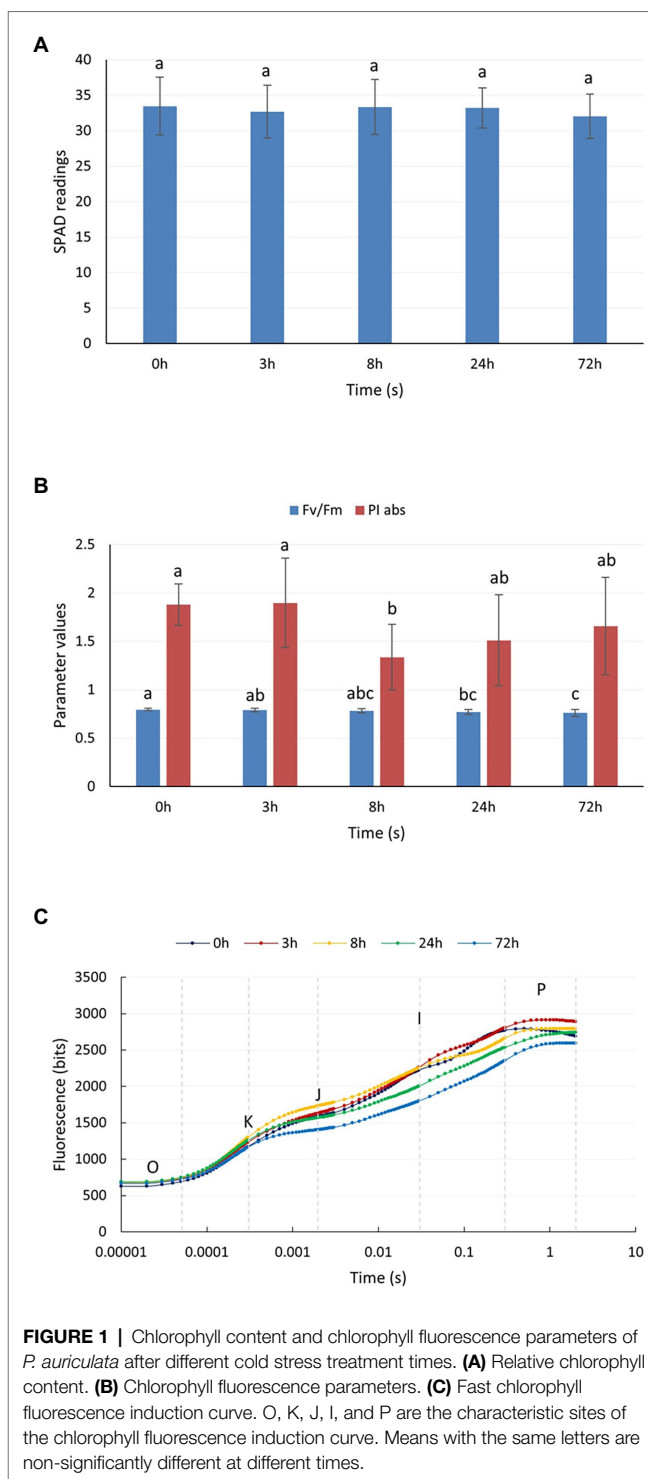


FIGURE 1 | Chlorophyll content and chlorophyll fluorescence parameters of *P. auriculata* after different cold stress treatment times. **(A)** Relative chlorophyll content. **(B)** Chlorophyll fluorescence parameters. **(C)** Fast chlorophyll fluorescence induction curve. O, K, J, I, and P are the characteristic sites of the chlorophyll fluorescence induction curve. Means with the same letters are non-significantly different at different times.

a decrease at 24 h, and then maintained a relatively stable value (**Figure 2C**). The MDA content started to show a significant increase at 8 h, peaked at 24 h, and then stopped increasing (**Figure 2D**). This observation indicates that the accumulation of ROS after cold stress was significant, but the value stabilized after 24 h. Thus, after 24 h, these three protective enzymes may play an important role in the cold tolerance of *P. auriculata*.

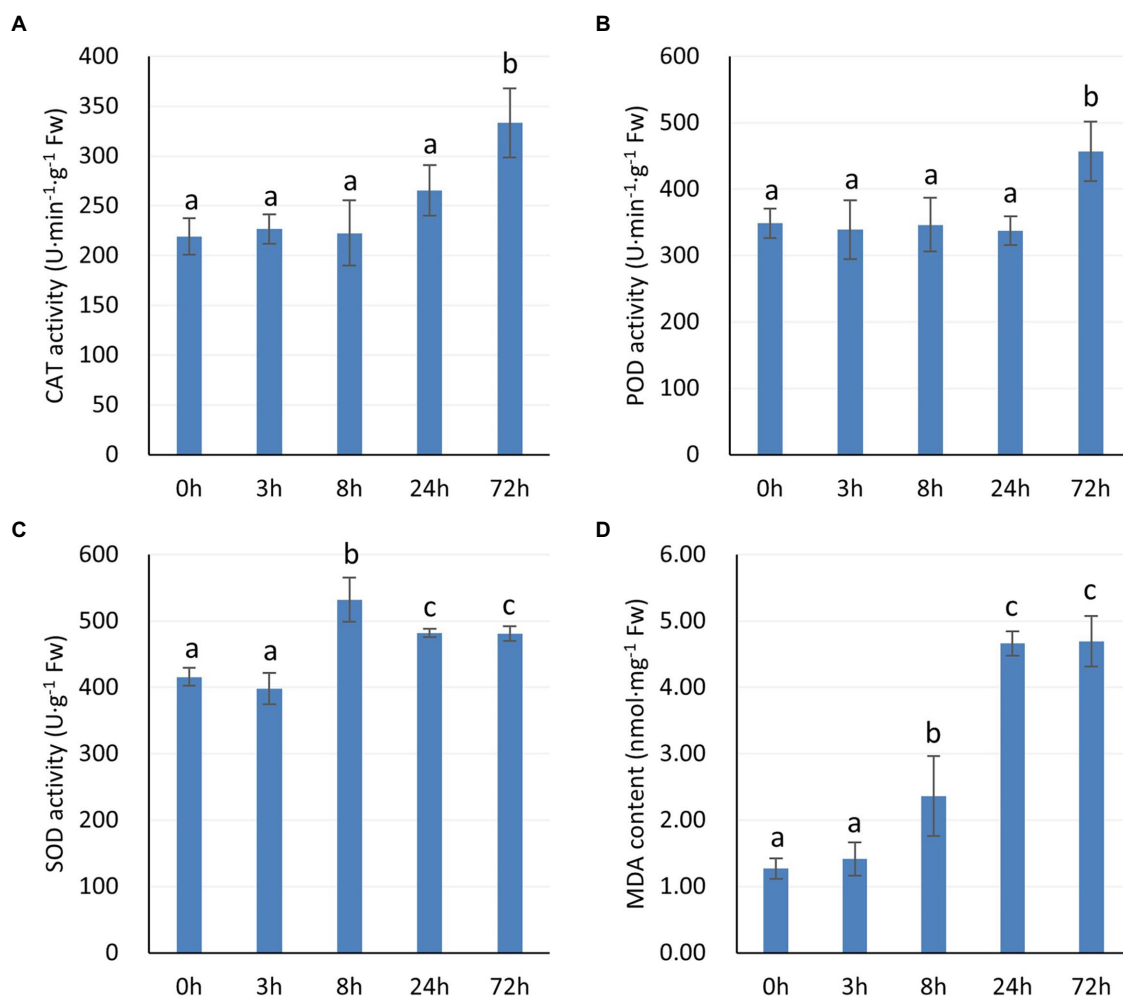


FIGURE 2 | Activities of protective enzymes and MDA content in *P. auriculata* after different cold stress treatment times. **(A)** CAT activity. **(B)** POD activity. **(C)** SOD activity. **(D)** MDA content. Means with the same letters are non-significantly different at different times.

RNA-Seq and Assembly and Differential Expression Analysis

Transcriptome sequencing of 15 samples (three biological replicates) was conducted, and a total of 118.16 Gb of clean data was obtained. The amount of clean data for each sample reached 6.18 Gb, with a Q30 base percentage of 93.79% and above. A total of 40,726 unigenes were obtained after assembly. Among them, there were 14,037 unigenes with lengths above 1 kb. The unigenes were functionally annotated with the NR (Deng et al., 2006), Swiss-Prot (Apweiler et al., 2004), KEGG (Kanehisa et al., 2004), COG (Tatusov et al., 2000), KOG (Koonin et al., 2004), GO (Ashburner et al., 2000), and Pfam (finn et al., 2014) databases, obtaining a total of 17,554 unigene annotations. Selected unigenes of interest were subjected to RT-qPCR analysis, the reliability of the RNA-seq results was verified, and the expression trends of all the selected genes were found to be consistent with the RNA-seq results (Supplementary Figure S2).

Four different cold stress treatment times were compared with 0h as the control, and the comparison combinations were as follows: S1 (0h vs. 1h), S2 (0h vs. 3h), S3 (0h vs. 8h), and S4 (0h vs. 24h). Analysis of DEGs and related pathways was performed. The number of DEGs increased with increasing cold stress treatment time. For S1, there were only 53 DEGs, but for S4, 2,578 DEGs were obtained. Notably, the differences in the number of upregulated and downregulated genes for S1, S2, and S3 were not significant. However, the number of upregulated genes (1524) was much higher than the number of downregulated genes (1054) for S4 (Supplementary Figure S3). This may be related to the positive response of related genes in the process of plant resistance to cold stress.

KEGG Pathway Identification

KEGG enrichment factor analysis of DEGs was performed for the four comparison combinations. We collated the pathways with a Q-value ≤ 0.6 (Supplementary Figure S4). For S1, which represented the initial stage of cold stress response, only a

small number of DEGs were annotated. Zeatin biosynthesis (ko00908) was found to be a downregulated pathway, which implies that zeatin may be involved in the stress signaling response at an early stage. For S2, two pathways of lipid metabolism, namely, linoleic acid metabolism (ko00591) and alpha-linolenic acid metabolism (ko00592), were upregulated. In particular, one of the catabolic products of linolenic acid is jasmonic acid (JA), an important growth regulator involved in the cold stress response. At the same time, upregulation of the secondary metabolite synthesis pathway tropine, piperidine, and pyridine alkaloid biosynthesis (ko00960) was also observed. This result may be related to the plant defense. ABC transporters (ko02010) and pentose and glucuronate interconversions (ko00040) were downregulated, which may indicate a slowdown in plant metabolism under cold stress. For S3, plant hormone signal transduction (ko04075) was upregulated, confirming our previous hypothesis. Further analysis of this pathway revealed that all three genes associated with JA signaling, namely, *JAR1*, *JAZ*, and *MYC2* (**Supplementary Figure S5**), were upregulated. Brassinosteroid biosynthesis (ko00905) and photosynthesis-antenna proteins (ko00196) were downregulated in S3 and S4. The downregulation of photosynthesis-antenna proteins was consistent with the chlorophyll fluorescence results, explaining the reduction in photochemical efficiency of the plants after cold stress.

Transcription Factor Prediction and CBF-Mediated Pathway Annotation

The transcription factors were predicted, and the results of the top 20 predictions are shown in **Supplementary Figure S6**. The three most abundant transcription factors belonged to the AP2/ERF-ERF (65), bHLH (55), and NAC (55) families. In addition, other transcription factors, such as those of the MYB (39), WRKY (35), and bZIP (21) families, which may be involved in the cold stress response, were also predicted. We focused on the expression of CBF/DREB1 transcription factors that are important for the regulation of cold stress in plants. Finally, c18703.graph_c0 was targeted. This unigene was annotated as *DREB1A* and started to be upregulated at S2, with expression peaking at S3 and starting to decline at S4 (**Figure 3**). The *DREB1A* expression pattern was fully consistent with that of CBF-mediated cold stress response genes (Su et al., 2010). Annotation analysis was conducted for several upstream genes and hormone signaling pathways that may be involved in CBF regulation. However, most of the genes were not significantly differentially expressed (**Figure 3**), but the pathways involved in JA regulation appeared to be differentially expressed. *MYC2*, an upstream positive regulator of *ICE*, had two unigenes that were significantly upregulated in S2 and S4 and one unigene that was significantly downregulated in S4. *JAR1*, located upstream of *MYC2*, is a positive regulator of *MYC2*, and *JAZ* is a negative regulator. However, both of these genes were found to be significantly upregulated. This is a complex set of mixed regulators, and we hypothesize that other signaling pathways are involved, but further clarification is required. However, based on the expression of *MYC2*, we hypothesize that JA is most

likely involved in the response to cold stress in *P. auriculata* and positively regulates the expression of CBFs. In addition, we annotated the downstream CORs that may be regulated by *DREB1A*. The annotated CORs were divided into two main categories: RDs and ERDs. There was no significant difference in the expression of RDs, but the expression of *ERD4* and *ERD7* was significantly different at different treatment times, with expression gradually increasing, peaking at S4 and lagging behind that in *DREB1A* (**Figure 3**). The expression pattern of these two genes was fully consistent with the expression pattern of CORs in response to cold stress (Shi et al., 2018). Therefore, we suggest that *DREB1A* may be a key transcription factor involved in the regulation of cold stress in *P. auriculata* and regulates the two CORs downstream to promote cold resistance.

Isolation and Characterization of PaDREB1A

Total RNA was extracted from *P. auriculata* leaves after 8 h of cold stress treatment and reverse transcribed to cDNA as a template. The CDS of the *DREB1A* gene obtained from RNA-seq was used to design multiple primer pairs for PCR amplification. The gel electrophoresis map showed a bright band at 750 bp. The band was determined to match the size of the target gene 789 bp (**Supplementary Figure S7**) and was named *PaDREB1A* (Accession number: MZ686430). *PaDREB1A* encodes 262 amino acids and has a predicted molecular mass of 29.1 kDa. SMART analysis showed that it contains a typical AP2 domain. Multiple sequence alignment with the other five homologous *DREB1A* proteins showed high conservation of its AP2 domain compared with those from other plant species (**Figure 4A**). Notably, the conserved amino acid residue in the AP2 domain was changed from V to L at position 91 and from A to V at position 108, unlike in other plants. Phylogenetic analysis showed that the closest *PaDREB1A* relative was the *Chenopodium quinoa* *DREB1A*-like protein (**Figure 4B**).

Overexpression of PaDREB1A Enhanced Cold Tolerance

To investigate the role of *PaDREB1A* in cold stress, the *pCAMBIA1302-PaDREB1A-EGFP* vector was constructed through *A. tumefaciens*-mediated transformation of *A. thaliana*. T0 generation plants were screened for resistance to hygromycin, and 22 strains were obtained. A total of 16 strains showed stable expression after a universal primer assay of the vector (**Supplementary Figure S8A**). After RT-qPCR, two positive transformants, namely, DRE-11 and DRE-13, were selected as the two most highly expressed strains (**Supplementary Figure S8B**). These transformants were again screened for hygromycin resistance and used as the third generation for the subsequent experiment. Adult plants grown in soil for 4 weeks were used for the cold stress treatment. WT plants showed symptoms of extensive leaf wilting after 8 h of freezing treatment at -6°C . WT plants (after 24 h of cold acclimation at 4°C) were significantly more resistant to freezing, with only some leaf edges wilted.

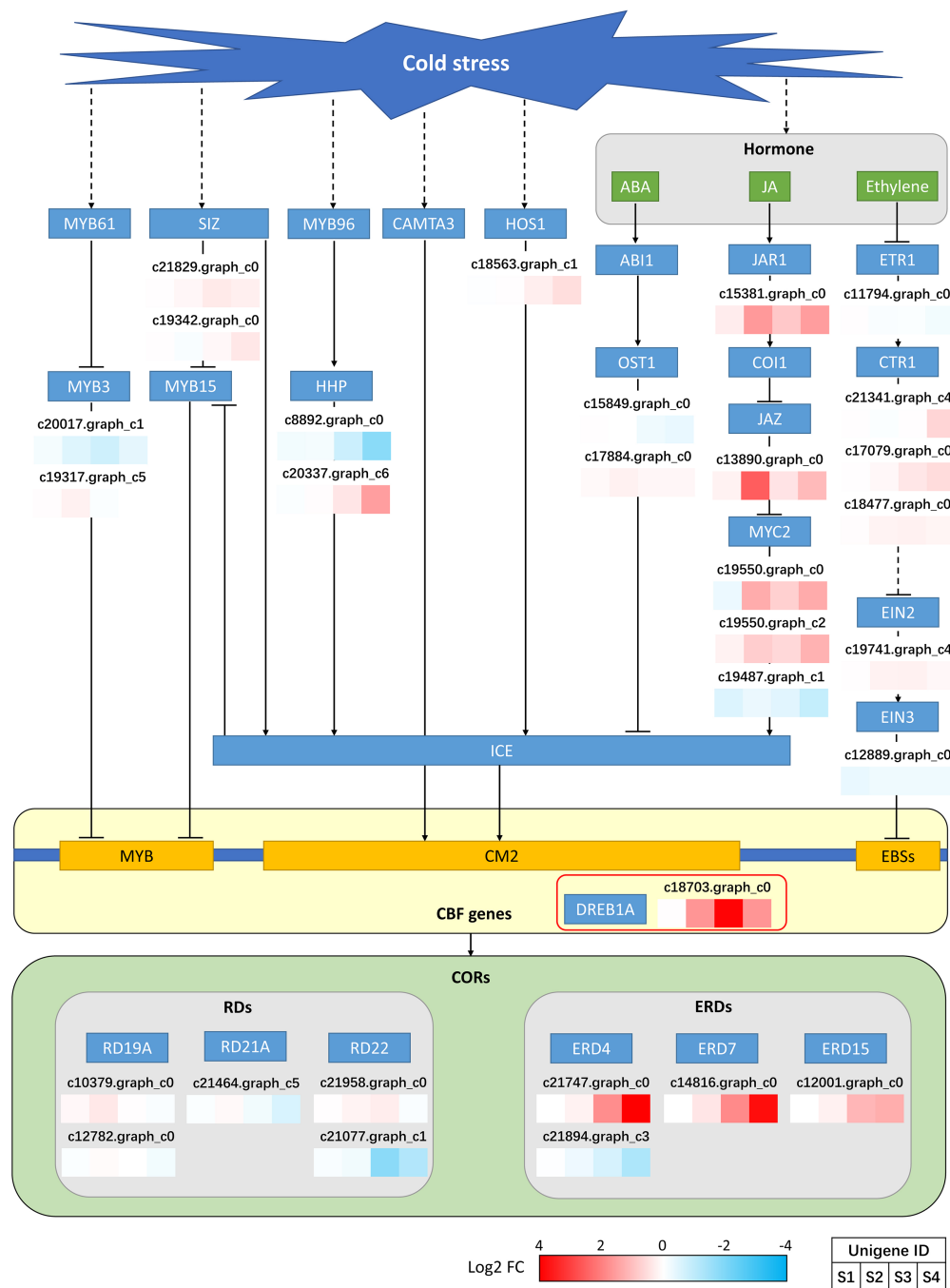


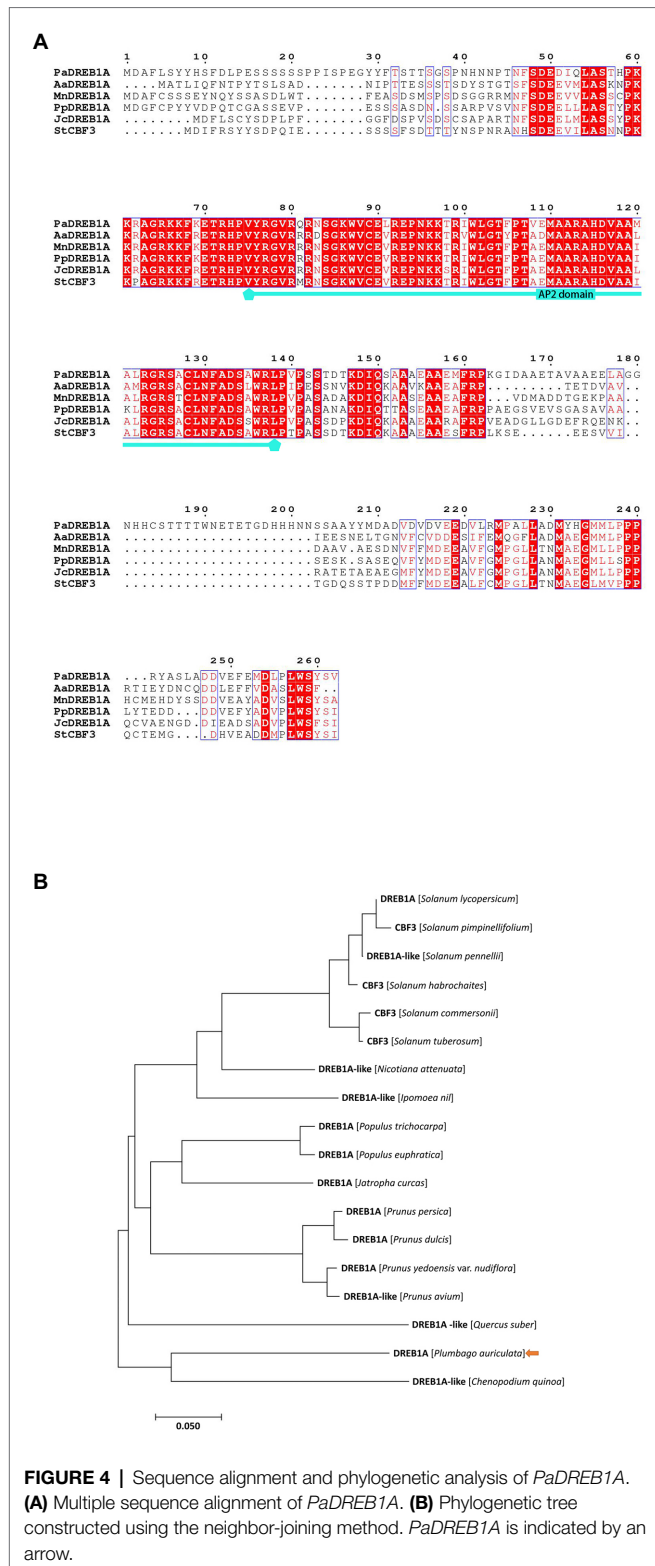
FIGURE 3 | Expression of CBF-mediated upstream and downstream genes in *P. auriculata* after different cold stress treatment times.

Both transgenic strains showed significantly less leaf damage after freezing treatment than the WT plants without cold domestication, especially DRE-13, which exhibited frost resistance close to that of the plants after cold domestication (Figure 5). After a longer recovery period of 72 h, all strains had withered leaves, but showed similar results as before. WT plants without cold acclimation had the most withered leaves. The damage of DRE-13 was similar to that

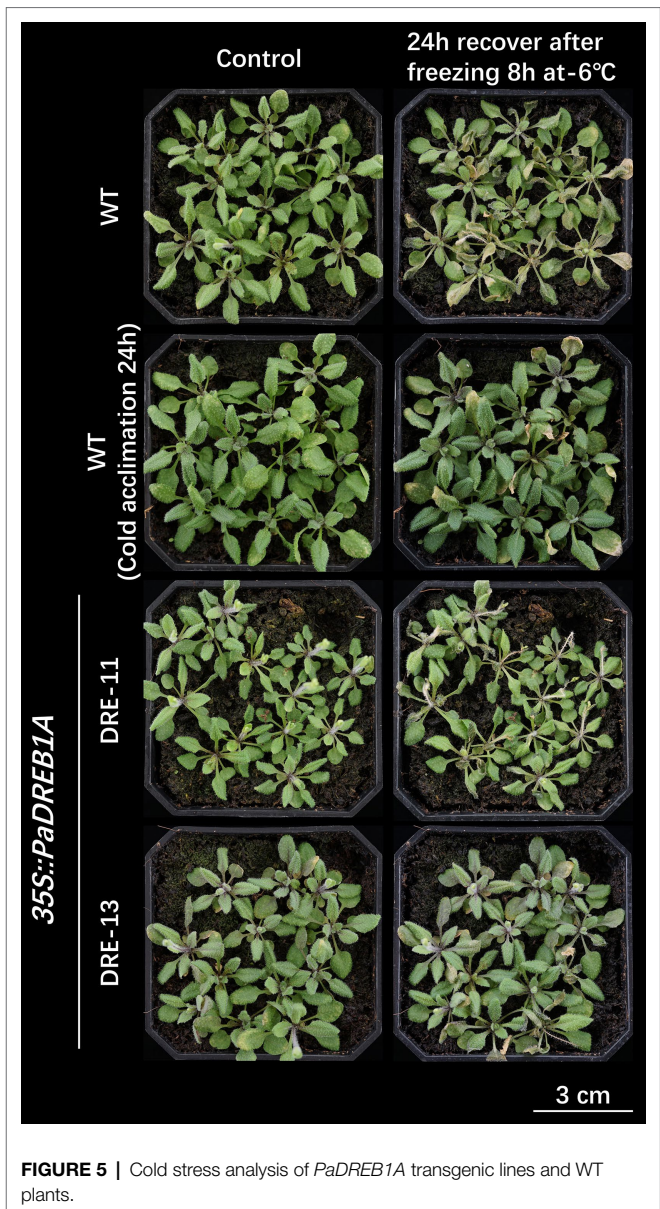
of WT plants after cold acclimation, with less damage (Supplementary Figure S9).

Overexpression of PaDREB1A Protected the Photosynthetic System Under Cold Stress

As shown in Figure 6A, similar to the results reported in section “Chlorophyll Content and Chlorophyll Fluorescence



Parameters of *P. auriculata* Under Cold Stress,” neither WT nor the two transgenic strains showed a significant difference in relative chlorophyll content after 72 h of cold stress at 4°C. We hypothesized that a low temperature of 4°C would



not have a significant effect on the chlorophyll content of the plants in a short period of time. Therefore, freezing treatment was conducted based on the observations in section “Overexpression of *PaDREB1A* Enhanced Cold Tolerance.” We subjected the three plants to freezing treatment at -4°C for 8 h, allowed them to recover at room temperature for 3 days, and then measured the chlorophyll content in the leaves, and the data appeared to be significantly different. The WT plants were significantly more severely affected, with a significantly lower chlorophyll content (24.87 ± 1.51) than that of the two transgenic strains (29.33 ± 2.46 ; 30.88 ± 1.91).

The chlorophyll fluorescence parameters more sensitively reflected the impact of stress on the plant photochemical system than the chlorophyll content. WT plants had significantly higher

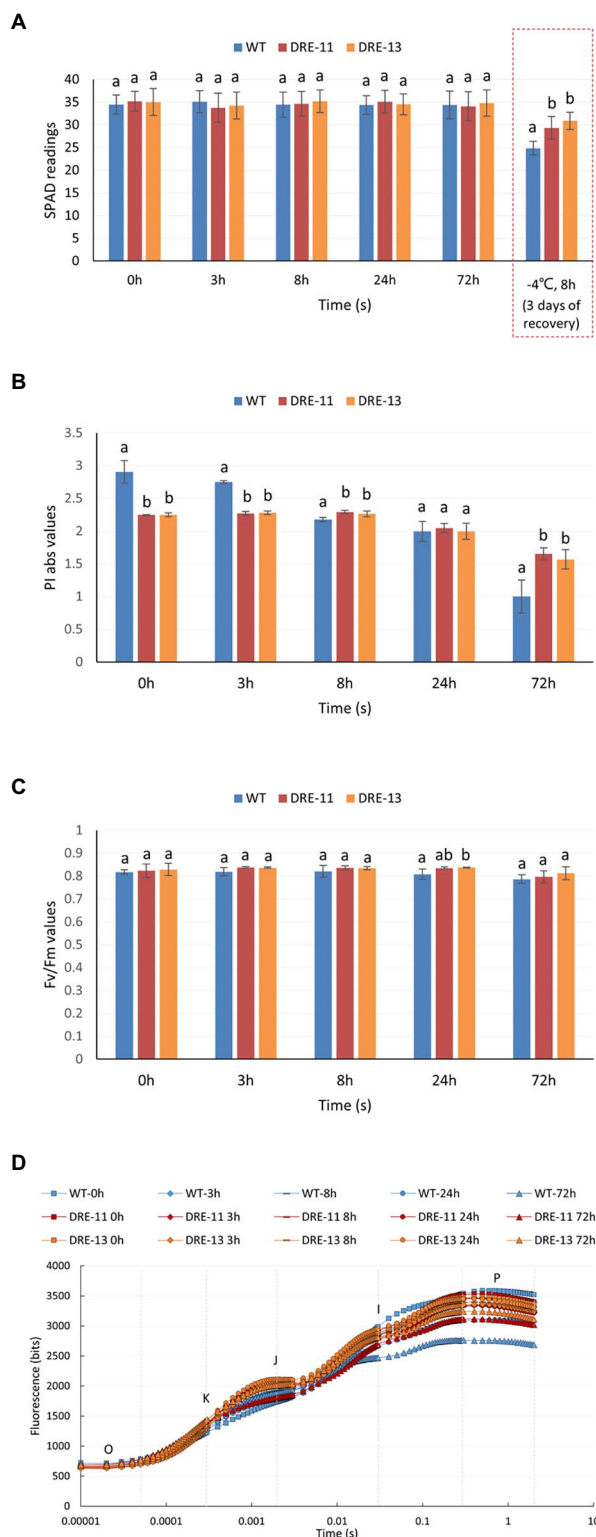


FIGURE 6 | Chlorophyll content and chlorophyll fluorescence parameters of *PaDREB1A* transgenic lines and WT plants after different cold stress treatment times. **(A)** SPAD readings. The dotted box shows an additional set of ice stress tests. **(B)** PI abs values and **(C)** Fv/Fm values. Means with the same letters are non-significantly different for different transgenic lines and WT plants. **(D)** Fast chlorophyll fluorescence induction curve. O, K, J, I, and P are the characteristic sites.

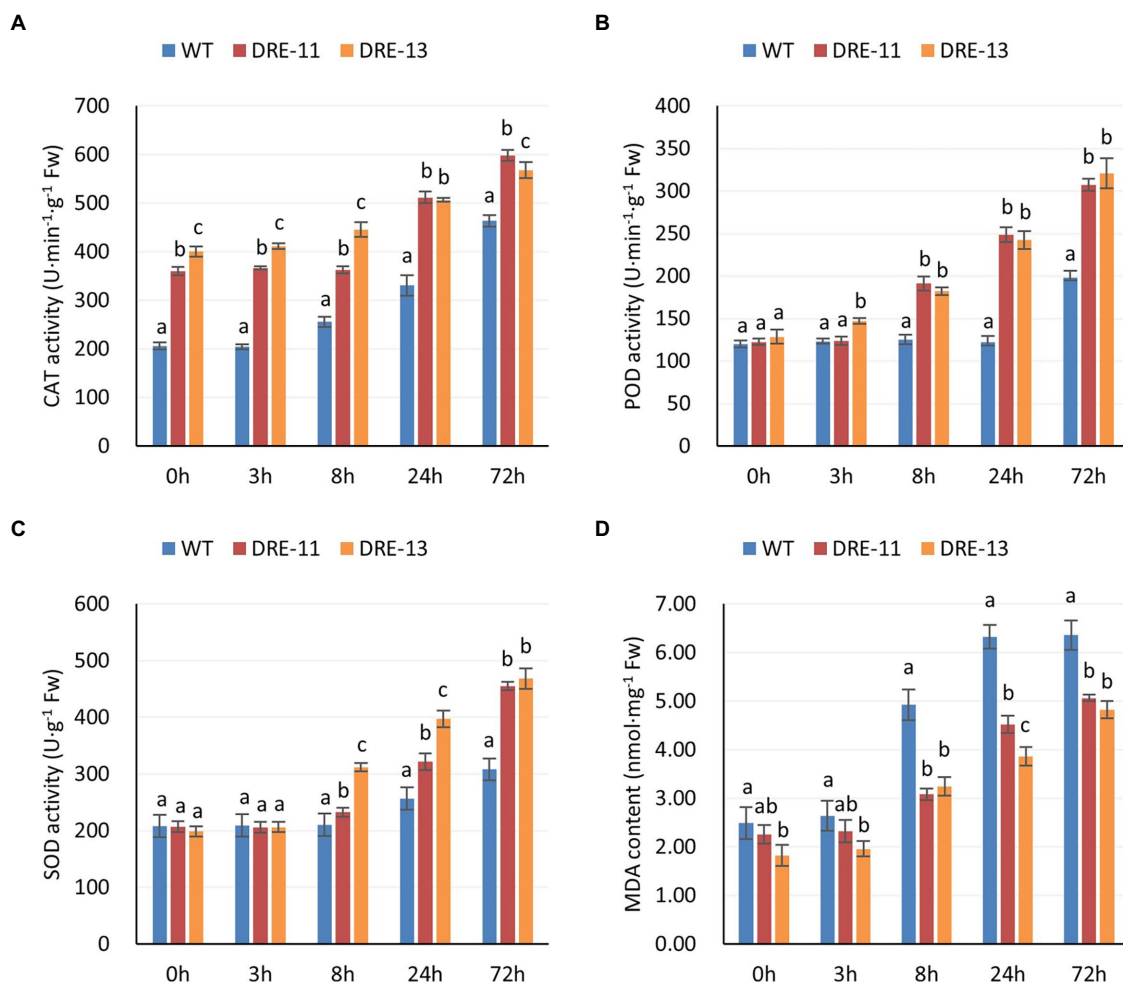


FIGURE 7 | Activities of protective enzymes and MDA content of *PaDREB1A* transgenic lines and WT plants after different cold stress treatment times. **(A)** CAT activity. **(B)** POD activity. **(C)** SOD activity. **(D)** MDA content. Means with the same letters are non-significantly different for different transgenic lines and WT plants.

values of PI abs than the two transgenic strains before cold stress (**Figure 6B**). This indicated that the transgenic strains may have a lower maximum photochemical efficiency than the WT plants. However, WT plants were significantly more sensitive to low temperature; their PI abs values were already on par with those of the two transgenic strains after 24h of treatment, while they were already much lower than those of the two transgenic strains at 72h. In contrast, the PI abs values of the two transgenic strains DRE-11 and DRE-13 changed moderately. Neither WT nor transgenic plants showed significant differences in Fv/Fm (**Figure 6C**). Fv/Fm is more stable than the value of *P*, but it is also less sensitive. No significant change in Fv/Fm was observed in this study, indicating that the plant may have suffered from cold stress at an early stage. The chlorophyll fluorescence induction curves showed similar results to those shown in *P. auriculata* (**Figure 1C**). WT plants showed different degrees of decrease in the curve at all stress time points, especially at 72h, when the I point had almost completely disappeared. Again, this represents a

significant impact on photochemical efficiency. In contrast, the two transgenic strains, especially DRE-13, were less strongly affected than the WT plants, as the curves started to show only a very slight decrease at 72h (**Figure 6D**).

Overexpression of PaDREB1A Increased the ROS Scavenging Capacity

CAT, SOD, and POD all play important roles in the scavenging of ROS in plants. CBFs can enhance the expression of downstream CORs and thus indirectly enhance the ROS scavenging mechanism in plants. As shown in **Figure 7**, both transgenic strains showed higher CAT activity than the WT plants even when they were not under cold stress, and the levels remained significantly higher at subsequent times (**Figure 7A**). In contrast, the SOD and POD activities did not show a significant difference at the beginning of the stress period. However, their activities soon significantly exceeded those of the WT plants with time (**Figures 7B,C**). The MDA content is an indicator of the extent

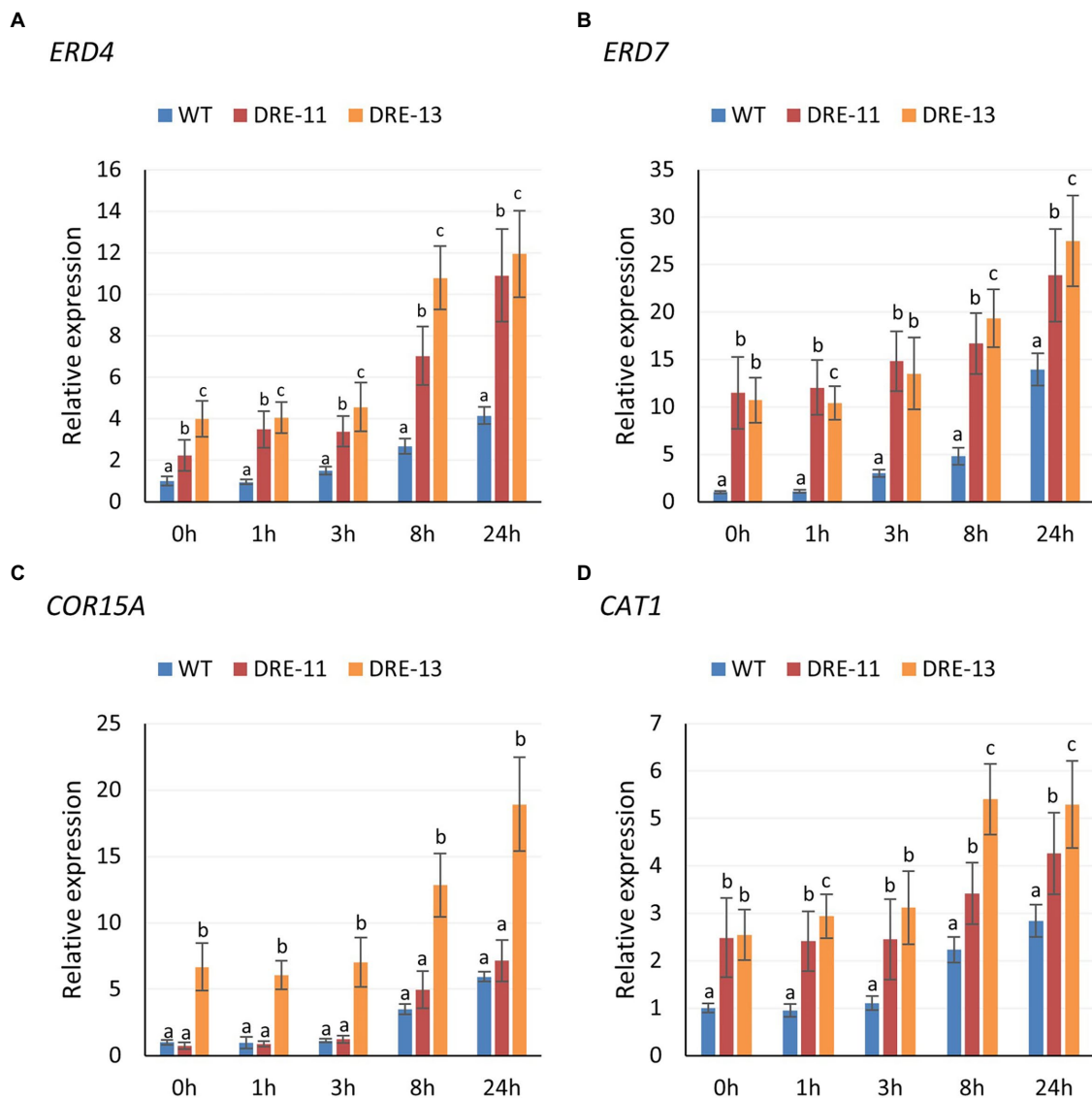


FIGURE 8 | Expression levels of *CORs* (A, *ERD4*; B, *ERD7*; C, *COR15A*) and (D) *CAT1* of *PaDREB1A* transgenic lines and WT plants after different cold stress treatment times. Means with the same letters are non-significantly different for different transgenic lines and WT plants.

of lipid peroxidation in plants. As shown in **Figure 7D**, the MDA content of WT plants was significantly higher than that of the two transgenic strains, and this difference was more pronounced in the 8h samples. These results indicate that overexpression of *PaDREB1A* enhanced the scavenging ability of ROS in the plants and reduced the oxidative damage of plants under cold stress.

Overexpression of *PaDREB1A* Upregulated the Expression Levels of *CORs* and *CAT1*

Since we found that two *COR* genes, namely, *ERD4* and *ERD7*, were upregulated with *PaDREB1A* overexpression in the transcriptome data, we hypothesized that *PaDREB1A* could

similarly upregulate *COR* gene expression downstream in *A. thaliana*. We selected three *CORs*, including the previously mentioned *ERD4*, *ERD7*, and *COR15A*, for RT-qPCR assays. We also determined the change in *CAT1* expression due to the significant enhancement of ROS scavenging ability. The results revealed that the expression of *ERD4* and *ERD7* was significantly upregulated in transgenic plants compared with WT plants, as expected from our transcriptomic results (**Figures 8A,B**). However, for *COR15A*, only DRE-13 showed significantly upregulated expression, while the expression level in DRE-11 was close to that in WT plants (**Figure 8C**). In addition, the *CAT1* expression levels in both transgenic plants were also significantly higher than those in WT plants. This again demonstrated that overexpression of *PaDREB1A* could

enhance the ROS scavenging level in the plants (**Figure 8D**). Although the expression of *ERD4*, *ERD7*, and *CAT1* was enhanced in both transgenic strains, the expression level in DRE-13 was significantly stronger than that in DRE-11 at the late stage of stress. This result may be one of the reasons for the enhanced cold stress tolerance of the transgenic plants.

DISCUSSION

Among all physiological processes in plants, photosynthesis is the most sensitive to the effects of low temperature. Cold stress can disrupt the chloroplast structure, decrease the chlorophyll content, and impair the electron transport function in plants. SPAD values have been widely used to assess the decrease in chlorophyll content caused by various abiotic stresses on plants. In pepper (*Capsicum frutescens*), leaves subjected to cold stress exhibited a significant decrease in SPAD values (Odhiambo et al., 2018). Similar findings have been obtained in other plants, and the extent of this decrease depends on the species itself (Miedema, 1982). In this study, we found that the SPAD values of *P. auriculata* under cold stress remained almost unchanged for 72 h. This result indicates that the chloroplasts of *P. auriculata* leaves were not structurally damaged by cold stress treatment at 4°C for a short period of time, and the chlorophyll level was maintained. Chlorophyll fluorescence reflects damage to PSII in plant leaves exposed to abiotic stress, and the data can be obtained quickly and efficiently without damaging the leaves. The maximum photochemical efficiency of PSII (Fv/Fm) is one of the most important chlorophyll fluorescence parameters. PI abs is the most sensitive of all chlorophyll fluorescence parameters, responding rapidly to subtle changes (Baker and Rosenqvist, 2004; Baker, 2008). These parameters have been widely used in response to cold stress in plants, such as soybean, tomato, and maize (Guy et al., 1997; Skrudlik et al., 2000; Cao et al., 2015). For *P. auriculata*, cold stress treatment at 4°C for 72 h caused a decrease in the photochemical efficiency of *P. auriculata* leaves but did not produce irreversible destructive damage. Many studies have shown that cold stress can cause ROS accumulation in plants, trigger membrane lipid oxidation, and activate elevated protective enzyme activities (Faize et al., 2011; Bhattacharjee, 2013; Diaz-Vivancos et al., 2013). Similar results were obtained in this study, where the CAT, SOD, and POD activities in the leaves of *P. auriculata* gradually increased with the duration of cold stress. However, we found that the CAT and POD activities did not peak. That is, the activities of these protective enzymes may be further increased if the stress time is further prolonged. However, the MDA content did not increase further between 24 h and 72 h for any plants, which indicates that the ROS content in the leaves of *P. auriculata* was well controlled and that further membrane lipid oxidation did not occur.

Several results from the current study show that cold stress can upregulate the tropane, piperidine, and pyridine alkaloid biosynthesis pathways. Song et al. (2020) found that this pathway in Tartary buckwheat (*Fagopyrum tataricum*) is also upregulated under cold stress. Accumulation of these substances may

be induced at low temperature and promote cold tolerance. Similar trends have also been observed in maize and wild banana (*Musa itinerans*; Liu et al., 2018; Li et al., 2019). In this study, we also found that the tropane, piperidine, and pyridine alkaloid biosynthesis pathways were significantly upregulated in *P. auriculata* after cold stress, and we thus hypothesize that *P. auriculata* may have a similar mechanism to resist cold stress. In addition, we noted that another pathway, pentose and glucuronate interconversions, was also significantly upregulated under cold stress. This phenomenon has also been found in *Cardiocrinum cathayanum* and may significantly improve its resistance to cold (Wang et al., 2020). In fact, upregulation of the pentose and glucuronate interconversions pathway has been found in a variety of plants, and this upregulation may be an important mechanism leading to plant cold tolerance (Gong et al., 2018; Zhang et al., 2020). JAs are composed of JA and its derivatives, such as methyl jasmonate (MeJA) and jasmonoyl-isoleucine, which play a role in growth and development as well as in biotic and abiotic stress responses (Ding et al., 2021). It has been widely demonstrated that cold stress can induce endogenous JA accumulation and act as an upstream signal for ICE-CBF to positively regulate cold tolerance in *A. thaliana* (Hu et al., 2013). As found in tomato, cold stress was able to induce JA production, and JA signaling further activated the CBF pathway to increase cold tolerance (Wang et al., 2016). MYC2 is a major regulator of the JA signaling pathway and directly interacts with ICE1 to jointly activate cold tolerance in banana (Zhao et al., 2013). MdMYC2 can activate the G-BOX element in the *MdCBF1* promoter of apple (*Malus × domestica*) to improve freezing tolerance. MdJAZ1/4 can bind to MdMYC2 and act as a negative regulator to reduce the expression of MdMYC2 and downstream CBFs (Wang et al., 2019). In this study, transcriptome analysis of *P. auriculata* under cold stress repeatedly upregulated the pathways involved in JA synthesis and signal transduction (linoleic acid metabolism, ko00591; plant hormone signal transduction, ko04075), and it was further observed that *JAR1*, *JAZ*, and *MYC2*, genes directly related to JA signaling, were upregulated. The upregulated genes included *JAR*, which is located most far upstream of and positively regulates the CBF gene; *JAZ*, which is located downstream and is a negative regulator; and *MYC2*, which is located most far downstream of and positive regulates ICE and CBF. According to the results of transcriptome analysis, MYC2 expression in *P. auriculata* was upregulated in S2. We hypothesize that endogenous JA may play a positive regulatory role in the CBF signaling pathway. However, this regulation was complex, and multiple unigenes were annotated to the same genetic locus. Moreover, inconsistent expression was observed, and both the positive regulator *JAR* and the negative regulator *JAZ* appeared to be upregulated in S2. Thus, it may be the case that there are other signaling pathways involved in regulation. Our findings suggest that JA may be an important signaling substance for the upstream regulation of CBFs in *P. auriculata*, but the mode of regulation of its signaling pathway is not clear from the present information and requires further study.

Cold stress leads to a decrease in photosynthesis, resulting in an increase in the total amount of excess excitation energy (Payton et al., 2001). If the excess light energy is

not dissipated in a timely manner, the photosynthetic system can be damaged even under low light (Demmig-Adams and Adams, 1992), causing photoinhibition (Allen and Ort, 2001). In this study, all cold stress experiments were carried out under dark conditions to avoid interference from further damage to the photosynthetic system by photoinhibition. The decrease in photosynthesis in *P. auriculata* was partly caused by the decrease in enzyme activity at low temperatures and the disruption of the membrane system by ROS. Transcriptome analysis was performed, and the results showed significant downregulation of the photosynthesis–antenna protein (ko00196) pathway in both S3 and S4. The downregulated genes were involved mainly in the light-harvesting chlorophyll protein complex (LHC) system of *Lhca4*, *Lhcb1*, and *Lhcb3* (Supplementary Figure S10). We believe that this is a rational response for plants to autonomously regulate the reduction of light energy uptake to allow plants to protect themselves from cold stress, which can mitigate photoinhibition and cause further damage.

To date, CBF1 (DREB1B), CBF2 (DREB1C), and CBF3 (DREB1A) have been identified successively in *A. thaliana* (Gilmour et al., 1998; Liu et al., 1998). These factors can bind to the DRE/CRT regulatory element CCGAC (Baker et al., 1994). This element is mostly found in the promoter region of *COR* genes (Medina et al., 2011). There is high similarity (>85%) among the three *CBF1*–*CBF3* genes, suggesting that they may have originated from the same gene (Gilmour et al., 1998; Medina et al., 1999). Overexpression of *CBF1*, *CBF2*, and *CBF3* substantially increased the frost resistance of plants and significantly induced the expression of *COR* genes in plants (Liu et al., 1998). In this study, we identified only *CBF3* (DREB1A) but did not detect expression of *CBF1* (DREB1B) and *CBF2* (DREB1C). Researchers have found similar results in tomato. Only *CBF1* expression was found to be induced by cold stress, and only three *CORs* were involved downstream, much fewer than the 30 found in *A. thaliana*. The findings also suggested that the cold stress response pattern of tropical plants may be different from that of conventional plants (Zhang et al., 2004). In *P. auriculata*, also a standard tropical plant, only *CBF3* and two *CORs* (*ERD4*, *ERD7*) were detected at low temperatures, which may contribute to the fact that tropical plants are much less tolerant to low temperatures than conventional plants. Indeed, although CBF, now known to be the most important transcription factor involved in the response to cold stress, has also been demonstrated to be present in a wide range of plants, its expression varies considerably among different species, especially those from the tropics (Carvallo et al., 2011). This unique phenomenon in tropical plants may represent a breakthrough in breeding for improved cold tolerance.

Overexpression of *PaDREB1A* in *A. thaliana* not only significantly enhanced freezing tolerance but also protected the photosynthetic system and enhanced the ROS scavenging mechanism in the plants at low temperatures. In addition, *CORs* of *A. thaliana* could also be upregulated by *PaDREB1A*. These experimental results were consistent with expectations

and similar to those of other studies (Cominelli et al., 2005; Nakashima et al., 2009). In addition, *CAT1* also appeared to be upregulated, which could be an important reason for the increased activity of the protective enzyme *CAT*. However, in both transgenic strains, for *COR15A*, only DRE-13 showed upregulated expression, while DRE-11 showed almost the same expression as the WT plants. Moreover, the cold tolerance of DRE-13 also seemed to be higher than that of DRE-11, with differences appearing among the different transgenic strains. We speculate that this difference may have been caused by the difference in the gene insertion location, where in some strains, the insertion site caused partial disruption of the original gene function. Notably, overexpression of *PaDREB1A* in *A. thaliana* resulted in higher cold tolerance. However, we also found slow growth and smaller leaves in most transgenic lines compared to WT plants (Figure 5). This trait does not seem to be correlated with the expression level of *PaDREB1A* if the transgenic strains are likely to show this trait. Several studies have shown that overexpression of *CBF* leads to plant dwarfing and delayed flowering (Gilmour et al., 2004; Park et al., 2015), but in this study, only slow growth was observed, and flowering time was not affected. It has been shown that overexpression of *CBF1* can activate a decrease in gibberellic acid (GA) content in plants, resulting in a high level of accumulation of the DELLA protein, a negative regulator of the GA signaling pathway, leading to growth inhibition, which can be relieved by exogenous application of GA (Achard et al., 2008). This suggests that this slow growth may be related to the influence of CBFs on hormone metabolism.

In conclusion, we identified *PaDREB1A* as a key transcription factor in *P. auriculata* under cold stress. Overexpression of *PaDREB1A* in *A. thaliana* enhanced freezing resistance, protected the photosynthetic system, and enhanced the ROS scavenging mechanism under cold stress. The enhancement of these cold tolerance-related indicators may be achieved by *PaDREB1A* through the activation of downstream *CORs* and other related genes.

DATA AVAILABILITY STATEMENT

The datasets presented in this study can be found in online repositories. The names of the repository/repositories and accession number(s) can be found at: PRJNA797114.

AUTHOR CONTRIBUTIONS

ZZ: data curation. WL: formal analysis and writing—original draft. SG: methodology. TL: project administration. YD: validation. LJ and SG: writing—review and editing. All authors contributed to the article and approved the submitted version.

FUNDING

This work was supported by the Sichuan Science and Technology Program (2021YFYZ0006).

ACKNOWLEDGMENTS

The authors would like to thank Guohua Zhang at Sichuan Agricultural University for providing the *Arabidopsis* plants.

REFERENCES

- Achard, P., Gong, F., Cheminant, S., Alioua, M., Hedden, P., and Genschik, P. (2008). The cold-inducible CBF1 factor-dependent signaling pathway modulates the accumulation of the growth-repressing DELLA proteins via its effect on gibberellin metabolism. *Plant Cell* 20, 2117–2129. doi: 10.1105/tpc.108.058941
- Allen, D. J., and Ort, D. R. (2001). Impacts of chilling temperatures on photosynthesis in warm-climate plants. *Trends Plant Sci.* 6, 36–42. doi: 10.1016/S1360-1385(00)01808-2
- Apweiler, R., Bairoch, A., Wu, C. H., Barker, W. C., Boeckmann, B., Ferro, S., et al. (2004). UniProt: the universal protein knowledgebase. *Nucleic Acids Res.* 32, 115D–1119D. doi: 10.1093/nar/gkh131
- Ashburner, M., Ball, C. A., Blake, J. A., Botstein, D., Butler, H., Cherry, J. M., et al. (2000). Gene ontology: tool for the unification of biology. *Nat. Genet.* 25, 25–29. doi: 10.1038/75556
- Baker, N. R. (2008). Chlorophyll fluorescence: a probe of photosynthesis in vivo. *Annu. Rev. Plant Biol.* 59, 89–113. doi: 10.1146/annurev.arplant.59.032607.092759
- Baker, N. R., and Rosenqvist, E. (2004). Applications of chlorophyll fluorescence can improve crop production strategies: an examination of future possibilities. *J. Exp. Bot.* 55, 1607–1621. doi: 10.1093/jxb/erh196
- Baker, S. S., Wilhelm, K. S., and Thomashow, M. F. (1994). The 5'-region of *Arabidopsis thaliana* cor15a has cis-acting elements that confer cold-, drought- and ABA-regulated gene expression. *Plant Mol. Biol.* 24, 701–713. doi: 10.1007/BF00029852
- Bhattacharjee, S. (2013). Heat and chilling induced disruption of redox homeostasis and its regulation by hydrogen peroxide in germinating rice seeds (*Oryza sativa* L., cultivar Ratna). *Physiol. Mol. Biol. Plants* 19, 199–207. doi: 10.1007/s12298-012-0159-x
- Bilka, A., and Sowiński, P. (2010). Closure of plasmodesmata in maize (*Zea mays*) at low temperature: a new mechanism for inhibition of photosynthesis. *Ann. Bot.* 106, 675–686. doi: 10.1093/aob/mcq169
- Cao, X., Jiang, F., Wang, X., Zang, Y., and Wu, Z. (2015). Comprehensive evaluation and screening for chilling-tolerance in tomato lines at the seedling stage. *Euphytica* 205, 569–584. doi: 10.1007/s10681-015-1433-0
- Carvallo, M. A., Pino, M. T., Jeknić, Z., Zou, C., Doherty, C. J., Shiu, S. H., et al. (2011). A comparison of the low temperature transcriptomes and CBF regulons of three plant species that differ in freezing tolerance: *Solanum commersonii*, *Solanum tuberosum*, and *Arabidopsis thaliana*. *J. Exp. Bot.* 62, 3807–3819. doi: 10.1093/jxb/err066
- Chassot, A., Stamp, P., and Richner, W. (2001). Root distribution and morphology of maize seedlings as affected by tillage and fertilizer placement. *Plant Soil* 231, 123–135. doi: 10.3929/ethz-b-000422942
- Chinnusamy, V., Zhu, J. K., and Sunkar, R. (2010). Gene regulation during cold stress acclimation in plants. *Meth Mol Biol* 639, 39–55. doi: 10.1007/978-1-60761-702-0_3
- Cominelli, E., Galbiati, M., Vavasseur, A., Conti, L., Sala, T., Vuylsteke, M., et al. (2005). A guard-cell-specific MYB transcription factor regulates stomatal movements and plant drought tolerance. *Curr. Biol.* 15, 1196–1200. doi: 10.1016/j.cub.2005.05.048
- Demmig-Adams, B., and Adams III, W. W. (1992). Carotenoid composition in sun and shade leaves of plants with different life forms. *Plant Cell Environ.* 15, 411–419. doi: 10.1111/j.1365-3040.1992.tb00991.x
- Deng, Y. Y., Li, J. Q., Wu, S. F., Zhu, Y. P., Chen, Y. W., and He, F. C. (2006). Integrated nr database in protein annotation system and its localization. *Comput. Eng.* 32, 71–72. doi: 10.1109/INFOCOM.2006.241
- Diaz-Vivancos, P., Faize, M., Barba-Espin, G., Faize, L., Petri, C., Hernández, J. A., et al. (2013). Ectopic expression of cytosolic superoxide dismutase and ascorbate peroxidase leads to salt stress tolerance in transgenic plums. *Plant Biotechnol. J.* 11, 976–985. doi: 10.1111/pbi.12090
- Ding, F., Wang, C., Xu, N., Wang, M., and Zhang, S. (2021). Jasmonic acid-regulated putrescine biosynthesis attenuates cold-induced oxidative stress in tomato plants. *Sci. Hort.* 288:110373. doi: 10.1016/j.scienta.2021.110373
- Dutilleul, C., Garmier, M., Noctor, G., Mathieu, C., Chétrit, P., Foyer, C. H., et al. (2003). Leaf mitochondria modulate whole cell redox homeostasis, set antioxidant capacity, and determine stress resistance through altered signaling and diurnal regulation. *Plant Cell* 15, 1212–1226. doi: 10.1105/tpc.009464
- Faize, M., Burgos, L., Faize, L., Piqueras, A., Nicolas, E., Barba-Espin, G., et al. (2011). Involvement of cytosolic ascorbate peroxidase and Cu/Zn-superoxide dismutase for improved tolerance against drought stress. *J. Exp. Bot.* 62, 2599–2613. doi: 10.1093/jxb/erq432
- Ferrero, V., De Vega, C., Stafford, G. I., Van Staden, J., and Johnson, S. D. (2009). Heterostyly and pollinators in *Plumbago auriculata* (Plumbaginaceae). *S. Afr. J. Bot.* 75, 778–784. doi: 10.1016/j.sajb.2009.06.014
- Finn, R. D., Bateman, A., Clements, J., Coghill, P., Eberhardt, R. Y., Eddy, S. R., et al. (2014). Pfam: the protein families database. *Nucleic Acids Res.* 42, D222–D230. doi: 10.1093/nar/gkt1223
- Gilmour, S. J., Fowler, S. G., and Thomashow, M. F. (2004). *Arabidopsis* transcriptional activators CBF1, CBF2, and CBF3 have matching functional activities. *Plant Mol. Biol.* 54, 767–781. doi: 10.1023/B:PLAN.0000040902.06881.d4
- Gilmour, S. J., Zarka, D. G., Stockinger, E. J., Salazar, M. P., Houghton, J. M., and Thomashow, M. F. (1998). Low temperature regulation of the *Arabidopsis* CBF family of AP2 transcriptional activators as an early step in cold-induced COR gene expression. *Plant J.* 16, 433–442. doi: 10.1046/j.1365-3113X.1998.00310.x
- Gong, X. X., Yan, B. Y., Hu, J., Yang, C. P., Li, Y. J., Liu, J. P., et al. (2018). Transcriptome profiling of rubber tree (*Hevea brasiliensis*) discovers candidate regulators of the cold stress response. *Genes & Genomics* 40, 1181–1197. doi: 10.1007/s13258-018-0681-5
- Guy, S., Berger, M., and Planchon, C. (1997). Response to low temperature in dinitrogen fixing soybeans. *Plant Sci.* 123, 67–75. doi: 10.1016/S0168-9452(96)04572-4
- Hafeez, B. B., Zhong, W., Fischer, J. W., Mustafa, A., Shi, X., Meske, L., et al. (2013). Plumbagin, a medicinal plant (*Plumbago zeylanica*)-derived 1, 4-naphthoquinone, inhibits growth and metastasis of human prostate cancer PC-3M-luciferase cells in an orthotopic xenograft mouse model. *Mol. Oncol.* 7(3), 428–439. doi: 10.1016/j.molonc.2012.12.001
- Hannah, M. A., Wiese, D., Freund, S., Fiehn, O., Heyer, A. G., and Hincha, D. K. (2006). Natural genetic variation of freezing tolerance in *Arabidopsis*. *Plant Physiol.* 142, 98–112. doi: 10.1104/pp.106.081141
- Hanson, H. I., Eckberg, E., Widenberg, M., and Olsson, J. A. (2021). Gardens' contribution to people and urban green space. *Urban For. Urban Green.* 63:127198. doi: 10.1016/j.ufug.2021.127198
- Hu, Y., Jiang, L., Wang, F., and Yu, D. (2013). Jasmonate regulates the inducer of CBF expression—c-repeat binding factor/DRE binding factor1 cascade and freezing tolerance in *Arabidopsis*. *Plant Cell* 25, 2907–2924. doi: 10.1105/tpc.113.112631
- Jaglo, K. R., Kleff, S., Amundsen, K. L., Zhang, X., Haake, V., Zhang, J. Z., et al. (2001). Components of the *Arabidopsis* C-repeat/dehydration-responsive element binding factor cold-response pathway are conserved in *Brassica napus* and other plant species. *Plant Physiol.* 127, 910–917. doi: 10.1104/pp.127.3.910
- Jaglo-Ottosen, K. R., Gilmour, S. J., Zarka, D. G., Schabenberger, O., and Thomashow, M. F. (1998). *Arabidopsis* CBF1 overexpression induces COR genes and enhances freezing tolerance. *Science* 280, 104–106. doi: 10.1126/science.280.5360.104
- Kanehisa, M., Goto, S., Kawashima, S., Okuno, Y., and Hattori, M. (2004). The KEGG resource for deciphering the genome. *Nucleic Acids Res.* 32, 277D–2280D. doi: 10.1093/nar/gkh063
- Kasuga, M., Miura, S., Shinozaki, K., and Yamaguchi-Shinozaki, K. (2004). A combination of the *Arabidopsis* DREB1A gene and stress-inducible rd29A

SUPPLEMENTARY MATERIAL

The Supplementary Material for this article can be found online at <https://www.frontiersin.org/articles/10.3389/fpls.2022.760460/full#supplementary-material>

- promoter improved drought-and low-temperature stress tolerance in tobacco by gene transfer. *Plant Cell Physiol.* 45, 346–350. doi: 10.1093/pcp/pch037
- Koonin, E. V., Fedorova, N. D., Jackson, J. D., Jacobs, A. R., Krylov, D. M., Makarova, K. S., et al. (2004). A comprehensive evolutionary classification of proteins encoded in complete eukaryotic genomes. *Genome Biol.* 5, R7–R28. doi: 10.1186/gb-2004-5-2-r7
- Kramer, D. M., Johnson, G., Kiirats, O., and Edwards, G. E. (2004). New fluorescence parameters for the determination of QA redox state and excitation energy fluxes. *Photosynth. Res.* 79, 209–218. doi: 10.1023/B:PRES.0000015391.99477.0d
- Li, W., Gao, S., Li, Q., Shen, P., Li, Y., Hu, D., et al. (2020). Transcriptome profiling of *Plumbago auriculata* lam. In response to cold stress. *Acta Physiol. Plant.* 42, 1–18. doi: 10.1007/s11738-020-03082-4
- Li, M., Sui, N., Lin, L., Yang, Z., and Zhang, Y. (2019). Transcriptomic profiling revealed genes involved in response to cold stress in maize. *Funct. Plant Biol.* 46, 830–844. doi: 10.1071/FP19065
- Li, Y. C., He, S. M., He, Z. X., Li, M., Yang, Y., Pang, J. X., et al. (2014). Plumbagin induces apoptotic and autophagic cell death through inhibition of the PI3K/Akt/mTOR pathway in human non-small cell lung cancer cells. *Cancer Lett.* 344, 239–259. doi: 10.1016/j.canlet.2013.11.001
- Liang, L. H., Mei, X., Lin, F., Xia, J., Liu, S. J., and Wang, J. H. (2009). Effect of low temperature stress on tissue structure and physiological index of cashew young leaves. *Ecol. Environ. Sci.* 18, 317–320.
- Liu, W., Cheng, C., Lin, Y., XuHan, X., and Lai, Z. (2018). Genome-wide identification and characterization of mRNAs and lncRNAs involved in cold stress in the wild banana (*Musa itinerans*). *PLoS One* 13:e0200002. doi: 10.1371/journal.pone.0200002
- Liu, Q., Kasuga, M., Sakuma, Y., Abe, H., Miura, S., Yamaguchi-Shinozaki, K., et al. (1998). Two transcription factors, DREB1 and DREB2, with an EREBP/AP2 DNA binding domain separate two cellular signal transduction pathways in drought- and low-temperature-responsive gene expression, respectively. *Arabidopsis. The Plant Cell* 10, 1391–1406. doi: 10.1105/tpc.10.8.1391
- Long, S. P., Humphries, S., and Falkowski, P. G. (1994). Photoinhibition of photosynthesis in nature. *Annu. Rev. Plant Biol.* 45, 633–662. doi: 10.1146/annurev.pp.45.060194.003221
- Medina, J., Catalá, R., and Salinas, J. (2011). The CBFs: three Arabidopsis transcription factors to cold acclimate. *Plant Sci.* 180, 3–11. doi: 10.1016/j.plantsci.2010.06.019
- Medina, J., Bargues, M., Terol, J., Pérez-Alonso, M., and Salinas, J. (1999). The Arabidopsis CBF gene family is composed of three genes encoding AP2 domain-containing proteins whose expression is regulated by low temperature but not by abscisic acid or dehydration. *Plant Physiol.* 119, 463–470. doi: 10.1104/pp.119.2.463
- Miedema, P. (1982). The effects of low temperature on *Zea mays*. *Adv. Agron.* 35, 93–128. doi: 10.1016/S0065-2113(08)60322-3
- Nakashima, K., Ito, Y., and Yamaguchi-Shinozaki, K. (2009). Transcriptional regulatory networks in response to abiotic stresses in Arabidopsis and grasses. *Plant Physiol.* 149, 88–95. doi: 10.1104/pp.108.129791
- Neill, S., Desikan, R., and Hancock, J. (2002). Hydrogen peroxide signalling. *Curr. Opin. Plant Biol.* 5, 388–395. doi: 10.1016/S1369-5266(02)00282-0
- Novillo, F., Medina, J., and Salinas, J. (2007). Arabidopsis CBF1 and CBF3 have a different function than CBF2 in cold acclimation and define different gene classes in the CBF regulon. *Proc. Natl. Acad. Sci.* 104, 21002–21007. doi: 10.1073/pnas.0705639105
- Odhambo, M. O., Wang, X. C., de Antonio, P. I. J., Shi, Y. Y., and Zhao, B. (2018). Effects of root-zone temperature on growth, chlorophyll fluorescence characteristics and chlorophyll content of greenhouse pepper plants grown under cold stress in southern China. *Russ. Agric. Sci.* 44, 426–433. doi: 10.3103/S1068367418050130
- Ozturk, I., Ottosen, C. O., and Ritz, C. (2013). The effect of temperature on photosynthetic induction under fluctuating light in *Chrysanthemum morifolium*. *Acta Physiol. Plant.* 35, 1179–1188. doi: 10.1007/s11738-012-1157-x
- Park, S., Lee, C. M., Doherty, C. J., Gilmour, S. J., Kim, Y., and Thomashow, M. F. (2015). Regulation of the Arabidopsis CBF regulon by a complex low-temperature regulatory network. *Plant J.* 82, 193–207. doi: 10.1111/tpj.12796
- Payton, P., Webb, R., Korniyev, D., Allen, R., and Holaday, A. S. (2001). Protecting cotton photosynthesis during moderate chilling at high light intensity by increasing chloroplastic antioxidant enzyme activity. *J. Exp. Bot.* 52, 2345–2354. doi: 10.1093/jexbot/52.365.2345
- Qin, F., Sakuma, Y., Li, J., Liu, Q., Li, Y. Q., Shinozaki, K., et al. (2004). Cloning and functional analysis of a novel DREB1/CBF transcription factor involved in cold-responsive gene expression in *Zea mays* L. *Plant Cell Physiol.* 45, 1042–1052. doi: 10.1093/pcp/pch118
- Qiu, J. R., Xiang, X. Y., Wang, J. T., Xu, W. X., Chen, J., Xiao, Y., et al. (2020). MfPIF1 of resurrection plant *Myrothamnus flabellifolia* plays a positive regulatory role in responding to drought and salinity stresses in Arabidopsis. *Int. J. Mol. Sci.* 21, 3011. doi: 10.3390/ijms21083011
- Rapacz, M. (2007). Chlorophyll a fluorescence transient during freezing and recovery in winter wheat. *Photosynthetica* 45, 409–418. doi: 10.1007/s11099-007-0069-2
- Shi, Y., Ding, Y., and Yang, S. (2018). Molecular regulation of CBF signaling in cold acclimation. *Trends Plant Sci.* 23, 623–637. doi: 10.1016/j.tplants.2018.04.002
- Skrudlik, G., Bączek-Kwinta, R., and Kościelniak, J. (2000). The effect of short warm breaks during chilling on photosynthesis and the activity of antioxidant enzymes in plants sensitive to chilling. *J. Agron. Crop Sci.* 184, 233–240. doi: 10.1046/j.1439-037x.2000.00377.x
- Song, Y., Jia, Z., Hou, Y., Ma, X., Li, L., Jin, X., et al. (2020). Roles of DNA methylation in cold priming in Tartary buckwheat. *Front. Plant Sci.* 11, 222. doi: 10.3389/fpls.2020.608540
- Spitz, D. R., and Oberley, L. W. (1989). An assay for superoxide dismutase activity in mammalian tissue homogenates. *Anal. Biochem.* 179, 8–18. doi: 10.1016/0003-2697(89)90192-9
- Stockinger, E. J., Gilmour, S. J., and Thomashow, M. F. (1997). Arabidopsis thaliana CBF1 encodes an AP2 domain-containing transcriptional activator that binds to the C-repeat/DRE, a cis-acting DNA regulatory element that stimulates transcription in response to low temperature and water deficit. *Proc. Natl. Acad. Sci.* 94, 1035–1040. doi: 10.1073/pnas.94.3.1035
- Strauss, A. J., Krüger, G. H. J., Strasser, R. J., and Van Heerden, P. D. R. (2006). Ranking of dark chilling tolerance in soybean genotypes probed by the chlorophyll a fluorescence transient OJIP. *Environ. Exp. Bot.* 56(2), 147–157. doi: 10.1016/j.envexpbot.2005.01.011
- Su, C. F., Wang, Y. C., Hsieh, T. H., Lu, C. A., Tseng, T. H., and Yu, S. M. (2010). A novel MYBS3-dependent pathway confers cold tolerance in rice. *Plant Physiol.* 153, 145–158. doi: 10.1104/pp.110.153015
- Tatusov, R. L., Galperin, M. Y., Natale, D. A., and Koonin, E. V. (2000). The COG database: a tool for genome-scale analysis of protein functions and evolution. *Nucleic Acids Res.* 28, 33–36. doi: 10.1093/nar/28.1.33
- Uddling, J., Gelang-Alfredsson, J., Piikki, K., and Pleijel, H. (2007). Evaluating the relationship between leaf chlorophyll concentration and SPAD-502 chlorophyll meter readings. *Photosynth. Res.* 91, 37–46. doi: 10.1007/s11200-006-9077-5
- Wang, X. F., Ye, Y. J., Fan, M. Y., Chen, L., Ma, T., and Wan, Z. B. (2020). Effects of temperature on Transcriptome profiles in *Cardiocrinum cathayanum* leaves. *Russ. J. Plant Physiol.* 67, 1105–1115. doi: 10.1134/S1021443720060199
- Wang, Y., Xu, H., Liu, W., Wang, N., Qu, C., Jiang, S., et al. (2019). Methyl jasmonate enhances apple cold tolerance through the JAZ-MYC2 pathway. *Plant Cell, Tissue and Organ Culture (PCTOC)* 136, 75–84. doi: 10.1007/s11240-018-1493-7
- Wang, Y. X., Ya, H. U., Chen, B. H., Zhu, Y. F., Dawuda, M. M., and Svetla, S. (2018). Physiological mechanisms of resistance to cold stress associated with 10 elite apple rootstocks. *J. Integr. Agric.* 17, 857–866. doi: 10.1016/S2095-3119(17)61760-X
- Wang, F., Guo, Z., Li, H., Wang, M., Onac, E., Zhou, J., et al. (2016). Phytochrome A and B function antagonistically to regulate cold tolerance via abscisic acid-dependent jasmonate signaling. *Plant Physiol.* 170, 459–471. doi: 10.1104/pp.15.01171
- Xie, C., Mao, X., Huang, J., Ding, Y., Wu, J., Dong, S., et al. (2011). KOBAS 2.0: a web server for annotation and identification of enriched pathways and diseases. *Nucleic Acids Res.* 39, W316–W322. doi: 10.1093/nar/gkr483
- Yamaguchi-Shinozaki, K., and Shinozaki, K. (2006). Transcriptional regulatory networks in cellular responses and tolerance to dehydration and cold stresses. *Annu. Rev. Plant Biol.* 57, 781–803. doi: 10.1146/annurev.arplant.57.032905.105444

- Yin, Y. J., Chen, C. J., Guo, S. W., Li, K. M., Ma, Y. N., Sun, W. M., et al. (2018). The fight against *Panax notoginseng* root-rot disease using zingiberaceae essential oils as potential weapons. *Front. Plant Sci.* 9, 1346. doi: 10.3389/fpls.2018.01346
- Zhang, Q., Shan, C. H., Ning, M., Zhao, X. X., Du, H. F., Cai, W. C., et al. (2020). Transcriptome profiling of gold queen Hami melons under cold stress. *Russ. J. Plant Physiol.* 67, 888–897. doi: 10.1134/S1021443720050209
- Zhang, X., Fowler, S. G., Cheng, H., Lou, Y., Rhee, S. Y., Stockinger, E. J., et al. (2004). Freezing-sensitive tomato has a functional CBF cold response pathway, but a CBF regulon that differs from that of freezing-tolerant *Arabidopsis*. *Plant J.* 39, 905–919. doi: 10.1111/j.1365-3113X.2004.02176.x
- Zhao, M. L., Wang, J. N., Shan, W., Fan, J. G., Kuang, J. F., Wu, K. Q., et al. (2013). Induction of jasmonate signalling regulators MaMYC2s and their physical interactions with MaICE1 in methyl jasmonate-induced chilling tolerance in banana fruit. *Plant Cell Environ.* 36, 30–51. doi: 10.1111/j.1365-3040.2012.02551.x

Conflict of Interest: The authors declare that this research was conducted in the absence of any commercial or financial relationships that could be construed as a potential conflict of interest.

Publisher's Note: All claims expressed in this article are solely those of the authors and do not necessarily represent those of their affiliated organizations, or those of the publisher, the editors and the reviewers. Any product that may be evaluated in this article, or claim that may be made by its manufacturer, is not guaranteed or endorsed by the publisher.

Copyright © 2022 Li, Gao, Lei, Jiang, Duan, Zhao, Li, Shi and Yang. This is an open-access article distributed under the terms of the Creative Commons Attribution License (CC BY). The use, distribution or reproduction in other forums is permitted, provided the original author(s) and the copyright owner(s) are credited and that the original publication in this journal is cited, in accordance with accepted academic practice. No use, distribution or reproduction is permitted which does not comply with these terms.



Inositol Improves Cold Tolerance Through Inhibiting *CBL1* and Increasing Ca^{2+} Influx in Rapeseed (*Brassica napus* L.)

Lei Yan, Liu Zeng, Ali Raza[†], Yan Lv, Xiaoyu Ding, Yong Cheng and Xiling Zou^{*}

Key Laboratory of Biology and Genetic Improvement of Oil Crops, Ministry of Agriculture, Oil Crops Research Institute of the Chinese Academy of Agricultural Sciences, Wuhan, China

OPEN ACCESS

Edited by:

Andy Pereira,
University of Arkansas, United States

Reviewed by:

Surinder Banga,
Punjab Agricultural University, India
Xiao-Li Tan,
Jiangsu University, China
Lalit Dev Tiwari,
Agricultural Research Organization
(ARO), Israel

*Correspondence:

Xiling Zou
zouxiling@gmail.com

†ORCID:

Ali Raza
orcid.org/0000-0002-5120-2791

Specialty section:

This article was submitted to
Plant Abiotic Stress,
a section of the journal
Frontiers in Plant Science

Received: 14 September 2021

Accepted: 07 February 2022

Published: 17 March 2022

Citation:

Yan L, Zeng L, Raza A, Lv Y, Ding X,
Cheng Y and Zou X (2022) Inositol
Improves Cold Tolerance Through
Inhibiting *CBL1* and Increasing Ca^{2+}
Influx in Rapeseed (*Brassica napus* L.).
Front. Plant Sci. 13:775692.
doi: 10.3389/fpls.2022.775692

Rapeseed (*Brassica napus* L.) is an important oilseed crop worldwide. However, its productivity is significantly affected by various abiotic stresses, including cold stress. Among various stresses, cold stress is an important abiotic factor affecting plant growth, yield, and quality. The calcium channels are regarded as key pathways affecting cold tolerance in plants. Thus, improvement in cold tolerance is of great significance for crop improvement. The current study was designed to examine the beneficial role of exogenous inositol in improving cold stress tolerance in rapeseed. From the RNA-seq results, we identified 35 differently expressed genes encoding different inositol enzymes. The results show that inositol (a cyclic polyol) positively regulated cold tolerance by increasing calcium ion (Ca^{2+}) influx in rapeseed. Furthermore, we found that the expression of calcineurin B-like (*CBL1*) gene was inhibited by inositol. On the other hand, overexpressed plant mediated the Ca^{2+} flux under cold stress suggesting the key role of inositol- Ca^{2+} pathway in cold tolerance. Moreover, the overexpression of *BnCBL1-2* in *Arabidopsis* represented that transgenic plants mediated the Ca^{2+} flux highlighting the vital role of the inositol- Ca^{2+} pathway in conferring cold stress. Our study provides new insights into rapeseed cold tolerance mechanism and introduces a feasible method to improve the cold tolerance of rapeseed quickly.

Keywords: chilling stress, calcium ion, gene expression, transgenic plant, signaling pathways, stress tolerance

INTRODUCTION

Cold stress, including chilling ($>0^{\circ}\text{C}$) and freezing ($<0^{\circ}\text{C}$) temperature, is one of the main abiotic factors affecting plant growth and productivity (Xin and Browse, 2000). In past years, the mechanism underlying plant cold tolerance has been extensively studied, and numerous components, such as transcription factors, amino acid metabolites, phosphatases, and protein kinases, have been identified in cold signaling pathways (Chinnusamy et al., 2003; Kou et al., 2018; Ding et al., 2019; Raza et al., 2021). Among them, the *CBF* (*C-repeat binding factors*)-*COR* (*cold-responsive*) signaling pathway is the most well-known. In this pathway, *CBFs* genes are rapidly induced by cold stress and then bind to the promoter regions of *COR* genes to activate their transcription (Chinnusamy et al., 2007; Shi et al., 2015;

Jia et al., 2016; Zhao et al., 2016). The *COR* genes encode a series of osmolyte and cryoprotective proteins to protect the plant against cold stress (Ding et al., 2019). In addition, various hormones, including abscisic acid (ABA), brassinosteroids, ethylene, etc., play an important role in cold stress signaling pathways by regulating the expression level of stress-responsive genes (Chen and Gusta, 1983; Huang et al., 2017; Tan et al., 2017; Rubio et al., 2019).

In addition to CBF-COR signaling and hormone-induced pathways, calcium ions (Ca^{2+}) also play an essential role in regulating plant cold response. Cytosolic Ca^{2+} are rapidly increased by cold stress, which is considered as one of the earliest cold signaling events in plants (Knight et al., 1996; Ding et al., 2019). The plasma membrane and endoplasmic reticulum-localized G protein regulator *COLD1* (CHILLING TOLERANCE DIVERGENCE1) coupled with *RGA1* (RICE G PROTEIN α SUBUNIT1) were found to improve the cold tolerance by regulating the influx of intracellular Ca^{2+} in rice (Ma et al., 2015). Some studies also indicated that Ca^{2+} might act as an important secondary messenger mediating low-temperature sensing in plants. For instance, CDPKs (Ca^{2+} -dependent protein kinases), CBLs (calciurein B-like), CIPKs (CBL-interacting protein kinases), and ANNEXIN1 (Ca^{2+} permeable transporter) were shown to modulate the cold tolerance in plants (Cheong et al., 2003; Abbasi et al., 2004; Komatsu et al., 2007; Weckwerth et al., 2015; Li et al., 2019; Liu et al., 2020). Inositol is a cyclic polyol that participates in numerous physiological processes, including signal transduction and stress adaptation in plants (Loewus and Murthy, 2000). A recent study shows that the overexpression of the rice inositol-coding gene (*OsIMP*) increases the accumulation of inositol and cold tolerance in tobacco by regulating the antioxidant enzyme activities (Zhang et al., 2017). However, the inositol-induced cold stress tolerance mechanism is yet to be reported.

Rapeseed (*Brassica napus* L.) is an important overwintering oilseed crop globally. It is mainly grown in the Yangtze River Basin of China, Canada, Central, and Northern Europe. Nevertheless, its yield parameters have been significantly altered due to the increased exposure to cold stress (Huang et al., 2021; Raza, 2021). In January 2008, south China suffered severe freezing weather, which reduces the rapeseed yield by 10.9% (Zhang et al., 2008). Therefore, there is a dire need to examine the molecular and biochemical mechanisms to enhance rapeseed production. Over the past few years, several attempts have been made to identify the cold-responsive mechanisms in rapeseed. For instance, Zeng et al. (2018) identified eight conserved, and two novels differentially expressed miRNAs that positively regulate cold stress tolerance in rapeseed. Previous studies showed six cold-tolerant rapeseeds cultivars and C18 had a higher ability to regulate hormonal, osmotic, and antioxidative activity along with gene transcriptional level than in cold-sensitive cultivar (C20) under cold stress (Yan et al., 2018, 2019). Only a few cold-responsive genes have been identified in rapeseed, and most of them are homologous to *CBF* or *COR*, including *BnCBF5*, *BnCBF17*, and *BnCOR25* (Savitch et al., 2005; Chen et al., 2011).

In this study, the comparison of transcriptomes was performed between cold-tolerant (C18) and cold-sensitive (C20) cultivars. The transcriptome results indicated that inositol was involved in the cold response. Therefore, rapeseed seedlings were treated with exogenous inositol to identify the possible mechanism of inositol-mediated cold tolerance. The results showed that inositol increased the expression of *CORs* genes independent of *CBF* or *ABA* and improved cold tolerance of rapeseed by increasing Ca^{2+} influx. In addition, we revealed that a feedback regulatory pathway composed of inositol, *CBL1*, and Ca^{2+} playing a key role in cold-induced cytoplasmic calcium accumulation and cold tolerance in rapeseed.

MATERIALS AND METHODS

Plant Materials, Freezing Stress, and RNA Isolation

The seeds of C18 (cold-tolerant) and C20 (cold-sensitive) cultivars were provided by the Oil Crops Research Institute, Chinese Academy of Agricultural Sciences (Wuhan, China). Rapeseed seedlings were grown in small pots having soil in a growth chamber with a 16-/8-h light/dark cycle at 22°C. Then, the 21-day-old seedlings (three-leaf stage) were placed in low-temperature incubators at 4°C for 24 h. Cold stress was imposed at a temperature of 2°C for 1 h, and then the temperature was reduced gradually to 0°C, −2°C for 1 h, respectively. The leaf samples from all the seedlings grew under corresponding controls (22°C when sampled under 2°C, 0°C and −2°C), 2°C, 0°C and −2°C were collected, frozen in liquid nitrogen, and stored at −80°C for RNA extraction and further use. *Arabidopsis* freezing treatment was carried out as described by Zhao et al. (2016). RNA extraction and purification were performed as described in Yan et al. (2019). Using the above-mentioned samples, the RNA-seq was performed using the Illumina Hiseq 2000 (LC, Science, and Houston, TX) platform, and then the raw reads were generated. The whole experiment was carried out with three biological replications.

Analysis of RNA Sequencing Data

Raw data were processed with Fast QC 10.1 software and filtered by removing the unqualified reads. The descriptive statistics for the clean data, such as Q20, Q30, and GC content, were calculated. The clean reads of each library were mapped to the *Brassica napus* L. genome using Hisat 2.0 software to count the mapping rate.¹ The remaining sequences were considered as clean reads (the corresponding data have been submitted into the database of National Center for Biotechnology Information, Short Read Archive (NCBI, SRV) with accession number PRJNA562064). Fragment per kilobase of exon per million fragments mapped (FPKM) value was used to evaluate the gene expression level.

¹<https://www.genoscope.cns.fr/brassicanapus/>

Identification and Analysis of DEGs

The DEGseq R package was used to identify differentially expression genes (DEGs). The integration of a $p < 0.05$ and an absolute value of $\log_2 \text{ratio} > 1$ were used to identify DEGs. Gene ontology (GO)² and MapMan³ analysis were performed for the functional analysis of DEGs.

qRT-PCR Analysis

The above-mentioned RNA samples were used for qRT-PCR analysis. The primers were designed using Primer 5.0 software and listed in **Supplementary Table S5**. The *Brassica napus* actin gene-specific primer (GeneBank: AF111812) was used as a control to normalize the expression data (Wang et al., 2014). The qRT-PCR was carried out with the TransStart Tip Green qPCR SuperMix (TransGen, China) on StepOnePlus real-time PCR system (Applied Biosystems, United States). The condition for PCR was as follows: 95°C for 30s and 40 cycles of 95°C for 10s, followed by 60°C for 30s (extension and signal acquisition). The relative expression levels were calculated using the $2^{-\Delta\Delta C_t}$ method.

Measurement of Endogenous Inositol and ABA Concentrations

Endogenous inositol and ABA concentration were estimated using the ELISA kit produced by You Xuan Biological Technology Co. Ltd. (Shanghai, China). A total of 0.1g of leaves was homogenized in chilled pestle and mortar using the 50 mmol L⁻¹ phosphate buffer (pH 7.4). The homogenate was centrifuged at 4,000 rpm for 10 min. Then, the supernatant was collected into another tube to measure the inositol concentration following the kit manufacturer's instructions.

Application of Exogenous Inositol

The 21-day-old seedlings of four cold-sensitive cultivars (Zheyu21, Ningyou18, C06, and C20) were pretreated with different concentrations (0.1, 0.5, 1.0, 2.0, 5.0, and 8.0 g L⁻¹) of inositol solution, and the CK plants were treated with water. The seedlings were divided into two groups. In the first group, the seedlings were treated with freezing stress (−2°C) immediately, and the second group seedlings were treated with freezing stress (−2°C) 2 days after the pretreatment with inositol. After the freezing treatment, the survival rate was evaluated as described in our previous report (Yan et al., 2018).

Ca²⁺ Flux

Net Ca²⁺ fluxes of leaves of 21-day-old seedlings were measured at the YoungerUSA Xuyue (Beijing) BioFunction Institute by using Non-invasive Micro-test Technology (NMT100 Series®, YoungerUSA LLC, Amherst, MA 01002, United States) Xuyue (Beijing) Sci. & Tech. Co., Ltd., Beijing, China, and imFluxes V2.0 (YoungerUSA LLC, Amherst, MA 01002, United States) Software (Ma et al., 2015).

Cloning of *CBL1-2* and Identification of Transgenic Plants

The CDS of *BnCBL1-2* was cloned by primers 5'-ATGGGCTGCTTCCACTCAA-3' and 5'-TCATGTGGCAATC TCATCGAC-3' and inserted into binary vector pBCXUN (ubiquitin promoter) linearized with *Sma* I and *Bam*HI enzymes. The recombinant plasmid pBCXUN-BnCBL1-2 (**Supplementary Figure S5**) was introduced into *Agrobacterium tumefaciens* strain GV3101 using the heat shock method. *Agrobacterium*-mediated transformation of *Arabidopsis* was carried out as described by Clough and Bent (1998).

To check the effect of exogenous inositol on cold-responsive markers gene (*CBFs*, and *CORs*) and ABA contents, the 21-day-old seedlings of C20 were sprayed with 0.5 g L⁻¹ of inositol solution water (control). Then, the seedlings were divided into two groups. One group continued to grow under 22°C, and the other was treated at 4°C for 1 h. After 1 h, green leaves were harvested and were stored at −80°C for the qRT-PCR.

Similarly, the 21-day-old seedlings of C20 were used to evaluate the transient effect of exogenous inositol on *CBLs* genes. The seedlings were subjected to the cold stress as 4°C for 1, 2, 4, 8, 12, and 24 h, 2°C for 1 h, 0°C for 1 h, and −2°C for 1 h. Green leaves were harvested at each time point and were stored at −80°C for the qRT-PCR. Meantime, the seedlings with the pretreatment of inositol and water under 22°C were also harvested as the CK. For durative effect, the cold stress was imposed after cold acclimation of 4°C for 24 h to 21-day-old seedlings of C20. The cold stress treatment was set as 2°C for 1 h, 0°C for 1 h, and −2°C for 1 h. The pretreatment of inositol and the harvest of samples were the same as the explained earlier. The primers used for qRT-PCR are shown in **Supplementary Table S5**.

Statistical Data Analysis

Statistical analysis were performed using SPSS statistical package (SPSS Student version 15.0). Significant differences were evaluated using the two-tailed Student's t-test or one-way ANOVA and Duncan's test. All test differences at $p \leq 0.05$ were considered to be significant. All the error bars were SD (Standard Deviation) value.

RESULTS

Inositol Phosphate Pathway Had Been Enriched and Displayed Differences Between C18 and C20

C18 and C20 were verified to be cold-tolerant and cold-sensitive cultivars in previous morphological and physiological experiments (Yan et al., 2018, 2019). To identify the molecular mechanism of cold tolerance, the two cultivars were exposed to 2°C, 0°C, −2°C, and 22°C (CK, control) for cold stress treatment and 36 cDNA libraries (two genotypes × six treatments × three biological replicates) were constructed for RNA-seq (**Supplementary Figure S1**). After a series of processing, such as filtering and quality control (**Supplementary Table S1**), the

²<http://www.geneontology.org>

³<https://mapman.gabipd.org/mapman/>

sequencing data were used for further analysis. With the criterion of $|\log_2FC| > 1$ and q value < 0.05 , a total of 31,392 DEGs were identified between cold stress and corresponding control.

Further, these DEGs were subjected to GO enrichment. The results of GO molecular function enrichment showed oxidoreductase activity, asparagine synthase (glutamine-hydrolyzing) activity, NADP binding, and phosphoric ester hydrolase activity were enriched in S1, S2, S3 (cold-sensitive cultivar C20 under 2°C, 0°C, -2°C compared to 22°C); oxidoreductase activity, asparagine synthase (glutamine-hydrolyzing) activity, catalytic activity, glutamate-ammonia ligase activity, and inositol-3-phosphate synthase activity were enriched in T1, T2, T3 (cold-tolerant cultivar C18 under 2°C, 0°C, -2°C compared to 22°C; **Figure 1**). The functional enrichment analysis by Mapman indicated that the pathway of inositol phosphate was enriched (**Supplementary Figure S2**). Inositol biosynthesis and degradation were enriched under cold stress, and 35 related DEGs were identified to be differentially expressed (**Figure 2A**). Of these 35 DEGs, 28 DEGs are involved in inositol biosynthesis, encoding three enzymes (hexokinase HXK, myo-inositol-1-phosphate synthase MIPS, and inositol monophosphate IMPase), and seven DEGs involved in inositol degradation, encoding myo-inositol oxygenase (MIOX; **Figure 2A**). Among these 35 DEGs, 14 DEGs were randomly selected for qRT-PCR-based validation. The expression patterns for these DEGs were generally consistent between RNA-seq and qRT-PCR data (**Supplementary Figure S3**), indicating the reproducibility of the RNA-seq data.

Among different HXK genes, two HXK2 genes were upregulated in response to cold stress in both cultivars, and one HXK3 and HXK4 were upregulated in C20. Seven HXK3 were downregulated in both cultivars (C18 and C20; **Figure 2A**). MIPS catalyzes the conversion of glucose 6-phosphate to myo-inositol 1-phosphate, which is a rate-limiting step of the inositol biosynthetic pathway in plants. All the eight DEGs encoding MIPS were increased in both cultivars under cold stress; however, the genes in C18 had a stronger increasing trend than that in C20. For IMPase, eight upregulated DEGs were identified in C18 under 2°C, while there were only four upregulated genes identified in C20 (**Figure 2A**). Notably, the expression trends have varied under 0°C and -2°C. For instance, more MIOXs genes were downregulated in C18 than C20 under cold stress. Especially under 0°C, seven downregulated MIOXs were identified in C18, and only three downregulated MIOXs were found in C20. The different expression patterns of genes responsible for myo-inositol biosynthesis and degradation between C18 and C20 might result in higher endogenous inositol accumulation in C18 than in C20 (**Figure 2A**).

Endogenous Inositol Content Increased in C18 and Decreased in C20 With Varying Temperature

The endogenous inositol concentration in C18 was 18.9 ng g⁻¹ and 20.1 ng g⁻¹ under 2°C and CK, and there was no significant difference. With the continually dropping temperature, the inositol content in C18 increased significantly (22.4 and 22.2 ng g⁻¹ under 0°C and -2°C treatment) compared to control conditions

(16.9 and 17.4 ng g⁻¹; **Figure 2B**). The inositol content of C20 under 2°C (19.2 ng g⁻¹) was higher than that under CK (16.4 ng g⁻¹). Notably, at 0°C, there were no significant differences (18.7 and 18.0 ng g⁻¹). However, the inositol content (15.9 ng g⁻¹) of C20 under -2°C was decreased compared to control (20.4 ng g⁻¹; **Figure 2B**). In a nutshell, the results showed that endogenous inositol concentration increased in C18 and decreased in C20 with the gradually dropping temperature.

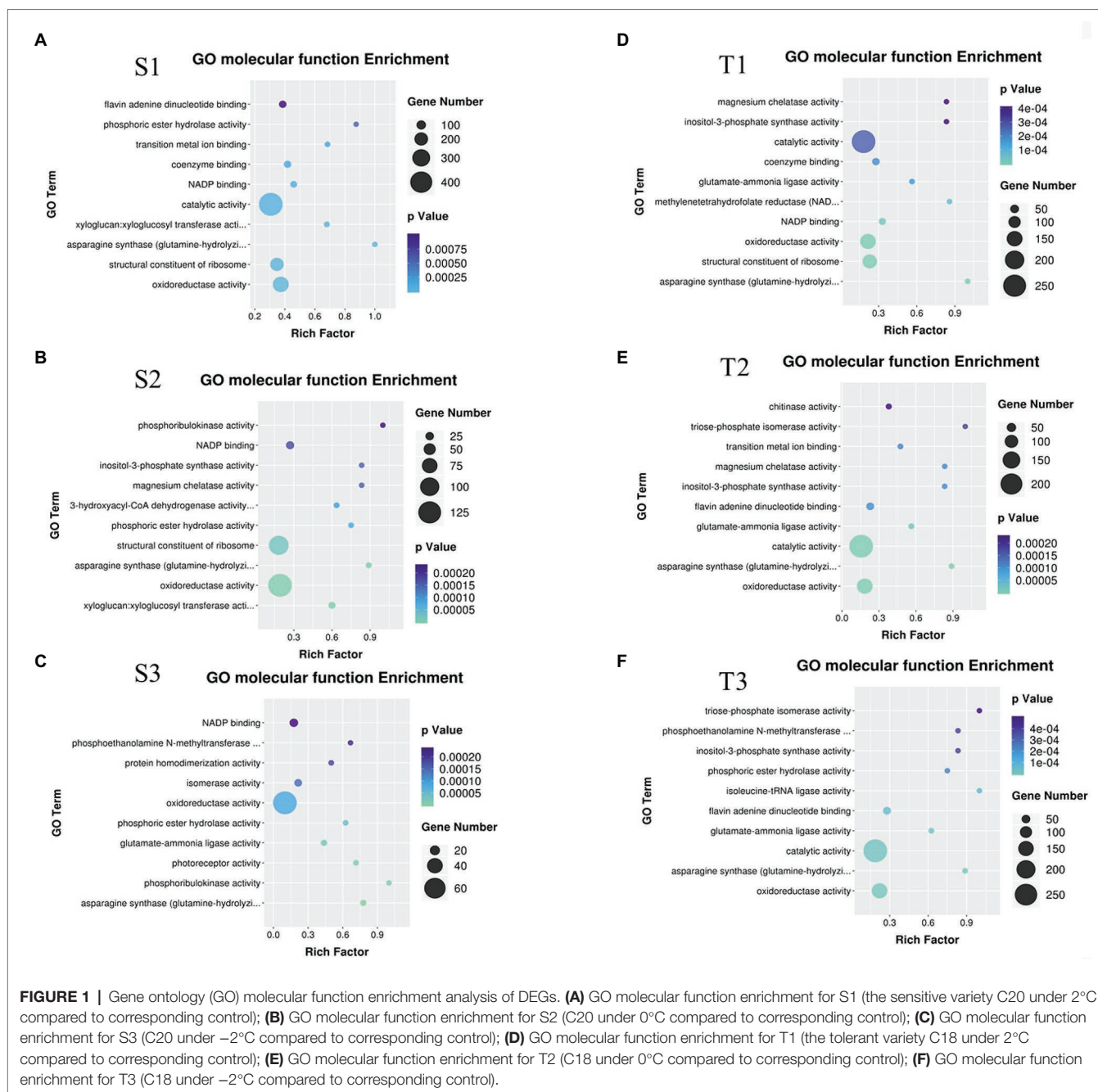
Exogenous Application of Inositol Improved Cold Tolerance In Rapeseed

To investigate the effect of inositol on cold tolerance in rapeseed, four representative sensitive cultivars (Zheyu21, Ningyou18, C06, and C20; Yan et al., 2018) were chosen to be treated with exogenous inositol under cold stress. The results presented that all the sensitive varieties with inositol pretreatment were found to be more cold-tolerant than CK (**Figures 2C,D**). Interestingly, control seedlings were failed to survive under -2°C. At the same time, the treated cultivars showed better performed. The survival rate of Zheyu21, Ningyou18, C06, and C20 was 79, 46, 17, and 46%, respectively, when pretreated with optimum concentration of inositol 1.0 g L⁻¹, 2.0 g L⁻¹, 0.1 g L⁻¹, and 0.5 g L⁻¹, respectively (**Figures 2C,D**).

Exogenous Inositol Application Increased the Expression of CORs Gene via a Pathway Independent of CBF or ABA

To clarify signal transduction of inositol, the relation was explored between inositol and known signaling pathways involved in cold stress, such as the CBF pathway. Therefore, the expression of several markers genes, including CBFs and CORs were analyzed after exogenous inositol pretreatment. Under 22°C, the expression of *BnCBF1*, *BnCBF2*, and *BnCBF4* was slightly increased after exogenous inositol application (**Figures 3A,B**). However, at 4°C, the expression of *BnCBF1*, *BnCBF2*, and *BnCBF4* was decreased dramatically compared with CK. The result showed that exogenous inositol increased cold tolerance, not by increasing the expression of CBFs. Besides, the expression pattern of CORs after exogenous inositol application was also analyzed. Under 22°C, the expressions of *BnCOR6.6*, *BnCOR15*, and *BnCOR25* increased significantly after exogenous inositol application (**Figure 3C**). At 4°C, the expression level of *BnCOR6.6* and *BnCOR15* was increased in inositol-treated seedlings than CK. However, for the expression of *BnCOR25*, there was no significant difference between the inositol treatment and CK.

Considering the expression of *BnCOR25* is regulated by ABA (Chen et al., 2011), the ABA concentration of seedlings after exogenous inositol application was detected. The results showed that, under 0°C and -2°C, there was no significant difference for ABA concentration between inositol treatment and CK (**Figure 3D**). In addition, the genes involved in CBF or ABA pathway were explored in the transcriptome data, and there was no difference of expression between C18 and C20 cultivars under cold stress (**Supplementary Table S2**). All of the above evidence indicated that exogenous inositol increased cold tolerance, not through the ABA pathway, but maybe by regulating the expression levels of cold-responsive marker genes.



Inositol Increased Ca^{2+} Influx Under Cold Stress

After excluding the CBF and ABA pathway, it is speculated that the mechanism of inositol improving cold tolerance may be related to Ca^{2+} flux. Therefore the Ca^{2+} flux value in C20 seedlings treated with water and inositol was evaluated. Under 22°C, the initial Ca^{2+} flux value of inositol and water treated seedlings was 370.1 and 60.3 $\text{pmol cm}^{-2} \text{ s}^{-1}$, respectively (the positive value represents Ca^{2+} efflux, and a negative value represents Ca^{2+} influx). Under 4°C, the Ca^{2+} influx of inositol and water treated seedlings increased by 195.5 and 108.7 $\text{pmol cm}^{-2} \text{ s}^{-1}$, respectively, and the Ca^{2+} flux value finally reached 175.6

and -48.4 $\text{pmol cm}^{-2} \text{ s}^{-1}$, respectively (Figures 4A,B). Compared with the control, inositol treatment led to a stronger calcium influx. The results suggested that inositol increased Ca^{2+} influx under cold stress, resulting in enhanced cold tolerance in rapeseed.

Inositol Inhibited *BnCBL1-2* Under Cold Stress

In our study, inositol was proved to increase Ca^{2+} influx under cold stress which resulted in enhanced cold tolerance in rapeseed. In other studies, the combination of different concentrations of inositol and Ca^{2+} significantly promoted the growth of Chinese cabbage and pepper seedlings (Liu et al., 2017; Yang et al., 2017).

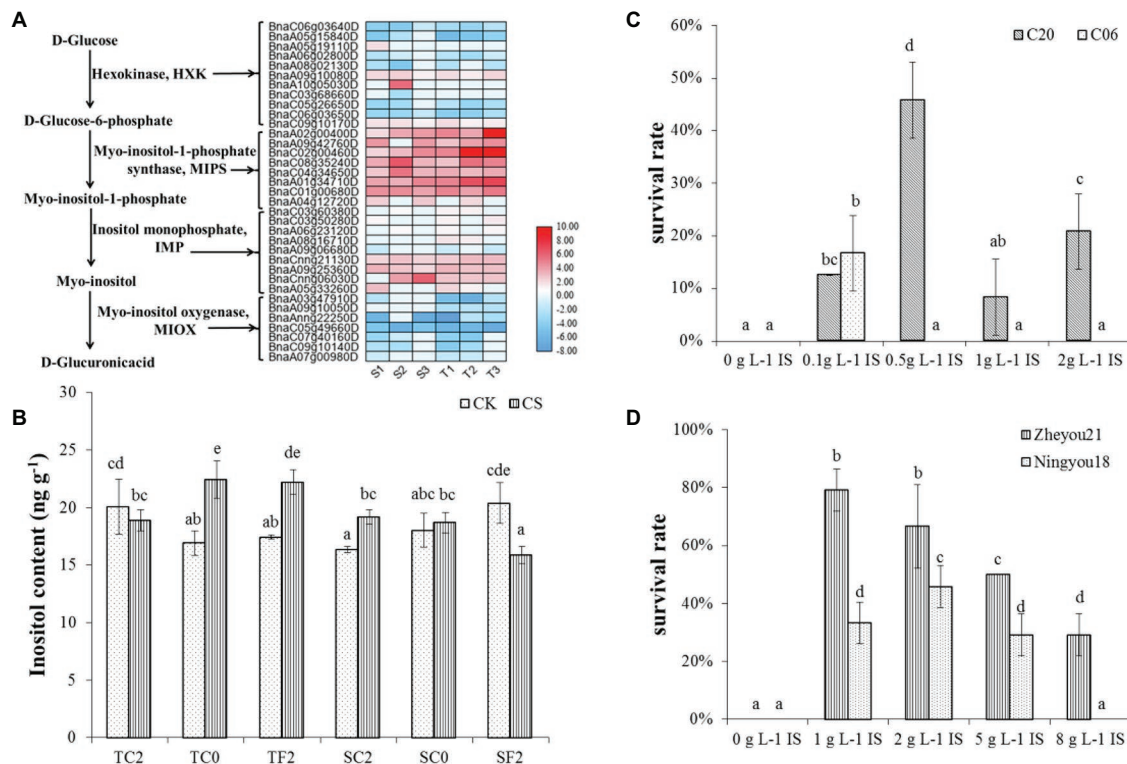


FIGURE 2 | Inositol involved in cold tolerance in rapeseed. **(A)** The expression analysis of DEGs involved inositol biosynthesis and degradation. Heat map data is log2 (Fold change). T1: the tolerant variety C18 under 2°C compared to corresponding control; T2: C18 under 0°C compared to corresponding control; T3: C18 under -2°C compared to corresponding control; S1: the sensitive variety C20 under 2°C compared to corresponding control; S2: C20 under 0°C compared to corresponding control; S3: C20 under -2°C compared to corresponding control. **(B)** Endogenous inositol concentrations under different cold treatment. TC2: C18 under 2°C; TC0: C18 under 0°C; TF2: C18 under -2°C; SC2: C20 under 2°C; SC0: C20 under 0°C; SF2: C20 under -2°C; CS: cold stress; CK: 22°C. Values were means of three replications, and the bars were represented the standard error of means. Different letters were represented significant differences according to Duncan's multiple range test ($p < 0.05$). **(C,D)** Exogenous inositol improved the cold tolerance of rapeseed. IS: inositol.

Then, we identified all the Ca^{2+} related gens in both the transcriptome of C18 and C20, and 351 DEGs were obtained to be different expressed in C18 and C20 (Supplementary Table S3). It has also been reported that some calcium sensors, such as *CBL1*, act as a rate-limiting factor to response to stress signals (Cheong et al., 2003). Of these 351 DEGs, there were four *CBL1*s. The expression of all the four *BnCBL1*s was increased in C20 under cold stress. There were no significant differences of expressions of *BnCBL1-3* and *BnCBL1-4* in C18 under cold stress. The expressions of *BnCBL1-1* and *BnCBL1-2* were decreased in C18 under cold stress (Supplementary Table S4). The result indicated that *BnCBL1* might be involved in signaling in cold tolerance. With the pretreatment of exogenous inositol, the expression of *BnCBL1-2* decreased in C20 under freezing stress (Supplementary Figure S4). *BnCBL1-2* was overexpressed in *Arabidopsis*, and two lines, *BnCBL1-2-1* and *BnCBL1-2-8*, were selected. After the cold treatment at -4°C for 3h, approximately 41% of WT and 7–18% of *CBL1*-overexpressing plants recovered from the freezing treatment. The survival rate of transgenic lines was significantly lower than WT plants (Figures 5C,D). The results indicated that overexpression of *BnCBL1-2* reduced cold tolerance.

The further experiment showed that overexpression of *BnCBL1-2* reduced cold tolerance and Ca^{2+} flux (Figures 5E,F). This research also revealed that inositol inhibited the expression of *BnCBL1-2* (*BnaA01g08510D*) under cold stress. Therefore, it is proposed there is a mechanism that inositol regulates the Ca^{2+} signaling and the expression of *CBL1* (Figure 6), which is a brand-new signal pathway under cold stress in plants.

Overexpressing *BnCBL1-2* Weaken the Ability of Ca^{2+} Influx Regulation in Plants

The Ca^{2+} flux was measured in WT and transgenic *Arabidopsis* with overexpressing *BnCBL1-2*. Under normal condition (22°C), in mesophyll cells, the initial Ca^{2+} flux values were 94.7, 35.6, and 61.7 pmol cm⁻² s⁻¹, respectively in WT, and overexpressing (*BnCBL1-2\textbackslash*u20131 and *BnCBL1-2\textbackslash*u20138) transgenic plants. Under cold stress (4°C), the Ca^{2+} flux of WT, overexpressing (*BnCBL1-2\textbackslash*u20131 and *BnCBL1-2\textbackslash*u20138) plants in mesophyll cells were -117.2, -101.8, and -41.1 pmol cm⁻² s⁻¹, respectively (Figures 5E,F). Compared with overexpressing *BnCBL1-2* plants, WT plants showed more Ca^{2+} efflux under normal conditions and more Ca^{2+} influx under cold stress, suggesting a stronger ability in Ca^{2+} regulation.

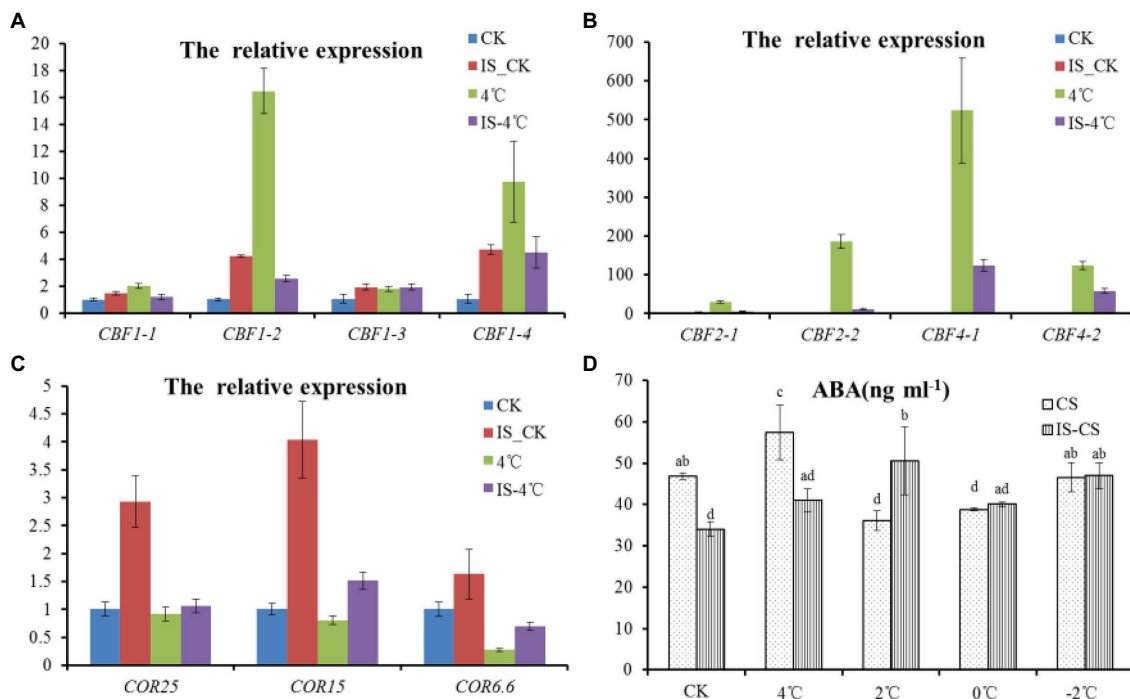


FIGURE 3 | Expression patterns of *CBFs*, *CORs*, and ABA content with exogenous inositol under cold stress. **(A)** The expression patterns of *CBF1* (*CBF1-1*–*CBF1-4*) with exogenous inositol under cold stress; **(B)** The expression patterns of *CBF2* (*CBF2-1* and *CBF2-2*) and *CBF4* (*CBF4-1* and *CBF4-2*) with exogenous inositol under cold stress; **(C)** The expression patterns of *CORs* (*COR25*, *COR15*, and *COR6.6*) with exogenous inositol under cold stress; **(D)** ABA content change with exogenous inositol under cold stress. CK: 22°C; 4°C: 4°C treatment for 1 h; IS-CK: 22°C for 1 h with 0.5 g L⁻¹ of exogenous inositol; IS-4°C: 4°C for 1 h with 0.5 g L⁻¹ of exogenous inositol.

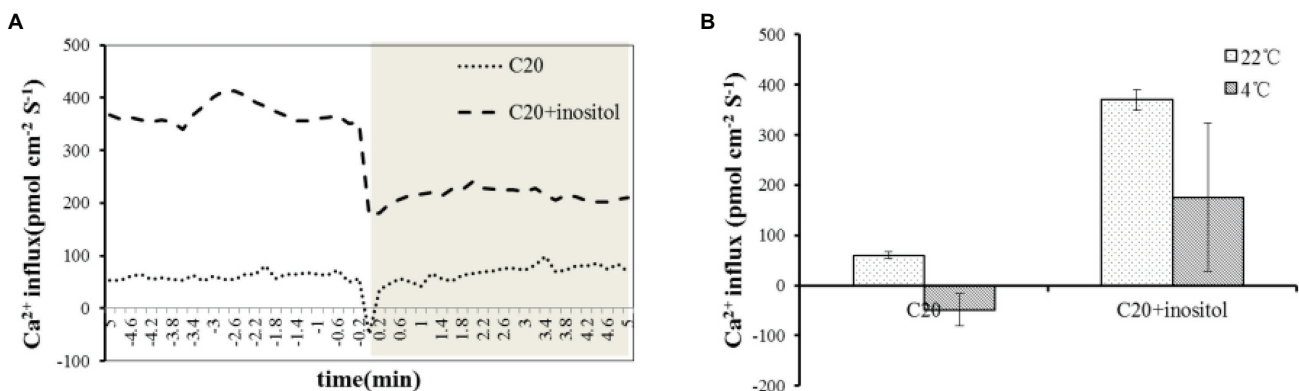


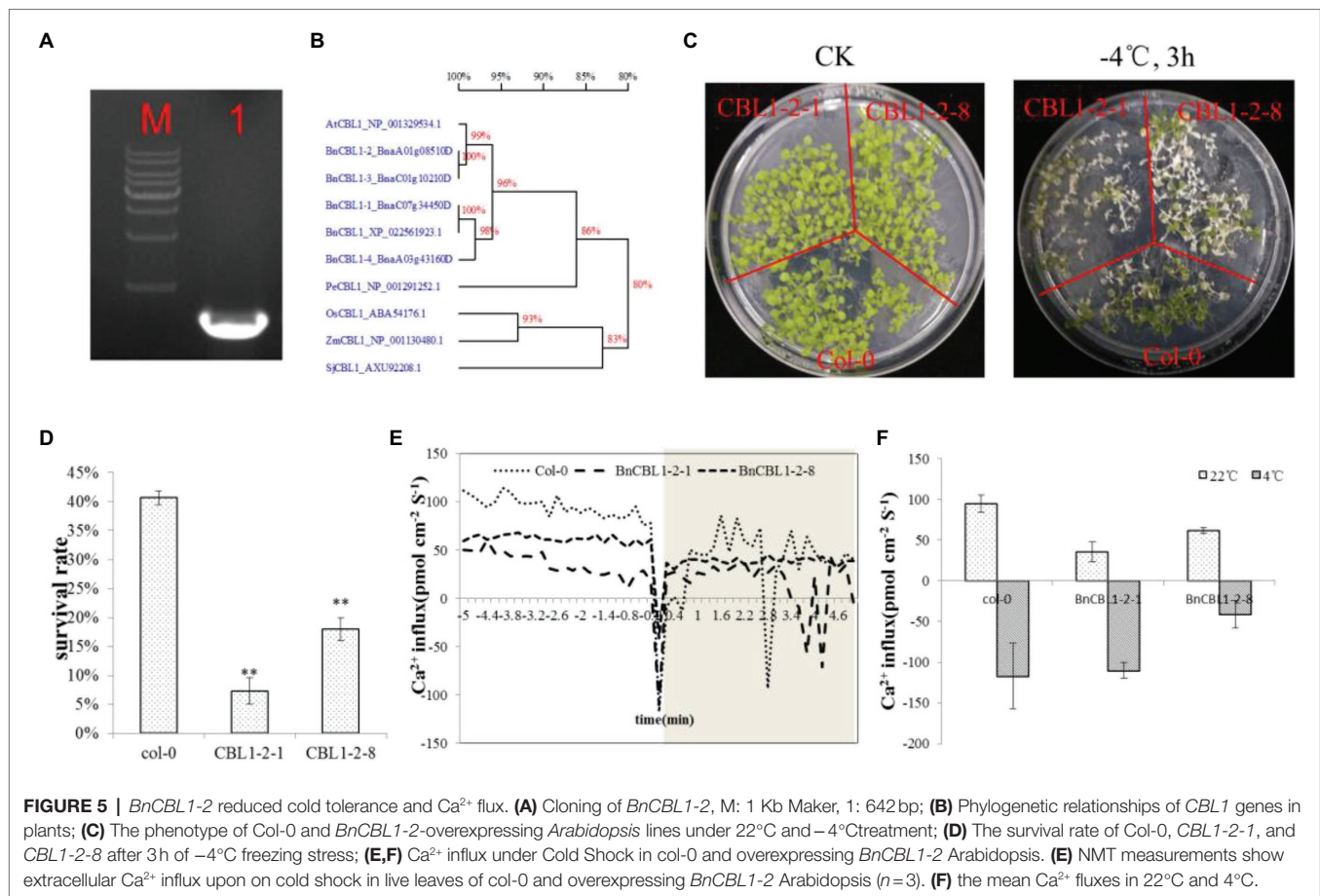
FIGURE 4 | Ca²⁺ influx upon Cold Shock in C20 spayed water and inositol. **(A)** NMT measurements show extracellular Ca²⁺ influx upon cold shock in live leaves of C20 spayed with water and inositol ($n=3$). **(B)** The mean Ca²⁺ fluxes in 22°C and 4°C.

DISCUSSION

Inositol Improved Cold Tolerance in Rapeseed

The best understood cold signaling pathway is the *ICE-CBF* transcriptional cascade, and the *CBF* genes play crucial roles in this cascade. In this study, three *CBF* related DEGs, *BnaA03g13620D* (homologous to *AtCBF1*), *BnaAnng34260D* (homologous to *AtCBF1*), and *BnaA10g07630D* (homologous to *AtCBF4*) were identified (Supplementary Table S2). The

BnCBF4 (*BnaA10g07630D*) was overexpressed in *Arabidopsis*, and the plants had a retarded flowering period (data not shown), which was similar to the previous studies (Jaglo-Ottosen et al., 1998; Gilmour et al., 2004). Overexpression of *CBFs* not only improved freezing tolerance but also led to dwarfism and late flowering (Jaglo-Ottosen et al., 1998; Gilmour et al., 2004). Therefore, the *CBFs* are not ideal target genes in transgenic breeding due to their negative effects. Previous transcriptome analysis showed that only 12% of the cold-responsive genes were controlled by *CBFs* (Fowler and Thomashow, 2002), which



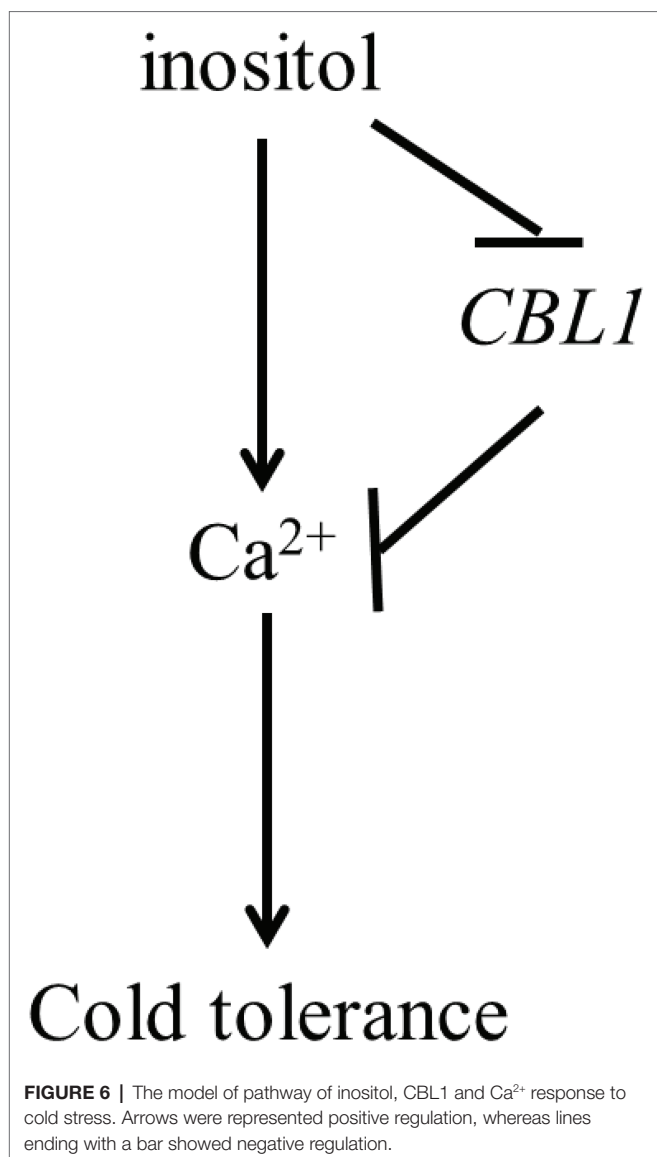
indicated there were other unexplored important pathways responding to cold stress.

Inositol, a cyclic polyol, is involved in various physiological processes and participates in programmed cell death, pathogen resistance, and stress adaptation in plants (Bohnert et al., 1995; Chaouch and Noctor, 2010; Bruggeman et al., 2014). In *Medicago falcata*, the concentration of inositol increased significantly under low temperature, and the inositol concentration in *Medicago falcata* (cold-tolerant) was higher than *Medicago sativa* (cold-sensitive) at 5°C (Tan et al., 2013). In animals, inositol was also reported to be involved in cold tolerance. For instance, the inositol concentrations increased up to 400-fold and peaked at 147 nmol mg⁻¹ fresh mass in overwintering flies during the winter (Vesala et al., 2012). Previous investigations also reported that inositol alleviated the damage of cold stress on maize and rice seedlings (You et al., 2000; Guo et al., 2014; Yao and Xia, 2014). When inositol was used as a seed coating, it significantly increased the germination rate and fresh weight in maize under cold stress (Yu et al., 2009). Notably, the combination of different concentrations of inositol and Ca^{2+} significantly promoted the growth of Chinese cabbage and pepper seedlings (Liu et al., 2017; Yang et al., 2017). In this study, inositol-3-phosphate synthase activity was enriched in T1, T2, T3, and S2 (Figure 1), and C18 showed higher inositol biosynthesis gene expression and lower degradation gene expression than in C20 (Figure 2A). Further, the endogenous

inositol concentration was increased in C18, and decreased in C20 with the continually dropping temperature (Figure 2B), suggesting the crucial role of inositol in cold tolerance. Besides, exogenous application of inositol increases cold tolerance of all four sensitive rapeseed cultivars (Figures 2C,D). Briefly, these results indicated that inositol played an important role in cold tolerance in rapeseed.

A New Signaling Pathway of Inositol Regulated Ca^{2+} and *CBL1* Modulates Cold Tolerance

As a secondary messenger, Ca^{2+} are participate in many biological processes and plays a critical role in signaling pathways under stress conditions in plants. Under stress, stress signals typically boost the Ca^{2+} levels over the threshold and activate calcium sensors. In this study, inositol positively regulated cold tolerance by increasing Ca^{2+} influx in rapeseed. Inositol is an important precursor of inositol phospholipids (Downes and Macphie, 1990). Phosphatidylinositol (4, 5) P₂ are hydrolyzed by phospholipase C (PLC) to InsP₃ and diacylglycerol (DAG). In animal cells, InsP₃ activate InsP₃ receptor (Ca^{2+} channel) and release Ca^{2+} (Valluru and Van den Ende, 2011). These outcomes suggest that there is a crosstalk between the signal pathway of inositol and Ca^{2+} in improving cold stress tolerance.



Some calcium sensors, such as *CBL1*, act as a rate-limiting factor in response to stress signals (Cheong et al., 2003). In *Arabidopsis*, *CBL1* improved the salt and drought stress tolerance but decreased cold stress tolerance (Cheong et al., 2003). Overexpression of *BnCBL1* improved tolerance to high salinity and low phosphate conditions in rapeseed (Chen et al., 2012). In this study, inositol increased Ca^{2+} influx under cold stress (Figures 4A,B), 351 Ca^{2+} DEGs and found *CBL1*s had different expression trend in both cultivars. Among different *CBL1*s, there were no significant differences in the expression levels of *BnCBL1-3* and *BnCBL1-4*. On the other hand, the expression levels of *BnCBL1-1* and *BnCBL1-2* were decreased in C18 under cold stress, whereas the expressions of four *BnCBL1*s increased in C20 under cold stress (Supplementary Table S4). Moreover, exogenous inositol decreases the expression of *BnCBL1-2* in C20 under freezing stress (Supplementary Figure S4). Overexpression of *BnCBL1-2* reduced cold tolerance and Ca^{2+} flux (Figures 5E,F). It was assumed that overexpression of *BnCBL1-2* may disturb the Ca^{2+} homeostasis in plants, leading to the failure in sending cold signals to the downstream

signaling pathway. This research also revealed that inositol inhibited the expression of *BnCBL1-2* (*BnaA01g08510D*) under cold stress. Therefore, it is proposed there is a mechanism that inositol regulates the Ca^{2+} signaling and the expression of *CBL1* (Figure 6), which is a brand-new signal pathway under cold stress in plants.

CONCLUSION

Rapeseed is considered one of the most important and economical oilseed crops around the world. However, cold stress significantly affects its growth and production in China. Therefore, the current study identified an inositol-mediated mechanism that helps in improving cold stress tolerance in rapeseed seedlings. Briefly, our results show that inositol positively regulated the cold tolerance by increasing Ca^{2+} influx in rapeseed. Inositol also inhibited the expression of the *CBL1* gene under stress conditions. Besides, overexpressed *Arabidopsis* plants mediated the Ca^{2+} flux under cold stress suggesting the key role of the inositol- Ca^{2+} pathway in cold tolerance in rapeseed. Therefore, future works should focus on how inositol interacts and regulates the expression of cold-responsive marker genes that help mitigate the adverse effect of cold stress on plants.

DATA AVAILABILITY STATEMENT

The original contributions presented in the study are publicly available in NCBI under accession number PRJNA562064.

AUTHOR CONTRIBUTIONS

LY conducted the experiment, analyzed the data, and wrote the paper. LY and AR wrote and revised the manuscript. LZ and XD provided the reagents and materials. YL, YC, and XZ helped in the relevant literature. XZ supervised the study, designed the experiment, and revised the paper. All authors contributed to the article and approved the submitted version.

FUNDING

This work was supported by the National Key Research and Development Program (2017YFD0101700), Agricultural Science and Technology Innovation Program of CAAS, and CARS-12.

ACKNOWLEDGMENTS

We thank all the members of the Key Laboratory of Biology and Genetic Improvement of Oil Crops, Oil Crops Research Institute, Chinese Academy of Agricultural Sciences (CAAS), Wuhan, China, for their support throughout the study.

SUPPLEMENTARY MATERIAL

The Supplementary Material for this article can be found online at <https://www.frontiersin.org/articles/10.3389/fpls.2022.775692/full#supplementary-material>

REFERENCES

- Abbasi, F., Onodera, H., Toki, S., Tanaka, H., and Komatsu, S. (2004). OsCDPK13, a calcium-dependent protein kinase gene from rice, is induced by cold and gibberellin in rice leaf sheath. *Plant Mol. Biol.* 55, 541–552. doi: 10.1007/s11103-004-1178-y
- Bohnert, H. J., Nelson, D. E., and Jensen, R. G. (1995). Adaptations to environmental stresses. *Plant Cell* 7, 1099–1111. doi: 10.2307/3870060
- Bruggeman, Q., Garmier, M., de Bont, L., Soubigou-Taconnat, L., Mazubert, C., Benhamed, M., et al. (2014). The polyadenylation factor subunit CLEAVAGE AND POLYADENYLATION SPECIFICITY FACTOR30: a key FACTOR of programmed cell death and a regulator of immunity in *Arabidopsis*. *Plant Physiol.* 165, 732–746. doi: 10.1104/pp.114.236083
- Chaouch, S., and Noctor, G. (2010). Myo-inositol abolishes salicylic acid-dependent cell death and pathogen defence responses triggered by peroxisomal hydrogen peroxide. *New Phytol.* 188, 711–718. doi: 10.1111/j.1469-8137.2010.03453.x
- Chen, T. H., and Gusta, L. V. (1983). Absciscic acid-induced freezing resistance in cultured plant cells. *Plant Physiol.* 73, 71–75. doi: 10.1104/pp.73.1.71
- Chen, L., Ren, F., Zhou, L., Wang, Q. Q., Zhong, H., and Li, X. B. (2012). The Brassica napus calcineurin B-like 1/CBL-interacting protein kinase 6 (CBL1/CIPK6) component is involved in the plant response to abiotic stress and ABA signalling. *J. Exp. Bot.* 63, 6211–6222. doi: 10.1093/jxb/ers273
- Chen, L., Zhong, H., Ren, F., Guo, Q. Q., Hu, X. P., and Li, X. B. (2011). A novel cold-regulated gene, COR25, of Brassica napus is involved in plant response and tolerance to cold stress. *Plant Cell Rep.* 30, 463–471. doi: 10.1007/s00299-010-0952-3
- Cheong, Y. H., Kim, K. N., Pandey, G. K., Gupta, R., Grant, J. J., and Luan, S. (2003). CBL1, a calcium sensor that differentially regulates salt, drought, and cold responses in *Arabidopsis*. *Plant Cell* 15, 1833–1845. doi: 10.1105/tpc.012393
- Chinnusamy, V., Ohta, M., Kanrar, S., Lee, B. H., Hong, X., Agarwal, M., et al. (2003). ICE1: a regulator of cold-induced transcriptome and freezing tolerance in *Arabidopsis*. *Genes Dev.* 17, 1043–1054. doi: 10.1101/gad.1077503
- Chinnusamy, V., Zhu, J., and Zhu, J. K. (2007). Cold stress regulation of gene expression in plants. *Trends Plant Sci.* 12, 444–451. doi: 10.1016/j.tplants.2007.07.002
- Clough, S. J., and Bent, A. F. (1998). Floral dip: a simplified method for agrobacterium-mediated transformation of *Arabidopsis thaliana*. *Plant J.* 16, 735–743. doi: 10.1046/j.1365-3113.1998.00343.x
- Ding, Y., Shi, Y., and Yang, S. (2019). Advances and challenges in uncovering cold tolerance regulatory mechanisms in plants. *New Phytol.* 222, 1690–1704. doi: 10.1111/nph.15696
- Downes, C. P., and Macphree, C. H. (1990). Myo-inositol metabolites as cellular signals. *Eur. J. Biochem.* 193, 1–18. doi: 10.1111/j.1432-1033.1990.tb19297.x
- Fowler, S., and Thomashow, M. F. (2002). *Arabidopsis* transcriptome profiling indicates that multiple regulatory pathways are activated during cold acclimation in addition to the CBF cold response pathway. *Plant Cell* 14, 1675–1690. doi: 10.1105/tpc.003483
- Gilmour, S. J., Fowler, S. G., and Thomashow, M. F. (2004). *Arabidopsis* transcriptional activators CBF1, CBF2, and CBF3 have matching functional activities. *Plant Mol. Biol.* 54, 767–781. doi: 10.1023/B:PLAN.0000040902.06881.d4
- Guo, Y. F., Gan, L. J., Zhu, C. H., Li, G. J., and Xia, K. (2014). Cold resistance of rice seedlings exposed to inositol. *Jiangsu J. Agr. Sci.* 30, 1216–1221 (in Chinese).
- Huang, X., Shi, H., Hu, Z., Liu, A., Amombo, E., Chen, L., et al. (2017). ABA is involved in regulation of cold stress response in Bermudagrass. *Front. Plant Sci.* 8:1613. doi: 10.3389/fpls.2017.01613
- Huang, H., Yan, L., Zhang, Y., Raza, A., Zeng, L., Lv, Y., et al. (2021). Study on the mechanism of exogenous serotonin improving cold tolerance of rapeseed (*Brassica napus* L.) seedlings. *Plant Growth Regul.* 94, 161–170. doi: 10.1007/s10725-021-00700-0
- Jaglo-Ottosen, K. R., Gilmour, S. J., Zarka, D. G., Schabenberger, O., and Thomashow, M. F. (1998). *Arabidopsis* CBF1 overexpression induces COR genes and enhances freezing tolerance. *Science* 280, 104–106. doi: 10.1126/science.280.5360.104
- Jia, Y., Ding, Y., Shi, Y., Zhang, X., Gong, Z., and Yang, S. (2016). The cbfs triple mutants reveal the essential functions of CBFs in cold acclimation and allow the definition of CBF regulons in *Arabidopsis*. *New Phytol.* 212, 345–353. doi: 10.1111/nph.14088
- Knight, H., Trewavas, A. J., and Knight, M. R. (1996). Cold calcium signaling in *Arabidopsis* involves two cellular pools and a change in calcium signature after acclimation. *Plant Cell* 8, 489–503. doi: 10.1105/tpc.8.3.489
- Komatsu, S., Yang, G., Khan, M., Onodera, H., Toki, S., and Yamaguchi, M. (2007). Over-expression of calcium-dependent protein kinase 13 and calreticulin interacting protein 1 confers cold tolerance on rice plants. *Mol. Gen. Genomics.* 277, 713–723. doi: 10.1007/s00438-007-0220-6
- Kou, S., Chen, L., Tu, W., Scossa, F., Wang, Y., Liu, J., et al. (2018). The arginine decarboxylase gene *adc1*, associated to the putrescine pathway, plays an important role in potato cold-acclimated freezing tolerance as revealed by transcriptome and metabolome analyses. *Plant J.* 96, 1283–1298. doi: 10.1111/tjp.14126
- Li, P., Zheng, T., Li, L., Zhuo, X., Jiang, L., Wang, J., et al. (2019). Identification and comparative analysis of the CIPK gene family and characterization of the cold stress response in the woody plant *Prunus mume*. *Peer J* 7:e6847. doi: 10.7717/peerj.6847
- Liu, Q., Ding, Y., Shi, Y., Ma, L., Wang, Y., Song, C., et al. (2020). The calcium transporter ANNEXIN1 mediates cold-induced calcium signaling and freezing tolerance in plants. *EMBO J.* 40:e104559. doi: 10.15252/emboj.2020104559
- Liu, T. W., Yang, W. J., Wang, F., Jiang, H. M., Yang, Z., and Xu, J. M. (2017). Synergistic effects of inositol and calcium on growth and development of Chinese cabbage seedlings. *J. Changjiang Vegetables* 14, 65–70 (in Chinese).
- Loewus, F. A., and Murthy, P. P. (2000). Myo-inositol metabolism in plants. *Plant Sci.* 150, 1–19. doi: 10.1016/S0168-9452(99)00150-8
- Ma, Y., Dai, X., Xu, Y., Luo, W., Zheng, X., Zeng, D., et al. (2015). COLD1 confers chilling tolerance in rice. *Cell* 160, 1209–1221. doi: 10.1016/j.cell.2015.01.046
- Raza, A. (2021). Eco-physiological and biochemical responses of rapeseed (*Brassica napus* L.) to abiotic stresses: consequences and mitigation strategies. *J. Plant Growth Regul.* 40, 1368–1388. doi: 10.1007/s00344-020-10231-z
- Raza, A., Su, W., Hussain, M. A., Mehmood, S. S., Zhang, X., Cheng, Y., et al. (2021). Integrated analysis of Metabolome and Transcriptome reveals insights for cold tolerance in rapeseed (*Brassica napus* L.). *Front. Plant Sci.* 12:721681. doi: 10.3389/fpls.2021.721681
- Rubio, S., Noriega, X., and Pérez, F. J. (2019). Absciscic acid (ABA) and low temperatures synergistically increase the expression of CBF/DREB1 transcription factors and cold-hardiness in grapevine dormant buds. *Ann. Bot.* 123, 681–689. doi: 10.1093/aob/mcy201
- Savitch, L. V., Allard, G., Seki, M., Robert, L. S., Tinker, N. A., Huner, N. P., et al. (2005). The effect of overexpression of two brassica CBF/DERE1-like transcription factors on photosynthetic capacity and freezing tolerance in *Brassica napus*. *Plant Cell Physiol.* 46, 1525–1539. doi: 10.1093/pcp/pci165
- Shi, Y., Ding, Y., and Yang, S. (2015). Cold signal transduction and its interplay with phytohormones during cold acclimation. *Plant Cell Physiol.* 56, 7–15. doi: 10.1093/pcp/pcu115
- Tan, T., Sun, Y., Peng, X., Wu, G., Bao, F., He, Y., et al. (2017). *ABSCISIC ACID INSENSITIVE3* is involved in cold response and freezing tolerance regulation in *Physcomitrella patens*. *Front. Plant Sci.* 8:1599. doi: 10.3389/fpls.2017.01599
- Tan, J., Wang, C., Xiang, B., Han, R., and Guo, Z. (2013). Hydrogen peroxide and nitric oxide mediated cold- and dehydration-induced myo-inositol phosphate synthase that confers multiple resistances to abiotic stresses. *Plant Cell Environ.* 36, 288–299. doi: 10.1111/j.1365-3040.2012.02573.x
- Valluru, R., and Van den Ende, W. (2011). Myo-inositol and beyond—emerging networks under stress. *Plant Sci.* 181, 387–400. doi: 10.1016/j.plantsci.2011.07.009
- Vesala, L., Salminen, T. S., Košťál, V., Zahradníčková, H., and Hoikkala, A. (2012). Myo-inositol as a main metabolite in overwintering flies: seasonal metabolomic profiles and cold stress tolerance in a northern drosophilid fly. *J. Exp. Biol.* 215, 2891–2897. doi: 10.1242/jeb.069948

- Wang, Z., Fang, H., Chen, Y., Chen, K., Li, G., Gu, S., et al. (2014). Overexpression of *BnWRKY33* in oilseed rape enhances resistance to *Sclerotinia sclerotiorum*. *Mol. Plant Pathol.* 15, 677–689. doi: 10.1111/mpp.12123
- Weckwerth, P., Ehler, B., and Romeis, T. (2015). ZmCPK1, a calcium-independent kinase member of the *Zea mays* CDPK gene family, functions as a negative regulator in cold stress signalling. *Plant Cell Environ.* 38, 544–558. doi: 10.1111/pce.12414
- Xin, Z., and Browse, J. (2000). Cold comfort farm: the acclimation of plants to freezing temperatures. *Plant Cell Environ.* 23, 893–902. doi: 10.1046/j.1365-3040.2000.00611.x
- Yan, L., Cai, J. S., Gao, L. B., Huang, B., Ma, H. Q., Liu, Q., et al. (2018). Identification method and selection of cold tolerance in rapeseed (*Brassica napus* L.). *Chinese J. Oil Crop Sci.* 40, 074–083 (in Chinese).
- Yan, L., Tariq, S., Cheng, Y., Lü, Y., Zhang, X. K., and Zou, X. L. (2019). Physiological and molecular responses to cold stress in rapeseed (*Brassica napus* L.). *J. Integr. Agric.* 18, 2742–2752. doi: 10.1016/S2095-3119(18)62147-1
- Yang, W. J., Wang, Y. T., Liu, T. W., and Xu, J. M. (2017). Research on synergistic action of inositol and calcium ion to growth and development of pepper seedlings. *Acta Agr. Jiangxi* 29, 16–19 (in Chinese).
- Yao, H., and Xia, K. (2014). Mitigative effect of inositol on low temperature stress of maize seedlings. *Crops* 04, 133–138 (in Chinese).
- You, J. H., Yang, W. J., and Li, X. L. (2000). Effects of inositol on chilling resistance of corn seedlings. *J. Northeast Normal University* 03, 44–46 (in Chinese).
- Yu, M. Y., Wang, X., Zhang, W. W., and Li, Y. F. (2009). Effects of inositol seed-coating on seed germination and seedling growth in maize under low temperature stress. *J. Maize Sci.* 17, 80–82, 86 (in Chinese).
- Zeng, X., Xu, Y., Jiang, J., Zhang, F., Ma, L., Wu, D., et al. (2018). Identification of cold stress responsive microRNAs in two winter turnip rape (*Brassica rapa* L.) by high throughput sequencing. *BMC Plant Biol.* 18:52. doi: 10.1186/s12870-018-1242-4
- Zhang, R. X., Qin, L. J., and Zhao, D. G. (2017). Overexpression of the OsIMP gene increases the accumulation of inositol and confers enhanced cold tolerance in tobacco through modulation of the antioxidant enzymes' activities. *Genes* 8:179. doi: 10.3390/genes8070179
- Zhang, X., Zhang, C., Liao, X., and Wang, H. (2008). Investigation on 2008' low temperature and freeze injure on winter rape along Yangtze River. *Chinese J. Oil Crop Sci.* 30, 122–126 (in Chinese).
- Zhao, C., Zhang, Z., Xie, S., Si, T., Li, Y., and Zhu, J. K. (2016). Mutational evidence for the critical role of CBF transcription factors in cold acclimation in *Arabidopsis*. *Plant Physiol.* 171, 2744–2759. doi: 10.1104/pp.16.00533

Conflict of Interest: The authors declare that the research was conducted in the absence of any commercial or financial relationships that could be construed as a potential conflict of interest.

Publisher's Note: All claims expressed in this article are solely those of the authors and do not necessarily represent those of their affiliated organizations, or those of the publisher, the editors and the reviewers. Any product that may be evaluated in this article, or claim that may be made by its manufacturer, is not guaranteed or endorsed by the publisher.

Copyright © 2022 Yan, Zeng, Raza, Lv, Ding, Cheng and Zou. This is an open-access article distributed under the terms of the Creative Commons Attribution License (CC BY). The use, distribution or reproduction in other forums is permitted, provided the original author(s) and the copyright owner(s) are credited and that the original publication in this journal is cited, in accordance with accepted academic practice. No use, distribution or reproduction is permitted which does not comply with these terms.

Advantages of publishing in Frontiers



OPEN ACCESS

Articles are free to read
for greatest visibility
and readership



FAST PUBLICATION

Around 90 days
from submission
to decision



HIGH QUALITY PEER-REVIEW

Rigorous, collaborative,
and constructive
peer-review



TRANSPARENT PEER-REVIEW

Editors and reviewers
acknowledged by name
on published articles

Frontiers

Avenue du Tribunal-Fédéral 34
1005 Lausanne | Switzerland

Visit us: www.frontiersin.org

Contact us: frontiersin.org/about/contact



REPRODUCIBILITY OF RESEARCH

Support open data
and methods to enhance
research reproducibility



DIGITAL PUBLISHING

Articles designed
for optimal readership
across devices



FOLLOW US

@frontiersin



IMPACT METRICS

Advanced article metrics
track visibility across
digital media



EXTENSIVE PROMOTION

Marketing
and promotion
of impactful research



LOOP RESEARCH NETWORK

Our network
increases your
article's readership